UNIVERSITY OF TURIN

Department of Clinical and Biological Sciences

PhD in Experimental Medicine and Therapy

Cycle XXXII

New antiviral approaches against known and emerging viruses

Thesis' author: **Rachele Francese**

Supervisor: Prof. David Lembo

PhD Programme Co-ordinator: Prof. Pasquale Pagliaro

Academic years of enrolment: 2016-2020

Code of scientific discipline: MED07

INDEX

7. STUDY OF THE ANTIVIRAL ACTIVITY OF HUMAN MILK AGAINST EMERGING FLAVIVIRUSES

8. ANALYSIS OF THE EFFECT OF HOLDER PASTEURIZATION AND HIGHT TEMPERATURE-SHORT TIME PASTEURIZATION ON MILK'S ANTIVIRAL PROPERTIES

PREFACE

I am writing my PhD thesis during the COVID-19 pandemic that dramatically changed our lives. This current situation makes clearer to me that viral infections represent a global challenge and we need to keep working hard in the fighting against both known and emerging viruses. Viral infections have indeed a significant impact on the societies, both in terms of death toll and economically. Furthermore, numerous viruses are still without a specific and safe antiviral drug and some viruses are developing resistance against the current therapies. All these elements, along with the constant emergence of new viruses, represented the driving force of my research projects.

During my PhD course, I investigated two different, but in some way complementary, lines of research. The first one was mainly focused on the discovery of new antiviral drugs or new antiviral strategies for the treatment and prevention of infectious viral diseases. The second line of research was instead aimed at studying the antiviral properties of human milk, both against viruses of pediatric clinical relevance or against recently emerged human pathogens. I was fascinated, and I still am, by this exceptional biofluid able to confer a natural protection against infections during the most vulnerable time of our life.

These multidisciplinary studies were performed in collaboration with national and international Universities and were designed with the aim to fulfill unmet medical needs. Important associations in the field of human milk banking and pediatric healthcare also supported some studies. In the following sections, I reviewed the recent literature on the presented research fields with an overview on the viruses of interest and a description of the analyzed molecules/compounds/biological fluids. Each section is closed by a brief description of the aim of the study followed by produced publications.

1. THE ANTIVIRAL THERAPY

The development of a safe and effective antiviral drug is a difficult task and several factors hinder this process:

1)   Viruses are obligate intracellular parasites that largely depend on the host cell biosynthetic machinery for their replication. Therefore, antiviral drugs can target only a limited number of virus-specific metabolic functions without harming the host;

2)   Most of these functions are specific for each virus, making it difficult to develop broad-spectrum antivirals active against diverse viruses that cause similar symptoms;

3)   The antivirals developed against some viruses treat the acute disease but do not cure the latent infection. This results in recurrent or chronic diseases that require treatment for longer periods;

4)   Many of the approved antiviral drugs present unfavorable pharmacokinetic features (mainly due to limited adsorption) that increase the dose to be administered daily or prolonge the treatment period with consequent severe side effects, negative patient compliance and the favorable environment for viruses to develop resistance.

The list of viral diseases for which antiviral therapies are available is still relatively short. About one hundred fifty antiviral drugs have been approved for the use in humans so far (1–3). They are mostly directed against the chronic infections caused by immunodeficiency virus (HIV-1), hepatitis B virus (HBV), hepatitis C virus (HCV), and herpesviruses such as herpes simplex viruses type I and II (HSV-1 and HSV-2) and cytomegalovirus (CMV). Only a few drugs were approved to treat acute infections, mainly influenza (Fig. 1).

Approvals Per Indication

43
17
8
11
4
5

48.9% HIV-1
19.3% HCV
9.1%   HBV
12.5% CMV, HSV
4.6%   Influenza
5.7%   Other
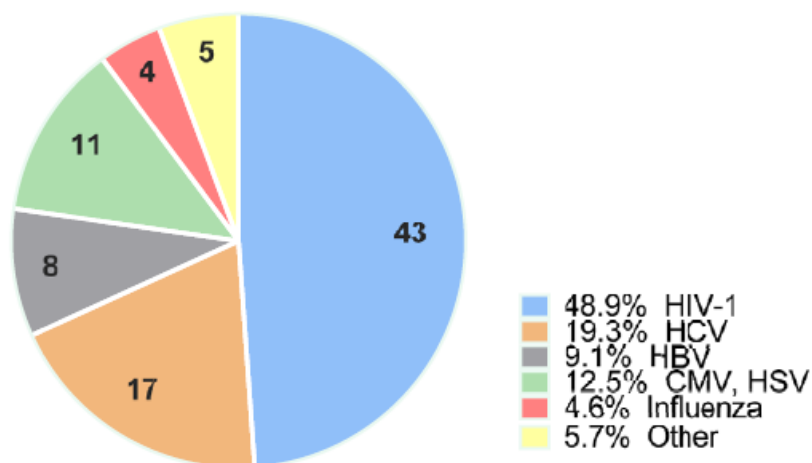
Figure 1: Proportion and number of US FDA antiviral drug approvals per indication (4)

Between the approved antiviral agents, twenty-one are broad-spectrum antivirals (BSAAs), i.e. compounds targeting viruses belonging to two or more viral families. This type of molecules could provide additional protection of the general population from emerging and re-emerging viral diseases, reinforcing the arsenal of available antiviral options. Although the concept of BSAAs has been around for almost 50 years, the field received a new impetus with recent outbreaks of Ebola, Zika, Dengue, influenza and other viral infections, the discovery of novel host-directed agents, as well as development of drug repositioning methodology (5,6). A large majority of the approvals were for small molecules and virus-targeting agents over large molecules (interferons, monoclonal antibodies and one oligonucleotide) and host-targeting therapies.

The available antivirals function using several mechanisms of action that include inhibition of viral penetration, uncoating, nucleic acid synthesis, integration of viral DNA into host genome, maturation, and exit from host cells. Nevertheless, the current antiviral clinical trials indicate a departure from classical targets (polymerase, protease…) with oligonucleotide-based therapeutics, cell fusion inhibitors, capsid-assembly modulators, and an array of novel host-based mechanisms (4,7,8) (Fig. 2).
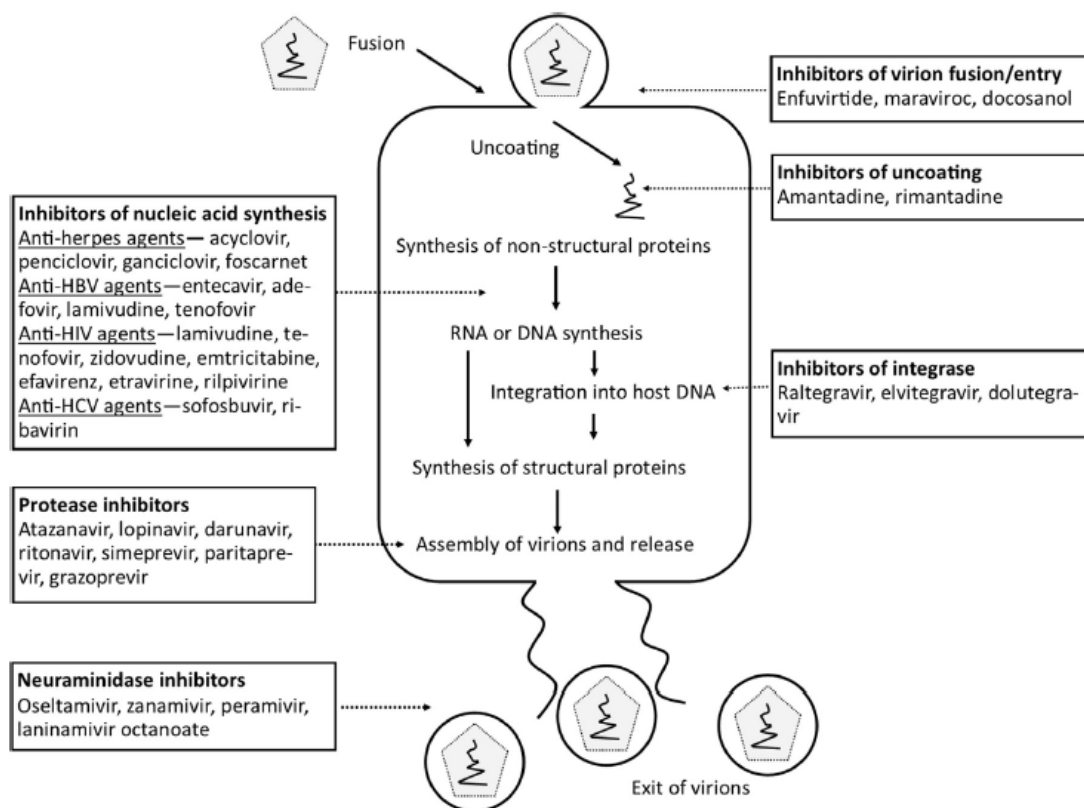
Figure 2: Mechanisms of action of most common types of antivirals (7)

Combination therapies, approved during the last years, especially for the treatment of HIV-1 and HCV infections, are employed to prevent the emergence of drug resistance by inhibiting viral replication at multiple points in the viral life cycle.

Nowadays, administration of antivirals remains the only way to combat HIV, HCV, HSV, respiratory syncytial virus (RSV), and CMV infections. On the other hand, despite big efforts from the scientific community, many viral infections are targeted only by vaccines, such as hepatitis A virus (HAV), rotavirus (HRoV), mumps, varicella and the current pandemic severe acute respiratory syndrome coronavirus 2 (SARS-CoV2). Furthermore, there are some viral infections against which we do not have any preventive or therapeutic tools, such as Zika virus (ZIKV), West-Nile virus (WNV) and other known and emerging viruses.

In this context, the first line of research of my PhD course was addressed to identify new antiviral molecules between compounds of different origins and different properties (chemically synthetized molecules, cholesterol derived molecules, plant extracts and compounds from ethno-medicine). I focused my attention on the emerging ZIKV and on the well-known HRoV that I will present in details in the next dedicated sections (paragraph 2.1 and 3.1 respectively).

2. STUDY OF NEW ANTIVIRAL MOLECULES AGAINST THE EMERGING ZIKA VIRUS

2.1 Overview on the emerging zika virus

ZIKV belongs to the *Flaviviridae* family, which also includes Dengue virus (DENV), WNV, Yellow fever virus (YFV), Japanese encephalitis virus (JEV) and Usutu virus (USUV). ZIKV is mostly transmitted by *Aedes aegypti* mosquitos, but sexual, vertical and blood transmissions have also been reported (9–11).

ZIKV is a positive sense, single-strand RNA virus with a genome size of approximately 10.8 kilobases. The RNA is translated into a single polyprotein encoding 3 structural proteins—capsid (C); membrane (M), which is generated from its precursor premembrane (prM); and envelope (E)—as well as 7 nonstructural proteins—NS1 (involved in RNA replication and particle assembly), NS2A (RNA replication and immune evasion), NS2B (cofactor of NS3), NS3 (major viral protease), NS4A (cofactor of NS3), NS4B (RNA replication and immune evasion) and NS5 (RNA synthesis and modification)—which are essential for viral replication. Immature virions are spiky, have a diameter of 60 nm, and display 60 projections of trimers of prM-E heterodimers. Mature virions, in contrast, are smaller (diameter of 50 nm) and have a smooth surface, which is formed by a herringbone-like array of 90 E protein homodimers oriented parallel to the viral membrane (12,13). Viral envelope protein E intermediates membrane fusion by receptor-mediated endocytosis mostly through C-type lectin receptors family from the host-cell. Although, cellular lipid receptors, such as TIM (T-cell immunoglobulin mucin) and TAM (Receptor tyrosine kinases: TYRO3, AXL and MER) receptor families showed to mediate ZIKV entry by interactions that do not involve protein E, but occur between negatively charged lipids, such as phosphatidylserine (PS), present in the viral membrane. Studies *in vivo* showed that cells of the reproductive tract (spermatogonia, sperm, Sertoli and Leydig cells) and from cerebral cortex and hippocampus are permissive to ZIKV infection in mice. More importantly, using an *in vitro* approach, cell culture experiments demonstrated the ability of ZIKV to infect human cells, such as skin fibroblasts, uterine fibroblasts, primary placental trophoblasts and Hofbauer cells, endometrial stromal cells, and neural progenitor cells (14). ZIKV structure and replicative cycle are schematically presented in Figure 3.
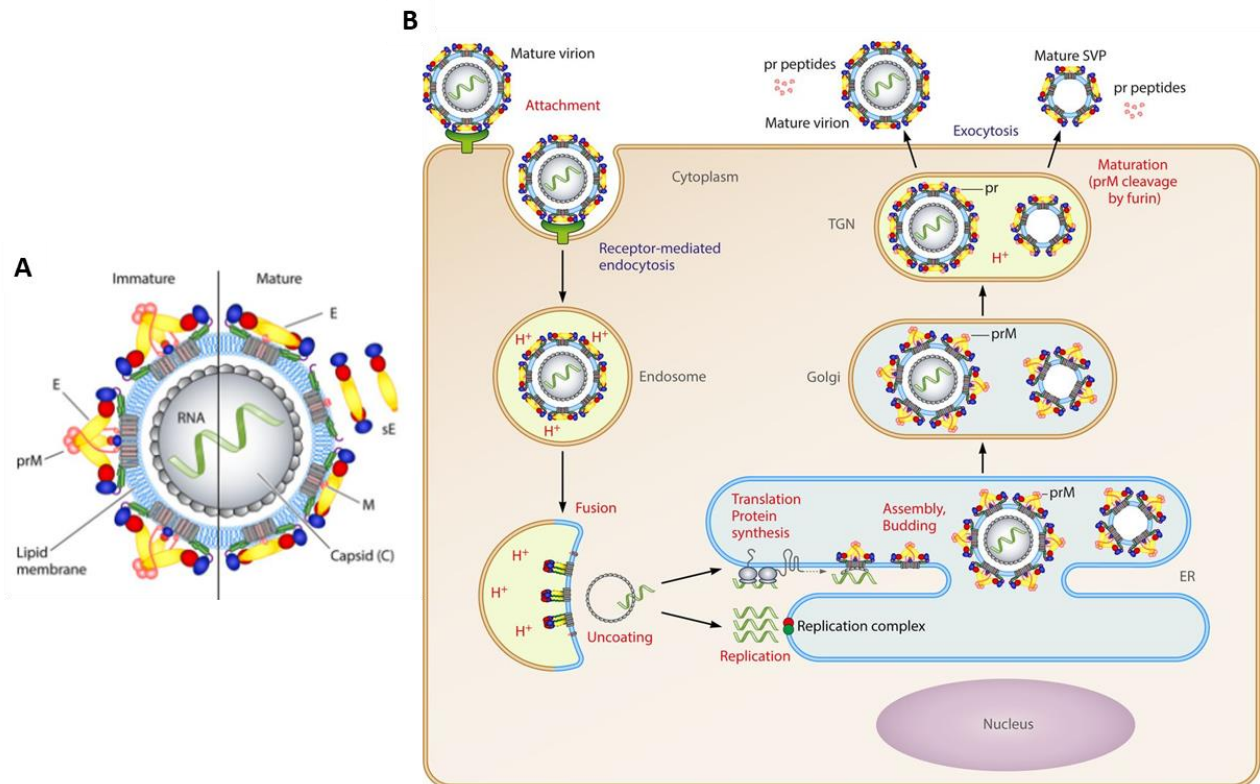
Figure 3: ZIKV structure (A) and ZIKV replicative cycle (B) (Adapted from Heinz et al.(12)). ZIKV enters cells by receptor-mediated endocytosis and fuses its membrane by an acidic-pH-triggered mechanism in the endosome to release the viral RNA. The positive-stranded genomic RNA serves as the only viral mRNA and leads to the synthesis of a polyprotein that is co- and post-translationally processed into three structural and seven nonstructural proteins. Virus assembly takes place at the ER membrane and leads to the formation of immature virions, which are further transported through the exocytic pathway. The acidic pH in the trans-Golgi network (TGN) causes structural changes that allow the cleavage of prM by the cellular protease furin and lead to the herringbone-like arrangement of E. At acidic pH, the cleaved pr part remains associated with the particles (preventing premature fusion in the TGN) and falls off at the neutral pH of the extracellular environment. Subviral particles (SVPs) are formed as a by-product of virion assembly and contain a lipid membrane and prM-E complexes but lack a capsid. SVPs are transported, processed, and released like whole virions

In symptomatic individuals (around 18% of cases), ZIKV causes a mild illness characterized by fever, rash, headache, conjunctivitis, joint and muscle pain. The incubation period is 4-11 days and the symptoms disappear in approximately a week (15). However, unlike other flaviviruses, ZIKV is associated to two main neurological complications: the Guillain-Barré Syndrome in adults and the now termed Zika Congenital Syndrome (CSZ), a variety of neurological impairments in fetus and infants of women infected during pregnancy. The incidence of ZIKV-associated Guillain–Barré syndrome is estimated to be 2 to 3 cases per 10,000 ZIKV infections. Acute inflammatory demyelinating polyneuropathy, acute motor axonal neuropathy, and the Miller–Fisher syndrome (a subset of the Guillain–Barré syndrome characterized by ophthalmoplegia, ataxia, and areflexia) have also been observed in these patients. The prognosis of ZIKV-associated Guillain–Barré syndrome is

similar to that of Guillain–Barré syndrome associated with other infectious or noninfectious processes; however, findings from a case–control study suggest that ZIKV-associated Guillain–Barré syndrome results in higher morbidity and more frequent cranial neuropathy. (16). On the other hand, the main clinical manifestations of CZS are severe microcephaly resulting in a partially collapsed skull, intracranial calcifications, eye abnormalities, limb contractures, high muscle tone and hearing loss. Child outcomes vary according to the extent of the brain damage (17). Vertical transmission has been estimated to occur in 26% of fetuses of ZIKV-infected mothers. The newborns have a 5 to 14% risk of CZS and a 4 to 6% risk of ZIKV-associated microcephaly. Although ZIKV infection in any trimester of pregnancy may cause CZS, the risk is greatest with infections occurring in the first trimester. The absence of clinical and radiologic abnormalities indicative of CZS at birth does not exclude the risk of abnormalities later in life (16). All the possible outcomes of ZIKV infection are schematically reported in Figure 4.
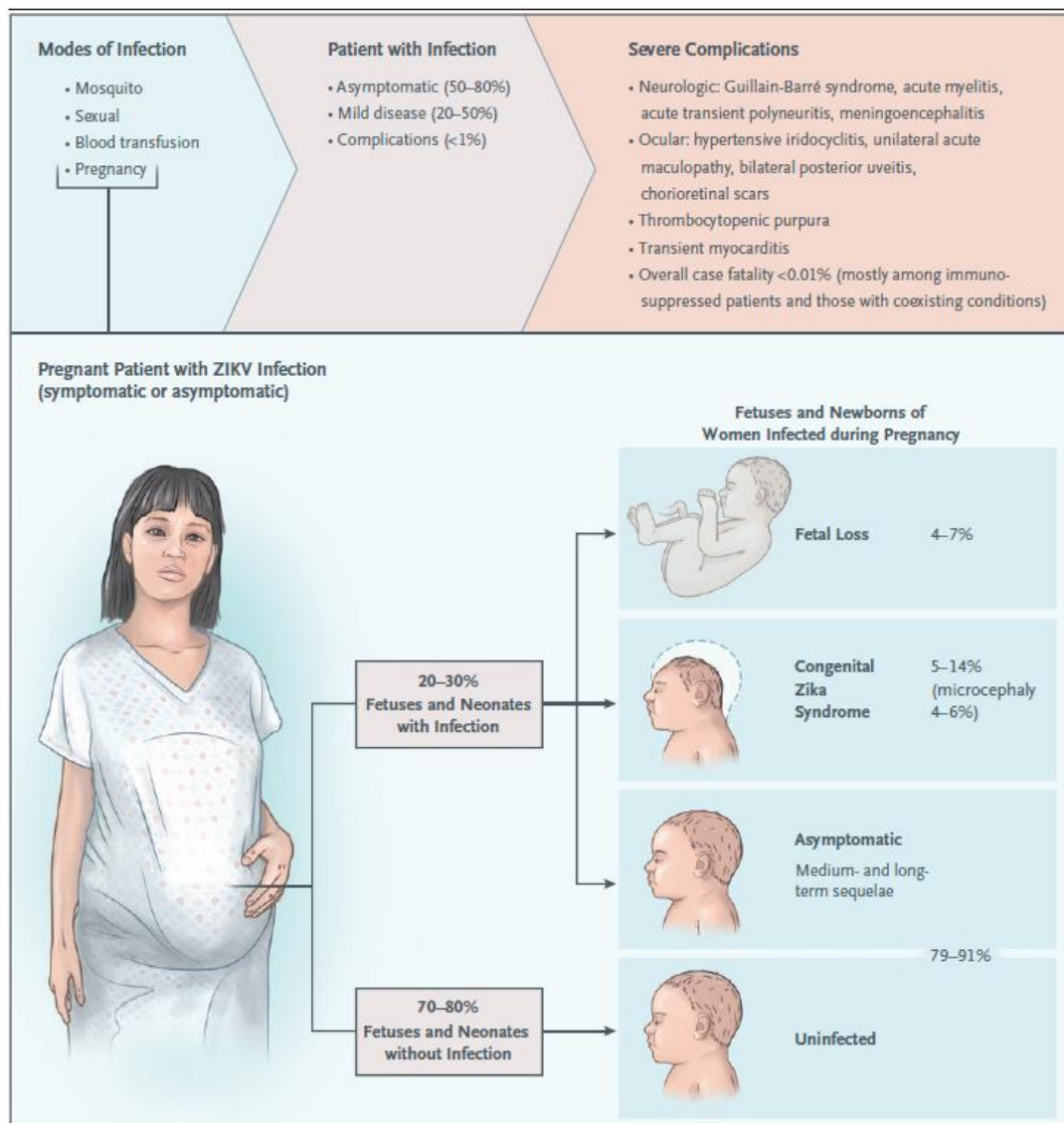
Figure 4: Zika Virus Transmission and Clinical Features (16)

The first case of ZIKV human infection was reported in 1950 in Africa, but its potential effect on public health was not recognized until the virus caused outbreaks in the Pacific from 2007 to 2015 and began spreading throughout the Americas in 2015. This last major epidemic counted, at its peak, more than 500 000 ZIKV cases and around 3000 cases of CZS, driving the World Health Organization to declare a public health emergency of international concern (18). Although transmission of ZIKV has declined in the Americas, the virus still poses a public health threat, as shown by outbreaks and infection clusters reported in some regions, such as India, Southeast Asia and Africa (19). At present, we do not have the tools to predict where and when the next large epidemic will happen, but the large numbers of susceptible persons residing in *Aedes*-infested regions make a reemergence of ZIKV likely.

Since the beginning of the pandemic, great efforts have been carried out, but nowadays still no vaccine or specific antiviral against ZIKV is available. The best way to prevent ZIKV infection is to avoid mosquito bites and the treatment of infected patients is palliative, involving analgesics and antipyretics (20,21). The discovery of an antiviral drug against ZIKV is a huge challenge, since it must be efficient and safe as any drug, but also be able to cross the placental barrier and the blood–brain barrier. Until now, this necessity has not been met.

I have been working on ZIKV since the end of 2016, when the number of ZIKV infections in the world was at its peak. In particular two different ZIKV strains have been the subject of my PhD research, the MR766, belonging to the African lineage and the HPF2013, belonging to the Asian one. They were selected as representative members of the two lineages in which ZIKV can be classified. The Asian-lineage ZIKV are responsible for the latest epidemics and are considered to be less virulent than the African ones, because of the lower infection rate, the lower viral production, the poor induction of early cell death and the lower immuno-stimulation in different models. These characteristics allow the virus to cause a prolonged infection within the central nervous system of fetus that could be the cause of its association with neurological impairments. On the contrary, the African lineage-ZIKV can result in a more acute infection, but they were not the cause of human outbreaks until now (22). Part of my PhD project was focused on the discovery of new antiviral agents against both ZIKV strains. Two different approaches have been investigated *in vitro* and they are deeply described in the 2.2 and 2.3 sections that are closed by produced publications.

2.2 The polyoxometalates

Polyoxometalates (POMs) are a class of negatively charged inorganic compounds recently used in biomedical research. POMs are anionic clusters of oxygen atoms and early transitional metal ions in

their highest oxidation states, such as tungsten (W^{VI}), molybdenum (Mo^{VI}) and vanadium (V^V). POMs can be classified into two groups:

- isopolyanions, composed of one type of metal (M) and oxygen (O), $[M_mO_y]^{p-}$;
- heteropolyanions, composed of one type of metal (M), oxygen (O) and a heterogroup (X), $[X_xM_mO_y]^{q-}$

Heteropolyanions are sub-classified based on core structure, which can vary in the number of oxygen and metal atoms. Examples are Anderson-Evans type $[XM_6O_{24}]^{n-}$, Keggin type POM $[XM_{12}O_{40}]^{n-}$ and Dawson type $[X_2M_{18}O_{62}]^n$ (Figure 5)(23).
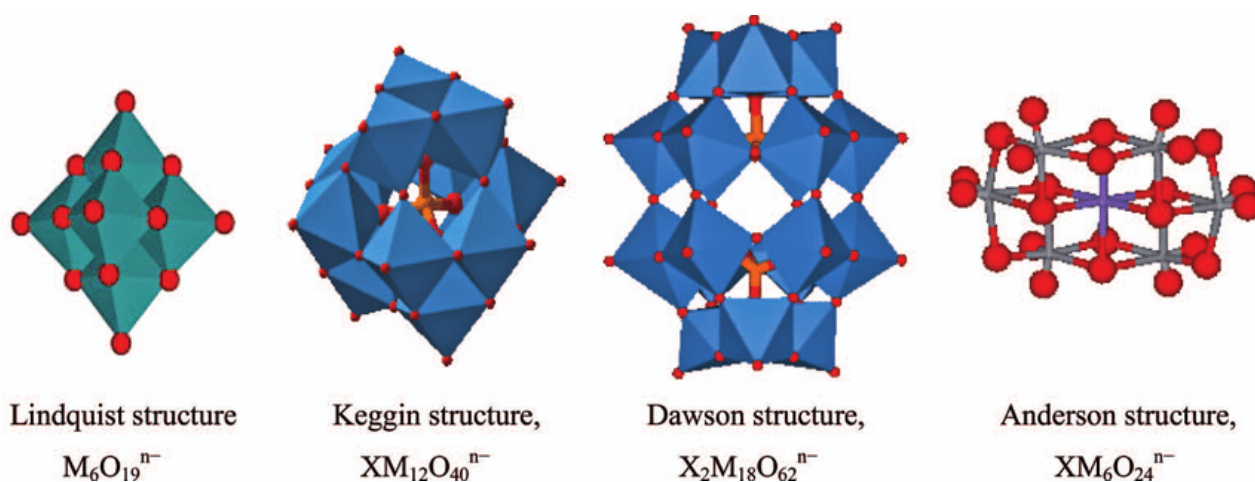
Figure 5: Some examples of common POMs structures (23)

POMs are a large family of compounds, characterized by structural and compositional variety and consequently various physical, chemical and biological properties. POMs are easily tunable at the molecular level in order to modify shape, size, surface distribution of charge, redox potential and acidity. Furthermore, POMs can be linked to an organic group or incorporated in biological matrices, in order to make the ion more compatible with physiological conditions, to lower the toxicity, and to improve cellular target delivery. Indeed, nearly every molecular property that affects the recognition between POMs and biological targets and the bioavailability of POMs can be modified, making them an interesting tool in biomedicine. In addition, the simple and highly reproducible methods and the favorable relative cost/efficiency ratio for POMs' synthesis, compared to organic pharmaceutical representatives, are other attractive features for POMs' clinical application. Inorganic POMs, organic-inorganic hybrid POMs and POM-based nanocomposites are the most common forms of POMs employed in biomedical research (24–26).

Recently, POMs were studied for a wide range of biological activities, such as for treatment of infectious diseases, diabetes, cancer and neurological diseases (27–29). In particular, POMs were already been investigated for their antiviral activity both *in vitro* and *in vivo* studies. Shigeta *et al.*(30) examined *in vitro* a panel of titanium- and vanadium-substituted POMs which exhibited antiviral activity against HIV-1, influenza virus type A, respiratory syncytial virus, parainfluenza virus type 2, Dengue virus and SARS coronavirus 1 (SARS-CoV1). Moreover, Wang *et al.*(31) identified a tri-niobium-containing POM which exerted anti-Influenza A, -Influenza B, -HSV-1, -HSV-2, -HIV-1, and -HBV activity and, a more recent article, shows that the polyoxometalate compound POM-12 has anti-flavivirus activity, with minimal cytotoxicity in cell culture system (32). Some limitations have been highlighted in the field of polyoxometalates in medicine, especially for their inorganic nature. At physiological pH, several POM salts are poorly soluble in water or thermodynamically unstable and therefore can undergo degradation or transformation in toxic metabolites (28). POMs used in biological studies must be truly solution-stable at physiological pH and in other physico-chemical conditions, in order to allow the clinical administration with the most suitable route (oral, topical, nasal and/or systemic) (18).

2.2.1 Publications

Francese R, Civra A, Rittà M, Donalisio M, Argenziano M, Cavalli R, Mougharbel AS, Kortz U, Lembo D. Anti-zika virus activity of polyoxometalates. Antiviral Res. 2019 Mar; 163:29-33. doi: 10.1016/j.antiviral.2019.01.005. Epub 2019 Jan 14. PMID: 30653996

Considering the previously demonstrated broad-spectrum antiviral activity of POMs and the need of a treatment for ZIKV infections, in the present article (*Francese et al.*) we investigated the anti-ZIKV activity of a minilibrary of three POMs, the Anderson-Evans type $[TeW_6O_{24}]^{6-}$ (**TeW$_6$**) and the Keggin-type $[TiW_{11}CoO_{40}]^{8-}$ (**TiW$_{11}$Co**) and $[Ti_2PW_{10}O_{40}]^7$ (**Ti$_2$PW$_{10}$**). The study was performed in close collaboration with the chemist group of Prof. Ulrich Kortz, from Jacobs University (Bremen, Germany), that synthesized and characterized the POMs according to the published procedures. The Innovative Pharmaceutical and Cosmetic Technology and Nanotechnology Group of Prof. Roberta Cavalli (Turin University) determined the physico-chemical characteristics (pH, osmolarity, Zeta potential) and the biocompatibility of the three POMs. They have been found stable in aqueous solution up to 6 months stored at 4°C, they showed good biocompatibility in hemolysis assay, and their tonicity and pH values were suitable for *in vitro* biological studies. These molecules were subsequently tested *in vitro* against two different ZIKV strains, the MR766 and the HPF13,

belonging to the African and the Asian lineage respectively. All POMs showed good antiviral activity against both strains, with Ti_2PW_{10} showing the most promising activity (EC_{50} in the low micromolar range) and the most favorable selectivity index (SI). These features prompted us to focus on the study of the mechanism of action of Ti_2PW_{10} against both ZIKV strains. The evidence accumulated in our study clearly demonstrated that Ti_2PW_{10} hampers the entry process of ZIKV into the host cells and is able to reduce the viral progeny production. These results suggest that the polyanion Ti_2PW_{10} could be a good starting point to develop an effective therapeutic to treat ZIKV infection.

Anti-zika virus activity of polyoxometalates

Rachele Francese[a], Andrea Civra[a], Massimo Rittà[a], Manuela Donalisio[a], Monica Argenziano[b], Roberta Cavalli[b], Ali S. Mougharbel[c], Ulrich Kortz[c,**], David Lembo[a,*]

[a] Department of Clinical and Biological Sciences, Laboratory of Molecular Virology and Antiviral Research, University of Turin, S. Luigi Gonzaga Hospital, Orbassano Turin, Italy
[b] Department of Drug Science and Technology, Innovative Pharmaceutical and Cosmetic Technology and Nanotechnology Group, University of Turin, Italy
[c] Department of Life Sciences and Chemistry, Jacobs University, Campus Ring 1, 28759 Bremen, Germany

ARTICLE INFO

ABSTRACT

Zika virus (ZIKV) is an emerging infectious viral pathogen associated with severe fetal cerebral anomalies and the paralytic Guillain-Barrè syndrome in adults. It was the cause of a recent global health crisis following its entrance into a naïve population in the Americas. Nowadays, no vaccine or specific antiviral against ZIKV is available. In this study, we identified three polyoxometalates (POMs), the Anderson-Evans type $[TeW_6O_{24}]^{6-}$ (TeW_6), and the Keggin-type $[TiW_{11}CoO_{40}]^{8-}$ (TiW_{11}Co), and $[Ti_2PW_{10}O_{40}]^{7-}$ (Ti_2PW_{10}), that inhibit ZIKV infection with EC_{50}s in the low micromolar range. Ti_2PW_{10}, the POM with the greatest selectivity index (SI), was selected and the step of ZIKV replicative cycle putatively inhibited was investigated by specific antiviral assays. We demonstrated that Ti_2PW_{10} targets the entry process of ZIKV infection and it is able to significantly reduce ZIKV progeny production. These results suggest that the polyanion Ti_2PW_{10} could be a good starting point to develop an effective therapeutic to treat ZIKV infection.

ZIKV is an enveloped positive-strand RNA virus belonging to the *Flaviviridae* family and mostly transmitted by *Aedes aegypti mosquitos* (Saiz et al., 2016). Sexual, vertical and blood transmissions have also been reported (Musso et al., 2015; Mlakar et al., 2016; Motta et al., 2016). In symptomatic individuals (around 18% of cases), ZIKV causes a mild illness characterized by fever, rash, headache, conjunctivitis, joint and muscle pain (Paixão et al., 2016); this clinical presentation is similar to that of other arbovirus infections, such as chikungunya and dengue virus. However, unlike other flavivirus, ZIKV is associated to two main neurological complications: the Guillain-Barré Syndrome in adults and the now termed Zika Congenital Syndrome (CSZ), a variety of neurological impairments in fetus and infants of women infected during pregnancy. The main congenital manifestations, developed in nearly one third of these newborns, are severe microcephaly, resulting in a partially collapsed skull, intracranial calcifications, eyes abnormalities, redundant scalp skin, arthrogryposis and clubfoot (Mlakar et al., 2016; Rasmussen et al., 2016; Cao-Lormeau et al., 2016; Brasil et al., 2016). Specifically, the risk of microcephaly, with a catastrophic impact on the socioeconomic status of affected families, was reported to be 1–13% during the first trimester and negligible during second and third trimesters (McCarthy, 2016).

ZIKV can be classified into two lineages (African and Asian) and three genotypes (West African, East African, and Asian), differing in pathogenicity and virulence. The Asian-lineage ZIKV, responsible for the latest epidemics (on Yap Island and Micronesia in 2007, in French Polinesya in 2013 and in the Americas in 2016), is considered to be less virulent than the African one, because of the lower infection rate, the lower viral production, the poor induction of early cell death and the lower immuno-stimulation in different models. These characteristics allow the virus to cause a prolonged infection within the central nervous system of fetus that could be the cause of its association with neurological impairments. On the contrary, the African lineage-ZIKV can result in a more acute infection (Duffy et al., 2009; Cao-Lormeau et al., 2014; Simonin et al., 2017; Shao et al., 2017; Beaver et al., 2018).

The last major epidemic in the Americas, in 2016, counted 177614 confirmed ZIKV cases and 2552 cases of CSZ at the end of the year, driving the World Health Organization to declare a public health emergency of international concern (CDC; PAHO WHO,). Since then, great efforts have been carried out, but nowadays still no vaccine or specific antiviral against ZIKV is available (Richner and Diamond, 2018; Saiz and Martín-Acebes, 2017). The best way to prevent ZIKV infection is to avoid mosquito bites and the treatment of infected

---

Table 1
Characteristics of POM aqueous solutions.

POM sample	pH	Osmolarity (mOsm)	Zeta potential (mV)
TeW_6	5.65	324	- 6.06 ± 3.11
$TiW_{11}Co$	5.45	320	- 6.95 ± 3.49
Ti_2PW_{10}	6.25	316	- 5.31 ± 1.95

patients is palliative, involving analgesics and antipyretics. In this context, ZIKV infection presents a huge challenge to the global health system and the search for efficient antivirals is absolutely necessary. To this aim, we investigated *in vitro* the anti-ZIKV activity of a minilibrary of three polyoxometalates (POMs). POMs are discrete, anionic metal-oxo complexes of early *d* block metal ions in high oxidation states (e.g. W^{VI}, Mo^{VI}, V^V) with a very large structural and compositional variety and a multitude of associated physicochemical properties (Pope, 1983; Pope and Müller, 1991; Pope and Kortz, 2012). POMs are usually synthesized in aqueous acidic media, but some selected species are also stable at pH 7–8. In fact, POMs have been investigated for many years as potentially useful agents in medicine, mainly for their antiviral, antitumoral, and antibacterial properties (Sarafianos et al., 1996; Rhule et al., 1998; Hasenknopf, 2005; Mauracher et al., 2014; Giang et al., 2015; Yang et al., 2016; Selman et al., 2018). Here, we decided to investigate the following three solution-stable POMs, the Anderson-Evans type $[TeW_6O_{24}]^{6-}$ (TeW_6) (Schmidt et al., 1986), and the Keggin-type $[TiW_{11}CoO_{40}]^{8-}$ ($TiW_{11}Co$) (Chen and Liu, 1997), and $[Ti_2PW_{10}O_{40}]^{7-}$ (Ti_2PW_{10}) (Domaille and Knoth, 1983), which were all synthesized according to the published procedures. The size of all three polyanions is in the range of 1 nm diameter. The purity (≥95%) of the compounds was confirmed by NMR and IR (Data available in Supplementary info). Some of these POMs have already been used in biological studies. For instance, Ti_2PW_{10} showed interesting results in the inhibition of acetylcholinesterase activity while maintaining low toxicity levels (Čolović et al., 2017). On the other hand, TeW_6 showed good activity against diabetes and Alzheimer's disease (Ilyas et al., 2014; Iqbal et al., 2013).

In order to perform *in vitro* biological assays, we first prepared aqueous solutions of TeW_6, $TiW_{11}Co$, and Ti_2PW_{10} and we determined their physico-chemical characteristics (pH, osmolarity, Zeta potential) (Table 1) and their biocompatibility. The POMs were stable in aqueous solution up to 6 months stored at 4 °C. Indeed, a concentration decrease of 3.25, 5.05 and 4.45% was observed for TeW_6, $TiW_{11}Co$ and Ti_2PW_{10} respectively, after 6 months. In the hemolysis assay, no significant hemolysis caused by the POM solutions was observed, indicating good biocompatibility. (Data available in Supplementary info). The tonicity and pH values were suitable for the following cell experiments.

Therefore, to evaluate the anti-Zika virus activity of the three POMs, we performed virus inhibition assays against two Zika virus strains, the 1947 Uganda MR766 and the 2013 French Polynesia HPF2013, representing the African and the Asian lineage respectively. The cells were treated with decreasing concentrations of POMs before, during

and after infection, in order to use a complete protection assay. As shown in Table 2, all three POMs were active against both ZIKV strains with half maximal effective concentrations (EC_{50}s) ranging from 0.63 to 2.52 μM. Moreover, in order to assess the specificity of the anti-ZIKV activity of the POMs, they were tested against the human rotavirus (HRoV), an unrelated RNA virus belonging to the Reoviridae family. Interestingly, we did not observe any inhibition. Next, to exclude the possibility that this antiviral activity was due to a cytotoxic effect of the POMs, viability assays were carried out on uninfected cells, challenged with the compounds under the same conditions as the virus inhibition assays. The CC_{50}s were different for all the three POMs (TeW_6 CC_{50} = 210.1 μM, $TiW_{11}Co$ CC_{50} = 97.08 μM, Ti_2PW_{10} CC_{50} > 225 μM), and demonstrated that they are not toxic at the concentrations used in the antiviral assays. The Selectivity Index (SI) of Ti_2PW_{10} was the most favorable one, so we decided to concentrate our research on the study of the mechanism of action of this polyanion. All the experiments were performed with the two Zika virus strains used for the initial screening. We first investigated whether the antiviral activity of Ti_2PW_{10} was exerted via direct inactivation of the viral particles. The ZIKV particles were incubated with a concentration of Ti_2PW_{10} that reduces almost completely the virus infection (EC_{90}) and then the viral titer was determined at high dilutions at which the polyanion was no longer active when added to cells. As depicted in Fig. 1A, there was no significant difference between the titer of treated virus and the titer of untreated control, demonstrating that Ti_2PW_{10} is not able to impair extracellular viral particles. Having excluded the viral particle as the target of the antiviral activity of Ti_2PW_{10}, further experiments were performed to investigate whether this polyanion acted directly on cells or on essential steps of the ZIKV replicative cycle. Vero cells were pretreated with decreasing dilutions of the polyanion for 2 h before virus infection; as reported in Fig. 1B, the infection of both ZIKV strains was not inhibited even at the highest tested concentration. Hence, we explored the possibility that Ti_2PW_{10} treatment could affect the early steps of the ZIKV replicative cycle. Binding assays were performed allowing the virus to bind host cell surface in the presence of a high concentration of Ti_2PW_{10}. The results (Fig. 2A) demonstrated that the treatment did not significantly reduce (p > 0.05) the titer of viral particles bound to the cell surface, thus suggesting that the inhibition occurs at a post-binding stage. To verify this hypothesis, we treated cells immediately after virus attachment, i.e. during virus entry into the host cell. In this case (Fig. 2B), we observed a marked antiviral activity of Ti_2PW_{10} against both, MR766 and HPF2013, ZIKV strains (EC_{50} = 1.11 and 1.25 μM respectively). To exclude an additional antiviral action of Ti_2PW_{10} on the last steps of the ZIKV replicative cycle, we executed focus reduction assays adding the polyanion to cells immediately after virus entry into the host cell (post-entry assay). We stopped the treatment at 24 h post-infection, i.e. at the end of the first replicative cycle, in order to avoid inhibition of the entry step of the upcoming viral progeny. As shown in Fig. 2C, the post-entry treatment did not reduce virus infectivity, suggesting that only the entry step is

Table 2
Antiviral activity of TeW_6, $TiW_{11}Co$ and Ti_2PW_{10}.

Compound	Virus	EC_{50} (μM) (95% CI)	EC_{90} (μM) (95% CI)	CC_{50} (μM) (95% CI)	SI
TeW_6	MR766	2.52 (1.87–3.39)	9.47 (4.41–20.35)	210.1 (161.3–273.6)	83.37
	HPF2013	0.71 (0.53–0.96)	6.12 (3.29–11.39)	210.1 (161.3–273.6)	295.91
	HRoV	n.a.	n.a.	> 75	–
$TiW_{11}Co$	MR766	1.04 (0.80–1.35)	5.19 (2.87–9.38)	97.08 (51.36–183.5)	93.34
	HPF2013	0.70 (0.57–0.87)	1.41 (1.02–1.94)	97.08 (51.36–183.5)	138.68
	HRoV	n.a.	n.a.	> 75	–
Ti_2PW_{10}	MR766	0.63 (0.51–0.78)	3.51 (2.19–5.63)	> 225	> 357.14
	HPF2013	0.70 (0.59–0.84)	2.78 (1.82–4.25)	> 225	> 321.42
	HRoV	n.a.	n.a.	> 75	–

EC_{50}: half maximal effective concentration; EC_{90}: 90% effective concentration; CC_{50}: half maximal cytotoxic concentration; SI: selectivity index; n.a.: not assessable; CI: confidence interval.
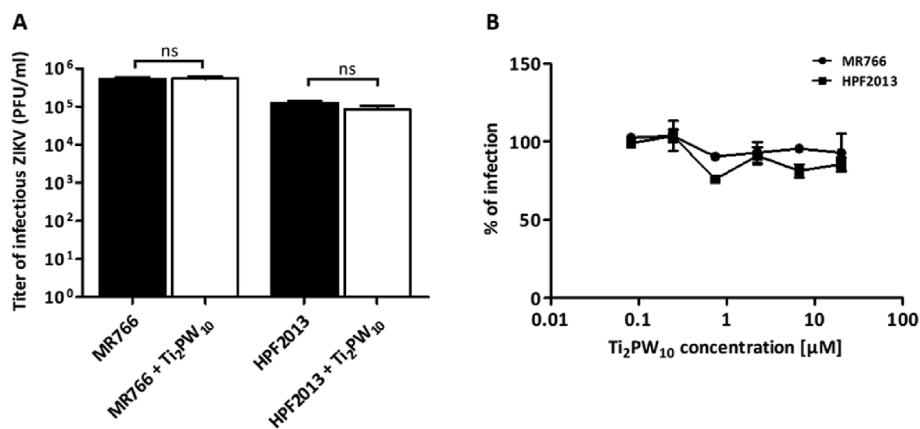
Fig. 1. Ti_2PW_{10} does not impair extracellular ZIKV particles and the cells pre-treatment does not affect viral infection. Panel A shows the evaluation of the virucidal effect of Ti_2PW_{10} on infectious ZIKV particles. Approximately 10^5 PFU of ZIKV (MR766 or HPF2013) plus EC_{90} of Ti_2PW_{10} were added to MEM and mixed in a total volume of $100\,\mu L$. The mixture was incubated for 2 h at 37 °C then diluted serially to the non-inhibitory concentration of the test polyanion; the residual viral infectivity was determined by viral plaque assay. Panel B displays the effect of cells pre-treatment with Ti_2PW_{10}. Vero cells were pre-treated with serial dilutions of Ti_2PW_{10} for 2 h before infection. After washing, cells were infected with ZIKV and the number of viral plaques was evaluated after 72 h. In panels A, the viral titers are expressed as PFU/ml and are shown as mean plus SEM for three independent experiments. In panels B, the number of viral plaques in the treated samples is expressed as a percentage of the untreated control and each point represents mean and SEM for three independent experiments. Experimental details are described in the Supplementary data file.
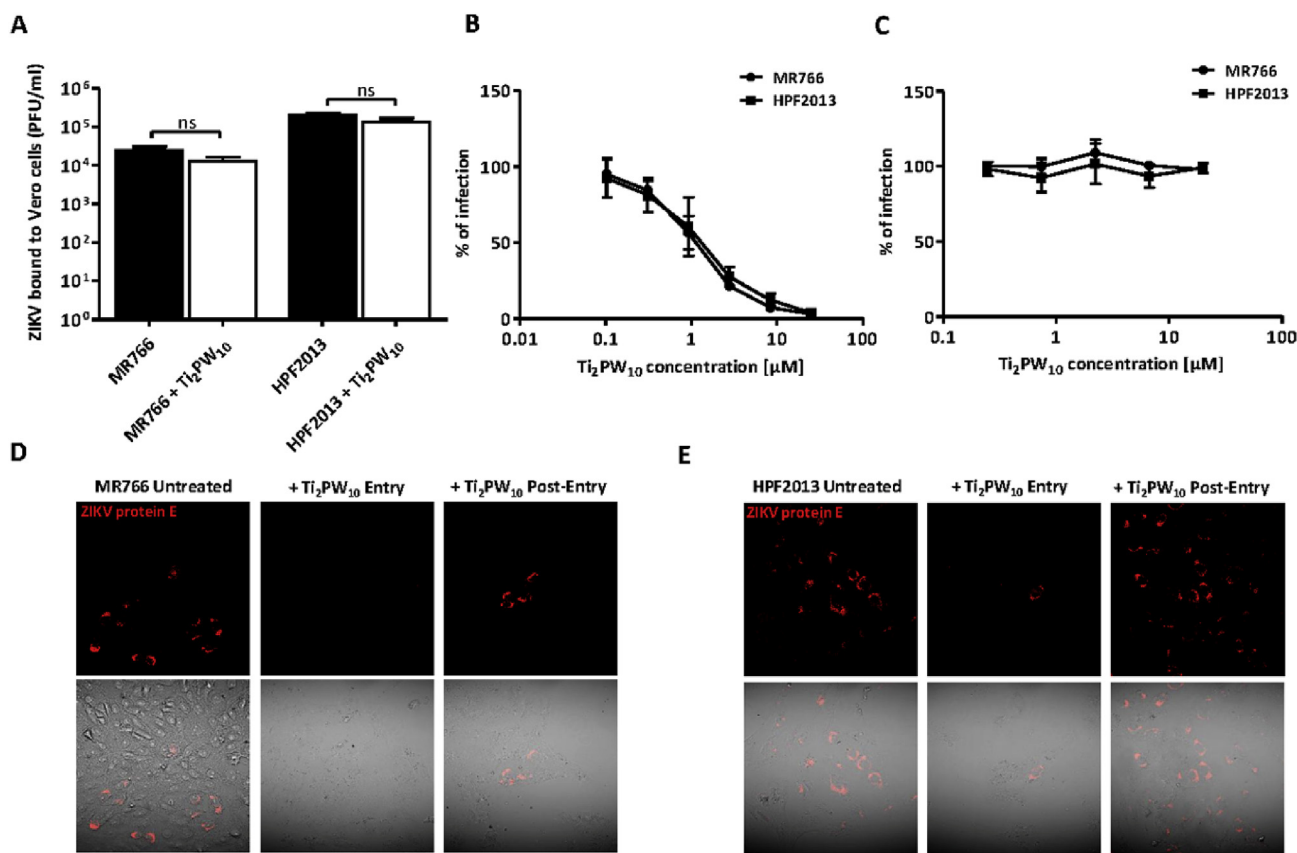
Fig. 2. Ti_2PW_{10} hampers the entry process of ZIKV into the host cell. In the binding assay (2A), ZIKV particles (MR766 or HPF2013, MOI = 3) were allowed to attach to cells in presence of Ti_2PW_{10} (EC_{90}) for 2 h on ice. Cells were then washed to remove the unbound virus and subsequently subjected to three rounds of freeze-thawing to release bound virus. The lysate was clarified and the cell-bound virus titer was determined by viral plaque assay. Here, the viral titers are expressed as PFU/ml and are shown as mean plus SEM for three independent experiments. For the entry assay (2B), ZIKV (MR766 or HPF2013) was adsorbed for 2 h at 4 °C on pre-chilled Vero cells. After the removal of the unbound virus, the temperature was shifted to 37 °C to allow the entry of pre-bound virus in presence of serial dilutions of Ti_2PW_{10}. Subsequently, unpenetrated virus was inactivated with an incubation with citrate buffer followed by 3 washes. The number of viral plaques was evaluated after 72 h. For the post-entry assay (2C), the same protocol of the entry assay was performed, but adding the polyanion after the incubation with citrate buffer for 24 h. The number of infected cells was assessed by indirect immunostaining after 24 h, in order to avoid the inhibition of the entry step of the upcoming viral progeny. In panels B, C, the number of viral plaques or infected cells in the treated samples is expressed as a percentage of the untreated control and each point represents mean and SEM for three independent experiments. In Fig. 2D (MR766) and 2E (HPF2013), the entry and the post-entry assays were performed with a concentration of Ti_2PW_{10} corresponding to EC_{99}. After 30 h of infection, cells were fixed and subjected to immunofluorescence. The ZIKV protein E is visualized in red. All experimental details are described in the Supplementary data file.

targeted by Ti_2PW_{10}. To confirm the inhibition of the ZIKV entry step, immunofluorescence experiments were performed by adding the polyanion (EC_{99}) during the virus entry step or immediately after the entry phase (post-entry). As reported in Fig. 2D (experiments with MR766)

and Fig. 2E (experiments with HPF2013), it was possible to detect a strong red signal of ZIKV protein E only in the untreated and in the post-entry treated samples. The number of red infected cells in the post-entry treated samples was comparable to the one of the untreated control. On
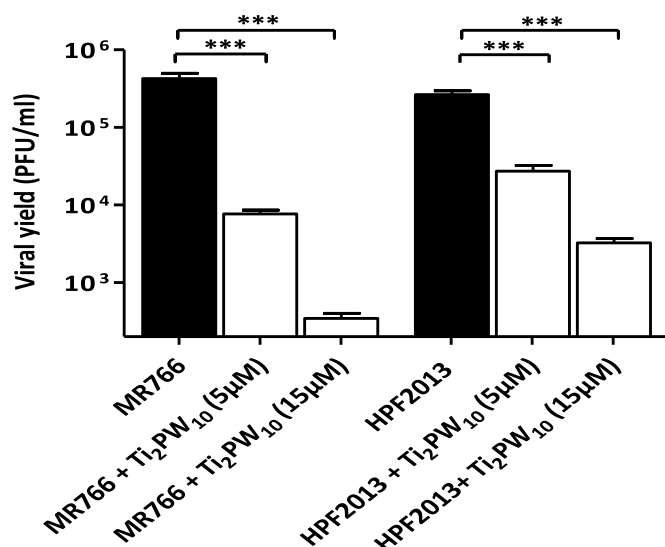
Fig. 3. Ti$_2$PW$_{10}$ reduces ZIKV progeny production. To test the ability of **Ti$_2$PW$_{10}$** compound to inhibit multiple cycles of ZIKV replication, Vero cells were treated and infected with a mixture of Ti$_2$PW$_{10}$ (5 μM or 15 μM) and ZIKV (MR766 or HPF2013, MOI = 0.001) for 2 h at 37 °C. The virus inoculum was then removed and cells were incubated with medium containing the compound (5 μM or 15 μM) until control cultures displayed extensive cytopathology. Supernatants were clarified and cell-free virus infectivity titers were determined by the plaque assay. The viral titers are expressed PFU/ml and are shown as mean plus SEM for three independent experiments. (***P$_{Tstud}$ < 0.001).

the contrary, the number of infected cells in the entry-treated samples was considerably reduced. All together these data indicate that the entry step is the target of the **Ti$_2$PW$_{10}$** antiviral activity. Finally, to complete the *in vitro* analysis of the antiviral potential of **Ti$_2$PW$_{10}$** against ZIKV strains, virus yield reduction assays were performed by treating cells during and after infection and allowing multiple cycles of viral replication to occur before measuring the production of infectious viruses. The results (Fig. 3) demonstrated that **Ti$_2$PW$_{10}$** significantly reduces the viral progeny production of both ZIKV strains (p < 0.001).

Previously, researchers focused on the antiviral properties of POMs because they are generally nontoxic to normal cells. Indeed, several studies reported the broad spectrum antiviral activities of POMs against different types of respiratory-viruses, as RSV, FluV A, FluV B, PfluV and SARS (Barnard et al., 1997; Shigeta et al., 2006), against HCV and DENV (Shigeta et al., 2003, 2006; Qi et al., 2013), belonging to the same family of ZIKV, and against others, as HIV, HSV-1, HSV-2 and HBV (Rhule et al., 1998; Shigeta et al., 2003; Wang et al., 2014). Herein, we showed that three heteropolytungstates, never tested before as antiviral agents, are endowed with a strong antiviral activity against ZIKV and we demonstrated their good biocompatibility. For the first time, POMs have been tested against two ZIKV strains and we can now include ZIKV in the list of pathogens targeted by the wide spectrum of action of POMs. Of note, we did not observe any inhibition against the human rotavirus, a taxonomically unrelated RNA virus. All together these results indicate that **TeW$_6$**, **TiW$_{11}$Co** and **Ti$_2$PW$_{10}$** exert a specific and not strain-restricted anti-ZIKV effect. In future experiments, we will investigate the antiviral action of **TeW$_6$**, **TiW$_{11}$Co** and **Ti$_2$PW$_{10}$** against other RNA and DNA viruses.

Some other POMs have already been investigated for their mechanism of action, which commonly depends on their shape, size and composition. Various studies reported on the inhibition of the early steps of an infection: for instance, Shigeta et al. (2003), demonstrated that the tri-vanadium-containing sandwich-type polyanion [(VO)$_3$(SbW$_9$O$_{33}$)$_2$]$^{11-}$ affects the binding of HIV to the cell membrane and the syncytium formation between HIV-infected and uninfected

cells; another biochemical study (Wang et al., 2014), reports that the ability of the tri-niobium-containing Keggin ion [SiW$_9$Nb$_3$O$_{40}$]$^{7-}$ to prevent the binding and fusion process of different viruses is mainly due to its localization on the cell surface; finally, Barnard et al. (1997), indicate the alteration of the attachment step as the primary mode of RSV inhibition by POMs of several structural classes. Consistent with these findings, we demonstrated that **Ti$_2$PW$_{10}$** acts as inhibitor of the entry process of ZIKV into the host cell. By contrast, no inhibition was observed at the binding stage. Further experiments are necessary to identify the cellular localization of this polyanion and to clarify its molecular mechanism of action.

In conclusion, we have discovered that the Keggin-type POM **Ti$_2$PW$_{10}$** inhibits ZIKV infection by hampering the entry process of the virus into the host cell. Since specific antivirals against ZIKV are not available, this polyanion could be a good starting point for the development of novel and efficient antiviral pharmaceuticals.

Declaration of interest

None.

Acknowledgements

Abbreviations

|	
ZIKV	zika virus
HRoV	human rotavirus
RSV	respiratory syncytial virus
FluV A	influenza virus type A
FluV B	influenza virus type B
PfluV	parainfluenza virus
SARS	severe acute respiratory syndrome
HCV	hepatitis C virus
DENV	dengue virus
HIV	human immunodeficiency virus
HSV-1	herpes simplex virus type 1
HSV-2	herpes simplex virus type 2
HBV	hepatitis B virus
POMs	polyoxometalates
EC$_{50}$	half maximal effective concentration
EC$_{90}$	90% effective concentration
CC$_{50}$	half maximal cytotoxic concentration
SI	selectivity index
n.a.	not assessable
CI	confidence interval
PFU	plaque forming unit
PFU/ml	plaque forming unit per ml

Appendix A. Supplementary data

Supplementary data to this article can be found online at https://doi.org/10.1016/j.antiviral.2019.01.005.

References

Barnard, D.L., Hill, C.L., Gage, T., Matheson, J.E., Huffman, J.H., Sidwell, R.W., I Otto, M., Schinazi, R.F., 1997. Potent inhibition of respiratory syncytial virus by polyoxometalates of several structural classes. Antivir. Res. 34, 27–37. https://doi.org/10.1016/S0166-3542(96)01019-4.

Beaver, J.T., Lelutiu, N., Habib, R., Skountzou, I., 2018. Evolution of two major zika virus lineages: implications for Pathology, immune response, and vaccine development. Front. Immunol. 9, 1640. https://doi.org/10.3389/fimmu.2018.01640.

Brasil, P., Pereira, J.P., Moreira, M.E., Nogueira, R.M.R., Damasceno, L., Wakimoto, M., Rabello, R.S., Valderramos, S.G., Halai, U.-A., Salles, T.S., Zin, A.A., Horovitz, D., Daltro, P., Boechat, M., Raja Gabaglia, C., Carvalho de Sequeira, P., Pilotto, J.H.,

Medialdea-Carrera, R., Cotrim da Cunha, D., Abreu de Carvalho, L.M., Pone, M., Machado Siqueira, A., Calvet, G.A., Rodrigues Baião, A.E., Neves, E.S., Nassar de Carvalho, P.R., Hasue, R.H., Marschik, P.B., Einspieler, C., Janzen, C., Cherry, J.D., Bispo de Filippis, A.M., Nielsen-Saines, K., 2016. Zika virus infection in pregnant women in Rio de Janeiro. N. Engl. J. Med. 375, 2321–2334. https://doi.org/10.1056/NEJMoa1602412.

CDC, https://www.cdc.gov/zika/reporting/case-counts.html, (accessed May 2018).

Cao-Lormeau, V.M., Roche, C., Teissier, A., Robin, E., Berry, A.L., Mallet, H.P., Sall, A.A., Musso, D., 2014. Zika virus, French polynesia, South pacific, 2013. Emerg. Infect. Dis. 20, 1085–1086. https://doi.org/10.3201/eid2006.140138.

Cao-Lormeau, V.M., Blake, A., Mons, S., Lastere, S., Roche, C., Vanhomwegen, J., Dub, T., Baudouin, L., Teissier, A., Larre, P., Vial, A.L., Decam, C., Choumet, V., Halstead, S.K., Willison, H.J., Musset, L., Manuguerra, J.C., Despres, P., Fournier, E., Mallet, H.P., Musso, D., Fontanet, A., Neil, J., Ghawché, F., 2016. Guillain-Barré syndrome outbreak caused by ZIKA virus infection in French Polynesia. Lancet Lond. Engl. 387, 1531–1539. https://doi.org/10.1016/S0140-6736(16)00562-6.

Chen, Y., Liu, J., 1997. Synth. React. Inorg. Met. Org. Chem. 27, 234.

Čolović, M.B., Medić, B., Ćetković, M., Stevović, T.K., Stojanović, M., Ayass, W.W., Mougharbel, A.S., Radenković, M., Prostran, M., Kortz, U., 2017. Toxicity evaluation of two polyoxotungstates with anti-acetylcholinesterase activity. Toxicol. Appl. Pharmacol. 333, 68–75. https://doi.org/10.1016/j.taap.2017.08.010.

Domaille, P.J., Knoth, W.H., 1983. Ti2W10PO407- and [CpFe(CO)2Sn]2W10PO385-. preparation, properties, and structure determination by tungsten-183 NMR. Inorg. Chem. 22, 818–822. https://doi.org/10.1021/ic00147a023.

Duffy, M.R., Chen, T.-H., Hancock, W.T., Powers, A.M., Kool, J.L., Lanciotti, R.S., Pretrick, M., Marfel, M., Holzbauer, S., Dubray, C., Guillaumot, L., Griggs, A., Bel, M., Lambert, A.J., Laven, J., Kosoy, O., Panella, A., Biggerstaff, B.J., Fischer, M., Hayes, E.B., 2009. Zika virus outbreak on Yap Island, Federated States of Micronesia. N. Engl. J. Med. 360, 2536–2543. https://doi.org/10.1056/NEJMoa0805715.

Giang, H., Ly, T., Absillis, G., Janssens, R., Proost, P., Parac-Vogt, T.N., 2015. Highly amino acid selective hydrolysis of myoglobin at aspartate residues as promoted by Zirconium(IV)-substituted polyoxometalates. Angew. Chem. Int. Ed. 54, 7391–7394. https://doi.org/10.1002/anie.201502000.

Hasenknopf, B., 2005. Polyoxometalates: introduction to a class of inorganic compounds and their biomedical applications. Front. Biosci. 10, 275–287. https://doi.org/10.2741/1527.

Ilyas, Z., Shah, H.S., Al-Oweini, R., Kortz, U., Iqbal, J., 2014. Antidiabetic potential of polyoxotungstates: in vitro and in vivo studies. Metallomics 6, 1521–1526. https://doi.org/10.1039/c4mt00106k.

Iqbal, J., Barsukova-Stuckart, M., Ibrahim, M., Ali, S.U., Khan, A.A., Kortz, U., 2013. Polyoxometalates as potent inhibitors for acetyl and butyrylcholinesterases and as potential drugs for the treatment of Alzheimer's disease. Med. Chem. Res. 22, 1224–1228. https://doi.org/10.1007/s00044-012-0125-8.

Mauracher, S.G., Molitor, C., Al-Oweini, R., Kortz, U., Rompel, A., 2014. Latent and active abPPO4 mushroom tyrosinase cocrystallized with hexatungstotellurate(VI) in a single crystal. Acta Crystallogr., Sect. D 70, 2301–2315. https://doi.org/10.1107/S1399004714013777.

McCarthy, M., 2016. BMJ, Microcephaly risk with Zika infection is 1-13% in first trimester, study shows, vol. 353. pp. i3048. https://doi.org/10.1136/bmj.i3048.

Mlakar, J., Korva, M., Tul, N., Popović, M., Poljšak-Prijatelj, M., Mraz, J., Kolencet, M., Rus, K.R., Vipotnik, T.V., Vodušek, V.F., Vizjak, A., Pižem, J., Petrovec, M., Županc, T.A., 2016. Zika virus associated with microcephaly. N. Engl. J. Med. 374, 951–958. https://doi.org/10.1056/NEJMoa1600651.

Motta, I.J.F., Spencer, B.R., Cordeiro da Silva, S.G., Arruda, M.B., Dobbin, J.A., Gonzaga, Y.B.M., Arcuri, I.P., Tavares, R.C.B.S., Atta, E.H., Fernandes, R.F.M., Costa, D.A., Ribeiro, L.J., Limonte, F., Higa, L.M., Voloch, C.M., Brindeiro, R.M., Tanuri, A., Ferreira, O.C., 2016. Evidence for transmission of zika virus by platelet transfusion. N. Engl. J. Med. 375, 1101–1103. https://doi.org/10.1056/NEJMc1607262.

Musso, D., Roche, C., Robin, E., Nhan, T., Teissier, A., Cao-Lormeau, V.-M., 2015. Potential sexual transmission of zika virus. Emerg. Infect. Dis. 21, 359–361. https://doi.org/10.3201/eid2102.141363.

PAHO WHO, https://www.paho.org/hq/index.php?option=com_content&view=article &id=12390%3Azika-cumulative-cases&catid=8424%3Acontents&Itemid=42090& lang=en, (accessed May 2018).

Paixão, E.S., Barreto, F., da Glória Teixeira, M., da Conceição, N., Costa, M., Rodrigues, L.C., 2016. Epidemiology, and clinical manifestations of zika: a systematic review. Am. J. Public Health 106, 606–612. https://doi.org/10.2105/AJPH.2016.303112.

Pope, M.T., 1983. Heteropoly and Isopoly Oxometalates. Springer, Berlin.

Pope, M.T., Kortz, U., 2012. Polyoxometalates. In: Encyclopedia of Inorganic and Bioinorganic Chemistry. John Wiley. https://doi.org/10.1002/9781119951438.eibc0185.pub2.

Pope, M.T., Müller, A., 1991. Polyoxometalate chemistry: an old field with new dimensions in several disciplines. Angew. Chem., Int. Ed. Engl. 30, 34–48. https://doi.org/10.1002/anie.199100341.

Qi, Y., Xiang, Y., Wang, J., Qi, Y., Li, J., Niu, J., Zhong, J., 2013. Inhibition of hepatitis C virus infection by polyoxometalates. Antivir. Res. 100, 392–398. https://doi.org/10.1016/j.antiviral.2013.08.025.

Rasmussen, S.A., Jamieson, D.J., Honein, M.A., Petersen, L.R., 2016. Zika virus and birth defects — reviewing the evidence for causality. N. Engl. J. Med. 374, 1981–1987. https://doi.org/10.1056/NEJMsr1604338.

Rhule, J.T., Hill, C.L., Judd, D.A., Schinazi, R.F., 1998. Polyoxometalates in medicine. Chem. Rev. 98, 327–358. https://doi.org/10.1021/cr960396q.

Richner, J.M., Diamond, M.S., 2018. Zika virus vaccines: immune response, current status, and future challenges. Curr. Opin. Immunol. 53, 130–136. https://doi.org/10.1016/j.coi.2018.04.024.

Saiz, J.C., Martín-Acebes, M.A., 2017. The race to find antivirals for zika virus. Antimicrob. Agents Chemother. 61. https://doi.org/10.1128/AAC.00411-17.

Saiz, J.-C., Vázquez-Calvo, Á., Blázquez, A.B., Merino-Ramos, T., Escribano-Romero, E., Martín-Acebes, M.A., 2016. Zika virus: the latest newcomer. Front. Microbiol. 7, 496. https://doi.org/10.3389/fmicb.2016.00496.

Sarafianos, S.G., Kortz, U., Pope, M.T., Modak, M.J., 1996. Mechanism of polyoxometalate-mediated inactivation of DNA polymerases: an analysis with HIV-1 reverse transcriptase indicates specificity for the DNA-binding cleft. Biochem. J. 319, 619–626. https://doi.org/10.1042/bj3190619.

Schmidt, K., Schrobilgen, G., Sawyer, J., 1986. Hexasodium hexatungstotellurate(VI) 22-hydrate. Acta Crystallogr. Sect. C Cryst. Struct. Commun. 42, 1115–1118. https://doi.org/10.1107/S0108270186093204.

Selman, M., Rousso, C., Bergeron, A., Son, H.H., Krishnan, R., El-Sayes, N.A., Varette, O., Chen, A., Le Boeuf, F., Tzelepis, F., Bell, J.C., Crans, D.C., Diallo, J.S., 2018. Multimodal potentiation of oncolytic virotherapy by vanadium compounds. Mol. Ther. 26 (1), 56–69. https://doi.org/10.1016/j.ymthe.2017.10.014.

Shao, Q., Herrlinger, S., Zhu, Y.N., Yang, M., Goodfellow, F., Stice, S.L., Qi, X.P., Brindley, M.A., Chen, J.F., 2017. The African Zika virus MR-766 is more virulent and causes more severe brain damage than current Asian lineage and dengue virus, vol. 144. The Company of Biologists, pp. 4114–4124. https://doi.org/10.1242/dev.156752.

Shigeta, S., Mori, S., Kodama, E., Kodama, J., Takahashi, K., Yamase, T., 2003. Broad spectrum anti-RNA virus activities of titanium and vanadium substituted polyoxotungstates. Antivir. Res. 58, 265–271. https://doi.org/10.1016/S0166-3542(03)00009-3.

Shigeta, S., Mori, S., Yamase, T., Yamamoto, N., Yamamoto, N., 2006. Anti-RNA virus activity of polyoxometalates. Biomed. Pharmacother. 60, 211–219. https://doi.org/10.1016/j.biopha.2006.03.009.

Simonin, Y., van Riel, D., Van de Perre, P., Rockx, B., Salinas, S., 2017. Differential virulence between Asian and African lineages of Zika virus. PLoS Neglected Trop. Dis. 11. https://doi.org/10.1371/journal.pntd.0005821.

Wang, J., Liu, Y., Xu, K., Qi, Y., Zhong, J., Zhang, K., Li, J., Wang, E., Wu, Z., Kang, Z., 2014. Broad-spectrum antiviral property of polyoxometalate localized on a cell surface. ACS Appl. Mater. Interfaces 6, 9785–9789. https://doi.org/10.1021/am502193f.

Yang, P., Lin, Z., Bassil, B.S., Alfaro-Espinoza, G., Ullrich, M.S., Li, M.-X., Silvestru, C., Kortz, U., 2016. Tetra-antimony(III)-bridged 18-tungsto-2-arsenates(V), [(LSb(III))4(A-α-As(V)W9O34)2](10-) (L = Ph, OH): turning bioactivity on and off by ligand substitution. Inorg. Chem. 55, 3718–3720. https://doi.org/10.1021/acs.inorgchem.6b00107.

2.3 Medicinal plants as natural sources of antiviral compounds

An alternative and complementary strategy to the classical approaches in the antiviral research field is the study of medicinal plants as natural sources of phytochemicals, such as polyphenols and alkaloids. In fact, therapeutically interesting and important drugs can be developed from plant sources which are used in traditional systems of medicines. Furthermore, there is currently the need of a scientific evidence for the use of plant derivatives in medicine, since they are frequently administered without a scientific background supporting their employment.

People are using herbal medicines from centuries for safety, efficacy, cultural acceptability and lesser side effects. Plants and plant products have been utilized with varying success to cure and prevent diseases throughout history. In China, as example from recent years, traditional herbal medicine played a prominent role in the strategy to contain and treat severe acute respiratory syndrome (SARS). According to WHO, 80% of African populations currently use some form of traditional herbal medicine and the worldwide annual market for these products approaches US$ 60 billion (33). The active plant derived substances could be found in various parts of the plant like roots, leaves, shoots and bark and they are used in the form of crude extracts, infusions or plasters for the treatment of many infectious diseases. In particular, hundreds of plant extracts with antiviral effect were recognized by numerous scientific productions reporting both *in vitro* and *in vivo* studies (34). As example, Akram M et al. recently reviewed the antiviral potential of medicinal plants against HIV, HSV, influenza, hepatitis, and coxsackievirus documenting fifty-four medicinal plants, from 36 different families, having antiviral activity against the listed viruses (35). On the contrary, other studies focused on the antiviral effect of plant derivatives against emerging viruses such as DENV, ZIKV, SARS-CoV2, Chikungunya virus (CHIKV) and others (36–39). I chose to mention only some of the most recent works in this field, since the detailed description of the extensive literature on plants antiviral properties is not the main goal of this thesis.

2.3.1 *Punica granatum*: the pomegranate plant

With the aim to identify new and effective antiviral compounds against ZIKV, the second approach that I explored during my PhD course was the study of medicinal plant extracts endowed with antiviral activity. The most promising results, reported in the 2.3.2 section, were obtained with the analysis of the antiviral properties of *Punica granatum*.

Punica granatum L. (Lythraceae family), commonly known as pomegranate, is a domesticated tree that is widely grown as an evergreen in tropical regions and as a deciduous tree in temperate areas. It is an ancient plant that is well known in folk medicine and is becoming increasingly popular as a functional food and nutraceutical source due to its high polyphenol content, not only in the edible

part, but also in other parts of the fruit and plant, including the peel, bark, leaves, and flowers (40). Pomegranate is a rich source of a wide variety of compounds with beneficial physiological activities, in particular antioxidative, anti-inflammatory, and anti-cancerous properties (41). Nearly every part of the plant has been tested for antimicrobial activity, and roles in the suppression of enteric infections, food preservation, wound healing, as well as gut and oral health, have been demonstrated (42). Most antiviral studies have been performed on the fruit's peel and juice, and it has been found that extracts exerted inhibitory activity against HSV-2, HIV-1, and the influenza virus (43–45). Little information has been reported on pomegranate leaf extracts, compared to other edible and nonedible parts of the plant, although some recent studies have indicated that they may be an important source of specialized bioactive metabolites and they possess a broad range of biological properties, such as in vitro antioxidant, anti-inflammatory, anticholinesterase, and antiproliferative activities (46). Our research focused on this less investigated part of the plant: the leaf.

2.3.2 Publications

Acquadro S, Civra A, Cagliero C, Marengo A, Rittà M, Francese R, Sanna C, Bertea C, Sgorbini B, Lembo D, Donalisio M, Rubiolo P. *Punica granatum Leaf Ethanolic Extract and Ellagic Acid as Inhibitors of Zika Virus Infection*. *Planta Med. 2020 Sep 16. doi: 10.1055/a-1232-5705. Epub ahead of print. PMID: 32937663.*

The article *Acquadro et al.* is the result of a study conducted in close collaboration with the group of Prof. Patrizia Rubiolo affiliated to the Department of Drug Science and Technology of the University of Turin. In this study, we explored the cytotoxicity and the anti-ZIKV activity of pomegranate leaf ethanolic crude extracts, as well as the corresponding fractions and phytoconstituents. Leaves were collected from various sites in Italy and Greece, after different vegetative periods (summer and autumn) and in different years (2017 and 2018) and their phytochemical and biomolecular characterization were performed. These analyses showed that the pomegranate leaf ethanolic extract is characterized by hydrolysable tannins, flavonoids, and triterpenes and that its phytochemical pattern is stable and does not depend on geographical conditions or season. Furthermore, no differences were found in the *ITS* and *psbA-trnH* sequences extracted from leaves collected in different sites. Subsequently, we demonstrated that pomegranate leaf extract and its fractions are active against the MR766 and the HPF2013 ZIKV strains. Of the 11 phenolic and triterpenic compounds isolated from the crude extract, ellagic acid was the one possessing the anti-ZIKV activity, with EC_{50} values of 30.86 μM for MR766 and 46.23 μM for HPF2013. We demonstrated

that this compound acts by preventing ZIKV cell infection and reduce the transmission of extracellular free virus at high titers. Our data demonstrated the anti-ZIKV activity of pomegranate leaf extract for the first time and indicated ellagic acid as a possible candidate compound for preventive and therapeutic interventions aimed at impairing the chain of ZIKV congenital transmission. Moreover, leaf collection is sustainable, as it does not cause damage to the plant during spring pruning or in the fall. Further work must still be done to elucidate the cellular targets involved in this antiviral action and to assess ellagic acid's clinical potential.

Punica granatum Leaf Ethanolic Extract and Ellagic Acid as Inhibitors of Zika Virus Infection

Authors

Stefano Acquadro[1]*, Andrea Civra[2]*, Cecilia Cagliero[1], Arianna Marengo[1], Massimo Rittà[2], Rachele Francese[2], Cinzia Sanna[3], Cinzia Bertea[4], Barbara Sgorbini[1] 🆔, David Lembo[2], Manuela Donalisio[2], Patrizia Rubiolo[1] 🆔

Affiliations

1 Department of Drug Science and Technology, University of Turin, Turin, Italy
2 Department of Clinical and Biological Sciences, University of Turin, Orbassano, Italy
3 Department of Environmental and Life Sciences University of Cagliari, Cagliari, Italy
4 Department of Life Sciences and Systems Biology, University of Turin, Turin, Italy

Correspondence

Prof. Patrizia Rubiolo
Department of Drug Science and Technology,
University of Turin
Via Pietro Giuria 9, 10125 Turin, Italy
Phone: + 39 01 16 70 71 73, Fax: + 39 01 12 36 76 61
patrizia.rubiolo@unito.it

Correspondence

Prof. Manuela Donalisio
Department of Clinical and Biological Sciences,
University of Turin
Regione Gonzole 10, 10043 Orbassano (To), Italy
Phone: + 39 01 16 70 54 27, Fax: + 39 01 19 03 86 39
manuela.donalisio@unito.it

🌐 Supporting information available online at http://www.thieme-connect.de/products

ABSTRACT

Zika virus, an arthropod-borne flavivirus, is an emerging healthcare threat worldwide. Zika virus is responsible for severe neurological effects, such as paralytic Guillain-Barrè syndrome, in adults, and also congenital malformations, especially microcephaly. No specific antiviral drugs and vaccines are currently available, and treatments are palliative, but medicinal plants show great potential as natural sources of anti-Zika phytochemicals. This study deals with the investigation of the composition, cytotoxicity, and anti-Zika activity of *Punica granatum* leaf ethanolic extract, fractions, and phytoconstituents. *P. granatum* leaves were collected from different areas in Italy and Greece in different seasons. Crude extracts were analyzed and fractionated, and the pure compounds were isolated. The phytochemical and biomolecular fingerprint of the pomegranate leaves was determined. The antiviral activities of the leaf extract, fractions, and compounds were investigated against the MR766 and HPF2013 Zika virus strains *in vitro*. Both the extract and its fractions were found to be active against Zika virus infection. Of the compounds isolated, ellagic acid showed particular anti-Zika activities, with EC_{50} values of 30.86 μM for MR766 and 46.23 μM for HPF2013. The mechanism of action was investigated using specific antiviral assays, and it was demonstrated that ellagic acid was primarily active as it prevented Zika virus infection and was able to significantly reduce Zika virus progeny production. Our data demonstrate the anti-Zika activity of pomegranate leaf extract and ellagic acid for the first time. These findings identify ellagic acid as a possible anti-Zika candidate compound that can be used for preventive and therapeutic interventions.

*   These authors contributed equally to this work.

ABBREVIATIONS

Aut	autumn samples
BHK-21	baby hamster kidney cell
BLAST	basic local alignment search tool
BSTFA	*N,O*-Bis(trimethylsilyl) trifluoroacetamide
CC_{50}	50%-cytotoxic concentrations
CI	confidence intervals
ESI	electrospray ionization
FDA	Food and Drug Administration
HBeAg	hepatitis B e antigen
HBV	hepatitis B virus
HIV-1	human immunodeficiency virus type 1
HPV	human papilloma virus
HSV-2	herpes simplex virus type 2
I_s	linear retention indices
ITS	internal transcribed spacer
MEM	minimum essential medium
MOI	multiplicity of infection
MTS	3-(4,5-Dimethylthiazol-2-yl)-5-(3-carboxy-methoxyphenyl)-2-(4-sulfophenyl)-2H-tetra-zolium, inner salt;
PC	principal component
PDA	photo diode array
PFU	plaque-forming unit
PG	*Punica granatum*
PGL8	*Punica granatum* leaf extract 8
Prep	preparative
psbA-trnH	chloroplast photosystem II protein D1
RP	reverse phase
RSD	relative standard deviation
SI	selectivity index
SIM	selected ion monitoring
SPE	solid phase extraction
SRM	selected reaction monitoring
Sum	summer samples
VACV	vaccinia virus
WHO	World Health Organization
ZIKV	Zikavirus

Introduction

ZIKV is a mosquito-borne virus that belongs to the Flaviviridae family. It is primarily transmitted by the bite of an infected mosquito from the *Aedes* genus, mainly *Aedes aegypti*, in tropical and subtropical regions [1]. Outbreaks of ZIKV disease have been recorded in Africa, the Americas, Asia, and the Pacific, and it is considered a global emerging healthcare threat. Since *Aedes albopictus* has the capability to be a vector for ZIKV, other countries in temperate regions, such as the Mediterranean basin, are potentially at risk [2]. ZIKV is usually responsible for asymptomatic or mild self-limiting dengue-like diseases, which are characterized by fever, rash, conjunctivitis, arthralgia, and malaise. During the recent outbreak in Brazil, it has been associated with severe neurological effects, such as Guillain-Barré syndrome and meningoencephalitis, in adults, and congenital malformations, espe-

cially microcephaly, in infants born to infected mothers [3]. Despite the severity of ZIKV complications, there are currently no FDA-approved vaccines. No specific antiviral drugs are currently available, and treatments are palliative and mainly directed towards the relief of symptoms [1]. For these reasons, new effective preventive and therapeutic strategies against ZIKV infection are urgently needed. Harnessing the potential of medicinal plants as natural sources of anti-ZIKV phytochemicals, such as polyphenols and alkaloids [4], is a complementary and alternative strategy. *Punica granatum* L. (Lythraceae family), commonly known as pomegranate, is a domesticated tree that is widely grown as an evergreen in tropical regions and as a deciduous tree in temperate areas. It is an ancient plant that is well known in folk medicine and is becoming increasingly popular as a functional food and nutraceutical source due to its high polyphenol content, not only in the edible part, but also in other parts of the fruit and plant, including the peel, bark, leaves, and flowers [5]. Pomegranate is a rich source of a wide variety of compounds with beneficial physiological activities, in particular antioxidative, anti-inflammatory, and anti-cancerous properties [6]. Nearly every part of the plant has been tested for antimicrobial activity, and roles in the suppression of enteric infections, food preservation, wound healing, as well as gut and oral health, have been demonstrated [7]. Most antiviral studies have been performed on the fruit's peel and juice, and it has been found that extracts exerted inhibitory activity against HSV-2, HIV-1, and the influenza virus [8–10]. Little information has been reported on pomegranate leaf extracts, compared to other edible and nonedible parts of the plant, although some recent studies have indicated that they may be an important source of specialized bioactive metabolites and they possess a broad range of biological properties, such as *in vitro* antioxidant, anti-inflammatory, anticholinesterase, and antiproliferative activities [5, 11, 12]. This study explores the cytotoxicity and anti-ZIKV activity of pomegranate leaf ethanolic extracts, as well as of the corresponding fractions and phytoconstituents after a phytochemical and biomolecular characterization of the leaves, which were collected from various sites, after different vegetative periods, and in different years.

Results and Discussion

Preliminary tests were carried out on a reference pomegranate leaf ethanolic extract (PGL8) to investigate its anti-ZIKV activity in a specific virus plaque reduction assay against the African lineage strain, 1947 Uganda MR766. A range of extract concentrations were added before and during the infection, as well as after the removal of the virus inoculum. As reported in **Fig. 1S**, Supporting Information, the extract exerts remarkable antiviral activity, generating dose-response curves. Under these conditions, the extract reduced the number of viral plaques with an EC_{50} value of 11.4 µg/mL (▶ **Table 1**). To exclude the possibility that antiviral activity was due to cytotoxicity, cells were treated with the serially diluted extract and added to the cell culture medium for 72 h at 37°C, and the cellular viability was then determined by MTS assay. The CC_{50} values were above 100 µg/mL, indicating that the antiviral activity observed was not due to cytotoxicity (▶ **Table 1**, **Fig. 2S**, Supporting Information). Since the extract was resus-

► **Table 1** Anti-ZIKV-MR766 activity of the pomegranate leaf ethanolic extract (PGL8).

Virus	Sample	EC$_{50}$[a] (µg/mL) (95% CI[b])	EC$_{90}$[c] (µg/mL) (95% CI)	CC$_{50}$[d] (µg/mL) (95% CI)	CC$_{90}$[e] (µg/mL) (95% CI)	SI[f]
MR766	PGL8	11.40 (7.84–16.57)	75.32 (25.7–113.3)	123.60 (104.0–146.7)	443 (313.3–559.2)	10.84
HSV-2	PGL8	3.29 (1.64–6.56)	120.20 (18.5–224.1)	154.90 (112.3–213.7)	1633 (860–2023.3)	47.08
Vaccinia virus	PGL8	n.a.[g]	n.a	–	–	n.a.
	Fractions	**EC$_{50}$ (µg/mL) (95% CI)**	**EC$_{90}$ (µg/mL) (95% CI)**	**CC$_{50}$ (µg/mL) (95% CI)**	**CC$_{90}$ (µg/mL) (95% CI)**	**SI**
MR766	PGSum85	16.20 (12.4–21.2)	95.27 (45.5–129.5)	76.10 (48.4–120)	143 (74.5–184.4)	4.69
	PGAut85	10.40 (7.08–15.2)	43.96 (17.3–111.7)	73.40 (51.6–104)	156 (88.3–216.2)	7.05
	PGSum95	n.a.	n.a.	14.20 (12.3–16.4)	32.20 (22.3–46.6)	–
	PGAut95	n.a.	n.a.	17.50 (11.9–25.8)	37.20 (18–76.6)	–

[a] EC$_{50}$: half maximal effective concentration; [b] CI: confidence interval; [c] EC$_{90}$: 90% effective concentration; [d] CC$_{50}$: half maximal cytotoxic concentration; [e] CC$_{90}$: 90% cytotoxic concentration; [f] SI: selectivity index; [g] n.a.: not assessable

pended in a DMSO/H$_2$O solution (50%/50%), a control sample with equal volumes of DMSO/H$_2$O was included in all cell-culture experiments in order to rule out the possibility of the solvent having a cytotoxic effect. The SI, which measures the preferential antiviral activity of a drug in relation to its cytotoxicity, was 10.84. Two unrelated DNA viruses, HSV-2 and VACV, were assessed in order to evaluate the antiviral specificity of PGL8. As reported in ► **Table 1**, the extract exerted relevant inhibitory activity against HSV-2, with an SI of 47.08. These data confirmed the anti-HSV-2 effect that had been observed in extracts derived from pomegranate fruit, including the rind and juice [8]. By contrast, we did not observe any inhibition of VACV infectivity.

The characterization of the pomegranate leaf ethanolic extract (sample PGL8) was carried out by HPLC-PDA-MS/MS and GC-MS after derivatization with bis(trimethylsilyl)trifluoroacetamide to obtain trimethylsilyl derivatives, and 3 different chemical classes of specialized metabolites were revealed: phenolics, flavonoids, and triterpenes. A list of the identified and putatively identified compounds is reported in ► **Table 2**, while the HPLC-PDA and GC-MS profile are found in **Figs. 3S** and **4S**, Supporting Information, respectively. In accordance with the current literature, flavones and flavonols are the most representative specialized metabolites in the extract and often exist as glycosides of luteolin, apigenin, and quercetin. Ellagic acid is the most abundant compound, while hydrolyzable tannins, such as punicalins and punicalagins, which are markers of the other parts of the pomegranate plant, were not detected. In addition, the presence of a pseudomolecular ion at m/z 455, in negative mode, with a fragment at m/z 407 (M-HCHO-H$_2$O−H)$^-$, and of a pseudomolecular ion at m/z 457, in negative ionization mode, in the LC-MS profiles indicates the presence of triterpenoid molecules, but with evident coelution. A GC-MS analytical platform was therefore used and enabled oleanolic, betulinic, and ursolic acids to be identified after their derivatization in the extract.

To ensure consistent quality and reproducible activity in the pomegranate leaf extracts, genotypic and phenotypic stability were evaluated by comparing the phytochemical and biomolecular patterns of leaves that belonged to plants of different origins

(see **Table 1S**, Supporting Information) that were harvested in different vegetative periods (summer and autumn) and in different years (2017 and 2018).

HPLC-PDA-MS/MS and GC-MS profiles were qualitatively consistent, and all markers were detected in all of the samples. Quantitation results, reported in **Table 2S**, Supporting Information, showed differences in the abundances of some compounds in the leaf extracts. The repeatability results showed that RSD% never exceeded 5%, while intermediate precision in the different extracts showed RSD% of below 15%. The accuracy of the data was determined by comparing, when available, the UV and MS quantification results, and the RSD% never exceeded 20%. Principal component analysis was then applied to highlight similarities and differences between the samples. ► **Fig. 1** reports the score and loading plots of the PC1 against the PC2, showing homogenous sample distribution in the score plot (no cluster of samples are formed) and a good explained variance (39.14% for PC1 and 19.72% for PC2). No clear discrimination between the samples was observed, although the Aut show slightly higher contents of ellagic acid and its hexoside (both positively correlated with PC2, as can be seen in the loading plot). In general, the few differences in the phenolics and triterpenes can be ascribed to phenotypical variability and environmental factors.

To further confirm the quality and reproducibility of the pomegranate leaf extracts, a genotypic fingerprint of the collected leaves was obtained using a DNA barcoding approach [16]. The nuclear *ITS* region and the *psbA-trnH* genes were amplified and sequenced for each site from which pomegranate leaf samples were harvested. The sequences were deposited in the GenBank (**Table 3S**, Supporting Information) and compared to those present in the database (59 *P. granatum ITS* sequences originating from India, Iran, and China and 27 *P. granatum psbA-trnH* sequences from Iran, Tunisia, China, and Italy [Apulia, Latium, Sardinia, Padua and Trieste]).

Figs. 5S and **6S**, Supporting Information, report no variation in the *ITS* and *psbA-trnH* nucleotide composition for the 11 sites, suggesting that these biomolecular markers are stable. A consensus sequence for each DNA region was obtained from the align-

▶ **Table 2** List of identified and putatively identified compounds in leaf extract. Each compound is referred through its relative retention time, UV maxima λ absorption, molecular formula, pseudomolecular ions (ESI⁺ and ESI⁻), ion fragments generated by Product Ion Scan mode (PIS), and identified or tentatively identified compound names. The identification confidence value and the literature reference that indicates the presence of the compounds in pomegranate are also reported.

N°	RT (min)	λmax (nm)	Molecular formula	[M + H]⁺	[M – H]⁻	Supp. MW	MS²⁺ m/z	MS²⁻ m/z	Compound name	Identif. conf.[b]	Ref.
1[a]	1.649	272	$C_7H_6O_5$	/	169	170		125 110	Gallic acid	1	[13]
2	7.373	314	$C_{15}H_{18}O_8$	/	325	326		163 145	Coumaric acid hexoside	2	[14]
3	11.657	273 357	$C_{13}H_8O_8$	/	291	292		247	Brevifolin – carboxyl acid	2	[14]
4	14.364	268		801 151	799	800	151	301	Ellagic derivative	2	[13]
5	19.032	270 350		611	935 655 609	610	151	301 137	Ellagitannin	3	
6	19.420	251 360	$C_{20}H_{16}O_{13}$	465	463	464	/	301	Ellagic acid glucoside	2	[13]
7	24.091	274 365	$C_{41}H_{28}O_{27}$	953	951	952	/	933 301	Galloyl- HHDP- DHHDP-hexoside (Granatin B)	2	[13]
8[a]	24.366	253 347	$C_{21}H_{20}O_{11}$	449	447	448	287	285	Luteolin 7-O-glucoside	1	[14]
9[a]	25.994	252 366	$C_{14}H_6O_8$		301	302	/	284 229 185	Ellagic acid	1	[13]
9a[a]	25.994		$C_{27}H_{30}O_{16}$	611	609	610			Rutin	1	[13]
10[a]	27.426	255 353	$C_{21}H_{20}O_{12}$	465	463	464	303 229 153	301 255 151	Quercetin 3-O-glucoside	1	[13]
11[a]	28.885	266 336	$C_{21}H_{20}O_{10}$	433	431	432	271	269	Apigenin 7-O-glucoside	1	[14]
12	30.971	268 332		433	431	432	271	269 195 151 117	Apigenin glycoside	3	
13[a]	31.719	267 337	$C_{21}H_{20}O_{11}$	449	447	448	287	285 257	Luteolin 4'-O-glucoside	1	[13]
14	33.223	268 340		449	447	448	287 153	285 151	Luteolin glycoside 1	3	
15	37.253	268 340		419	417	418	287 153	285 257 175 151	Luteolin glycoside 2	3	
16[a]	42.958	252 347	$C_{15}H_{10}O_6$	287	285	286	153 135 117	171 151 133 115	Luteolin	1	[13]
17[a]	45.538	267 336	$C_{15}H_{10}O_5$	271	269	270	163 153 119	151 117	Apigenin	1	[14]
*	50.201	–	$C_{30}H_{48}O_3$	457	455	456	333 239 191 189	407	Oleanolic acid	1	[14]

cont.

► **Table 2** *Continued*

N°	RT (min)	λmax (nm)	Molecular formula	[M + H]⁺	[M – H]⁻	Supp. MW	MS²⁺ m/z	MS²⁻ m/z	Compound name	Identif. conf.ᵇ	Ref.
*	50.201	–	$C_{30}H_{48}O_3$	457	455	456	333 239 191 189	407	Betulinic acid	1	[14]
*	50.201	–	$C_{30}H_{48}O_3$	457	455	456	333 239 191 189	407	Ursolic acid	1	[14]

ᵃ Compounds identified by comparing with reference standards; ᵇ An identification confidence according to the request of the Chemical Analysis Working Group (CAWG, 2007) [15] is indicated: Level 1:Identified compound (A minimum of 2 independent orthogonal data (such as retention time and mass spectrum) compared directly to an authentic reference standard; Level 2: Putatively annotated compound (compound identified by analysis of spectral data and similarity to bibliographic data); Level 3: putatively characterized class compound; Level 4: unknown compound.
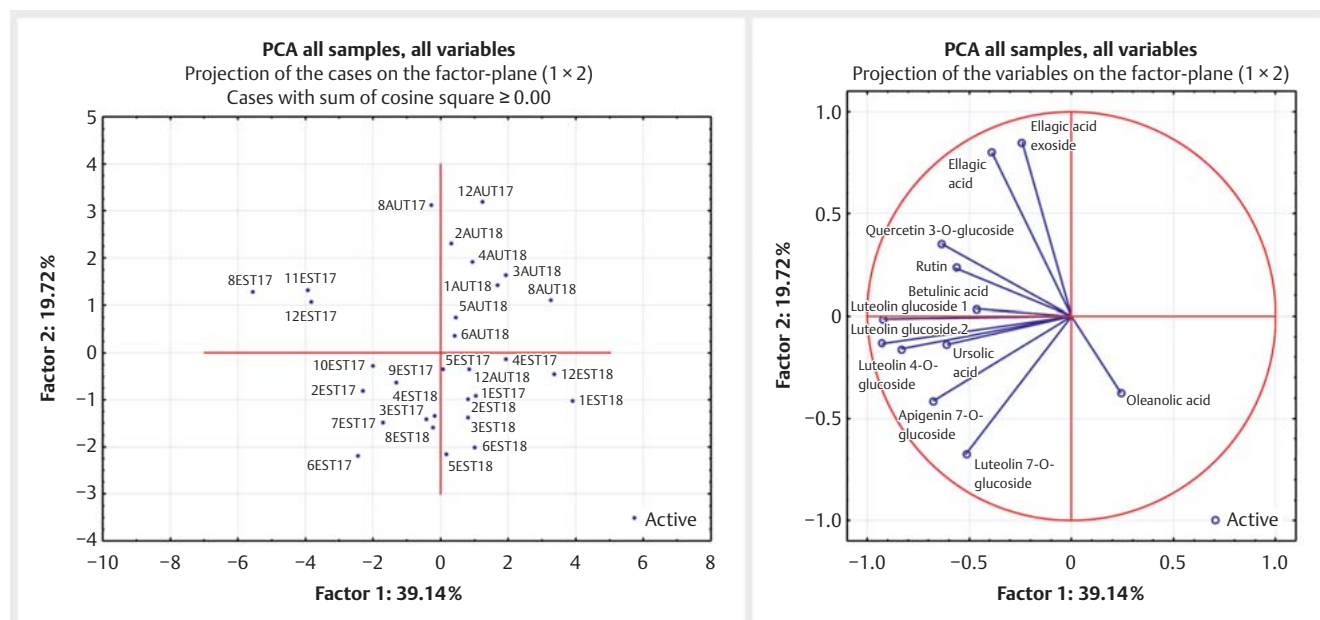
► **Fig. 1** Score plot (**a**) and loading plot (**b**) of the principal component analysis relative to the quantity of the main markers of the pomegranate's leaf extracts.

ment of all the samples. A BLAST alignment of the consensus, with all the data present in the database, showed a percentage of identity among the *P. granatum* sequences that ranged from 100% to 96.89% for *ITS,* and from 100% to 97.64% for *psbA-trnH,* confirming intraspecies stability and higher interspecies variability. Interestingly, the comparison with *psbA-trnH* from Italian regions (accession numbers: HG765008, HG765007, HG765006, HG765005), showed 100% similarity, supporting the stability of the species in Italy.

Based on the data obtained from the phytochemical characterization, representative summer and autumn pool extracts were created.

A bio-guided fractionation procedure was performed to attribute the antiviral activity to a specific fraction and/or single com-

ponents of the pomegranate leaf extracts. The summer and autumn extracts were submitted to SPE fractionation, resulting in 2 fractions: a phenolic fraction (yield 73%) eluted with methanol/water 85:15 (PGAut85, PGSum85), and a triterpenoid fraction (yield 5%) eluted with methanol/water 95:05 (PGAut95, PGSum95). **Table 2S**, Supporting Information, reports the quali-quantitative composition of the 4 samples. The phenolic fraction was characterized by ellagic acid, rutin, apigenin, quercetin, and luteolin glycosides. In the PGAut85 fraction, ellagic acid was the most abundant compound, while, in the PGSum85 one, luteolin 4′-O-glucoside was the main compound, although a good amount of ellagic acid was detected. The triterpenoid fraction was characterized by oleanolic, betulinic, and ursolic acids.

▶ **Table 3** Anti-ZIKV-MR766 activity of phenolic and triterpenic compounds. For each concentration tested, the percentage of infection in comparison to control is reported as mean value ± SD. The molarities of the compounds is reported in square brackets, referred to 3.7 µg/mL, 11 µg/mL, and 33 µg/mL concentrations, respectively.

Compounds	3.7 µg/mL	11 µg/mL	33 µg/mL
Apigenin	99.0 ± 7.1 [13.7 µM]	n. a.[a] [40.7 µM]	n. a. [122.1 µM]
Apigenin 7-O-glucoside	103.6 ± 8.9 [8.5 µM]	101.2 ± 3.7 [25.4 µM]	102.5 ± 2.8 [76.2 µM]
Betulinic acid	99.3 ± 1.1 [8.1 µM]	101.5 ± 6.4 [24.1 µM]	95.5 ± 10.7 [72.3 µM]
Luteolin	102.9 ± 4.1 [13 µM]	n. a. [38.5 µM]	n. a. [115.5 µM]
Luteolin 4-O-glucoside	103.0 ± 1.4 [8.3 µM]	96.0 ± 5.7 [24.5 µM]	102.8 ± 8.8 [73.6 µM]
Luteolin 7-O-glucoside	105.0 ± 5.7 [8.3 µM]	102.0 ± 11.3 [24.5 µM]	100.0 ± 3.3 [73.6 µM]
Oleanolic acid	99.5 ± 9.2 [8.1 µM]	103.8 ± 3.2 [24.1 µM]	104.3 ± 6.7 [72.3 µM]
Quercetin 3-O-glucoside	105.5 ± 6.4 [8.0 µM]	103.1 ± 9.8 [23.8 µM]	106.5 ± 4.6 [71.3 µM]
Rutin	103.3 ± 9.5 [6.1 µM]	95.4 ± 20.6 [18.0 µM]	107 ± 2.4 [54.1 µM]
Ursolic acid	100.0 ± 11.9 [8.1 µM]	79.7 ± 2.3 [24.1 µM]	n. a. [72.3 µM]
Ellagic acid	83.8 ± 11.5 [12.2 µM]	43.3 ± 1.3 [36.4 µM]	0.0 ± 0.0 [109.2 µM]

Betulinic acid, oleanolic acid, ursolic acid, apigenin were resuspended in a DMSO/H_2O solution (70%/30%); apigenin 7-O-glucoside, luteolin, luteolin 4-O-glucoside, luteolin 7-O-glucoside, quercetin 3-O-glucoside, rutin, and ellagic acid were were resuspended in a DMSO solution. [a] n. a.: not assessable

▶ **Table 4** Anti-ZIKV activity of ellagic acid.

	Virus	EC_{50}[a] (µM) (95% CI[b])	EC_{90}[c] (µM) (95% CI[b])	CC_{50}[d] (µM)	SI[e]
Commercial ellagic acid	MR766	36.22 (28.91–45.37)	93.05 (53.17–162.8)	496.5	13.7
	HPF2013	20.99 (16.48–26.74)	53.23 (31.11–91.09)	496.5	23.7
Isolated ellagic acid	MR766	30.86 (26.02–36.6)	42.64 (33.98–53.51)	446.85	14.5
	HPF2013	46.23 (37.88–56.41)	141.2 (85.90–232.0)	446.85	9.7

[a] EC_{50}: half maximal effective concentration; [b] CI: confidence interval; [c] EC_{90}: 90% effective concentration; [d] CC_{50}: half maximal cytotoxic concentration; [e] SI: selectivity index. Ellagic acid was resuspended in a DMSO solution.

As reported in ▶ **Table 1** and **Fig. 7S**, Supporting Information, both the PGAut85 and PGSum85 fractions were active against ZIKV at increasing doses with EC_{50} values of 10.40 and 16.20 µg/mL, respectively. However, no PG95 fractions exerted antiviral activity. No statistical differences were observed in the EC_{50} values of the summer and autumn fractions, confirming the demonstrated similar chemical compositions of the pomegranate leaves. The main components of the PG85 and PG95 fractions were therefore tested. A preliminary screening was performed to test the activity of the phenolic and triterpenic compounds at 3 doses (33, 11, 3.7 µg/mL) against the MR766 strain by treating cells before, during, and after infection. ▶ **Table 3** demonstrates that ellagic acid was active against ZIKV infection in a dose-dependent manner. No inhibitory effect was observed at any dose for the other compounds. These data, obtained on cell cultures, did not confirm the predictive inhibitory activity of luteolin, apigenin, and rutin as inhibitors of the ZIKV NS2B-NS3 protease, as identified by molecular docking [17, 18]. Furthermore, the ability of quercetin 3-O-glucoside to inhibit ZIKV in vitro, as reported in the literature, was not reproduced [19]. According to our data, ellagic acid showed the highest antiviral activity against ZIKV and was therefore isolated from the pomegranate extract by Prep-LC and se-

lected for further study. The isolated ellagic acid was characterized by ^{1}H NMR, and its spectrum compared with that of the commercial standard (**Fig. 8S**, Supporting Information). The purity of the compound was determined by HPLC-PDA and calculated to be > 97%.

To confirm the inhibition of ZIKV infectivity that the isolated ellagic acid demonstrated in the preliminary standard plaque reduction assay, a wider range of concentrations was tested against the MR766 strain in order to determine the EC_{50} values. High inhibitory activity was observed with an EC_{50} value of 30.86 µM (▶ **Table 4**, **Fig. 2a**). It is worth noting that the compound was also active against the Asian lineage strain, 2013 French Polynesia HPF2013, with an EC_{50} of 46.23 µM, indicating the broad spectrum of its action against different ZIKV strains. These data were confirmed using the commercially available standard, endowed with comparable EC_{50} values (▶ **Table 4** and **Fig. 2b**). To corroborate the inhibition of ZIKV infectivity by ellagic acid, immunofluorescence experiments that incubated fixed cells with a flavivirus group antigen antibody, were performed in the same conditions as described previously for both MR766 and HPF2013. As reported in ▶ **Figs. 2c** and **d**, the analysis by confocal laser scanning microscope revealed a strong red signal from ZIKV protein E in the
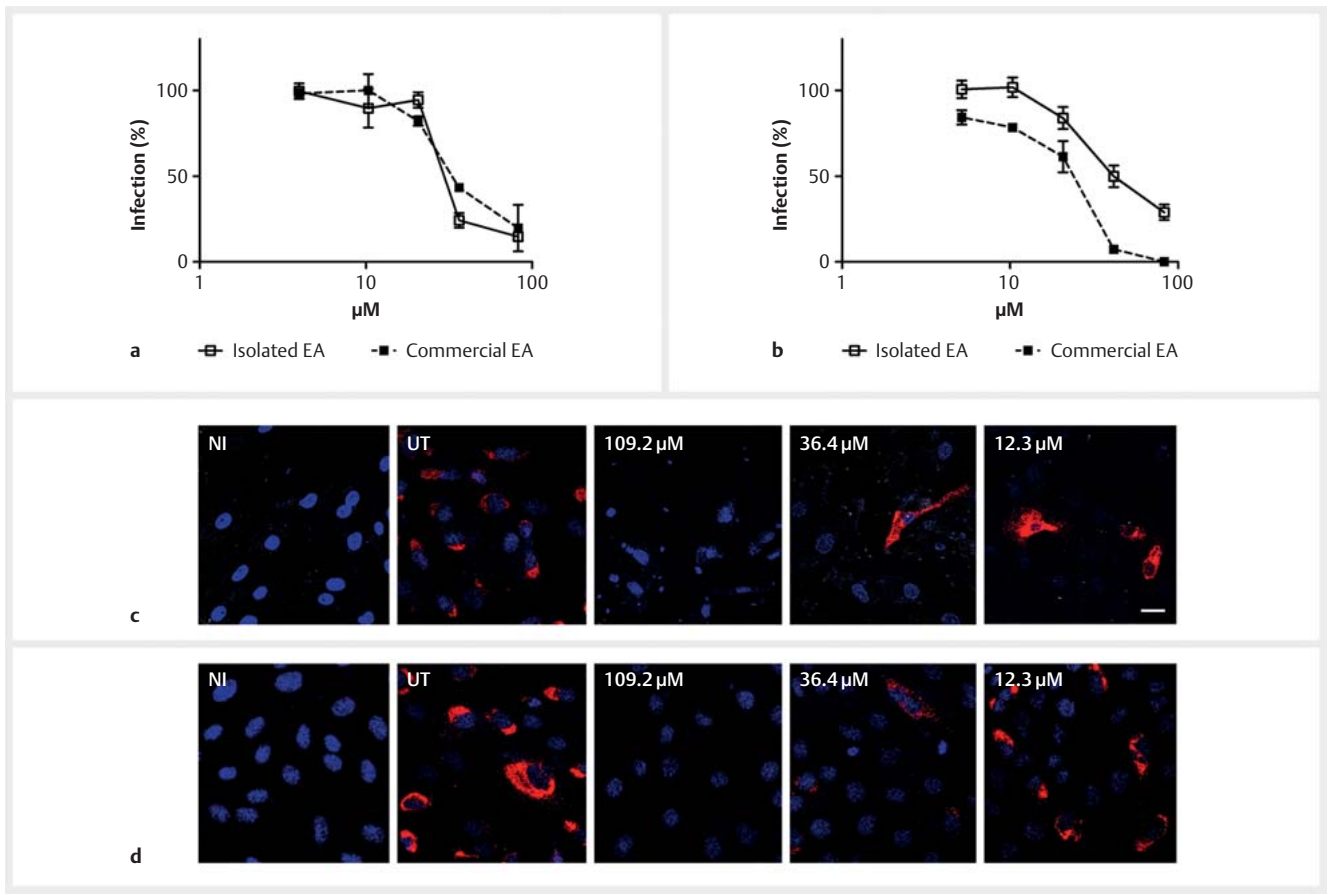
▶ **Fig. 2** Panels **a** and **b**. Plaque reduction assays infecting cells with MR766 (panel **a**) and HPF2013 (panel **b**) in the presence of isolated and commercial ellagic acid. Vero cells were treated with ellagic acid prior to infection, during the infection period, and after the infection for 72 h. Results are reported as percentage of infection in comparison to untreated controls (Y-axis); the concentrations tested are reported on X-axis. Error bars represent the standard error of the mean for 3 independent experiments. Panel **c** and **d**. Representative MR766 foci (panel **c**) and HPF2013 foci (panel **d**) in Vero cells by immunofluorescence assay. Vero cells were treated with ellagic acid before, during, and after the infection. The ZIKV protein E is visualized in red, nuclei in blue. NI: not infected; UT: untreated. Scale bar, 20 μm. Ellagic acid was resuspended in a DMSO solution.

cytosol of untreated cells. A dose-dependent signal was observed in treated cells; the highest tested dose (109.2 μM) completely inhibited the infectivity of both strains, while the number of infected cells was considerably reduced at 36.4 μM.

Recently, the antiviral activity of ellagic acid, which had been isolated from other plants, has been demonstrated *in vitro* against different RNA viruses, such as the influenza virus, Ebola virus, hepatitis C virus, and HIV-1 [20–23]. Furthermore, ellagic acid has revealed potential activity against HBV infection due to its hepatoprotective properties and ability to effectively block HBeAg secretion in cells [24]. By contrast, ellagic acid partially inhibited HSV-2 infection [8]. Herein, we have demonstrated, for the first time, the antiviral activity of pomegranate-derived ellagic acid against ZIKV, a member of the Flaviviridae family. Previously, other polyphenols, such as delphinidin and epigallocatechin gallate, have been shown to have antiflaviviral effects [25]. Our data have demonstrated that the isolated ellagic acid inhibited, *in vitro,* the infection of 2 lineages, the African one, which is responsible for more acute infection, and Asian ZIKV, which is associated with neurological impairments [26]. Interestingly, the compound also

exerted adulticidal activity against *Aedes aegypti* mosquito, the main vector of the virus [27].

As ellagic acid was identified as an inhibitor compound of ZIKV infectivity, further studies were performed to elucidate its mechanism of action. Firstly, we tested the ability of isolated ellagic acid to reduce ZIKV progeny production *in vitro* by performing a virus yield reduction assay. The experimental procedure for this assay is similar to the one described for the viral plaque reduction assay, but the viral titers of the samples were evaluated after infection. As reported in ▶ **Fig. 3**, 109.2 and 36.4 μM concentrations significantly reduced the production of infectious viruses 100- and 10-fold, respectively.

A virucidal assay was performed to investigate the possible direct virus-inactivating activity of the isolated compound on both MR766 and HPF2013. To this aim, 10^5 pfu of the ZIKV strains and the compound, at the dose corresponding to the EC_{90} values, were mixed and incubated for 2 h at either 4 or 37 °C. As reported in **Fig. 9S**, Supporting Information, no inhibition by the isolated ellagic acid was observed under any experimental conditions either for MR766 or HPF2013, thus excluding the possibility that the di-
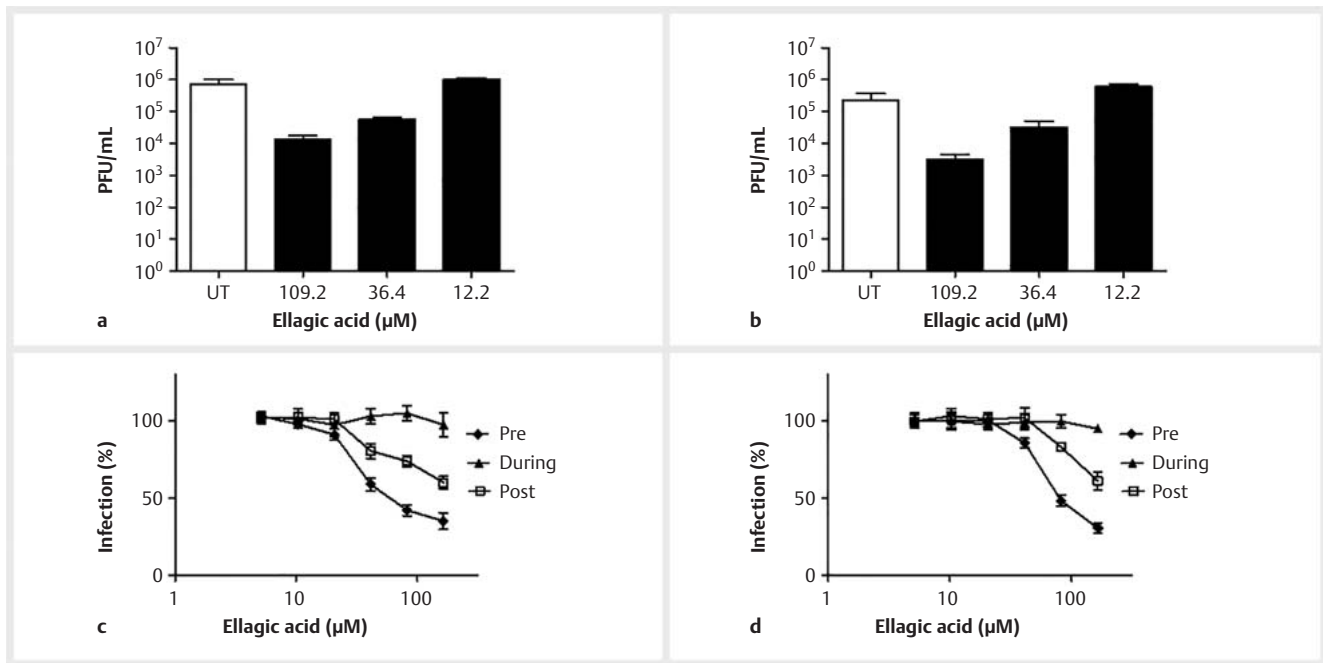
▶ **Fig. 3** Panel **a** and **b**. Virus yield reduction assays. Effects of isolated ellagic acid on multiple cycles of MR766 (panel **a**) and HPF2013 (panel **b**) replication. Viral titers are expressed as PFU/mL. Error bars represent the standard error of the mean for 3 independent experiments (p < 0.05). Panel **c** and **d**. Time of addition assays with isolated ellagic acid. Vero cells were treated with compound prior to infection (pre-treatment), during the infection period (during infection), or after infection (post-treatment) with MR766 (panel **c**) and HPF 2013 (panel **d**). Data are reported as percentage of infection in comparison to untreated control. Error bars represent the standard error of the means for 3 independent experiments. Ellagic acid was resuspended in a DMSO solution.

rect inactivation of extracellular virus particles may be a mode of antiviral action. The time-of-addition assay allowed us to investigate the stage of the virus replication cycle at which the compound acts by targeting the cellular surface or intracellular processes. To this aim, the compound was added to the cells at different times of infection only before, during, or after infection. In all of the experiments, DMSO-treated infected cells were used as controls, and plaque-formation inhibition was evaluated. ▶ **Fig. 3c** shows that the isolated compound exerted inhibitory activity against the MR766 strain in a dose-response manner, when added 2 h before infection, with an EC_{50} value of 74.48 µM. By contrast, inhibition was absent in the during-treatment assay, whereas weak inhibition was observed at the higher doses tested in the post-treatment assay. These data were confirmed using the HPF2013 (panel **d**) strain with inhibitory activity being observed in the pre-treatment assay with a value of 93.01 µM. The ability to inhibit viral infection during the pre-treatment assay was also observed when cells were treated with the commercial compound (data not shown). These data suggest that ellagic acid primarily reduces cell susceptibility to virus infection by tethering to the cell surface.

Our results demonstrate that ellagic acid did not affect the ZIKV infection by directly inactivating the virus particles. The time-of-addition experiments indicated that ellagic acid, added before viral exposure, suppressed viral replication, which suggests that, mechanistically, the compound interferes with the cell surface, likely masking ZIKV receptors, including Axl9, on target cells,

prior to viral/cell membrane fusion. Similar ellagic acid activity was observed against HIV-1. However, in this case, it was also shown to be able to specifically block viral integrase activity [21]. Furthermore, ellagic acid has been observed to have a HPV-preventive effect in clinical trials; women treated with the ellagic acid complex were less likely to be diagnosed with an abnormal Pap smear at 6 months [28].

The absence of activity when the compound was added, with the virus, to the cells indicates that it did not impair the early intracellular steps of viral replication or viral targets. This hypothesis was confirmed by performing a binding assay, and it was shown that a high concentration of isolated compound did not inhibit the binding of either MR766 or HPF2013 to the host-cell surface (**Fig. 10S**, Supporting Information).

Further studies are required to clarify whether the anti-ZIKV activity of ellagic acid may also occur indirectly via an alteration in the innate response of the infected target cells. In recent years, ellagic acid has gained attention due to its antioxidant, anticancer, anti-allergic, and anti-inflammatory activities. Its antioxidant properties have been associated with hepatoprotective activity, the attenuation of liver injury during hepatitis B infection, and with therapeutic effects on the survival of influenza-challenged mice, in combination with an antiviral drug and an immunomodulator [29, 30].

Our current data suggest that ellagic acid may be a promising candidate for the development of a novel anti-ZIKV compound.

Further structural modifications might be needed to improve its selectivity index.

In summary, we have demonstrated, for the first time, that pomegranate leaf extract and its fractions possess anti-ZIKV activity. The lack of a protective vaccine and specific treatment against ZIKV has prompted us to develop safe and effective anti-ZIKV compounds that are also able to prevent infection by impairing the chain of congenital transmission. The pomegranate leaf ethanolic extract is characterized by hydrolyzable tannins, flavonoids, and triterpenes; its phytochemical pattern is stable and does not depend on geographical conditions or season. Furthermore, no differences were found in the *ITS* and *psbA-trnH* sequences extracted from leaves collected in different sites. Moreover, leaf collection is sustainable as it does not cause damage to the plant during spring pruning or in the fall. Ellagic acid was identified, from among the isolated constituents, as an interesting antiviral compound for its inhibitory activity, and its ability to prevent infection and reduce the transmission of extracellular free virus at high titers. Further work must still be done to elucidate the cellular targets involved in this antiviral action and to assess ellagic acid's clinical potential as a preventive and/or therapeutic compound.

Materials and Methods

Plant materials

P. granatum leaves were collected from different sites in Sardinia, and occasionally other Italian regions, and in Greece from June to October 2017 and 2018 (**Table 1S**, Supporting Information). Sample 8 was from the botanical garden of the University of Cagliari, Italy. All individuals sampled from other sites were collected randomly. Voucher specimens (**Table 1S**, Supporting Information) were deposited at the Cagliari's botanical garden and at the Department of Drug Science and Technology of the University of Turin. The fresh plant materials were dried at 40 °C to constant weight.

Chemicals

LC-MS grade acetonitrile, HPLC-grade methanol, pyridine, BSTFA, formic acid (> 98 % purity), ellagic acid, rutin, and apigenin were purchased from Merck. De-ionized water (18.2 MΩ cm) was obtained from a Milli-Q purification system (Millipore). Luteolin, apigenin 7-*O*-glucoside, quercetin 3-*O*-glucoside, luteolin 7-*O*-glucoside, luteolin 4′-*O*-glucoside, betulinic acid, oleanolic acid, and ursolic acid were obtained from Extrasynthese.

Ethanolic extract preparation

Two extracts were prepared from each sample; 0.500 g of dried and ground powder was extracted using an ultrasonic bath (Soltec, Sonica S3 EP 2400) operating at 40 KHz with 10 mL of ethanol, 3 times for 10 min each. The supernatants were combined and centrifuged at 5000 rpm for 10 min, poured into a glass balloon, and evaporated in a rotary evaporator under vacuum at a temperature below 50 °C. In order to reduce chlorophyll interference, 30 mg of crude extract were resuspended in 1 mL of methanol/water (20:80, v/v), loaded onto a Bond Elut Jr 500 mg SPE-C18 cartridge (Agilent Technologies), eluted with 8 mL of methanol/water (95:5, v/v), and evaporated in a rotary evaporator. Pool samples, obtained by mixing the leaves that were harvested in summer (PGSum) and autumn (PGAut), were also created and extracted in the same way.

HPLC-PDA-MS/MS analysis

For each extract, a 10 mg/mL stock solution in methanol was prepared, subsequently diluted with acetonitrile/water (95:5, v/v), and filtered through a 13 mm diameter, 0.22 μm PTFE syringe hydrophilic filter before HPLC-PDA-MS/MS analyses. Each extract (5 μL) was analyzed using a Shimadzu Nexera X2 system equipped with a photodiode array detector SPD-M20A that was connected, in series, to a Shimadzu LCMS-8040 triple quadrupole system outfitted with an ESI source (Shimadzu). The chromatographic conditions were: column: Ascentis Express RP-Amide (10 cm × 2.1 mm, 2.7 μm, Supelco); mobile phases: A water/formic acid (999:1, v/v) and B acetonitrile/formic acid (999:1, v/v); flow rate: 0.4 mL/min; column temperature: 30 °C; gradient: 5 % B for 5 min, 5–25 % B in 35 min, 25–100 % B in 10 min, 100 % B for 1 min. UV spectra were acquired over the 220–450 nm wavelength range. The mass spectrometer operation conditions and identification criteria were as reported by Marengo et al. [31]. Quantitation was performed using the external standard calibration method via UV (at the λ max for each compound) and SRM acquisition in ESI⁺ (collision energy: 35.0 V for ESI⁺, dwell time: 20). The results are expressed as mg of compound per g of dried leaves (mg/g). When the commercial standard was not available, quantification was based on the UV calibration curves of compounds belonging to the same chemical class. The calibration ranges, λ max, SRM transitions, and analytical performance of the method are reported in **Table 5S**, Supporting Information. Analyses were performed in triplicate. All data were processed using LabSolution software (Shimadzu).

GC-MS analysis

GC analysis were carried out on a Shimadzu 2010 GC unit that was coupled to a Shimadzu QP2010 Mass spectrometer and that made use of a MPS-2 multipurpose sampler (Gerstel). The derivatization of the extracts was performed with bis(trimethylsilyl)trifluoroacetamide to obtain trimethylsilyl derivatives, as reported by Rubiolo et al. [32]. GC-MS analyses were carried out on a MEGA-1 column (100 % methylpolysiloxane, 15 m × 0.18 mm d_c, 0.18 μm d_f) from MEGA S.r.l. (Milan, Italy). Analytical conditions: injector temperature: 300 °C, transfer line temperature: 320 °C, carrier gas: He (0.8 ml/min), split ratio 1:10. Temperature program: 50 °C (2 min)//5 °C/min//300 °C. MS conditions: source temperature: 200 °C, ionization mode: electron impact (70 eV), scan rate: 0.2 u/s, mass range: 100–650 *m/z*. Compounds were identified via comparisons of mass spectra and I_s, calculated versus a C9-C25 hydrocarbon mixture, with those reported in the literature. The identity of the triterpenoids was confirmed by the co-injection of commercially available standards. The quantitation of the triterpenoids was performed in SIM-acquisition mode using the external standard calibration method, according to Rubiolo et al. [32] (**Table 6S**, Supporting Information). Data were processed using Shimadzu GCMS Solution software (Shimadzu)

DNA extraction, PCR amplification and sequencing

The DNA extraction, PCR amplification, and sequencing of the *ITS* and *psbA-trnH* regions were performed according to Marengo et al. [16] without modifications. **Table 4S**, Supporting Information, reports the list of primers used in PCR and sequencing.

SPE-C18 cartridge and Prep-LC fractionation

Crude PGSum and PGAut ethanolic extracts were fractionated using a SPE-C18 cartridge: 30 mg of each crude extract were resuspended in 1 mL of methanol/water (20 : 80, v/v), loaded onto the Bond Elut Jr 500 mg SPE-C18 cartridge, first eluted with 5 mL of methanol/water 85 : 15, v/v (PG85) and subsequently with 5 mL of methanol/water 95 : 05, v/v (PG95). Both fractions were evaporated to dryness. Fraction PGAut85, at a concentration of 40 mg/mL, was injected into a Shimadzu LC-10AT system to isolate the ellagic acid. Chromatographic conditions: column: Ascentis Express RP-Amide (15 cm × 10 mm, 5 µm, Supelco) mobile phases: see HPLC-PDA-MS/MS analysis; flow rate: 1 mL/min; column temperature: 30 °C; gradient program: 10% B for 1 min, 10–30% B in 60 min, 30–51% B in 9 min, 51–100% B in 1 min, 100% B for 4 min; injection volume: 100 µL. Ellagic acid was collected via multiple injections, the organic solvent was evaporated with a rotary evaporator, and the sample was subsequently freeze-dried. The purity of the isolated ellagic acid was confirmed via a HPLC-PDA-MS/MS analysis at a concentration of 1 mg/ml in methanol and was calculated as a percentage peak area at 254 nm. Isolated and commercial ellagic acid were also characterized by ^{1}H NMR. Spectra were collected in deuterated DMSO using a JEOL ECZR600 (600 MHz) nuclear magnetic resonance (NMR) spectrometer.

Cell cultures

African green monkey fibroblastoid kidney cells (Vero cells, ATCC CCL-81) were grown as monolayers in Eagle's MEM (Sigma-Aldrich) with 10% heat-inactivated FBS (Sigma-Aldrich) and 1% antibiotic solution (penicillin-streptomycin, Sigma-Aldrich) in a humidified 5% CO_2 atmosphere at 37 °C. The antiviral assays, against ZIKV and HSV-2, were performed on Vero cells. BHK-21 cells (ATCC CCL-10) were grown in DMEM 10% FBS and used for antiviral assays against the VACV. The embryonic human kidney cells (293 T) (ATCC CRL-3216) were grown as monolayer in DMEM 10% FBS supplemented with 1% Glutamax-I (Invitrogen).

Viruses

Two ZIKV strains were used to investigate the antiviral potential of pomegranate: the 1947 Uganda MR766 and the 2013 French Polynesia HPF2013, representing the African and the Asian lineages respectively. The viruses were produced via the transfection of 293T cells with 2 plasmids (pCDNA6.2 Zika MR766 Intron3115 HDVr MEG 070916 5 and pCDNA6.2 Zika HPF2013 3864,9388Intron HDVr MEG091316 2) kindly provided by Prof. F. Di Cunto and Prof. M. J. Evans, and were propagated and titered in Vero cells, as described in Francese et al. [26]. The HSV-2 strain (ATCC VR-540) was propagated, collected, and titrated, via plaque assay, on Vero cells [33]. The VACV, ATCC VR-1354 strain was propagated, collected, and titrated, via plaque assay, on BHK-21 cells.

Viability assay

Cell viability was assessed using the MTS assay, as described in Donalisio et al. [34]. PGL8, PGAut85, and PGSum85 were resuspended in a DMSO/H_2O solution (50%/50%), at 10 mg/mL concentration; PGAut95 and PGSum95 were resuspended in a DMSO/H_2O solution (87.5%/12.5%) at 2.5 mg/mL concentration; ellagic acid was resuspended in DMSO at 10 mg/mL concentration. The effects of the extract, fractions, and ellagic acid on Vero cells viability were evaluated at 24 and 72 h. CC_{50} and 95% CI were determined using Prism 5 software (Graph-Pad Software).

Inhibition assays

The anti-ZIKV activity of the extract, fractions, and ellagic acid was determined using a viral plaque reduction assay on Vero cells as described in Francese et al. [26]. For the HSV-2 and VACV plaque reduction assays, the cells were infected with virus at MOI 0.001 and 0.006 PFU/cell, respectively; the cells were fixed and the plaques were counted at 24 (HSV-2) and 72 h (VACV) post infection. PGL8, PGAut85, and PGSum85 were resuspended in a DMSO/H_2O solution (50%/50%) at 10 mg/mL concentration; PGAut95 and PGSum95 were resuspended in a DMSO/H_2O solution (87.5%/12.5%) at 2.5 mg/mL concentration. Betulinic acid, oleanolic acid, ursolic acid, and apigenin were resuspended in a DMSO/H_2O solution (70%/30%) at 7 mg/mL concentration; apigenin 7-*O*-glucoside, luteolin, luteolin 4-*O*-glucoside, luteolin 7-*O*-glucoside, quercetin 3-*O*-glucoside, rutin, and ellagic acid were resuspended in DMSO at 10 mg/mL concentration. The concentrations that reduced viral infectivity by 50% (half maximal effective concentration, EC_{50}) and concentrations that reduced viral infectivity by 90% (effective concentration-90, EC_{90}) were calculated using the software Prism. The results are reported for 3 independent experiments. The selectivity index (SI) was calculated as the ratio CC_{50}/EC_{50}.

Virus inactivation assay

Ellagic acid preparations were investigated for their ability to directly inactivate ZIKV particles at 4 °C and 37 °C [26]. Ellagic acid was resuspended in DMSO at 10 mg/mL concentration.

Time-of-addition assays

Serial dilutions of ellagic acid were either added to Vero cells before infection for 2 h at 37 °C, during infection with MR766 (MOI 0.005), or after the infection [33]. Ellagic acid was resuspended in DMSO at 10 mg/mL concentration.

Immunofluorescence assay

Vero cells that were seeded on coverslips were treated with serial doses of plant-isolated ellagic acid for 2 h prior to infection, for 2 h during infection with MR766 (MOI 1), and for 30 h after the absorption process, at 37 °C. The experiment was performed as described in Francese et al. [26], with the exception of the nucleic staining, which was performed using DAPI (Sigma-Aldrich) 0.5 µg/mL for 10 min at room temperature. Ellagic acid was resuspended in DMSO at 10 mg/mL concentration.

Virus yield reduction assay

The experiment was conducted as described in Francese et al. [26]. Ellagic acid was resuspended in DMSO at 10 mg/mL concentration.

Binding assay

The experiment was conducted as described in Francese et al. [26]. Ellagic acid was resuspended in DMSO at 10 mg/mL concentration.

Statistical analysis

Antiviral data were analyzed using the Student's t-test and F-test on GraphPad Prism version 5.00 software, as appropriate. The Student's t-test was used to compare viral titers in virus inactivation assays. Significance was reported for p-value < 0.05. Principal component analysis was carried out using Statistica 10 (StatSoft. Inc.) software. Sequence quality and alignment were performed as reported by Marengo et al. [16].

Supporting Information

Anti-ZIKV activity of a reference pomegranate leaf ethanolic extract PGL8 (**Fig. 1S**); cell viability assays (**Fig. 2S**); LC chromatograms of the pomegranate leaf extract PGL8 (**Fig. 3S**); GC-MS chromatograms of the pomegranate leaf extract PGL8 (**Fig. 4S**); comparison of *ITS* sequences between the 11 *P. granatum* samples (**Fig. 5S**); comparison of *psbA-trnH* sequences between the 11 *P. granatum* samples (**Fig. 6S**); anti-MR766 activity of PGSum85, PGSum95, PGAut85, and PGAut95 (**Fig. 7S**); ^{1}H 600 MHz NMR of ellagic acid isolated with LC-Prep and of the commercial standard reference (**Fig. 8S**); inactivation of MR766 particles by isolated ellagic acid (**Fig. 9S**); effect of isolated ellagic acid on virus binding to cells (**Fig. 10S**); location, coordinates, and code of pomegranate leaf samples (**Table 1S**); concentration of phenolic compounds and triterpenes in the different pomegranate leaf extracts and in the fractions (**Table 2S**); list of the sequences obtained from *P. granatum* samples deposited in GenBank (**Table 3S**); list of primers used in PCR and sequencing (**Table 4S**); quantification method, linearity range, R^2, and calibration curve of the main compounds by UV and SRM methods (**Table 5S**); and target ion, qualifier ions, linearity range, R^2, and calibration curve of triterpenoids quantified by GC-MS (**Table 6S**) are available as Supporting Information.

Contributors' Statement

Conception and design: C. Sanna; C. Bertea; C. Cagliero; B. Sgorbini; D. Lembo; M. Donalisio; P. Rubiolo. Data collection: C. Sanna; S. Acquadro; A. Civra; A. Marengo; R. Francese; M. Rittà. Analysis and interpretation: S. Acquadro; A. Civra; A. Marengo; R. Francese; M. Rittà; C. Cagliero; C. Sanna; C. Bertea; B. Sgorbini; D. Lembo; M. Donalisio; P. Rubiolo. Statistical analysis: S. Acquadro; A. Civra; A. Marengo; R. Francese; M. Rittà; C. Cagliero; C. Bertea; B. Sgorbini; D. Lembo; M. Donalisio; P. Rubiolo. Drafting of the manuscript: S. Acquadro; A. Civra; A. Marengo; R. Francese; M. Rittà. Critical revision of the manuscript: C. Sanna; C. Bertea; C. Cagliero; B. Sgorbini; D. Lembo; M. Donalisio; P. Rubiolo.

Conflict of Interest

The authors declare that they have no conflict of interest.

References

[1] Saiz JC, Vazquez-Calvo A, Blazquez AB, Merino-Ramos T, Escribano-Romero E, Martin-Acebes MA. Zika virus: the latest newcomer. Front Microbiol 2016; 7: 496

[2] WHO. Zika virus [WWW Document], n.d. Available at https://www.who.int/news-room/fact-sheets/detail/zika-virus. Accessed April 5, 2020

[3] Blázquez AB, Saiz JC. Neurological manifestations of Zika virus infection. World J Virol 2016; 5: 135–143

[4] Batista MN, Braga ACS, Campos GRF, Souza MM, Matos RPA, Lopes TZ, Candido NM, Lima MLD, Machado FC, Andrade STQ, Bittar C, Nogueira ML, Carneiro BM, Mariutti RB, Arni RK, Calmon MF, Rahal P. Natural products isolated from oriental medicinal herbs inactivate Zika virus. Viruses 2019; 11: 49

[5] Fellah B, Bannour M, Rocchetti G, Lucini L, Ferchichi A. Phenolic profiling and antioxidant capacity in flowers, leaves and peels of Tunisian cultivars of *Punica granatum* L. J Food Sci Technol 2018; 55: 3606–3615

[6] Vucic V, Grabez M, Trchounian A, Arsic A. Composition and potential health benefits of pomegranate: a review. Curr Pharm Des 2019; 25: 1817–1827

[7] Howell AB, D'Souza DH. The pomegranate: Effects on bacteria and viruses that influence human health. Evid Based Complement Alternat Med 2013; 2013: 606212

[8] Arunkumar J, Rajarajan S. Study on antiviral activities, drug-likeness and molecular docking of bioactive compounds of *Punica granatum* L. to herpes simplex virus-2 (HSV-2). Microb Pathog 2018; 118: 301–309

[9] Haidari M, Ali M, Ward Casscells S, Madjid M. Pomegranate (*Punica granatum*) purified polyphenol extract inhibits influenza virus and has a synergistic effect with oseltamivir. Phytomedicine 2009; 16: 1127–1136

[10] Neurath AR, Strick N, Li YY, Debnath AK. *Punica granatum* (Pomegranate) juice provides an HIV-1 entry inhibitor and candidate topical microbicide. BMC Infect Dis 2004; 4: 41

[11] Bekir J, Mars M, Souchard JP, Bouajila J. Assessment of antioxidant, anti-inflammatory, anti-cholinesterase and cytotoxic activities of pomegranate (*Punica granatum*) leaves. Food Chem Toxicol 2013; 55: 470–475

[12] Boggula N, Peddapalli H. Phytochemical analysis and evaluation of *in vitro* antioxidant activity of punica granatum leaves. Int J Pharmacogn Phytochem Res 2017; 9: 1110–1118

[13] Abdulla R, Mansur S, Lai H, Ubul A, Sun G, Huang G, Aisa HA. Qualitative analysis of polyphenols in macroporous resin pretreated pomegranate husk extract by HPLC-QTOF-MS. Phytochem Anal 2017; 28: 465–473

[14] Wu S, Tian L. Diverse phytochemicals and bioactivities in the ancient fruit and modern functional food pomegranate (*Punica granatum*). Molecules 2017; 22: 1606

[15] Sumner LW, Amberg A, Barrett D, Beale MH, Beger R, Daykin CA, Fan TWM, Fiehn O, Goodacre R, Griffin JL, Hankemeier T, Hardy N, Harnly J, Higashi R, Kopka J, Lane AN, Lindon JC, Marriott P, Nicholls AW, Reily MD, Thaden JJ, Viant MR. Proposed minimum reporting standards for chemical analysis Chemical Analysis Working Group (CAWG) Metabolomics Standards Initiative (MSI). Metabolomics 2007; 3: 211–221

[16] Marengo A, Maxia A, Sanna C, Mandrone M, Bertea CM, Bicchi C, Sgorbini B, Cagliero C, Rubiolo P. Intra-specific variation in the little-known Mediterranean plant *Ptilostemon casabonae* (L.) Greuter analysed

through phytochemical and biomolecular markers. Phytochemistry 2019; 161: 21–27

[17] Roy A, Lim L, Srivastava S, Lu Y, Song J. Solution conformations of Zika NS2B-NS3pro and its inhibition by natural products from edible plants. PLoS One 2017; 12: e0180632

[18] Yadav R, Selvaraj C, Aarthy M, Kumar P, Kumar A, Singh SK, Giri R. Investigating into the molecular interactions of flavonoids targeting NS2B-NS3 protease from ZIKA virus through in-silico approaches. J Biomol Struct Dyn 2020. doi:10.1080/07391102.2019.1709546

[19] Wong G, He S, Siragam V, Bi Y, Mbikay M, Chretien M, Qiu X. Antiviral activity of quercetin-3-beta-O-D-glucoside against Zika virus infection. Virol Sin 2017; 32: 545–547

[20] Cui Q, Du R, Anantpadma M, Schafer A, Hou L, Tian J, Davey RA, Cheng H, Rong L. Identification of ellagic acid from plant rhodiola rosea L. as an anti-Ebola virus entry inhibitor. Viruses 2018; 10: 152

[21] Promsong A, Chuenchitra T, Saipin K, Tewtrakul S, Panichayupakaranant P, Satthakarn S, Nittayananta W. Ellagic acid inhibits HIV-1 infection in vitro: Potential role as a novel microbicide. Oral Dis 2018; 24: 249–252

[22] Reddy BU, Mullick R, Kumar A, Sudha G, Srinivasan N, Das S. Small molecule inhibitors of HCV replication from pomegranate. Sci Rep 2014; 4: 5411

[23] Tran TT, Kim M, Jang Y, Lee HW, Nguyen HT, Nguyen TN, Park HW, Le Dang Q, Kim JC. Characterization and mechanisms of anti-influenza virus metabolites isolated from the Vietnamese medicinal plant Polygonum chinense. BMC Complement Altern Med 2017; 17: 162

[24] Shin MS, Kang EH, Lee YI. A flavonoid from medicinal plants blocks hepatitis B virus-e antigen secretion in HBV-infected hepatocytes. Antiviral Res 2005; 67: 163–168

[25] Lee JL, Loe MWC, Lee RCH, Chu JJH. Antiviral activity of pinocembrin against Zika virus replication. Antiviral Res 2019; 167: 13–24

[26] Francese R, Civra A, Ritta M, Donalisio M, Argenziano M, Cavalli R, Mougharbel AS, Kortz U, Lembo D. Anti-Zika virus activity of poly-oxometalates. Antiviral Res 2019; 163: 29–33

[27] Ajaegbu EE, Danga SP, Chijoke IU, Okoye FB. Mosquito adulticidal activity of the leaf extracts of *Spondias mombin* L. against *Aedes aegypti* L. and isolation of active principles. J Vector Borne Dis 2016; 53: 17–22

[28] Morosetti G, Criscuolo AA, Santi F, Perno CF, Piccione E, Ciotti M. Ellagic acid and *Annona muricata* in the chemoprevention of HPV-related pre-neoplastic lesions of the cervix. Oncol Lett 2017; 13: 1880–1884

[29] Garcia-Nino WR, Zazueta C. Ellagic acid: pharmacological activities and molecular mechanisms involved in liver protection. Pharmacol Res 2015; 97: 84–103

[30] Pavlova EL, Simeonova LS, Gegova GA. Combined efficacy of oseltamivir, isoprinosine and ellagic acid in influenza A(H3N2)-infected mice. Biomed Pharmacother 2018; 98: 29–35

[31] Marengo A, Maxia A, Sanna C, Bertea CM, Bicchi C, Ballero M, Cagliero C, Rubiolo P. Characterization of four wild edible *Carduus* species from the Mediterranean region via phytochemical and biomolecular analyses. Food Res Int 2017; 100: 822–883

[32] Rubiolo P, Casetta C, Cagliero C, Brevard H, Sgorbini B, Bicchi C. *Populus nigra* L. bud absolute: a case study for a strategy of analysis of natural complex substances. Anal Bioanal Chem 2013; 405: 1223–1235

[33] Ghosh M, Civra A, Ritta M, Cagno V, Mavuduru SG, Awasthi P, Lembo D, Donalisio M. *Ficus religiosa* L. bark extracts inhibit infection by herpes simplex virus type 2 in vitro. Arch Virol 2016; 161: 3509–3514

[34] Donalisio M, Quaranta P, Chiuppesi F, Pistello M, Cagno V, Cavalli R, Volante M, Bugatti A, Rusnati M, Ranucci E, Ferruti P, Lembo D. The AGMA1 poly(amidoamine) inhibits the infectivity of herpes simplex virus in cell lines, in human cervicovaginal histocultures, and in vaginally infected mice. Biomaterials 2016; 85: 40–53

3. STUDY OF NEW ANTIVIRAL MOLECULES AGAINST THE HUMAN ROTAVIRUS

3.1 Overview on the human rotavirus

HRoV is a double-stranded RNA virus belonging to the *Reoviridae* family. It is transmitted by the fecal-oral route, directly from person to person, or indirectly via contaminated fomites.

HRoV genome consists of 11 segments of double-stranded RNA encoding six structural proteins (VP1–VP4, VP6, and VP7) and six non-structural proteins (NSP1–NSP6). The mature virion is a triple-layered particle (TLP) about 100 nm in diameter and consists of an inner layer (the core) composed of the viral proteins VP1 and VP2, an intermediate layer (the inner capsid made of VP6), and an outer layer (the outer capsid consisting of VP7 and projections of VP4), with VP4 being the major determinant of tropism and receptor binding. The proteolytic cleavage of VP4 by trypsin is essential for optimum rotavirus infectivity and produces two subunits, VP5* and VP8*, which remain associated with the virion (47).
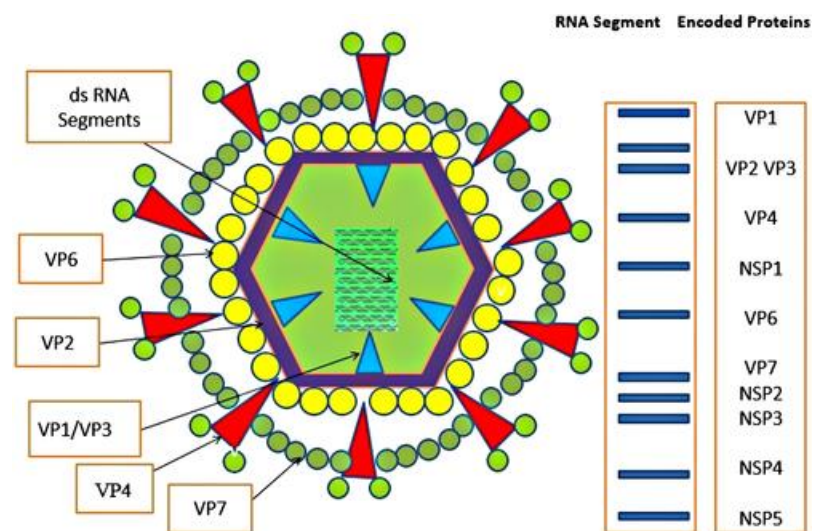
Figure 6: Rotavirus particle structure (47)

HRoV entry into the host cell is a multistep process that implicates the sequential interaction of the VP4-derived peptides (VP5* and VP8*) and VP7 with different cell surface molecules. VP8* has been implicated in the initial attachment to the host cell through the interaction with glycans, whereas VP5* and VP7 have been associated in post-attachment interactions. Proposed non-glycan HRoV co-receptors include integrins $\alpha v\beta 3$ and $\alpha x\beta 2$ for VP7 and $\alpha 2\beta 1$ for VP5*. Additionally, heat shock cognate protein 70 (Hsc70) has been implicated as a putative co-receptor recognized by VP5* (48).

Subsequently, HRoV exploits the endocytic route to enter cells. Various human strains, such as HRoV Wa, WI61, and DS-1, travel along this intracellular path to reach the late endosomes (LEs). Once inside the LEs, a sequence of molecular transformations in the outer-layer proteins VP7 and VP4 strips the proteins from the virion and delivers into the cytosol an inner capsid particle, known as the double-layered particle or DLP. These initial entry steps are the target of the anti-HRoV molecules, 25HC and 27HC, tested in our article *Civra et al.* The later steps of the HRoV replicative cycle are schematically described in Figure 7.
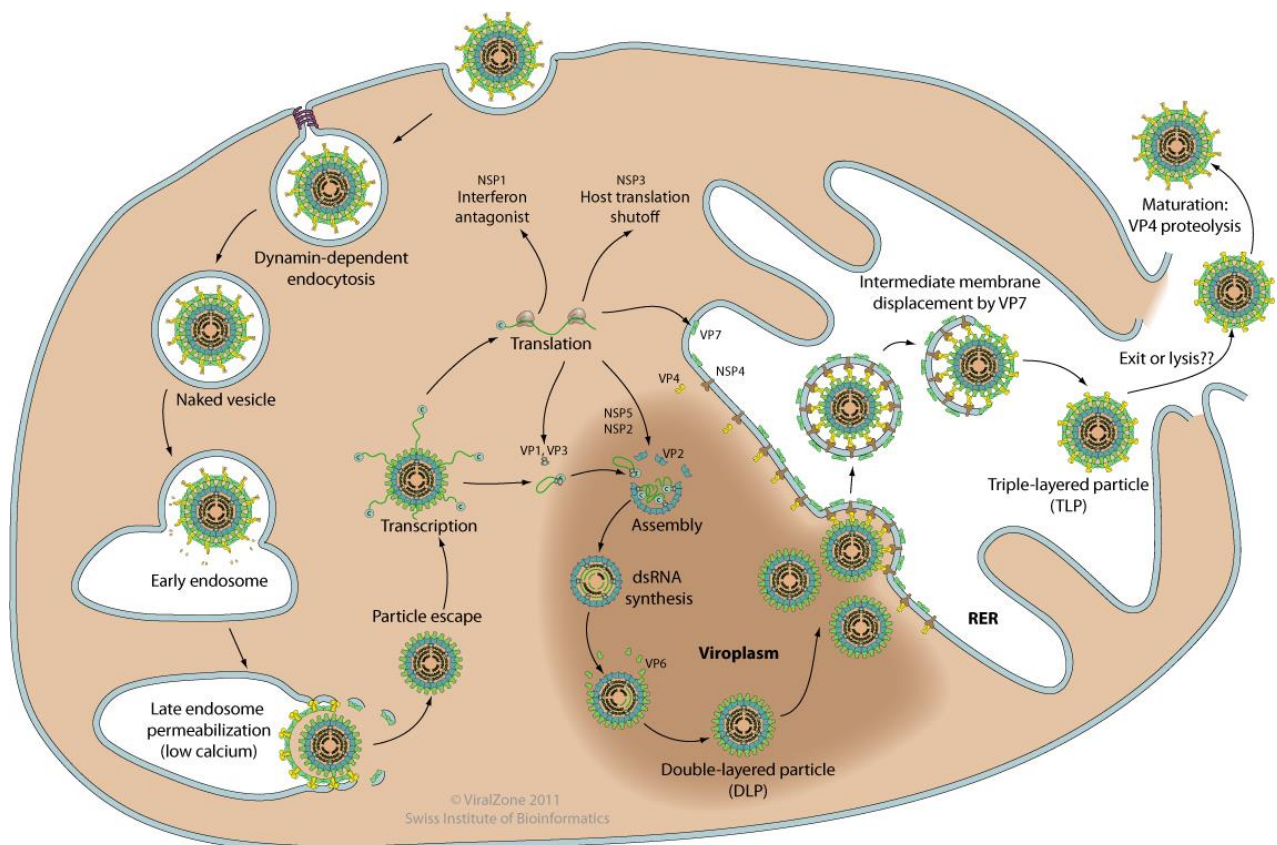
Figure 7: Schematic representation of rotavirus replicative cycle. 1) Attachment of the viral VP4 protein to host receptors mediates clathrin-dependent endocytosis of the virus into the host cell. 2) Particles are partially uncoated in endolysosomes (loss of the VP4-VP7 outermost layer), and penetrate into the cytoplasm via permeabilization of host endosomal membrane. 3) Early transcription of the dsRNA genome by viral polymerase occurs inside these DLPs 4) The nascent (+)RNAs are extruded into the cytoplasm and serve as template for viral proteins synthesis. 5) Progeny cores with replicase activity are produced in cytoplasmic virus factories (viroplasms). This implies synthesis of complementary (-)RNA and initial steps of viral morphogenesis. 5) Late transcription occurs in these progeny cores. 6) At the periphery of virus factories, these core are coated with VP6, forming immature DLPs that bud across the membrane of the endoplasmic reticulum, acquiring a transient lipid membrane which is modified with the ER resident viral glycoproteins NSP4 and VP7; these enveloped particles also contain VP4. As the particles move towards the interior of the ER cisternae, the transient lipid membrane and the nonstructural protein NSP4 are lost, while the virus surface proteins VP4 and VP7 rearrange to form the outermost virus protein layer. 7) Mature virions are released presumably following cell death(49).

21

Rotavirus causes an acute gastroenteritis in infants and young children and is associated with profuse watery diarrhea, projectile vomiting and fever. The virus replicates in the enterocytes of the small intestine, causing extensive damage to the microvilli and resulting in malabsorption and loss of fluids and electrolyte.

Nearly every child in the world under 5 years of age is at the risk of rotavirus infection. HRoV causes approximately 2 million hospitalizations and 25 million outpatient cases annually, with more than 90% deaths occurring in developing countries of Asia and Africa (47). According to a recent study conducted by Tate and colleagues (50), the number of rotavirus deaths in children <5 years of age declined from 528 000 in 2000 to 215 000 in 2013. This was possible because of the concurrent efforts of the two globally licensed live-attenuated oral vaccines. The same authors also estimated that 22% of all rotavirus deaths under five years of age occurred in India in 2013 and four countries (India, Nigeria, Pakistan and the Democratic Republic of the Congo) accounted approximately half (49%) of all rota-deaths under age five. Groups at increased risk for rotavirus infection include children who are hospitalized or in community care centers and undernourished and/or immunodeficient children (51). Moreover, since exclusive breast-feeding was found to be associated with a lower incidence of rotavirus gastroenteritis (52,53), non-exclusively breastfed children are considered an additional group more vulnerable to rotavirus infections.

To date no specific antiviral drug against rotavirus infection is available. Clinical management is directed towards early replacement of fluid losses using oral rehydration at home. However, with more extensive fluid losses there may be a need for intravenous rehydration provided in hospital settings. No other therapy is required in previously healthy individuals and the condition is self-limiting (54).

There are two globally licensed live-attenuated oral vaccines, Rotarix (GSK, Belgium) and RotaTeq (Merck & Co. Inc., USA), first introduced in the USA in 2006. Recently, two Indian-produced live-attenuated oral vaccines named Rotavac (Bharat Biotech, India) and RotaSIIL (Serum Institute of India Pvt., India) have been pre-licensed in 2018, to be used globally against HRoV infections, but their use is still largely restricted to India and partly Africa. Apart from these, there are other regionally licensed live-attenuated oral vaccines such as LLR-37 from Lanzhou Biologicals (Chengguan District, China) and Rotavin-M from Polyvac (Center for Research and Production of Vaccines and Biologicals, Vietnam) (55). Recently, Burnett et al. reported that Rotarix and RotaTeq are effective in preventing hospitalizations due to rotavirus diarrhea, with higher efficacy in high- and middle-income countries than in low- income countries. (56). In particular, Rotarix effectiveness against laboratory-confirmed rotavirus among children younger than 12 months old was 86% in low-mortality countries and 63% in high-mortality countries and RotaTeq effectiveness was 86% and 66%

respectively. This lower efficacy in low-income countries could be attributed to several factors, including the nature of the circulating rotavirus strains, trans-placentally acquired maternal rotavirus-specific antibodies in infant, co-infections (such as norovirus and enteric bacterial infections), microbiota, body immune-status, and general nutritional status (55).

The current problems related to the low efficacy of rotavirus vaccines in some Regions and the relative high mortality rate indicate that a specific anti-HRoV drug is still a necessity. In this context, part of my PhD research was addressed to fulfill this unmet medical need. Similar to the anti-ZIKV projects previously described, two different approaches have been investigated *in vitro,* the first analyzing cholesterols oxidation products as anti-HRoV agents (3.2 section) and the second exploring the antiviral properties of plants commonly used in Turkish folk medicine (3.3 section).

3.2 The oxysterols

Oxysterols are a family of cholesterol oxidation derivatives that contain an additional hydroxyl, epoxide or ketone group in the sterol nucleus and/or a hydroxyl group in the side chain of the cholesterol molecule. Normocholesterolemic healthy individuals contain a mixture of these compounds in their peripheral blood, accounting for 1–5% of total cholesterol. A small part of this oxysterol haematic pool is derived from exogenous origins, i.e. oxysterols originating from cholesterol-rich food that have undergone non-enzymatic oxidation. The rest are of endogenous origin. Some endogenous oxysterols are the result of enzymatic hydroxylation of cholesterol at specific sites of the molecule and are almost ubiquitous in the human body, while other endogenous oxysterols result from the non-enzymatic attack of a variety of oxidant species. This latter pathway is greatly enhanced in sites of inflammation compared to non-inflamed areas of the body (Figure 8) (57). Several among the various cholesterol oxidation products of enzymatic origin contribute to physiological functions: they are intermediates of pregnenolone and steroid hormone synthesis (58) and target nuclear receptors (e.g., the liver X receptor [LXR] and the estrogen receptor α [ER α]), cellular membrane receptors (e.g., C-X-C motif chemokine receptor 2 [CXCR2]) and transport proteins (e.g., insulin induced gene protein [INSIG], Niemann-Pick protein 1 [NPC1], oxysterol binding protein [OSBP] and its related proteins [ORPs])(59–63). In contrast, the oxysterols derived from cholesterol autoxidation, a not-regulated and therefore potentially harmful biochemical reaction, appear to be more likely involved in pathophysiological processes associated with inflammation and oxidative stress (64–66).
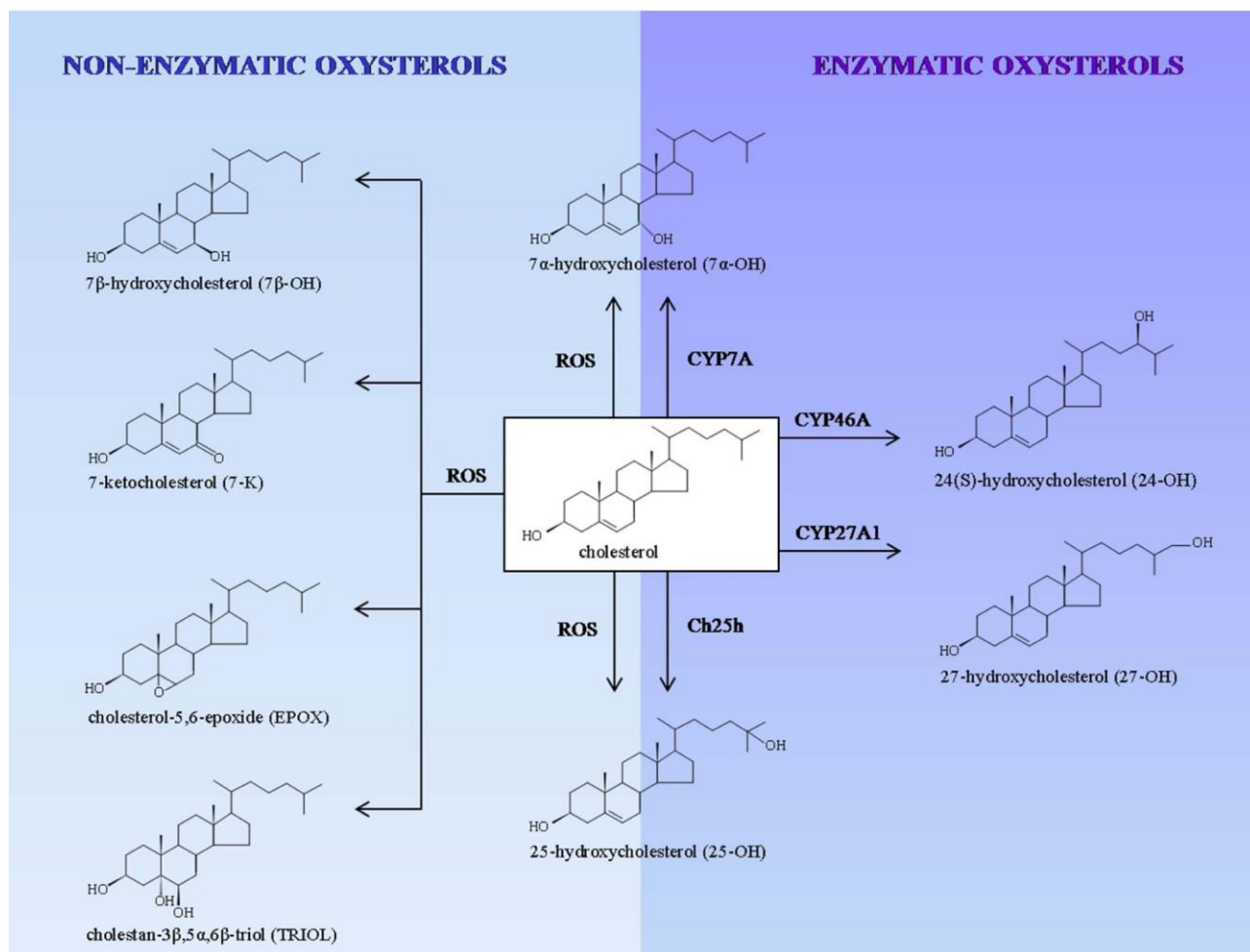
Figure 8: Representation of the main oxysterols recognised to date for their potential involvement in human pathophysiology. They are subdivided into the following three groups: oxysterols of enzymatic origin; oxysterols of non-enzymatic origin; and oxysterols produced via both enzymatic and non-enzymatic pathways (57). Notably, we studied 25-OH and 27-OH as antiviral molecules against HRoV.

In recent years, a growing body of evidence points to a significant role of some oxysterols in host nonspecific antiviral defences.

The bulk of the studies has focused on 25-hydroxycholesterol (25HC) that was shown to act as a physiological interferon (IFN)-induced effector of innate immunity against viral infections (67) and to inhibit the replication of a wide spectrum pathogenic viruses (57,68). Indeed, it was demonstrated that 25HC inhibits both enveloped viruses, i.e., those with a phospholipidic bilayer outside the proteic capsid such as human immunodeficiency virus (HIV), herpes simplex virus type 1 (HSV-1), varicella zoster virus (VZV), Nipah virus (NiV), Ebola virus (EBOV), ZIKV, hepatitis C virus (HCV), orthomixovirus, and non-enveloped viruses such as human rhinovirus (HRhV), human papillomavirus (HPV), and HRoV (57,69–71). The mechanisms underlying this broad antiviral action are still under investigation and the available studies are mostly focused on enveloped viruses. The

reported antiviral mechanisms of action are multiple and include the inhibition of virus adsorption, entry, and release by manipulating cholesterol metabolism; inhibition of virus replication through direct interactions with viral components; inhibition of virus infection by modulating innate immunity and virus-specific adaptive immunity; and the activation of the integrated stress response (ISR), changing the endocytic transport patterns and other mechanisms (72). Of note, other side chain oxysterols have been found to exert potent antiviral action *in vitro*. The enzymatically-produced oxysterol 27- hydroxycholesterol (27HC), the most common oxysterols in the peripheral blood of healthy individuals, was shown to block the infection of murine cytomegalovirus, HRhV, HRoV, HPV and HSV-1/HSV-2. Interestingly, 27HC is not induced by IFN, thus indicating that the innate-immune response to virus infections involving lipid sterol effectors is only partially dependent on IFN stimulation and might even occur in its absence through 27HC. A third oxysterol containing a hydroxyl group in its side chain, namely 24-hydroxycholesterol (24HC), has been reported to inhibit the murine cytomegalovirus and the 22(S)-hydroxycholesterol was shown to be active against HBV (57).

During the first part of my PhD course, I focused my attention on 25HC and 27HC with the aim to clarify the mechanisms underlying their protective effects against non-enveloped viruses and to discover novel antiviral mechanisms and targets potentially exploitable for a new generation of antiviral molecules.

The following publications were performed in close collaboration with the Pathology group of Prof. Giuseppe Poli (University of Turin).

3.2.1 Publications

Civra A, Francese R, Gamba P, Testa G, Cagno V, Poli G, Lembo D. 25-Hydroxycholesterol and 27-hydroxycholesterol inhibit human rotavirus infection by sequestering viral particles into late endosomes. Redox Biol. 2018 Oct;19:318-330. doi: 10.1016/j.redox.2018.09.003. Epub 2018 Sep 5. PMID: 30212801; PMCID: PMC6138790.

The group of Prof. Lembo has been investigating the antiviral potential of oxysterols since 2014. The present study is the natural continuation of the study by Civra et al. (73), in which they showed that 25HC and 27HC are endowed with marked antiviral activity against three pathogenic non-enveloped viruses, i.e. HPV-16, HRoV and HRhV. That study allowed to expand the broad

antiviral spectrum of 25HC, that were thought to be to be limited to viruses with envelope until that moment. Therefore, the mechanisms underlying the protective effect of cholesterol oxidation products against non-enveloped viruses are still largely unexplored. The few available studies showed that 25HC markedly reduce the accumulation of phosphatidylinositol 4-phosphate (PI4P) in the Golgi apparatus, a crucial event for the assembly of HRhV replicative machinery, by targeting members of the OSBP family I (74,75). To get insight into this field, we investigated the antiviral activity of 25HC and 27HC against the non-eveloped HRoV. We demonstrated that both oxysterols affect the final step of viral entry into the host cells by inducing an accumulation of cholesterol in the late endosomes (LEs), thereby sequestering viral particles inside these vesicles. This study discloses a totally novel mechanism of two oxysterols of enzymatic origin and demonstrates that lipid involvement as host restriction strategy is an area of focus which holds great promise to discover novel mechanisms and redox active lipid factors to develop innovative approaches for antiviral therapy.

Civra A, Colzani M, Cagno V, Francese R, Leoni V, Aldini G, Lembo D, Poli G. <u>*Modulation of cell proteome by 25-hydroxycholesterol and 27-hydroxycholesterol: A link between cholesterol metabolism and antiviral defense.*</u> *Free Radic Biol Med. 2020 Mar;149:30-36. doi: 10.1016/j.freeradbiomed.2019.08.031. Epub 2019 Sep 13. PMID: 31525455; PMCID: PMC7126780.*

In this second study, we deeply explored the broad-spectrum antiviral potential of 25HC and 27HC by analysing their possible modulation of cell proteome. We carried out a technically advanced proteomic screening in a cell model system (Hela cells) commonly employed to *in vitro* test the antiviral efficacy of a wide variety of compounds. We demonstrated that both 25HC and 27HC can down-regulate the junction adhesion molecule-A (JAM-A) and the cation independent isoform of mannose-6-phosphate receptor (MPRci), two crucial molecules for the replication of all those viruses that exploit adhesion molecules and the endosomal pathway to enter and diffuse within target cells. These results contributed to clarifying the complex and multiple mechanisms of action of oxysterols that partially mediate the host innate antiviral defense.

Research paper

25-Hydroxycholesterol and 27-hydroxycholesterol inhibit human rotavirus infection by sequestering viral particles into late endosomes

Andrea Civra, Rachele Francese, Paola Gamba, Gabriella Testa, Valeria Cagno[1], Giuseppe Poli*, David Lembo*

Department of Clinical and Biological Sciences, University of Turin, Regione Gonzole 10, 10043 Orbassano, TO, Italy

ABSTRACT

A novel innate immune strategy, involving specific cholesterol oxidation products as effectors, has begun to reveal connections between cholesterol metabolism and immune response against viral infections. Indeed, 25-hydroxycholesterol (25HC) and 27-hydroxycholesterol (27HC), physiologically produced by enzymatic oxidation of cholesterol, act as inhibitors of a wide spectrum of enveloped and non-enveloped human viruses. However, the mechanisms underlying their protective effects against non-enveloped viruses are almost completely unexplored. To get insight into this field, we investigated the antiviral activity of 25HC and 27HC against a non-enveloped virus causing acute gastroenteritis in children, the human rotavirus (HRV). We found that 25HC and 27HC block the infectivity of several HRV strains at 50% inhibitory concentrations in the low micromolar range in the absence of cell toxicity. Both molecules affect the final step of virus penetration into cells by preventing the association of two cellular proteins: the oxysterol binding protein (OSBP) and the vesicle-associated membrane protein-associated protein-A (VAP-A). By altering the activity of these cellular mediators, 25HC and 27HC disturb the recycling of cholesterol between the endoplasmic reticulum and the late endosomes which are exploited by HRV to penetrate into the cell. The substantial accumulation of cholesterol in the late endosomal compartment results in sequestering viral particles inside these vesicles thereby preventing cytoplasmic virus replication. These findings suggest that cholesterol oxidation products of enzymatic origin might be primary effectors of host restriction strategies to counteract HRV infection and point to redox active lipids involvement in viral infections as a research area of focus to better focus in order to identify novel antiviral agents targets.

Introduction

Innate immune response is the first line of defense during the earliest hours of exposure to a novel pathogen. Its mechanisms are non-specific and rely on a group of proteins and phagocytic cells that quickly activate to help destroy invaders. Alongside these pathways, a novel innate immune strategy has begun to reveal connections between cholesterol metabolism and immune response against viral infections. [1–3].

The most widely studied effector of this branch of innate immunity is an oxysterol, 25-hydroxycholesterol (25HC) [1,2]. Oxysterols contain 27 carbon atoms per molecule and are derived from cholesterol by both enzymatic and nonenzymatic oxidation [4–6]. Several among the various cholesterol oxidation products of enzymatic origin contribute to physiological functions: they are intermediates of pregnenolone and steroid hormone synthesis [7] and target nuclear receptors (e.g., the liver X receptor [LXR] and the estrogen receptor α [ER α]), cellular membrane receptors (e.g., C-X-C motif chemokine receptor 2 [CXCR2]) and transport proteins (e.g., insulin induced gene protein [INSIG], Niemann-Pick protein 1 [NPC1], oxysterol binding protein [OSBP] and

its related proteins [ORPs]) [8–13]. In contrast, the oxysterols derived from cholesterol autoxidation, a not-regulated and therefore potentially harmful biochemical reaction, appear to be more likely involved in pathophysiological processes associated with inflammation and oxidative stress [4,5,14].

In 2013 Blanc and colleagues provided in vitro findings indicating that 25HC acts as a physiological interferon (IFN)-induced effector of innate immunity against viral infections [1]. They reported that 25HC was the only oxysterol synthesized and secreted by macrophages upon IFN treatment or virus infection and that transcription factor Stat1 directly couples IFN-stimulated signaling to regulation of the cholesterol hydroxylase gene (Ch25h) encoding the 25HC-synthesizing enzyme.

Unlike known antiviral small molecules that target highly specific viral determinants, thus showing a restricted spectrum of activity, 25HC inhibits the replication of a wide spectrum of pathogenic viruses. This includes both enveloped viruses, i.e., those with a phospholipidic bilayer outside the proteic capsid such as human immunodeficiency virus (HIV), herpes simplex virus type 1 (HSV-1), varicella zoster virus (VZV) murine cytomegalovirus (MCMV), vesicular stomatitis virus (VSV), Ebola virus (EBOV), Zika virus, hepatitis C virus, and

---

Table 1
Antirotavirus activity of oxysterols (MA104 cells).

Oxysterols	HRV strain	EC$_{50}$[a] (µM) – 95% CI[b]	EC$_{90}$[c] (µM) – 95% CI	CC$_{50}$[d] (µM) –95% CI	SI[e]
25HC	Wa	0.16 (0.12–0.20)	1.37 (0.75–2.40)	> 150	> 938
	WI61	0.09 (0.08–0.12)	0.28 (0.16–0.46)	> 150	> 1667
	HRV408	0.12 (0.09–0.16)	0.42 (0.23–0.74)	> 150	> 1250
	HRV248	0.11 (0.07–0.18)	1.26 (0.47–3.38)	> 150	> 1364
	DS-1	0.27 (0.14–0.53)	5.77 (1.15–28.89)	> 150	> 556
27HC	Wa	0.26 (0.22–0.31)	1.73 (1.21–2.47)	> 150	> 577
	WI61	0.19 (0.14–0.27)	0.74 (0.35–1.55)	> 150	> 790
	HRV408	0.40 (0.26–0.62)	4.56(1.62–12.82)	> 150	> 375
	HRV248	0.23 (0.12–0.46)	3.84 (0.80–18.39)	> 150	> 652
	DS-1	0.72 (0.49–1.06)	5.85 (2.43–14.06)	> 150	> 208

n.a. not assessable.
[a] EC$_{50}$ half-maximal effective concentration.
[b] CI confidence interval.
[c] EC$_{90}$ 90% effective concentration.
[d] CC$_{50}$ half maximal cytotoxic concentration
[e] SI selectivity index.

orthomixovirus [1,2,15–19], and non-enveloped viruses such as human rhinovirus (HRhV) [20–22], human papillomavirus (HPV), and human rotavirus (HRV) [21].

This unprecedented range of antiviral properties is ascribable to the ability of 25HC to modulate cellular lipid metabolism and transport, thereby modifying the composition and structure of cellular and subcellular membranes [23,24]. Since viral pathogens have to pass through cellular lipid membranes or hijack them to assemble their replicative machinery, regulation of the lipid composition of cellular and subcellular membranes looks like a particularly smart and effective strategy to counteract viral invasion from a strictly evolutionary point of view.

The mechanisms underlying the antiviral activity of 25HC have been extensively investigated for a number of enveloped viruses: 25HC might alter the lipid composition of cellular membranes, thus hampering the fusion between the viral envelope and the cytoplasmic lipid bilayer that allows some enveloped viruses to penetrate into the host cell [1]. This oxysterol directly changes cell membrane properties by inserting itself into the lipid bilayer [2]. Moreover, various studies on 25HC-induced host response to HCV infection clearly correlated this protective action with an imbalance in the mevalonate pathway by the oxysterol [17,25–27], implying the inhibition of cholesterol synthesis and depletion of non-sterol isoprenoid products, in this way impairing cholesterol membrane content and protein prenylation [17,25–28]. Of note, our group showed that 25HC but also a second enzymatically synthesized oxysterol, 27-hydroxycholesterol (27HC) can stimulate the release of interleukin 6 (IL6) and are endowed with an anti-HSV-1 activity which is apparently non-unrelated to the viral entry inhibition [19].

By contrast, the mechanisms underlying the protective effects of cholesterol oxidation products against non-enveloped viruses are largely unexplored, with the unique exception of HRhV [22] and 25HC as the only oxysterol examined so far [22]. In fact, this oxysterol has been shown to markedly reduce the accumulation of phosphatidylinositol 4-phosphate (PI4P) in the Golgi apparatus, a crucial event for the assembly of HRhV replicative machinery, by targeting members of the OSBP family I [20,22].

With regard to non-enveloped viruses, we previously described the antiviral activity exerted by 25HC and 27HC, particularly against HRV [21]. We investigated the mechanism of action of 25HC and 27HC against HRV to shed a light on an almost totally unexplored scenario, which may hold promise to reveal novel antiviral mechanisms and targets, likely exploitable for a new generation of antiviral molecules.

HRV belongs to the reoviridae family and represents one of the leading causes of infective gastroenteritis in children [29]. Its genome consists of 11 segments of double-stranded RNA encoding six structural proteins (VP1–VP4,VP6, and VP7) and six non-structural proteins (NSP1–NSP6). The mature virion is a triple-layered particle (TLP) about 100 nm in diameter and consists of an inner layer (the core) composed of the viral proteins VP1 and VP2, an intermediate layer (the inner capsid made of VP6), and an outer layer (the outer capsid consisting of VP7 and projections of VP4) [30,31], with VP4 being the major determinant of tropism and receptor binding [32–35].

HRVs exploit the endocytic route to enter cells. Various human strains, such as HRV Wa, WI61, and DS-1, travel along this intracellular path to reach the late endosomes (LEs) [36]. Once inside the LEs, a sequence of molecular transformations in the outer-layer proteins VP7 and VP4 strips the proteins from the virion (i.e., the TLP) and delivers into the cytosol an inner capsid particle, known as the double-layered particle or DLP [37].

Here we report on an original mechanism of antiviral action by oxysterols against HRV. We found that both 25HC and 27HC block HRV cell entry and replication by inducing an accumulation of cholesterol in the LEs, thereby sequestering viral particles inside these vesicles. These findings represent a step forward in our understanding the role oxysterols play as effectors of innate immunity against viral infections.

Results

Anti-HRV effect of 25HC and 27HC and their spectrum of activity

In a previous study, we reported on the inhibitory activity of 25HC and 27HC against the Wa strain of HRV [21]. To explore the spectrum of anti-HRV activity, 25HC and 27HC were tested against four additional HRV strains (WI61, HRV 408, HRV 248, DS-1) in MA104 cells. As shown in Table 1, the antiviral activity of both 25HC and 27HC is not strain-restricted, with EC$_{50}$ values falling in the low micromolar range and favorable selectivity index (SI) for all the HRV strains tested. Both oxysterols inhibited HRV infection in a dose-dependent fashion (Fig. 1). The antiviral potency of 25HC was significantly (p$_{Ftest}$ < 0.001) higher than that of 27HC against each strain tested. Since most of the assays of the mechanism of action described below were performed by testing 25HC and 27HC against high viruses/target cell ratios (MOI, multiplicity of action), we verified that both molecules were able to inhibit HRV infectivity also under these conditions. Indeed, they significantly inhibited HRV infectivity to a maximum of 90% even at high MOI (MOI 10) (Fig. 3). Finally, 25HC and 27HC were also tested against HRV infection of human intestinal Caco2 cell line to determine whether their antiviral activity was influenced by the cellular model. The two oxysterols displayed a strong antiviral effect in both MA104 and Caco2 cells, two quite different cellular models (Tables 1 and 2; Figs. 1 and 2), thus indicating that their activity is not cell line dependent.

Fig. 1. Antiviral activity of 25HC and 27HC against HRV strains Wa (A), DS-1 (B), HRV 408 (C), WI61 (D), and HRV 248 (E) on MA104 cells. Cells were treated for 20 h with increasing concentrations of oxysterols and then infected. Viral infections were detected as described in the Material and Methods section. The percentage infection was calculated by comparing treated and untreated wells. The results are means and SEM for triplicates.

Table 2
Antirotavirus activity of oxysterols (Caco2 cells).

Oxysterols	HRV strain	EC$_{50}$[a] (µM) – 95% CI[b]	EC$_{90}$[c] (µM) – 95% CI	CC$_{50}$[d] (µM) –95% CI	SI[e]
25HC	Wa	0.19 (0.14–0.25)	1.26 (0.61–2.60)	> 150	> 789
	WI61	0.25(0.20–0.31)	0.83(0.50–1.38)	> 150	> 600
	HRV408	0.42(0.36–0.48)	2.30(1.66–3.18)	> 150	> 357
	HRV248	0.21(0.16–0.28)	1.04(0.55–1.94)	> 150	> 714
	DS-1	0.43 (0.29–0.63)	2.42 (1.04–5.63)	> 150	> 349
27HC	Wa	0.44 (0.34–0.56)	2.50 (1.45–4.29)	> 150	> 341
	WI61	0.34(0.22–0.53)	2.43(0.90–6.59)	> 150	> 441
	HRV408	0.81(0.60–1.09)	3.78(1.94–7.36)	> 150	> 185
	HRV248	0.41(0.35–0.48)	2.70(1.90–3.83)	> 150	> 366
	DS-1	0.45 (0.34–0.61)	2.62 (1.37–5.03)	> 150	> 333

n.a. not assessable.

[a] EC$_{50}$ half-maximal effective concentration.
[b] CI confidence interval.
[c] EC$_{90}$90% effective concentration.
[d] CC$_{50}$ half maximal cytotoxic concentration.
[e] SI selectivity index.

25HC and 27HC inhibit HRV-cell penetration

Specific assays were performed to identify which step(s) of the HRV replicative cycle was inhibited by the two oxysterols. Time-of-addition assays showed that 25HC and 27HC exerted their highest antiviral efficacy when added to cells 20 h before infection (Fig. 4A-B). By contrast, when the treatment was performed after viral infection, no antiviral effect was observed. These data suggest that both oxysterols modify the cellular milieu so as to render the cells less susceptible to HRV most likely by targeting cellular determinants essential for virus
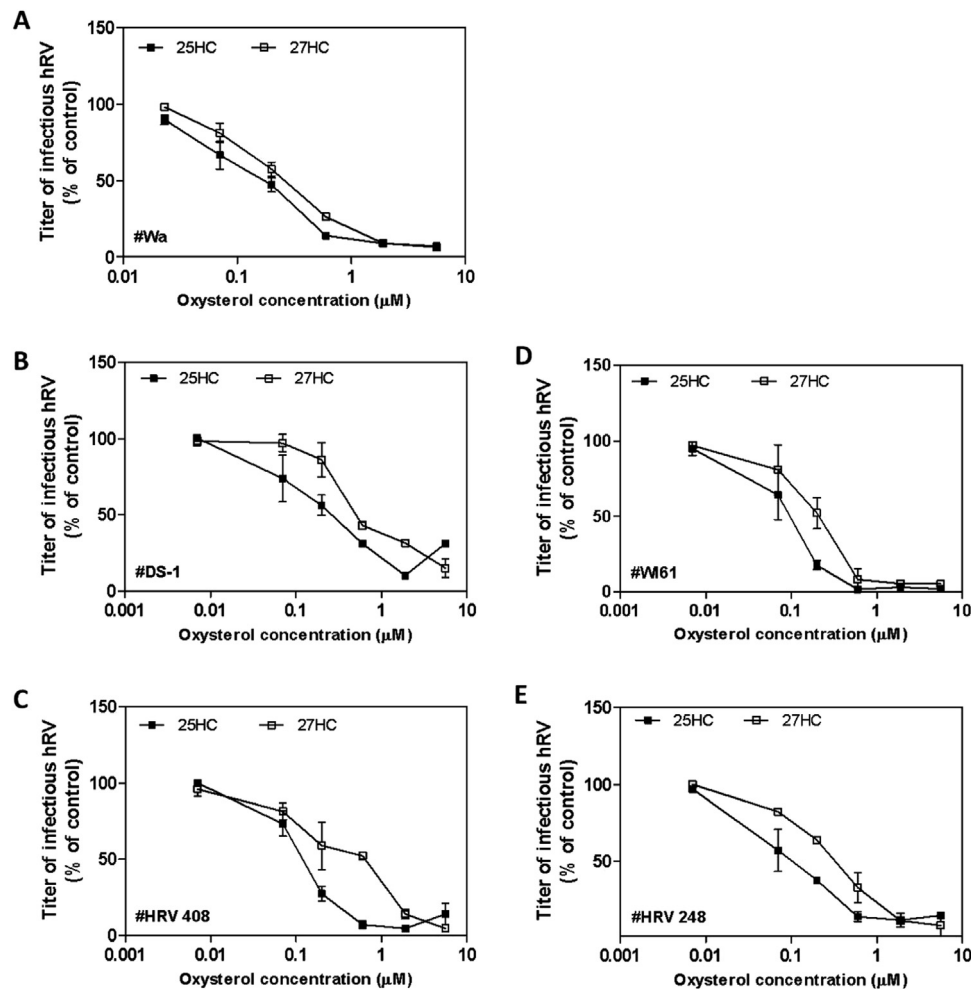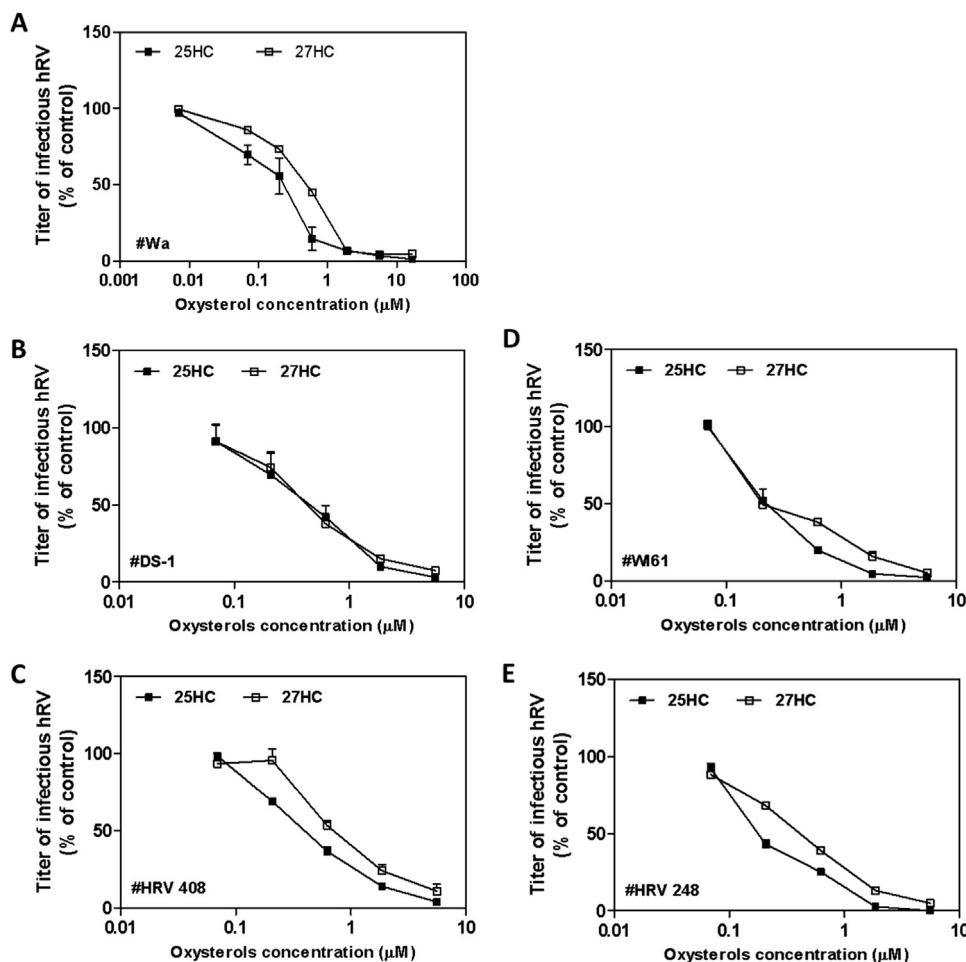
Fig. 2. Antiviral activity of 25HC and 27HC against HRV strains Wa (A), DS-1 (B), HRV 408 (C), WI61 (D), and HRV 248 (E) on Caco2 cells. The results are means and SEM for triplicates.
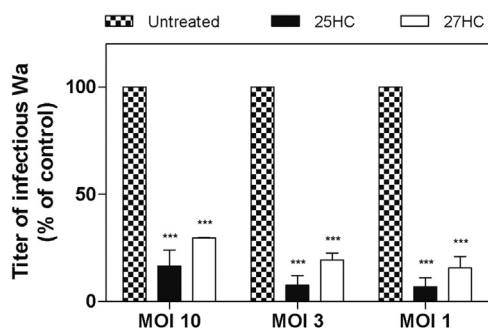

Fig. 3. Antiviral activity of 25HC and 27HC against HRV Wa at multiplicity of infection (MOI) 10, 3, and 1 on MA104 cells. Cells were treated for 20 h with 25HC or 27HC at EC90 concentrations and then infected. Viral infections were detected as described in the Material and Methods section. The percentage infection was calculated by comparing treated and untreated wells. The results are means and SEM for triplicates. ***$p_{ANOVA} < 0.001$.

penetration or replication. Of note, as displayed in Fig. 4C, the indirect immunocytochemistry clearly shows that no deposition of neo-synthetized HRV antigen occurs in both MA104 and Caco2 cells at 20 h post infection, when infection was stopped by fixing cells. Taken together, these results suggested that 25HC and 27HC were able to affect the steps of the HRV replicative cycle occurring before HRV protein synthesis. For this reason, we investigated the effect of oxysterols on the earliest steps of HRV replication, i.e. virus binding and penetration. Binding assay experiments clearly showed that treatment with both

25HC and 27HC had no effect on HRV attachment to the cell surface (Fig. 5 panel A).

In a second set of experiments, we assessed the ability of the oxysterols to alter HRV entry kinetics into the cells. Both 25HC and 27HC significantly ($0.001 < p_{ANOVA} < 0.05$) hampered normal virus-cell penetration, when measured as a function of viral particles that enter cells and carry out a single replication cycle (Fig. 5B). Consistent with previous results (Fig. 1), 25HC affected HRV entry kinetics more potently than 27HC.

HRV penetration into the host cell is a complex event involving receptor-mediated endocytosis, LE membrane permeabilization, and release of the virus particle into the cytoplasm where viral replication occurs. Interestingly, when we forced by means of Lipofectamine the infection of an ethylene glycol tetraacetic acid (EGTA)-inactivated HRV suspension, thereby bypassing viral entry through endocytosis, 25HC and 27HC showed no antiviral activity (Fig. 5C). Consistently with these results, when we added oxysterols on infected cells after NH₄Cl treatment (i.e. after the HRV exit from LEs) no antiviral activity was measurable (Fig. 5D). More importantly, we analyzed the intracellular localization of HRV 8 h post-inoculum, when most of the virus particles have already escaped from the LEs and replicate in the cytoplasm where newly synthesized viral proteins accumulate. As expected, confocal immune microscopy revealed that the viral antigen VP6 was mostly diffused in the cytoplasm of untreated infected cells (Fig. 6). By contrast, in both the 25HC- and the 27HC-treated cells, almost all VP6 co-localized with a marker of LEs (Rab-7). Taken together, these results indicate that 25HC and 27HC affect HRV entry by sequestering the virus particles penetrating the LEs and preventing their replication in the cytoplasm.
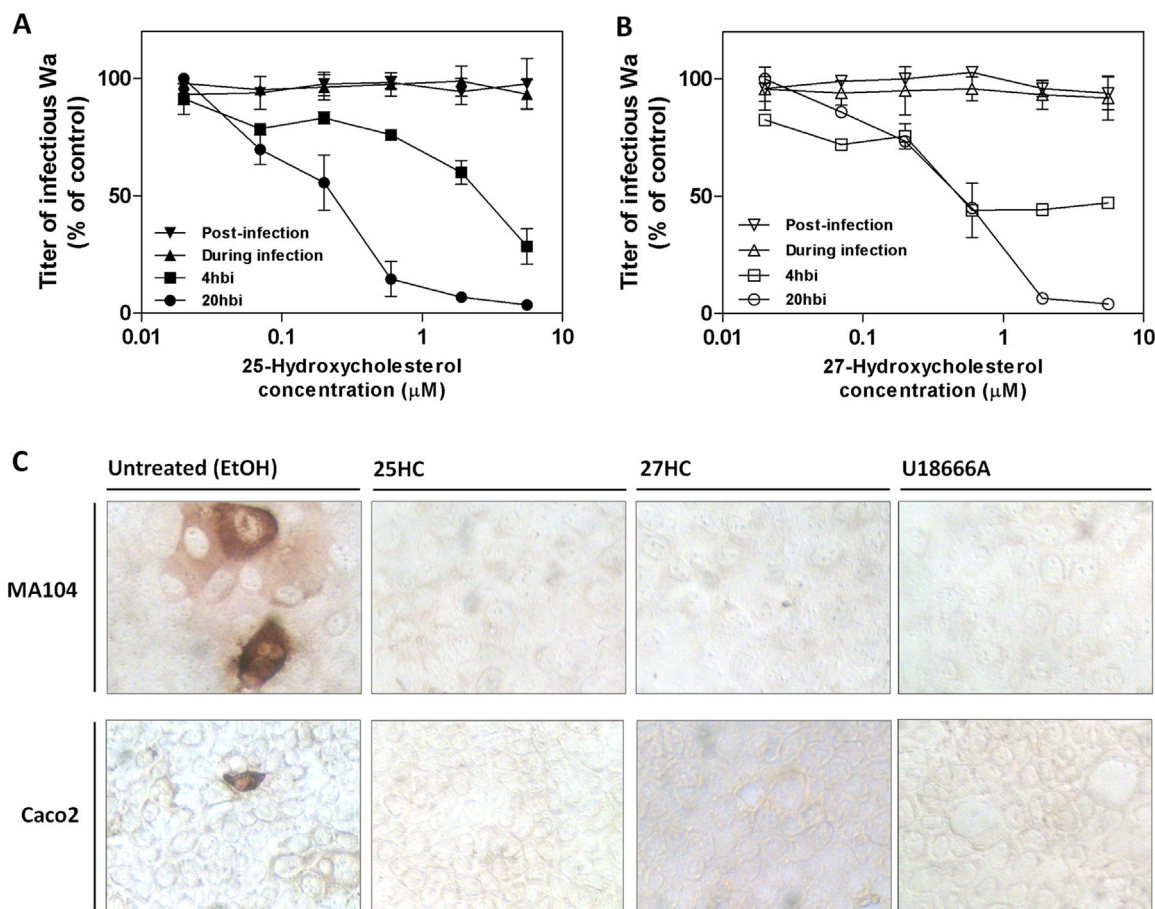
Fig. 4. Time of addition experiments. Panels A and B: time-of-addition experiments were performed by treating cells with 25HC(A) or 27HC(B) for 20 h or 4 h before infection, for 1 h during infection or by adding the oxysterols immediately after infection. The infectivity titers of virus in the treated samples are expressed as a percentage of the titer obtained in the absence of treatment. Error bars represent the standard error of the mean (SEM) of 3 independent experiments. Panel C shows the effect of oxysterols on deposition of neosynthetized VP6 antigen as assessed by immunocytochemistry. Infected MA104 or Caco2 cell lines were fixed at 20 h post-infection and stained with anti-VP6 antibody.

OSBP and VAP-A are cellular determinants of 25HC and 27HC anti-HRV activity

To elucidate the mechanism by which 25HC and 27HC block HRV penetration in the LEs, we focused our attention on the cellular protein OSBP, one of the main intracellular interactors of oxysterols. Proteins that prevent OSBP association with the vesicle-associated membrane protein-associated protein A (VAP-A) are known to disrupt intracellular cholesterol homeostasis, leading to cholesterol accumulation on the LEs membrane. This event has been shown to inhibit the entry of specific enveloped viruses [38,39]. Although this mechanism has been postulated only for enveloped viruses, we hypothesized that the model of a "greasy response" to viral infection - as defined by Tanner and colleagues in 2013 [39] - could fit with our results (Fig. 6). In specific assays to verify whether this mechanism applies to the anti-HRV activity of oxysterols, first we used co-immunoprecipation assays to assess whether physical interaction between OSBP and VAP-A was disrupted in 25HC- or 27HC-treated MA104 cells.

Immunoprecipitation of VAP-A co-immunoprecipitated OSBP in untreated cells and the reverse was demonstrated (Fig. 7A). Co-immuneprecipitation was specific since neither VAP-A nor OSBP was detected in the immunoprecipitates obtained with an unrelevant antibody used as a negative control. This result was consistent with previous studies that showed a physical interaction between OSBP and VAP-A. Interestingly, we found that the association of OSBP to VAP-A was disrupted in the 25HC- or 27HC-treated cells. Control experiments showed that the treatment did not down-regulate OSBP and VAP-A

protein levels (Fig. 7B). To explore whether OSBP and VAP-A play a role in the antiviral activity exerted by 25HC or 27HC, we performed target identification by siRNA sensitization (TISS) assay. This assay allows to evaluate whether knockdown of OSBP or VAP-A results in enhanced sensitivity to suboptimal concentrations of 25HC or 27HC.

Silencing of the expression of both proteins by specific siRNA improved the antiviral efficacy of both 25HC and 27HC (Fig. 8A-B-D-E). By contrast, no effect was observed when the cells were transfected with a non-targeting siRNA. A slight but significant ($p_{ANOVA} < 0.01$) block of HRV infectivity was measurable in the OSBP- and VAP-A-silenced untreated cells (Fig. 8C-F). Taken together, these results prove that OSBP and VAP-A are cellular determinants of the anti-HRV activity elicited by 25HC and 27HC.

25HC and 27HC induce cholesterol accumulation in LEs

We next investigated by confocal immunomicroscopy whether treatment of MA104 cells with 25HC or 27HC induces cholesterol accumulation in LEs. As a positive control, cells were treated with U18666A, an amphipathic steroid 3-β-[2-(diethylamine)ethoxy] androst-5-en-17-one that blocks the exit of free cholesterol from the LE compartment. Cholesterol accumulation was visualized by filipin, a fluorescent polyene antibiotic that binds to cholesterol but not to esterified sterols. As compared to the untreated cells, cholesterol accumulation was observed in the LEs of the cells treated with the oxysterols or U18666A, along with enlargement of the LE compartment (Fig. 9). Like 25HC and 27HC, U18666A was found to be endowed with anti-
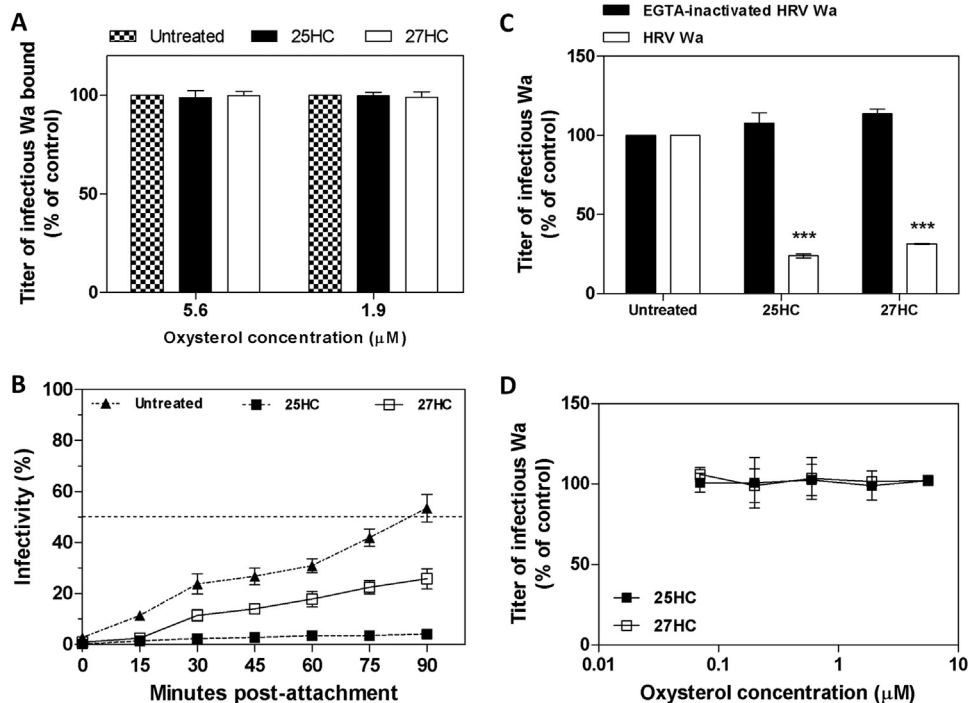
Fig. 5. Evaluation of the step of HRV inhibited by 25HC and 27HC. Panel A shows the effect of oxysterols on binding to the MA104 cell surface. On the *y* axis, the infectious titer of Wa bound to cells is expressed as a % of the titer bound to control untreated MA104 cells. Error bars represent the SEM of 3 independent experiments. Panel B: HRV Wa entry kinetics on treated or untreated MA104 cell monolayers. Virus was inoculated at 4 °C for 1 h, then temperature was shifted to 37 °C. HRV-cell penetration was stopped with EGTA in PBS at fixed time points. On the *y* axis, the number of infected cells in the treated or untreated samples is expressed as a percentage of infected cells when no EGTA wash was performed, which was taken as 100% entry. Each point represents mean and SEM for triplicates. Panel C: Effect of oxysterols on the infectivity of EGTA-inactivated HRV Wa transfected with lipofectamine (black bars) or trypsin-activated HRV Wa (white bars). MA104 cells were treated 20 h before inoculums. Panel D: Effect of oxysterols when added after HRV escape from LEs. Cells were infected for 45 min, treated with 25 mM of NH_4Cl for 15 min, then oxysterols were added. In panels C-D, the percentage infection was calculated by comparing treated and untreated wells. The results are means and SEM for triplicates. ***$p_{ANOVA} < 0.001$.

HRV activity (Table 3; Fig. 10A, B, C, D, E), even when the cells were infected with high MOIs (Fig. 10F), it was not endowed with antiviral activity when added after HRV escape from LEs (Fig. 10G), when cells were infected with an HRV suspension that skipped the endocytosis steps (Fig. 10H), and it blocked the viruses penetrating inside the LEs (Fig. 10I).

Discussion

Here we show that 25HC and 27HC sequester HRV Wa inside LEs and that both are endowed with antiviral activity against the LEs-dependent strains Wa, WI61, and DS-1, as well as against strains HRV248 and HRV408. Physiologic concentrations of 25HC and 27HC range from
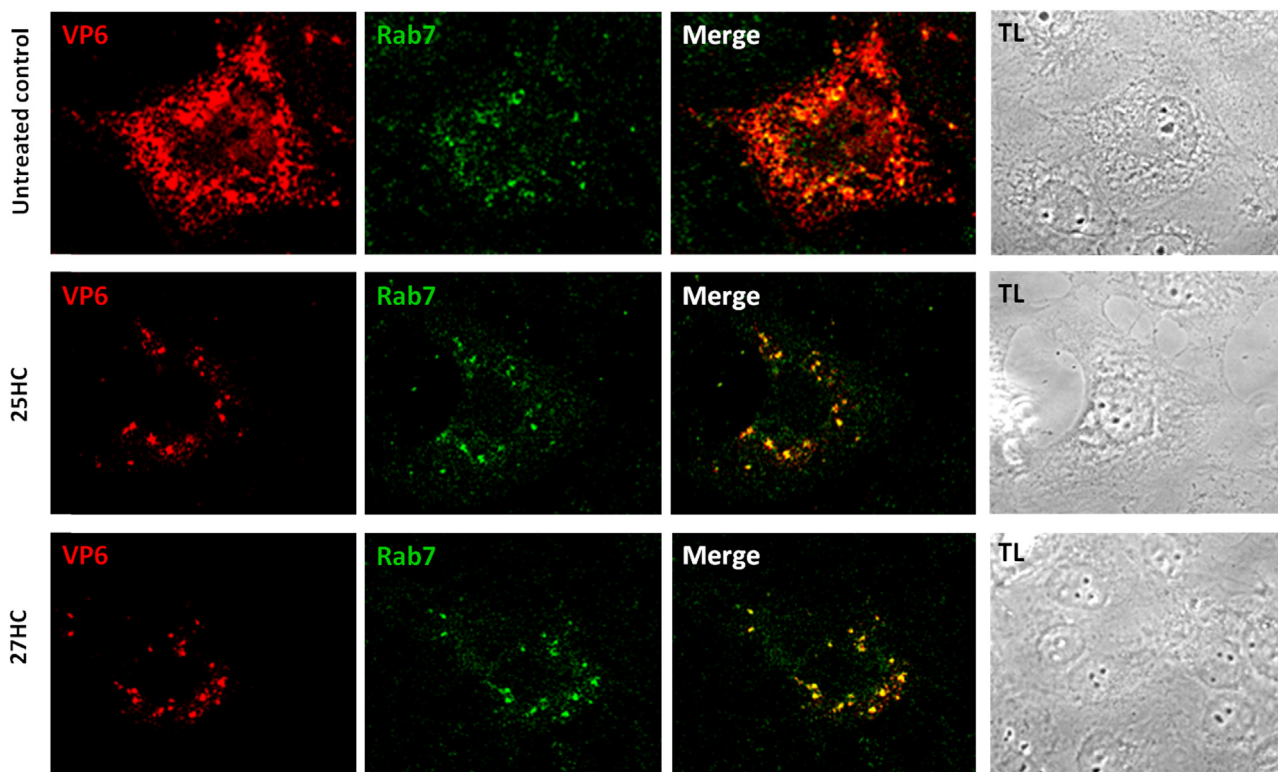
Fig. 6. Intracellular localization of HRV VP6 antigen as assessed by immunofluorescence experiments. Infected MA104 were fixed at 8 h post-infection and stained with anti-VP6 antibody (red signal) and anti-Rab7 antibody (green signal). The inserts in the right panels show the merged signals.

Fig. 7. Panel A: effect of 25HC or 27HC treatment on the interaction of OSBP and VAP-A, as assessed by coimmune precipitation experiments. A total amount of 500 μg of proteins extracted from treated or untreated cells was pulled-down with anti-VAP-A antibody (upper insert) or anti-OSBP antibody (lower insert) overnight at 4 °C. A control (Ctrl(-)) pull-down was performed with or anti-VP6 antibody. The precipitated proteins were analyzed by immunoblotting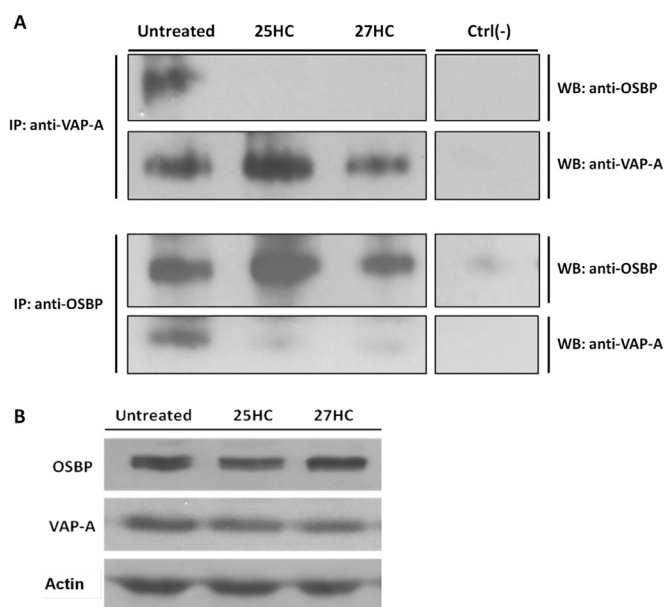. IP: immune precipitation; WB: Western blot. Panel B: effect of 25HC or 27HC treatment on the expression of OSBP and VAP-A. Actin blotting was used as normalization.

1 to 25 μg/L for 25HC and from 25 to 250 μg/L for 27HC. The average EC_{50}s of 25HC against HRV strains are 0.15 μM as assessed on MA104 cells (corresponding to 60 μg/L), and 0.30 μM on Caco2 (corresponding to 121 μg/L), being at supraphysiologic levels. Notably, average EC_{50}s of 27HC are 0.36 μM on MA104 cells (corresponding to 145 μg/L), and 0.49 μM on Caco2 (corresponding to 197 μg/L), being both in the physiologic range of concentrations of this oxysterol. The intracellular localization of HRV particles was assessed in immunofluorescence experiments using a specific antibody directed to the intermediate capsid protein VP6: since this antibody does not recognize the whole TLP particle (VP6 is hidden beneath the external capsid), we can assume that the HRV particles sequestered in the LEs of the oxysterol-treated cells are DLPs. This suggests that oxysterols do not inhibit the disassembly of the HRV external capsid (which would lead to permeabilization of the LEs membrane), but rather they somehow modify the LE milieu that halts the release of DLPs from LEs. Accumulation of cholesterol within LE compartments has been shown to alter their function, significantly impairing the infection of certain enveloped viruses that enter the cell through endocytosis, such as Influenza A virus (IAV), vescicular stomatitis virus (VSV), and dengue virus [38, 40, 41].

Oxysterols are implicated in endosomal cholesterol homeostasis through their interaction with OSBP. Mammalian OSBP and OSBP-related proteins (ORPs) constitute a large eukaryotic gene family characterized by a conserved C-terminal sterol-binding domain [42]. Their primary function is to transfer cholesterol, ergosterol or oxysterols between target membranes and/or to transduce sterol-dependent signals at these points of contact [43,44]. The OSBP possess N-terminal pleckstrin homology (PH) domains that interact with phosphatidylinositol (PI) phosphates [45,46] and two phenylalanines (FF) in an acidic tract (FFAT) motif that bind the vesicle-associated membrane protein–associated protein A (VAP-A) on the cytoplasmic surface of the endoplasmic reticulum (ER; 47, 48). The complex VAP-A-OSBP mediates the transport of de novo synthesized cholesterol from the ER to other intracellular organelles.

A recent study by Amini-Bavil-Olyaee and colleagues investigating OSBP/VAP-A-mediated cholesterol shuttling as a cellular restriction mechanism of innate immunity against enveloped viruses showed that interferon-inducible transmembrane protein 3 (IFITM3) expression induces substantial accumulation of cholesterol within LE compartments in a VAP-A binding dependent manner [38]. IFITM3 was found to interact with VAP-A and prevent its association with OSBP, so inducing a marked accumulation of cholesterol in multivesicular bodies and LEs; the latter event inhibited the fusion of intraluminal virion-containing vesicles with endosomal membranes, thereby blocking virus release into the cytosol of IAV and VSV.

To this end, Tanner and Lee commented on a novel and intriguing antiviral mechanism they called "the greasy response" to viral infections: IFITM3 expressed at LE compartments interacts with VAP-A and disrupts the ER resident complex between OSBP and VAP-A, leading to cholesterol accumulation in LE, thus blocking virus entry [39]. An eventual involvement of oxysterol (the highest affinity ligands of OSBP) was never demonstrated.

In the present study, we demonstrate for the first time that oxysterols can trigger this antiviral mechanism, and that this restriction strategy can block the infectivity of a non-enveloped virus. Consistent with previous data showing 25HC-induced translocation of OSBP from the ER (where VAP-A is localized) to the Golgi [49], we show that treatment with 25HC prevents the association of OSBP to VAP-A. More interestingly, we report that even 27HC can abolish OSBP-VAP-A interaction. Accordingly, both 25HC and 27HC appeared to induce a substantial accumulation of cholesterol in the LE compartment.

In agreement with our initial hypothesis, the antiviral effect of oxysterols was potentiated in the cells in which the expression of either OSBP or VAP-A was silenced. The silencing of these proteins in the untreated cells exerted a partial block of HRV infectivity, thus stressing the involvement of these two proteins in HRV replication.

The present report also provides proof of concept that accumulation of cholesterol within LEs is an effective anti-HRV mechanism. While many studies have demonstrated the wide spectrum of antiviral activity of U18666A against enveloped viruses [50–52], we provide the first evidence of its antiviral potential against a non-enveloped virus. This cationic amphiphile causes a significant block of HRV infectivity even at high MOIs by inducing cholesterol accumulation on LEs and sequestering HRV inside them. This finding opens the way to the search for small anti-HRV molecules endowed with this molecular mechanism.

Cholesterol accumulation on the membrane of LEs leads to several dramatic modifications of this intracellular compartment. Our results show that cholesterol accumulation in the larger cholesterol-enriched LEs in the 25HC-, 27HC-, and U18666A-treated cells leads to enlargement of LEs. Moreover, Sobo and colleagues showed that cholesterol accumulation dramatically perturbs the back fusion of intraluminal vesicles with the limiting membrane and intra-organellar trafficking [53]. Inhibition of back fusion events is expected to severely interfere with the sorting and trafficking of the proteins that cycle between intraluminal and limiting membranes, as was shown for the cation-dependent mannose-6-phosphate receptor (CD-M6PR; 53). LE-dependent HRVs are strictly dependent on the presence of the CD-M6PR on such vesicles to become uncoated and exit the endosomal system [37]. These cholesterol-induced perturbations of the LE compartment provide a reasonable explanation for why cholesterol accumulation blocks HRV particles inside these organelles.

In conclusion, both 25HC and 27HC appear to exert a remarkable anti-HRV effect, based at least on the impairment of the OSBP/VAP-A interplay and on abnormal cholesterol accumulation within LEs, the last gate for the virus to enter the cytosol. Indeed, since these side chain oxysterols have been shown to drive a number of biochemical reactions within the cells [14], their direct action on LE structure and function cannot be excluded.

This study discloses a totally novel mechanism of two oxysterols of enzymatic origin suggesting that, besides 25HC, other members of this
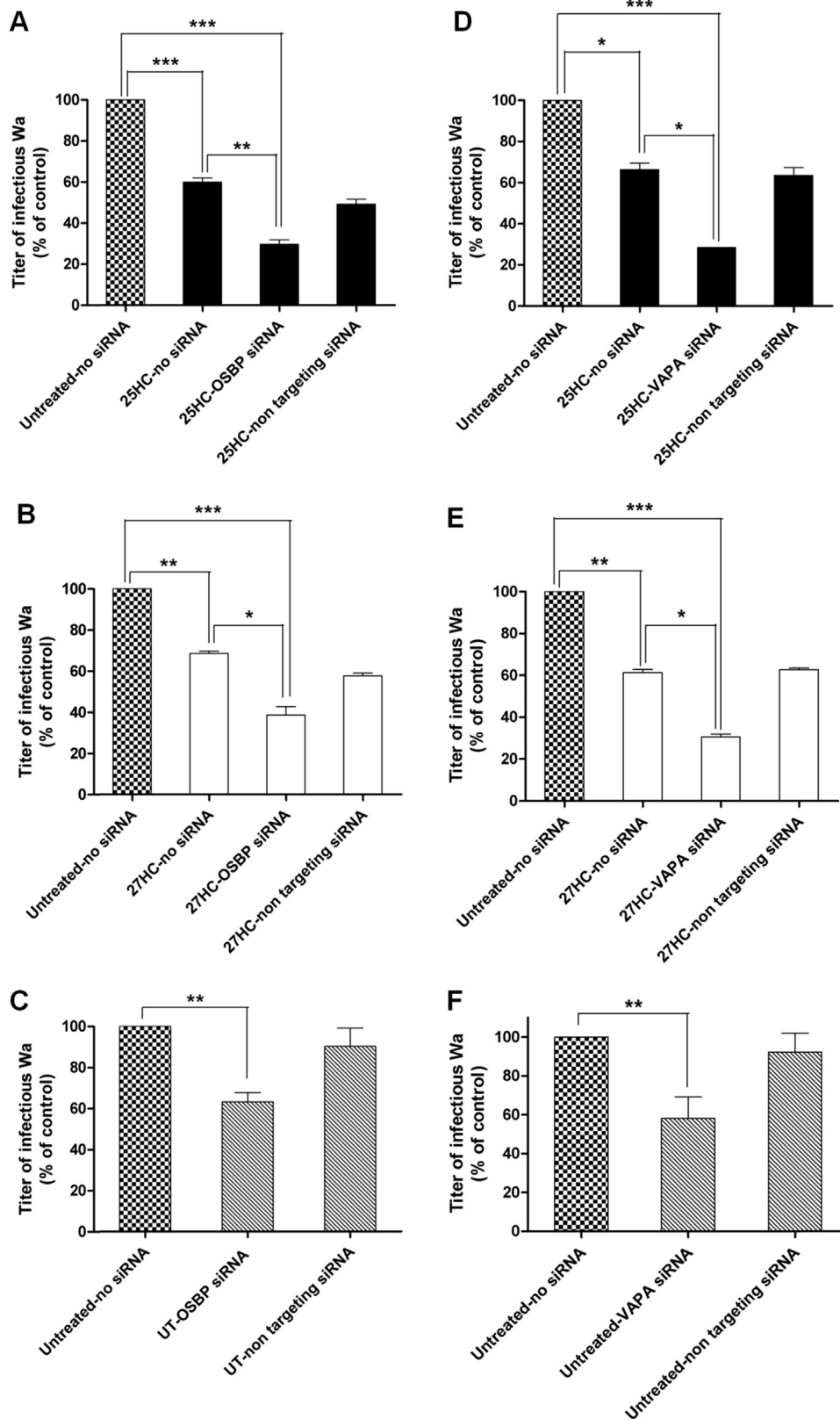
Fig. 8. Effect of OSBP silencing (panels A, B, and C) or VAP-A silencing (panels D, E, and F) by short interfering RNA (siRNA) transfection on the antiviral activity of 25HC or 27HC. Cells were transfected for 72 h with 20 nM of anti-OSBP siRNA, anti-VAP-A siRNA or control non-interfering siRNA. Cells were then treated for 20 h with oxysterols at sub-optimal concentrations and finally infected with HRV Wa. Viral infections were detected as described in the Material and Methods section. The infectivity titers of virus in the treated samples are expressed as a percentage of the titer obtained in the absence of treatment. Error bars represent the standard error of the mean (SEM) of 3 independent experiments.*$p_{ANOVA} < 0.05$; **$p_{ANOVA} < 0.01$; ***$p_{ANOVA} < 0.001$.

family could be actively involved in the innate immunity response against viruses. To these end, our results demonstrate that lipid involvement as host restriction strategy is an area of focus which, with the recent advances in technology, holds great promise to discover novel mechanisms and redox active lipid factors to develop innovative approaches for antiviral therapy.
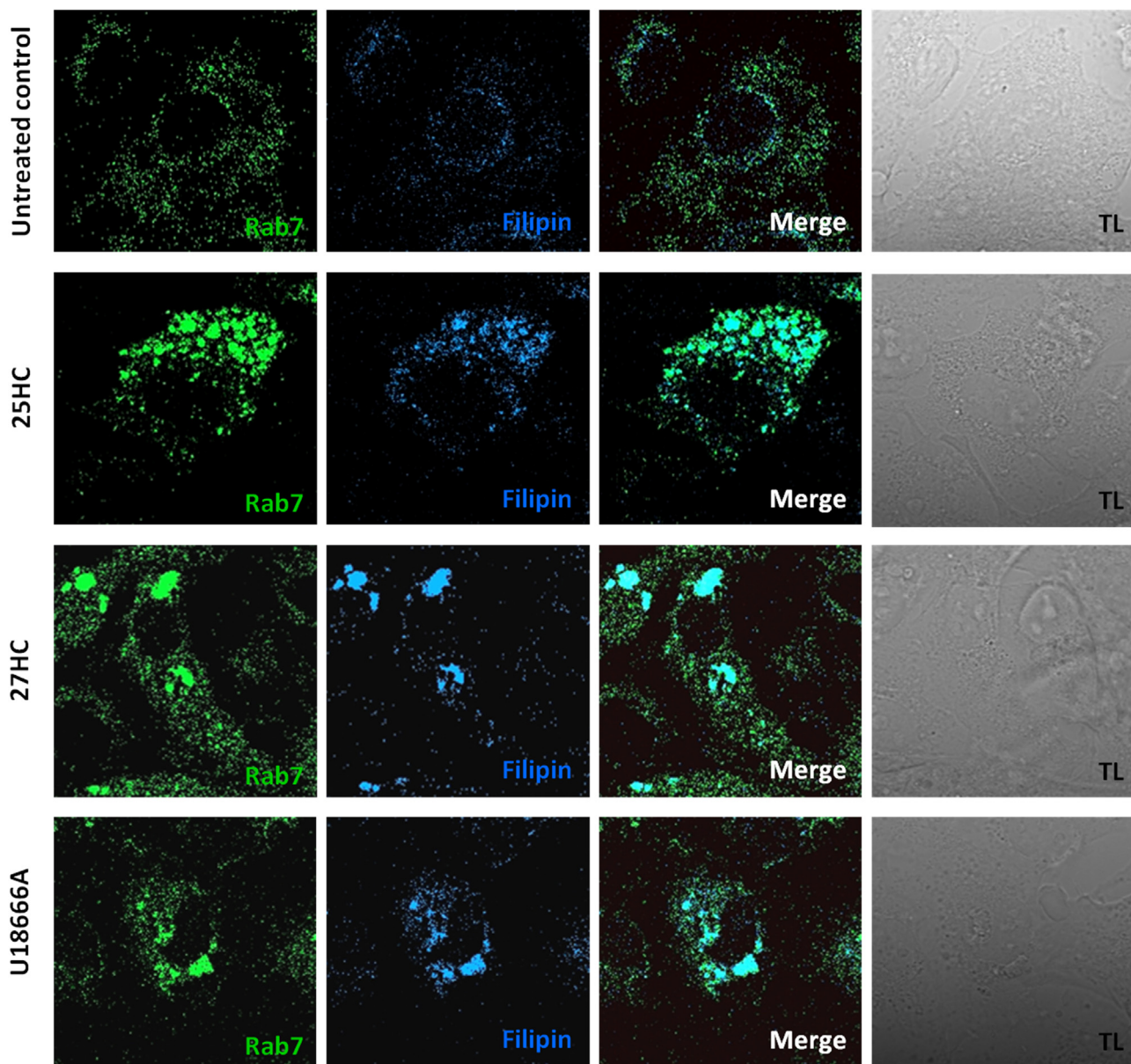
Fig. 9. Effect of 25HC or 27HC on intracellular localization of cholesterol. Positive control experiments were performed by treating cells with U18666A. Treated or untreated MA104 were fixed at 20 h post-treatment and intracellular cholesterol was stained with filipin (blue signal)and late endosomes with anti-Rab7 antibody (green signal). The inserts in the right panels show the merged signals.

Table 3
Antirotavirus activity of U18666A (MA104 cells).

Treatment	HRV strain	EC_{50}[a] (µM) – 95% CI[b]	EC_{90}[c] (µM) – 95% CI	CC_{50}[d] (µM) –95% CI	SI[e]
U18666A	Wa	1.44 (1.17–1.78)	11.66 (7.63–17.83)	219.3 (180.6–266.4)	152.29
	WI61	7.84 (7.08–8.68)	20.89 (16.72–26.09)	219.3 (180.6–266.4)	27.97
	HRV408	2.14 (1.55–2.95)	12.04 (5.94–24.42)	219.3 (180.6–266.4)	102.47
	HRV248	2.63 (1.74–3.80)	17.60 (7.05–43.94)	219.3 (180.6–266.4)	83.38
	DS-1	5.84(4.76–7.16)	19.87 (12.43–31.74)	219.3 (180.6–266.4)	37.56

n.a. not assessable.

[a] EC_{50} half-maximal effective concentration.

[b] CI confidence interval.

[c] EC_{90}90% effective concentration.

[d] CC_{50} half maximal cytotoxic concentration.

[e] SI selectivity index.
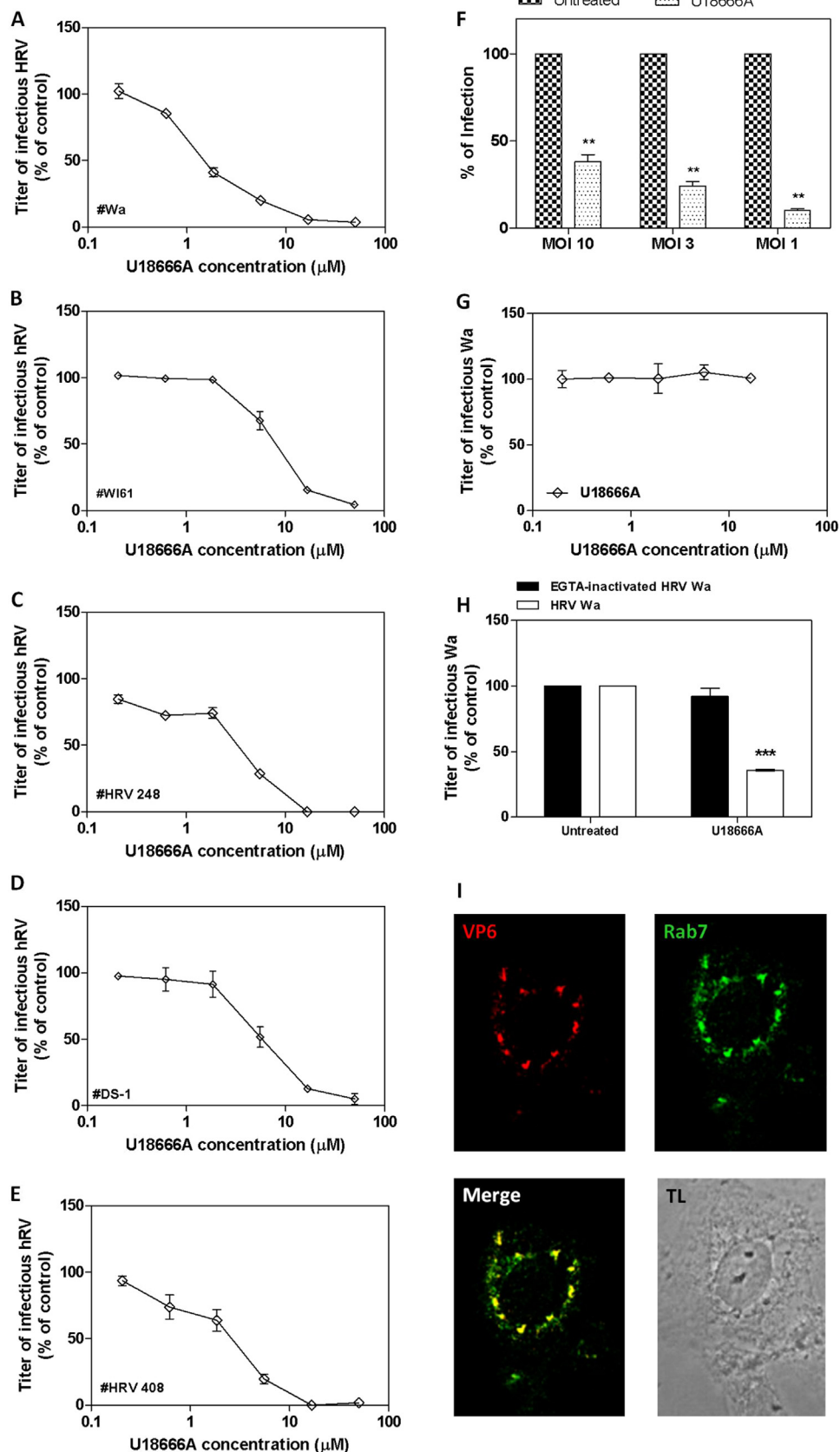
Fig. 10. Assessment of the antiviral activity of U18666A against HRV strains and assessment of its mechanism of action. Cells were treated for 20 h with increasing concentrations of U18666A and then infected with HRV Wa (A), WI61 (B), HRV 248 (C), DS-1 (D), and HRV 408 (E). Viral infections were detected as described in the Material and Methods section. The percentage infection was calculated by comparing treated and untreated wells. The results are means and SEM for triplicates.***$p_{ANOVA} < 0.001$. Panel F: cells were treated with 1.9 μM of U18666A for 20 h, then infected with high multiplicities of infection (MOIs) of HRV Wa. The percentage infection was calculated by comparing treated and untreated wells. The results are means and SEM for triplicates.**$p_{ANOVA} < 0.01$. Panel G: effect of oxysterols when added after HRV escape from LEs. Cells were infected for 45 min, treated with 25 mM of NH_4Cl for 15 min, then oxysterols were added. Panel H: effect of oxysterols on the infectivity of EGTA-inactivated HRV Wa transfected with lipofectamine (black bars) or trypsin-activated HRV Wa (white bars). MA104 cells were treated 20 h before inoculums. * **$p_{ANOVA} < 0.001$ Panel I: intracellular localization of HRV VP6 antigen as assessed by immunofluorescence experiments. Infected MA104 were fixed at 8 h post-infection and stained with anti-VP6 antibody (red signal) and anti-Rab7 antibody (green signal). The inserts in the right panels show the merged signals.

Materials and methods

Cell line and viruses

African green monkey kidney epithelial cells (MA104) and human epithelial colorectal adenocarcinoma cells (Caco-2) were propagated in Dulbecco's Modified Eagle Medium (DMEM; Sigma, St. Louis, MO, USA) supplemented with 1% (v/v) Zell Shield (Minerva Biolabs, Berlin, Germany) and heat inactivated, 10% (v/v) fetal bovine serum (Sigma). Human rotavirus (HRV) strains Wa (ATCC® VR-2018), WI61 (ATCC® VR-2551), HRV 408 (ATCC® VR-2273), HRV 248 (ATCC® VR-2274), DS-1 (ATCC® VR-2550) were purchased from ATCC (American Type Culture Collection, Rockville, MD, USA); virus was activated with 5 µg/ml of porcine pancreatic trypsin type IX (Sigma) for 30 min at 37 °C and propagated in MA104 cells using DMEM containing 0.5 µg of trypsin per ml as described previously [54]. Viral titers are expressed as focus-forming unit (FFU) per ml.

Antibodies and reagents

25HC and 27HC (Sigma) were dissolved in sterile ethanol at concentrations ranging from 2.75 mM to 3 mM. U18666A was purchased from Millipore (Darmstadt, Germany) and dissolved in sterile dimethyl sulfoxide (DMSO) to a concentration of 5 mM. Mouse monoclonal antibody (MAb) directed to human rotavirus VP6 (2B4) was purchased from Covalab (Villeurbanne, France). The rabbit polyclonal antibodies directed to VAP-A (H-40: sc-98890) and Rab 7 (H-50: sc-10767) were purchased from Santa Cruz Biotechnology, Inc. (Dallas, TX, USA). The rabbit polyclonal antibody directed to OSBP (C2C3) was purchased from GeneTex (Irvine, CA, USA). The rabbit polyclonal antibody to OSBP-N-terminal (ab192990) was purchased from Abcam (Cambridge, UK). The mouse monoclonal antibody directed to actin (MAB1501R) was purchased from Millipore. The secondary antibody peroxidase-conjugated AffiniPure F(ab')2 Fragment Goat Anti-Mouse IgG (H + L) was purchased from Jackson ImmunoResearch Laboratories Inc. (West Grove, PA, USA). The secondary antibodies anti-mouse IgG horseradish (HRP)-linked (NA931V) and anti-rabbit IgG HRP-linked (NA934V) were purchased from GE Healthcare UK (Chalfont St Giles, UK). The secondary antibodies goat anti-rabbit IgG-FITC (sc-2012) and goat anti-mouse IgG-R (sc-2092) were purchased from Santa Cruz Biotechnology, Inc.

Antiviral assays

The antiviral efficacy of the oxysterols was determined by focus reduction assay on confluent MA104 or Caco2 cell monolayers plated in 96-well trays, as described elsewhere [21]. Cells were treated for 20 h at 37 °C with 25HC, 27HC or U18666A at concentrations ranging from 0.07 to 16.7 µM (corresponding to 28.2 and 6724 µg/L for both oxysterols, and 29.7 and 7082 µg/L for U18666A). Control samples (100% of infectivity) were prepared by treating cells with culture medium supplemented with equal volumes of ethanol or DMSO, corresponding to 0.6% (v/v) to 0.0014% (v/v) in cell media. Cells were then washed with medium and infected with HRV at a multiplicity of infection (MOI) of 0.02 FFU/cell for 1 h, unless otherwise stated. Alternatively, MA104 cells were treated for 20 h with 25HC, 27HC, or U18666A at respective EC90 concentrations and then infected for 1 h with HRV Wa at MOIs 10, 3, and 1. Experiments with EGTA-inactivated HRV were performed by treating trypsin activated HRV Wa for 15 min with 1.5 mM EGTA at room temperature. Infection was then performed for 1 h at 37 °C in presence of Lipofectamine (Invitrogen Carlsbad, CA). This technique represents a useful strategy to skip viral penetration through endocytosis while delivering in cytoplasm HRV DLPs ready to start viral RNA transcription [55]. After infection, cells were washed with medium and incubated at 37 °C in a humidified incubator in 5% (vol/vol) CO$_2$–95% (vol/vol) air until fixed. For time-of-addition assays,

serial dilutions of oxysterols were added on cells alternatively 20 h or 4 h before infection or during infection or post-infection. Alternatively, cells were infected with trypsin-activated HRV Wa for 45 min at 37 °C, then medium supplemented with 25 mM NH$_4$Cl was added. This technique inhibits endosome acidification thereby sequestering HRV particles that are still inside the endosomes, while permitting the replication of those that already escaped from LEs [56]. After 15 min of incubation at 37 °C, oxysterols in presence of 25 mM NH$_4$Cl were added. After each one of these treatment/infection protocols, cells were incubated for 16 h, then fixed with cold acetone-methanol (50:50), and viral titers were determined by indirect immunostaining. Blockade of viral infectivity is expressed as mean % ± standard error of the mean (SEM).

Cell viability assay

Cells were seeded at a density of 5×10^3/well in 96-well plates and treated the next day with oxysterols 25HC, 27HC, or U18666A at concentrations ranging from 0.07 to 150 µM (corresponding to 28.2 and 60400 µg/L for both oxysterols, and 29.7 and 63609 µg/L for U18666A) to generate dose-response curves. Control samples (100% of viability) were prepared by treating cells with culture medium supplemented with equal volumes of ethanol, corresponding to 0.6% (v/v) to 0.0025% (v/v) in cell media. After 24 h of incubation, cell viability was determined using a CellTiter 96 Proliferation Assay Kit (Promega, Madison, WI, USA) and following the manufacturer's instructions. Absorbances were measured using a Microplate Reader (Model 680, Bio-Rad Laboratories, Hercules, CA, USA) at 490 nm. Viability of oxysterol-treated cells is expressed as a percentage relative to cells incubated with culture medium supplemented with equal volumes of ethanol.

Rotavirus-cell binding assay

Rotavirus-cell binding assays were performed as described previously [54]. Confluent MA104 cell monolayers in 24-well trays were treated with 25HC or 27HC at 1.8 µM or 5.6 µM. After 20 h, cells were washed with fresh medium and cooled on ice. Trypsin-activated virus, which had been cooled to 4 °C, was allowed to attach to cells for 1 h (MOI = 3 FFU/cell) at 4 °C. After a washing with cold DMEM, the cells were subjected to two rounds of freeze-thawing and then incubated at 37 °C for 30 min with 10 µg/ml porcine trypsin to release bound virus. The lysates were clarified by low speed centrifugation for 10 min. Cell-bound virus titers were determined by indirect immunostaining as above.

Rotavirus-cell entry assay

Confluent MA104 cell monolayers in 96-well plates were treated with 25HC or 27HC at concentrations ranging from 0.07 to 16.7 µM. After 20 h, cells were washed twice with DMEM and cooled on ice for 20 min. Trypsin-activated virus, which had been cooled to 4 °C, was adsorbed to cells on ice for 1 h at 4 °C (MOI = 0.2 FFU/cell) to ensure virus attachment but not entry. Unbound viruses were then washed, warmed medium was added, and the plates were incubated at 37 °C in humidified atmosphere to allow entry. At fixed timepoints (0, 15, 30, 45, 60, 75, 90 min after virus-cell attachment), the medium in the wells was aspirated, and viral particles still present on the cell surface were detached by two quick washes with 3 mM EGTA in PBS, followed by incubation in warm medium. After reaching the last timepoint (90 min), the plates were placed into a CO2 incubator, and the infection was left to proceed for an additional 16 h. The cells were then fixed and stained by indirect immunostaining as described above. The amount of virus that entered at each time point was compared to the amount of virus that entered when no EGTA wash was performed, which was taken as 100% entry.

Immunoblotting

Cells were lysed in denaturing conditions, unless otherwise stated. Extracted proteins were denatured by boiling for 5 min, then separated by sodium dodecyl sulfate–12% polyacrylamide gel electrophoresis (SDS-12% PAGE) and transferred to a polyvinylidene difluoride (PVDF) membrane. Membranes were blocked overnight at 4 °C with PBS, 0.1% Tween 20, and milk powder 10%. Membranes were then incubated with primary antibodies for 1 h at 37 °C, washed 4 times with PBS, 0.1% Tween 20, and 15% milk powder, then incubated for 1 h at 37 °C with secondary antibodies coupled with HRP and washed extensively prior to developing by the enhanced chemiluminescence method. The band density was compared using ImageJ software, and the intensity of the actin bands was used to normalize values. Where possible, the results are expressed as a percentage, by comparing treated cells with cells incubated with culture medium alone.

Immunofluorescence experiments

Subconfluent MA104 cell monolayers plated on coverslips in 24-well plates were treated with 25HC, 27HC or U18666A at 1.8 µM. After 20 h, cells were infected with trypsin-activated rotavirus Wa (MOI = 10 FFU/cell) for 8 h at 37 °C. Cells were washed twice with PBS and then fixed in cold acetone-methanol (50:50). Cells were blocked with 1% BSA for 30 min and then incubated with primary antibodies diluted in blocking buffer for 1 h followed by three washes in PBS with 0.05% Tween 20 and incubation with secondary antibodies diluted in blocking buffer for 1 h. After washing three times with PBS, coverslips were mounted and analyzed on a confocal fluorescence microscope (LSM510, Carl Zeiss, Jena, Germany).

Co-immunoprecipitation experiments

MA104 cells were treated with 5.6 µM of 25HC or 27HC for 2 h at 37 °C and then lysed in non-denaturing conditions (Tris HCl pH8 20 mM, NaCl 137 mM, NP40 1%, EDTA 2 mM, and 1X protease inhibitor mixture). The extracted proteins (500 µg) were incubated with 0.5 µg of VAP-A antibody, rabbit polyclonal to OSBP-N-terminal or anti-VP6 antibody overnight at 4 °C. Protein A-Sepharose (15 µl in PBS with 0.1% Triton X-100) was added for 1 h at 4 °C. Sepharose beads were collected by centrifugation and washed four times with 1 ml of PBS containing 1% NP40. The samples were heated to 97 °C in SDS sample buffer, separated by SDS-PAGE, and analyzed by immunoblotting.

siRNA transfection experiments

Caco2 cells (2×10^4) were transfected with 20 nM of siRNA against OSBP, VAP-A or with control non-interfering siRNAs. Each sample of transfected or untransfected cells was seeded in different wells in a 24-well tray and cultured for 72 h at 37 °C (5% CO_2). Cells were treated with suboptimal concentrations (EC_{50}) of 25HC or 27HC for 20 h, and then infected with HRV Wa (MOI 0.02 FFU/cell) as previously described. After 16 h, cells were fixed and subjected to indirect immunostaining to assess blockade of virus infectivity.

Quantitative real-time reverse transcription (RT)-PCR

The levels of siRNA-mediated silencing of OSBP or VAP-A expression were assessed by quantitative real-time reverse transcription (RT)-PCR. Briefly, extraction of total RNA from transfected or untransfected Caco2 cells was performed 72 h after transfection using TRIzol Reagent (Applied Biosystems, Monza, Italy). Concentration and purity of the extracted RNA were assessed by spectrophotometry (A260/A280). Later, 2 µg of RNA were reverse transcribed by using a High-Capacity cDNA Reverse Transcription Kit (Applied Biosystems). Quantitative RT-PCR was performed with 30 ng of cDNA using TaqMan Gene Expression Assay kits for OSBP and β-actin, TaqMan Fast Universal PCR Master Mix, and 7500 Fast Real-Time PCR System (Applied Biosystems). For each gene, threshold cycles (Ct) were determined and results were normalized using β-actin. Relative quantification was performed using a previously published mathematical method [57].

Statistical analysis

Where possible, half-maximal antiviral effective concentration (EC_{50}) values were calculated by regression analysis using the dose-response curves generated from the experimental data using GraphPad PRISM 7 (GraphPad Software, San Diego, CA, USA). The 50% cytotoxic concentration (CC_{50}) was determined using logarithmic viability curves. Where possible, a selectivity index (SI) was calculated by dividing the CC_{50} by the EC_{50} value. EC_{50} values were compared using the sum-of-squares F test. One-way ANOVA, followed by Bonferroni test, was used to assess the statistical significance of the differences between treated and untreated samples, where appropriate. Significance was set at the 95% level.

Acknowledgements

References

[1] M. Blanc, W.Y. Hsieh, K.A. Robertson, K.A. Kropp, T. Forster, G. Shui, P. Lacaze, S. Watterson, S.J. Griffiths, N.J. Spann, A. Meljon, S. Talbot, K. Krishnan, D.F. Covey, M.R. Wenk, M. Craigon, Z. Ruzsics, J. Haas, A. Angulo, W.J. Griffiths, C.K. Glass, Y. Wang, P. Ghazal, The transcription factor STAT-1 couples macrophage synthesis of 25-hydroxycholesterol to the interferon antiviral response, Immunity 38 (2013) 106–118.
[2] S.Y. Liu, R. Aliyari, K. Chikere, G. Li, M.D. Marsden, J.K. Smith, O. Pernet, H. Guo, R. Nusbaum, J.A. Zack, A.N. Freiberg, L. Su, B. Lee, G. Cheng, Interferon-inducible cholesterol-25-hydroxylase broadly inhibits viral entry by production of 25-hydroxycholesterol, Immunity 38 (2013) 92–105.
[3] S.Y. Bah, P. Dickinson, T. Forster, B. Kampmann, P. Ghazal, Immune oxysterols: role in mycobacterial infection and inflammation, J. Steroid Biochem. Mol. Biol. 169 (2017) 152–163.
[4] G. Leonarduzzi, B. Sottero, G. Poli, Oxidized products of cholesterol: dietary and metabolic origin, and proatherosclerotic effects, J. Nutr. Biochem. 13 (2002) 700–710.
[5] G. Leonarduzzi, P. Gamba, B. Sottero, A. Kadl, F. Robbesyn, R.A. Calogero, F. Biasi, E. Chiarpotto, N. Leitinger, A. Sevanian, G. Poli, Oxysterol-induced up-regulation of MCP-1 expression and synthesis in macrophage cells, Free Radic. Biol. Med. 39 (2005) 1152–1161.
[6] V. Mutemberezi, O. Guillemot-Legris, G.G. Muccioli, Oxysterols: from cholesterol metabolites to key mediators, Prog. Lipid Res. 64 (2016) 152–169.
[7] V. Luu-The, Assessment of steroidogenesis and steroidogenic enzyme functions, J. Steroid Biochem. Mol. Biol. 137 (2013) 176–182.
[8] T. Jakobsson, E. Treuter, J.A. Gustafsson, K.R. Steffensen, Liver X receptor biology and pharmacology: new pathways, challenges and opportunities, Trends Pharmacol. Sci. 33 (2012) 394–404.
[9] R. Lappano, A.G. Recchia, E.M. De Francesco, T. Angelone, M.C. Cerra, D. Picard, M. Maggiolini, The cholesterol metabolite 25-hydroxycholesterol activates estrogen receptor alpha-mediated signaling in cancer cells and in cardiomyocytes, PLoS One 6 (2011) e16631.
[10] L. Raccosta, R. Fontana, D. Maggioni, C. Lanterna, E.J. Villablanca, A. Paniccia, A. Musumeci, E. Chiricozzi, M.L. Trincavelli, S. Daniele, C. Martini, J.A. Gustafsson, C. Doglioni, S.G. Feo, A. Leiva, M.G. Ciampa, L. Mauri, C. Sensi, A. Prinetti, I. Eberini, J.R. Mora, C. Bordignon, K.R. Steffensen, S. Sonnino, S. Sozzani, C. Traversari, V. Russo, The oxysterol-CXCR2 axis plays a key role in the recruitment of tumor-promoting neutrophils, J. Exp. Med. 210 (2013) 1711–1728.
[11] A. Radhakrishnan, Y. Ikeda, H.J. Kwon, M.S. Brown, J.L. Goldstein, Sterol-regulated transport of SREBPs from endoplasmic reticulum to Golgi: oxysterols block transport by binding to Insig, Proc. Natl. Acad. Sci. USA 104 (2007) 6511–6518.
[12] R.E. Infante, L. Abi-Mosleh, A. Radhakrishnan, J.D. Dale, M.S. Brown, J.L. Goldstein, Purified NPC1 protein. I. Binding of cholesterol and oxysterols to a 1278-amino acid membrane protein, J. Biol. Chem. 283 (2008) 1052–1063.
[13] V.M. Olkkonen, S. Li, Oxysterol-binding proteins: sterol and phosphoinositide sensors coordinating transport, signaling and metabolism, Prog. Lipid Res. 52 (2013) 529–538.
[14] B. Vurusaner, G. Leonarduzzi, P. Gamba, G. Poli, H. Basaga, Oxysterols and mechanisms of survival signaling, Mol. Asp. Med. 49 (2016) 8–22.
[15] C. Moog, A.M. Aubertin, A. Kirn, B. Luu, Oxysterols, but not cholesterol, inhibit

human immunodeficiency virus replication in vitro, Antivir. Chem. Chemother. 9 (1998) 491–496.

[16] E.S. Gold, A.H. Diercks, I. Podolsky, R.L. Podyminogin, P.S. Askovich, P.M. Treuting, A. Aderem, 25-Hydroxycholesterol acts as an amplifier of inflammatory signaling, Proc. Natl. Acad. Sci. USA 111 (2014) 10666–10671.

[17] A.I. Su, J.P. Pezacki, L. Wodicka, A.D. Brideau, L. Supekova, R. Thimme, S. Wieland, J. Bukh, R.H. Purcell, P.G. Schultz, F.V. Chisari, Genomic analysis of the host response to hepatitis C virus infection, Proc. Natl. Acad. Sci. USA 99 (2002) 15669–15674.

[18] M. Iwamoto, K. Watashi, S. Tsukuda, H.H. Aly, M. Fukasawa, A. Fujimoto, R. Suzuki, H. Aizaki, T. Ito, O. Koiwai, H. Kusuhara, T. Wakita, Evaluation and identification of hepatitis B virus entry inhibitors using HepG2 cells overexpressing a membrane transporter NTCP, Biochem. Biophys. Res. Commun. 443 (2014) 808–813.

[19] V. Cagno, A. Civra, D. Rossin, S. Calfapietra, C. Caccia, V. Leoni, N. Dorma, F. Biasi, G. Poli, D. Lembo, Inhibition of herpes simplex-1 virus replication by 25-hydroxycholesterol and 27-hydroxycholesterol, Redox Biol. 12 (2017) 522–527.

[20] M. Arita, H. Kojima, T. Nagano, T. Okabe, T. Wakita, H. Shimizu, Oxysterol-binding protein family I is the target of minor enviroxime-like compounds, J. Virol. 87 (2013) 4252–4260.

[21] A. Civra, V. Cagno, M. Donalisio, F. Biasi, G. Leonarduzzi, G. Poli, D. Lembo, Inhibition of pathogenic non-enveloped viruses by 25-hydroxycholesterol and 27-hydroxycholesterol, Sci. Rep. 4 (2014) 7487.

[22] P.S. Roulin, M. Lötzerich, F. Torta, L.B. Tanner, F.J. van Kuppeveld, M.R. Wenk, U.F. Greber, Rhinovirus uses a phosphatidylinositol 4-phosphate/cholesterol counter-current for the formation of replication compartments at the ER-Golgi interface, Cell Host Microbe 16 (2014) 677–690.

[23] J.G. Cyster, E.V. Dang, A. Reboldi, T. Yi, 25-Hydroxycholesterols in innate and adaptive immunity, Nat. Rev. Immunol. 14 (2014) 731–743.

[24] D. Lembo, V. Cagno, A. Civra, G. Poli, Oxysterols: an emerging class of broad spectrum antiviral effectors, Mol. Asp. Med. 49 (2016) 23–30.

[25] S.M. Sagan, Y. Rouleau, C. Leggiadro, L. Supekova, P.G. Schultz, A.I. Su, J.P. Pezacki, The influence of cholesterol and lipid metabolism on host cell structure and hepatitis C virus replication, Biochem. Cell Biol. 84 (2006) 67–79.

[26] C. Wang, M. Gale Jr., B.C. Keller, H. Huang, M.S. Brown, J.L. Goldstein, J. Ye, Identification of FBL2 as a geranylgeranylated cellular protein required for hepatitis C virus RNA replication, Mol. Cell 18 (2005) 425–434.

[27] J. Ye, C. Wang, R. Sumpter Jr., M.S. Brown, J.L. Goldstein, M. Gale Jr., Disruption of hepatitis C virus RNA replication through inhibition of host protein geranylgeranylation, Proc. Natl. Acad. Sci. USA 100 (2003) 15865–15870.

[28] J.P. Pezacki, S.M. Sagan, A.M. Tonary, Y. Rouleau, S. Bélanger, L. Supekova, A.I. Su, Transcriptional profiling of the effects of 25-hydroxycholesterol on human hepatocyte metabolism and the antiviral state it conveys against the hepatitis C virus, BMC Chem. Biol. 9 (2009) 2.

[29] K.L. Kotloff, J.P. Nataro, W.C. Blackwelder, D. Nasrin, T.H. Farag, S. Panchalingam, Y. Wu, S.O. Sow, D. Sur, R.F. Breiman, A.S. Faruque, A.K. Zaidi, D. Saha, P.L. Alonso, B. Tamboura, D. Sanogo, U. Onwuchekwa, B. Manna, T. Ramamurthy, S. Kanungo, J.B. Ochieng, R. Omore, J.O. Oundo, A. Hossain, S.K. Das, S. Ahmed, S. Qureshi, F. Quadri, R.A. Adegbola, M. Antonio, M.J. Hossain, A. Akinsola, I. Mandomando, T. Nhampossa, S. Acácio, K. Biswas, C.E. O'Reilly, E.D. Mintz, L.Y. Berkeley, K. Muhsen, H. Sommerfelt, R.M. Robins-Browne, M.M. Levine, Burden and aetiology of diarrhoeal disease in infants and young children in developing countries (the Global Enteric Multicenter Study, GEMS): a prospective, case-control study, Lancet 382 (2013) 209–222.

[30] A.L. Shaw, R. Rothnagel, C.Q. Zeng, J.A. Lawton, R.F. Ramig, M.K. Estes, B.V. Prasad, Rotavirus structure: interactions between the structural proteins, Arch. Virol. Suppl. 12 (1996) 21–27.

[31] M. Yeager, J.A. Berriman, T.S. Baker, A.R. Bellamy, Three-dimensional structure of the rotavirus haemagglutinin VP4 by cryo-electron microscopy and difference map analysis, EMBO J. 13 (1994) 1011–1018.

[32] K.L. Graham, P. Halasz, Y. Tan, M.J. Hewish, Y. Takada, E.R. Mackow, M.K. Robinson, B.S. Coulson, Integrin-using rotaviruses bind alpha2beta1 integrin alpha2 I domain via VP4 DGE sequence and recognize alphaXbeta2 and alphaVbeta3 by using VP7 during cell entry, J. Virol. 77 (2003) 9969–9978.

[33] J.E. Ludert, N. Feng, J.H. Yu, R.L. Broome, Y. Hoshino, H.B. Greenberg, Genetic mapping indicates that VP4 is the rotavirus cell attachment protein in vitro and in vivo, J. Virol. 70 (1996) 487–493.

[34] D.M. Bass, E.R. Mackow, H.B. Greenberg, Identification and partial characterization of a rhesus rotavirus binding glycoprotein on murine enterocytes, Virology 183 (1991) 602–610.

[35] C.D. Kirkwood, R.F. Bishop, B.S. Coulson, Attachment and growth of human rotaviruses RV-3 and S12/85 in Caco-2 cells depend on VP4, J. Virol. 72 (1998) 9348–9352.

[36] M.A. Díaz-Salinas, D. Silva-Ayala, S. López, C.F. Arias, Rotaviruses reach late endosomes and require the cation-dependent mannose-6-phosphate receptor and the activity of cathepsin proteases to enter the cell, J. Virol. 88 (2014) 4389–4402.

[37] E.C. Settembre, J.Z. Chen, P.R. Dormitzer, N. Grigorieff, S.C. Harrison, Atomic model of an infectious rotavirus particle, EMBO J. 30 (2011) 408–416.

[38] S. Amini-Bavil-Olyaee, Y.J. Choi, J.H. Lee, M. Shi, I.C. Huang, M. Farzan, J.U. Jung, The antiviral effector IFITM3 disrupts intracellular cholesterol homeostasis to block viral entry, Cell Host Microbe 13 (2013) 452–464.

[39] L.B. Tanner, B. Lee, The greasy response to virus infections, Cell Host Microbe 13 (2013) 375–377.

[40] M. Lakadamyali, M.J. Rust, X. Zhuang, Endocytosis of influenza viruses, Microbes Infect. 6 (2004) 929–936.

[41] S.N. Pattanakitsakul, J. Poungsawai, R. Kanlaya, S. Sinchaikul, S.T. Chen, V. Thongboonkerd, Association of Alix with late endosomal lysobisphosphatidic acid is important for dengue virus infection in human endothelial cells, J. Proteome Res. 9 (2010) 4640–4648.

[42] M. Lehto, V.M. Olkkonen, The OSBP-related proteins: a novel protein family involved in vesicle transport, cellular lipid metabolism, and cell signalling, Biochim. Biophys. Acta 2003 (1631) 1–11.

[43] W.A. Prinz, Non-vesicular sterol transport in cells, Prog. Lipid Res. 46 (2007) 297–314.

[44] M.H. Ngo, T.R. Colbourne, N.D. Ridgway, Functional implications of sterol transport by the oxysterol-binding protein gene family, Biochem. J. 429 (2010) 13–24.

[45] T.P. Levine, S. Munro, Targeting of Golgi-specific pleckstrin homology domains involves both PtdIns 4-kinase-dependent and -independent components, Curr. Biol. 12 (2002) 695–704.

[46] T.P. Levine, S. Munro, The pleckstrin homology domain of oxysterol-binding protein recognises a determinant specific to Golgi membranes, Curr. Biol. 8 (1998) 729–739.

[47] J.P. Wyles, C.R. McMaster, N.D. Ridgway, Vesicle-associated membrane protein-associated protein-A (VAP-A) interacts with the oxysterol-binding protein to modify export from the endoplasmic reticulum, J. Biol. Chem. 277 (2002) 29908–29918.

[48] C.J. Loewen, A. Roy, T.P. Levine, A conserved ER targeting motif in three families of lipid binding proteins and in Opi1p binds VAP, EMBO J. 22 (2003) 2025–2035.

[49] A. Goto, X. Liu, C.A. Robinson, N.D. Ridgway, Multisite phosphorylation of oxysterol-binding protein regulates sterol binding and activation of sphingomyelin synthesis, Mol. Biol. Cell 23 (2012) 3624–3635.

[50] C.J. Shoemaker, K.L. Schornberg, S.E. Delos, C. Scully, H. Pajouhesh, G.G. Olinger, L.M. Johansen, J.M. White, Multiple cationic amphiphiles induce a Niemann-Pick C phenotype and inhibit Ebola virus entry and infection, Plos One 8 (2013) e56265.

[51] M.K. Poh, G. Shui, X. Xie, P.Y. Shi, M.R. Wenk, F. Gu, U18666A, an intra-cellular cholesterol transport inhibitor, inhibits dengue virus entry and replication, Antivir. Res. 93 (2012) 191–198.

[52] T. Takano, K. Tsukiyama-Kohara, M. Hayashi, Y. Hirata, M. Satoh, Y. Tokunaga, C. Tateno, Y. Hayashi, T. Hishima, N. Funata, M. Sudoh, M. Kohara, Augmentation of DHCR24 expression by hepatitis C virus infection facilitates viral replication in hepatocytes, J. Hepatol. 55 (2011) 512–521.

[53] K. Sobo, I. Le Blanc, P.P. Luyet, M. Fivaz, C. Ferguson, R.G. Parton, J. Gruenberg, F.G. van der Goot, Late endosomal cholesterol accumulation leads to impaired intra-endosomal trafficking, PLoS One 2 (2007) e851.

[54] A. Civra, M.G. Giuffrida, M. Donalisio, L. Napolitano, Y. Takada, B.S. Coulson, A. Conti, D. Lembo, Identification of equine lactadherin-derived peptides that inhibit rotavirus infection via integrin receptor competition, J. Biol. Chem. 290 (2015) 12403–12414.

[55] M. Gutiérrez, P. Isa, C. Sánchez-San Martin, J. Pérez-Vargas, R. Espinosa, C.F. Arias, S. López, Different rotavirus strains enter MA104 cells through different endocytic pathways: the role of clathrin-mediated endocytosis, J. Virol. 84 (2010) 9161–9169.

[56] M. Soliman, J.Y. Seo, D.S. Kim, J.Y. Kim, J.G. Park, M.M. Alfajaro, Y.B. Baek, H.E. Cho, J. Kwon, J.S. Choi, M.I. Kang, S.I. Park, K.O. Cho, Activation of PI3K, Akt, and ERK during early rotavirus infection leads to V-ATPase-dependent endosomal acidification required for uncoating, PLoS Pathog. 14 (2018) e1006820.

[57] J.K. Livak, T.D. Schmittgen, Analysis of relative gene expression data using real-time quantitative PCR and the 2(-Delta Delta C(T)) method, Methods 25 (2001) 402–408.

Original article

Modulation of cell proteome by 25-hydroxycholesterol and 27-hydroxycholesterol: A link between cholesterol metabolism and antiviral defense

Andrea Civra[a],[1], Mara Colzani[b],[1], Valeria Cagno[c], Rachele Francese[a], Valerio Leoni[d], Giancarlo Aldini[b], David Lembo[a], Giuseppe Poli[a],*

[a] Department of Clinical and Biological Sciences, University of Torino at San Luigi Hospital, Orbassano, Torino, Italy
[b] Department of Pharmaceutical Sciences, Università degli Studi di Milano, Milan, Italy
[c] Department of Molecular Microbiology, University of Geneva, Geneva, Switzerland
[d] Department of Laboratory Medicine, University of Milano-Bicocca, School of Medicine, Hospital of Desio, Milan, Italy

ABSTRACT

Physiological cholesterol metabolism implies the generation of a series of oxidized derivatives, whose oxysterols are by far the most investigated ones for their potential multifaceted involvement in human pathophysiology. In this regard, noteworthy is the broad antiviral activity displayed by defined side chain oxysterols, in particular 25-hydroxycholesterol (25HC) and 27-hydroxycholesterol (27HC). Although their antiviral mechanism(s) may vary depending on virus/host interaction, these oxysterols share the common feature to hamper viral replication by interacting with cellular proteins. Here reported is the first analysis of the modulation of a cell proteome by these two oxysterols, that, besides yielding additional clues about their potential involvement in the regulation of sterol metabolism, provides novel insights about the mechanism underlying the inhibition of virus entry and trafficking within infected cells. We show here that both 25HC and 27HC can down-regulate the junction adhesion molecule-A (JAM-A) and the cation independent isoform of mannose-6-phosphate receptor (MPRci), two crucial molecules for the replication of all those viruses that exploit adhesion molecules and the endosomal pathway to enter and diffuse within target cells.

1. Introduction

Over the last few years solid evidence has been provided of a remarkable antiviral effect of defined oxysterols, essentially of enzymatic origin [1–3]. These cholesterol derived molecules proved to be effective in inhibiting the replication of a wide span of viral pathogens, characterised by highly divergent replicative strategies and structural features. In this relation, the most studied member of this family has certainly been 25-hydroxycholesterol (25HC), a physiological oxysterol whose production by the enzyme 25-cholesterol hydroxylase was proven to be interferon-inducible [1,2]. Moreover, a similarly strong inhibition of the replication of both enveloped and non-enveloped viruses was demonstrated to be exerted as well by 27-hydroxycholesterol (27HC) [4–6], the product of the ubiquitous

mitochondrial enzyme 27-cholesterol hydroxylase [7] and by far the most represented oxysterol in human plasma [8]. This unprecedented antiviral spectrum relies at least in part on the ability of oxysterols to modify the composition of cellular and subcellular membranes that all viral pathogens have to cross in order to enter the host cells or hijack their replicative machinery. These oxysterol-induced modifications can be triggered by different mechanisms such as (A) the direct interaction of oxysterols with cellular membranes, (B) the interaction with cellular proteins involved in cholesterol shuttling between intracellular membranes [such as the oxysterol-binding protein 1 (OSBP)]], (C) the modulation of the expression of enzymes involved in cholesterol metabolism, by binding specific nuclear receptors such as the liver X receptor [LXR] and the estrogen receptor α [ER α] [3], or, last but not least, (D) a suitable potentiation of the initial inflammatory reaction by

---

Abbreviations:

		FBS	fetal bovine serum
		DDA	data dependent acquisition
25HC	25-hydroxycholesterol	CID	collision induced dissociation
27HC	27-hydroxycholesterol	AUG	automatic gain control
NFKB2	NF-kappa-B p100 subunit	FDR	peptide false discovery rates
LC	liquid chromatography	SDS-12% PAGE	sodium dodecyl sulphate-12% polyacrylamide gel electrophoresis
MS	mass spectrometry		
SILAC	stable isotope labelling by amino acids in cell culture	PVDF	polyvinylidene difluoride
IFITM3	interferon-induced transmembrane protein 3	PBS	phosphate buffered saline
MPRci	cation independent mannose-6-phosphate receptor	EDTA	ethylenediaminetetraacetic acid
JAM-A	junctional adhesion molecule A	OSBP1	oxysterol binding protein 1
LE	late endosomes	LXR	liver X receptor
DMEM	Dulbecco's modified Eagle's medium	ER α	estrogen receptor α

---

cells under viral attack, for instance through a redox-dependent up-regulation of NF-kB-driven overproduction of pro-inflammatory cytokines, in particular IL-6 [4].

Aiming at investigating the mechanism(s) behind such an important property of these side chain oxysterols, we deemed useful to afford the analysis of their possible modulation of cell proteome. To date, just two reports investigated the effect of not enzymatic 7-oxysterols on vascular cells proteome [9,10], while no data are so far accessible as far as side-chain and at the same enzymatic oxysterols are concerned.

2. Materials and Methods

2.1. Antibodies and reagents

The mouse monoclonal antibody directed to JAM-A (J10.4: sc-53623) was purchased from Santa Cruz Biotechnology, Inc. (Dallas, TX, USA). The mouse monoclonal antibody directed to actin (MAB1501R) was purchased from Millipore. The secondary antibody anti-mouse IgG horseradish (HRP)-linked (NA931V) was purchased from GE Healthcare UK (Chalfont St Giles, UK). 25HC and 27HC (Sigma) were dissolved in sterile ethanol at 3 mM.

2.2. Cell culture and SILAC labelling

Human epithelial adenocarcinoma HeLa cells (ATCC® CCL-2™) and African green monkey kidney epithelial cells (MA104) were propagated in Dulbecco's modified Eagle's medium (DMEM) (Gibco-BRL, Gaithersburg, MD) supplemented with heat-inactivated 10% fetal bovine serum (FBS) (Gibco/BRL) and 1% penicillin-streptomycin solution 100X (EuroClone), at 37 °C in an atmosphere of 5% of CO_2. HeLa cells were SILAC-labelled using SILAC DMEM (#89985, ThermoScientific) deficient in lysine and arginine, supplemented with 10% dialyzed fetal bovine serum (Invitrogen). To this medium, the appropriate amino acids were added as follows: unlabelled L-lysine (Lys0) and L-arginine (Arg0) (both from Sigma) were used to obtain light-labelled cells, and $^{13}C_6{}^{15}N_4$ L-arginine (Arg10, CNLM-539, Cambridge Isotope Laboratory) and $^{13}C_6{}^{15}N_2$ L-lysine (Lys8, CNLM-291, Cambridge Isotope Laboratory) were used to obtain heavy-labelled cells. The final amino acid concentration corresponded to the standard DMEM composition (*i.e.* 84 mg/l arginine and 146 mg/l lysine). Cells were cultured for at least seven replications to achieve complete labelling. Full protein labelling was verified by geLC-MS analysis (data not shown) [11].

2.3. Oxysterol treatment and preparation of cell extracts

Exponentially growing HeLa cells (either unlabelled or SILAC-labelled) were seeded in 10 cm dishes. After 24 h, cells were treated for 20 h with 25HC or 27HC at 5 μM in SILAC DMEM supplemented with 2% dialyzed FBS. Control samples were prepared by treating cells with culture medium supplemented with equal volumes of ethanol,

corresponding to 0.17% (v/v) in cell media. For each oxysterol, a "direct" and a "reverse" protocol were performed according to the following scheme: for the "direct" experiment unlabelled HeLa cells were chosen as untreated control, while labelled HeLa cells were oxysterol-treated; for the "reverse" experiment, unlabelled HeLa were oxysterol-treated, while labelled HeLa were chosen as untreated control. After 20 h from treatment, cells were washed twice with phosphate buffered saline containing ethylenediaminetetraacetic acid (PBS/EDTA), trypsinized, washed with PBS and counted.

2.4. Protein extraction and digestion

Heavy-labelled and light-unlabelled HeLa cells were mixed in 1:1 proportion (5 million:5 million) to form direct and reverse SILAC samples, i.e. the four samples "direct 25HC", "reverse 25HC", "direct 27HC" and "reverse 27HC". The mixed cells were pelleted and solubilized in Laemmli sample buffer (Bio-Rad) and dithiothreitol 50 mM, to extract proteins. The protein extract was centrifuged to pellet cellular debris (10 min, 16,000 g, 4 °C); 50 μg of the clarified protein extracts were loaded on sodium dodecyl sulphate (SDS) polyacrylamide gel (any kD Mini Protean TGX, Bio-Rad). After protein electrophoresis (200 V for 25 min), the gel was stained with Coomassie blue (Bio-Safe, Bio-Rad). Each lane, corresponding to one SILAC sample, was cut into 14 subsequent bands of different molecular weight, in order to obtain a rough fractionation of the sample. Each gel slice was reduced with 10 mM dithiothreitol (Sigma) in 50 mM ammonium bicarbonate (Sigma) for 30 min at 56 °C and alkylated on cysteine residues by incubation with 55 mM iodoacetamide (Sigma) in 50 mM ammonium bicarbonate for 45 min at RT in the dark. Proteins were in-gel digested overnight using 1 μg of trypsin (sequencing grade, Roche) solubilized in 50 mM ammonium bicarbonate, for each gel slice. Peptides were extracted from gel firstly with 30% acetonitrile/0.3% formic acid and then with 100% acetonitrile; the two extractions of each gel slice were pooled. Eluted peptides were dried in a vacuum concentrator (Martin Christ) and solubilized in 12 μl of 0.1% formic acid.

2.5. Mass spectrometry analysis

Five μl peptides solubilized in 0.1% formic acid were loaded on a nano C18 column (PicoFrit C18 HALO, 90 Å, 75 μm ID, 2.7 μm, New Objective) by an RSLCnano System Ultimate 3000 (Dionex) controlled by the software Chromeleon Xpress (Dionex, version 6.80). Peptides were separated using a 90 min linear gradient (from 1% acetonitrile, 0.1% formic acid to 40% acetonitrile, 0.1% formic acid) and on-line electrosprayed into an LTQ Orbitrap XL mass spectrometer equipped with a nanospray ion source (both Thermo). The mass spectrometer operated in data dependent acquisition (DDA) mode, controlled by the software Xcalibur (version 2.0.7, Thermo) to acquire both full MS spectra in the *m/z* range 320–1400 (resolution 1×10^5 FWHM at *m/z* 400) and MS/MS spectra obtained by collision induced dissociation

A. Civra, et al.

(CID) of the 6 most abundant multi-charged ions. Automatic gain control (AUG) was set at 1×10^6 for the acquisition of full MS spectra and at 1×10^5 for MS/MS spectra. To avoid redundancy, after two subsequent occurrences in less than 30 s, precursor ions already selected for fragmentation were dynamically excluded for 45 s.

2.6. Protein identification and quantification

The software MaxQuant [12] (version 1.5.1.2) was used to extract peaks from spectra and to match them against the human protein database (downloaded on December 03.12.2014 from UniProt, 66922 entries). Mass values were re-calibrated using the "first search" option. The following main search was performed using the following parameters: enzyme = trypsin, maximum number of missed cleavages = 2, MS mass tolerance = 5 ppm, MS/MS mass tolerance = 0.3 Da, variable modification = oxidation of Met, fixed modification = carbamidomethylation of Cys. Spectra collected from the 14 fractions of the 4 SILAC samples were analysed simultaneously, by specifying the correct experimental design of the direct and reverse assays. The "re-quantify" and "match between runs" options were selected. The decoy mode based on the reverse database was activated; peptide false discovery rates (FDR) was set to 0.05 and protein FDR was set to 0.01.

2.7. Analysis of SILAC data

The four SILAC samples, namely "direct 25HC", "reverse 25HC", "direct 27HC" and "reverse 27HC" were analysed simultaneously to increase the number of protein identification and quantification. Then, the 25HC- and 27HC-treated samples were analysed separately, by considering the reverse and direct assay as independent replicate analyses. Rigorous quality filters were used to filter the "raw" protein list obtained by MaxQuant; only proteins identified by two peptides and at least by 1 unique peptide (in both replicates) were considered as genuine identifications and analysed further. Then only proteins quantified by at least two peptides (in both replicates) were analysed further.

For each replicate, the distribution of protein ratio was used to detect proteins up- and down-regulated by oxysterols, using as threshold the 5th and 95th percentile of the ratio distribution. Proteins with heavy/light (H/L) ratio > 95th percentile in the direct assay and < 5th percentile in the reverse assay were considered as up-regulated by oxysterols, while proteins with H/L ratio < 5th percentile in the direct assay and > 95th percentile in the reverse assay were considered down-regulated by oxysterols. Normalized SILAC ratio values, provided by MaxQuant, were used for protein quantification (instead of raw ratio), in order to eliminate experimental bias due to variation in the overall content of heavy and light proteins in each sample.

The list of proteins modulated by the oxysterols was analysed using STRING (version 10) to detect interactions between them and to perform enrichment analysis of gene ontology (GO) categories and KEGG pathways, which were considered "enriched" if the probability of finding the observed number of proteins was < 0.05.

2.8. Immunoblotting

In order to validate the results of SILAC proteomic analysis, an immunoblot was performed. Briefly, HeLa cells or MA104 cells were plated in 6 well plates and treated with 25HC or 27HC at 5 μM, when they reached confluence. Control samples were prepared by treating cells with culture medium supplemented with equal volumes of ethanol, corresponding to 0.17% (v/v) in cell media. After 20 h, cells were washed twice with sterile PBS, harvested and lysed in denaturing conditions. Extracted proteins were denatured by boiling for 5 min, then separated by 12%-SDS polyacrylamide gel electrophoresis (SDS-12% PAGE) and transferred to a polyvinylidene difluoride (PVDF) membrane. Membranes were blocked overnight at 4 °C with PBS, 0.1%

Tween 20, and milk powder 10%. Membranes were then incubated with the primary antibody for 1 h at 37 °C, washed 4 times with PBS, 0.1% Tween 20, and 15% milk powder, then incubated for 1 h at 37 °C with the secondary antibody coupled with horseradish peroxidase and washed extensively prior to developing by the enhanced chemiluminescence method. The bands' density was compared using ImageJ software, and the intensity of the actin bands was used to normalize values. Where possible, the results were expressed as a percentage, by comparing treated cells with cells incubated with culture medium alone. Statistically significant differences ($p < 0.05$) were assessed by one-way analysis of variance (one-way ANOVA).

3. Results and discussion

3.1. Detection of proteins modulated by 25HC and 27HC

HeLa cells were challenged 20 h at 37 °C in the presence or in the absence of 25HC or 27HC, at the final concentration of 5 μM, an oxysterol dose and an incubation time that previously showed to fully abolish Rhinovirus and Rotavirus replication [5]. Notably, the half maximal cytotoxic concentration (CC_{50}) of both oxysterols was shown to be > 150 μM [5].

In order to obtain a first, large-scale and unbiased view of the effect of the two oxysterols 25HC and 27HC on cells, we applied quantitative proteomics as approach to detect variations of protein expression upon the incubation of model cells with 25HC and/or 27HC.

In particular, stable isotope labelling in cell culture (SILAC) was used as fully established and reliable method to obtain large-scale protein quantification [13]. The HeLa cell line was exploited as model system, not only because largely employed in *in vitro* antiviral studies, including those related to oxysterols [4,5,14–17], but also because successfully applied to several SILAC-based studies [13,18], also in the field of virology [19–21].

According to the SILAC strategy, heavy- and light-labelled cells were treated in vitro with 25HC, 27HC or vehicle (sterile-filtered ethanol). After mixing heavy and light cells in 1:1 ratio, proteins were extracted, fractionated, digested, analysed by mass spectrometry, identified, and relatively quantified according to heavy/light SILAC ratios. Overall, more than 3000 proteins were identified in samples obtained from 25HC- and 27HC-treated cells (Table 1).

Rigorous quality filters were applied to focus the analysis on high quality data (as described in the Materials and Methods section). After filtering, the total numbers of proteins genuinely identified and quantified were 2262 and 2,287, in HeLa cells respectively treated with 25HC and 27HC. The overlap between replicate analyses was remarkable: 87.5% of the proteins were identified and quantified in both direct and reverse 25HC assays, and 83.2% of the proteins in the case of the 27HC assays.

Quality filters were applied to focus on genuine identifications and quantifications.

Table 1
Number of proteins identified and quantified in HeLa cells treated with 25HC and 27HC.

	N. of proteins	
	25-HC	27-HC
protein identification (raw)	3081	3135
- reverse database	3043	3105
- contaminants	3008	3068
- id. based on modifications	2965	3025
≥2 peptides/protein	2364	2393
≥1 unique peptide/protein	2319	2341
≥2 SILAC ratio/protein	2262	2287
up-regulated proteins	18	8
down-regulated proteins	38	33

Proteins modulated by 25HC and 27HC were detected by applying 5th and 95th percentile thresholds at the distribution of SILAC ratio obtained in each sample.

Notably, since the main task of the here reported proteomic analysis was to investigate possible mechanisms underlying the antiviral effect displayed in a quite similar way by both oxysterols, we focused on those proteins whose cellular expression was either increased or decreased upon both 25HC and 27HC treatments.

For the sake of completeness, the whole list and details of proteins modulated by each oxysterol are provided in Supplementary Tables S1-S4.

3.2. Proteins up-regulated by both 25HC and 27HC

Table 2 reports the proteins up-regulated in both 25HC- and 27HC-treated HeLa cells, as compared to control cells treated with vehicle.

Among the proteins up-regulated by both oxysterols, only nuclear factor-kappa-B p100 subunit (NFKB2), a transcription factor playing a role in inflammation and immune functions, might actually be related to viral infections but also to the antiviral properties of the two side chain oxysterols. p100 is the precursor protein of NF-kB2/p52; the processing of p100 is signal-dependent and highly inducible, and it selectively degrades the C-terminal portion of the precursor protein, working as an alternative mechanism for NF-kB activation. Indeed, several viruses have been shown to activate NF-kB signalling, usually in the first stages of the infection and in a transient way [22–25]. The NF-kB-dependent induction of inflammatory cytokines synthesis would then contribute to counteract cell invasion by viral particles [26–28] and the recognized pro-inflammatory properties of oxysterols [29,30] could potentiate the cytokine production provoked by the virus, as actually demonstrated in cells infected with Herpes Simplex type 1 virus (HSV-1) [4]. However, even if the proteomic result regarding NF-kB2 well fits with the recent available literature, the same finding should be taken with care due to the high CV observed (Table 2).

3.3. Proteins down-regulated by both 25HC and 27HC

Listed in Table 3 are the proteins down-regulated in both 25HC- and 27HC-treated HeLa cells.

The large majority of the proteins whose cellular content resulted to be significantly reduced by HeLa treatment with 25HC or 27HC is related to lipid synthesis and metabolism or more specifically to sterol synthesis and metabolism. This finding was somehow expected, still the proteome analysis of oxysterol treated cells provided for the first time, to our knowledge, meaningful and precious data. For instance, both investigated oxysterols strongly down-regulated cellular levels of hydroxymethylglutaryl-CoA (HMG-CoA) synthase, the key regulatory enzyme of the cholesterol synthetic pathway. This is consistent with previous literature, showing that 25-HC is a HMG-CoA reductase and synthase inhibitor [31] and, by means of this mechanism, it conveys an antiviral state in treated cells, particularly against flaviviruses, including hepatitits C virus [32]. Moreover, both oxysterols can down-regulate the expression of isopentenyl-diphosphate delta-isomerase 1, a crucial regulatory enzyme in the synthesis of isoprenoids. Interestingly,

an excessive protein isoprenylation is correlated to cardiovascular and age-related disease [33], while the two oxysterols would act as quenchers of isoprenoids' synthesis.

Out of 19 cellular proteins found to be down-regulated by both 25HC and 27HC, three are most likely implicated in viral entry and replication, namely interferon-induced transmembrane protein 3 (IFITM3/Q01628), cation independent mannose-6-phosphate receptor (MPRci/P11717) and junctional adhesion molecule A (JAM-A/Q9Y624) (Table 3).

IFITM3 actually appears to be an antiviral protein inducible by α and γ interferons and acting as restriction factor inhibiting the cell entry of a number of enveloped viruses, such as influenza A virus, Marburg and Ebola filoviruses, SARS coronavirus [34]. IFITM3, like IFITM2, predominantly localizes at the endosomal level and most likely interferes with endocytosis-mediated viral entry and progression in the late endosomes, as observed for IFITM2 in the case of African swine fever virus [35]. Thus, these findings would exclude the IFITM3 falling off induced by 25HC and 27HC as a mechanism underlying their proved antiviral activity.

3.4. Reduced expression of MPRci and JAM-A proteins: two likely antiviral mechanisms of 25HC and 27HC

Contrary to the observed reduction of IFITM3, the down-regulation of MPRci and JAM-A cellular levels as exerted by 25HC and 27HC appears to support the antiviral properties displayed by these side chain oxysterols.

MPRci, together with the cation dependent isoform MPRcd, is one of the specialized transporters of newly synthesized lysosomal factors, including cathepsins, from the Golgi apparatus to late endosomes (LE) [36]. It was very recently demonstrated that most rotavirus strains need the Golgi-LEs transporters MPRci and Sortilin-1 and their cargo cathepsins to efficiently infect Caco-2 and MA104 cells [37]. In this relation, both 25HC and 27HC proved to markedly inhibit rotavirus replication in the same cell lines [5,6]. In the report of Diaz-Salinas and colleagues [37], at least cathepsins B, L and S were involved in the Golgi-LE traffic modulated by MPRci. SILAC experiments showed a significant down-regulation of cathepsin D only in HeLa cells treated with 25HC and not with 27HC (Supplementary Material, Table S2). It cannot be excluded that also this isoform could contribute to the infectivity of at least defined rotavirus strains. More importantly, MPR appears to be pivotal for the replication of several other viruses. Vaccinia virus protein p37 localizes to the LE and interacts with proteins associated with LE-derived transport vesicle biogenesis such as MPR to facilitate assembly of extracellular forms of virus [38]. The HSV glycoprotein D (gD), which is essential for this virus to enter cells, can efficiently bind to MPRci, an interaction that plays a role in virus entry and egress [39]. In a recent study, Dohgu and colleagues showed that the MPR is involved in both the replicative cycle and the dissemination of human immunodeficiency virus (HIV-1), facilitating the passing of HIV-1 through the blood brain barrier [40].

It must be outlined the fact that Sortilin-1 was not among the proteins whose cellular level was diminished by the oxysterol treatment, thus a MPRci independent Golgi-LE pathway may compensate the

Table 2

Proteins up-regulated by both 25HC and 27HC

1st ID UniProt	1st Protein name	average ratio 25HC	CV (%) 25HC	average ratio 27HC	CV (%) 27HC
Q00653	Nuclear factor-kappa-B p100 subunit	**1.692**	31.0	**1.399**	13.29
Q96QD8	Sodium-coupled neutral amino acid transporter 2	**1.731**	8.3	**1.379**	11.22
Q00534	Cyclin-dependent kinase 6	**1.280**	6.5	**1.223**	4.89
Q8IZV5	Retinol dehydrogenase10	**1.238**	6.1	**1.212**	6.44
O00762	Ubiquitin-conjugating enzyme E2 C	**1.310**	4.1	**1.194**	5.19
Q99595	Mitochondrial import inner membrane translocase subunit Tim17-A	**1.323**	12.3	**1.184**	2.52

CV: coefficient of variation.

Table 3
Proteins down-regulated by both 25HC and 27HC

1st ID UniProt	1st Protein name	average ratio 25HC	CV (%) 25HC	average ratio 27HC	CV (%) 27HC
P37268	Squalene synthase	0.262	38.5	0.164	26.80
O00767	Acyl-CoA desaturase	0.221	19.3	0.229	1.47
Q01581	Hydroxymethylglutaryl-CoA synthase, cytoplasmic	0.291	45.3	0.287	38.50
Q13907	Isopentenyl-diphosphate Delta-isomerase 1	0.483	11.8	0.457	7.48
Q16850	Lanosterol 14-alpha demethylase	0.619	26.4	0.535	23.53
Q9UBM7	7-Dehydrocholesterol reductase	0.594	5.4	0.592	5.03
Q01628	Interferon-induced trans membrane protein3	0.544	13.0	0.615	11.71
P49327	Fatty acid synthase	0.670	4.8	0.648	4.82
Q9BWD1	Acetyl-CoA acetyltransferase, cytosolic	0.709	7.9	0.691	9.42
P14324	Farnesylpyrophosphate synthase	0.743	6.2	0.711	2.33
Q15738	Sterol-4-alpha-carboxylate 3-dehydrogenase, decarboxylating	0.726	6.1	0.726	1.87
Q9Y624	Junctional adhesion molecule A	0.626	15.3	0.737	16.42
P11717	Cation-independent mannose-6-phosphate receptor	0.658	1.9	0.766	3.23
P05413	Fatty acid-binding protein, heart	0.786	1.1	0.767	9.07
P53396	ATP-citrate synthase	0.798	3.1	0.771	5.14
Q99933	BAG family molecular chaperone regulator 1	0.782	8.7	0.784	7.03
Q15796	Mothers against decapentaplegic homolog (SMAD2)	0.792	2.2	0.796	1.49
P53007	Tricarboxylate transport protein, mitochondrial	0.796	1.6	0.811	3.30
Q96CP2	FLYWCH family member 2	0.799	3.3	0.849	3.82

CV: coefficient of variation.

specific decrease of a given transporter [41]. However, an actual co-involvement of oxysterol-induced deficit of cell MPRci in the protective effect of 25HC and 27HC against rotavirus infection [5,6] could be reinforced by the evidence that defined rotavirus strains, including the human ones, utilize the tight junction protein JAM-A as a co-receptor to enter enterocyte cells [42]. Solid proofs are actually available indicating that several virus families exploit various tight junction proteins to enter, replicate or even exit the target cells, being JAM-A used by reovirus and rotavirus to facilitate the infection process [43].

Of note, JAM-A and MPRci have a different localization in the cell, being the first bounded to the plasma membrane and the second to cytoplasmic membranes. Hence, the tight junction protein appears the first and critical target of viruses, then reaching LE in a second step to enter into the cytosol from those vesicles.

3.5. Confirmation of JAM-A down regulation in HeLa and MA104 cells

The modulation of JAM-A expression by 25HC and 27HC was assessed by immunoblot analysis. The treatment of HeLa cell line with 25HC or 27HC significantly ($p_{ANOVA} < 0.05$) decreased JAM-A protein level by about 40% and 60% respectively (Fig. 1 A, B). The modulation was comparable to the SILAC ratios obtained in the proteomic analysis,

corresponding to 0.626 in the direct assay and 0.737 in the reverse assay. These results were further confirmed by immunoblotting on 25HC- or 27HC-treated MA104 cells (Fig. 1C, D).

3.6. Modulation of cholesterol and isoprenoid metabolism by 25HC and 27HC

A quite large portion of the proteins that resulted to be either up- or down regulated by one or both the oxysterols of enzymatic origin considered in the present study are involved in the cholesterol or the isoprenoid metabolism. The evidence here provided of a likely modulation of these key cell metabolic pathways by 25HC and/or 27HC is certainly preliminary and in need of deeper investigation by other groups more focused on sterol metabolism. Still, the data reported here should provide some useful clues for such a more focused research.

4. Conclusions

In the present study, we carried out a technically advanced proteomic screening in a cell model system (HeLa cell line) commonly employed to in vitro test the antiviral efficacy of a wide variety of compounds. Cellular treatment was performed at a concentration of the
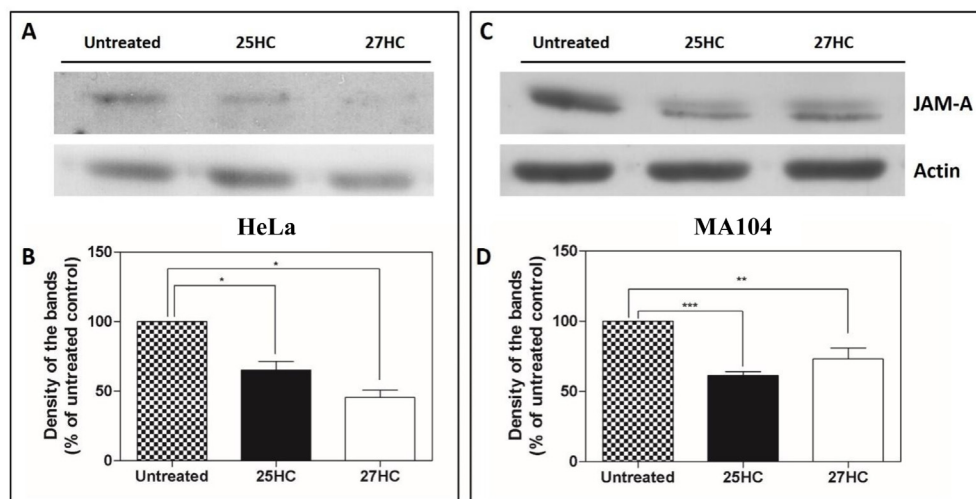
Fig. 1. **Western blotting validation of the 25HC- and 27HC-exerted down-regulation of JAM-A protein level in two different cell lines.** Cells were incubated 20 h at 37 °C in the presence or in the absence of 25HC or 27HC at 5 μM final concentration. Panels A–C: JAM-A immunoblots were assessed in HeLa and MA104 cells respectively and normalized against actin. Panel B–D: the density of the bands obtained in HeLa and MA104 cells was calculated by means of ImageJ software, using the intensity of the actin bands for values normalization. Results were expressed as percent values as to untreated cells, taken as control. Error bars represent the standard error of the mean (SEM) of two independent experiments in duplicate. Statistically significant differences were assessed by one way analysis of variance (one way ANOVA). $*p_{ANOVA} < 0.05$; $**p_{ANOVA} < 0.01$; $***p_{ANOVA} < 0.001$.

two oxysterols (5 μM) demonstrated to significantly inhibit viral replication of a large number of viral pathogens, without inducing any cytotoxicity at all [1,4–6].

Focusing on the antiviral activity of the two oxysterols, we identified two new mechanisms of inhibition of virus entry and diffusion within infected cells. Indeed, both 25HC and 27HC were shown able to down-regulate the junction adhesion molecule-A and the cation independent isoform of mannose-6-phosphate receptor, two crucial molecules for a number of viruses to exert infection.

This research communication is the first report on cell proteome modulation by two side chain oxysterols, i.e. 25HC and 27HC, certainly of primary interest in human pathophysiology. The two oxysterols were shown by our group to further up-regulate the redox sensitive transcription factor NF-kB in virus infected cells, by this way boosting the cellular pro-inflammatory reaction against the virus itself [4]. In addition, we previously reported that the survival signalling triggered by low micromolar concentrations of 27HC in the human pro-monocytyc U-937 cell line was dependent on a rapid and transient activation of NADPH-oxidase with consequent H_2O_2 production [44,45]. These findings are thus indicating a promising way to deeper elucidate the actual contribution of redox reactions in the antiviral effects of 25HC and 27HC.

Acknowledgements

Appendix A. Supplementary data

Supplementary data to this article can be found online at https://doi.org/10.1016/j.freeradbiomed.2019.08.031.

References

[1] S.-L. Liu, R. Aliyari, K. Chikere, G. Li, M.D. Marsden, J.K. Smith, O. Pernet, H. Guo, R. Nusbaum, J.A. Zack, A.N. Freiberg, L. Su, B. Lee, G. Cheng, Interferon-inducible cholesterol-25-hydroxylase broadly inhibit viral entry by production of 25-hydroxycholesterol, Immunity 38 (2013) 92–105.

[2] M. Blanc, W.Y. Hsieh, K.A.: Robertson, K.A. Kropp, T. Forster, G. Shui, P. Lacaze, S. Watterson, S.J. Griffiths, N.J. Spann, A. Meljon, S. Talbot, K. Krishnan, D.F. Covey, M.R. Wenk, M. Craigon, Z. Ruzsics, J. Haas, A. Angulo, W.J. Griffiths, C.K. Glass, Y. Wang, P. Gazhal, The transcription factor STAT-1 couples macrophage synthesis of 25-hydroxycholesterol to the interferon antiviral response, Immunity 38 (2013) 106–118.

[3] D. Lembo, V. Cagno, A. Civra, G. Poli, Oxysterols: an emerging class of broad spectrum antiviral effectors, Mol. Asp. Med. 49 (2016) 23–30.

[4] V. Cagno, A. Civra, D. Rossin, S. Calfapietra, C. Caccia, V. Leoni, N. Dorma, F. Biasi, G. Poli, D. Lembo, Inhibition of herpes simplex-1 virus replication by 25-hydroxycholesterol and 27-hydroxycholesterol, Redox Biol. 12 (2017) 522–527.

[5] A. Civra, V. Cagno, M. Donalisio, F. Biasi, G. Leonarduzzi, G. Poli, D. Lembo, Inhibition of pathogenic non-enveloped viruses by 25-hydroxycholesterol and 27-hydroxycholesterol, Sci. Rep. 4 (2014) 7487, https://doi.org/10.1038/srep07487.

[6] A. Civra, R. Francese, P. Gamba, G. Testa, V. Cagno, G. Poli, D. Lembo, 25-Hydroxycholesterol and 27-hydroxycholesterol inhibit human rotavirus infection by sequestering viral particles into late endosomes, Redox Biol. 19 (2018) 318–330.

[7] X. Li, P. Hylemon, W.M. Pandak, S. Ren, Enzyme activity assay for cholesterol 27-hydroxylase in mitochondria, J. Lipid Res. 47 (2006) 1507–1512.

[8] V. Leoni, C. Caccia, Potential diagnostic applications of side chain oxysterols analysis in plasma and cerebrospinal fluid, Biochem. Pharmacol. 86 (2013) 26–36.

[9] L.J. Ward, S.A. Liunggren, H. Karlsson, W. Li, X.M. Yuan, Exposure to atheroma-relevant 7-oxysterols causes proteomic alterations in cell death, cellular longevity, and lipid metabolism in THP-1 macrophages, PLoS One 12 (2017) e0174475, , https://doi.org/10.1371/journal.pone.0174475.

[10] L. Rosa-Fernandes, L.M.F. Maselli, N.Y. Maeda, G. Palmisano, S.P. Bydlowski, Outside-in, inside-out: proteomic analysis of endothelial stress mediated by 7-ketocholesterol, Chem. Phys. Lipids 207 (Pt B) (2017) 231–238.

[11] F. Schmidt, M. Strozynski, S.S. Salus, H. Nilsen, B. Thiede, Rapid determination of amino acid incorporation by stable isotope labelling with amino acids in cell culture (SILAC), Rapid Commun. Mass Spectrom. 21 (2007) 3919–3926.

[12] J. Cox, M. Mann, MaxQuant enables high peptide identification rates, individualized p.p.b.-range mass accuracies and proteome-wide protein quantification, Nat. Biotechnol. 26 (2008) 1367–1372.

[13] S.E. Ong, M. Mann, A practical recipe for stable isotope labeling by amino acids in cell culture (SILAC), Nat. Protoc. 1 (2006) 2650–2660.

[14] P.S. Roulin, M. Lötzerich, F. Torta, L.B. Tanner, F.J. van Kuppeveld, M.R. Wenk, U.F. Greber, Rhinovirus uses a phosphatidylinositol 4-phosphate/cholesterol counter-current for the formation of replication compartments at the ER-Golgi interface, Cell Host Microbe 16 (2014) 677–690.

[15] P.S. Roulin, L.P. Murer, U.F. Greber, A single point mutation in the Rhinovirus 2B protein reduces the requirement for phosphatidylinositol 4-kinase class III beta in viral replication, J. Virol. 92 (2018), https://doi.org/10.1128/JVI.01462-18 e01462-18.

[16] A. Doms, T. Sanabria, J.N. Hansen, N. Altan-Bonnet, G.H. Holm, 25-Hydroxycholesterol production by the cholesterol-25-hydroxylase Interferon-stimulated gene restricts mammalian Reovirus infection, J. Virol. 92 (2018), https://doi.org/10.1128/JVI.01047-18 e01047-18.

[17] H. Wang, J.W. Perry, A.S. Lauring, P. Neddermann, R. De Francesco, A.W. Tai, Oxysterol-binding protein is a phosphatidylinositol 4-kinase effector required for HCV replication membrane integrity and cholesterol trafficking, Gastroenterology 146 (2014) 1373–1385.

[18] M. Hilger, M. Mann, Triple SILAC to determine stimulus specific interactions in the Wnt pathway, J. Proteome Res. 11 (2012) 982–994.

[19] K.M. Coombs, HeLa cell response proteome alterations induced by mammalian reovirus T3D infection, Virol. J. 10 (2013) 202, https://doi.org/10.1186/1743-422X-10-202.

[20] L.K. Zhang, F. Chai, H.Y. Li, G. Xiao, L. Guo, Identification of host proteins involved in Japanese encephalitis virus infection by quantitative proteomics analysis, J. Proteome Res. 12 (2013) 2666–2678.

[21] Y.W. Lam, V.C. Evans, K.J. Heesom, A.I. Lamond, D.A. Matthews, Proteomics analysis of the nucleolus in adenovirus-infected cells, Mol. Cell. Proteom. 9 (2010) 117–130.

[22] L. Havard, S. Rahmouni, J. Boniver, P. Delvenne, High levels of p105 (NFKB1) and p100 (NFKB2) proteins in HPV16-transformed keratinocytes: role of E6 and E7 oncoproteins, Virology 331 (2005) 357–366.

[23] I. Ersing, K. Bernhardt, B.E. Gewurz, NF-κB and IRF7 pathway activation by epstein-barr virus latent membrane protein 1, Viruses 5 (2013) 1587–1606.

[24] G. Jiang, S. Dandekar, Targeting NF-κB signaling with protein kinase C agonists as an emerging strategy for combating HIV latency, AIDS Res. Hum. Retrovir. 31 (2015) 4–12.

[25] R.M.G. Da Costa, M.M.S.M. Bastos, R. Medeiros, P.A. Oliveira, The NFκB signaling pathway in papillomavirus-induced lesions: friend or foe? Anticancer Res. 36 (2016) 2073–2083.

[26] T.H. Mogensen, J. Melchjorsen, L. Malmgaard, A. Casola, S.R. Paludan, Suppression of proinflammatory cytokine expression by herpes simplex virus type 1, J. Virol. 78 (2004) 5883–5890.

[27] A.J. Chucair-Elliott, C. Conrady, M. Zheng, C.M. Kroll, T.E. Lane, D.J. Carr, Microglia-induced IL-6 protects against neuronal loss following HSV-1 infection of neural progenitor cells, Glia 62 (2014) 1418–1434.

[28] E.A. Murphy, J.M. Davis, A.S. Brown, M.D. Carmichael, A. Ghaffarm, E.P. Mayer, Effect of IL-6 deficiency on susceptibility to HSV-1 respiratory infection and intrinsic macrophage antiviral resistance, J. Interferon Cytokine Res. 28 (2008) 589–595.

[29] G. Leonarduzzi, P. Gamba, S. Gargiulo, F. Biasi, G. Poli, Inflammation-related gene expression by lipid oxidation-derived products in the progression of atherosclerosis, Free Radic. Biol. Med. 52 (2012) 19–34.

[30] S. Gargiulo, G. Testa, P. Gamba, E. Staurenghi, G. Poli, G. Leonarduzzi, Oxysterols and 4-hydroxy-2-nonenal contribute to atherosclerotic plaque destabilization, Free Radic. Biol. Med. 111 (2017) 140–150.

[31] J.P. Pezacki, S.M. Sagan, A.M. Tonary, Y. Rouleau, S. Bélanger, L. Supekova, A.I. Su, Transcriptional profiling of the effects of 25-hydroxycholesterol on human hepatocyte metabolism and the antiviral state it conveys against the hepatitis C virus, BMC Chem. Biol. 9 (2009), https://doi.org/10.1186/1472-6769-9-2.

[32] J.F. Osuna-Ramos, J.M. Reyes-Ruiz, R.M. Del Ángel, The role of host cholesterol during Flavivirus infection, Front. Cell. Infect. Microbiol. 8 (2018), https://doi.org/10.3389/fcimb.2018.00388.

[33] D. Perez-Sala, Protein isoprenylation in biology and disease: general overview and perspectives from studies with genetically engineered animals, Front. Biosci. 12 (2007) 4456–4472.

[34] I.C. Huang, C.C. Bayley, J.L. Weyer, S.R. Radoshitzky, M.M. Becker, A.L. Brass, A.A. Ahmed, X. Chi, L. Dong, L.E. Longobardi, D. Boltz, J.H. Kuhn, S.J. Elledge, S. Bavari, M.R. Denison, H. Choe, M. Farzan, Distinct patterns of IFITM-mediated restriction of filoviruses, SARS coronavirus, and influenza A virus, PLoS Pathog. 7 (2011) e1001258, , https://doi.org/10.1371/journal.ppat.1001258.

[35] R. Muñoz-Moreno, M.A. Cuesta-Geijo, C. Martinez-Romero, L. Barrado-Gil, I. Galindo, A. Garcia-Sastre, A. Covadonga, Antiviral role of IFITM proteins in African Swine Fever virus infection, PLoS One 11 (2016) e0154366, , https://doi.org/10.1371/journal.pone.0154366.

[36] T. Braulke, J.S. Bonifacino, Sorting of lysosomal proteins, Biochim. Biophys. Acta 1793 (2009) 605–614.

[37] M.A. Díaz-Salinas, L.A. Casorla, T. López, S. López, C.F. Arias, Most rotavirus strains require the cation-independent mannose-6-phosphate receptor, sortilin-1, and cathepsins to enter cells, Virus Res. 245 (2018) 44–51.

[38] Y. Chen, K.M. Honeychurch, G. Yang, C.M. Byrd, C. Harver, D.E. Hruby, R. Jordan, Vaccinia virus p37 interacts with host proteins associated with LE-derived transport vesicle biogenesis, Virol. J. 6 (2009) 44, https://doi.org/10.1186/1472-6769-9-2.

[39] M. Gary-Bobo, P. Nirdé, A. Jeanjean, A. Morère, M. Garcia, Mannose 6-phosphate receptor targeting and its applications in human diseases, Curr. Med. Chem. 14 (2007) 2945–2953.

[40] S. Dohgu, J.S. Ryerse, S.M. Robinson, W.A. Banks, Human immunodeficiency virus-1 uses the mannose-6-phosphate receptor to cross the blood-brain barrier, PLoS One

7 (2012) e39565, , https://doi.org/10.1371/journal.pone.0039565.

[41] M.F. Coutinho, M.J. Prata, S. Alves, A shortcut to the lysosome: the mannose-6-phosphate-independent pathway, Mol. Genet. Metab. 107 (2012) 257–266.

[42] J.M. Torres-Flores, D. Silva-Ayala, M.A. Espinoza, S. López, C.F. Arias, The tight junction protein JAM-A functions as coreceptor for rotavirus entry into MA104 cells, Virology 475 (2015) 172–178.

[43] J.M. Torres-Flores, C.F. Arias, Tight junctions go viral!, Viruses 7 (2015) 5145–5154.

[44] B. Vurusaner, P. Gamba, G. Testa, S. Gargiulo, F. Biasi, C. Zerbinati, L. Iuliano, G. Leonarduzzi, H. Basaga, G. Poli, Survival signaling elicited by 27-hydroxycholesterol through the combined modulation of cellular redox state and ERK/Akt phosphorylation, Free Radic. Biol. Med. 77 (2014) 376–385.

[45] B. Vurusaner, G. Leonarduzzi, P. Gamba, G. Poli, H. Basaga, Mol. Asp. Med. 49 (2016) 8–22.

3.3 Plants from Turkish flora as natural source of anti-rotavirus molecules

The study of medicinal plants as alternative source of novel active antiviral compounds has been deeply described in the 2.4 paragraph. We explored medicinal plants also against HRoV. In particular, we investigated the anti-HRoV action of the crude extracts of *Ballota macrodonta*, *Salvia cryptantha* and *Rindera lanata*, three plants from Turkish flora. *Rindera lanata* (Figure 9), the one exhibiting the more interesting antiviral action, belongs to the Boraginaceae family that counts about 2000 species in the world. The genus *Rindera* includes about 25 species distributed mainly in Central and Western Asia (76), four of which growing in Turkey, namely *R. lanata*, *R. caespiota*, *R. albida* and *R. dumani*. Rindera species are widely known as "Yünlü gelin" and used as an anti-inflammatory agent in Anatolian folk medicine (77) and to alleviate joint pains in Iranian folk medicine (78).

Figure 9: *Rindera Lanata* (Boraginaceae)

3.3.1 Publications

Civra A, Francese R, Sinato D, Donalisio M, Cagno V, Rubiolo P, Ceylan R, Uysal A, Zengin G, Lembo D. <u>In vitro screening for antiviral activity of Turkish plants revealing methanolic extract of Rindera lanata var. lanata active against human rotavirus.</u> BMC Complement Altern Med. 2017 Jan 24;17(1):74. doi: 10.1186/s12906-017-1560-3. PMID: 28118832; PMCID: PMC5260038.

This international study was performed in collaboration with researchers of Selcuk University, Konya, Turkey, and is the first paper that I ever published. With the view to discovering novel antiviral compounds against HRoV, we first screened *Ballota macrodonta*, *Salvia cryptantha* and *Rindera lanata* extracts by focus reduction assay and we reported that *Rindera lanata* methanolic extract was the one exerting the most interesting antiviral action. Furthermore, we demonstrated that

R. lanata extract targets the early steps of HRoV infection, likely by hampering virus penetration into the cells. The quantification of identified phenolic compounds in the methanol extract of *Rindera Lanata* by LC MS/MS revealed the presence of hesperidin, a phenolic compound already known to have anti-HRoV activity. Considering the favorable selectivity index and the anti-HRoV activity against multiple rotavirus strains, we concluded that the *R.lanata* extract is a promising starting material for a bioguided-fractionation aimed at identifying antiviral compounds.

CrossMark

In vitro screening for antiviral activity of Turkish plants revealing methanolic extract of *Rindera lanata* var. lanata active against human rotavirus

Andrea Civra[1], Rachele Francese[1], Davide Sinato[1], Manuela Donalisio[1], Valeria Cagno[1], Patrizia Rubiolo[2], Ramazan Ceylan[3], Ahmet Uysal[4], Gokhan Zengin[3] and David Lembo[1*]

Abstract

Background: Human rotavirus (HRoV) is the leading cause of severe gastroenteritis in infants and children under the age of five years. No specific antiviral drug is available for HRoV infections and the treatment of viral diarrhea is mainly based on rehydration and zinc treatment. In this study, we explored medicinal plants endemic to Turkey flora as a source of anti-HRoV compunds.

Methods: We performed an antiviral screening on *Ballota macrodonta*, *Salvia cryptantha* and *Rindera lanata* extracts by focus reduction assay. The extract with the highest selectivity index (SI) was selected; its antiviral activity was further confirmed against other HRoV strains and by virus yield reduction assay. The step of viral replicative cycle putatively inhibited was investigated by in vitro assays.

Results: The methanolic extract of *R. lanata* (Boraginaceae) showed the most favourable selectivity index. This extract exhibited a dose-dependent inhibitory activity against three different HRoV strains (EC_{50} values ranging from 5.8 μg/ml to 25.5 μg/ml), but was inactive or barely active against other RNA viruses, namely human rhinovirus and respiratory syncytial virus. The *R. lanata* extract targets the early steps of HRoV infection, likely by hampering virus penetration into the cells.

Conclusion: These results make the *R. lanata* methanolic extract a promising starting material for a bioguided-fractionation aimed at identifying anti-HRoV compounds. Further work is required to isolate the active principle and assess its clinical potential.

Background

Gastroenteritis accounts for almost 20% of the deaths of children under five years (National Collaborating Centre for Women's and Children's Health. 2012). Viruses cause approximately 70% of acute gastroenteritis, with rotavirus infection frequently implicated in cases that require hospitalization [1, 2]. Human rotavirus (HRoV, family Reoviridae, genus Rotavirus) is responsible for 114 million episodes of diarrhea, 25 million clinic visits, 2.4 million hospital admissions, and more than 500,000 deaths in children up to age 5 occur worldwide annually [3]. While most of the episodes are mild, about 10% of cases lead to dehydration requiring a doctor visit, and in resource-constrained nations, one in 250 children will die from this dehydration [4–7]. In Europe, HRoV infection accounts for more than 50% of hospitalizations for gastroenteritis and about one-third of emergency department visits [1, 4, 8]. At present, the treatment of viral diarrhea is based on fluid replacement and zinc treatment in order to prevent dehydration and to decrease the severity and duration. So far, no specific antiviral drug is available to treat HRoV infections. Discovering novel, safe and effective antiviral molecules is a difficult task. One strategy is to explore plants as a source of novel active compounds due to the

* Correspondence: david.lembo@unito.it
[1]Department of Clinical and Biological Sciences, University of Torino, S. Luigi Gonzaga Hospital, Regione Gonzole, 10, 10043 Orbassano, Torino, Italy
Full list of author information is available at the end of the article

Civra *et al. BMC Complementary and Alternative Medicine* (2017) 17:74

Page 2 of 8

large structural diversity of natural products. Indeed, several studies reported on anti-HRoV activity by plant extracts [9–14]. In this context, we performed an antiviral screening of three plants endemic to Turkey flora and here we report on the anti-HRoV activity of *Rindera lanata* (Boraginaceae). Boraginaceae is a plant family represented by about 2,000 species in the world [15]. The genus *Rindera* includes about 25 species distributed mainly in Central and Western Asia [16], four of which growing in Turkey, namely *R. lanata*, *R. caespiota*, *R. albida* and *R. dumani*. *Rindera* species are widely known as "Yünlü gelin" and used as an anti-inflammatory agent in Anatolian folk medicine [17]. *R. lanata* is used to alleviate joint pains in Iranian folk medicine [18]. However, to the best of our knowledge, *R. lanata* was neither traditionally used nor scientifically investigated for antiviral properties. The present study reports the anti-HRoV potency, the spectrum of antiviral activity, and the probable mechanisms of antiviral action of the *R. lanata* methanol extract.

Methods

Chemicals
Quinic acid (>98%), malic acid (>99%), cholorogenic acid (>95%), protocatechuic acid (>97%), caffeic acid (>98%), *p*-coumaric acid (>98%), rosmarinic acid (>96%), rutin (>94%), hesperidin (>97%) and hyperoside (>97%) were purchased from Sigma-Aldrich (Germany). Apigenin (>99%) and rhamnetin (>99%) were purchased from Fluka (Germany).

Plant material and extraction
Taxonomic identification of the plant materials were confirmed by the senior taxonomist Dr. Murad Aydin Sanda, from the Department of Biology, Selcuk University. The voucher specimens were deposited at the Konya Herbarium of Department of Biology, Selcuk University, Konya-Turkey. *Rindera lanata* (Lam.) Bunge var. *lanata* (Lam.) Bunge (family: Boraginaceae) was collected from Balcilar-Taskent, Konya-Turkey, May 2014, (Voucher No: GZ 1410). *Salvia cryptantha* Montbret et Aucher ex Bentham (family: Lamiaceae) was provided by Selcuk University, Aladdin Keykubat Campus, Yukselen village- Campus road, Konya-Turkey, June 2014, (Voucher No: GZ 1421). *Ballota macrodonta* Boiss. et Bal (family: Lamiaceae): was collected from Camardi, Mazmili Mountain, Nigde-Turkey, June 2014 (Voucher No: 1425).

The plant materials were dried at room temperature. The air-dried aerial parts (leaves, stem, flowers) were collected as a mix (10 g) and were macerated with 250 mL of methanol at room temperature for 24 h. Methanol was then removed with a rotary evaporator at 40 °C. The extracts were stored at +4 °C until analyzed.

Yield of these extracts were 17.83%, 14.86% and 4.90%, respectively.

For both cell viability assays and infectivity assays, the extracts were reconstituted in sterile methanol, to a concentration of 25 mg/ml. Every experiment was performed with freshly resuspended extracts.

LC-MS/MS analysis
LC-MS/MS analyses of the phenolic compounds were performed on a Shimadzu Nexera UHPLC system coupled to a triple quadrupole LC-MS8040 system equipped with an ESI source operating in both positive and negative ionization modes. The liquid chromatograph was equipped with LC-30 AD binary pumps, DGU-20A3R degasser, CTO-10ASvp column oven and SIL-30 AC autosampler. The chromatographic separation was performed on a C18 reversed-phase Inertsil ODS-4 (150 mm × 4.6 mm, 3 μm particle size, GL Sciences, The Netherlands) analytical column. The column was maintained at 40 °C. The elution gradient consisted of mobile phase with eluent A (water, 5 mM ammonium formate and 0.1% formic acid) and eluent B (methanol, 5 mM ammonium formate and 0.1% formic acid). The mobile phase gradient was as follows; from 40% to 90% eluent B in 20 min, then 90% B for 4 min. The flow rate of the mobile phase was 0.5 mL/min and the injection volume 4 μL.

MS conditions were: interface temperature; 350 °C, DL temperature; 250 °C, heat block temperature; 400 °C, nebulizing gas flow (Nitrogen); 3 L/min and drying gas flow (Nitrogen); 15 L/min. LC-MS/MS data were collected and processed by LabSolutions software (Shimadzu, Kyoto, Japan). The multiple reaction monitoring (MRM) mode was used to quantify the analytes by adopting two or three transitions per compound, the first one for quantitative purposes and the second and/or the third one for confirmation. These analytical conditions have been successfully used to analyze other plant matrices [19–21].

Cell lines and viruses
African green monkey kidney epithelial cells (MA104) and human epithelial adenocarcinoma HeLa cells (ATCC® CCL-2) were propagated in Dulbecco's Modified Eagle Medium (DMEM; Sigma, St. Louis, MO) supplemented with 1% (v/v) Zell Shield (Minerva Biolabs, Berlin, Germany) and heat inactivated, 10% (v/v) fetal bovine serum (Sigma). Human epithelial cells HEp-2 (ATCC® CCL-23) were grown as monolayers in Eagle's minimal essential medium (MEM) (Gibco/BRL, Gaithersburg, MD) supplemented with 10% FBS and 1% antibiotic-antimycotic solution. HRoV strains Wa (ATCC® VR-2018), HRoV 408 (ATCC® VR-2273) and DS-1 (ATCC® VR-2550) were purchased from ATCC; virus was activated with 5 μg/ml of porcine pancreatic

Civra *et al. BMC Complementary and Alternative Medicine* (2017) 17:74

Page 3 of 8

trypsin type IX (Sigma, St. Louis, Mo.) for 30 min at 37 °C and propagated in MA104 cells by using DMEM containing 0.5 μg of trypsin per ml as described previously [22]. Respiratory Syncytial Virus (RSV) strain A2 (ATCC® VR-1540) was propagated in HEp-2 and titrated by the indirect immunoperoxidase staining procedure using an RSV monoclonal antibody (Ab35958; Abcam, Cambridge, United Kingdom) as described previously [23]. Human rhinovirus (HRhV) 1A (ATCC® VR-1559) was cultured in HeLa cells, at 34 °C, in a humidified 5% CO_2 incubator. When the full cytopathic effect (CPE) developed, cells and supernatants were harvested, pooled, frozen and thawed three times, clarified and stored at –70 °C. HRhV titers were determined by the standard plaque method as described previously [22].

Cell viability assay

Cells were seeded at a density of 5×10^3/well in 96-well plates and treated the following day with serially-diluted methanol extracts of *B. macrodonta*, *S. cryptantha* or *R. lanata* (1.2 μg/ml to 1666 μg/ml) to generate dose–response curves. Control wells (100% of viability) were prepared by treating cells with equal volumes of methanol, corresponding to 6.7% (v/v) to 0.0048% (v/v) in cell media. After 24 h of incubation, cell viability was determined using the CellTiter 96 Proliferation Assay Kit (Promega, Madison, WI, USA), and following the manufacturer's instructions. Absorbances of both treated (Abs_T) and untreated (Abs_{METH}) samples were measured using a Microplate Reader (Model 680, BIORAD) at 490 nm. The % of cell viability was calculated according to the following formula: (Abs_T X 100)/Abs_{METH}. The 50% cytotoxic concentration (CC_{50}) was determined using logarithmic viability curves. Where possible, a selectivity index (SI) was calculated by dividing the CC_{50} by the EC_{50} value.

Rotavirus inhibition assays

The anti-HRoV efficacy of methanol extracts of *B. macrodonta*, *S. cryptantha* and *R. lanata* was determined by focus reduction assay. Assays of inhibition of rotavirus infectivity were carried out with confluent MA104 cell monolayers plated in 96-well trays, as described elsewhere [22]. Cells were treated for 2 h at 37 °C with methanol extract of *R. lanata*, at concentrations ranging from 1.2 to 300 μg/ml in serum-free medium prior to virus addition. HRoV infection was performed at a multiplicity of infection (MOI) of 0.02 for 1 h at 37 °C, in presence of the methanol extract unless otherwise stated. Infected cells were washed with serum-free medium, fresh methanol extract was added, and cells were incubated in this medium at 37 °C in a humidified incubator in 5% (vol/vol) CO_2–95% (vol/vol) air. For time of addition assays, serial dilutions of extracts were added on cells alternatively 2 h before infection or during infection or post infection.

Control samples were prepared by treating cells with culture medium supplemented with equal volumes of methanol and taken as 100% of infection. After 16 h of incubation, infected cells were fixed with cold acetone-methanol (50:50), and viral titers determined by indirect immunostaining by using a mouse monoclonal antibody directed to human rotavirus VP6 (0036; Villeurbanne, France), and the secondary antibody peroxidase-conjugated AffiniPure F(ab')$_2$ Fragment Goat Anti-Mouse IgG (H + L) (Jackson ImmunoResearch Laboratories Inc., 872 W. Baltimore Pike, West Grove, PA 19390). Blockade of viral infectivity is expressed as mean % ± SD. Where possible, anti-viral effective concentration (EC_{50}) values were calculated by regression analysis using the dose–response curves generated from the experimental data, using PRISM 4 (GraphPad Software, San Diego, CA, U.S.A.).

RSV inhibition assay

HEp-2 cells were first seeded (at 8×10^3 cells/well) in 96 well plate. The methanol extract of *R. lanata* was serially diluted in medium (from 300 to 0.4 μg/ml) and incubated with cells for 2 h at 37 °C, then mixtures of extracts and virus (MOI 0.01) were added to cells to allow the viral adsorption for 3 h at 37 °C; the monolayers were then washed and overlaid with 1.2% methylcellulose medium containing serial dilutions of extract. Control wells (100% of infection) were prepared by treating cells with equal volumes of methanol. Three days post-infection, cells were fixed with cold methanol and acetone (50:50) for 1 min and subjected to RSV-specific immunostaining. Immunostained plaques were counted, and the percent inhibition of virus infectivity was determined by comparing the number of plaques in treated wells with the number in untreated control wells.

Rhinovirus inhibition assay

HeLa cells were first seeded (at 8×10^4 cells/well) in 24 well plates. 24 h later the methanol extract of *R. lanata* was serially diluted in medium (from 300 μg/ml to 0.4 μg/ml) and added to cell monolayers. After 2 h of incubation (37 °C, 5% CO_2), medium was removed and infection was performed with 200 μL/well with HRhV 1A (MOI 0.0002) and different concentrations of the extract. The infected cells were incubated at 34 °C for 1 h, then washed with medium, and overlaid with a 1:1 combination of 1.6% SeaPlaque Agarose and 2X DMEM containing the extract. Control wells (100% of infection) were prepared by treating cells with equal volumes of methanol. The plates were incubated at 34 °C for 3 days. After incubation, the plates were fixed with 7.5% formaldehyde (Fluka) and stained with crystal violet (Sigma, St. Louis, Mo.). The number of plaques formed was counted.

Civra *et al. BMC Complementary and Alternative Medicine* (2017) 17:74

Page 4 of 8

Assay of rotavirus yield

To test the ability of *R. lanata* extract to inhibit multiple cycles of HRoV replication, confluent MA104 cells in 24-well trays were infected with trypsin-activated Wa rotavirus (MOI 0.02) for 1 h at 37 °C and washed as above. Cells were incubated in medium supplemented with 0.5 μg/ml porcine trypsin and 1.2, 3.6, 11, 33, 100, 300 μg/ml of *R. lanata* extract. Infected cells and cell supernatants were harvested at 48 h post infection and virus titers determined by indirect immunostaining of MA104 cell monolayers inoculated with serial dilutions of the samples. The assay was performed in triplicate. One-way analysis of variance (ANOVA), followed by the Bonferroni test, was used to assess the statistical significance of differences in virus titers. Significance was set at 95% level.

Virus inactivation assay

Trypsin-activated HRoV Wa was incubated for 2 h at 4 °C in presence of 100 μg/ml of *R. lanata* extract. After this incubation, both treated and untreated viruses were titrated. Viral yields were determined by indirect immunostaning, by counting the number of infective events at dilutions at which the extract was no more active (i.e. 1:1024, 1:2048, 1:4096).

Entry assays

In order to test the effect of *R. lanata* methanol extract on the rotavirus-cell penetration process, an entry assay was performed. Briefly, MA104 cells were cultured to confluence in 96-well trays; cells were washed twice with DMEM and then cooled on ice for 20 min. Activated virus, which had been cooled to 4 °C, was allowed

Table 1 Antiviral activity of *R. lanata*, *B. macrodonta* and *S. cryptantha* methanolic extract against HRoV Wa

HRoV strain	Source	EC50[a] (μg/ml) – 95% C.I.[b]	CC50[c](μg/ml)	SI[d]
Wa	*Salvia cryptantha*	16.3 (9.0–29.6)	134.8	8.3
	Ballota macrodonta	8.1 (6.9–9.7)	445.5	55
	Rindera lanata	5.8 (4.6–7.2)	1179	205

[a]EC$_{50}$ half maximal effective concentration
[b]C.I. confidence interval
[c]CC$_{50}$ half maximal cytotoxic concentration
[d]SI selectivity index

to attach to cells on ice for 1 h at 4 °C, at a MOI of 0.02. Cells were washed three times, then *R. lanata* methanol extract was added to the cells (at concentrations ranging from 1.2 μg/ml to 300 μg/ml) and virus particles were allowed to penetrate inside cells for 1 h at 37 °C. The entry of the viral particles was stopped with two quick washes with 3 mM EGTA in PBS, which releases the outer layer of the virions and causes the particles to detach from the cell surface [24, 25]; finally, cells were incubated with warm DMEM. After 16 h, cells were fixed and blockade of virus entry were determined by focus reduction assay as described above, and expressed as mean percentages of untreated control ± SEM. Significant differences were assessed by one way ANOVA, using PRISM 4 (GraphPad Software, San Diego, California, USA).

Rotavirus cell-binding assay

Confluent MA104 cell monolayers in 24-well trays were washed, incubated with *R. lanata* methanol extract for 2 h at 37 °C and cooled on ice for 20 min in the continuing presence of the extract. Trypsin-activated virus,

Table 2 Quantification of identified phenolic compounds in methanol extract of *Rindera lanata* by LC ESI MS/MS in negative ionization mode

Analytes	RT	[M-H]⁻(m/z)	MS^2 (m/z)	Equation	Amount[a]
Quinic acid	3.36	190.95	85, 93	$f(x) = 33.66x + 25133$	2318.60 ± 111.29
Malic acid	3.60	133.05	115, 71	$f(x) = 93.61x-5673$	9381.66 ± 497.23
Chlorogenic acid	5.29	353	191	$f(x) = 48.98x + 26780$	23.63 ± 1.16
Protocatechuic acid	5.51	152.95	109, 108	$f(x) = 36.86x + 6197$	32.3 ± 1.65
Caffeic acid	7.11	178.95	135, 134, 89	$f(x) = 1585x + 83958$	13.53 ± 0.70
p-Coumaric acid	9.17	162.95	119, 93	$f(x) = 73.53x + 27064$	173.59 ± 8.85
Rosmarinic acid	9.19	358.9	161, 133	$f(x) = 18.02x + 1149$	706.38 ± 34.61
Rutin	9.67	609.1	300, 271, 301	$f(x) = 51.88 + 3841$	101.89 ± 5.09
Hesperidin	9.69	611.1	303, 465	$f(x) = 1975.77 + 105641$	399.74 ± 19.59
Hyperoside	9.96	463.1	300, 301	$f(x) = 0.98x + 827$	118.00 ± 5.78
Apigenin	16.73	268.95	151, 117	$f(x) = 543.79 + 18525$	0.10 ± 0.005
Rhamnetin	18.41	314.95	165, 121, 300	$f(x) = 110.09 + 632.44$	0.23 ± 0.014

RT: Retention time
[M-H]⁻: Deprotonated ions of the standard compounds
MS^2: MRM fragments for the related molecular ions
[a]Values in μg/g (w/w) of plant methanol extract

Civra *et al. BMC Complementary and Alternative Medicine* (2017) 17:74

Page 5 of 8

which had been cooled to 4 °C, was allowed to attach to cells on ice for 1 h (MOI = 3) in presence of *R. lanata* methanol extract. Cells were washed with cold DMEM, followed by addition of cold DMEM. Cells were subjected to two rounds of freeze-thawing, incubated at 37 °C for 30 min with 10 μg/ml porcine trypsin to release bound virus, and the lysate clarified by low speed centrifugation for 10 min. Cell-bound virus titers were determined by indirect immunostaining as above. Significant differences were assessed by Student's *t*-test, using PRISM 4 (GraphPad Software, San Diego, California, USA).

Results

R. lanata methanolic extract is endowed with anti-HRoV activity

In a first set of experiments, we tested the anti-HRoV activity of *R. lanata*, *B. macrodonta* and *S. cryptantha* methanolic extracts against HRoV Wa. Results depicted in Table 1 show that all the methanolic extracts were endowed with anti-HRoV activity, with EC_{50}s ranging from 5.8 to 16.3 μg/ml. To exclude the possibility that the antiviral activity might depend on a cytotoxic effect, cell viability assays were performed on uninfected cells, challenged with the extracts under the same conditions as the antiviral assays. Control wells were prepared by treating cells with equal volumes of methanol, corresponding to 6.7% (v/v) to 0.0048% (v/v) in cell media: these low volumes of methanol were non cytotoxic and did not influence viral replication (data not shown). As shown in Table 1, *R. lanata* showed the most favourable selectivity index (SI), i.e. 205. Therefore, we focused our research on *R. lanata* methanolic extract. Firstly, we performed LC-MS/MS analysis to identify and quantify phenolic components that characterize *R. lanata* methanolic extract, in order to make sure of the reproducibility of our study and to ensure that the results of future studies will be comparable to the ones of this research. The LC-MS/MS analysis allowed to identify and quantify twelve phenolic compounds in *R. lanata* methanolic extract and the results are listed in Table 2. Malic acid (9381.66 μg/g extract) and quinic acid (2318.60 μg/g) were found to be major phenolic component followed by rosmarinic acid (706.38 μg/g) hesperidin (399.74 μg/g

extract), *p*-coumaric acid (173.59 μg/g extract), and hyperoside (118.00 μg/g extract). In accordance with these results, *R. lanata* belongs to the Boraginaceae family, characterized by the presence of rosmarinic acid and related components [26]

To assess the spectrum of anti-HRoV activity, the extract was tested against two additional HRoV strains, namely HRoV 408 and DS-1. The results reported in Table 3 clearly show that the extract was effective in inhibiting the infectivity of both strains tested, although to a different extent, with EC_{50} values of 25.5 μg/ml and 14.3 μg/ml respectively. The specificity of the anti-HRoV activity was assessed by performing antiviral assays against two unrelated viruses, namely the rhinovirus (HRhV) and the respiratory syncytial virus (RSV). These were selected for being both RNA viruses as HRoV and representative of naked (HRhV) or enveloped (RSV) viruses. The methanolic extract of *R. lanata* did not show any antiviral activity against HRhV (Table 4) while it was possible to calculate an EC_{50} against RSV (45.3 μg/ml). However, the selectivity index was very low (4), suggesting that the anti-RSV activity was mainly an expression of a cytotoxic effect (Table 4). Taken together, the results presented so far demonstrate

Table 4 Antiviral activity of *R. lanata* methanolic extract against HRhV 1A and RSV A2

Virus	EC_{50}^a (μg/ml) – 95% C.I.[b]	CC_{50}^c(μg/ml)	SI^d
HRhV 1A	n.a.	804.3	n.a.
RSV A2	45.28 (30.20–67.88)	183.9	4.1

[a]EC50 half maximal effective concentration
[b]C.I. confidence interval
[c]CC50 half maximal cytotoxic concentration
[d]SI selectivity index
n.a. not assessable

Table 3 Antiviral activity of *R. lanata* methanolic extract against HRoV strains

HRoV strain	EC_{50}^a (μg/ml) – 95% C.I.[b]	CC_{50}^c(μg/ml)	SI^d
HRoV408	25.5 (15.6–41.6)	1179	46
DS-1	14.3 (6.7–30.2)	1179	83

[a]EC$_{50}$ half maximal effective concentration
[b]C.I. confidence interval
[c]CC$_{50}$ half maximal cytotoxic concentration
[d]SI selectivity index

Fig. 1 Effect of methanol extract of *R. lanata* on multiple cycles of HRoV-Wa replication. Cells were treated after virus infection at the given concentrations. The titer of HRoV in the treated samples is expressed as focus-forming units per ml (FFU/ml). Error bars represent the SD of the mean of 3 independent experiments. One-way analysis of variance (ANOVA), followed by the Bonferroni test, was used to assess the statistical significance of differences in virus titers. Significance was set at the 95% level. *$p < 0.05$; ***$p < 0.001$

Civra *et al. BMC Complementary and Alternative Medicine* (2017) 17:74

Page 6 of 8

Fig. 2 Time-of-addition experiments were performed by treating cells with *R. lanata* methanolic extract for 2 h before infection (*B*), for 1 h during infection (*C*) or immediately after infection (*D*). Control experiments were performed by treating cells both before and during viral inoculum (*A*). The infectivity titers of virus in the treated samples are expressed as a percentage of the titer obtained in theuntreated control. Error bars represent the SD of the mean of 3 independent experiments
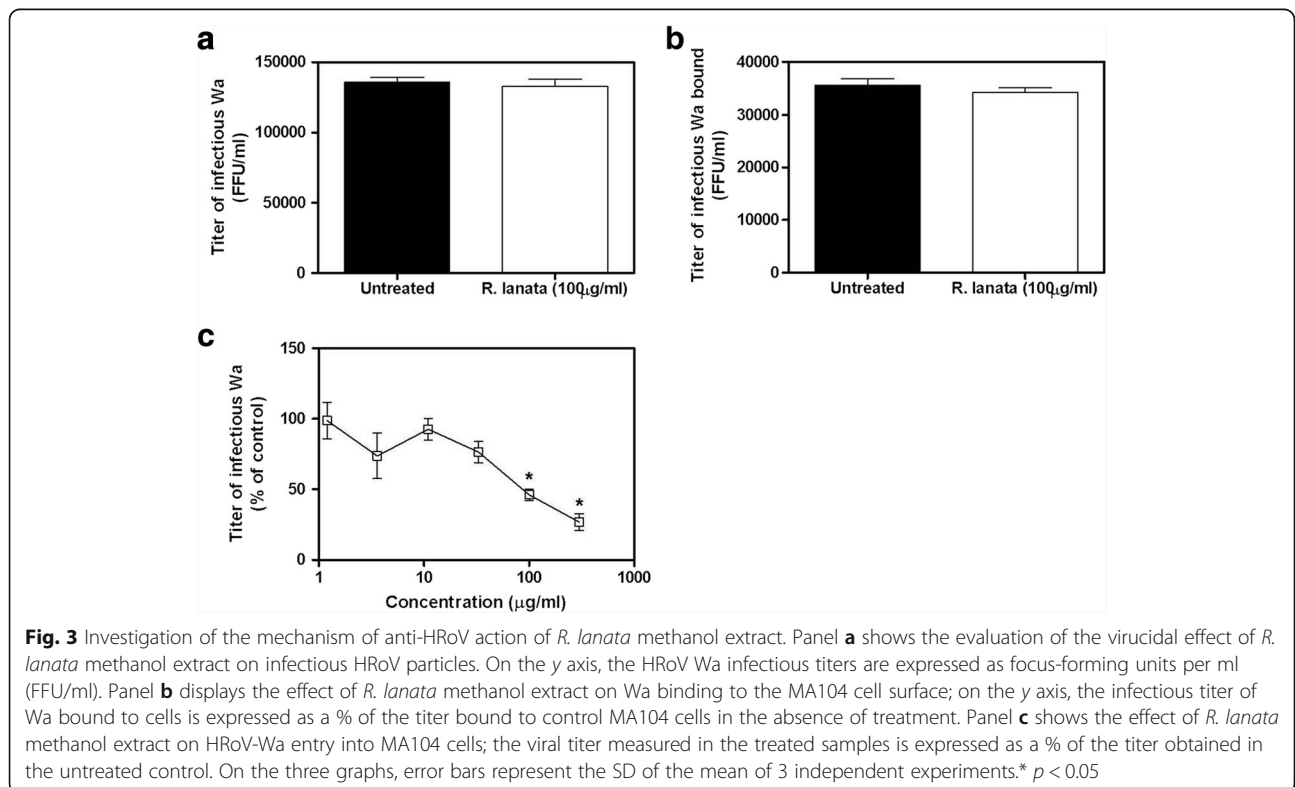
that the *R. lanata* methanolic extract exerts a specific anti-HRoV effect which is not strain restricted.

To investigate further the extract antiviral efficacy, a virus yield reduction assay was performed by treating cells after viral inoculum, and titrating viral progeny. We chose this experimental setting because represents a stringent kind of test, allowing multiple cycles of

replication to occur before measuring antiviral activity. Figure 1 shows that the extract significantly ($0.001 < p_{ANOVA} < 0.05$) reduced the titer of HRoV progeny in a dose-dependent manner. This result confirms that *R. lanata* methanolic extract affects HRoV replication, likely by targeting a specific step of viral replication.

R. lanata methanolic extract inhibits viral infectivity by targeting the early steps of viral infection

To investigate the step of viral replication inhibited by the extract, we performed time of addition assays by treating cells with serial dilutions of extract 2 h before infection or during infection or post-infection. The results, depicted in Fig. 2, show that the first two treatment protocols were active while the latter was not, suggesting a probable activity of the extract on the early steps of HRoV infection. To explore this hypothesis, more stringent tests were performed to assess the putative target of the extract (i.e. the viral particle or the virus-cell interactions). Firstly, we assessed the extract ability to directly inactivate the virus particle by incubating HRoV with a high concentration (100 μg/ml) of methanolic extract and then measuring the viral titer at dilutions corresponding at concentrations that are not antiviral when added on cells. Results depicted in Fig. 3a demonstrate that the methanolic extract did not inactivate the virus particles. Having excluded the virus particle as a target of the antiviral activity of the extract, we explored the possibility that the interaction between

Fig. 3 Investigation of the mechanism of anti-HRoV action of *R. lanata* methanol extract. Panel **a** shows the evaluation of the virucidal effect of *R. lanata* methanol extract on infectious HRoV particles. On the *y* axis, the HRoV Wa infectious titers are expressed as focus-forming units per ml (FFU/ml). Panel **b** displays the effect of *R. lanata* methanol extract on Wa binding to the MA104 cell surface; on the *y* axis, the infectious titer of Wa bound to cells is expressed as a % of the titer bound to control MA104 cells in the absence of treatment. Panel **c** shows the effect of *R. lanata* methanol extract on HRoV-Wa entry into MA104 cells; the viral titer measured in the treated samples is expressed as a % of the titer obtained in the untreated control. On the three graphs, error bars represent the SD of the mean of 3 independent experiments.* $p < 0.05$

Civra *et al. BMC Complementary and Alternative Medicine* (2017) 17:74

Page 7 of 8

the viral particles and the cell surface could be affected by the extract. To this aim HRoV-cell binding assays were performed. The results (Fig. 3b) demonstrate that the treatment did not reduce significantly ($p > 0.05$) the titer of virus particles bound to the surface of treated cells, thus suggesting that inhibition occurs at a post-binding stage. To verify this hypothesis, entry assays were performed by treating cells during virus penetration. Figure 3c shows that the *R. lanata* methanolic extract significantly reduced HRoV infectivity in a dose-dependent manner when added immediately after the virus-cell attachment step (i.e. during cell penetration).

Discussion

Several recent studies demonstrate that plant extracts are deeply explored for their antiviral potential against HRoV [9–14, 27–29].

In this study we show that the methanolic extract of *R. lanata* is endowed with anti-HRoV activity. Although several molecules inside this crude extract can contribute to its effect, each one acting through a specific mechanism, some preliminary conclusions can be drawn on the main mechanism of antiviral action. The treatment with the methanolic extract of *R. lanata* does not alter the ability of HRoV to attach on the host cell surface, as shown by the results of the binding experiments; moreover, the results of the virus inactivation assays rule out a direct antiviral effect of any component of *R. lanata* methanolic extract. By contrast, the results suggest that inhibition takes place at a post-attachment stage, since no antiviral effect is shown when the methanolic extract is added on cells 1 h after the viral inoculum (Fig. 2) - i.e. when the entry process already started and the 30% of the inoculated HRoV particles already entered inside cells [30]. Nevertheless, since the inhibition of entry is not complete it is likely that other, yet unidentified mechanisms, contribute to the overall antiviral activity of the extract. Of note, cells pre-treatment with the extract affects their susceptibility to the HRoV infection (Fig. 2) suggesting that the extract may target cellular functions required for virus replication. Among the major phenolic compounds present in the methanol extract of *R. lanata* hesperidin is known to a have anti-HRoV activity [31] and might be responsible, at least in part, to the anti-HRoV effect of the extract.

Conclusion

In conclusion, the favorable selectivity index and the anti-HRoV activity against multiple viral strains make the *R.lanata* extract a promising starting material for a bioguided-fractionation aimed at identifying anti-HRoV compounds. Further work remains to be done in order to isolate the active principle, elucidate its mechanism of action and assess its clinical potential.

Authors' information

AC is post doctoral fellow researcher working in the Laboratory of Molecular Virology, University of Turin, Italy.
RF and DS are post graduate researchers working in the Laboratory of Molecular Virology, University of Turin, Italy.
GZ is a research assistant working at the University of Selcuk.
AU is an assistant Professor working at the University of Selcuk.
RC is a phD student working at the University of Selcuk.
MD is an assistant Professor working in the Laboratory of Molecular Virology, University of Turin, Italy.
VC is post doctoral fellow researcher working in the Laboratory of Molecular Virology, University of Turin, Italy.
PR is Professor, Senior lecturer working in the Laboratory of Phytoanalysis at the Department of Drug Science and Technology, University of Turin, Italy.
DL is Professor, Head of the Laboratory of Molecular Virology, University of Turin, Italy. He is also Donalisio's, Civra's, Cagno's, Francese's and Sinato's research supervisor.

Competing interests

The authors declare that they have no competing interests.

Consent for publication

Not applicable.

Ethics approval and consent to participate

This information is not relevant for the study.

Author details

[1]Department of Clinical and Biological Sciences, University of Torino, S. Luigi Gonzaga Hospital, Regione Gonzole, 10, 10043 Orbassano, Torino, Italy. [2]Dipartimento di Scienza e Tecnologia del Farmaco, Università degli Studi di Torino, 10125 Torino, Italy. [3]Department of Biology, Science Faculty, Selcuk University, Konya, Turkey. [4]Deparment of Medicinal Laboratory, Vocational School of Health Services, Selcuk University, Konya, Turkey.

Civra *et al. BMC Complementary and Alternative Medicine* (2017) 17:74

Page 8 of 8

References

1. Guarino A, Dupont C, Gorelov AV, Gottrand F, Lee JK, Lin Z, Lo Vecchio A, Nguyen TD, Salazar-Lindo E. The management of acute diarrhea in children in developed and developing areas: from evidence base to clinical practice. Expert Opin Pharmacother. 2012;13:17–26.
2. Albano F, Bruzzese E, Bella A, Cascio A, Titone L, Arista S, Izzi G, Virdis R, Pecco P, Principi N, Fontana M, Guarino A. Rotavirus and not age determines gastroenteritis severity in children: a hospital-based study. Eur J Pediatr. 2007;166:241–7.
3. Kotloff KL, Nataro JP, Blackwelder WC, Nasrin D, Farag TH, Panchalingam S, Wu Y, Sow SO, Sur D, Breiman RF, Faruque AS, Zaidi AK, Saha D, Alonso PL, Tamboura B, Sanogo D, Onwuchekwa U, Manna B, Ramamurthy T, Kanungo S, Ochieng JB, Omore R, Oundo JO, Hossain A, Das SK, Ahmed S, Qureshi S, Quadri F, Adegbola RA, Antonio M, Hossain MJ, Akinsola A, Mandomando I, Nhampossa T, Acácio S, Biswas K, O'Reilly CE, Mintz ED, Berkeley LY, Muhsen K, Sommerfelt H, Robins-Browne RM, Levine MM. Burden and aetiology of diarrhoeal disease in infants and young children in developing countries (the Global Enteric Multicenter Study, GEMS): a prospective, case–control study. Lancet. 2013;382:209–22.
4. Forster J, Guarino A, Parez N, Moraga F, Román E, Mory O, Tozzi AE, de Aguileta A, Wahn U, Graham C, Berner R, Ninan T, Barberousse C, Meyer N, Soriano-Gabarró M, Rotavirus Study Group. Hospital-based surveillance to estimate the burden of rotavirus gastroenteritis among European children younger than 5 years of age. Pediatrics. 2009;123:393–400.
5. Parashar UD, Gibson CJ, Bresee JS, Glass RI. Rotavirus and severe childhood diarrhea. Emerg Infect Dis. 2006;2:304–6.
6. de Rougemont A, Kaplon J, Pillet S, Mory O, Gagneur A, Minoui-Tran A, Meritet JF, Mollat C, Lorrot M, Foulongne V, Gillet Y, Nguyen-Bourgain C, Alain S, Agius G, Lazrek M, Colimon R, Fontana C, Gendrel D, Pothier P, French Rotavirus Network. Molecular and clinical characterization of rotavirus from diarrheal infants admitted to pediatric emergency units in France. Pediatr Infect Dis J. 2011;30:118–24.
7. Palumbo E, Branchi M, Malorgio C, Siani A, Bonora G. Diarrhea in children: etiology and clinical aspects. Minerva Pediatr. 2010;62:347–51.
8. Guarino A, Ansaldi F, Ugazio A, Chiamenti G, Bona G, Correra A, Di Pietro P, Mele G, Sapia MG, Società Italiana di Pediatria. [Italian Pediatrician's consensus statement on anti-Rotavirus vaccines]. Minerva Pediatr. 2008;60:3–16.
9. Alfajaro MM, Kim HJ, Park JG, Ryu EH, Kim JY, Jeong YJ, Kim DS, Hosmillo M, Son KY, Lee JH, Kwon HJ, Ryu YB, Park SJ, Park SI, Lee WS, Cho KO. Anti-rotaviral effects of Glycyrrhiza uralensis extract in piglets with rotavirus diarrhea. Virol J. 2012;9:310.
10. Cecílio AB, de Faria DB, Oliveira Pde C, Caldas S, de Oliveira DA, Sobral ME, Duarte MG, Moreira CP, Silva CG, de Almeida VL. Screening of Brazilian medicinal plants for antiviral activity against rotavirus. J Ethnopharmacol. 2012;14:975–81.
11. Gonçalves JL, Lopes RC, Oliveira DB, Costa SS, Miranda MM, Romanos MT, Santos NS, Wigg MD. In vitro anti-rotavus activity of some medicinal plants used in Brazil against diarrhea. J Ethnopharmacol. 2005;99:403–7.
12. Knipping K, Garssen J, Van't Land B. An evaluation of the inhibitory effects against rotavirus infection of edible plant extracts. Virol J. 2012;9:137.
13. Roner MR, Tam KI, Kiesling-Barrager M. Prevention of rotavirus infections in vitro with aqueous extracts of Quillaja Saponaria Molina. Future Med Chem. 2013;2:1083–97.
14. Téllez MA, Téllez AN, Vélez F, Ulloa JC. In vitro antiviral activity against rotavirus and astrovirus infection exerted by substances obtained from Achyrocline bogotensis (Kunth) DC. (Compositae). BMC Complement Altern Med. 2005;15:428.
15. Ozcan T. Analysis of the total oil and fatty acid composition of seeds of some Boraginaceae taxa from Turkey. Plant Syst Evol. 2008;274:143–53.
16. Bigazzi M, Nardi E, Selvi F. Palynological Contribution to the Systematics of Rindera and the Allied Genera Paracaryum and Solenanthus (Boraginaceae-Cynoglosseae). Willdenowia 2006;36:37–46.
17. Altundag E, Ozturk M. Ethnomedicinal studies on the plant resources of east Anatolia, Turkey. Procedia Soc Behav Sci. 2001;19:756–77.
18. Mosaddegh M, Naghibi F, Moazzeni H, Pirani A, Esmaeili S. Ethnobotanical survey of herbal remedies traditionally used in Kohghiluyeh va Boyer Ahmad province of Iran. J Ethnopharmacol. 2012;141:80–95.
19. Ertaş A, Bog AM, Yılmaz MA, Yeşil Y, Aşimi N, Kaya MS, Temel H, Kolak U. Chemical compositions by using LC-MS/MS and GC-MS and biological activities of Sedum sediforme (Jacq.) Pau. J Agric Food Chem. 2014;62:4601–9.
20. Ertas A, Bog AM, Yilmaz MA, Yesil Y, Tel G, Temel H, Hasimi N, Gazioglu I, Ozturk M, Ugurlu P. A detailed study on the chemical and biological profiles of essential oil and methanol extract of Thymus nummularius (Anzer tea): Rosmarinic acid. Ind Crops Prod. 2005;67:336–45.
21. Ceylan R, Kathanic J, Zengin G, Matic S, Aktumsek A, Borojab T, Stanic S, Mihailovic V, Gulerd OG, Boga M, Yılmazf MA. Chemical and biological fingerprints of two Fabaceae species (Cytisopsis dorycniifolia and Ebenus hirsuta): Are they novel sources ofnatural agents for pharmaceutical and food formulations? Ind Crops Prod. 2016;84:254–62.
22. Civra A, Cagno V, Donalisio M, Biasi F, Leonarduzzi G, Poli G, Lembo D. Inhibition of pathogenic non-enveloped viruses by 25-hydroxycholesterol and 27-hydroxycholesterol. Sci Rep. 2014;4:7487.
23. Cagno V, Donalisio M, Civra A, Volante M, Veccelli E, Oreste P, Rusnati M, Lembo D. Highly sulfated K5 Escherichia coli polysaccharide derivatives inhibit respiratory syncytial virus infectivity in cell lines and human tracheal-bronchial histocultures. Antimicrob Agents Chemother. 2014;58:4782–94.
24. Cohen J, Laporte J, Charpilienne A, Scherrer R. Activation of rotavirus RNA polymerase by calcium chelation. Arch Virol. 1979;60:177–86.
25. Estes MK, Graham DY, Smith EM, Gerba CP. Rotavirus stability and inactivation. J Gen Virol. 1979;43:403–9.
26. Petersen M. Rosmarinic acid: new aspects. Phytochem Rev. 2013;12:207–27.
27. Sun Y, Gong X, Tan JY, Kang L, Li D, Vikash, Yang J, Du G. In vitro Antiviral Activity of Rubia cordifolia Aerial Part Extract a Rotavirus. Front Pharmacol. 2016 Sep 13;7:308
28. Alfajaro MM, Rho MC, Kim HJ, Park JG, Kim DS, Hosmillo M, Son KY, Lee JH, Park SI, Kang MI, Ryu YB, Park KH, Oh HM, Lee SW, Park SJ, Lee WS, Cho KO. Anti-rotavirus effects by combination therapy of stevioside and Sophora flavescens extract. Res Vet Sci. 2014;96(3):567–75.
29. Chingwaru W, Majinda RT, Yeboah SO, Jackson JC, Kapewangolo PT, Kandawa-Schulz M, Cencic A. Tylosema esculentum (marama) tuber and bean extracts Are strong antiviral agents against rotavirus infection. Evid Based Complement Alternat Med. 2011;2011:284795.
30. Gutiérrez M, Isa P, Sánchez-San Martin C, Pérez-Vargas J, Espinosa R, Arias CF, López S. Different rotavirus strains enter MA104 cells through different endocytic pathways: the role of clathrin-mediated endocytosis. J Virol. 2010;84:9161–9.
31. Bae EA, Han MJ, Lee M, Kim DH. In vitro inhibitory effect of some flavonoids on rotavirus infectivity. Biol Pharm Bull. 2000;23:1122–4.

4. INNOVATIVE ANTIVIRAL AIR FILTERS IN THE FIGHTING AGAINST RESPIRATORY VIRUSES

4.1 Respiratory viruses of interest

Acute upper and lower respiratory infections are a major public health problem and a leading cause of morbidity and mortality worldwide. At greatest risk are young children, the elderly, the chronically ill, and the immunosuppressed subjects. A range of different viruses can cause respiratory tract infections and the most important are influenza viruses (FluV), respiratory syncytial virus (RSV), parainfluenza virus (HPIV), metapneumovirus (HMPV), rhinoviruses (HRhV), adenovirus and the emerging coronavirus SARS-CoV 2. (79)

These viruses, which have a nanometer size, can be transmitted through three different transmission routes: contact (direct or indirect), droplet and aerosol transmission. Contact transmission refers to direct virus transfer from an infected person to a susceptible individual (i.e., via contaminated hands) or indirect virus transfer via intermediate objects. Transmission of virus through the air can occur via droplets or aerosols that are generated during coughing, sneezing or talking. Droplets (> 5 µm in diameter) remain only shortly in air and they can be dispersed over short distances (<1 m) contaminating surfaces and objects. Aerosols (droplet nuclei < 5 µm in diameter) have a slow settling velocity, thus they remain suspended in the air longer and they can be dispersed over long distances. Transmission via each of these three routes is complex and depends on many variables such as environmental factors (e.g., humidity and temperature), crowding of people, but also on host factors such as receptor distribution throughout the respiratory tract. Differences in virus shedding between individuals also contribute to the transmissibility rate, especially in the case of superspreaders (80).

Viruses are now recognized as common causal pathogens in severe disease. Recent systematic reviews and meta-analyses, performed before the current COVID19 pandemic, revealed that in adults, 25% of patients with community-acquired pneumonia was viral. This percentage is higher in children under 5, due to the large proportion of cases caused by RSV. In adults, the contributions of identified viral etiologies were 8% for influenza viruses, 6% for rhinoviruses, 3% for coronaviruses, and 2% for RSV. In children under 5 with low respiratory tract infections, strong causal associations for RSV, influenza viruses, parainfluenza viruses and HMPV were found in comparison with healthy controls, and less so for adenoviruses, bocaviruses, and coronaviruses (81,82).

During my PhD course, I focused my attention on three respiratory viruses, the RSV, the FluV and the HRhV. They were selected as representative members of the respiratory virus category. In the last months of the fourth year, I also started to investigate new antiviral approaches against human coronaviruses. The main characteristics of the three viruses are described below.

The *Human Respiratory Syncytial Virus (RSV)* belongs to the *Paramyxiviridae* family and to the genus *Pneumovirus.* It is an enveloped, negative sense, single stranded RNA virus. The structure of RSV consists of a bilipid-layer-envelope surrounding a ribonucleoprotein core, with several membrane proteins, one of which functions in attachment to host cells (G protein), and one of which functions in fusion to host cells (F protein). There is only one serotype of RSV, but it is classified into two strains, "A" and "B," with differences consisting of variation in the structure of several structural membrane proteins, most especially the attachment protein. The virion structure and the steps of viral replicative cycle necessary for the understanding of our publications are schematically presented in Figure 10.
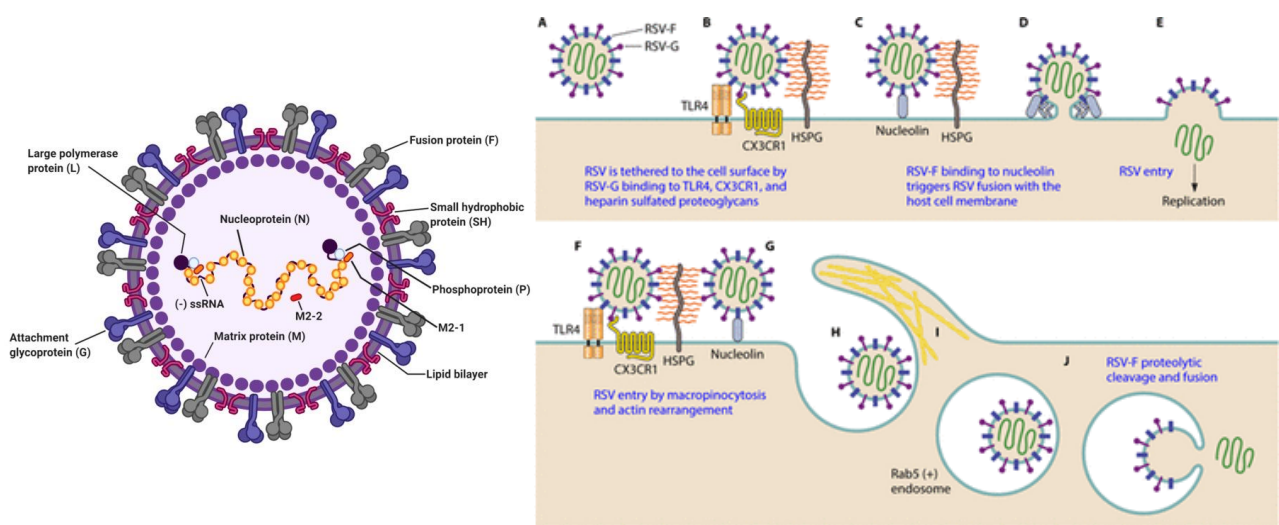

Figure 10: The RSV virion (100–350 nm in diameter) consists of a nucleocapsid packaged in a lipid envelope derived from the host cell plasma membrane. The RSV envelope contains three viral transmembrane surface glycoproteins: the large glycoprotein G, the fusion protein F, and the small hydrophobic SH protein. The nonglycosylated matrix M protein is present on the inner face of the envelope. There are four nucleocapsid/polymerase proteins: the nucleoprotein N, the phosphoprotein P, the transcription processivity factor M2-1, and the large polymerase subunit L (83); Candidate receptors of RSV (A) such as TLR4, CX3CR1, and HSPG (B) bind to the RSV-G glycoprotein and act to tether the virus particle to the cell surface. Cell surface nucleolin is also involved in the entry process (C) by triggering fusion of the virus and host cell membranes by binding to the RSV-F fusion glycoprotein (D). The virion fuses with the cell membrane and enters the cell (E). Host cell macropinocytosis of RSV is also a route of entry for RSV (F). It is unclear which receptors are involved in this process (G). Internalization of the virion (H) is dependent on actin rearrangement, phosphatidylinositol 3-kinase activity, and host cell (I) early endosomal Rab5+ vesicles where proteolytic cleavage of the RSV-F protein triggers delivery of the capsid contents into the host cells by fusion of the virus and endosomal membranes (J). The replication occurs entirely in the cytoplasm, a positive sense RNA is generated by viral polymerase and it is used as a template for negative sense RNA to be encapsidated in new virions and for protein synthesis (84).

After inoculation into the nasopharyngeal or conjunctival mucosa, the virus spreads into the respiratory tract, where it infects the apical ciliated epithelial cells. Host inflammatory immune response is triggered, including both humoral and cytotoxic T-cell activation, and a combination of viral cytotoxicity and the host's cytotoxic response cause necrosis of respiratory epithelial cells, leading to small airway obstruction and plugging by mucus, cellular debris, and DNA. More severe cases may also include alveolar obstruction. Other effects include ciliary dysfunction with impaired mucus clearance, airway edema, and decreased lung compliance (85). Through these pathogenetic mechanisms, RSV is the leading cause of lower respiratory tract infections, such as bronchiolitis and pneumonia, in infants and young children worldwide. The risk factors for severe RSV disease include premature birth, low birth weight, bronchopulmonary dysplasia, congenital heart disease, immunodeficiency, and the timing of birth in relation to the winter season (86). RSV causes also severe morbidity and mortality in the elderly, particularly in those with chronic obstructive pulmonary disease (87). Worldwide, RSV is responsible for approximately 33 million lower respiratory tract illnesses, three million hospitalizations, and up to 199,000 childhood deaths. The hospitalization of RSV patients in the United States produces an annual economic burden of approximately $500 million, and considerable further costs can be added to this figure as a result of outpatient care (85,88).

The management of RSV infection is primarily a matter of treating symptoms, and antiviral treatment is limited to the use of ribavirin, a drug which has controversial activity and is associated with significant side effects. Palivizumab, a humanized monoclonal antibody with activity against the RSV membrane fusion protein, has been approved for the immune prophylaxis of RSV infection in high-risk prematurely born infants. However, a major problem with palivizumab is its high cost, which may lead to the progressive restriction of its use. Vaccines and therapeutic interventions for RSV infection remain a target of intense scientific interest (89).

Influenza viruses (FluVs) are members of the *Orthomyxoviridae* family and belong to the four genera Alphainfluenzavirus (Influenza A virus, FluVA), Betainfluenzavirus (Influenza B virus, FluVB), Gammainfluenzavirus (FluVC) and Deltainfluenzavirus (FluVD) The four genera differ in host range and pathogenicity. FluVA and FluVB cause seasonal epidemics of disease known as the flu season. Only FluVA pose a significant risk of zoonotic infection, host switch and the generation of pandemics, i.e., global epidemics of flu disease. A pandemic can occur when a new and very different FluVA emerges that both infects people and has the ability to spread efficiently between them. FluVC infections generally cause mild illness and are not thought to cause human flu epidemics. Influenza D viruses primarily affect cattle and are not known to infect or cause illness in people. (90,91) .

All FluVs possess a uniquely segmented, single-stranded, negative-sense RNA genome. Depending on the influenza type, there are seven (FluVC) or eight (FluVA and FluVB) segments; each segment contains one or two genes that code for various proteins. The viral genome is enclosed in a nucleocapsid that is surrounded by a lipid envelope. FluV A contains 11 genes on eight segments encoding for 11 proteins, including the surface glycoproteins hemagglutinin (HA) and neuraminidase (NA), a nucleoprotein (NP), the matrix proteins M1 and M2, the nonstructural proteins NS1 and NS2, and the core proteins PA, PB1 (polymerase basic 1), PB1-F2, and PB2. The HA glycoprotein mediates binding to sialic acid residues on the host cell surface and membrane fusion and virus entry, while NA functions to cleave sialic acid and release new virus particles from the surface of infected cells (79).

Influenza A viruses are divided into subtypes based on the surface protein HA and NA. There are 18 different hemagglutinin subtypes and 11 different neuraminidase subtypes. While there are potentially 198 different influenza A subtype combinations, only 131 subtypes have been detected in nature. Current subtypes of FluVA that routinely circulate in people include: A(H1N1) and A(H3N2). FlvA subtypes can be further broken down into different genetic "clades" and "sub-clades" (90).

FluVs structure and replicative cycle are summarized in Figure 11.
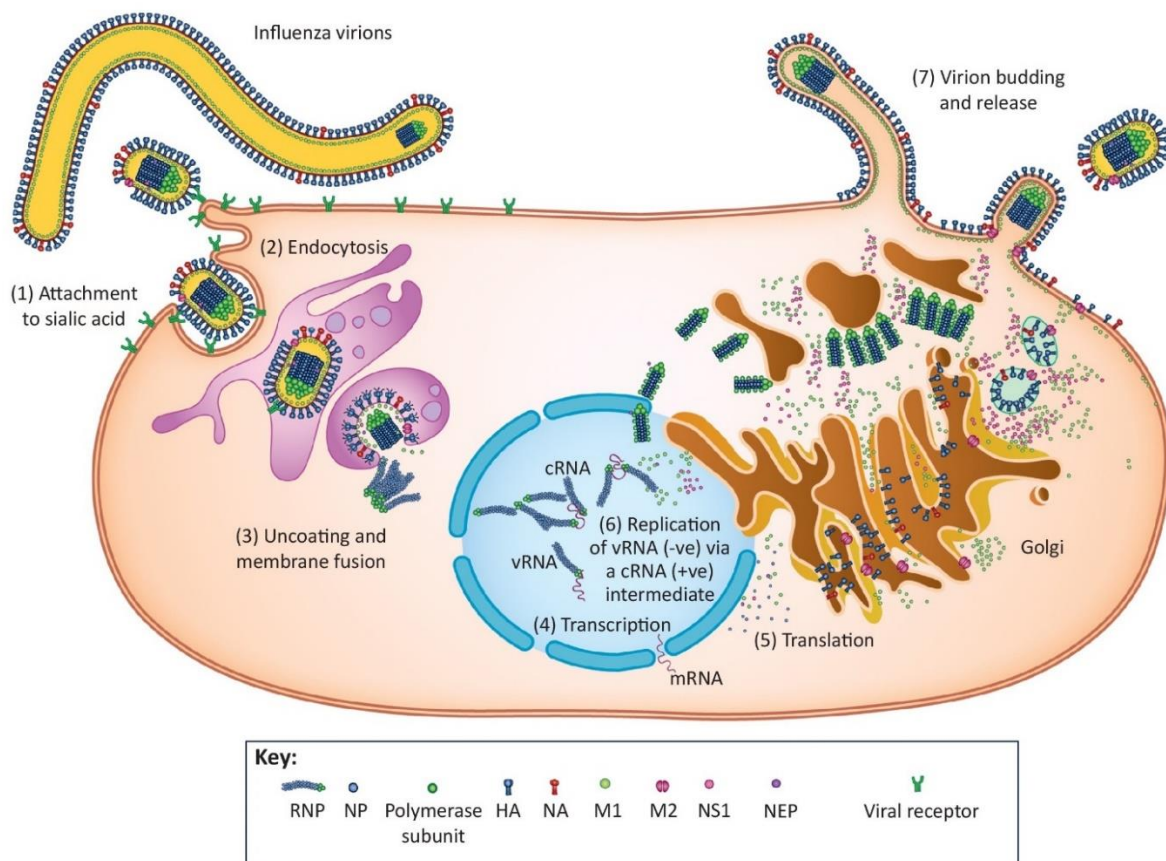

Figure 11: This infographic briefly summarizes FluVA structure and replication cycle (91).

FluV can replicate in the epithelial cells of both the upper and lower respiratory tract. It causes an acute respiratory disease characterized by fever, coryza, cough, headache, prostration, malaise, and inflammation of the upper respiratory tree and trachea. In most cases, pneumonic involvement is not clinically prominent. People of all ages are afflicted, but the prevalence is greatest in school-age children; disease severity is greatest in infants, the aged, pregnant women and those with underlying illnesses. People with chronic pulmonary or cardiac disease, or diabetes mellitus, are at high risk of developing severe complications from FluVA, which may include hemorrhagic bronchitis, pneumonia (primary viral or secondary bacterial), and death (92).

Worldwide, these annual epidemics result in about 3 to 5 million cases of severe illness, and about 290 000 to 650 000 respiratory deaths. In industrialized countries most deaths associated with influenza occur among people age 65 or older. The effects of seasonal influenza epidemics in developing countries are not fully known, but research estimates that 99% of deaths in children under 5 years of age with influenza related lower respiratory tract infections are found in developing countries (93).

Two classes of anti-influenza drugs, adamantane derivatives (amantadine and rimantadine) and neuraminidase inhibitors (zanamivir, oseltamivir and peramivir), are available. The recently circulating FluVA and FluVB are susceptible to neuraminidase inhibitors, but amantadine and rimantadine are not recommended because of resistance to these drugs and also because they are not effective against influenza B viruses. Oseltamivir and zanamivir are recommended for all individuals with suspected or confirmed influenza requiring hospitalization and patients in high-risk groups. Vaccination is the best approach to prevent influenza infections annually. However, due to frequent mutations in the surface glycoprotein HA, FluVA acquire enough mutations each year to escape the protection of the annually formulated vaccines, and some of them show a high level of resistance against antiviral drugs. A universal influenza vaccine that can neutralize all types of FluV is still not available (94). In this context, FluV continue to pose a significant threat to both life and economy.

Human rhinoviruses (HRVs) are single-stranded, positive-sense, RNA (ssRNA) nude viruses, belonging to *Picornaviridae* family and *Enterovirus* genus. The viral genome consists of a single gene whose translated protein is cleaved by virally encoded proteases to produce 11 proteins. Four proteins, VP1, VP2, VP3, and VP4, make up the viral capsid that encases the RNA genome, while non-structural proteins are involved in viral genome replication and assembly. The VP1, VP2, and VP3 proteins account for the virus antigenic diversity, while VP4 anchors the RNA core to the capsid. There are 60 copies each of the four capsid proteins, giving the virion an icosahedral structure, with a canyon in VP1 that serves as the site of attachment to cell surface receptors (Figure 12). More than

90% of known HRV serotypes, the "major group," utilize the cell surface receptor intercellular adhesion molecule 1 (ICAM-1), while the "minor group" attaches to and enters cells via the low-density lipoprotein receptor (LDLR). Some of the major-group HRVs also use heparan sulfate as an additional receptor (95). The replicative cycle is schematically reported in Figure 12.
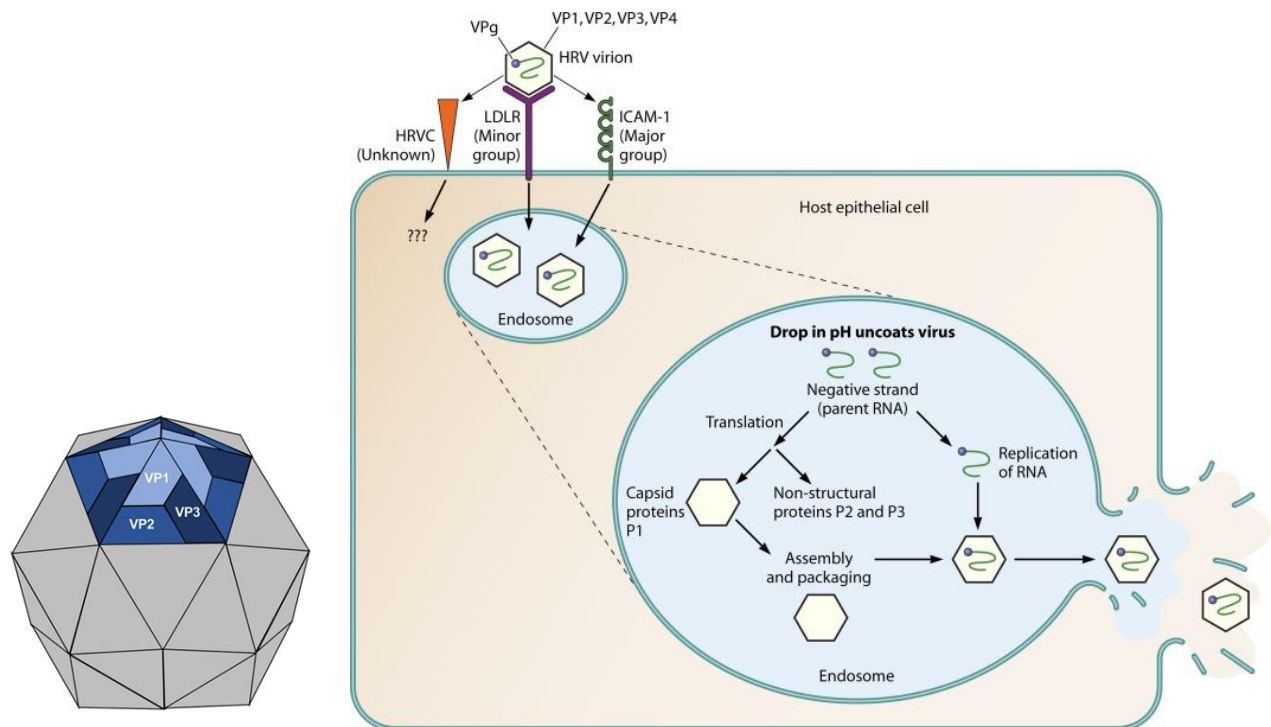

Figure 12: Schematic representation of HRV capsid structure and viral replication in airway epithelial cells. Depending on the receptor type, virus uptake occurs via clathrin-dependent or -independent endocytosis or via macropinocytosis. A drop in the pH leads to viral uncoating. RNA is replicated as well as translated into structural (capsid) and nonstructural proteins. The virion is then assembled and packaged prior to cellular export via cell lysis. (95)

Sequencing studies of the HRV genome revealed the existence of more than 160 strains, which were divided into three major species, namely HRV-A (containing 80 serotypes), HRV-B (containing 32 serotypes) and HRV-C species (65 serotypes). (95).

HRV is the main etiological agent of common cold, a mild seasonal disease affecting the upper respiratory tract. It causes one-half to two-thirds of this self-limiting condition worldwide, with nearly 62 million cases only in the United States. Each year children can be infected from 8- to 12-times, while adults can be infected 2- to 3-times, especially in spring and winter periods. While other respiratory viruses, such as FluV and RSV, destroy airway epithelial cells, HRV is seldom associated with cytopathology of the upper respiratory tract. However, HRV alters epithelial cell barrier function thereby facilitating the transmigration of pathogens and complication of respiratory diseases (95). While mild and self-limiting in immunocompetent hosts, HRV infection is associated with

bronchiolitis in infants, pneumonia in the immunosuppressed and exacerbations of pre-existing pulmonary conditions such as asthma or chronic obstructive pulmonary disease and cystic fibrosis. In the context of these pathologies, HRV can exert not only a direct damage on the respiratory epithelium as a result of the lytic cycle of the virus replication, but it also stimulates innate and adaptive host immune responses, triggering the inflammatory pathways of the patient and thereby worsening the clinical outcome (96).

No antivirals or vaccines are currently available against HRV (86). Therefore, HRV infections and HRV induced exacerbations of respiratory pathologies still represent a significant economic cost upon healthcare infrastructure and an important public health problem.

4.2 The co-sputtering technology to confer direct virucidal activity to various substrates

As previously described, the spread of endemic or emerging viral respiratory pathogens is difficult to control. This is particularly true in our modern world characterized by growth in the human population, urbanization, close interactions between human and animal populations, climate change, and increases in international travel and trade. Vaccination is the most powerful weapon that humans have to prevent viral diseases, but despite big efforts from the scientific community, this approach is not always possible. Indeed, considering the respiratory viruses described in point 4.1 and matter of this thesis, only FluV can be prevented by an effective annual vaccine. Besides, as the current COVID19 pandemic teaches us, new viral respiratory pathogens are emerging with increasing frequency and have potentially devastating impacts on the population worldwide. In the absence of an effective vaccine or antiviral drug, the best opportunities to prevent the global spread of a new pathogen or to control new outbreaks from well-known respiratory viruses are rapid and early identification systems and individual and government control measures (97). In this context, we conducted a project in close collaboration with the Polytechnic of Turin, in particular with the group of Prof. Monica Ferraris from the Dept. of Applied Science and Technology. This group recently patented a method, named co-sputtering technic, for the application of an antibacterial and antiviral coating to different substrates (98). This invention allows to obtain a coating having, at the same time, both antimicrobial properties and a high resistance to thermal and mechanical wear for an extended period of time. Briefly, the process consists in the deposition through a cathodic pulverization of silica and silver nanoclusters on a plurality of substrates that must not be contaminated by microorganisms, such as surfaces of medical and surgical instruments, surfaces of filters for air conditioning plants and all objects and fomites that could be a vehicle of transmission of human pathogens. The final thickness of the coating ranges between 15 nm and 500 nm and not only silver, but also other metallic material such as copper and zinc, can be deposited via co-sputtering. Nevertheless, our collaborators

chosen silver as preferred material to confer antiviral activity, due its previously and extensively demonstrated antiviral properties (99–105).

The main goal of our joined project was the development of efficient air control technology able to capture contaminated aerosols and directly inactivate microorganisms for maintaining a safe indoor air environment and protecting people. In particular, current Heating, Ventilating, and Air Conditioning (HVAC) systems can handle and mitigate the air-transmission of disease, capturing and retaining both particulates and microorganisms in the air filter. Nevertheless, they are predisposed to microbial colonization, stimulated also by dirt accumulation in the long term, inadequate filter maintenance, and the presence of cooling coil condensate or other moisture sources. All these elements can reduce the HVCA system efficiency making people at risk. The application of an antibacterial and antiviral coating to air filters can therefore improve the efficiency of these HVCA systems and consequently contributing to ensure efficient control measures. To this end, we evaluated the antiviral activity against respiratory viruses of the silver nanoclusters/silica composite coating deposited on glass-fiber and metallic air filters.

Finally, we also evaluated the antiviral properties of this coating when deposited on cotton textiles used to produce working clothes and individual protective equipment.

4.2.1   Publications

Balagna C, Francese R, Perero S, Lembo D, Ferraris M. <u>Nanostructured composite coating endowed with antiviral activity against human respiratory viruses deposited on fibre-based air filters</u>. Surface and Coating Technology – Available online 17 January 2021, 126873. https://doi.org/10.1016/j.surfcoat.2021.126873

With this work we aimed to respond to the necessity of an efficient HVAC system, able to capture and inactivate viruses- and bacteria-rich aerosols, thus preserving a safe indoor air environment and protecting people. We evaluated the virucidal activity of the silver nanoclusters/silica composite coating deposited via co-sputtering technique on glass, on metallic fiber-based air filters as well as on cotton textiles. We selected three human respiratory viruses, RSV, FluVA, and HRV as representative members of the respiratory virus category. Performing *in vitro* experiments, we demonstrated that the coated air filters and cotton textile are endowed with strong virucidal activity against RSV and FluVA, but not against HRV. Our results indicated that the silver nanocluster/silica coating deposited on the air filters (and cotton textiles) can lead to an important

contribution to the viral biological risk restraint. This technology can improve the current prevention and safety procedures in the health sector, but also in crowded places such as public transport, schools, offices, gyms, and sports facilities.

Nanostructured composite coating endowed with antiviral activity against human respiratory viruses deposited on fibre-based air filters

C. Balagna [a,*], R. Francese [b], S. Perero [a], D. Lembo [b], M. Ferraris [a]

[a] *Dept. of Applied Science and Technology, Politecnico di Torino, Corso Duca degli Abruzzi 24, 10129 Torino, Italy*
[b] *Dept. of Clinical and Biological Sciences, University of Turin, San Luigi Gonzaga Hospital, Regione Gonzole 10, 10043 Orbassano, TO, Italy*

ABSTRACT

The widespread of viral airborne diseases is becoming a critical problem for human health and safety, not only for the common cold and flu, but also considering more serious infection as the current pandemic COVID-19. Even if the current heating, ventilating and air conditioning (HVAC) systems limit the disease transmission by air, the air filters are susceptible to microbial colonization. In addition, viruses spread via droplets (aerosol) produced by direct or indirect contact with infected people. In this context, the necessity of an efficient HVAC system, able to capture and inactivate viruses- and bacteria-rich aerosols, thus preserving a safe indoor air environment and protecting people, is of enormous importance. The aim of this work is the assessment of the antiviral properties of a silver nanoclusters/silica composite coating deposited via co-sputtering technique on glass, on metallic fibre-based air filters as well as on cotton textiles. The selected human respiratory viruses are: *respiratory syncytial virus* (RSV), the human *rhinovirus* (HRV) and the *influenza* virus type A (FluVA). The coated air filters show that the nanostructured coating develops a strong virucidal activity against RSV and FluVA, but not against the HRV.

1. Introduction

Air-transmitted pathogens as bacteria, fungi or viruses are the cause of several airborne diseases, from common colds or influenza to even more acute respiratory illnesses, like the Severe Acute Respiratory Syndrome (SARS) and the current pandemic of COVID-19, caused by the coronavirus SARS-CoV-2. The widespread of airborne diseases becomes a crucial problem, especially, for indoor and crowded places such as public transport, kindergartens, offices, gyms and sports facilities, or in hospital where the risk of infectious disease transmission for patients, workers, and visitors is further increased. An exposure to airborne microorganisms for a long time together with a poor air quality reduces people comfort and productivity [1,2] and increases the risk of adverse health effects development [3,4]. For this, a clean indoor air environment has to be preserved considering that in the world, people spend most of their time indoor, on average about 90% [5,6].

Current Heating, Ventilating and Air Conditioning (HVAC) systems are able to handle and mitigate the air-transmission of disease. HVAC system reduces the circulation of microorganisms in the air, as they capture and retain both particulates and microorganisms in the air filters [7]. However, air filter is predisposed to microbial colonization,

stimulating also by dirt accumulation in the long term, inadequate filter maintenance and the presence of cooling coil condensate or other moisture sources [7,8]. The respiratory viruses spread efficiently among humans through the air, via droplets (aerosol) or via direct or indirect contact with contaminated people, or via contaminated hands and objects, causing outbreaks that are difficult to control [9].

Besides its well-known antibacterial and antifungal broad-spectrum effect [10–12], silver recently demonstrated also antiviral properties [13]. Studies, performed in vitro, proved that silver nanoparticles are able to directly inactivate and prevent the infection of adenovirus type 3 [14] and have efficient inhibitory activity on H1N1 influenza A virus [15]. Few studies are more specific to antiviral air filters. In particular, silica particles decorated with silver nanoparticles, deposited on air filter media, demonstrated effective antiviral behaviour, towards aerosolized bacteriophage MS2 in a continuous airflow condition, without altering filtration performance [16]. Only silver nanoparticles, deposited on air filter, demonstrated similar results even if the dust particles loaded on the filtration media reduced the antimicrobial effect of the metallic agent [17].

The aim of this work is the evaluation of the antiviral effect of a silver nanocluster/silica composite coating deposited on fibre-based air filters

via co-sputtering through a patented procedure [31]. Over the past ten years, authors developed this nanostructured composite coating [19–21] for several applications, from biomedical implants [22,23], to mobile phones [24], natural and technical textiles [25,26], aerospace structures [27,28], and also glass-fibre air filters [29], but evaluating only antibacterial and antifungal effect. In a recent short communication, authors' preliminary demonstrated the virucidal effect of the silver nanoclusters/silica composite coating deposited on disposable facemask towards SARS-CoV-2 [30].

In this study, the nanostructured coating was tested against representative members of the respiratory virus category of human origin, instead of bacteriophage as in the previously mentioned study [16]. Specifically, the respiratory syncytial virus (RSV) is the most frequent cause of paediatric bronchiolitis and pneumonia [31]; the human rhinovirus (HRV) is the major etiologic agent of the common cold [32]; influenza virus type A (FluVA) is the cause of the well-known respiratory disease that annually results in about 3 to 5 million cases of severe illness [33].

2. Materials and methods

2.1. Coating deposition and characterization

A nanostructured composite coating was deposited on several air filters by means of radio frequency (RF) co-sputtering technique. The nanostructured coating was a composite thin layer (thickness of 300 nm) of silica matrix which homogeneously embedded silver nanoclusters [20,21]. The selected substrates were glass-fibre and stainless-steel fibre-based air filters, supplied by Sagicofim Spa and GV Filtri Spa, respectively. A cotton fabric, supplied by Tessitura Fratelli Ballesio Srl, was used as fibre-based substrate for other kinds of application as the personnel protective clothes. The deposition process was patented by authors [18,19]. The coatings were deposited using the sputtering equipment (Microcoat™ MS450) with two cathodes, one of silver target (Sigma-Aldrich™ 99.99% purity) and one of silica target (Franco Corradi S.r.l.TM 99.9% purity). The deposition was performed in pure argon atmosphere for 80 min, operating in RF mode for silica (power 200 W) and in DC mode for silver (power 1 W) under a pressure of 5.5 dPa (corresponding to 5.5×10^{-3} mbar). The water-cooled targets have different diameters, 6 in. for silica and 1 for silver. The distance between targets and substrates was 14 cm. The co-sputtering process parameters were optimized as reported in the previous studies for cotton substrate [25], other textile materials [26,28] and glass-fibre air filter [29].

Morphology of the coated and uncoated filters was observed by means of scanning electron microscopy (Field Emission Scanning Electron Microscope FESEM, QUANTA INSPECT 200, Zeiss SUPRATM 40™) equipped with Energy Dispersive Spectroscopy (EDS, EDAX PV 9900™), used for detecting the composition of all the samples. EDS analysis was performed on three different areas at low magnification ($100\times$) for a statistical analysis.

Silver release tests quantified silver ions released into water from the coated filters up to 14 days. For this test, coated filters with dimension of about $1cm^2$ of area were dipped into 25 ml of MilliQ water. Silver ion content was analysed after 3 h, 24 h, and 3, 7 and 14 days of immersion using silver photometer (Hanna Instruments™). Each measurement was done in triplicate.

2.2. Cells and viruses

Madin-Darby Canine Kidney cells (MDCK) (ATCC® CCL-34), human epithelial cells (Hep-2) (ATCC® CCL-23) and human epithelial adenocarcinoma cells (HeLa) (ATCC® CCL-2) were cultured in Dulbecco's modified Eagle's medium (DMEM; Sigma, St. Louis, MO), supplemented with heat-inactivated 10% (v/v) fetal bovine serum (FBS) (Sigma). All media were supplemented with 1% (v/v) penicillin/streptomycin solution (Euroclone, Milan, Italy) and cells were grown at 37 °C in an

atmosphere of 5% of CO_2. The A/H3N2 strain A/Christchurch/28/03 (FluVA) (Italian National Institute of Health) was propagated in MDCK cells by using MEM containing 1 μg/ml of IX type porcine pancreatic trypsin (Sigma, St. Louis, Mo) [34] and titrated by means of the plaque assay. The A2 (ATCC VR-1540) respiratory syncytial virus (RSV) strain was propagated in Hep-2 and titrated by means of the indirect immunoperoxidase staining procedure. Human rhinovirus (HRV) 1A (ATCC®VR-1559™) was produced in HeLa cells, at 33 °C, in a humidified 5% CO_2 incubator and titrated by means of plaque assay.

2.3. Virus titration by plaque assay

To evaluate the HRV titre, HeLa cells were seeded in 96-well plates, reaching 60%–70% confluence at the time of infection. The HRV suspension was serially diluted in DMEM supplemented with 2% FBS and inoculated on cells at 33 °C for 1 h. After this time, cells were washed with medium and overlaid with a 1:1 combination of 1.6% SeaPlaque Agarose (BioWhittaker Molecular Applications) and $2 \times$ DMEM. After an incubation at 33 °C for 3 days, the plates were fixed and stained with 0.1% of crystal violet solution for 30 min to allow the plaque count. To evaluate the FluVA titre, subconfluent MDCK cells in 96 well plates were inoculated with increasing dilutions of virus prepared in cold DMEM with 2% of FBS. After 2 h of adsorption at 37 °C, the virus inoculum was removed, cells overlaid with 1.6% SeaPlaque Agarose solution supplemented with 2 μg/ml of trypsin and incubated at 37 °C for 72 h. Cells were then fixed and coloured with 0.1% of crystal violet solution. The RSV titration was performed on Hep-2 cells in 96 well plates. Cells, seeded at a density of 9×10^3 cells/well, were inoculated with serial dilutions of RSV suspension for 3 h at 37 °C. Subsequently, the inoculum was removed and cells were overlaid with 1.2% methylcellulose and incubated at 37 °C. After 72 h, cells were fixed with acetone-methanol (50:50). The number of syncytia were determined by indirect immunostaining by using an RSV monoclonal antibody (Ab35958; Abcam, Cambridge, the United Kingdom) and a secondary antibody peroxidase-conjugated AffiniPure F(ab')2 Fragment Goat Anti-Mouse IgG (H + L) (Jackson ImmunoResearch Laboratories Inc., 872 W. Baltimore Pike, West Grove, PA 19390) [35].

Virus titration was performed in duplicate for each dilution and the virus titre was estimated as plaque forming units per ml (PFU/ml) by counting the number of plaques at an appropriate dilution.

2.4. Antiviral tests

Approximately 1.5×10^5 viral particles (RSV, FluVA, HRV) were suspended in a final volume of 500 μl of DMEM supplemented with 2% of FBS. The mixture was incubated with coated or uncoated filters (cut into pieces of 1 cm² and sterilized at 170 °C for 1 h) with a gentle oscillation for 1 h 30 min RT. As control (referred to untreated in the text), 1.5×10^5 viral particles were incubated under the same conditions of time and temperature, but without any filter. After this incubation, the mixture was collected and the residual viral infectivity was calculated by means of plaque assay and compared with the untreated control. The results are presented as the mean values from three independent experiments (mean ± SEM). One-way ANOVA, followed by Bonferroni test, was used to assess the statistical significance of the differences between treated and untreated samples, where appropriate (significance was set at $P < 0.05$). Fig. 1 reports the schematic representation of the procedure.

3. Results and discussion

3.1. Coating deposition and characterization

The glass and metallic fibre-based substrates were selected as materials used for air filters whereas cotton is used for other type of applications as an example the realization of personnel protective devices.
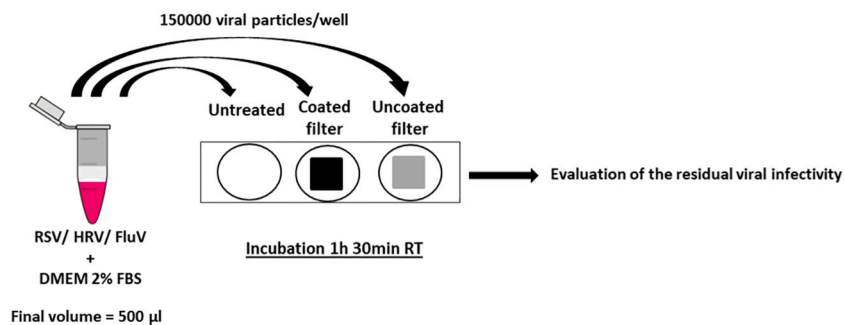
Fig. 1. Schematic representation of the antiviral test procedure. Viral particles were incubated with coated or uncoated cotton or filters (metallic or glass-fibre filter) or left untreated. After 1 h 30 min at room temperature the residual viral infectivity was calculated and compared with the untreated control.
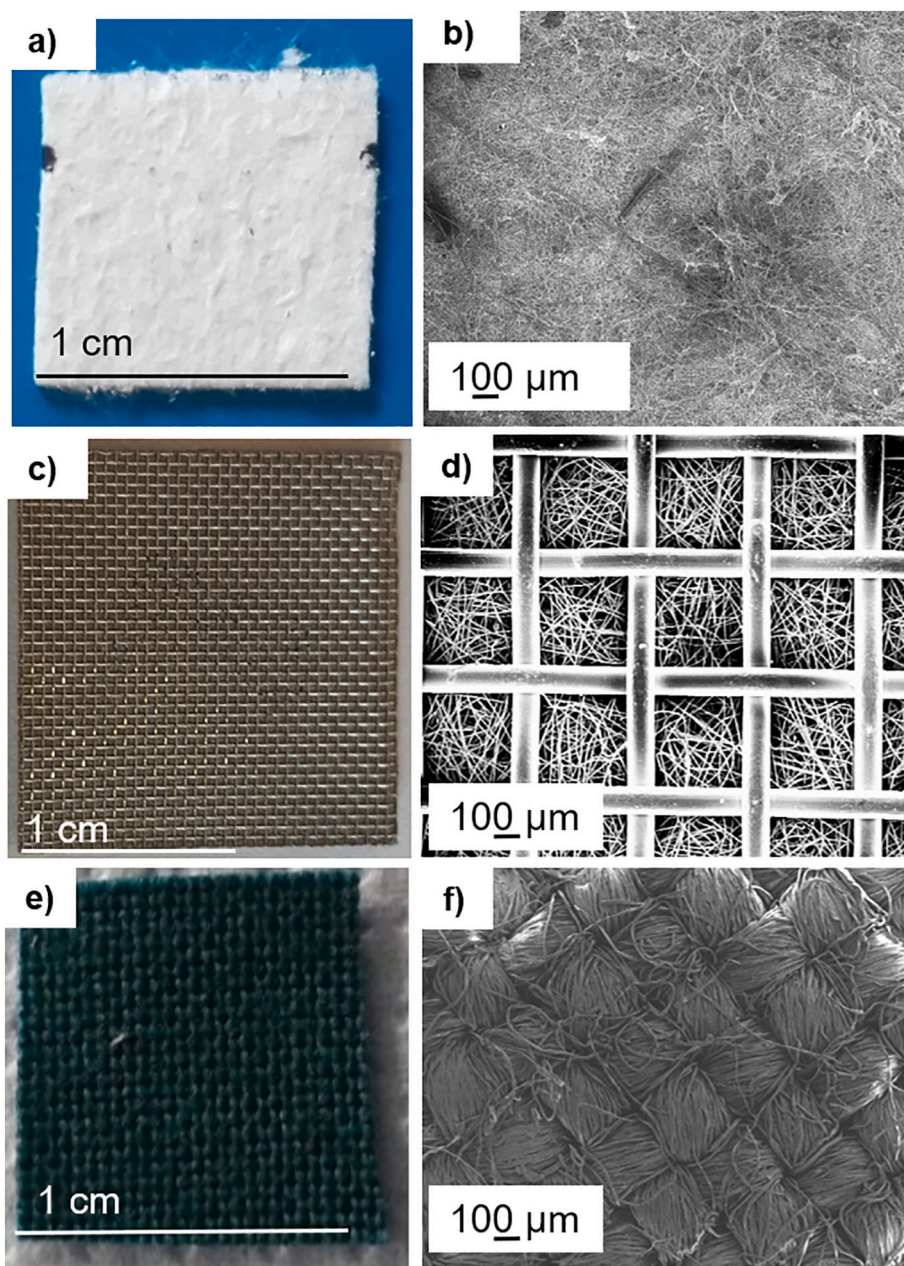
Fig. 2. Photographs of substrates and the relative FESEM images for observing morphology at low magnification: (a), (b) glass-fibre filter; (c), (d) metallic filter; (e), (f) cotton.

Fig. 2 reports the photographs and the relative surface morphology observed at FESEM of the uncoated substrates. Glass-fibre air filter (Fig. 2a, b) was white coloured (Fig. 2a) and characterized by randomly oriented glass-fibres as observed in FESEM images (Fig. 2b). Higher magnified-micrograph relative to the fibres orientation was reported in the Fig. 2b of previous work [29]. Metallic air filter (Fig. 2c, d) is composed of a regular metal grid over randomly arranged metallic fibres. Lastly, woven cotton fabric (Fig. 2e, f) is green dyed with warp and weft fibres.

Fig. 3 reports the comparison of the fibres surface morphology before and after coating deposition. The silver nanocluster/silica composite coating, deposited by means of co-sputtering technique, visibly changed the surface morphology of the fibres of all the used substrates. The smooth uncoated glass fibres (Fig. 3a) became rougher with a globular morphology after the coating deposition (Fig. 3b). This surface microstructure was already observed for the substrates treated in the previous papers [25,29]. The same modification occurred in the case of metallic air filter and cotton. In the first, the circular bands visible on the uncoated fibre (Fig. 3c) completely disappeared with the presence of silver nanocluster/silica composite coating (Fig. 3d). In the second, the uniform composite coating (Fig. 3f) uniformly covered the uncoated cotton (Fig. 3e) and the stripes were not visible anymore. Silver nanoclusters appear as bright particles (dimensions less than 50 nm) dispersed into the silica matrix. They were well noticeable (red-circled in Fig. 3b,d,f) on the surfaces of both coated metallic air filter and cotton and less visible on the glass fibre filter as they were surrounded by silica matrix. As already observed for the glass fibre filter and cotton in the previous works [25,29], the silver nanocluster/composite coating covered the fibre of all the here studied substrates without altering filtration

performance, and the filters porosity remained unchanged (no closed or obstructed pores).

Fig. 4 shows the compositional analysis, comparing the EDS graphs between uncoated and coated substrates. The analysis confirmed the presence of silver nanocluster/silica composite coating through the detection of the two main elements of the deposited layer, Si and Ag as reported in the previous works relative to the substrate of cotton and glass-fibre filter [25,29]. The original composition of uncoated glass-fibre filter is mainly based on Si, Na, Ca, Al and Ba (Fig. 4a). After coating deposition, the amount of Si slightly increased of about 1 at.% due to the silica matrix and Ag peaks appears (Fig. 4b). Ag amount is about 2.3 at.%. The metallic air filter is composed of stainless steel and the main detected elements are Fe, Cr, Mn, Ni with trace of S and Si (Fig. 4c). Si peak intensity and, so, the relative atomic percentage increased from 0.7 to 5.4 at.% and Ag peaks (amount about 1.7 at.%) were identified on the surface of the coated sample (Fig. 4d). In the case of cotton, naturally composed of C and O with an external contamination of Ca (Fig. 3e), Si and Ag peaks appeared in the coated textile (Fig. 4f), with an amount of about 3.4 and 2.3 at.%, respectively.

Fig. 5 reports the curve of the silver ion release from all the coated substrates in distilled water at RT. The acquisition of the data relative to the amount of silver ions was done up to 14 days. The trend of the silver ions release is progressive and very similar for both the air filter samples, reaching the maximum quantity at about 0.25 and 0.3 ppm for metallic filter and glass-fibre filter, respectively. The curve relative to cotton used as model substrate is characterized by an abrupt release of ions after 3 h, a decrement after 1 day and a further increment after 3 days, achieving higher value (about 0.55 ppm) then the data reported for the two air filters. This is probably due to the water absorption by cotton, differently

Fig. 3. FESEM images relative to the substrates fibres before and after the deposition of silver nanoclusters/silica composite coating: (a) uncoated and (b) coated glass-fibre filter; (c) uncoated and (d) coated metallic filter; (e) uncoated and (f) coated cotton. Silver nanoclusters in red circles.

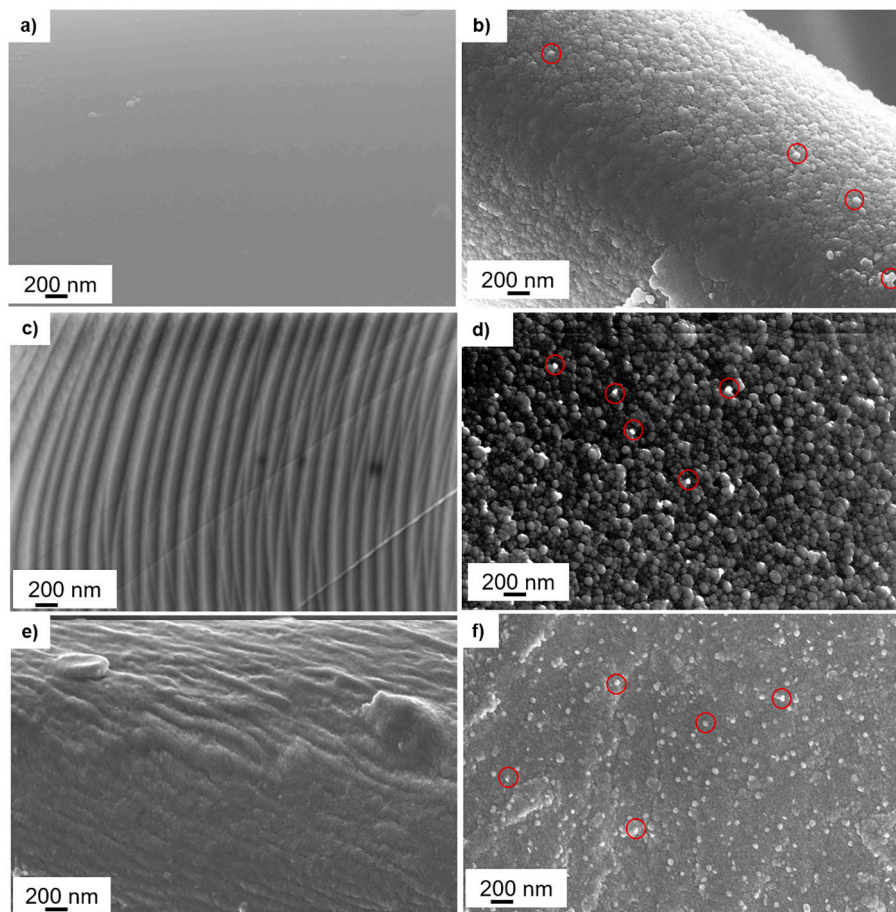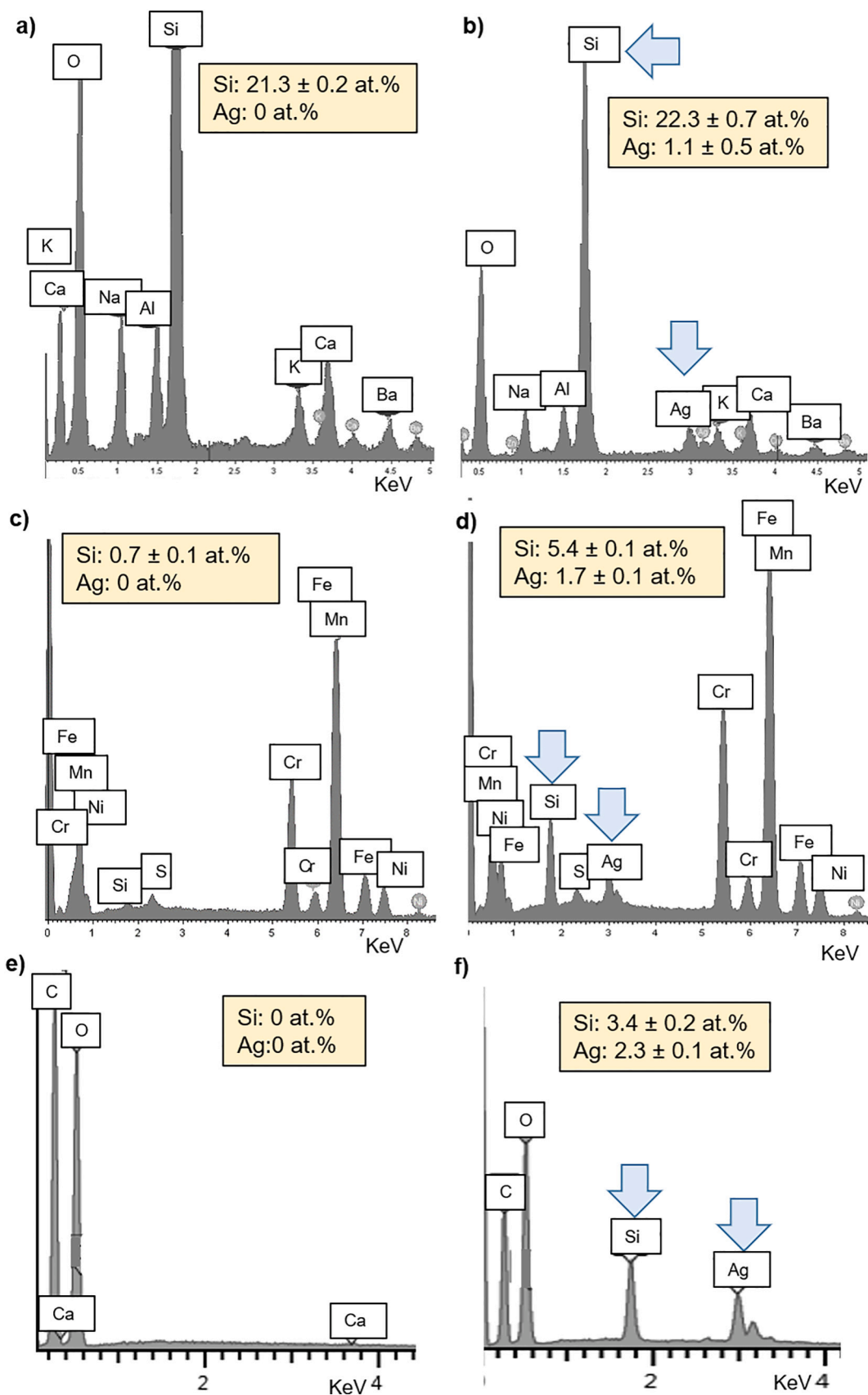**Fig. 4.** EDS analysis relative to the substrates fibres before and after the deposition of silver nanoclusters/silica composite coating: (a) uncoated and (b) coated glass-fibre filter; (c) uncoated and (d) coated metallic filter; (e) uncoated and (f) coated cotton.
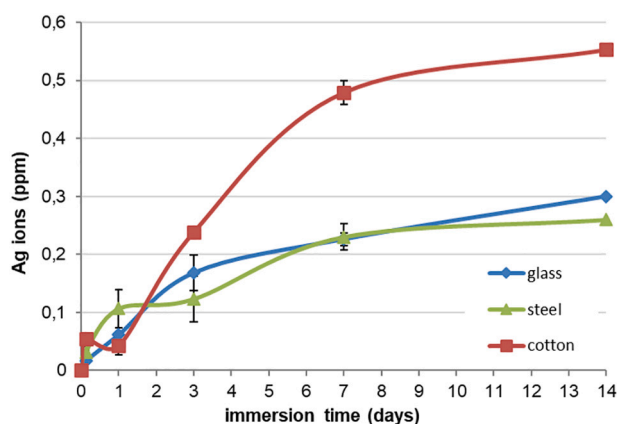
Fig. 5. Silver ion release up to 14 days in water at RT of the coated substrates: glass-fibre air filter (glass); metallic air filter (steel) and cotton textile (cotton).

from glass-fibre and metallic filter. For all substrates, the maximum quantity of ions detected into water after 14 days remained in the range of antimicrobial behaviour without reaching the toxic limit for human cells (10 ppm) [36,37]. Even if the curves did not reach a plateau after 14 days, it can be supposed that the amount of ion release is not going to exceed the toxicity threshold (10 ppm). Moreover, it must be underlined that HVAC system and in general air filters did not work immersed in water or any other aqueous solution, but in a moisture environment, so the silver release test into water up to 14 days could be considered a very harsh analysis.

3.2. Antiviral tests

The antiviral assays were performed in order to investigate the virucidal activity of the silver nanoclusters/silica composite coating by simulating the passage of viral particles through the filters. Possible dust contamination of the air filters was not considered in this test as dirt accumulation usually occurs after long period of exposition. The results obtained from the experiments with RSV, HRV and FluVA are reported in Table 1 and schematically presented in Fig. 6(a, b and c respectively), comparing all the substrates. The first set of experiments was carried out with the cotton as model substrate, to setup the procedure and to verify the antiviral action of the nanostructured composite coating against only two of the respiratory viruses, the respiratory syncytial virus (RSV) and the rhinovirus (HRV) (Fig. 6a, b). As reported in Fig. 6(a), the coated cotton significantly reduces the number of infectious RSV particles if compared with the uncoated cotton and the untreated (which refers to the viral particles incubated under the same conditions of temperature and time but without testing any samples). The reduction of RSV titre visible between both the cotton samples and the control is probably due to an aspecific absorption of the medium containing viral particles to the cotton substrate (Untreated: 7954 ± 511 PFU/ml; Uncoated cotton: 2482 ± 377 PFU/ml; Coated cotton: 62 ± 10 PFU/ml). On the contrary,

Table 1
Data relative to the plaque forming unit per ml (PFU/ml) for the untreated, the cotton textile, the glass-fibre filter and the metallic filter (coated and uncoated), against RSV, HRV and FluVA.

Samples		Plaque forming unit per ml (PFU/ml)		
		RSV	HRV	FluVa
Untreated	/	7954 ± 511	4731 ± 939	7819 ± 754
Cotton textile	Uncoated	2482 ± 377	4680 ± 256	/
	Coated	62 ± 10	6640 ± 989	/
Glass fibre filter	Uncoated	9013 ± 988	2800 ± 560	8241 ± 1513
	Coated	18 ± 3	3680 ± 160	140 ± 26
Metallic filter	Uncoated	8400 ± 1200	3467 ± 525	6054 ± 1430
	Coated	323 ± 41	2773 ± 282	220 ± 116

any virucidal activity against HRV was observed. In fact, as shown in Fig. 6(b), the coated cotton does not reduce the HRV titre if compared to the uncoated cotton treated sample (Untreated: 4731 ± 939 PFU/ml; Uncoated cotton: 4680 ± 256 PFU/ml; Coated cotton: 6640 ± 989 PFU/ml). This result could be attributed to the different structural conformation of these two viruses. In general, the protein capsid of naked viruses (as HRV) is less susceptible to environmental conditions (desiccation, detergents, pH, temperature…) than the lipid bilayer wrapping enveloped viruses (as RSV).

Having verified the feasibility of the antiviral procedure and the antiviral action of the nanostructured silver nanocluster/silica composite coating, the antiviral tests were performed with the metallic and the glass-fibre filters, adding also the FluVA virus, in order to conduct a significant screening against respiratory viruses. As reported in Fig. 6(a) and as expected, the nanostructured silver nanocluster/silica composite coating exerts a virucidal effect against RSV regardless of the type of filter (metallic or glass-fibre filter) on which it is deposed. There was indeed a significant reduction of RSV titre between both the coated samples and the uncoated one but no significant difference was observed comparing the antiviral effect of the coated samples. As shown in Fig. 6 (b) and in accordance with the results obtained with the cotton substrate, any significant inhibition of HRV titre was observed. On the contrary, the antiviral tests performed with the FluVA (Fig. 6c) showed that the silver nanocluster/silica composite coating significantly inhibits influenza virus infectivity. Also, in this case, the nature of the substrate did not influence the antiviral effect of the coating. These results are in line with previous papers demonstrating the antiviral activity of silver nanoparticles (Ag NPs) against these two human pathogens [38–41]. Despite the antiviral mechanism of AgNPs is still unclear, some hypotheses have been put forward. AgNPs have been proposed to interfere with viral replication by binding viral surface glycoproteins and therefore preventing the attachment and entry of the virus into the host cell or by crossing the cell membrane and actively blocking cellular factors necessary for viral replication. The experimental settings, here presented, allowed excluding the second mechanism of action, because cells and Ag nanoclusters did not come in contact. In this case, it is possible to assume that the virus is structurally altered or inactivated in such way that cell infection is no more possible, after interacting with the Ag nanoclusters embedded into the composite coating. Considering that the test was performed with samples immersed into a liquid solution, a second hypothesis could be ascribable also to the antiviral effect of silver ions, released from the nanoclusters. In fact, according to the data reported in Fig. 5, it was demonstrated that the ion release in water began in the first 3 h with a trend of progressive increment. In addition, skin test, performed in [25], demonstrated that silica matrix completely trapped silver nanoclusters, avoiding in this way the release of them into the surrounding environment. In addition, the porous morphology of silica allowed Ag ion release also from the nanoclusters disposed into the innermost matrix areas. In this way, the homogenous distribution of the nanoclusters inside the matrix increased ions amount. Here, no antiviral action of the silver nanoclusters/silica composite coating against HRV was reported. This phenomenon could be attributed to the different structural conformation of this virus with respect to the other two viruses. In general, the protein capsid of naked viruses (as HRV) is less susceptible to environmental conditions (desiccation, detergents, pH, temperature…) than the lipid bilayer wrapping enveloped viruses (as RSV and FluVA). To the best of our knowledge, no reports are available against the antiviral effect of silver nanoparticles against the human rhinovirus. Thanks to the premise about the promising results on virucidal effect of the silver nanoclusters/silica composite coating towards SARS-CoV-2 on disposable facemask [30], the coated filtering substrates, described in this paper, will be shortly investigated in details their antiviral activity against viruses belonging to *Coronaviridae* family.
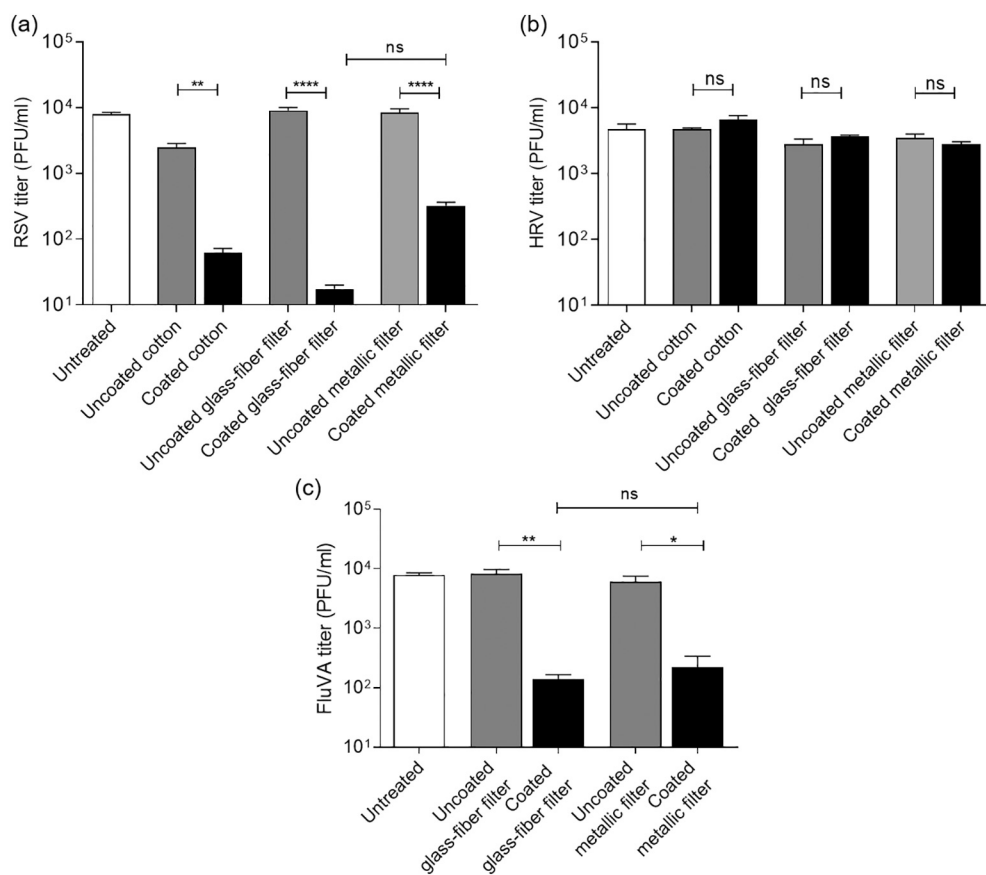
Fig. 6. Antiviral tests performed with the cotton textile, the glass-fibre filter and the metallic filter against (a) RSV, (b) HRV and (c) FluVA. The coated and the uncoated samples are compared. The untreated refers to the viral particles incubated under the same conditions of temperature and time but without testing any samples. The viral titre is reported on the Y-axis and expressed as plaque forming unit per ml (PFU/ml). On the X-axis the type of treatment is reported. ****pANOVA<0.0001; **pANOVA<0.01; *pANOVA<0.05; ns: not significant.

4. Conclusions

In conclusion, the nanostructured silver nanoclusters/silica composite coating effectively coated glass-fibre and metallic air filters and the cotton textile. The filtration performance was not reduced as the coating was conformal deposited only on the fibres, maintaining unaltered the filter porosity. Even if the air filter will find the final application in a moisture surrounding environment, the release test in water demonstrate that the silver ions were released without reaching the toxicity threshold after 14 days. The results obtained from the antiviral tests, simulating a close contact between infectious viral aerosol and air filters, demonstrated that the silver nanoclusters/silica composite coating is characterized by a strong virucidal activity against RSV and FluVA. The reduction of RSV titre resulted of almost three orders of magnitude between coated and uncoated glass-fibre filters and more than one order of magnitude between coated and uncoated metallic filters. Instead, the nanostructured coating is able to reduce FluVA titre of about two orders of magnitude, independently of the filters used as substrate, compared to the uncoated filters or the control. Here, no antiviral action of the silver nanoclusters/silica composite coating against HRV was reported.

In this study, the antiviral action of the nanostructured coating was tested, performing the experiments in a liquid environment with an incubation time of hour and half. In future tests, it will be interesting to assess the ability of silver nanocluster/silica composite coating to inactivate viral aerosols in a shorter time and to inactivate infectious viruses after their aerosolization. On the other hand, tests could be performed in order to evaluate the possible effect of dust accumulation on the air filter on the antiviral efficacy. The silver nanocluster/silica coating deposited on the air filters (and masks), can lead to an important contribution to the antiviral biological risk restraint, especially but not only in the health sector. In fact, it can improve the current prevention

and safety procedures, also in crowded places or in the public transport, kindergartens, offices, gyms and sports facilities. In addition, staff and workers operating in critical conditions such as hospitals, conflict areas or regions affected by natural disasters or pandemics, could benefit of the antiviral air filters. Furthermore, the antiviral coating can confer an add value to the protective clothing such as gowns, masks or gloves.

CRediT authorship contribution statement

C. Balagna: Funding acquisition, Project administration, Investigation, Conceptualization, Writing – original draft, Writing – review & editing. **R. Francese:** Investigation, Methodology, Writing – original draft, Writing – review & editing. **S. Perero:** Methodology, Writing-review & editing. **D. Lembo:** Supervision, Writing- review & editing. **M. Ferraris:** Supervision, Funding acquisition, Project administration, Writing- review & editing.

Declaration of competing interest

The authors declare that they have no known competing financial interests or personal relationships that could have appeared to influence the work reported in this paper.

Acknowledgment

References

[1] K.W. Tham, Indoor air quality and its effects on humans - a review of challenges and developments in the last 30 years, Energy Build. 130 (2016) 637–650, https://doi.org/10.1016/j.enbuild.2016.08.071.

[2] G. Liu, M. Xiao, X. Zhang, C. Gal, X. Chen, L. Liu, S. Pan, J. Wu, L. Tang, D. Clements-Croome, A review of air filtration technologies for sustainable and healthy building ventilation, Sustain. Cities Soc. 32 (2017) 375–396, https://doi.org/10.1016/j.scs.2017.04.011.

[3] K. Kim, E. Kabir, S.A. Jahan, Airborne bioaerosols and their impact on human health, J. Environ. Sci. 67 (2018) 23–35, https://doi.org/10.1016/j.jes.2017.08.027.

[4] J. Douwes, P. Thorne, N. Pearce, D. Heederik, Bioaerosol health effects and exposure assessment: progress and prospects, Ann. Occup. Hyg. 47 (2003) 187–200, https://doi.org/10.1093/annhyg/meg032.

[5] N.E. Kepleis, W.C. Nelson, W.R. Ott, J.P. Robinson, A.M. Tsang, P. Switzer, J. V. Behar, S.C. Hern, W.H. Engelmann, The national human activity pattern survey (NHAPS): a resource for assessing exposure to environmental pollutants, J. Expo. Anal. Environ. Epidemiol. 11 (2001) 231–252, https://doi.org/10.1038/sj.jea.7500165.

[6] European Commission Press Release Database, Indoor air pollution: new EU research reveals higher risks than previously thought, IP/03/1278. https://europa.eu/rapid/press-release_IP-03-1278_en.htm, 2003 (accessed 22 September 2003).

[7] M. Möritz, H. Peters, B. Nipko, H. Rüden, Capability of air filters to retain airborne bacteria and molds in heating, ventilating and air-conditioning (HVAC) systems, Int. J. Hyg. Environ. Health 203 (2001) 401–409, https://doi.org/10.1078/1438-4639-00054.

[8] H.C. Flemming, Biofilms and environmental protection, Wat Sci. Tech. 27 (1993) 1–10, https://doi.org/10.2166/wst.1993.0528.

[9] J.S. Kutter, M.I. Spronken, P.L. Fraaij, R.A.M. Fouchier, S. Herfst, Transmission routes of respiratory viruses among humans, Curr. Opin. Virol. 28 (2018) 142–151, https://doi.org/10.1016/j.coviro.2018.01.001.

[10] S.P. Deshmukh, S.M. Patil, S.B. Mullani, S.D. Delekar, Silver nanoparticles as an effective disinfectant: a review, Mater. Sci. Eng. C 97 (2019) 954–965, https://doi.org/10.1016/j.msec.2018.12.102.

[11] M. Rai, A. Yadav, A. Gade, Silver nanoparticles as a new generation ofantimicrobials, Biotechnol. Adv. 27 (2009) 76–83, https://doi.org/10.1016/j.biotechadv.2008.09.002.

[12] T.C. Dakal, A. Kumar, R.S. Majumdar, V. Yadav, Mechanistic basis of antimicrobial actions of silver nanoparticles, Front. Microbiol. 7 (2016) 1831, https://doi.org/10.3389/fmicb.2016.01831.

[13] R. Ciriminna, Y. Albo, M. Pagliaro, New antivirals and antibacterials based on silver nanoparticles, Chem. Med. Chem. 15 (2020) 1619–1623, https://doi.org/10.1002/cmdc.202000390.

[14] N. Chen, Y. Zheng, J. Yin, X. Li, C. Zheng, Inhibitory effects of silver nanoparticles against adenovirus type 3 in vitro, J. Virol. Methods 193 (2013) 470–477, https://doi.org/10.1016/j.jviromet.2013.07.020.

[15] D. Xiang, Q. Chen, L. Pang, C. Zheng, Inhibitory effects of silver nanoparticles on H1N1 influenza A virus in vitro, J.Virol. Methods 178 (2011) 137–142, https://doi.org/10.1016/j.jviromet.2011.09.003.

[16] Y.H. Joe, K. Woo, J. Hwang, Fabrication of an anti-viral air filter with SiO2–Ag nanoparticles and performance evaluation in a continuous airflow condition, J. Hazard. Mater. 280 (2014) 356–363, https://doi.org/10.1016/j.jhazmat.2014.08.013.

[17] Y.H. Joe, D.H. Park, J. Hwang, Evaluation of Ag nanoparticle coated air filter against aerosolizedvirus: anti-viral efficiency with dust loading, J. Hazard. Mater. 301 (2016) 547–553, https://doi.org/10.1016/j.jhazmat.2015.09.017.

[18] M. Ferraris, C. Balagna, S. Perero, Method for the Application of an Antiviral Coating to a Substrate and Relative Coating, 2019 (WO2019/082001).

[19] M. Ferraris, D. Chiaretta, M. Fokine, M. Miola, E. Verné, Pellicole antibatteriche ottenute da sputtering e procedimento per conferire proprietà antibatteriche ad un substrato TO2008A000098, 2008.

[20] M. Ferraris, S. Perero, M. Miola, S. Ferraris, E. Verné, J. Morgiel, Silver nanocluster– silica composite coatings with antibacterial properties, Mater. Chem. Phys. 120 (2010) 123–126, https://doi.org/10.1016/j.matchemphys.2009.10.034.

[21] M. Ferraris, S. Perero, M. Miola, S. Ferraris, G. Gautier, G. Maina, G. Fucale, E. Verne, Chemical, mechanical, and antibacterial properties of silver nanocluster– silica composite coatings obtained by sputtering, Adv. Eng. Mater. 12 (2010) B276–B282, https://doi.org/10.1002/adem.200980076.

[22] G. Muzio, S. Perero, M. Miola, M. Oraldi, S. Ferraris, E. Vernè, F. Festa, R. A. Canuto, V. Festa, M. Ferraris, Biocompatibility versus peritoneal mesothelial cells of polypropylene prostheses for hernia repair, coated with a thin silica/silver layer, J Biomed Mater Res B Appl Biomater 105 (2016) 1586–1593, https://doi.org/10.1002/jbm.b.33697.

[23] F. Baino, S. Ferraris, M. Miola, S. Perero, E. Verné, A. Coggiola, D. Dolcino, M. Ferraris, Novel antibacterial ocular prostheses: proof of concept and physico-chemical characterization, Mater. Sci. Eng. 60 (2016) 467–474, https://doi.org/10.1016/j.msec.2015.11.075.

[24] M. Miola, S. Perero, S. Ferraris, A. Battiato, C. Manfredotti, E. Vittone, D. Del Vento, S. Vada, G. Fucale, M. Ferraris, Silver nanocluster-silica composite antibacterial coatings for materials to be used in mobile telephones, Appl. Surf. Sci. 313 (2014) 107–115, https://doi.org/10.1016/j.apsusc.2014.05.151.

[25] M. Irfan, S. Perero, M. Miola, G. Maina, A. Ferri, M. Ferraris, C. Balagna, Antimicrobial functionalization of cotton fabric with silver nanoclusters/silica composite coating via RF co-sputtering technique, Cellulose 24 (2017) 2331–2345, https://doi.org/10.1007/s10570-017-1232-y.

[26] C. Balagna, M. Irfan, S. Perero, M. Miola, G. Maina, D. Santella, A. Simone, Characterization of antibacterial silver nanocluster/silica composite coating on high performance Kevlar® textile, Surf. Coat. Technol. 321 (2017) 438–447, https://doi.org/10.1016/j.surfcoat.2017.05.009.

[27] C. Balagna, S. Perero, S. Ferraris, M. Miola, G. Fucale, C. Manfredotti, A. Battiato, D. Santella, E. Verné, E. Vittone, M. Ferraris, Antibacterial coating on polymer for space application, Mater. Chem. Phys. 135 (2012) 714–722, https://doi.org/10.1016/j.matchemphys.2012.05.049.

[28] C. Balagna, M. Irfan, S. Perero, M. Miola, G. Maina, M. Crosera, D. Santella, A. Simone, M. Ferraris, Antibacterial nanostructured composite coating on high performance Vectran™ fabric for aerospace structures, Surf. Coat. Technol. 373 (2019) 47–55, https://doi.org/10.1016/j.surfcoat.2019.05.076.

[29] C. Balagna, S. Perero, F. Bosco, C. Mollea, M. Irfan, M. Ferraris, Antipathogen nanostructured coating for air filters, Appl. Surf. Science 508 (2020), 145283, https://doi.org/10.1016/j.apsusc.2020.145283.

[30] C. Balagna, S. Perero, E. Percivalle, E. Vecchio Nepita, M. Ferraris, Virucidal effect against coronavirus SARS-CoV-2 of a silver nanocluster/silica composite sputtered coating, Open Ceramics 1 (2020) 100006, https://doi.org/10.1016/j.oceram.2020.100006.

[31] G. Piedimonte, M.K. Perez, Respiratory syncytial virus infection and bronchiolitis, Pediatr. Rev. 35 (2014) 519–530, https://doi.org/10.1542/pir.35-12-519.

[32] R. Turner, W. Lee, Rhinovirus, in: D. Richman, R. Whitley, F. Hayden (Eds.), Clinical Virology, ASM Press, Washington DC, 2009, pp. 1063–1082.

[33] World Health Organization, Influenza (Seasonal). https://www.who.int/news-room/fact-sheets/detail/influenza-(seasonal), 2018 (accessed 06 November 2018).

[34] K.J. Szretter, A.L. Balish, J.M. Katz, Influenza: propagation, quantification, and storage, Curr. Protoc. Microbiol. 15 (2006) 15G.1, https://doi.org/10.1002/0471729256.mc15g01s3.

[35] M. Donalisio, M. Rittà, R. Francese, A. Civra, P. Tonetto, A. Coscia, High temperature—short time pasteurization has a lower impact on the antiviral properties of human milk than holder pasteurization, Front. Pediatr. 6 (2018) 304, https://doi.org/10.3389/fped.2018.00304.

[36] W. Chen, Y. Liu, H.S. Courtney, M. Bettenga, C.M. Agrawal, J.D. Bumgardner, J. L. Ong, In vitro anti-bacterial and biological properties of magnetron co-sputtered silver-containing hydroxyapatite coating, Biomaterials 27 (2006) 5512–5517, https://doi.org/10.1016/j.biomaterials.2006.07.003.

[37] K. Jamuna-Thevi, S.A. Bakar, S. Ibrahim, N. Shahab, M.R.M. Toff, Quantification of silver ion release, in vitro cytotoxicity and antibacterial properties of nanostuctured Ag doped TiO2 coatings on stainless steel deposited by RF magnetron sputtering, Vacuum 86 (2011) 235–241, https://doi.org/10.1016/j.vacuum.2011.06.011.

[38] S. Nakamura, M. Sato, Y. Sato, N. Ando, T. Takayama, M. Fujita, M. Ishihara, Synthesis and application of silver nanoparticles (Ag NPs) for the prevention of infection in healthcare workers, Int. J. Mol. Sci. 20 (2019) 3620, https://doi.org/10.3390/ijms20153620.

[39] H.H. Lara, E.N. Garza-Treviño, L. Ixtepan-Turrent, D.K. Singh, Silver nanoparticles are broad-spectrum bactericidal and virucidal compounds, J. Nanobiotechnol. 3 (2011) 9–30, https://doi.org/10.1186/1477-3155-9-30.

[40] X.X. Yang, C.M. Li, C.Z. Huang, Curcumin modified silver nanoparticles for highly efficient inhibition of respiratory syncytial virus infection, Nanoscale 8 (2016) 3040, https://doi.org/10.1039/c5nr07918g.

[41] D. Morris, M. Ansar, J. Speshock, T. Ivanciuc, Y. Qu, A. Casola, R. Garofalo, Antiviral and immunomodulatory activity of silver nanoparticles in experimental RSV infection, Viruses 11 (2019) 732, https://doi.org/10.3390/v11080732.

5. THE WONDER OF HUMAN MILK

5.1 Human milk composition and biological properties

Human milk is an extremely complex and highly variable biofluid that has evolved over millennia to nourish infants, support their growth and to protect them from numerous diseases. A large body of literature has demonstrated the benefits of human milk in diminishing infant morbidity and mortality and in protecting against specific infections during the breastfeeding period (106,107). This is particularly relevant for premature infants (i.e. born before the 37th week of pregnancy) because, they often develop complications, namely chronic lung disease, retinopathy and necrotizing enterocolitis (NEC) (108). The World Health Organization (WHO), indeed, recommends exclusive breastfeeding for the first 6 months of life, with continued breastfeeding for up to 2 years or beyond (109).

Breast milk composition changes in response to many factors including time of lactation, length of gestation, maternal diseases, genotype and diet and is widely believed to be specifically tailored by each mother to precisely reflect the requirements of her infant. It contains many complex proteins, lipids and carbohydrates as source of nutrition for infants, but it also contains a myriad of biologically active components. These molecules possess diverse roles, both guiding the development of the infant immune system and intestinal microbiota (110).

More specifically, the mean macronutrient composition of mature term milk is estimated to be approximately 0.9 to 1.2 g/dL for protein, 3.2 to 3.6 g/dL for fat, and 6.7 to 7.8 g/dL for lactose. The most abundant proteins are casein, α-lactalbumin, lactoferrin, secretory immunoglobulin IgA, lysozyme, and serum albumin, while the fat content is characterized by high levels of palmitic and oleic acids. Many micronutrients vary in human milk depending on maternal diet and body stores, including vitamins A, B1, B2, B6, B12, D, and iodine (111).

On the other hand, human milk contains a variety of factors with medicinal qualities that have a profound role in infant survival and health. Bioactive components, are defined as elements that "affect biological processes or substrates and hence have an impact on body function or condition and ultimately health". Many of these factors act synergistically, such that consumption of human milk is superior to supplementation with individual factors or their combinations (112). More precisely, human milk contains numerous growth factors, such as epidermal growth factor (EGF), neuronal growth factors, vascular endothelial growth factor (VEGF), insulin-like growth factors (IGF), adiponectin and other hormones, that have wide-ranging effects on the intestinal tract, vasculature, nervous system, and endocrine system and are likely to play a role in determining infant growth (112). Other molecules protect infants against infection and inflammation and contribute in developing the infant immune system and intestinal microbiota. The specific protective components of human milk

are so numerous and multi-functional, that science is just beginning to understand their functions. Part of my PhD project was indeed focused on the discovery of new bioactive components of human milk able to confer protection against viral infections. Immunological factors detected in human milk include, firstly, immunoglobulins such as secretory IgA (SIgA), the most predominant form, followed by SIgG. These provide immunological protection to the infant, whilst its own immune system matures. Their levels reflect the infant needs, therefore their concentration decreases withing lactation (110). A set of innate, multi-functional molecules also provide significant protection against infection. Factors such as the Toll-like receptors (TLR-2 and TLR-4) provide efficient microbial recognition, working in synergy with the co-receptor CD14 and soluble CD14. Other compound such as lactoferrin, lactadherin, human milk oligosaccharides (HMO) and mucins have been demonstrated to confer both anti-viral and anti-bacterial properties to human milk. Cytokines and chemokines and a variety of cells, including macrophages, T cells, stem cells, and lymphocytes can be also included in the list of immunologic factors detected in human milk (112).

A complete description of the numerous human milk bioactive factors, along with the full description of their roles, are beyond the scope of this thesis. The following Table I, produced by Ballard & Morrow (112), schematically summarize the major bioactive components and their functions.

Table I. Major bioactive factors in human milk	
Component	**Function**
Cells	
Macrophages	Protection against infections
Stem cells	Regeneration and repair
Immunoglobulines	
IgA/sIgA	Pathogen binding inhibition
IgG	Anti-microbial, activation of phagocytosis (IgG1, IgG2, IgG3); anti-inflammatory, response to allergens (IgG4)
IgM	Agglutination, complement activation
Cytokines	

IL-6	Stimulation of the acute phase response, B cell activation, pro-inflammatory
IL-7	Increased thymic size and output
IL-8	Recruitment of neutrophilis, pro-inflammatory
IL-10	Repressing Th1-type inflammation, induction of antibody production, facilitation of tolerance
IFN-ɤ	Pro-inflammatory, stimulates Th1 response
TGFβ	Anti-inflammatory, stimulation of T cell phenotype switch
TNFα	Stimulates inflammatory immune activation
Chemokines	
G-CSF	Trophic factor in intestines
MIF	Macrophage Migratory Inhibitory Factor: Prevents macrophage movement, increases anti-pathogen activity of macrophages
Cytokine Inhibitors	
TNFRI and II	Inhibition of TNFα, anti-inflammatory
Growth Factors	
EGF	Stimulation of cell proliferation and maturation
HB-EGF	Protective against damage from hypoxia and ischemia
VEGF	Promotion of angiogenesis and tissue repair
NGF	Promotion of neuron growth and maturation
IGF	Stimulation of growth and development, increased RBCs and hemoglobin
Erythropoietin	Erythropoiesis, intestinal development
Hormones	
Calcitonin	Development of enteric neurons
Somatostatin	Regulation of gastric epithelial growth

Anti-microbial	
Lactoferrin	Acute phase protein, chelates iron, antibacterial, anti-oxidant
Lactadherin/ MFG E8	Anti-viral, prevents inflammation by enhancing phagocytosis of apoptotic cells
Metabolic hormones	
Adiponectin	Reduction of infant BMI and weight, anti-inflammatory
Leptin	Regulation of energy conversion and infant BMI, appetite regulation
Ghrelin	Regulation of energy conversion and infant BMI
Oligosaccharides & glycans	
HMOs	Prebiotic, stimulating beneficial colonization and reducing colonization with pathogens; reduced inflammation
Gangliosides	Brain development; anti-infectious
Glycosaminoglycans	Anti-infectious
Mucins	
MUC1	Block infection by viruses and bacteria
MUC4	Block infection by viruses and bacteria

Table I. Major bioactive components of human milk. Adapted from "Human Milk Composition: Nutrients and Bioactive Factors" (112)

During my PhD course, I investigated human milk always referring to its different stages of maturation. Milk is commonly classified into colostrum, transitional milk and mature milk; however, these are not distinct classes of milk, but refer to the gradual alteration in the content of milk throughout lactation. In particular, colostrum is produced in low quantities in the first few days after partum and is rich in immunologic components such as secretory IgA, lactoferrin, leukocytes, as well as developmental factors such as epidermal growth factor. Colostrum also contains relatively low

concentrations of both lactose and fat, indicating that its primary functions are immunologic and trophic rather than nutritional. Levels of sodium, chloride and magnesium are higher and levels of potassium and calcium are lower in colostrum than later milk. As tight junction closure occurs in the mammary epithelium, the sodium to potassium ratio declines and lactose concentration increases, indicating secretory activation and the production of transitional milk. Transitional milk shares some of the characteristics of colostrum but represents a period that support the nutritional and developmental needs of the rapidly growing infant, and typically occurs from 5 days to two weeks postpartum, after which milk is considered mature. In contrast to the dramatic shift in composition observed in the first month of life, human milk remains relatively similar in composition over the course of lactation (110).

5.2 Viruses and human milk: transmission or protection? A brief overview on the topic

Several viruses, listed in Table II, have been detected in breast milk, but rarely the detection of a virus into this biofluid corresponds to an infected or diseased infant. In fact, exclusive breast-feeding is not normally associated with any risk, even in the case of maternal infection. The main hazards of breast-feeding are exposure to the maternal viral pathogens HIV, human T-cell lymphotropic virus-1 (HTLV-1), and HCMV (113). However, even for these viruses the actual transmission risk is not fully understood. Paradoxically, despite daily exposure to HCMV, most preterm infants breastfed by HCMV seropositive mothers do not become infected and do not develop clinical signs or severe diseases (114,115). A similar observation has been made for infants breastfed by HIV positive mothers and it has been demonstrated that exclusive breastfeeding, regardless of the HIV status of the mother, led to a significant decrease in mother-to-child transmission compared with non-exclusive breastfeeding (116). This intriguing paradox could be explained by the intrinsic antiviral properties of human milk, that is therefore able to neutralize the virus infectivity or reduce the viral titer, thereby lowering the risk of acquiring a symptomatic infection. A multitude of antiviral components, that is still partially undiscovered, synergically mediates this protective activity. Table III summarizes the major antiviral compounds detected in breast milk so far.

In this context, part of my PhD research was addressed to study the intrinsic antiviral properties of human milk against known and emerging viruses, with the aim to contribute to clarifying the described paradox. Furthermore, I also investigated the mechanism underlying milk antiviral properties, particularly focusing on the discovery of new antiviral compounds. All publications in the field of human milk were carried out in close collaboration with the Neonatal Care Unit of the University of Turin directed by Prof. Enrico Bertino and were supported by the Italian Association of Donor Milk Banks (AIBLUD).

Table II. Viruses detected in human milk			
Known viruses			
HIV: Human immunodeficiency virus	HCMV: Human cytomegalovirus	HTLV-I/HTLV-II: Human T-lymphotropic virus	HPV: Human papilloma virus
VZV: Varicella-zoster virus	EBV: Epstein-Barr virus	HBV: Hepatitis B virus	HCV: Hepatitis C virus
HAV: Hepatitis A virus	HEV: Hepatitis E virus	HSV-1/HSV-2: Herpes simplex virus type 1/2	HHV-6: Human herpes virus 6
HHV-7: Human herpes virus 7	HHV-8: Human herpes virus 8	HMTV: Human mammary tumor virus	CVB3: Coxsackievirus B3
RuV: Rubella virus			
Emerging viruses			
EBOV: Ebola virus	CHIKV: Chikungunya virus	DENV: Dengue virus	WNV: West Nile virus
ZIKV: Zika virus	YFV: Yellow fever virus	SARS-CoV-2: Severe Acute Respiratory Syndrome coronavirus 2	ADNV: Andes virus
What's next?			

Table II: Viruses detected in human milk. This table results from the electronic search in Pubmed with the following keywords and MeSH terms: ("Milk, Human"[Majr] OR breast-milk*[title] OR human-milk*[title]) AND ("virology"[subheading] OR "Viruses"[Mesh] OR viru*[tiab] OR viral*[tiab])

Table III. Human milk antiviral compounds			
Antibodies (IgA/IgG)	Oligosaccharides	Lactoferrin	Lactadherine
Mucins	Oxysterols	Tenascin-C	Lipid compounds
Glycosaminoglycans	Cytokines	Extracellular vesicles	Glycolipids
Secretory leukocyte protease inhibitor (SLPI)	sTLR2	Lewis X	*Others yet undiscovered*

Table III: Viruses detected in human milk. This table results from the electronic search in Pubmed of the following keywords and MeSH terms: ("Milk, Human"[Mesh] OR breast-milk*[tiab] OR human-milk*[tiab]) AND (antiviral[tiab] OR anti-viral[tiab] OR "Antiviral Agents"[Mesh] OR "Antiviral Agents"[Pharmacological Action])

6. DISCOVERY OF NEW ANTIVIRAL COMPONENTS OF HUMAN MILK

6.1 Viruses of pediatric clinical relevance

The section number 6 of this thesis is mainly focused on three viruses of pediatric clinical relevance: RSV, HRoV and HCMV. HRoV and RSV and their involvement in the pediatric area have been extensively described in sections 3.1 and 4.1 respectively.

HCMV is an enveloped dsDNA virus, belonging to *Herpesviridae* family and to the *Betaherpesvirinae* subfamily. Compared to the other human herpes viruses, HCMV is the largest, with a diameter around 200-300 nanometres and a genome of ~235 kb encoding over 220 open reading frames (ORFs) and 165 genes. It establishes a lifelong latent infection following primary infection that can periodically reactivate with shedding of infectious viruses. Transmission usually occurs by direct and prolonged contact with bodily fluids, including saliva, urine, and breast milk. HCMV can also be transmitted from a seropositive mother to her child during pregnancy and represents the major infectious cause of congenital abnormalities. Healthy individuals are usually asymptomatic, while HCMV is of great concern in immunocompromised patients and in preterm infants who are more prone to develop symptomatic disease (117).

HCMV virion has the typical herpesvirus structure: the dsDNA is contained in an icosahedral nucleocapsid enveloped by a proteinaceous tegument and an outer bilayer lipid envelope (Figure 13). The capsid has a protein component, comprising at least five proteins contributing to the formation of 12 pentons, 150 hexons and 320 triplexes. The major capsid protein is pUL86, which is the most abundant protein component of the capsid (960 copies) and forms the penton and hexons. The intermediate compartment is the tegument, which comprise more than half of the total proteins found within infectious virions (118). The protein component of the tegument plays a double role: some proteins are fundamental from the assembly of the virion and the disassembling of the viral particle during the entry phase into cells, others are able to modulate the host cell response during the infection. The envelope, characterized by a lipid bilayer derived from the host cell, contains around 20 virus encoded glycoproteins, fundamental for cell attachment and penetration. These include glycoprotein B (gB), gH, gL, gM, gN and gO (117). As in all other herpesviruses the expression of gH/gL and gB is essential for virus entry into cells (119). HCMV gH/gL is able to assemble either with a third glycoprotein (gO) forming a trimer on virus envelope or with UL128-131 (formed by a binding of three proteins), mediating the entry of HCMV in different cell types (respectively in fibroblast and epithelial/endothelial). On the other hand, gB and gM/gN mediate the initial adsorption of HCMV onto heparan sulphate glycosaminoglycans (GAG), a process that increases HCMV surface concentration, promotes other interactions and triggers entry fusion. Moreover, gB has been indicated as a primary receptor binding protein, and it could also be able to engage EGFR (Epidermal Growth Factor Receptor) in certain cell types (119).
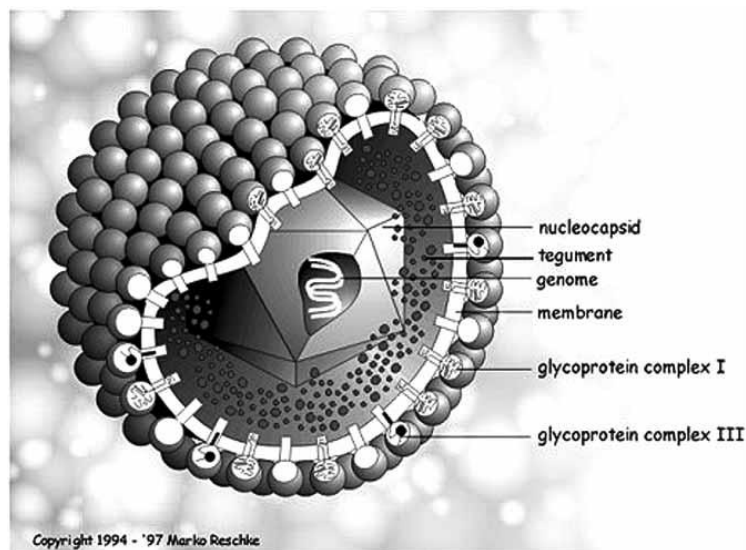

Figure 13: HCMV structure

The herpesvirus replicative cycle is divided into three major phases: initiation of infection, lytic replication and latency. After the infection occurs, the virus can either follow the lytic or the latent pathway, and it acquires the ability to reactivate to a lytic state after a long period of latency. A wide variety of human cell types can be infected by HCMV *in vivo*, and these include epithelial, endothelial, neuronal (astrocyte, oligodendrocyte and neuron), myeloid, macrophages, dendritic and fibroblast cells. Latent infection is granted by a myeloid cell population (precursor of monocytes, macrophages and dendritic cells) which remains in the bone marrow (120).

HCMV pathogenesis involves productive replication. The entire HCMV replicative cycle is schematically presented in Figure 14.
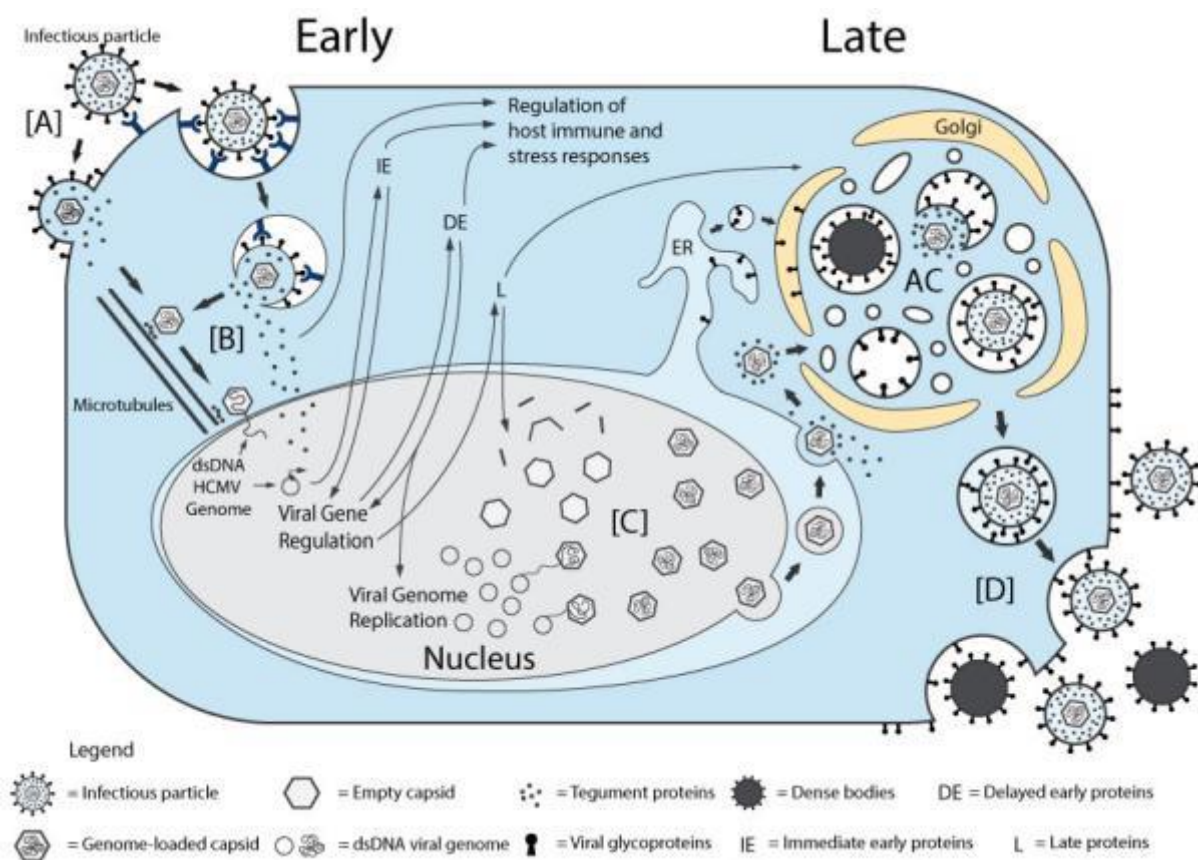

Figure 14. Overview of the HCMV life cycle (A) Infectious particles enter the cell through interaction with cellular receptors. Capsid and tegument proteins are delivered to the cytosol. (B) The capsid travels to the nucleus, where the genome is delivered and circularized. Tegument proteins regulate host cell responses and initiate the temporal cascade of the expression of viral I immediate early (IE) genes, followed by delayed early (DE) genes, which initiate viral genome replication, and late (L) genes. (C) Late gene expression initiates capsid assembly in the nucleus, followed by nuclear egress to the cytosol. Capsids associate with tegument proteins in the cytosol and are trafficked to the viral assembly complex (AC) that contains components of the endoplasmic reticulum (ER), Golgi apparatus and endosomal machinery. The capsids further acquire tegument and viral envelope by budding into intracellular vesicles at the AC. (D) Enveloped infectious particles are released along with non-infectious dense bodies (120).

HCMV is a common pathogen of global clinical relevance, with worldwide seroprevalence ranging from 56% to 94%. The viral spread in the global population is enormous, mainly due to the asymptomatic mode of infection, followed by a constant shedding of the virus through body fluids (e.g., milk, saliva, cervical secretions, and tears), which can last for months or even years (121). While HCMV infection is generally asymptomatic, it is particularly dangerous for immunocompromised individuals and congenitally infected newborns, who can be infected in utero, postnatally, or via breastfeeding. Indeed, HCMV is notoriously famous for its ability to cause congenital anomalies and long-term neurological sequelae in newborns. About one out of every 200 babies is born with congenital HCMV infection and even though most infants are asymptomatic, they may develop health problems at birth or later. In the most severe cases, congenital HCMV can cause the death of the unborn baby. In all other cases, the most clinically relevant signs at birth may include microcephaly, hepatosplenomegaly, retinitis, intrauterine growth restriction, seizures, rash, and jaundice. Some children with congenital HCMV infection may also suffer from long-term health problems, such as hearing loss, which can be present at birth or may develop later even in asymptomatic infants, developmental and motor delay, vision loss, and seizures (121,122). Premature infants, especially those with a birth weight below 1500 g or those of less than 32 weeks of gestational age, are at greatest risk of developing congenital disease through breastfeeding. Different studies showed that they may develop neutropenia, lymphocytosis, hepatosplenomegaly, and aggravation on respiratory status. A sepsis-like syndrome was also observed in some cases. Compared with term infants, preterm newborns have lower level of HCMV-specific IgG and often rapidly lose maternal IgG due to repeated blood sampling and transfusions (123). Furthermore, HCMV can also trigger the development of serious pathologies in solid organ or stem cell transplant recipients that are not always resolved by currently available antivirals, thereby leading in some cases to death (121,122). During solid organ transplantation, seropositive donors frequently (around 78%) transmit HCMV to seronegative recipients. On the other hand, approximately 40% of seropositive recipients reactivate latent HCMV or can be infected with new strains when treated with immunosuppressive drugs.

Despite increasing efforts, an effective vaccine against HCMV is currently missing, de facto leaving high-risk populations, chiefly immunocompromised patients and immunocompetent seronegative pregnant mothers, exposed to primary infection. Four compounds are currently approved for systemic treatment or prophylaxis of HCMV infections, ganciclovir (GCV) and its oral prodrug valganciclovir (VGCV), cidofovir (CDV), foscarnet (FOS), and, more recently, letermovir (LTV), but they are quite unsatisfactory due to the frequent occurrence of drug resistance and toxicity(124).

6.2 The human milk-derived extracellular vesicles (HM-EVs)

Despite the widely recognized health benefits of human milk, some intriguing mysteries still have to be solved, in particular about how specific components confer intrinsic protection against infections and how they contribute to the development of both infant's innate and adaptive immune functions. In the search of new antiviral components contained in human milk, we examined the antiviral potential of human milk-derived extracellular vesicles (HM-EVs).

Extracellular vesicles (EVs) are a heterogeneous group of secreted nanoparticles, often referred to as distinct subsets, such as "exosomes", "apoptosomes", "oncosomes", "microvesicles," and "platelet dust". They consist of lipid bilayer enclosed vesicles displaying a heterogeneous size ranging from 50 to 300 nm and they are released by most tissues and they have been identified in various biological fluids, such as urine, blood, cerebrospinal fluid, and breast milk. EVs can be taken up by other cells in which they release their molecular cargo (e.g. miRNA, mRNA, RNAs, enzymes, signalling proteins) playing a role in intercellular signalling, immune response, stem cell differentiation, neuronal function, tissue regeneration and viral replication (125).

Despite numerous studies that have investigated HM-EVs, their exact functions and their physiological concentrations are still largely unknown (126). HM-EVs function has been investigated both *in vitro* and *in vivo* suggesting that EVs play a role in immunomodulation and in protection from necrotizing enterocolitis (NEC) (126–128). RNA content of HM-EVs was examined by Karlsson et al. who identified a range of long noncoding RNAs implicated in the immune system [e.g., growth arrest-specific 5 (GAS5), ZNFX1 antisense RNA 1 (ZFAS1), steroid receptor RNA activator 1 (SRA1), and differentiation antagonizing non-protein coding RNA (DANCR)] and metabolism [e.g., GAS5, SRA1, colorectal neoplasia differentially expressed (CRNDE)] (129). It has also been reported the presence of immune-related miRNA (*miR-181a and miR-17)* in the EVs produced during the first 6 mounts of lactation, indicating EVs as delivery vehicles (130). HM EVs and HM-associated miRNAs may also play a role in the regulation of metabolism. Although this possibility is poorly understood in humans, some evidence has been obtained in other mammals. For instance, porcine EVs contain miRNAs associated with regulation of key metabolic pathways including the citrate cycle and glycerophospholipid metabolism (131). Both rat and mouse models showed differences in muscle physiology in those that received an oral gavage of EVs that were RNA sufficient versus those treated with RNA-depleted EVs (132). Some mechanistic evidence was also found to support a role of EV-associated miRNAs in the regulation of the mTORC1 pathway, a key regulator of both growth and development (133).

Proteins transported as EV cargo and surface EV-proteins have been identified as one of the mediators of EV functions. Using proteomics analysis of HM-EVs, van Herwijnen et al. revealed

\>600 proteins not previously detected in human milk and indicated that these proteins were associated with signal transduction, controlling inflammatory signaling pathway with a possible role in supporting the newborn's gut and immune system (134).

Interestingly, HM-EVs along with their microRNA and protein cargo have been shown to survive to *in vitro* pancreatic and gastric digestion, supporting the hypothesis that intact EV cargos are delivered to intestinal cells where they may elicit their functions (135,136). Furthermore, researchers recently demonstrated that exosomes from animal milk are long-lasting *in vivo* and accumulate in the intestinal mucosa, spleen, liver, heart or brain when administered orally or intravenously to mice and pigs (137,138).

Finally, the possible antiviral role of HM-EVs is still largely unexplored. The only available study reported that milk exosomes, a specific subclass of EVs, bind monocyte-derived dendritic cells (MDDCs) via DC-SIGN inhibiting HIV-1 infection of MDDCs and subsequent viral transfer to CD4 T cells.

Prompted by the abovementioned studies and with the aim to contribute to clarifying HM-EVs functions, we investigated the protective role of HM-EVs against HCMV, HRoV and RSV, three pathogens clinically relevant for infants and trigger of severe complications in preterm babies. The studies in the field of HM-EVs will shed light on their role in infant development and protection and will contribute to clarifying the milk exact composition. An additional rationale for examining HM EVs is for the possible therapeutic use of exogenously delivered EVs. This is already a fertile ground for research with multiple neonatal conditions targeted using mesenchymal stem cell (MSC)–derived EVs as "cell free" regenerative medicine (126). HM-EVs could become a therapeutic option for neonates whose mothers are unable to breastfeed and where receiving donor-expressed breast milk is difficult.

6.2.1 Publications

Donalisio M, Cirrincione S, Rittà M, Lamberti C, Civra A, Francese R, Tonetto P, Sottemano S, Manfredi M, Lorenzato A, Moro GE, Giribaldi M, Cavallarin L, Giuffrida MG, Bertino E, Coscia A, Lembo D. Extracellular Vesicles in Human Preterm Colostrum Inhibit Infection by Human Cytomegalovirus In Vitro. Microorganisms. 2020 Jul 21;8(7):1087. doi: 10.3390/microorganisms8071087. PMID: 32708203; PMCID: PMC7409124.

In the present study, we have addressed the question of whether breast milk-derived EVs could inhibit HCMV infection, and we have explored how EVs can affect the viral replicative cycle steps. Colostra were collected from mothers of preterm infants and EVs were derived and characterized. Performing specific antiviral assays *in vitro*, we confirmed the antiviral action of colostrum against HCMV and we demonstrated, for the first time, a remarkable antiviral activity of colostrum-derived EVs. The investigation of the mechanism of action has indicated that the anti-HCMV activity of EVs is not mediated by a direct inactivation of the viral particle, but rather by the inhibition of the viral attachment to the cell surface. Furthermore, we conducted "membrane shaving" experiments and a proteomic analysis of the shaved peptides with the aim of characterizing the potential molecular players of the antiviral activity. The significant reduction in the antiviral activity of EVs, after shaving experiments, suggests a crucial role of EV surface proteins in inhibiting viral infection. The proteomic analysis of the EV surfaceome revealed the contribution of immune components including antibodies (mainly IgA) and complement component proteins (C9 and C3) to antiviral activity. We found both milk proteins (caseins, whey proteins and milk fat membrane associated proteins) and proteins shared by different tissue cells and biological fluids. The common feature of the identified proteins is that their glycomoieties seem to play a crucial role in the interference mechanism between a virus and the host cells, acting as a point of cell-specific recognition for the virus particle and inhibiting its attachment on the cell surface. Overall, our results provide novel insights into the protective role of human colostrum against HCMV and indicate extracellular vesicles as new additional bioactive components of human milk.

The second study on the topic was carried out in parallel with the first one, but focusing on RSV and HRoV. Although the protective role of breastfeeding on respiratory and gastrointestinal infections caused by RSV and HRoV was well established, the intrinsic anti-RSV and anti-HRoV activity of human milk was poorly investigated until then. Therefore, we addressed this issue, in the context of preterm infants, by assessing the antiviral activity of human colostrum and by exploring whether the EVs contribute to its antiviral properties. To the best of our knowledge, we reported the intrinsic antiviral activity of human colostrum against RSV and HRoV for the first time. Furthermore, we found that EVs were endowed with anti-RSV and anti-HRoV activity, although to a different extent between mothers and, differently from the first study, we indicated that EVs inhibit HRoV and RSV by interfering with their entry into the host cells.

Taken together, our results confirmed that EVs can be added to the list of antiviral effectors contained in human milk and contributed to unraveling novel mechanisms underlying the functional role of human milk as a protective and therapeutic agent in preterm infants.

Extracellular Vesicles in Human Preterm Colostrum Inhibit Infection by Human Cytomegalovirus In Vitro

Manuela Donalisio [1,*,†], **Simona Cirrincione** [2,†], **Massimo Rittà** [1], **Cristina Lamberti** [2], **Andrea Civra** [1], **Rachele Francese** [1], **Paola Tonetto** [3], **Stefano Sottemano** [3], **Marcello Manfredi** [4], **Annalisa Lorenzato** [5,6], **Guido E. Moro** [7], **Marzia Giribaldi** [8], **Laura Cavallarin** [2], **Maria Gabriella Giuffrida** [2], **Enrico Bertino** [3], **Alessandra Coscia** [3,*] and **David Lembo** [1]

[1] Laboratory of Molecular Virology, Department of Clinical and Biological Sciences, University of Turin, 10043 Orbassano, Italy; massimo.ritta@unito.it (M.R.); andrea.civra@unito.it (A.C.); rachele.francese@unito.it (R.F.); david.lembo@unito.it (D.L.)

[2] Consiglio Nazionale delle Ricerche-Istituto di Scienze delle Produzioni Alimentari, 10095 Grugliasco (TO), Italy; simona.cirrincione@ispa.cnr.it (S.C.); cristina.lamberti@ispa.cnr.it (C.L.); laura.cavallarin@ispa.cnr.it (L.C.); gabriella.giuffrida@ispa.cnr.it (M.G.G.)

[3] Neonatal Intensive Care Unit, Department of Public Health and Pediatrics, University of Turin, 10126 Torino, Italy; paola.tonetto@unito.it (P.T.); stefano.sottemano@unito.it (S.S.); enrico.bertino@unito.it (E.B.)

[4] Center for Translational Research on Autoimmune and Allergic Disease (CAAD), University of Piemonte Orientale, 28100 Novara, Italy; marcello.manfredi@uniupo.it

[5] Candiolo Cancer Institute, FPO-IRCCS, 10060 Candiolo (TO), Italy; annalisa.lorenzato@unito.it

[6] Department of Oncology, University of Turin, 10060 Candiolo (TO), Italy

[7] Italian Association of Human Milk Banks, 20126 Milano, Italy; guidoemoro@tiscali.it

[8] Research Centre for Engineering and Agro-food Processing (CREA), 10135 Torino, Italy; marzia.giribaldi@crea.gov.it

* Correspondence: manuela.donalisio@unito.it (M.D.); alessandra.coscia@unito.it (A.C.); Tel.: +39-011-6705427 (M.D.); +39-011-3134437 (A.C.)

† These authors contributed equally to this work.

check for updates

Abstract: Breast milk is a complex biofluid that nourishes infants, supports their growth and protects them from diseases. However, at the same time, breastfeeding is a transmission route for human cytomegalovirus (HCMV), with preterm infants being at a great risk of congenital disease. The discrepancy between high HCMV transmission rates and the few reported cases of infants with severe clinical illness is likely due to the protective effect of breast milk. The aim of this study was to investigate the anti-HCMV activity of human preterm colostrum and clarify the role of colostrum-derived extracellular vesicles (EVs). Preterm colostrum samples were collected and the EVs were purified and characterized. The in vitro anti-HCMV activity of both colostrum and EVs was tested against HCMV, and the viral replication step inhibited by colostrum-purified EVs was examined. We investigated the putative role EV surface proteins play in impairing HCMV infection using shaving experiments and proteomic analysis. The obtained results confirmed the antiviral action of colostrum against HCMV and demonstrated a remarkable antiviral activity of colostrum-derived EVs. Furthermore, we demonstrated that EVs impair the attachment of HCMV to cells, with EV surface proteins playing a role in mediating this action. These findings contribute to clarifying the mechanisms that underlie the protective role of human colostrum against HCMV infection.

Keywords: HCMV; breastfeeding; preterm; colostrum; extracellular vesicles; antiviral

1. Introduction

Human milk (HM) is considered the most important biofluid for the nutrition of infants and for the development of a child's immune system by the World Health Organization [1]. HM provides protection against necrotizing enterocolitis, sepsis, enteric and respiratory infections and severe retinopathy and decreases the risk of death. For these reasons, the American Academy of Pediatrics recommends exclusive breastfeeding for the first 6 months of life, and colostrum is considered especially important for preterm newborns (up to one week postpartum) [2–4]. In spite of the well-known health benefits of HM, breastfeeding is also a common route for the mother-to-child transmission of human cytomegalovirus (HCMV), particularly in populations with a high HCMV seroprevalence. During lactation, the virus is shed into HM by almost every seropositive woman; maternal HCMV reactivation can already be detected in the colostrum and normally ends about three months after birth, as evidenced by PCR and viral culture analyses [5,6]. The postnatally acquired symptomatic HCMV infection rate is low in term infants, whereas preterm infants, especially those with a birth weight below 1500 g or those of less than 32 weeks of gestational age, are at the greatest risk of developing congenital disease through breastfeeding [5]. Systematic reviews have shown that breast milk-acquired HCMV infection with symptomatic disease is relatively rare [7,8]. The discrepancy of high HCMV transmission rates and the low number of reported infants with severe clinical illness are probably due to the protective effect of the components of breast milk against viral infection. We have recently demonstrated, in the context of preterm infants, that HM is endowed with intrinsic anti-HCMV properties, and their potency may vary according to the stage of lactation and the serological status of the mother [9]. Passive immunity is provided to newborns through a large number of soluble and cellular immune HM components, such as secretory immunoglobulins and leukocytes, as well as antimicrobial factors [10]. In this context, immunomodulatory and specific bioactive factors, such as lactoferrin, vitamin A and monolaurin, have been demonstrated to endow specific anti-HCMV properties. [11–13].

Extracellular vesicles (EVs) from human milk have recently become a subject of increasing interest for their protective role for infants [14]. EVs are complex structures, ranging from 50 to 300 nm in diameter, with an endosome-derived limiting membrane, secreted by a diverse range of cell types and found in all body fluids [15]. Milk EVs may originate from breast epithelial cells and from the macrophages and lymphocytes present in breast milk [16]. EVs have been found to be involved in cell–cell communication through the transfer of their cargos, which consist of microRNAs, noncoding RNAs, lipids and proteins from donor cells to recipient cells. Several current publications suggest an immune-regulatory role of milk EVs, especially exosomes, in both immune stimulation and toleration, and several studies have suggested their potential in immunotherapy [17,18]. Recent publications on the antiviral properties of EVs support the hypothesis that milk EVs are involved in the instruction of the protective role of the neonatal immune system [19]. In the present study, we have addressed the question of whether breast milk-derived EVs could inhibit HCMV infection, and we have explored how EVs can affect the viral replicative cycle steps. Furthermore, after conducting "membrane shaving" experiments, the antiviral activity of EVs was explored and a proteomic analysis of the shaved peptides was performed with the aim of characterizing the potential molecular players of antiviral activity.

2. Materials and Methods

2.1. Human Colostrum Collection

Colostrum samples (1–5 days postpartum, 15 mL each) were obtained from 13 healthy mothers admitted to the Sant'Anna Hospital (Città della Salute e della Scienza di Torino, Turin, Italy) for preterm delivery between February 2017 and January 2020. An ethical review process was not required for this study since it was not a clinical trial. Each milk donor involved in this research signed a written consent form in which the data protection of the mother and infant was assured. Moreover, the donors were informed that only milk samples stored in excess would be used for research purposes, and the study design was explained. The donors cleaned their hands and breasts according to the

Italian Human Milk Bank (HMB) guidelines [20]. Samples were collected, by means of an electric breast pump, in disposable sterile polypropylene Bisphenol-free bottles, to minimize the possibility of contamination. The main clinical characteristics of the study population are reported in Table 1.

Table 1. Main clinical characteristics of the study group.

Sample no.	Parity *	Breastfeeding afterPrevious Delivery(ies)	Type of Delivery
1	2002	Yes	CS
2	0000	-	CS
3	0000	-	CS
4	1001	Yes	CS
5	0000	-	S
6	1021	Yes	S
7	0000	-	CS
8	0000	-	CS
9	1001	Yes	CS
10	1001	Yes	CS
11	1001	-	S
12	0000	Yes	CS
13	1001	-	CS

* The numbers indicate full-term births, premature births, abortions and living children. CS: caesarean section; S: spontaneous delivery.

2.2. Colostrum Clarification and Extracellular Vesicle (EV) Isolation

Ten-milliliter colostrum samples were centrifuged at 2000× *g* for 10 min, and the defatted colostrum was transferred to a new tube and centrifuged at 12,000× *g* for 30 min. The aqueous supernatant fractions were filtered (0.45 μm pore size filter), and two volumes of filtered supernatants were incubated overnight with one volume of Exoquick Exosome Precipitation Solution (SBI, System Biosciences, Palo Alto, CA, USA) at 4 °C. The following day, the mixture was centrifuged at 1500 g for 30 min at 4 °C, and the precipitated EVs were resuspended in PBS. The protein concentration was determined by means of a Protein Assay (Bio-Rad, Hercules, CA, USA).

2.3. EV Characterization by Immunoblotting

The protein profile of the EVs was determined by immunoblotting, using human foreskin fibroblasts (HFF-1) as a control. The EV preparations and HFF-1 cells were lysed in an RIPA buffer (25 mM Tris-HCl pH 7.6, 150 mM NaCl, 1% NP-40, 1% sodium deoxycholate, 0.1% sodium dodecyl sulfate (SDS) with a protease inhibitor cocktail. The supernatants were analyzed for protein concentrations by means of the Bio-Rad Protein Assay (Bio-Rad). The extracted proteins were denatured in a Laemmli buffer (4% SDS, 20% glycerol, 10% β-mercaptoethanol, 0.004% bromophenol blue, 0.125 M tris-HCl pH 6.8) at 95 °C for 5 min. The lysates were fractionated onto 8.5% SDS-PAGE and transferred to a polyvinilidene difluoride membrane (Millipore, USA). The following primary antibodies were used: CD9, CD63, CD81 (1:1000; SBI System Biosciences) and calnexin (1:1000, Transduction Laboratories, San Jose, CA, USA).

2.4. Nanoparticle Tracking Analysis (NTA)

A nanoparticle tracking analysis system (NanoSight NS300, Malvern Instruments Ltd, Malvern, UK) was used to determine the particle size and particle concentration. EV preparations were diluted in PBS (1:8000) prior to analysis and quantified in triplicate. Data were reported as the number of particles/mL (n/mL).

2.5. Cell lines and Viruses

Low-passage-number (<30) HFF-1 (ATCC SCRC-1041) were grown as monolayers in Dulbecco's modified Eagle's medium (DMEM) (Sigma-Aldrich, Sain Louis, USA), supplemented with

15% heat inactivated fetal bovine serum (FBS) (Sigma-Aldrich) and a 1% antibiotic solution (penicillin–streptomycin, Sigma-Aldrich). A bacterial artificial chromosome-derived HCMV Towne strain, incorporating the green fluorescent protein (GFP) sequence, was propagated on HFF-1 [21]. HCMV Towne titers were determined on the HFF-1 cells by means of a fluorescence focus assay, as previously reported [9]. The HCMV AD169 laboratory strain (ATCC VR-538) was propagated on HFF-1 cells by infecting freshly prepared confluent monolayers in DMEM 2% FBS. When the whole monolayer displayed a clear cytopathic effect, the infected cell suspension was collected, and the viral supernatant was clarified by means of centrifugation. Viral stocks were aliquoted and stored at −80 °C. HCMV-AD169 titers were determined on the HFF-1 cells using the median tissue culture infective dose ($TCID_{50}$) method.

2.6. Cell Viability Assay

Colostrum samples and extracellular vesicles were investigated for their impact on cell viability by means of a 3-(4,5-dimethylthiazol-2-yl)-5-(3-carboxymethoxyphenyl)-2-(4-sulfophenyl)-2H-tetrazolium (MTS) assay, as described in Cagno et al. (2015) [22]. HFF-1 cells, pre-seeded at a 5×10^3/well density in 96-well plates in DMEM 10% FBS, were challenged with serial dilutions of the aqueous fraction of colostra and extracellular vesicles. After 5 days of incubation at 37 °C, the cell monolayers were washed three times with DMEM, and cell viability was assessed with a Cell Titer 96 Proliferation Assay Kit (Promega, Madison, WI, USA). An aliquot of 20 microliters of MTS reagent was added to 100 µL DMEM per well; the cells were incubated at 37 °C for 4 h. Absorbance was measured at 491 nm using a Multiskan FC Microplate Photometer (Thermo Scientific, Waltham, MA, USA). The percentage of absorbances of the treated cells to the cells incubated with only a culture medium was calculated, and the 50% cytotoxic concentrations (CC_{50}) and 95% confidence intervals (95% CI) were determined for the preterm colostra and colostrum-derived EVs using Prism software (Graph-Pad Software, San Diego, CA, USA).

2.7. HCMV Inhibition Assay

Pre-seeded HFF-1 cells (density 5×10^3 per well in 96-multiwell plates) were pre-incubated with serial dilutions of colostra (1:1 to 1:1024) and EVs (from 423 µg/mL to 0.41 µg/mL) for 1 h at 37 °C. Corresponding serial dilutions of colostra and EVs containing a constant amount of HCMV Towne at a multiplicity of infection (MOI) of 0.02 foci forming units (FFU)/cell or HCMV AD169 at a MOI of 0.03 plaque forming units (PFU)/cell were incubated for 1 h at 37 °C and were then added to pre-treated HFF-1 cells. Viral adsorption was performed for 2 h at 37 °C. The inocula were removed; then, the cells were washed and were then overlaid with a 1.2% methylcellulose DMEM medium 2% FBS. After 5 days of incubation at 37 °C, the HCMV Towne-infected cells and foci were visualized as green fibroblasts by means of fluorescence microscopy and counted. The results were reported as the percentage of fluorescent cells compared to the control. The HCMV AD169-infected cell monolayers, after 5 days of incubation at 37 °C, were fixed with cold methanol-acetone (1:1) for 1 min, permeabilized in PBS 0.1 % Triton X-100, treated with PBS–methanol (1:1) 0.6% H_2O_2 and subjected to HCMV-specific immunostaining with a specific anti-HCMV IEA monoclonal antibody (1:1500 dilution; 11-003, Argene, Verniolle, France). An UltraTech HRP Streptavidin–Biotin detection system was used (Beckman Coulter, Marseille, France). The immunostained cells and plaques were counted, and the percentage of the inhibition of virus infectivity was determined. The concentrations of colostra and EVs that produced a reduction of 50% and of 90% in the formation of HCMV Towne foci (effective concentration-50 (EC_{50}) and effective concentration-90 (EC_{90})) and of HCMV AD169 infectivity, in comparison with the controls, were calculated by means of Prism 5 software.

2.8. HCMV Inactivation Assay

Constant amounts of HCMV Towne (10^5 FFUs) were challenged with EVs at EC_{90} concentrations (as determined in the inhibition assay) in a final volume of 110 µL. The virus–EV mixtures were

incubated for 2 h at 37 °C. Both EV-treated and untreated HCMV mixtures were titrated to non-inhibitory concentrations on HFF-1 cells (density 5×10^3/well) by means of a foci assay. Viral infectivity was determined after 5 days of incubation at 37 °C by means of fluorescence microscopy. The titers of the EV-treated and untreated viral mixtures were analyzed by means of the Student's *t*-test. Significance was reported for $p < 0.05$.

2.9. Pre-Treatment Assay

HFF-1 cells (5×10^3/well density) were challenged with serial dilutions of EV preparations at 37 °C for 2 h. After washing, the cells were infected with HCMV Towne at a MOI of 0.02 FFU per cell for 2 h, washed and incubated with a 1.2% methylcellulose DMEM medium with 2% FBS. After 5 days of incubation at 37 °C, the infected cells and foci were visualized by means of fluorescence microscopy and counted. The EC_{50} values of the EV preparations were calculated using Prism 5 software.

2.10. Attachment Assay

Pre-chilled HFF-1 cells (5×10^3/well density) were infected with HCMV Towne at a MOI of 0.2 (FFU per cell) at 4 °C in the presence of serial dilutions of EV preparations. After one wash, to remove the unbound virus, the cells were shifted to 37 °C for 2 h. The outer virions were inactivated with acidic glycine (0.1 M glycine, 0.14 M NaCl, pH 3) for 2 min at RT. The cells were then washed three times, overlaid with a 1.2% methylcellulose DMEM medium 2% FBS and incubated at 37 °C for 5 days. The infected cells and foci were visualized by means of fluorescence microscopy and counted. The EC_{50} values of the EV preparations were calculated using Prism 5 software. All the experiments were performed in triplicate.

2.11. Entry Assay

HCMV Towne, at a MOI of 0.2 FFU/cell, was adsorbed for 2 h at 4 °C on pre-chilled HFF-1 cells (5×10^3/well density). After one wash to remove any unbound viral particles, the cells were treated with serial dilutions of EV preparations for 2 h at 37 °C. The outer virions were inactivated with acidic glycine for 2 min at RT. The cells were then washed three times, overlaid with a 1.2% methylcellulose DMEM medium 2% FBS and incubated at 37 °C for 5 days. The infected cells and foci were visualized by means of fluorescence microscopy and counted. The EC_{50} values of the EV preparations were calculated using Prism 5 software. All the experiments were performed in triplicate.

2.12. Post-Entry Assay

HCMV Towne, at a MOI of 0.2 FFU/cell, was adsorbed for 2 h at 4 °C on pre-chilled HFF-1 cells (5×10^3/well density). After one wash, the cells were shifted to 37 °C for 2 h. The outer virions were inactivated with acidic glycine for 2 min at RT. The cells were then washed three times, challenged with serial dilutions of EV preparations in a 1.2% methylcellulose DMEM medium 2% FBS and incubated at 37 °C for 5 days. The infected cells and foci were visualized by means of fluorescence microscopy and counted. The EC_{50} values of the EV preparations were calculated using Prism 5 software. All the experiments were performed in triplicate.

2.13. Data Analysis

The EC_{50} and EC_{90} concentrations were calculated by means of regression analysis and compared using the F-test by Prism 5 Software. The Student's *t*-test was used for the virus inactivation assay to compare the viral titers in the EV-treated and untreated samples, as well as for the attachment assay to compare the number of HCMV foci. A one-way ANOVA was used to compare HCMV infectivity in the attachment assays with the pooled peptides. Significance was reported for $p < 0.05$. All the experiments are presented and discussed as the means of the results of three independent experiments performed in duplicate.

2.14. Shaving of Extracellular Vesicles

An aliquot of 100 µL of EVs, resuspended in PBS, was mixed with an equal volume of 25 mM NH_4HCO_3. An aliquot of 3 µL of trypsin (1 µg/µL) (Promega, Madison, WI, USA) was added and the sample was incubated at 37 °C for 4 h under mild agitation in order to allow surface protein digestion. The shaved EVs were washed with sterile PBS using a 300 kDa Nanosep Centrifugal Device (Pall Corporation, New York, US) previously passivated for 1 h with 5% Tween80 and washed once with 70% ethanol, once with sterile ddH_2O and twice with 25 mM NH_4HCO_3. In order to obtain the tryptic peptide fraction, the solution that passed through the membrane was collected and further filtrated with 10kDa Nanosep. The peptides were then dried under vacuum (Concentrator 5301, Eppendorf AG, Hamburg, Germany) before LC–MS/MS analysis. As a control, the EV preparation was processed, as already described, without the trypsin digestion step.

2.15. ESI-Q-TOF Analysis of Peptides

LC–MS/MS analyses were performed using a micro-LC Eksigent Technologies (Dublin, USA) system with a stationary phase of a Halo Fused C18 column (0.5×100 mm, 2.7 µm; Eksigent Technologies, Dublin, USA). The injection volume was 4.0 µL and the oven temperature was set at 40 °C. The mobile phase was a mixture of 0.1% (v/v) formic acid in water (A) and 0.1% (v/v) formic acid in acetonitrile (B), which was eluted at a flow-rate of 15.0 µL/min at increasing concentrations of B; that is, from 2% to 40% in 30 min. Peptides were suspended in 10 µL of A. The LC system was interfaced with a 5600+ TripleTOF system (AB Sciex, Concord, Canada), equipped with a DuoSpray Ion Source and CDS (Calibrant Delivery System). Peptide identification was performed using the traditional data-dependent acquisition (DDA) method. The MS data were acquired with Analyst TF 1.7 (SCIEX, Concord, Canada).

2.16. Peptide Data Search

The MS files were searched using Mascot v. 2.4 software (Matrix Science Inc., Boston, MA, USA) with trypsin as the enzyme, a peptide mass tolerance of 50 ppm, an MS/MS tolerance of 0.1 Da, peptide charges set to 2^+, 3^+ and 4^+ and under consideration of the monoisotopic mass. The UniProtKB review database containing human proteins (Human Uniprot, version v.2018.02.01, 42,271 sequences) was used. Only the peptides with a higher peptide score than the peptide identity were considered for the protein identification. Moreover, only the proteins identified in at least two samples out of three were selected as shared proteins and subjected to further in silico analyses. In the case of common proteins identified with a single peptide, they were only included if they were identified with at least two peptides in another sample containing the same protein.

2.17. In Silico Analysis of Proteins

The 45 proteins selected as previously described were analyzed using three open-source tools. Cell Plock 2.0 (package Euk-mPLoc 2.0) (http://www.csbio.sjtu.edu.cn/bioinf/euk-multi-2/) was used to find the protein sub-localization, Protter version 1.0 (http://wlab.ethz.ch/protter/start/) was used to visualize the protein arrangement between the internal and external environment of the cell, and InterPro (https://www.ebi.ac.uk/interpro/) was used to classify the proteins according to the biological process in which they are involved.

3. Results and Discussion

3.1. Milk Sample Collection and Antiviral Activity of Colostrum-Derived Extracellular Vesicles (EVs) against HCMV

The first set of experiments was performed on 13 fresh colostrum samples (1–5 days postpartum) collected from healthy donor mothers admitted to the Sant'Anna Hospital of Turin (Città della Salute e della Scienza di Torino). This study group included mothers of preterm infants with gestational

ages ranging from 23 + 3 to 32 + 0 (weeks + day). The milk was collected in the hospital and kept at room temperature until it was delivered to the laboratory, where it was processed within two hours. The aqueous fraction derived from clarified colostrum is considered the most appropriate biological matrix for in vitro assays because of its lower impact on cell viability than whole milk [9]; it was therefore used as the starting material for the isolation of EVs with an ExoQuick preparation [23,24]. The EV pellet was dissolved in a small volume of PBS, and its protein concentration was determined. Vesicles purified from preterm colostra were characterized using nanoparticle tracking analysis to determine the size and particle concentration. The Nanosight instrument showed that most EVs were between 100–400 nm in diameter (mean size, 219.9 ± 28.7 nm, mode 184.4 nm; a representative analysis is reported in Figure 1A). The particle concentration of the milk EVs was roughly 1.00×10^{13} particles/mL. Minimal differences in size and concentration were observed for the different EV preparations. Protein lysates were prepared and Western blot analysis was performed to confirm the presence of exosomes in the EVs. The immunoblotting revealed that the colostrum-derived vesicles were positive for the CD63, CD9 and CD81 exosome-associated proteins, but negative for calnexin, which was only detected in the HFF-1 cell lysate. The negative calnexin signal indicated that the EVs did not contain an endoplasmic reticulum marker (Figure 1B) [25,26].

After the isolation and characterization of the EVs, colostrum samples and the corresponding isolated EVs were tested in vitro on HFF-1 cells against HCMV Towne strain expressing the GFP protein; the GFP marker facilitated the identification of infected cells. As reported in Table 2, we confirmed the net antiviral activity of colostrum against HCMV, with the presence of only moderate differences among samples; all the tested samples generated dose–response curves with a half maximal effective concentration (EC_{50} value) ranging from 38.71 μg protein/mL to 213.9 μg protein/mL. The observed variability in the anti-HCMV activity of human colostrum was likely related to the well-known interpersonal variability of HM composition and to the HCMV serostatus of the milk donors. Furthermore, we demonstrated a remarkable antiviral activity in all the EV preparations, with EC_{50}s ranging from 3.98 to 75.93 μg protein/mL.

Table 2. Anti-human cytomegalovirus (HCMV) activity of the colostra and colostrum-derived EVs.

	Sample no.	EC_{50}[a] (μg/mL) (95% CI [b])	EC_{90}[c] (μg/mL) (95% CI)
Colostra	1	67.33 (54.24–83.57)	190 (118.5–304.5)
	2	62.58 (50.45–77.63)	215 (133.9–345.3)
	3[d]	153.5 (129.5–182.1)	527.6 (359.1–775.1)
	4	152 (83.46–276.8)	581.8 (160.1–2115)
	5	115.7 (109.3–122.6)	306 (269.7–347.2)
	6	104.3 (84.02–129.5)	652.9 (404.6–1053)
	7	51.35 (28.24–93.38)	647.4 (170.6–2457)
	8	111.8 (90.67–137.9)	323.2 (204.3–511.6)
	9	149.7 (116.9–191.6)	920.1 (545.3–1552)
	10	38.71 (29.82–50.24)	738.3 (405.4–1345)
	11	125.3 (105.9–148.2)	356.8 (245.1–519.4)
	12	140.6 (107.9–198.4)	637.5 (431.6–941.5)
	13	213.9 (186.2–245.7)	413.9 (290.4–590)
Colostrum-derived EV	1	35.29 (23.91–52.08)	200.9 (85.08–474.4)
	2	8.84 (5.66–13.81)	120.4 (42.95–337.4)
	3[d]	41.56 (27.44–62.95)	222.2 (87.30–565.7)
	4	42.16 (27.33–65.02)	435.9 (168.3–1129)
	5	55.55 (49.31–62.58)	97.31 (69.92–135.4)
	6	19.68 (14.09–27.49)	479.6 (219.7–1047)
	7	3.98 (1.36–11.63)	844.1 (74.99–9501)
	8	21.96 (13.20–36.53)	277.2 (85.72–896.4)

Table 2. *Cont.*

Sample no.	EC$_{50}$[a] (µg/mL) (95% CI [b])	EC$_{90}$[c] (µg/mL) (95% CI)
9	75.93 (47.92–120.3)	625.1 (201.5–1940)
10	33.92 (14.31–80.38)	1324 (65.48–26763)
11	74.21 (62.6–113.3)	493.8 (246.8–988)
12	41.4 (32.7–64.59)	277.6 (159.7–482.4)
13	30.92 (22.27–42.94)	371 (187.3–735.1)

[a] EC$_{50}$: half maximal effective concentration; [b] CI: confidence interval; [c] EC$_{90}$: 90%-effective concentration; [d] HCMV multiplicity of infection (MOI) 0.3 FFU/cell.
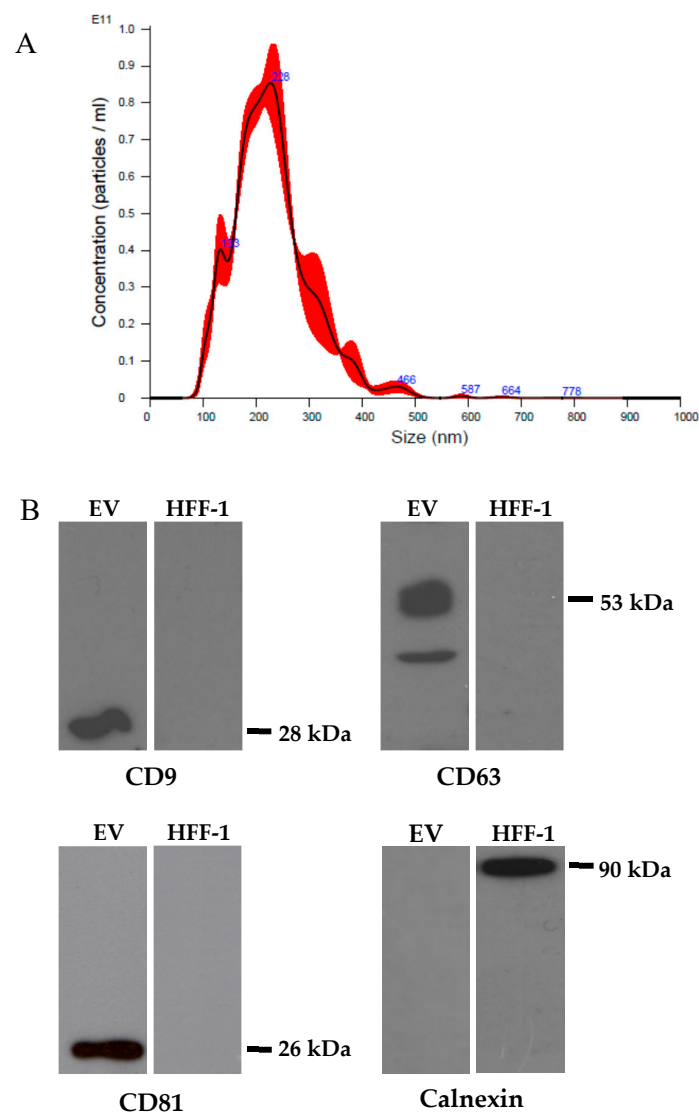

Figure 1. Characterization of the breast milk extracellular vesicles (EVs). (**A**): Representative analysis of an EV sample obtained from nanoparticle tracking analysis (NTA) using NanoSight. Size (nm) on the X-axis and concentration (number of particles/mL) on the Y-axis. The NTA showed that most EVs were between 100–400 nm in diameter (mean size, 219.9 ± 28.7 nm, mode 184.4 nm). (**B**): Profile of the colostrum-derived EVs obtained from immunoblotting. The CD9, CD63 and CD81 EV markers and the endoplasmic reticulum-related protein calnexin were analyzed. Human foreskin fibroblast (HFF-1) cell lysate was used as a control. The immunoblotting revealed that the colostrum-derived EVs were positive for CD63, CD9 and CD81 and negative for calnexin.

Figure 2 shows that a high number of GFP-expressing cells were visible in the untreated infected monolayers. On the other hand, the viral infectivity was completely abolished for the highest tested dose (423 μg/mL), and a reduced number of green cells was reported for lower EV doses. Interestingly, a high level of antiviral activity of the colostrum-derived EVs (an EC_{50} value of 41.56 μg protein/mL) was observed, even when a 10-fold greater viral inoculum was used (sample 3). Moreover, we excluded the possibility that the antiviral activity of the EVs was due to cytotoxicity, since the EVs did not affect the cellular viability when the cells were treated under the same conditions as the antiviral assays and processed by means of an MTS assay (CC_{50} values > 1000 μg/mL for all the EV preparations). Figure S1 reports cell viability data from assays performed on three representative EV preparations (EV samples 1, 2 and 3).
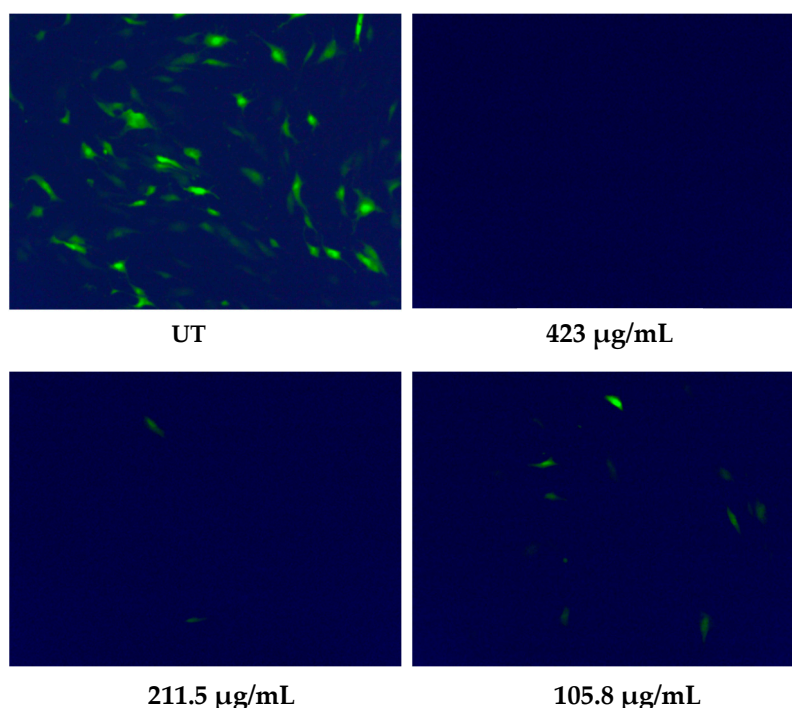

Figure 2. Anti-HCMV assay with colostrum-derived EVs. Representative HCMV foci (green fluorescent protein (GFP)-expressing, green) in the HFF-1 cell monolayers are reported for 423, 211.5 and 105.8 μg/mL EV protein concentrations, as obtained from the HCMV Towne inhibition assay; HCMV at MOI 0.3 FFU/cell. UT, untreated.

To the best of our knowledge, this is the first study to have reported the intrinsic antiviral activity of human colostrum-derived EVs against HCMV infection. Näslund et al. (2014) demonstrated a similar antiviral activity of breast milk exosomes and showed that milk exosomes, but not plasma exosomes, significantly reduced the productive HIV-1 infection of monocyte-derived dendritic cells by approximately 50%, compared with untreated cells, and blocked HIV-1 transfer from monocyte-derived dendritic cells to CD4+ T cells [19]. Only a few studies have reported a direct inhibition of viral infections by the extracellular vesicles of biological fluids. Extracellular vesicles isolated from semen, but not from the blood of HIV-1–infected individuals, inhibited HIV-1 replication in vitro [27]. Furthermore, exosome-like vesicles released from human tracheobronchial ciliated epithelium neutralized the infectivity of the influenza virus by up to 85–99% [28].

3.2. Colostrum-Derived Extracellular Vesicles Inhibit the Attachment of HCMV on Cells

In order to identify the major mechanism of action, three EV preparations (3, 6 and 10) were selected and subjected to further studies. First, a virus inactivation assay was performed in which the virus was incubated with an effective high concentration of EVs (EC_{90}) for 2 h at 37 °C and then

added to cells at dilutions at which the vesicles were no longer active. Figure 3A shows no significant differences in the viral titers between the treated and untreated samples, indicating that the vesicles did not impair infectivity by directly targeting viral particles. Having excluded virus inactivation activity, we then investigated whether the active EVs targeted the cell surface before the infection, thereby inhibiting infectivity. A pre-treatment assay was performed in which Vero cells were pre-treated with scalar protein concentrations of EVs for two hours prior to viral infection. Figure 3B shows that none of the tested EV preparations exerted inhibitory activity under these experimental conditions.
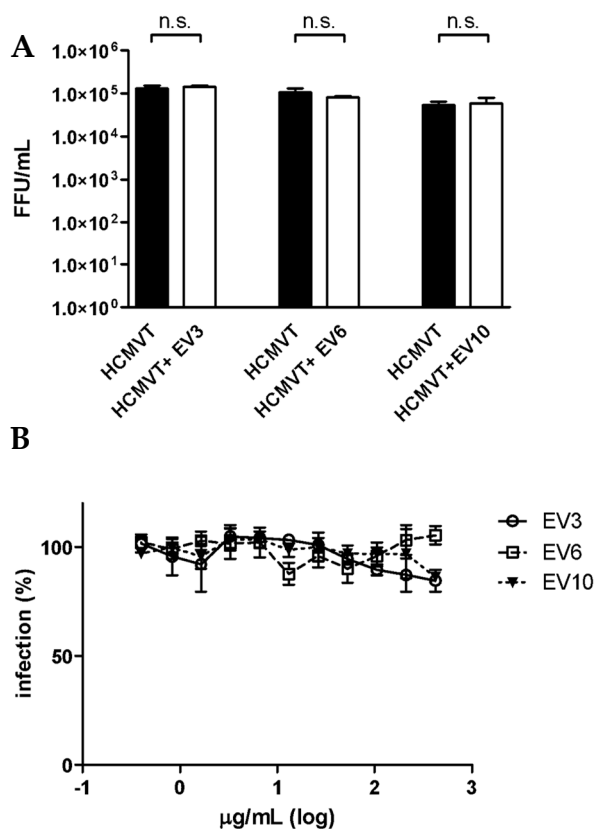

Figure 3. (**A**). Evaluation of the inactivation of HCMV by EVs. Three samples of EVs were investigated to evaluate the inactivation of the HCMV particles at 37 °C for 2 h. No significant differences in the viral titers were observed between the treated and untreated samples. The infectious titers are expressed on the Y-axis as FFU/mL. Black bar, HCMV; white bar, HCMV plus EV sample. Error bars represent the standard error of the means of three independent experiments. (**B**). Pre-treatment anti-HCMV assay. Three samples of EVs were challenged with HFF-1 cells for 2 h at 37 °C prior to HCMV infection. None of the EV preparations exerted inhibitory activity under these experimental conditions. Data are reported as the mean percentages of infection, in comparison with the control of three independent experiments.

We then evaluated the ability of EVs to impair the first steps of the HCMV replicative cycle, such as their attachment and entry into cells, by means of specific assays. First, we carried out an attachment assay, using an experimental condition in which the virus was allowed to bind to the surface of the host cells, in the presence or absence of EVs, but did not undergo cell entry. Figure 4A shows that all the EV preparations inhibited HCMV infectivity and generated dose–response curves with EC_{50} values ranging from 14.50 to 38.90 μg protein/mL. It should be highlighted that no statistically significant differences were observed for any of the investigated EV preparations ($p > 0.05$, Student's *t*-test) in the comparison between the number of HCMV foci in the untreated wells and those in the treated wells, with no active EV dilutions in the attachment assays, thus suggesting that the viral titers did not change. On the other hand, when EVs were added immediately after virus attachment to assess their ability to prevent entry (entry assay), no inhibition was observed for two EV preparations, and a weak

inhibition was observed at high doses for the sample 3-derived EVs (Figure 4B). Furthermore, in order to exclude the ability of EVs to impair the late intracellular steps of viral replication, vesicles were added immediately after the viral penetration of the host cells. The post entry assay, which is reported in Figure 4C, showed no inhibition of HCMV infectivity at the post-entry stage for any of the tested EV preparations.
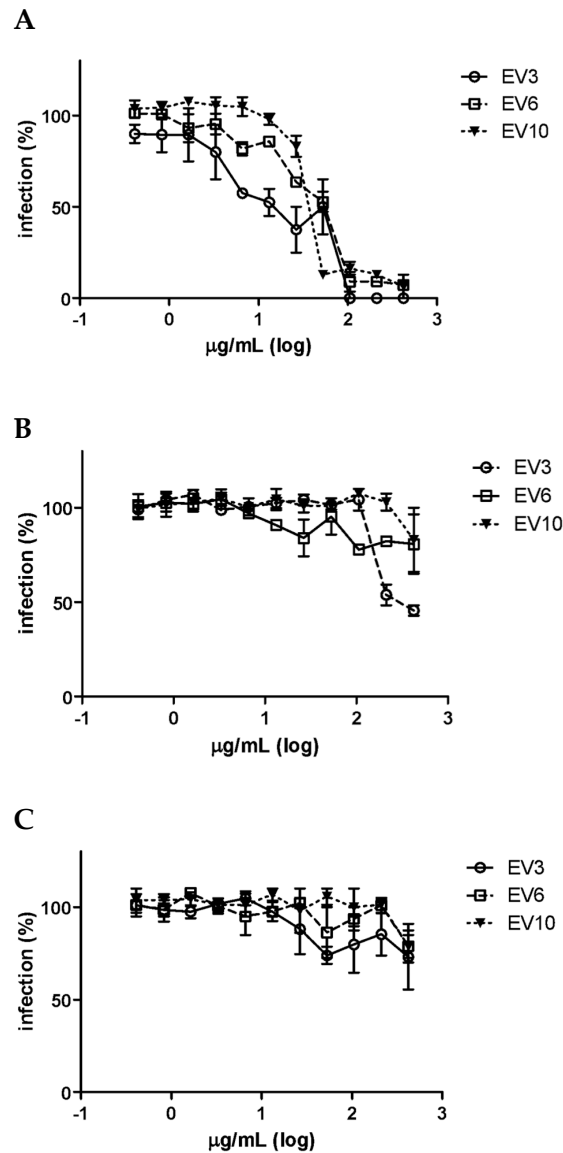

Figure 4. Effect of the colostrum-derived EV on the HCMV replicative cycle. (**A**) of the above figure shows the attachment assay; in this experimental condition, the virus was allowed to bind to the surface of the HFF-1 cells in the presence of EV but not to undergo cell entry. All the EV preparations inhibited HCMV Towne infectivity and generated dose–response curves. (**B**) shows the entry assay; in this experimental condition, the EVs were added to the HFF-1 cells immediately after virus attachment. No inhibition was observed for EV preparations 6 and 10, and a weak inhibition was observed for high doses for EV sample 3. (**C**) shows the post-treatment assay; the EVs were added to HFF-1 cells immediately after the viral penetration of the cells. No inhibition of HCMV infectivity was observed at the post-entry stage of infection for any of the EV preparations. Data are reported as the mean percentages of infection, compared with the control, for three independent experiments and for three EV preparations.

Overall, these findings demonstrate that human colostrum-derived EVs exert their antiviral activity by impairing the attachment of HCMV to the cell surface. This effect may be attributed to several EV components acting together, or to a single species/component, likely including proteins, glycoproteins and lipids which are present on the EV surface. These antiviral effectors might act through two distinct approaches: first, by binding to specific viral components while mimicking cellular receptors, or through a direct interaction with the cell, and masking cellular receptors, thereby competitively inhibiting virus attachment. Like viruses, EVs can also bind to the plasma membranes of other cells, enter them through either fusion or endocytosis and trigger specific reactions. These processes are mediated by specific EV proteins, and tetraspanins in particular [29].

3.3. Shaving of Extracellular Vesicles Significantly Reduced Their Anti-HCMV Activity

Shaving experiments were performed on three EV preparations (11, 12 and 13) to evaluate the ability of EVs to affect the interaction between the viral particles and the cell surface proteins. To this end, the EVs were subjected to trypsin digestion in order to shave the proteins that were present on the surface of the EVs. As a control, an aliquot of each EV preparation was subjected to the same shaving protocol but without digestion with trypsin. The shaved EVs were characterized using NanoSight to evaluate their size, which showed a reduction in diameter (mean size 188.2 nm, mode 138.9 nm) compared with intact EVs (mean size 219.9 nm, mode 184.4 nm) (Figure 5), while no diameter variations were reported for the control EVs.
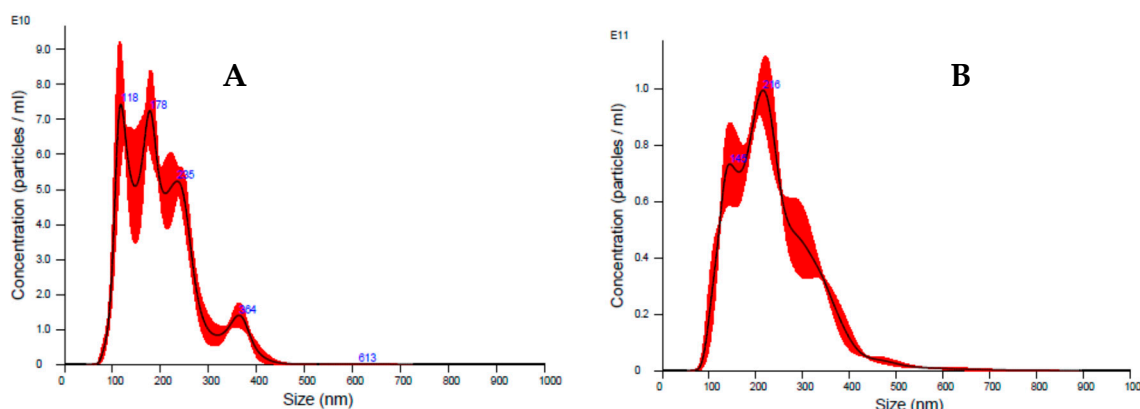

Figure 5. Characterization of shaved EVs. Representative analysis of a shaved EV sample (**A**), and intact EV (**B**) by means of nanoparticle tracking analysis (NTA) using NanoSight. The shaved EVs showed a reduction in diameter compared with the intact EVs. Size (nm) on the X-axis and concentration (number of particles/mL) on the Y-axis.

After shaving, the expected decrease in the number of EVs was observed, and the inhibition test data were therefore normalized to the decreased number of vesicles. Antiviral assays against the HCMV Towne strain were then performed by treating cells with intact, shaved and control EVs. As reported in Figure 6, the shaved EVs of the three preparations exerted a significantly reduced antiviral activity, compared with both the intact EV and control preparations. The EC_{50} values of the intact EVs were around 3.65×10^{10} particles/mL, while the EC_{50} values of the shaved EVs were in a range from 1.47×10^{11} to 4.61×10^{11} particles/mL. In order to validate these data, antiviral experiments were also performed against HCMV strain AD169—another laboratory reference strain. Again, the clarified colostrum exhibited a net anti-HCMV-AD169 activity (EC_{50} 163 µg/mL), and the intact colostrum-derived EVs exerted a high antiviral activity (EC_{50} 24.2 µg/mL), which was significantly reduced after the shaving experiments (shaved EVs, EC_{50} 201 µg/mL). Our results indicate that the proteins on the surface of EVs play a role in the antiviral mechanism of action of EVs.
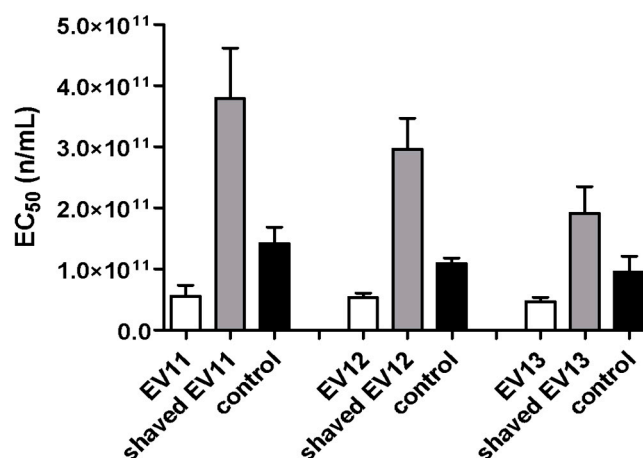
Figure 6. Anti-HCMV assays with EVs and shaved EVs. The antiviral activities of three EV preparations, shaved EVs and controls are reported as EC_{50} values obtained from an HCMV inhibition assay. The shaved EVs from three preparations (11, 12 and 13) exerted a significantly reduced antiviral activity compared with both the intact EV and the control preparations. The inhibition test data were normalized to the number of vesicles and expressed as the number of particles/mL (n/mL). Error bars represent the standard error of the means of three independent experiments.

3.4. Proteomic Analysis of EV Surfaceome

The shaved peptide mixture derived from the EV membrane surface proteins (surfaceome) was analyzed by means of LC–MS/MS in order to investigate the proteins that could be responsible for the EV antiviral properties (Table 3; more details are shown in Table S1).

Table 3. List of the 45 proteins shared between at least two samples out of three (samples 11, 12 and 13) identified by means of LC–MS/MS. The UNIPROT ID, the molecular weight (MW), the isoelectric point (pI) and the biological function are reported for each identified protein.

Uniprot Id	Description	MW	pI	Biological Function
O00300	Tumor necrosis factor receptor superfamily member 11B	45,996	8.66	Signaling pathway
O00391	Sulfhydryl oxidase 1	66,818	9.13	Oxidation-reduction process
O15232	Matrilin-3	52,816	6.25	Calcium ion binding
P00709	Alpha-lactalbumin	16,214	4.83	Lactose biosynthetic process
P01011	Alpha-1-antichymotrypsin	47,621	5.33	Proteolysis
P01024	Complement C3	187,030	6.02	Immune response
P01833	Polymeric immunoglobulin receptor	83,232	5.58	Immune response
P01834	Immunoglobulin kappa constant	11,758	6.11	Immune response
P01876	Immunoglobulin heavy constant alpha 1	37,631	5.99	Immune response
P02647	Apolipoprotein A-I	30,759	5.56	Lipid transport
P02649	Apolipoprotein E	36,132	5.65	Lipid transport
P02652	Apolipoprotein A-II	11,168	6.26	Lipid transport
P02748	Complement component C9	63,133	5.43	Immune response
P02788	Lactotransferrin	78,182	8.50	Immune response
P04114	Apolipoprotein B-100	515,283	6.58	Lipid transport
P04406	Glyceraldehyde-3-phosphate dehydrogenase	36,030	8.57	Glucose metabolic process
P05814	Beta-casein	25,366	5.52	Casein micelle formation
P06396	Gelsolin	85,698	5.90	Cell motility and contraction
P06858	Lipoprotein lipase	53,129	8.37	Lipid metabolic process
P07498	Kappa-casein	20,293	8.97	Casein micelle formation
P07602	Prosaposin	58,112	5.06	Lipid metabolic process
P07996	Thrombospondin-1	129,300	4.71	Adhesion
P08571	Monocyte differentiation antigen CD14	40,051	5.84	Immune response
P10451	Osteopontin	35,422	4.37	Adhesion
P10909	Clusterin	52,494	5.88	Protein folding/transport
P15291	Beta-1,4-galactosyltransferase 1	43,920	8.88	Carbohydrate metabolic process
P19835	Bile salt-activated lipase	79,272	5.13	Lipid metabolic process
P22897	Macrophage mannose receptor 1	165,905	6.11	Endocytosis
P23280	Carbonic anhydrase 6	35,366	6.51	Carbon metabolic process

Table 3. *Cont.*

Uniprot Id	Description	MW	pI	Biological Function
P23284	Peptidyl-prolyl cis-trans isomerase B	23,728	9.42	Protein folding/transport
P24821	Tenascin	240,853	4.79	Adhesion
P47710	Alpha-S1-casein	21,671	5.32	Calcium ion binding
P47989	Xanthine dehydrogenase/oxidase	146,330	7.86	Oxidation-reduction process
P49327	Fatty acid synthase	273,254	6.01	Oxidation-reduction process
P58499	Protein FAM3B	25,981	8.97	Insulin secretion
P60709	Actin, cytoplasmic 1	41,710	5.29	Cell motility and contraction
Q02809	Procollagen-lysine,2-oxoglutarate 5-dioxygenase 1	83,550	6.46	Oxidation-reduction process
Q08431	Lactadherin	43,105	8.47	Adhesion
Q13410	Butyrophilin subfamily 1 member A1	58,923	5.38	Milk-fat droplet release / immune response
Q14697	Neutral alpha-glucosidase AB	106,873	5.74	Carbohydrate metabolic process
Q6WN34	Chordin-like protein 2	49,643	6.75	Signaling pathway
Q96DA0	Zymogen granule protein 16 homolog B	22,725	6.74	Protein folding/transport
Q96S86	Hyaluronan and proteoglycan link protein 3	40,868	6.07	Adhesion
Q99102	Isoform 10 of Mucin-4	225,293	5.85	Adhesion
Q9H173	Nucleotide exchange factor SIL1	52,052	5.27	Protein folding/transport

The total number of identified proteins in the three analyzed samples was 258. Of these proteins, 45 were found to be shared between at least two samples out of three, and 16 were found in all the analyzed samples (Figure 7A). Sample 11 and sample 12 shared a higher number of proteins than sample 13, which seemed to be less rich in shaved peptides. Considering that only the proteins with an extracellular domain containing cutting sites for trypsin were identified, we believe that the number of identified proteins is adequate. As far as sub-localization is concerned, the extracellular proteins were most abundant, followed by the cell membrane proteins (Figure 7B). The analyses of the membrane protein coverage by the identified peptides showed that 98% of the peptides were located in the extracellular regions, thus demonstrating the effectiveness of the shaving protocol. The most frequently represented biological function categories were those related to the immune response and adhesion (Figure 7C), thus indicating that these are the key mechanisms involved in antiviral response.

The surfaceome proteomic analysis showed that 91% of the identified proteins had already been found in the HM EVs [17,30]. Some of them are already known for their antiviral properties, especially against HIV infection, whereas there are scarce data regarding their inhibitory effect on HCMV. Interaction with both the virus and the host cell receptors has been proposed as a mechanism of action for most of these proteins (e.g., clusterin, bile salt-activated lipase, tenascin, thrombospondin and osteopontin). Among the identified proteins, the most promising in terms of antiviral properties are components of the immune system (polymeric-Ig receptor precursor, Ig κ-chain C region, Ig heavy constant alpha 1 and complement C9 and C3), caseins (α-S1-casein, β-casein and k-casein), whey proteins (lactoferrin and α lactalbumin), milk fat globule-associated proteins (MFGP) (mucin MUC4, lactadherin, clusterin, bile salt-activated lipase, apolipoproteins and lipoprotein lipase), macrophage mannose receptor, tenascin, thrombospondin, gelsolin and osteopontin.

The components of the immunoglobulin superfamily—and IgAs in particular—are already known to be prominent in human breast colostrum and to provide newborns with passive immune protection. Among the complement proteins, complement component C9—which has here been identified for the first time in the HM EV fraction—is the major actor of the membrane attack complex (MAC), a multi-protein complex that forms pores in the plasma membrane of target pathogens or virally infected cells [31]. C9 polymerization is the product of a single gene that is sufficient to encode a pore-forming molecule targeted at an early stage by C3b (also identified in this study). C9 is a multi-domain protein that contains an N-terminal type-1 thrombospondin (TSP) domain, an LDL-receptor class A repeat, a number of potential transmembrane regions and a C-terminal EGF-like domain. The N-terminal TSP1 domain seems to be crucial in the molecular mechanism of the MAC assembly. The formation of a MAC on the viral surface and complement-mediated lysis seem to be essential for the reduction of viral titers in Zika virus infection [32].
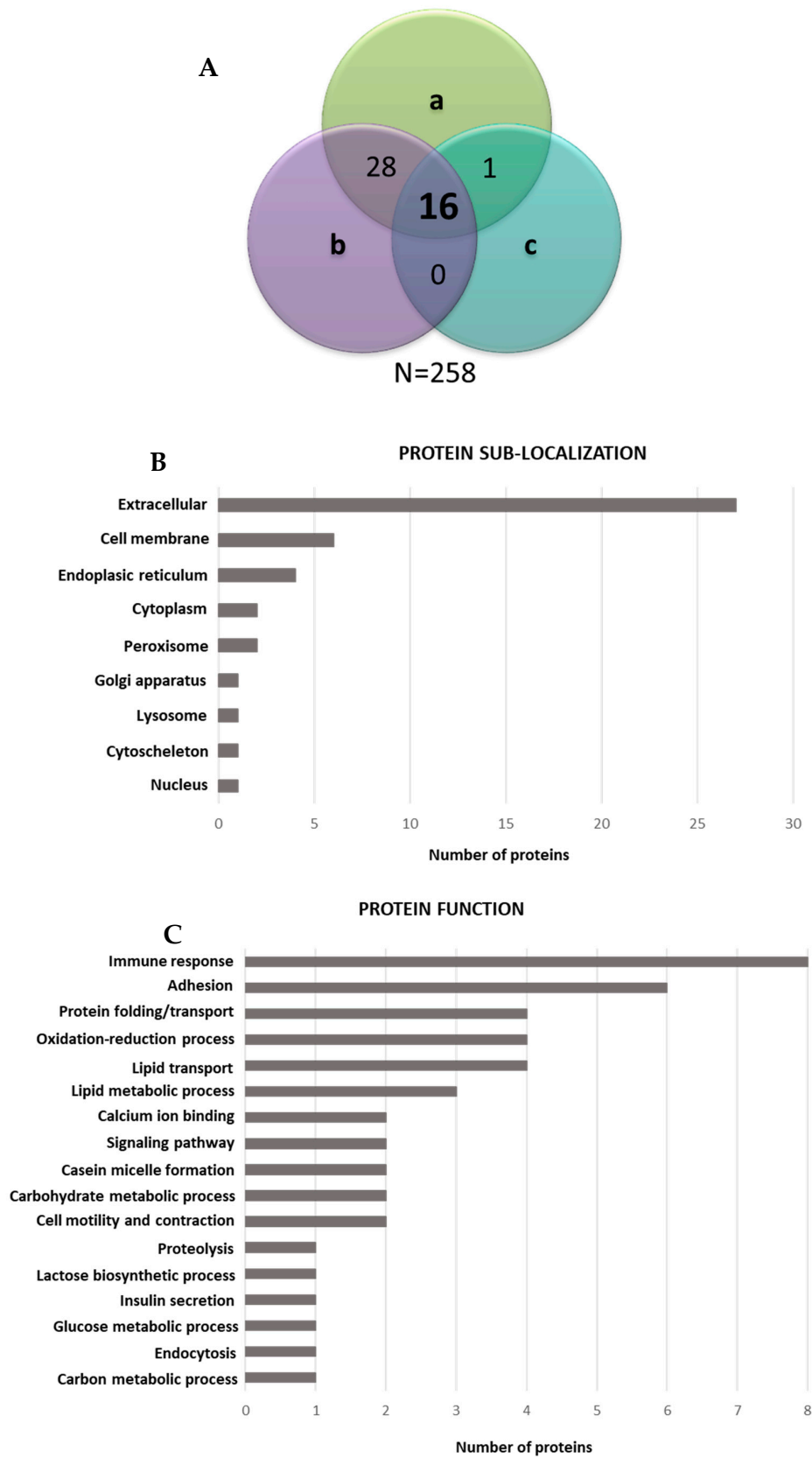
Figure 7. Venn diagrams showing the distribution of the identified proteins over samples 11 (a), 12 (b) and 13 (c). A total of 258 proteins were identified in all the samples (**A**). Histograms grouping the 45 shared proteins (identified in at least two out of the three analyzed samples) according to the sub-localization (**B**) and to the function (**C**).

Most of the proteins identified in our study are phosphorylated and/or glycosylated and thus function as soluble receptors that inhibit pathogen binding to the mucosal cell surface. Caseins, for instance, can exert their antiviral activity with both phospho-groups and glycans. K-casein has been reported to have anti-human rotavirus activity via the direct binding of glycans to the virus [33]. Among the whey proteins, lactoferrin (LF) has a well-known antiviral activity against HCMV as well as against the hepatitis C virus, poliovirus, enterovirus 71, BK polyomavirus, HIV-1 and the human papilloma virus [34]. The cationic N-terminal amino acid sequence of both human and bovine LF, which are rich in arginine and tryptophan, contributes to anti-HCMV activity [35]. Lactoferricin, mainly in the cyclic structure, which is derived from the LF N-terminal part by proteolytic cleavage with pepsin, primarily exhibits its antiviral effect on the cell surface, where it interferes between the virus and host cell receptors and thus blocks HCMV adsorption and entry [36]. Alpha-lactalbumin has also demonstrated antiviral activity against reovirus strain type 3 Dearing, for which a hemagglutination mechanism has been suggested [37].

Regarding milk fat membrane associated proteins, the involvement of human milk mucins in protection against virus infection has already been established. Purified mucin components (MUC1 and MUC4) are able to inhibit HIV-1 in vitro and prevent the transmission of HIV-1 from dendritic cells to CD4+ T cells [38,39]. Moreover, core 2 glycans of mucins bind to the rotavirus virion, thereby preventing the virus from recognizing the cellular receptors [40]. Furthermore, the presence of epithelial mucins, associated with a-2,6-linked sialic acid, on exosome-like vesicles from human tracheobronchial ciliated epithelium has been shown to contribute to their antiviral effect against the human influenza A virus, which is known to bind sialic acid. The antiviral activity was ablated by pre-treating EVs with neuraminidase, thus suggesting that the interaction between exosomes and the influenza A virus was sialic acid-dependent [28]. Milk exosomes instead act as a protective factor against the vertical transmission of HIV-1 by competing with the virus to bind to the cellular receptor dendritic cell-specific ICAM-3–grabbing non-integrin (DC-SIGN). This action was found to be due to the presence of the soluble MUC 1 on the exosome surface—a known DC-SIGN ligand [19]. Among the MFGPs, lactadherin (LA) is a glycoprotein that is able to attenuate the infectivity of rotavirus by interacting directly between the virus and its oligosaccharides, thus preventing the virus from attaching to the intestinal mucosa [41]. As already demonstrated for MUC1, the N-linked carbohydrate sequence containing sialic acids is an essential feature due to its antiviral activity, and the removal of sialic acid in fact results in a loss of its inhibitory activity [42]. Another MFGP is clusterin; although it is ubiquitously expressed, it is engaged in a variety of physiologic and pathologic processes, including inflammation, atherosclerosis and cancer. It may display different biological functions according to its glycosylation pattern [43]. Sabatte et al. (2011) demonstrated that semen clusterin is a high-affinity ligand of the C-type lectin receptor DC-SIGN and is responsible for the complete inhibition of HIV-1 recognition [44]. DC-SIGN is expressed by immature monocyte-derived dendritic cells (MDDC) and macrophage subsets and binds specific carbohydrate structures expressed on the pathogen surface, thereby mediating the internalization of different pathogens, including HCMV [45]. Moreover, Tripathi et al. (2013) demonstrated an interaction between the influenza A virus nucleoprotein and the host antiapoptotic factor clusterin, which is involved in host cell death induction [46]. A few other viruses, including the dengue virus and hepatitis D, also target clusterin to modulate host responses [47,48]. Bile salt-activated lipase (BSSL), like clusterin, is able to bind DC-SIGN and cause the inhibition of the HIV-1 transfer to CD4+ T cells [49]. Moreover, BSSL is effective against the Norwalk virus, probably because its tandem repeat O-glycosylated motifs attract the virus by acting as decoy receptors [50].

The macrophage mannose receptor (MRC1)—a single-pass transmembrane glycoprotein belonging to the C-type lectin family—has been investigated in great detail. It is found on the surface of most tissues—macrophages, dendritic cells and some lymphatic or liver endothelial cells—where it plays the role of capturing pathogens and removing them from circulation in the bloodstream [51]. As already demonstrated by Taylor et al. (2005), MRC1 is able to recognize specific sugar motifs (i.e., mannose modification) on pathogen membrane proteins and to mediate pathogen uptake [52]. It is able to interact

with different viruses (HIV-1, dengue, hepatitis B and influenza A). As recently reported by Sukegawa at al. (2018) with reference to HIV-1, MRC1 inhibits virus release and mediates HIV retention on the surface of virus-producing cells, thus causing a reduction in the progression of infection [53]. To the best of our knowledge, the possible involvement of MRC1 in the HCMV replication cycle has never been investigated. However, considering that MRC1 is expressed on the main target HCMV-infected cells, including macrophages and endothelial cells, its ability to bind viral glycoproteins and prevent cell surface attachment can be hypothesized. Further studies are required to confirm this mechanism of action.

Thrombospondin (TSP1) is an extracellular matrix glycoprotein with functional domains that is able to bind calcium, heparin, collagens, other matrix components and cell surface receptors, including CD36, heparan sulfate proteoglycans (HSPG) and integrins. It has been demonstrated that HCMV infection suppresses the expression of TSP1 and 2 in human fibroblasts, in human retinal glial cells and in primary fetal astrocytes, and this action is mainly mediated by HCMV immediate–early proteins [54,55]. Considering the early steps of the HCMV replicative cycle, viral attachment involves envelope glycoproteins, such as glycoprotein M and B (gM and gB), both of which bind to HSPGs on the cell surface. The virus then moves quickly to a more stable cell type-specific docking interaction, with one or more cellular surface receptors, including specific integrins, epidermal growth factor receptor (EGFR) and platelet-derived growth factor receptor (PDGFR)-α, which mediate HCMV attachment and entry [56]. Therefore, given the ability of TSP to bind several cellular receptors, including HSPG, it is possible to hypothesize that it might be able to competitively inhibit virus attachment.

Tenascin is a large, hexameric extracellular matrix glycoprotein that is heavily sialylated: each monomer contains an assembly domain, a region of epidermal growth factor-like repeats, a region of fibronectin type III-like domains and a fibrinogen-like globe [57]. Fouda et al. (2013) isolated tenascin from the HIV-neutralizing fraction of antibody-depleted breast milk [58]. It is able to mediate HIV-1 capture, to block virus-epithelial cell binding and to neutralize HIV-1 by binding to the HIV Envelope variable 3 loop in a charge-dependent manner, depending on the presence of sialic acid in its glycomoieties. Furthermore, Mangan et al. (2019) demonstrated that the interaction between the negatively charged fn domain of tenascin and the positively charged regions of the chemokine coreceptor binding site of HIV-Env is a likely mechanism of tenascin-mediated virus neutralization [59]. According to these data, it would be interesting to evaluate whether tenascin represents an innate mucosal antiviral factor that is present as an endogenous HCMV neutralizing protein in breast milk and to investigate its mechanism of action.

Another protein involved in the anti-HIV-1 mechanism of action is gelsolin, which belongs to the actin binding protein superfamily and is known to promote actin cytoskeleton remodeling. García-Expósito et al. (2013) demonstrated that gelsolin can compromise HIV-induced actin reorganization and the viral receptor capping events required for HIV-1 Env-mediated fusion, entry and infection. Therefore, gelsolin can constitute a barrier that restricts the HIV-1 infection of CD4+ lymphocytes in a pre-fusion step [60].

Finally, osteopontin is a multifunctional protein that is involved in both innate and adaptive immunity. Zhao et al. (2016) demonstrated that osteopontin is an essential positive regulator that protects the host from virus infection through the stabilization of the tumor necrosis factor receptor (TNFR)-associated factor 3, induction of interferon regulatory factor 3 activation and interferon beta (IFN-β) production [61].

3.5. Surface Peptide Mixtures Inhibit HCMV Attachment

The peptide mixtures derived from the EV shaving of preparations 12 and 13 were investigated for their anti-HCMV Towne potency. Pooled peptides were dissolved in 420 μL DMEM medium, and two different volumes of the samples were assessed in triplicate by means of an attachment assay. As reported in Figure 8, a significant dose-dependent HCMV inhibition of the viral attachment was observed, with slight variability between the two peptide pools. The 90 μL volumes from EVs 12

and 13 reduced HCMV attachment by 82.04% and 90.46% in comparison with the untreated control, respectively. The 50 μL EV preparations inhibited the viral attachment in the 49.5–66.16% range in comparison with the untreated control. These data suggest the direct involvement of EV surface peptides in the inhibition of viral attachment to cells. The incomplete inhibition of viral attachment from peptide mixtures may be attributed to changes in the structural folding of surface proteins due to enzymatic digestion. Considering these data, the identification of peptides by means of LC–MS/MS and the in silico characterization of the peptides will be performed with the aim of characterizing the peptides that are potentially responsible for the observed antiviral activity. The most promising peptides will then be synthetized for further antiviral in vitro experiments.
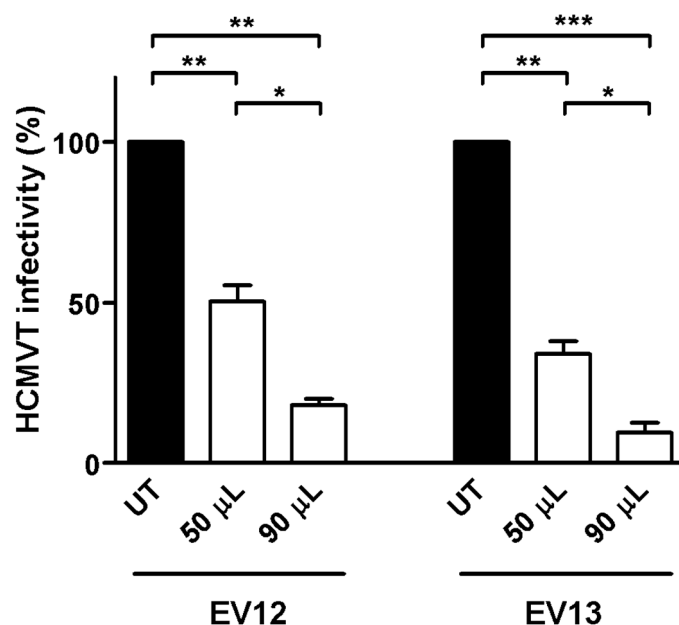

Figure 8. Effect of the peptides from shaved colostrum-derived EVs on the HCMV replicative cycle, as determined by means of the attachment assay. In this experimental condition, the virus was allowed to bind to the surface of HFF-1 cells in presence of EV but did not undergo cell entry. Peptides from both shaved EV preparations (12 and 13) were dissolved in 420 μL DMEM, and two different volumes were challenged. Both of the preparations inhibited the viral attachment in a dose–response manner in comparison with the untreated control. Data are reported as percentages of infection, in comparison with untreated controls for two shaved EV preparations, and compared by means of a one-way ANOVA (*, $p < 0.05$; **, $p < 0.01$; ***, $p < 0.001$). UT, untreated.

4. Conclusions

Overall, our results provide novel insights into the protective role of human colostrum against HCMV infection in reducing the risk of viral transmission from mother to child through breastfeeding. We have confirmed the anti-HCMV activity of human colostrum in vitro, and we have identified extracellular vesicles as additional antiviral effectors, together with well-known non-specific bioactive and immune components of human colostrum. The investigation of the mechanism of action has indicated that the anti-HCMV activity of EVs is not mediated by a direct inactivation of the viral particle, but rather by the inhibition of the viral attachment to the cell surface. The significant reduction in the antiviral activity of EVs, after shaving experiments, suggests a crucial role of EV surface proteins in inhibiting viral infection. The proteomic analysis of the EV surfaceome revealed the contribution of immune components including antibodies (mainly IgA) and complement component proteins (C9 and C3) to antiviral activity. Moreover, we identified several proteins which have proven antiviral properties against HIV infection but which have scarcely been characterized so far for their activity against HCMV. We found both milk proteins (caseins, whey proteins and milk fat membrane associated

proteins) and proteins shared by different tissue cells and biological fluids. The common feature of the identified proteins is that their glycomoieties seem to play a crucial role in the interference mechanism between a virus and the host cells, acting as a point of cell-specific recognition for the virus particle and inhibiting its attachment on the cell surface. Further studies are necessary to explore the involvement of the identified proteins and their glycan chain composition in the protective role of EVs against HCMV.

Supplementary Materials: The following are available online at http://www.mdpi.com/2076-2607/8/7/1087/s1. Table S1. List of the proteins identified by means of LC–MS/MS in at least two samples out of three. The protein score and the sequence of the detected peptides are reported for each protein. Figure S1. Cell viability assay. Evaluation of the effect of three EV preparations (EV1, EV2 and EV3) on HFF-1 viability at 5 days. The HFF-1 cells were treated under the same conditions as the antiviral assays and processed by means of an MTS assay. Data are reported as the percentages of viable cells in comparison with the controls, as determined by means of the MTS assay for 1000, 500, 250 and 125 μg/mL concentrations. Three independent experiments were performed.

Author Contributions: Conceptualization, D.L. and A.C. (Alessandra Coscia); Methodology, M.D., S.C. and M.G.; Validation, G.E.M., E.B., D.L. and L.C.; Formal Analysis, M.R., C.L., M.G.G. and M.M.; Investigation, R.F., A.C. (Andrea Civra), M.R., S.C., M.M. and A.L.; Resources, P.T. and S.S.; Data Curation, P.T., C.L. and A.C. (Andrea Civra); Writing—Original Draft Preparation, S.C. and M.D.; Writing—Review & Editing, M.D., E.B., A.C. (Alessandra Coscia) and M.G.G; Supervision, D.L. and A.C. (Alessandra Coscia); Project Administration, D.L. and L.C. All authors have read and agreed to the published version of the manuscript.

Conflicts of Interest: The authors declare no conflict of interest.

References

1. WHO | Guidelines on Optimal Feeding of Low Birth-Weight Infants in Low- and Middle-Income Countries. Available online: http://www.who.int/maternal_child_adolescent/documents/infant_feeding_low_bw/en/ (accessed on 13 March 2020).
2. Civardi, E.; Tzialla, C.; Baldanti, F.; Strocchio, L.; Manzoni, P.; Stronati, M. Viral Outbreaks in Neonatal Intensive Care Units: What We Do Not Know. *Am. J. Infect. Control* **2013**, *41*, 854–856. [CrossRef] [PubMed]
3. Eidelman, A.I. Breastfeeding and the Use of Human Milk: An Analysis of the American Academy of Pediatrics 2012 Breastfeeding Policy Statement. *Breastfeed. Med.* **2012**, *7*, 323–324. [CrossRef] [PubMed]
4. Moro, G.E.; Billeaud, C.; Rachel, B.; Calvo, J.; Cavallarin, L.; Christen, L.; Escuder-Vieco, D.; Gaya, A.; Lembo, D.; Wesolowska, A.; et al. Processing of Donor Human Milk: Update and Recommendations From the European Milk Bank Association (EMBA). *Front. Pediatr.* **2019**, *7*, 49. [CrossRef] [PubMed]
5. Hamprecht, K.; Goelz, R. Postnatal Cytomegalovirus Infection Through Human Milk in Preterm Infants: Transmission, Clinical Presentation, and Prevention. *Clin. Perinatol.* **2017**, *44*, 121–130. [CrossRef] [PubMed]
6. Manicklal, S.; Emery, V.C.; Lazzarotto, T.; Boppana, S.B.; Gupta, R.K. The "Silent" Global Burden of Congenital Cytomegalovirus. *Clin. Microbiol. Rev.* **2013**, *26*, 86–102. [CrossRef]
7. Doctor, S.; Friedman, S.; Dunn, M.S.; Asztalos, E.V.; Wylie, L.; Mazzulli, T.; Vearncombe, M.; O'Brien, K. Cytomegalovirus Transmission to Extremely Low-Birthweight Infants through Breast Milk. *Acta Paediatr.* **2005**, *94*, 53–58. [CrossRef]
8. Lanzieri, T.M.; Dollard, S.C.; Josephson, C.D.; Schmid, D.S.; Bialek, S.R. Breast Milk-Acquired Cytomegalovirus Infection and Disease in VLBW and Premature Infants. *Pediatrics* **2013**, *131*, e1937–e1945. [CrossRef]
9. Donalisio, M.; Rittà, M.; Tonetto, P.; Civra, A.; Coscia, A.; Giribaldi, M.; Cavallarin, L.; Moro, G.E.; Bertino, E.; Lembo, D. Anti-Cytomegalovirus Activity in Human Milk and Colostrum From Mothers of Preterm Infants. *J. Pediatr. Gastroenterol. Nutr.* **2018**, *67*, 654–659. [CrossRef]
10. Trend, S.; Strunk, T.; Lloyd, M.L.; Kok, C.H.; Metcalfe, J.; Geddes, D.T.; Lai, C.T.; Richmond, P.; Doherty, D.A.; Simmer, K.; et al. Levels of Innate Immune Factors in Preterm and Term Mothers' Breast Milk during the 1st Month Postpartum. *Br. J. Nutr.* **2016**, *115*, 1178–1193. [CrossRef]
11. Clarke, N.M.; May, J.T. Effect of Antimicrobial Factors in Human Milk on Rhinoviruses and Milk-Borne Cytomegalovirus In Vitro. *J. Med. Microbiol.* **2000**, *49*, 719–723. [CrossRef]

12. Ng, T.B.; Cheung, R.C.F.; Wong, J.H.; Wang, Y.; Ip, D.T.M.; Wan, D.C.C.; Xia, J. Antiviral Activities of Whey Proteins. *Appl. Microbiol. Biotechnol.* **2015**, *99*, 6997–7008. [CrossRef] [PubMed]

13. Wakabayashi, H.; Oda, H.; Yamauchi, K.; Abe, F. Lactoferrin for Prevention of Common Viral Infections. *J. Infect. Chemother.* **2014**, *20*, 666–671. [CrossRef] [PubMed]

14. Zempleni, J.; Aguilar-Lozano, A.; Sadri, M.; Sukreet, S.; Manca, S.; Wu, D.; Zhou, F.; Mutai, E. Biological Activities of Extracellular Vesicles and Their Cargos from Bovine and Human Milk in Humans and Implications for Infants. *J. Nutr.* **2017**, *147*, 3–10. [CrossRef] [PubMed]

15. Théry, C.; Zitvogel, L.; Amigorena, S. Exosomes: Composition, Biogenesis and Function. *Nat. Rev. Immunol.* **2002**, *2*, 569–579. [CrossRef]

16. Xanthou, M. Immune Protection of Human Milk. *Biol. Neonate* **1998**, *74*, 121–133. [CrossRef] [PubMed]

17. Admyre, C.; Johansson, S.M.; Qazi, K.R.; Filén, J.-J.; Lahesmaa, R.; Norman, M.; Neve, E.P.A.; Scheynius, A.; Gabrielsson, S. Exosomes with Immune Modulatory Features Are Present in Human Breast Milk. *J. Immunol.* **2007**, *179*, 1969–1978. [CrossRef]

18. Hock, A.; Miyake, H.; Li, B.; Lee, C.; Ermini, L.; Koike, Y.; Chen, Y.; Määttänen, P.; Zani, A.; Pierro, A. Breast Milk-Derived Exosomes Promote Intestinal Epithelial Cell Growth. *J. Pediatr. Surg.* **2017**, *52*, 755–759. [CrossRef]

19. Näslund, T.I.; Paquin-Proulx, D.; Paredes, P.T.; Vallhov, H.; Sandberg, J.K.; Gabrielsson, S. Exosomes from Breast Milk Inhibit HIV-1 Infection of Dendritic Cells and Subsequent Viral Transfer to CD4+ T Cells. *AIDS* **2014**, *28*, 171–180. [CrossRef]

20. Arslanoglu, S.; Bertino, E.; Tonetto, P.; De Nisi, G.; Ambruzzi, A.M.; Biasini, A.; Profeti, C.; Spreghini, M.R.; Moro, G.E.; Italian Association of Human Milk Banks Associazione Italiana Banche del Latte Umano Donato (AIBLUD: www.aiblud.org). Guidelines for the Establishment and Operation of a Donor Human Milk Bank. *J. Matern. Fetal Neonatal Med.* **2010**, *23*, 1–20. [CrossRef]

21. Marchini, A.; Liu, H.; Zhu, H. Human Cytomegalovirus with IE-2 (UL122) Deleted Fails to Express Early Lytic Genes. *J. Virol.* **2001**, *75*, 1870–1878. [CrossRef]

22. Cagno, V.; Donalisio, M.; Civra, A.; Cagliero, C.; Rubiolo, P.; Lembo, D. *In Vitro* Evaluation of the Antiviral Properties of Shilajit and Investigation of Its Mechanisms of Action. *J. Ethnopharmacol.* **2015**, *166*, 129–134. [CrossRef]

23. Qin, W.; Tsukasaki, Y.; Dasgupta, S.; Mukhopadhyay, N.; Ikebe, M.; Sauter, E.R. Exosomes in Human Breast Milk Promote EMT. *Clin. Cancer Res.* **2016**, *22*, 4517–4524. [CrossRef] [PubMed]

24. Zhou, Q.; Li, M.; Wang, X.; Li, Q.; Wang, T.; Zhu, Q.; Zhou, X.; Wang, X.; Gao, X.; Li, X. Immune-Related MicroRNAs Are Abundant in Breast Milk Exosomes. *Int. J. Biol. Sci.* **2012**, *8*, 118–123. [CrossRef] [PubMed]

25. ExoCarta: Exosome Markers. Available online: http://exocarta.org/exosome_markers (accessed on 13 March 2020).

26. Simons, M.; Raposo, G. Exosomes-Vesicular Carriers for Intercellular Communication. *Curr. Opin. Cell Biol.* **2009**, *21*, 575–581. [CrossRef] [PubMed]

27. Welch, J.L.; Kaddour, H.; Winchester, L.; Fletcher, C.V.; Stapleton, J.T.; Okeoma, C.M. Semen Extracellular Vesicles From HIV-1-Infected Individuals Inhibit HIV-1 Replication *In Vitro*, and Extracellular Vesicles Carry Antiretroviral Drugs In Vivo. *J. Acquir. Immune Defic. Syndr.* **2020**, *83*, 90–98. [CrossRef]

28. Kesimer, M.; Scull, M.; Brighton, B.; DeMaria, G.; Burns, K.; O'Neal, W.; Pickles, R.J.; Sheehan, J.K. Characterization of Exosome-like Vesicles Released from Human Tracheobronchial Ciliated Epithelium: A Possible Role in Innate Defense. *FASEB J.* **2009**, *23*, 1858–1868. [CrossRef]

29. Nolte-'t Hoen, E.; Cremer, T.; Gallo, R.C.; Margolis, L.B. Extracellular Vesicles and Viruses: Are They Close Relatives? *Proc. Natl. Acad. Sci. USA* **2016**, *113*, 9155–9161. [CrossRef]

30. Van Herwijnen, M.J.C.; Zonneveld, M.I.; Goerdayal, S.; Hoen, E.N.M.N.; Garssen, J.; Stahl, B.; Maarten Altelaar, A.F.; Redegeld, F.A.; Wauben, M.H.M. Comprehensive proteomic analysis of human milk-derived extracellular vesicles unveils a novel functional proteome distinct from other milk components. *Mol. Cell. Proteom.* **2016**, *15*, 3412–3423. [CrossRef]

31. Dudkina, N.V.; Spicer, B.A.; Reboul, C.F.; Conroy, P.J.; Lukoyanova, N.; Elmlund, H.; Law, R.H.P.; Ekkel, S.M.; Kondos, S.C.; Goode, R.J.A.; et al. Structure of the poly-C9 component of the complement membrane attack complex. *Nat. Commun.* **2016**, *7*, 1–6. [CrossRef]

32. Schiela, B.; Bernklau, S.; Malekshahi, Z.; Deutschmann, D.; Koske, I.; Banki, Z.; Thielens, N.M.; Würzner, R.; Speth, C.; Weiss, G.; et al. Active human complement reduces the zika virus load via formation of the membrane-attack complex. *Front. Immunol.* **2018**, *9*, 1–9. [CrossRef]

33. Inagaki, M.; Muranishi, H.; Yamada, K.; Kakehi, K.; Uchida, K.; Suzuki, T.; Yabe, T.; Nakagomi, T.; Nakagomi, O.; Kanamaru, Y. Bovine κ-casein inhibits human rotavirus (HRV) infection via direct binding of glycans to HRV. *J. Dairy Sci.* **2014**, *97*, 2653–2661. [CrossRef] [PubMed]

34. Mistry, N.; Drobni, P.; Näslund, J.; Sunkari, V.G.; Jenssen, H.; Evander, M. The anti-papillomavirus activity of human and bovine lactoferricin. *Antivir. Res.* **2007**, *75*, 258–265. [CrossRef] [PubMed]

35. Swart, P.J.; Kuipers, E.M.; Smit, C.; Van Der Strate, B.W.A.; Harmsen, M.C.; Meijer, D.K.F. Lactoferrin. In *Advances in Lactoferrin Research*; Spik, G., Legrand, D., Mazurier, J., Pierce, A., Perraudin, J., Eds.; Advances in Experimental Medicine and Biology, vol 443; Springer: Boston, MA, USA, 1998.

36. Andersen, J.H.; Osbakk, S.A.; Vorland, L.H.; Traavik, T.; Gutteberg, T.J. Lactoferrin and cyclic lactoferricin inhibit the entry of human cytomegalovirus into human fibroblasts. *Antivir. Res.* **2001**, *51*, 141–149. [CrossRef]

37. Iskarpatyoti, J.A.; Morse, E.A.; Paul McClung, R.; Ikizler, M.; Wetzel, J.D.; Contractor, N.; Dermody, T.S. Serotype-specific differences in inhibition of reovirus infectivity by human-milk glycans are determined by viral attachment protein σ1. *Virology* **2012**, *433*, 489–497. [CrossRef] [PubMed]

38. Saeland, E.; de Jong, M.A.W.P.; Nabatov, A.A.; Kalay, H.; Geijtenbeek, T.B.H.; van Kooyk, Y. MUC1 in human milk blocks transmission of human immunodeficiency virus from dendritic cells to T cells. *Mol. Immunol.* **2009**, *46*, 2309–2316. [CrossRef] [PubMed]

39. Mall, A.S.; Habte, H.; Mthembu, Y.; Peacocke, J.; De Beer, C. Mucus and Mucins: Do they have a role in the inhibition of the human immunodeficiency virus? *Virol. J.* **2017**, *14*, 1–14. [CrossRef]

40. Sun, X.; Dang, L.; Li, D.; Qi, J.; Wang, M.; Chai, W.; Zhang, Q.; Wang, H.; Bai, R.; Tan, M.; et al. Structural Basis of Glycan Recognition in Globally Predominant Human P[8] Rotavirus. *Virol. Sin.* **2020**, *35*, 156–170. [CrossRef]

41. Peterson, J.A.; Patton, S.; Hamosh, M. Glycoproteins of the Human Milk Fat Globule in the Protection of the Breast-Fed Infant against Infections. *Neonatology* **1998**, *74*, 143–162. [CrossRef]

42. Newburg, D.S. Neonatal protection by an innate immune system of human milk consisting of oligosaccharides and glycans. *J. Anim. Sci.* **2009**, *87*, 26–34. [CrossRef]

43. Wyatt, A.; Yerbury, J.; Poon, S.; Dabbs, R.; Wilson, M. Chapter 6: The Chaperone Action of Clusterin and Its Putative Role in Quality Control of Extracellular Protein Folding. *Adv. Cancer Res.* **2009**, *104*, 89–114. [CrossRef]

44. Sabatte, J.; Faigle, W.; Ceballos, A.; Morelle, W.; Rodríguez Rodrígues, C.; Remes Lenicov, F.; Thépaut, M.; Fieschi, F.; Malchiodi, E.; Fernández, M.; et al. Semen Clusterin Is a Novel DC-SIGN Ligand. *J. Immunol.* **2011**, *187*, 5299–5309. [CrossRef] [PubMed]

45. Švajger, U.; Anderluh, M.; Jeras, M.; Obermajer, N. C-type lectin DC-SIGN: An adhesion, signalling and antigen-uptake molecule that guides dendritic cells in immunity. *Cell. Signal.* **2010**, *22*, 1397–1405. [CrossRef] [PubMed]

46. Tripathi, S.; Batra, J.; Cao, W.; Sharma, K.; Patel, J.R.; Ranjan, P.; Kumar, A.; Katz, J.M.; Cox, N.J.; Lal, R.B.; et al. Influenza A Virus Nucleoprotein Induces Apoptosis in Human Airway Epithelial Cells: Implications of a Novel Interaction between Nucleoprotein and Host Protein Clusterin. *Cell Death Dis.* **2013**, *4*, e562. [CrossRef]

47. Kurosu, T.; Chaichana, P.; Yamate, M.; Anantapreecha, S.; Ikuta, K. Secreted complement regulatory protein clusterin interacts with dengue virus nonstructural protein 1. *Biochem. Biophys. Res. Commun.* **2007**, *362*, 1051–1056. [CrossRef] [PubMed]

48. Liao, F.T.; Lee, Y.J.; Ko, J.L.; Tsai, C.C.; Tseng, C.J.; Sheu, G.T. Hepatitis delta virus epigenetically enhances clusterin expression via histone acetylation in human hepatocellular carcinoma cells. *J. Gen. Virol.* **2009**, *90*, 1124–1134. [CrossRef] [PubMed]

49. Naarding, M.A.; Dirac, A.M.; Ludwig, I.S.; Speijer, D.; Lindquist, S.; Vestman, E.-L.; Stax, M.J.; Geijtenbeek, T.B.H.; Pollakis, G.; Hernell, O.; et al. Bile Salt-Stimulated Lipase from Human Milk Binds DC-SIGN and Inhibits Human Immunodeficiency Virus Type 1 Transfer to CD4+ T Cells. *Antimicrob. Agents Chemother.* **2006**, *50*, 3367–3374. [CrossRef]

50. Liu, B.; Newburg, D.S. Human milk glycoproteins protect infants against human pathogens. *Breastfeed. Med.* **2013**, *8*, 354–362. [CrossRef]

51.　Azad, A.K.; Rajaram, M.V.S.; Schlesinger, L.S. Exploitation of the Macrophage Mannose Receptor (CD206) in Infectious Disease Diagnostics and Therapeutics. *J. Cytol. Mol. Biol.* **2014**, *1*, 1–10. [CrossRef]

52.　Taylor, P.R.; Martinez-Pomares, L.; Stacey, M.; Lin, H.-H.; Brown, G.D.; Gordon, S. Macrophage Receptors and Immune Recognition. *Annu. Rev. Immunol.* **2005**, *23*, 901–944. [CrossRef]

53.　Sukegawa, S.; Miyagi, E.; Bouamr, F.; Farkašová, H.; Strebel, K. Mannose Receptor 1 Restricts HIV Particle Release from Infected Macrophages. *Cell Rep.* **2018**, *22*, 786–795. [CrossRef]

54.　Cinatl, J., Jr.; Bittoova, M.; Margraf, S.; Vogel, J.; Cinatl, J.; Preiser, W.; Doerr, H.W. Cytomegalovirus Infection Decreases Expression of Thrombospondin-1 and -2 in Cultured Human Retinal Glial Cells: Effects of Antiviral Agents. *J. Infect. Dis.* **2000**, *182*, 643–651. [CrossRef] [PubMed]

55.　Zhang, B.; Wang, Z.; Deng, B.; Wu, X.; Liu, J.; Feng, X. Identification of Enolase 1 and Thrombospondin-1 as serum biomarkers in HBV hepatic fibrosis by proteomics. *Proteome Sci.* **2013**, *11*, 30. [CrossRef] [PubMed]

56.　Nguyen, C.C.; Kamil, J.P. Pathogen at the gates: Human cytomegalovirus entry and cell tropism. *Viruses* **2018**, *10*, 704. [CrossRef] [PubMed]

57.　Midwood, K.S.; Hussenet, T.; Langlois, B.; Orend, G. Advances in tenascin-C biology. *Cell. Mol. Life Sci.* **2011**, *68*, 3175–3199. [CrossRef] [PubMed]

58.　Fouda, G.G.; Jaeger, F.H.; Amos, J.D.; Ho, C.; Kunz, E.L.; Anasti, K.; Stamper, L.W.; Liebl, B.E.; Barbas, K.H.; Ohashi, T.; et al. Tenascin-C Is an Innate Broad-Spectrum, HIV-1-Neutralizing Protein in Breast Milk. *Proc. Natl. Acad. Sci. USA* **2013**, *110*, 18220–18225. [CrossRef]

59.　Mangan, R.J.; Stamper, L.; Ohashi, T.; Eudailey, J.A.; Go, E.P.; Jaeger, F.H.; Itell, H.L.; Watts, B.E.; Fouda, G.G.; Erickson, H.P.; et al. Determinants of Tenascin-C and HIV-1 Envelope Binding and Neutralization. *Mucosal Immunol.* **2019**, *12*, 1004–1012. [CrossRef]

60.　García-Expósito, L.; Ziglio, S.; Barroso-González, J.; de Armas-Rillo, L.; Valera, M.S.; Zipeto, D.; Machado, J.D.; Valenzuela-Fernández, A. Gelsolin activity controls efficient early HIV-1 infection. *Retrovirology* **2013**, *10*, 39. [CrossRef]

61.　Zhao, K.; Zhang, M.; Zhang, L.; Wang, P.; Song, G.; Liu, B.; Wu, H.; Yin, Z.; Gao, C. Intracellular osteopontin stabilizes TRAF3 to positively regulate innate antiviral response. *Sci. Rep.* **2016**, *6*, 1–13. [CrossRef]

Original Research

Human Colostrum and Derived Extracellular Vesicles Prevent Infection by Human Rotavirus and Respiratory Syncytial Virus in Vitro

Andrea Civra, PhD[1*], Rachele Francese, MS[1*], Manuela Donalisio, PhD[1],
Paola Tonetto, MD[2], Alessandra Coscia, MD, PhD[2], Stefano Sottemano, MD[2] [iD],
Raffaella Balestrini, PhD[3], Antonella Faccio, MS[3], Laura Cavallarin, PhD[4],
Guido E. Moro, MD[5], Enrico Bertino, MD[2], and David Lembo, PhD[1]

Abstract

Background: It is known that breastfeeding protects the infant from enteric and respiratory infections; however, the antiviral properties of human milk against enteric and respiratory viruses are largely unexplored.

Research aims: To explore the antiviral activity of human preterm colostrum against rotavirus and respiratory syncytial virus and to assess whether the derived extracellular vesicle contribute to this activity.

Methods: We used a cross-sectional, prospective two-group non-experimental design. Colostra were collected from mothers of preterm newborns ($N = 10$) and extracellular vesicles were purified and characterized. The antiviral activity of colostra and derived extracellular vesicles were tested *in vitro* against rotavirus and respiratory syncytial virus and the step of viral replication inhibited by extracellular vesicles was investigated.

Results: Each sample of colostrum and colostrum-derived extracellular vesicles had significant antiviral activity with a wide interpersonal variability. Mechanism of action studies demonstrated that extracellular vesicles acted by interfering with the early steps of the viral replicative cycle.

Conclusion: We demonstrated the intrinsic antiviral activity of human colostrum against rotavirus and respiratory syncytial virus and we showed that extracellular vesicles substantially contribute to the overall protective effect. Our results contribute to unravelling novel mechanisms underlying the functional role of human milk as a protective and therapeutic agent in preterm infants.

Keywords

breastfeeding, colostrum, infectious disease, milk composition, prematurity

Background

Human milk (HM) is a complex biofluid containing nutrients and bioactive factors to support infant growth and development, along with its immune system. It also contains antimicrobial glycoproteins, which act like specific or non-specific pathogen recognition molecules (Ballard & Morrow, 2013). A large body of literature has demonstrated the benefits of HM in diminishing infant morbidity and mortality and in protecting against specific infections during the breastfeeding period (Bahl et al., 2005; Duijts et al., 2010). This is particularly relevant for preterm infants (i.e., born before the 37th week of pregnancy) because they often develop complications, namely chronic lung disease, retinopathy, and necrotizing enterocolitis (NEC; Collins et al., 2018). Interestingly, preterm colostrum (i.e., the milk produced during the first days after delivery), compared with the colostrum of term mothers, contains larger amounts of nutrients and immune factors (Gidrewicz & Fenton, 2014). Moreover, it stimulates the immature neonatal immune system by means of a prebiotic mechanism that provides bacteriostatic, bactericidal, antiviral, anti-inflammatory, and immunomodulatory protection against infections (Rodriguez et al., 2009), thus contributing to compensating against the immunological deficiency of preterm

Corresponding Author:
David Lembo, PhD, Department of Clinical and Biological Sciences, University of Torino, S. Luigi Gonzaga Hospital, Regione Gonzole, 10, Orbassano, Torino 10043, Italy.
Email: david.lembo@unito.it

infants. Despite these widely recognized health benefits of HM, some intriguing mysteries have yet to be solved, in particular about how specific components contribute to the development of an infant's innate and adaptive immune functions. Extracellular vesicles (EVs) are one of these components consisting of a heterogeneous population of vesicles that include exosomes and microvesicles. They consist of lipid bilayer enclosed vesicles displaying a heterogeneous size ranging from 50–200 nm, and they are released by most tissues, including HM (Admyre et al., 2007). EVs can be taken up by other cells in which they release their molecular cargo (e.g., miRNA, mRNA, RNAs, enzymes, signaling proteins) playing a role in intercellular signaling, immune response, stem cell differentiation, neuronal function, tissue regeneration, and viral replication (Baier et al., 2014; Benmoussa et al., 2016; Izumi et al., 2012; van der Pol et al., 2012). A potential role for milk-derived EVs in immune modulation has been suggested based on their protein and miRNA contents (Admyre et al., 2007; van Herwijnen et al., 2016; Zempleni et al., 2017; Zhou et al., 2012). Moreover, human milk-derived EVs (HM-EVs) have been found to have immunomodulatory properties on T cells. (Admyre et al., 2007). This has led to the hypothesis that EVs in HM could be involved in the instruction of the neonatal immune system. Besides this solid body of literature and the evidence that HM is a rich source of EVs (Torregrosa Paredes et al., 2014), the antiviral potential of HM-EVs has been largely unexplored. The only available studies reported that EVs and exosomes (a specific subclass of cell-derived EVs) were endowed with antiviral activity against human cytomegalovirus (CMV) and human immunodeficiency virus Type 1 (HIV-1), respectively (Donalisio et al., 2020; Näslund et al., 2014), suggesting that EVs may play a role in controlling viral infections in breastfed infants. This is particularly appealing since viruses are a relevant risk factor for the worsening of prognosis in preterm infants. Human rotavirus (HRoV) and respiratory syncytial virus (RSV) are well-known triggers of complications in preterm neonates, representing the most frequent causes of neonatal viral outbreaks in neonatal intensive care units (NICUs; Civardi et al., 2013). HRoV is the most common cause of pediatric diarrhea (Kotloff, 2017) and preterm infants are at a higher risk of complications and hospitalization than children born full term (Goveia et al., 2007). RSV infection often causes severe, and sometimes life-threatening respiratory disease in preterm infants (Figueras-Aloy et al., 2016). Therefore, the aims of this study were to explore the antiviral activity of human preterm colostrum against HRoV and RSV and to assess whether the derived EVs contribute to this activity.

Key Messages

- The intrinsic anti-rotavirus and anti-respiratory syncytial virus activity of human milk has been poorly investigated.
- Colostrum from preterm mothers is endowed with a significant antiviral activity against rotavirus and respiratory syncytial virus.
- Colostrum derived extracellular vesicles contribute to the colostrum antiviral activity interfering with the early steps of viral replication.
- We demonstrated novel mechanisms underlying the protective effect of human milk against viral infections.

Methods

Design

This was a cross-sectional, prospective two-group non-experimental design. This design enabled us to explore the anti-HRoV and anti-RSV activity of human colostrum and to evaluate the contribution of colostrum derived-EVs to the overall antiviral activity of this biofluid. The study was approved by the Ethical Committee of the Italian Association of Human Milk Banks (AIBLUD) in December 2016.

Setting and Relevant Context

This study was conducted using colostrum samples donated by mothers whose preterm infants had been admitted to the Neonatal Care Unit of the University, City of Health and Science Hospital of Turin. All participants resided in the Piedmont region, Italy.

Sample

Fresh colostrum samples (collected 1–5 days postpartum) were obtained from 10 healthy preterm mothers. We chose this number of replicates in order to avoid any variability of the results ascribable to the heterogeneity of the colostrum samples. Inclusion criteria were mothers giving birth to preterm infants with gestational ages ranging from 23 + 3 to 32 + 0 (weeks + day). The only exclusion criteria was term mothers.

[1]Laboratory of Molecular Virology and Antiviral Research, Department of Clinical and Biological Sciences, University of Turin, Italy
[2]Neonatal Care Unit of the University, City of Health and Science Hospital, Turin, Italy
[3]National Research Council - Institute for Sustainable Plant Protection (CNR-IPSP), Turin Unit, Italy
[4]Consiglio Nazionale delle Ricerche-Istituto di Scienze delle Produzioni Alimentari, Grugliasco (TO), Italy
[5]Italian Association of Human Milk Banks, Milan, Italy

*The authors Andrea Civra and Rachele Francese contributed equally to the work.

Measurement

Cell Lines and Viruses. African green monkey kidney epithelial cells (MA104; ATCC® CRL-2378.1), Hep-2 human epithelial cells (ATCC® CCL-23) and human foreskin fibroblasts (HFF-1; ATCC® SCRC-1041) were cultured as described above (Cagno et al., 2014, 2015; Civra et al., 2018). HRoV strain Wa (ATCC® VR-2018) and A2 RSV strain (ATCC VR-1540) were propagated as previously reported (Civra et al., 2018; Donalisio, Rittà, Francese, et al., 2018).

EV Characterization by Means of Western Blotting. The EV protein profile was analyzed by means of Western blotting. HFF cells were chosen as the control since they are a reliable and highly standardized human cell line and HFF cell lysate was used to verify the reactivity of the anti-calnexin primary antibody. Proteins were extracted in reducing conditions. Briefly, RIPA buffer was added to the EV pellet, or to HFF cells, for 10 min at RT. Soluble proteins were collected and quantified using a protein assay kit. Extracted proteins were separated by gel electrophoresis (SDS-8.5% PAGE). In each well, 20 µg of protein was loaded for the extracellular vesicles, and 3 µg of protein for the cellular extracts. The Western blot was performed as previously described (Civra et al., 2018). Primary antibodies: anti-CD63, anti-CD9, anti-CD81 (EXOAB-KIT-1, System Biosciences), and anti-calnexin (G65120-050, Transduction laboratories) were diluted 1:1000; secondary antibodies: goat anti-rabbit HRP (EXOAB-KIT-1, System Biosciences) and goat anti-mouse IgG (H+L; 115-036-003 Jackson Immuno Research) were diluted 1:10000. The blots were exposed for 10 min.

EV Characterization by Means of TEM. Seven µl of the purified EVs was allowed to adsorb into Formvar/Carbon-coated grids (Electron Microscopy Sciences). After washing, the grids were negatively stained with 0.5% uranyl acetate. The gold formvar/carbon-coated grids were then washed with 0.05 M Tris-buffered saline (TBS, pH 7.6), treated with normal goat serum, diluted 1:30 in TBS + 0.2% BSA for 15 min, and then incubated for 2 hr in the primary antibody anti-CD63 in the same buffer. After washing in TBS, the grids were incubated for 1 hr with a 5 nm colloidal gold conjugated goat anti-mouse IgG(Fc) antibody (AuroProbe) in TBS + BSA. After washing with TBS and water, the grids were subjected to the negative staining procedure. Images were captured with CM10 electron microscope (Philips, the Netherlands).

Nanoparticle Tracking Analysis (NTA). EVs samples were diluted in PBS (1:8000) to a final volume of 1 ml. A nanoparticle tracking analysis system (NanoSight NS300, Malvern Instruments Ltd., UK) was used to determine particle size and concentration/ml at the ideal particle per frame (50 particle/frame). NTA 3.2 Dev Build 3.2.16 software was used to perform the particles tracking analysis. Camera type: sCMOS; laser type: Blue488; camera level: 14; slider shutter: 1259; slider gain: 366; FPS 25.0; number of frames: 749; temperature: 25 °C; syringe pump speed: 30; detect threshold: 6; maximum jump distance: 9.6–10.5 pix.

Viability Cell Assay. Cell viability was assessed using the MTS [3-(4,5-dimethylthiazol-2-yl)-5-(3-carboxymethoxyphenyl)-2-(4-sulfophenyl)-2H-tetrazolium] assay as previously described (Cagno et al., 2014). Confluent MA104 and Hep2 cells in 96-well plates were treated with serial dilutions of colostrum or EVs under the same experimental conditions described for the virus inhibition assays. The 50% cytotoxic concentrations (CC_{50}) were determined using Prism software (GraphPad).

Virus Inhibition Assay. Confluent MA104 and the Hep2 cells in 96-well plates, were pre-treated with serial dilutions of colostrum (1:1–1:4096 parts) or EVs (423–0.19 µg protein/ml) for 1 hr at 37 °C. Simultaneously, mixtures of serial dilutions of colostrum, or EVs, and the same amount of virus were incubated for 1 hr at 37 °C at MOIs of 0.02 for HRoV and 0.01 for RSV. These mixtures were then added to cells and left for 1 hr, in the case of HRoV, or for 3 hr in the case of RSV. After two washes, the infected MA104 cells were incubated with a fresh medium for 16 hr at 37 °C, while the infected Hep2 cells were overlaid with a 1.2% methylcellulose medium for 72 hr at 37 °C. After 24 hr for HRoV and 72 hr for RSV, the cells were fixed with cold acetone-methanol (50:50). The HRoV-infected cells and RSV syncytia were detected by means of indirect immunostaining as reported beforehand (Civra et al., 2018; Donalisio, Rittà, Francese, et al., 2018).

Virus Inactivation Assay. Approximately 10^5 FFU of HRoV or RSV were incubated with a concentration of EVs, corresponding to EC_{90} in the virus inhibition assay. The HRoV-EV mixture was incubated for 1 hr at 37 °C, while the RSV-EV mixture was incubated for 3 hr at 37 °C. Both the treated and untreated viruses were then titrated to the non-inhibitory concentration of EVs and the residual viral infectivity was determined by means of indirect immunostaining. Statistical analysis was performed using Student's *t*-test.

Cell Pre-Treatment Assay. Confluent MA104 or Hep2 cells were pre-treated in 96 well plates with different concentrations of EVs (from 423 to 0.19 µg protein/ml) for 2 hr at 37 °C. After washing, the MA104 cells were infected with HRoV (MOI = 0.02) and left for 1 hr at 37 °C, while the Hep2 cells were infected with RSV (MOI = 0.01) and left for 3 hr at 37 °C. After two washes, the infected MA104 cells were incubated with a fresh medium and left for 16 hr at 37 °C and the infected Hep2 cells were overlaid with 1.2% methylcellulose medium and left for 72 hr at 37 °C. Subsequently, the cells were fixed and indirect immunostainings were performed.

Binding Assay. Pre-cooled viruses (HRoV or RSV, MOI = 3 FFU/ml) were allowed to attach to confluent MA104 or Hep2 (in 24 well-plates) in the presence of EVs (EC_{90}). After an incubation of 2 hr on ice, the cells were washed with a cold medium

Table 1. Main Clinical Characteristics of the Sample (*N* = 10).

Participant ID	Parity	BF after previous parturition(s)	Type of delivery
I	2002	Yes	CS
2	0000	-	CS
3	0000	-	CS
5	1001	-	CS
7	0000	-	S
8	1021	Yes	S
9	0000	-	CS
10	0000	-	CS
11	1001	Yes	CS
12	1001	Yes	CS

Note. BF = breastfeeding; parity refers to the number of previous pregnancies (the first number indicates infants born at term; the second number indicates infants born preterm; the third number indicates miscarriages; and the fourth number indicates living children); type of delivery: S = spontaneous delivery; CS = cesarean section. Missing values for BF after previous parturition = 5.

to remove any unbound virus. The cells were then subjected to three rounds of freeze-thawing to release any bound virus, and the lysate was clarified by means of low speed centrifugation for 10 min. The cell-bound virus titers were determined by means of indirect immunostaining. The presence of any significant differences was assessed by means of Student's *t*-test.

Entry Assay and Post-Entry Assay. HRoV and RSV, pre-cooled to 4 °C, were allowed to attach to cells on ice for 2 hr at 4 °C, at a MOI of 0.04 FFU/ml. The cells were then washed twice with a cold medium to remove the unbound virus and then incubated with serial dilutions of EVs (1269– 0.19 μg protein/ml) for 1 hr (HRoV-infected cells) or 3 hr (RSV-infected cells). During this incubation, the temperature was shifted to 37 °C to allow viral particles entry inside the cells. The entry of HRoV was stopped with a quick wash with 3 mM EGTA in PBS (PBS-EGTA; 23) and the unpenetrated RSV particles were inactivated with acidic glycine (Cagno et al., 2015) for 1 min at room temperature. After 2 washes, the MA104 cells were incubated with DMEM for 16 hr at 37 °C and the Hep2 cells were overlaid with a 1.2% methylcellulose medium for 72 h rat 37 °C. Alternatively, in the post-entry assays, increasing concentrations of EVs (from 1269 to 0.19 μg protein/ml) were added to the cultures in DMEM (HRoV-infected cells) or in a 1.2% methylcellulose medium (RSV-infected cells) after washing with PBS-EGTA and acidic glycine, respectively. The viral entry blockade was determined by indirect immunostaining.

Data Collection

Samples were collected between January 2017 and December 2018 by members the Neonatal Intensive Care Unit of Sant'Anna Hospital of Turin, under the supervision of the director, Professor Enrico Bertino. All experimental analyses were completed before December 2019. Each milk donor involved in this research

signed a written consent form, where the participant's data protection was assured. Participants were informed that only milk samples stored in excess would be used for research purposes. The donors were informed about the study design. Every participant signed a privacy informative. Every milk sample was coded with an identity number, and personal and sensitive data were kept in a database accessible only by clinicians who were members of the research team.

Milk samples were collected within 5 days of delivery. The donors cleaned their hands and breasts according to the Italian HMB guidelines (Arslanoglu et al., 2010) and the colostrum specimens were collected in sterile, bisphenol-free polypropylene bottles using a breast pump. The colostrum samples were transported to a laboratory, within 1 hr, for EVs isolation. The aqueous fraction of colostrum samples were obtained by means of two sequent centrifugations at $2000 \times g$ for 10 min and at $12000 \times g$ for 30 min. The supernatant was filtered (0.45 μm) and subsequently incubated with 2:1 v/v ratio of colostrum: ExoQuick solution (System Biosciences, CA) overnight at 4 °C. The EVs were then purified, according to the manufacturer's instructions. The EV pellet (in 1 x PBS) was quantified with a protein assay kit (Bio-Rad Laboratories, Munich), aliquoted and stored at −80°C until use. We have submitted all relevant data of our experiments to the EV-TRACK knowledgebase (EV-TRACK ID: EV200100; EV-TRACK consortium et al., 2017).

Data Analysis

All the results were presented as the mean values of two independent experiments (i.e., each sample of colostrum or EVs was tested twice for each experimental setting, then we calculated the average values from the data of these two independent experiments). The EC_{50} values of the inhibition curves were calculated from a regression analysis using GraphPad Prism software, Version 5.0 (GraphPad) by fitting a variable slope-sigmoidal dose-response curve. Statistical analysis was performed using Student's *t*-test, Bartlett test ($p_{Bartlett} < .0001$) followed by ANOVA Analysis of variance, or the *F*-test.

Results

Characteristics of the Sample

All the participant donors gave birth to preterm infants with gestational ages ranging from 23 + 3 to 32 + 0 (weeks + day). The main demographic characteristics of the study population are reported in Table 1.

Preterm Colostrum Collection and Colostrum-Derived EV Isolation and Characterization

The samples were clarified to obtain the aqueous fraction, which was subsequently divided into two parts; one part was used for the antiviral assays and the other was processed, with the ExoQuick kit (Wang, 2017), to isolate EV-like vesicles. The
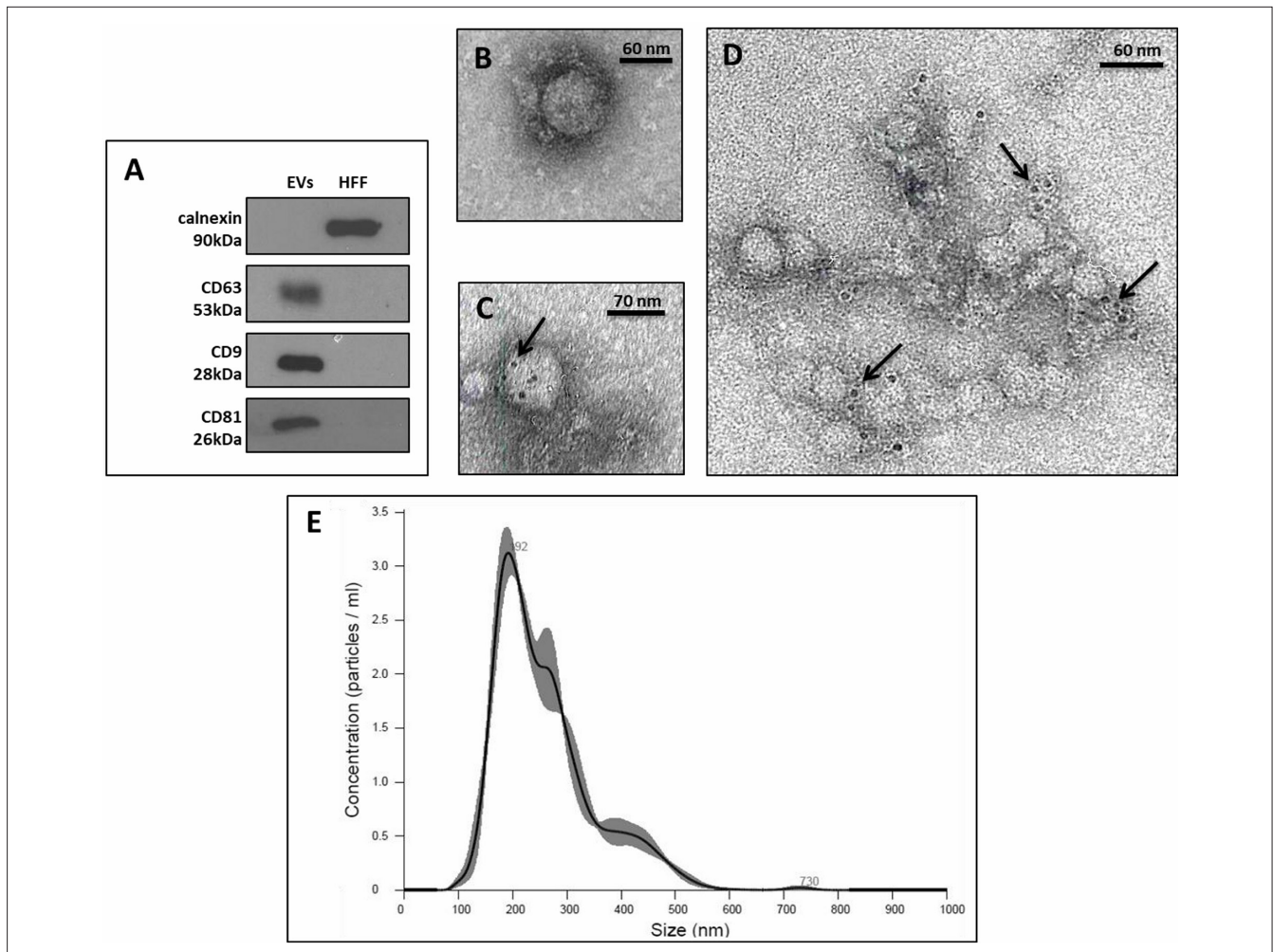
Figure 1. EVs Characterization. (1A) The protein profile of the EVs was analyzed by means of Western blotting, using Abs against the endoplasmatic reticulum-related protein calnexin and the EV marker proteins CD63, CD9, and CD81. HFF cell lysate was used as the positive control. (1B-1C-1D) Electron microscope images of the EVs. (1C-D) Abs against CD63 were detected with gold conjungated secondary antibodies (black arrows). (1E) Nanoparticle tracking analysis (NTA) NanoSight.

aqueous fraction was chosen as the preferred biological matrix because of its previously shown lower impact on cell viability (Donalisio, Rittà, Tonetto, et al., 2018). In order to confirm the extracellular nature of the extracted vesicles, we first examined the EV surface makers by means of Western blotting. As shown in Figure 1A, the EV lysate was positive for the three tetraspanines CD63, CD9, and CD81, which are known to be enriched in EVs from multiple tissue sources (Simons & Raposo, 2009; Théry et al., 2018), while it was negative for the contaminating endoplasmatic reticulum-related protein calnexin. Furthermore, as reported in Figure 1B–D and we confirmed the vesicular structure of the purified and CD63-immunolabeled EVs by means of transmission electron microscope (TEM) observation and we subsequently analyzed their size using NanoSight NTA (Figure 1E).

Extracted EVs presented a size distribution with a mean size of 258.8 nm (Mode: 196.1 ± 7.4 nm), and a concentration of

$4.96e+012 \pm 3.21e+010$ particles/ml. Therefore, we demonstrated the presence of heterogeneous-sized vesicle structures in milk EV isolates.

Preterm Colostrum and Derived EVs Inhibit HRoV and RSV Infection in Vitro

The first set of antiviral assays was performed to determine the antiviral activity of colostrum, collected from mothers of preterm infants, against HRoV and RSV. We showed that all samples exhibited antiviral activity against both HRoV and RSV, although to a different extent. Indeed, each single colostrum sample had different antiviral potency, with EC_{50}s ranging from 5.0 to 933.6 µg protein/ml for HRoV and from 65.5 to 1564 µg protein/ml for RSV (complete results are reported in Table 2). Next, we investigated whether EVs contribute to the anti-HRoV and the anti-RSV activity of human colostrum. We performed antiviral assays

Table 2. Antiviral Activity of Human Colostrum (*N* = 10).

Virus	Participant ID	EC$_{50}$ (µg/ml) (95% CI)	EC$_{90}$ (µg/ml) (95% CI)
HRoV	1	84.8 (68.1–105.7)	408.3 (252.5–660.2)
	2	290.7 (238.6–354.1)	756.6 (518.3–1104.0)
	3	108.8 (65.8–179.9)	233.1 (92.7–586.0)
	5	933.6 (493.0–1768.0)	4069 (991.1–16705.0)
	7	116.0 (97.1–138.6)	437.8 (297.4–644.5)
	8	260.5 (223.3–304.0)	550.9 (381.5–795.6)
	9	5.0 (2.4–10.8)	106.0 (24.1–466.4)
	10	563.5 (347.8–913.0)	3129.0 (1069.0–9162.0)
	11	194.4 (158.7–238.0)	920.9 (592.7–1431.)
	12	495.3 (397.1–618.0)	1414 (848.3–2358.0)
RSV	1	65.5 (54.3–79)	104.4 (67.7–161.2)
	2	138.7 (108.0–178.3)	373.9 (215.0–650.2)
	3	423.9 (345.1–520.6)	984.8 (685.6–1415.0)
	5	116.2 (87.2–154.8)	235.6 (147.2–377.0)
	7	143.6 (113.2–182.2)	463.8 (293.3–733.6)
	8	130.9 (85.6–200.0)	1095.0 (431.8–2776.0)
	9	179.0 (141.2–227.0)	678.7 (403.8–1141.0)
	10	1564.0 (901.5–2713.0)	15003.0 (4134.0–54444.0)
	11	1444.0 (629.0–3315.0)	30603.0 (3610.0–259425.0)
	12	591.2 (283.3–1234.0)	13194.0 (2355.0–73931.0)

Note. HRoV = human rotavirus; RSV = respiratory syncytial virus; EC$_{50}$ = half-maximal effective concentration, EC$_{90}$ = 90% effective concentration.

in which we treated cells and viruses with EVs before and during infection and we demonstrated that EVs were endowed with a significant antiviral activity against both viruses (Table 3). Notably, the EC$_{50}$ values, expressed as micrograms of EV proteins per ml, ranged from 17.6 µg protein/ml to 434.2 µg protein/ml for HRoV and from 29.5 µg protein/ml to 297.6 µg protein/ml for RSV, thus indicating a wide interpersonal variability. For example, the efficacy of EVs from colostrum ID #5 against HRoV was low, while it was not possible to calculate any anti-RSV activity of colostrum ID #11. Similar to the colostrum samples (data not shown), the antiviral activity of the EVs was not due to their cytotoxicity. In fact, there was no evidence of cytotoxicity in the cell viability assays (Figure 2), even for the highest tested concentration of EV proteins (1269.0 µg protein/ml).

EVs Alter the Early Steps of the HRoV and RSV Replicative Cycles

In order to identify the putative step of viral replication inhibited by EVs, we performed specific antiviral assays with three randomly selected EV populations. First, we investigated the ability of these vesicles to impair infectivity by directly targeting viral particles. To this aim, HRoV or RSV were incubated with EVs at high effective concentrations (EC$_{90}$) and the viral titer was then determined at dilutions at which the EVs were no longer active when added to

cells. As reported in Figure 3A, the EVs were not able to inactivate HRoV particles. On the other hand, EVs exhibited a moderate to null RSV inactivation activity (Figure 3B), which was not sufficient to justify the overall anti-RSV activity observed in the previously described infectivity assays. Therefore, having assessed that viral particles were not the major target of EVs, we focused on the early stages of viral replication. In order to explore whether the interaction between the viral particles and the cell surface could be affected by EVs, we carried out binding assays. We demonstrated (Figure 4A) that the EVs did not affect HRoV binding to the host cells. On the contrary, only one sample of EVs slightly, but significantly (*p* < .05), inhibited RSV-cell attachment (Figure 4B). Considering these results, we hypothesized that EV antiviral activity was mainly focused on a post-binding inhibition step of both viruses. To verify this, we performed entry inhibition assays by treating cells with EVs immediately after virus attachment, that is, during cell penetration. As depicted in Figure 4C, D and we demonstrated that EVs were able to inhibit the capacity of the pre-bound virus to infect cells, with EC$_{50}$ ranging from 124.5 µg protein/ml to 901.7 µg protein/ml for HRoV and from 42.3 µg protein/ml to 127.3 µg protein/ml for RSV. Finally, in order to rule out any influence of EVs on a post-entry stage, we analyzed the final steps of HRoV and RSV replication by treating cells with EVs immediately after viral penetration

Table 3. Antiviral Activity of Colostrum Derived Extracellular Vesicles (*N* = 10).

Virus	Participant ID	EC$_{50}$ (µg/ml) (95% CI)	EC$_{90}$ (µg/ml) (95% CI)
HRoV	1	59.3 (45.5–77.4)	345.2 (189.5–629.1)
	2	81.4 (54.2–122.3)	269.8 (114.8–634.3)
	3	34.4 (21.8–54.4)	77.8 (34.3–176.2)
	5	434.2 (145.1–1300.0)	1554.0 (42.5–56834.0)
	7	99.6 (88.9–111.5)	198.7 (151.7–260.2)
	8	140.3 (123.2–159.8)	255.9 (110.4–592.8)
	9	17.6 (8.4–37.1)	217.5 (41.3–1145.0)
	10	256.1 (152.7–429.7)	734.0 (246.3–2187.0)
	11	91.4 (73.9–112.9)	313.1 (200.0–490.1)
	12	135.8 (95.46–193.2)	498.2 (221.2–1122.0)
RSV	1	29.5 (23.9–36.4)	138.4 (86.6–220.7)
	2	58.1 (44.5–76.3)	165.5 (87.4–313.4)
	3	153.6 (119.4–197.7)	354.5 (167.4–750.8)
	5	52.9 (40.0–70.0)	97.79 (28.2–339.0)
	7	46.5 (28.0–77.0)	331 (119.6–915.6)
	8	74.0 (57.7–94.9)	310.8 (180.1–536.3)
	9	80.2 (50.4–127.6)	324.6 (118.2–891.1)
	10	297.6 (171.2–517.4)	3798 (655.6–22003.0)
	11	>423.0	n.a.
	12	138.5 (52.3–366.7)	1519.0 (113.8–20282.0)

Note. HRoV = human rotavirus; RSV = respiratory syncytial virus; EC$_{50}$ = half-maximal effective concentration; EC$_{90}$ = 90% effective concentration; n. a. = not assessable.
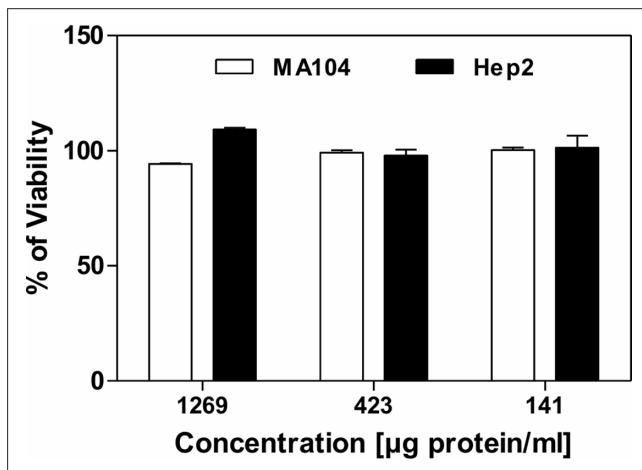

Figure 2. Evaluation of the Effect of the EVs on Cell Viability. Cells were treated with three doses of EVs under the same conditions as the antiviral assays. Cell viability was assessed with an MTS assay. The viability of the treated cells is expressed as a percentage, which was obtained by comparing the absorbances of the treated cells with those of the cells incubated with culture medium alone. Here, we report data of two representative viability assays. All the samples showed the same results. Error bars indicate the SEM of the mean of the independent duplicates. The *t*-test was used to analyze the results.

inside the host cells. We reported (Figure 4E and F) that no effect on the post-entry stages of either virus was exerted by EVs. Taking together these results, we showed that EVs can hamper the entry of HRoV and RSV inside the host cells. Interestingly, when the EVs were removed from the cells after a treatment of 2 hr before virus inoculum, neither HRoV nor RSV infectivity was inhibited (Figure 5A and B), thus suggesting that the simultaneous presence of EVs and viruses was necessary to disturb viral entry into host cells.

Discussion

Although the protective role of breastfeeding on respiratory and gastrointestinal infections by RSV and HRoV is well established (Figueras-Aloy et al., 2016; Lanari et al., 2013; Plenge-Bönig et al., 2010), the intrinsic anti-RSV and anti-HRoV activity of HM has been poorly investigated. We addressed this issue, in the context of preterm infants, by assessing the antiviral activity of human colostrum from preterm mothers and by exploring whether the EVs contribute to its antiviral properties.

The first notable finding was that all the colostrum samples were endowed with anti-RSV and anti-HRoV activity, although to differing extents from mother to mother. A similar variability had been reported (Donalisio, Rittà, Tonetto, et al.,

2018) and was in line with the well-known variability of HM composition between individuals (Gidrewicz & Fenton, 2014) and with differences in the mother's serostatus. To the best of our knowledge, we have reported the intrinsic antiviral activity of human colostrum against RSV and HRoV for the first time. However, previous researchers have attributed the protective role of breastfeeding against RSV and HRoV infections either to non-specific bioactive components or to specific antibodies (Asensi et al., 2006; Grover et al., 1997; Laegreid et al., 1986; Newburg et al., 1998; Superti et al., 1997; Yolken et al., 1992). In this study, our aim has been to explore whether additional antiviral components of human colostrum are at play. EVs are known to exert multiple biological activities (Admyre et al., 2007; Hata et al., 2010; Reinhardt et al., 2012; Zhou et al., 2012), but their role as antiviral effectors in HM has largely been unexplored. We found that EVs were endowed with anti-RSV and anti-HRoV activity, although to different extents between different mothers. An interesting scientific question was whether the maternal immunoglobulin levels against HRoV and RSV correlate with the efficacy of EVs: this could represent a hint for future studies. Performing the antiviral assays, we suggested that EVs inhibit HRoV and RSV by interfering with the early virus-cell interactions. The lack of antiviral activity in the pre-treatment assays rules out an antiviral mechanism involving the release of a molecular cargo able to induce a stable modification of the cell membrane or the intracellular environment in a way that makes cells resistant to virus replication. Interestingly, Näslund et al. (2014) showed that milk exosomes compete with HIV-1 for binding to DC-SIGN receptors on monocyte-derived dendritic cells, and in our previous article (Donalisio et al., 2020) we demonstrated that the anti-HCMV activity of milk EVs was mediated by the inhibition of the viral attachment to the host cell. In our current model, the EVs did not prevent the binding of RSV and HRoV to the cell surface but did affect their entry into the cells. Consistent with these findings, it was previously demonstrated that cells can take up EVs through a variety of endocytic pathways, including clathrin-dependent endocytosis and clathrin-independent pathways (e.g., macropinocytosis and phagocytosis; Feng et al., 2010; Yang et al., 2017). These events may perturb the virus penetration process by inducing a modification of the lipidic composition of the cellular membrane, if they occur concomitantly with a virus infection. In addition, it has been demonstrated that EVs exploit viral entry routes to deliver their cargo inside the target cells (Tian et al., 2014); it is thus likely that EVs compete with HRoV and RSV for the same penetration mechanisms.

Taken together, our results demonstrated that EVs contribute to the overall anti-RSV and anti-HRoV activity played by human colostrum in vitro and that they should be added to the list of antiviral effectors contained in this complex biofluid. Additional studies are required to assess whether the EVs could reach the intestinal lumen intact and be absorbed, in order to exert their antiviral action locally, against HRoV, or at distal body sites, against RSV. In this regard, researchers recently have demonstrated that milk exosomes are long-lasting *in vivo* (Luketic et al., 2007) and accumulate in the intestinal mucosa, spleen, liver, heart, or brain when administered orally or intravenously to mice and pigs (Manca et al., 2018). Finally, further studies are necessary to assess the spectrum of the antiviral activity of colostrum and milk-derived EVs against other viruses that are relevant pathogens for newborns.
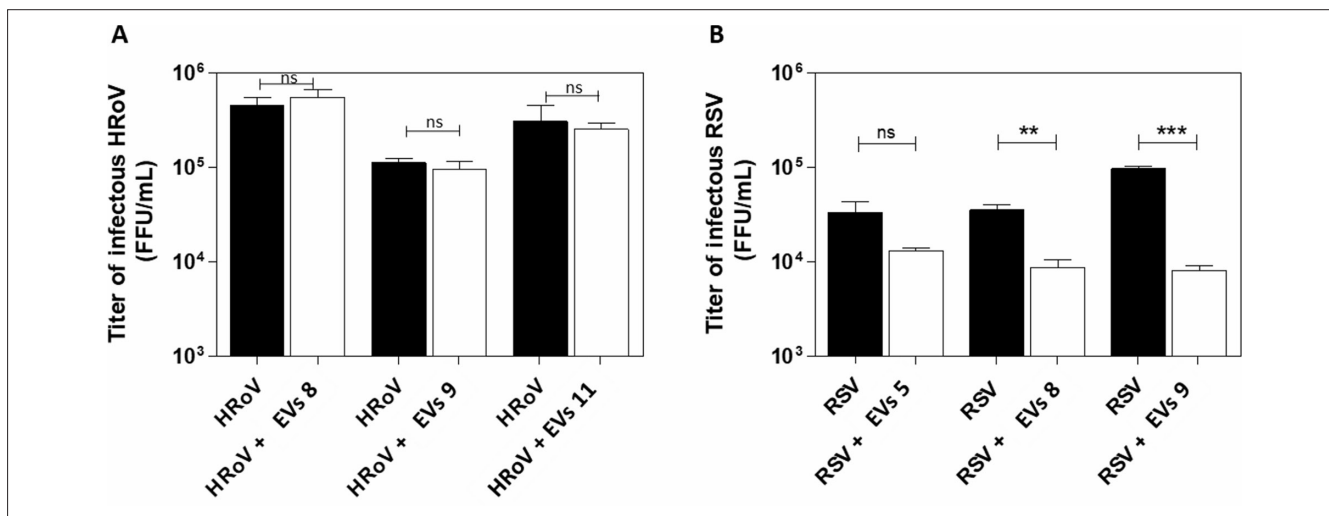

Figure 3. Evaluation of the Virucidal Effect of EVs on Infectious HRoV (3A) and RSV (3B). HRoV and RSV viral particles were pre-incubated with EVs at a concentration corresponding to EC90 in the virus inhibition assay, for 1hr (HRoV) or 3 hr (RSV) at 37 °C. The residual viral infectivity was then determined by means of indirect immunostaining and compared with the infectivity of the untreated control. Viral titers are expressed as FFU/ml and error bars represent the SD of the mean of the independent duplicates. The results of assays with three different EVs are reported. ** .001 < p (t-test) < .01; *** p (t-test) < .001; ns: not significant p (t-test) > .05.
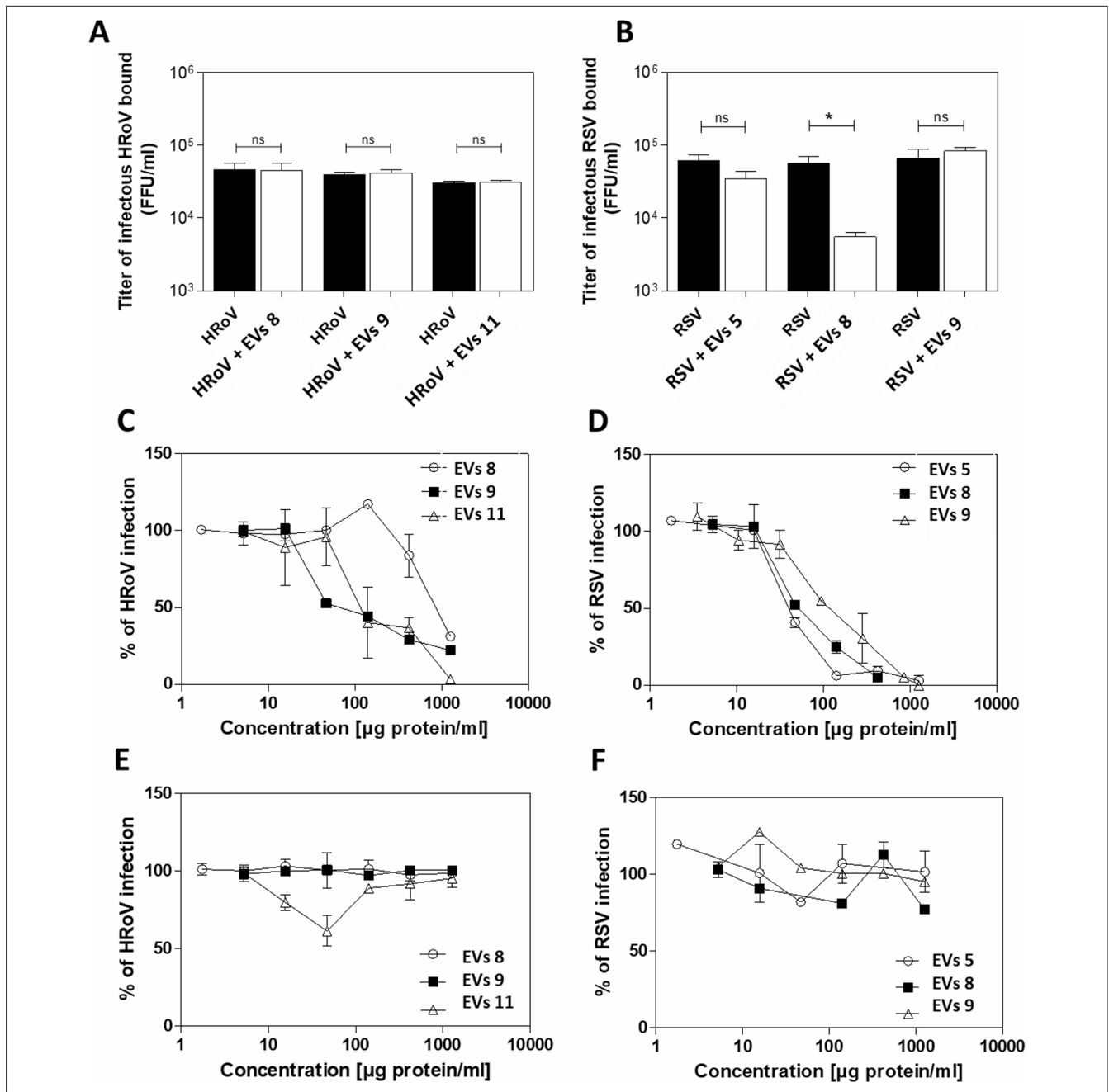
Figure 4. Investigation of the Putative Step of the Viral Replicative Cycle Inhibited by EVs. The results of assays with three different EV populations are reported. In the binding assay, HRoV (4A) and RSV (4B) were allowed to attach to cells in the presence of a high concentration of EVs for 2 hr on ice. Cells were then washed to remove the unbound virus and subsequently subjected to three rounds of freeze-thawing to release bound virus. The lysate was clarified and the cell-bound virus titer was assessed by means of indirect immunostaining and compared with the untreated control. Here, the viral titers are expressed as FFU/ml and are shown as mean ± SEM of the independent duplicates (* .01 < $p_{(t-test)}$ < .05; ns: not significant $p_{(t-test)}$ > .05). In the entry assay, cells were infected with HRoV (4C) or RSV (4D) at 4 °C to allow virus attachment. Next, serial dilutions of EVs were added to the cells and the temperature was shifted to 37 °C to allow virus entry into the cells. After 1hr (HRoV) or 3 hr (RSV), any unpenetrated virus was removed by washing with specific buffers. In the post-entry assay, cells were treated with serial dilutions of EVs immediately after HRoV (4E) or RSV (4F) infection. For the entry and the post-entry assay, the number of infected cells was detected by means of indirect immunostaining and expressed as a percentage of the untreated control. Error bars indicate the SD of the mean of the independent duplicates.
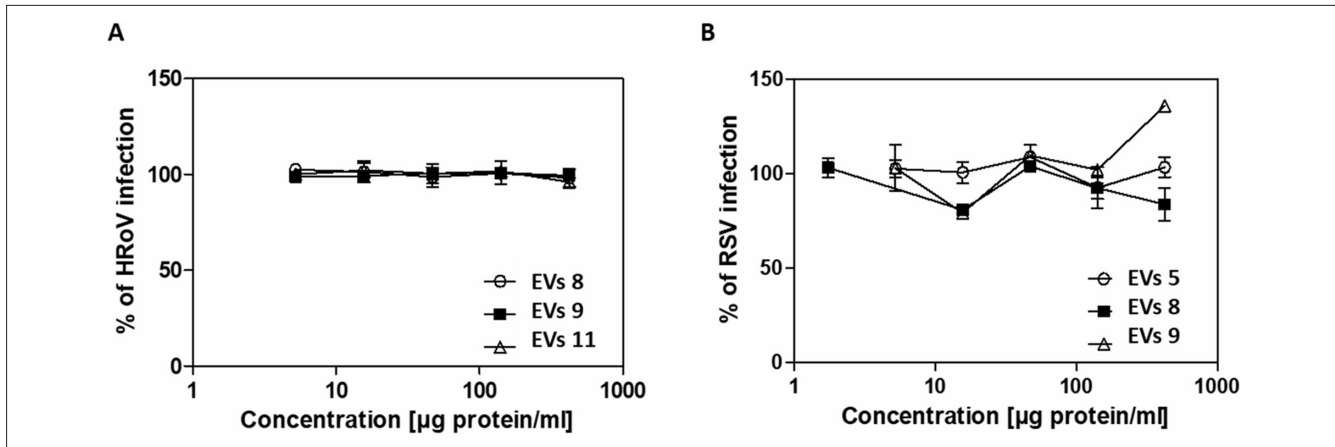
Figure 5. Pre-Treatment Assay. Cells were pre-treated with serial dilutions of EVs for 2 hr and then infected with HRoV (5A) or RSV (5B). The number of infected cells measured in the treated samples is expressed as a percentage of the number obtained in the untreated control. Error bars represent the SD of the mean of independent duplicates. Data of assays with three different EV populations are reported.

Limitations

According to the MISEV2018 guidelines (Théry et al., 2018), ExoQuick purification is considered a "high recovery and low specificity" method . While we chose this technique in order to optimize the chances of detecting any antiviral activity associated to EVs, we cannot exclude the presence of proteic contaminants or anti-viral molecules giving a partial contribution to the *in vitro* efficacy of our EVs preparations. More in depth experiments will be performed in order to identify the specific subpopulation of the EVs responsible for the major observed antiviral activity. Second, the anti-HRoV and anti-RSV activity of EVs was demonstrated *in vitro* and on a relatively small sample size. Therefore, further *in vivo* experiments are necessary to validate the actual antiviral protection conferred by EVs when ingested by a breast-fed infant.

Conclusion

We demonstrated the intrinsic anti-HRoV and anti-RSV activity of human colostrum and we showed that EVs contribute substantially to the overall protective effects. These results contribute to unravelling novel mechanisms underlying the functional role of human milk as a protective and therapeutic agent in preterm infants.

Editor's Note

JHL has a policy of not publishing references from predatory publishers. The references in the Reference List with * were published in journals whose publishers have been criticized by some academics for low standards of peer review, as well as some allegations of academic misconduct. Others have

felt these publishers have done their due diligence. Due to the importance of the topic covered in this review, we left the inclusion of these articles to the authors' discretion. The authors have reviewed all references and take responsibility for their quality.

Declaration of Conflicting Interests

Funding

ORCID iD

Stefano Sottemano, MD 🔵 https://orcid.org/0000-0002-1015-9862

References

Admyre, C., Johansson, S. M., Qazi, K. R., Filén, J.-J., Lahesmaa, R., Norman, M., Neve, E. P. A., Scheynius, A., & Gabrielsson, S. (2007). Exosomes with immune modulatory features are present in human breast milk. *Journal of Immunology*, *179*(3), 1969–1978. doi:10.4049/jimmunol.179.3.1969

Arslanoglu, S., Bertino, E., Tonetto, P., De Nisi, G., Ambruzzi, A. M., Biasini, A., Profeti, C., Spreghini, M. R., & Moro, G. E (2010). Guidelines for the establishment and operation of a donor human milk bank. *The Journal of Maternal-Fetal*

& Neonatal Medicine, *23*(suppl. 2), 1–20. doi:10.3109/14767058.2010.512414

Asensi, M. T., Martínez-Costa, C., & Buesa, J. (2006). Anti-rotavirus antibodies in human milk: Quantification and neutralizing activity. *Journal of Pediatric Gastroenterology and Nutrition*, *42*(5), 560–567. doi:10.1097/01.mpg.0000221892.59371.b3

Bahl, R., Frost, C., Kirkwood, B. R., Edmond, K., Martines, J., Bhandari, N., & Arthur, P. (2005). Infant feeding patterns and risks of death and hospitalization in the first half of infancy: Multicentre cohort study. *Bulletin of the World Health Organization*, *83*(6), 418–426. doi:/S0042-96862005000600009

Baier, S. R., Nguyen, C., Xie, F., Wood, J. R., & Zempleni, J. (2014). MicroRNAs are absorbed in biologically meaningful amounts from nutritionally relevant doses of cow milk and affect gene expression in peripheral blood mononuclear cells, HEK-293 kidney cell cultures, and mouse livers. *The Journal of Nutrition*, *144*(10), 1495–1500. doi:https://doi.org/10.3945/jn.114.196436

Ballard, O., & Morrow, A. L. (2013). Human milk composition: Nutrients and bioactive factors. *Pediatric Clinics of North America*, *60*(1), 49–74. doi:10.1016/j.pcl.2012.10.002

Benmoussa, A., Lee, C. H. C., Laffont, B., Savard, P., Laugier, J., Boilard, E., Gilbert, C., Fliss, I., & Provost, P. (2016). Commercial dairy cow milk microRNAs resist digestion under simulated gastrointestinal tract conditions. *The Journal of Nutrition*, *146*(11), 2206–2215. doi:10.3945/jn.116.237651

Cagno, V., Donalisio, M., Civra, A., Cagliero, C., Rubiolo, P., & Lembo, D. (2015). In vitro evaluation of the antiviral properties of Shilajit and investigation of its mechanisms of action. *Journal of Ethnopharmacology*, *166*, 129–134. doi:10.1016/j.jep.2015.03.019

Cagno, V., Donalisio, M., Civra, A., Volante, M., Veccelli, E., Oreste, P., Rusnati, M., & Lembo, D. (2014). Highly sulfated K5 Escherichia coli polysaccharide derivatives inhibit respiratory syncytial virus infectivity in cell lines and human tracheal-bronchial histocultures. *Antimicrobial Agents and Chemotherapy*, *58*(8), 4782–4794. doi:10.1128/AAC.02594-14

Civardi, E., Tzialla, C., Baldanti, F., Strocchio, L., Manzoni, P., & Stronati, M. (2013). Viral outbreaks in neonatal intensive care units: What we do not know. *American Journal of Infection Control*, *41*(10), 854–856. doi:10.1016/j.ajic.2013.01.026

Civra, A., Francese, R., Gamba, P., Testa, G., Cagno, V., Poli, G., & Lembo, D. (2018). 25-Hydroxycholesterol and 27-hydroxycholesterol inhibit human rotavirus infection by sequestering viral particles into late endosomes. *Redox Biology*, *19*, 318–330. doi:10.1016/j.redox.2018.09.003

Collins, A., Weitkamp, J.-H., & Wynn, J. L. (2018). Why are preterm newborns at increased risk of infection? *Archives of Disease in Childhood. Fetal and Neonatal Edition*, *103*(4), F391–F394. doi:https://doi.org/10.1136/archdischild-2017-313595

*Donalisio, M., Cirrincione, S., Rittà, M., Lamberti, C., Civra, A., Francese, R., Tonetto, P., Sottemano, S., Manfredi, M., Lorenzato, A., Moro, G. E., Giribaldi, M., Cavallarin, L., Giuffrida, M. G., Bertino, E., Coscia, A., & Lembo, D. (2020). Extracellular vesicles in human preterm colostrum inhibit infection by human cytomegalovirus in vitro. *Microorganisms*, *8*(7), 1087. doi:10.3390/microorganisms8071087

*Donalisio, M., Rittà, M., Francese, R., Civra, A., Tonetto, P., Coscia, A., Giribaldi, M., Cavallarin, L., Moro, G. E., Bertino, E., & Lembo, D. (2018). High temperature-short time pasteurization has a lower impact on the antiviral properties of human milk than holder pasteurization. *Frontiers in Pediatrics*, *6*, 304. doi:10.3389/fped.2018.00304

Donalisio, M., Rittà, M., Tonetto, P., Civra, A., Coscia, A., Giribaldi, M., Cavallarin, L., Moro, G. E., Bertino, E., & Lembo, D. (2018). Anti-cytomegalovirus activity in human milk and colostrum from mothers of preterm infants. *Journal of Pediatric Gastroenterology and Nutrition*, *67*(5), 654–659. doi:10.1097/MPG.0000000000002071

Duijts, L., Jaddoe, V. W. V., Hofman, A., & Moll, H. A. (2010). Prolonged and exclusive breastfeeding reduces the risk of infectious diseases in infancy. *Pediatrics*, *126*(1), e18–e25. doi:10.1542/peds.2008-3256

EV-TRACK Consortium, Van Deun, J., Mestdagh, P., Agostinis, P., Akay, Ö., Anand, S., Anckaert, J., Martinez, Z. A., Baetens, T., Beghein, E., Bertier, L., Berx, G., Boere, J., Boukouris, S., Bremer, M., Buschmann, D., Byrd, J. B., Casert, C., Cheng, L., . . .Hendrix, A. (2017). EV-TRACK: Transparent reporting and centralizing knowledge in extracellular vesicle research. *Nature Methods*, *14*(3), 228–232. doi:10.1038/nmeth.4185

Feng, D., Zhao, W.-L., Ye, Y.-Y., Bai, X.-C., Liu, R.-Q., Chang, L.-F., Zhou, Q., & Sui, S.-F. (2010). Cellular internalization of exosomes occurs through phagocytosis. *Traffic*, *11*(5), 675–687. doi:10.1111/j.1600-0854.2010.01041.x

Figueras-Aloy, J., Manzoni, P., Paes, B., Simões, E. A. F., Bont, L., Checchia, P. A., Fauroux, B., & Carbonell-Estrany, X. (2016). Defining the risk and associated morbidity and mortality of severe respiratory syncytial virus infection among preterm infants without chronic lung disease or congenital heart disease. *Infectious Diseases and Therapy*, *5*(4), 417–452. doi:10.1007/s40121-016-0130-1

Gidrewicz, D. A., & Fenton, T. R. (2014). A systematic review and meta-analysis of the nutrient content of preterm and term breast milk. *BMC Pediatrics*, *14*, 216. doi:10.1186/1471-2431-14-216

Goveia, M. G., Rodriguez, Z. M., Dallas, M. J., Itzler, R. F., Boslego, J. W., Heaton, P. M., DiNubile, M. J., & REST Study Team. (2007). Safety and efficacy of the pentavalent human-bovine (WC3) reassortant rotavirus vaccine in healthy premature infants. *The Pediatric Infectious Disease Journal*, *26*(12), 1099–1104. doi:10.1097/INF.0b013e31814521cb

Grover, M., Giouzeppos, O., Schnagl, R. D., & May, J. T. (1997). Effect of human milk prostaglandins and lactoferrin on

respiratory syncytial virus and rotavirus. *Acta Paediatrica*, *86*(3), 315–316. doi:10.1111/j.1651-2227.1997.tb08896.x

Hata, T., Murakami, K., Nakatani, H., Yamamoto, Y., Matsuda, T., & Aoki, N. (2010). Isolation of bovine milk-derived microvesicles carrying mRNAs and microRNAs. *Biochemical and Biophysical Research Communications*, *396*(2), 528–533. doi:10.1016/j.bbrc.2010.04.135

Izumi, H., Kosaka, N., Shimizu, T., Sekine, K., Ochiya, T., & Takase, M. (2012). Bovine milk contains microRNA and messenger RNA that are stable under degradative conditions. *Journal of Dairy Science*, *95*(9), 4831–4841. doi:10.3168/jds.2012-5489

Kotloff, K. L. (2017). The burden and etiology of diarrheal illness in developing countries. *Pediatric Clinics of North America*, *64*(4), 799–814. doi:10.1016/j.pcl.2017.03.006

Laegreid, A., Kolstø Otnaess, A. B., Orstavik, I., & Carlsen, K. H. (1986). Neutralizing activity in human milk fractions against respiratory syncytial virus. *Acta Paediatrica*, *75*(5), 696–701. doi:10.1111/j.1651-2227.1986.tb10276.x

Lanari, M., Prinelli, F., Adorni, F., Di Santo, S., Faldella, G., Silvestri, M., Musicco, M., & Italian Neonatology Study Group on RSV Infections. (2013). Maternal milk protects infants against bronchiolitis during the first year of life. Results from an Italian cohort of newborns. *Early Human Development*, *89*(Suppl. 1), S51–S57. doi:10.1016/S0378-3782(13)70016-1

Luketic, L., Delanghe, J., Sobol, P. T., Yang, P., Frotten, E., Mossman, K. L., Gauldie, J., Bramson, J., & Wan, Y. (2007). Antigen presentation by exosomes released from peptide-pulsed dendritic cells is not suppressed by the presence of active CTL. *Journal of Immunology*, *179*(8), 5024–5032. doi:10.4049/jimmunol.179.8.5024

Manca, S., Upadhyaya, B., Mutai, E., Desaulniers, A. T., Cederberg, R. A., White, B. R., & Zempleni, J. (2018). Milk exosomes are bioavailable and distinct microRNA cargos have unique tissue distribution patterns. *Scientific Reports*, *8*(1), 11321. doi:10.1038/s41598-018-29780-1

Näslund, T. I., Paquin-Proulx, D., Paredes, P. T., Vallhov, H., Sandberg, J. K., & Gabrielsson, S. (2014). Exosomes from breast milk inhibit HIV-1 infection of dendritic cells and subsequent viral transfer to CD4+ T cells. *AIDS*, *28*(2), 171–180. doi:10.1097/QAD.0000000000000159

Newburg, D. S., Peterson, J. A., Ruiz-Palacios, G. M., Matson, D. O., Morrow, A. L., Shults, J., Guerrero, M. L., Chaturvedi, P., Newburg, S. O., Scallan, C. D., Taylor, M. R., Ceriani, R. L., & Pickering, L. K. (1998). Role of human-milk lactadherin in protection against symptomatic rotavirus infection. *Lancet*, *351*(9110), 1160–1164. doi:10.1016/S0140-6736(97)10322-1

Plenge-Bönig, A., Soto-Ramírez, N., Karmaus, W., Petersen, G., Davis, S., & Forster, J. (2010). Breastfeeding protects against acute gastroenteritis due to rotavirus in infants. *European Journal of Pediatrics*, *169*(12), 1471–1476. doi:10.1007/s00431-010-1245-0

Reinhardt, T. A., Lippolis, J. D., Nonnecke, B. J., & Sacco, R. E. (2012). Bovine milk exosome proteome. *Journal of Proteomics*, *75*(5), 1486–1492. doi:10.1016/j.jprot.2011.11.017

Rodriguez, N. A., Meier, P. P., Groer, M. W., & Zeller, J. M. (2009). Oropharyngeal administration of colostrum to extremely low birth weight infants: Theoretical perspectives. *Journal of Perinatology*, *29*(1), 1–7. doi:10.1038/jp.2008.130

Simons, M., & Raposo, G. (2009). Exosomes—vesicular carriers for intercellular communication. *Current Opinion in Cell Biology*, *21*(4), 575–581. doi:10.1016/j.ceb.2009.03.007

Superti, F., Ammendolia, M. G., Valenti, P., & Seganti, L. (1997). Antirotaviral activity of milk proteins: Lactoferrin prevents rotavirus infection in the enterocyte-like cell line HT-29. *Medical Microbiology and Immunology*, *186*(2–3), 83–91. doi:10.1007/s004300050049

Théry, C., Witwer, K. W., Aikawa, E., Alcaraz, M. J., Anderson, J. D., Andriantsitohaina, R., Antoniou, A., Arab, T., Archer, F., Atkin-Smith, G. K., Ayre, D. C., Bach, J.-M., Bachurski, D., Baharvand, H., Balaj, L., Baldacchino, S., Bauer, N. N., Baxter, A. A., Bebawy, M., . . .Zuba-Surma, E. K. (2018). Minimal information for studies of extracellular vesicles 2018 (MISEV2018): A position statement of the International Society for Extracellular Vesicles and update of the MISEV2014 guidelines. *Journal of Extracellular Vesicles*, *7*(1), 1535750. doi:10.1080/20013078.2018.1535750

Tian, T., Zhu, Y.-L., Zhou, Y.-Y., Liang, G.-F., Wang, Y.-Y., Hu, F.-H., & Xiao, Z.-D. (2014). Exosome uptake through clathrin-mediated endocytosis and macropinocytosis and mediating miR-21 delivery. *Journal of Biological Chemistry*, *289*(32), 22258–22267. doi:10.1074/jbc.M114.588046

Torregrosa Paredes, P., Gutzeit, C., Johansson, S., Admyre, C., Stenius, F., Alm, J., Scheynius, A., & Gabrielsson, S. (2014). Differences in exosome populations in human breast milk in relation to allergic sensitization and lifestyle. *Allergy*, *69*(4), 463–471. doi:10.1111/all.12357

van der Pol, E., Böing, A. N., Harrison, P., Sturk, A., & Nieuwland, R. (2012). Classification, functions, and clinical relevance of extracellular vesicles. *Pharmacological Reviews*, *64*(3), 676–705. doi:10.1124/pr.112.005983

van Herwijnen, M. J. C., Zonneveld, M. I., Goerdayal, S., Nolte-'t Hoen, E. N. M., Garssen, J., Stahl, B., Maarten Altelaar, A. F., Redegeld, F. A., & Wauben, M. H. M. (2016). Comprehensive proteomic analysis of human milk-derived extracellular vesicles unveils a novel functional proteome distinct from other milk components. *Molecular & Cellular Proteomics*, *15*(11), 3412–3423. doi:10.1074/mcp.M116.060426

Wang, X. (2017). Isolation of extracellular vesicles from breast milk. *Methods in Molecular Biology*, *1660*, 351–353. doi:10.1007/978-1-4939-7253-1_28

Yang, M., Song, D., Cao, X., Wu, R., Liu, B., Ye, W., Wu, J., & Yue, X. (2017). Comparative proteomic analysis of milk-derived exosomes in human and bovine colostrum and mature milk samples by iTRAQ-coupled LC-MS/MS. *Food*

Research International*, *92*, 17–25. doi:10.1016/j.foodres.
2016.11.041

Yolken, R. H., Peterson, J. A., Vonderfecht, S. L., Fouts, E. T.,
Midthun, K., & Newburg, D. S. (1992). Human milk mucin
inhibits rotavirus replication and prevents experimental
gastroenteritis. *Journal of Clinical Investigation*, *90*(5),
1984–1991. doi:10.1172/JCI116078

Zempleni, J., Aguilar-Lozano, A., Sadri, M., Sukreet, S.,
Manca, S., Wu, D., Zhou, F., & Mutai, E. (2017). Biological
activities of extracellular vesicles and their cargos from
bovine and human milk in humans and implications for
infants. *The Journal of Nutrition*, *147*(1), 3–10. doi:10.3945/
jn.116.238949

Zhou, Q., Li, M., Wang, X., Li, Q., Wang, T., Zhu, Q.,
Zhou, X., Wang, X., Gao, X., & Li, X. (2012). Immune-
related microRNAs are abundant in breast milk exosomes.
International Journal of Biological Sciences, *8*(1), 118–123.
doi:10.7150/ijbs.8.118

7. STUDY OF THE ANTIVIRAL ACTIVITY OF HUMAN MILK AGAINST EMERGING FLAVIVIRUSES

7.1 Emerging flaviviruses of interest

The section number 7 is mainly focused on two emerging flaviviruses, namely ZIKV and Usutu virus (USUV). ZIKV has been extensively described in section 2.1.

The less-known USUV has recently attracted the attention of the scientific community due its potential for emergence and its extensive spread in Europe. As ZIKV, USUV is an arbovirus of the *Flaviviridae* family and of the *Flavivirus* genu*s*. It is a member of the Japanese encephalitis serocomplex and is phylogenetically close to Japanese encephalitis virus (JEV) and West Nile virus (WNV). Its name derives from the Usutu River in Swaziland, in Southern Africa, where it was first identified in 1959 in mosquitos. USUV has been isolated from numerous mosquito species, but *Culex pipiens* mosquitos are considered the most common vectors (139).

Briefly, USUV is an enveloped virus of approximately 40–60 nm in diameter, with a single-stranded RNA of positive polarity (Figure 15). The genome of USUV comprises a single open reading frame coding for a polyprotein of 3434 amino acids that, after cleavage, generates to three structural proteins (capsid C, premembrane prM and envelope E) and eight non-structural proteins (NS1/NS1', NS2a, NS2b, NS3, NS4a, 2K, NS4b and NS5). The capsid protein (C) forms the central body of the virion and is associated with the viral RNA. The prM protein is required for virion assembly and maturation of virions through the folding of the envelope glycoprotein (E) that participates in various aspects of the viral cycle such as attachment and fusion to the cell membrane. The non-structural proteins (NS) of USUV are associated with the endoplasmic reticulum to form replication complexes in which NS5 ensures viral RNA replication by its RNA-dependent RNA polymerase activity.
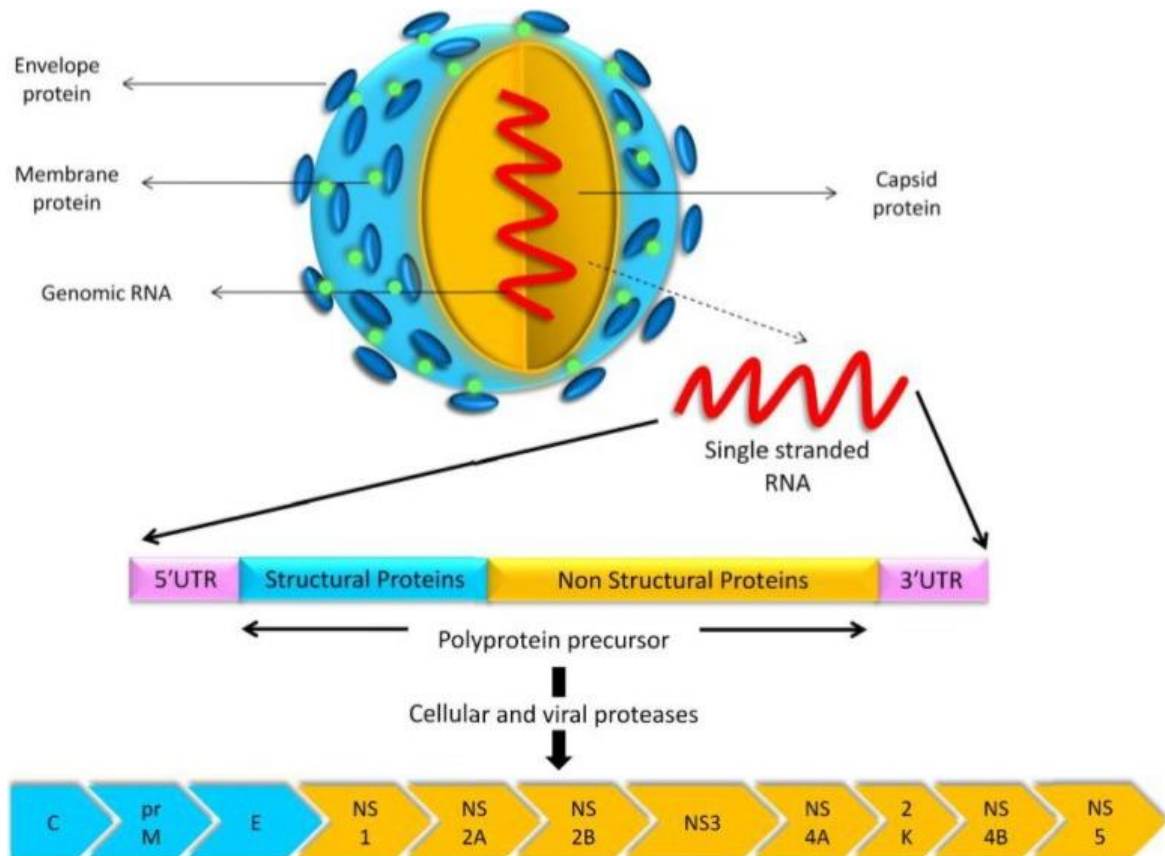
Figure 15. USUV model, its gene structure, and the proteins encoded by its genome. The polyprotein precursor is cleaved by cellular and viral proteases to yield three structural proteins (C, prM, and E) and eight non-structural proteins (NS1, NS2A, NS2B, NS3, NS4A, 2K, NS4B, and NS5) (139).

The early steps of USUV replicative cycle are not yet fully defined, but it has been demonstrated that different molecules play a role in flaviviruses attachment to cells. The most common attachment factors are negatively charged glycosaminoglycans (GAGs), which can be utilized by several flaviviruses, including DENV, WNV, JEV and tick-borne encephalitis virus (TBEV), as low-affinity attachment factors to concentrate the virus on cell surface. In addition, phosphatidylserine (PS) receptors' families, such as T-cell immunoglobulin (TIM) and TYRO3, AXL and MERTK (TAM), as well as integrins and C-type lectin receptors (CLRs), have been described as key factors during the initial steps of flavivirus cell invasion (140). As other flaviviruses, viral replication takes place in the cytoplasm of infected cells. The NS5 protein, which is highly conserved among USUV strains, has a methyltransferase domain required for the addition of the cap element at the 5′ end of the viral genomic RNA. Phylogenetic studies based on the nucleic acid sequence of the NS5 gene have shown that USUV strains isolated in different regions of the world can be divided into eight lineages: three African and five European, and that the level of genetic relatedness depends on their geographical origin and on the host from which they have been isolated (141). The strain of USUV employed in the study presented in section 7.3 belongs to one of the three African lineages.

The main USUV natural hosts are birds, with infection being reported to date in 93 different species. USUV is particularly pathogenic in a few species such as blackbirds (Turdus merula), gray owls (Strix nebulosa), and house sparrows (Passer domesticus). In these birds, the virus was detected in many organs such as the liver, heart, brain, and spleen and necrotic lesions were noted in these organs. Beyond infection of birds and humans, USUV has been detected in many mammalian species considered to be dead-end hosts. As is the case with WNV, horses are considered to be a sensitive host for USUV and it was also detected in bats, squirrels and rodents, in which the virus did not seem to cause the same severe pathogenicity as it does in birds. The expanding range of wild animals susceptible to USUV highlights its potential as an important emerging pathogen (142).

In humans, USUV infection (like WNV) is usually asymptomatic. Around 80 cases of subclinical infections have been described in blood donors or healthy patients in Italy, Serbia, the Netherlands, and Germany during the surveillance of WNV circulation. Nevertheless, seroprevalence studies suggested that USUV infections in humans may have been largely underestimated. Indeed, antibodies against USUV were detected in the blood of 0.01% to 1% of healthy blood donors in Germany and Italy, respectively. Higher seroprevalence was detected in serum samples collected from healthy individuals in Serbia (7.5%) and from forestry workers in Italy (18%). A large retrospective study, conducted on over 900 patients found a prevalence of 6.5% (142). Clinical disease with moderate flu-like (rash, fever, and headache) manifestations may also occur. The neurotropism of USUV represents a growing concern for human health. In more than 32 cases to date, indeed, severe neurological disorders, including facial paralysis, encephalitis, meningitis, and meningoencephalitis, in both immunocompromised and immunocompetent patients have been observed. However, the full clinical presentation of USUV infection needs to be better defined (142–144).

The increasing number of severe acute human cases, along with the avian mass mortality induced by this virus in Europe and numerous similarities with WNV biology and clinical manifestations, have prompted the improvement of surveillance programs and the development of experimental models to clarify the mechanisms underlying USUV pathogenesis and transmission (143,144).

No antivirals or vaccines are currently available against USUV virus. The only way to prevent this infection is to avoid mosquito bites.

7.2 Zika virus and Usutu virus in the context of breastfeeding

We studied ZIKV and USUV in the context of breastfeeding. As reported in Table II (section 5.2), previous reports have shown that some flaviviruses, such as DENV, WNV, YFV and ZIKV, can

occasionally be present in breast milk. Nevertheless, the transmission of flaviviruses through breastfeeding is still controversial. Human breastfeeding transmission was confirmed for only YFV and there was evidence of milk-related transmission of DENV, Powassan virus, WNV and ZIKV in animal studies (145–147). Probably due to the actual small number of human cases, the presence of USUV in breast milk is currently unknown, but its strong correlation with WNV suggests it could be possible.

With regard to ZIKV and more in details, ZIKV genome has been reported in breast milk from 3 to 33 days after maternal onset of fever and ZIKV infectious particles were also detected in this biofluid. The most recent systematic review on the topic, performed at the end of 2019 (148), concluded that human milk may be considered as a potentially infectious fluid. Nevertheless, the authors found no documented studies of the long-term complications in infants up to 32 months of age, with suspected, probable or confirmed ZIKV infection through human lactation, or evidence with respect to the human pathophysiology of the infection acquired through human lactation. The WHO recommends that mothers with possible or confirmed ZIKV infection continue to breastfeed, since the short and long-term health advantages of breastfeeding for both neonates and lactating mothers outweigh any potential risk of transmission.

Considering the reported evidence, we investigated the role of human milk in limiting ZIKV and USUV transmission from the mother to the child.

7.2.1 Publications

Francese R, Civra A, Donalisio M, Volpi N, Capitani F, Sottemano S, Tonetto P, Coscia A, Maiocco G, Moro GE, Bertino E, Lembo D. Anti-Zika virus and anti-Usutu virus activity of human milk and its components. PLoS Negl Trop Dis. 2020 Oct 7;14(10):e0008713. doi: 10.1371/journal.pntd.0008713. PMID: 33027261.

The present study was performed in close collaboration with the Neonatal Care Unit of Sant'Anna Hospital of Turin, directed by Prof. Enrico Bertino, that provided milk samples and with Prof.Volpi group of the University of Modena and Reggio Emilia, that isolated and characterized HM-glycosaminoglycans (GAGs). HM-EVs were, on the contrary, isolated and characterized directly in our Lab. The aim of this study was to explore the intrinsic protective role of human milk against the emerging ZIKV and USUV and to identify specific components contributing to this activity. We reported that human milk is endowed with anti-ZIKV and anti-USUV activity at all maturation stages and that it acts by altering virus attachment to the host cell. Furthermore, we indicated that this activity

is mediated, at least in part, by non-specific bioactive factors, including HM-EVs and HM-GAGs. Since the potential infectivity of human milk during ZIKV and USUV infection is still unclear, our data support the WHO recommendations about breastfeeding during ZIKV infection and could contribute to producing new guidelines for a possible USUV epidemic.

Anti-Zika virus and anti-Usutu virus activity of human milk and its components

**Rachele Francese[1], Andrea Civra[1], Manuela Donalisio[1], Nicola Volpi[2],
Federica Capitani[2], Stefano Sottemano[3], Paola Tonetto[3], Alessandra Coscia[3],
Giulia Maiocco[3], Guido E. Moro[4], Enrico Bertino[3], David Lembo[1]***

1 Department of Clinical and Biological Sciences, Laboratory of Molecular Virology and Antiviral Research, University of Turin, Orbassano (TO), Italy, **2** Department of Life Sciences, University of Modena and Reggio Emilia, Modena, Italy, **3** Department of Public Health and Pediatrics, Neonatal Intensive Care Unit, University of Turin, Turin, Italy, **4** Italian Association of Human Milk Banks (AIBLUD), Milan, Italy

* david.lembo@unito.it

Abstract

The benefits of human milk are mediated by multiple nutritional, trophic, and immunological components, able to promote infant's growth, maturation of its immature gut, and to confer protection against infections. Despite these widely recognized properties, breast-feeding represents an important mother-to-child transmission route of some viral infections. Different studies show that some flaviviruses can occasionally be detected in breast milk, but their transmission to the newborn is still controversial. The aim of this study is to investigate the antiviral activity of human milk (HM) in its different stages of maturation against two emerging flaviviruses, namely Zika virus (ZIKV) and Usutu virus (USUV) and to verify whether HM-derived extracellular vesicles (EVs) and glycosaminoglycans (GAGs) contribute to the milk protective effect.

Colostrum, transitional and mature milk samples were collected from 39 healthy donors. The aqueous fractions were tested *in vitro* with specific antiviral assays and EVs and GAGs were derived and characterized. HM showed antiviral activity against ZIKV and USUV at all the stages of lactation with no significant differences in the activity of colostrum, transitional or mature milk. Mechanism of action studies demonstrated that colostrum does not inactivate viral particles, but it hampers the binding of both flaviviruses to cells. We also demonstrated that HM-EVs and HM-GAGs contribute, at least in part, to the anti-ZIKV and anti-USUV action of HM.

This study discloses the intrinsic antiviral activity of HM against ZIKV and USUV and demonstrates the contribution of two bioactive components in mediating its protective effect. Since the potential infectivity of HM during ZIKV and USUV infection is still unclear, these data support the World Health Organization recommendations about breast-feeding during ZIKV infection and could contribute to producing new guidelines for a possible USUV epidemic.

Author summary

ZIKV and USUV are emerging flaviviruses that cause conditions ranging from mild febrile diseases to more sever outcomes. ZIKV is associated with microcephaly in newborns and USUV neurotropism represents a growing concern for human health. We studied these viruses in the context of breast-feeding. Breast-milk is a complex biofluid to nourish infants, support their growth and to protect them from numerous diseases, but it also represents a transmission route of several infections. It has been reported that flaviviruses can occasionally be detected in breast-milk, with limited information existing about their possible transmission through breast-feeding. We therefore explored the intrinsic protective role of human milk against ZIKV and USUV infections *in vitro* and we also assessed the contribution of specific components in mediating this activity. We demonstrated that human milk is endowed with anti-ZIKV and anti-USUV activity at all maturation stages and that it acts by altering virus attachment to the host cell. This activity is mostly due to non-specific bioactive factors, including extracellular vesicles and glycosaminoglycans. Our findings support the use of fresh milk (or from donor banks) as the food of choice for nutrition and protection of newborns in a possible context of ZIKV or USUV epidemics.

Introduction

Zika virus (ZIKV) and Usutu virus (USUV) are two emerging flaviviruses mostly transmitted by mosquitos. *Aedes aegypti* and *Culex pipiens* mosquitos are their major vectors respectively [1–3]. Most ZIKV and USUV infections are asymptomatic, but in symptomatic cases, they may cause conditions ranging from a mild febrile disease to more severe outcomes with neurological involvement.

ZIKV infection has been associated with the Guillain-Barré syndrome in adults and with a variety of neurological impairments, including microcephaly, in infants born to infected mothers [4,5]. It has caused a series of epidemics in the Americas, Asia and the Pacific in the past decade and it is now considered an important public health concern [6]. To date, 84 countries and territories have reported autochthonous transmission of ZIKV [7].

The less-known USUV has recently attracted the attention of the scientific community due its potential for emergence and its extensive spread in Europe [8,9]. It is phylogenetically closely related to West Nile virus (WNV) and it is maintained through an enzootic cycle between migratory birds and ornithophilic mosquitos, with humans representing incidental hosts [9]. Seroprevalence studies suggested that USUV infections in humans may have been largely underestimated, and many of them may be asymptomatic. The full clinical presentation of human severe USUV infection is still partially unknown, but cases of meningoencephalitis and facial paralysis have been reported and its neurotropism represents a growing concern for human health [10–12].

No antivirals or vaccines are currently available against either virus and the only way to prevent these infections is to avoid mosquito bites.

We studied ZIKV and USUV in the context of breastfeeding. Previous reports have shown that some flaviviruses, such as Dengue virus (DENV), WNV and Yellow fever virus (YFV), can occasionally be present in breast milk [13]. In particular, ZIKV RNA has been reported in breast milk from 3 to 33 days after maternal onset of fever and ZIKV infectious particles were also detected in this biofluid [14–18]. Nevertheless, this mode of transmission to the newborn is still controversial [19–25]. Probably due to the small number of human cases, the presence

of USUV in breast milk is currently unknown, but its strong correlation with WNV suggests it could be possible. Notwithstanding these evidences, the short and long-term health advantages of breastfeeding for both neonate and lactating mother outweigh any potential risk of transmission [26]. The World Health Organization (WHO) recommends indeed that mothers with possible or confirmed ZIKV infection continue to breastfeed [27].

Breast milk composition is extremely complex, individual-specific and variable according to the stage of lactation. It includes macro- and micronutrients and a wide variety of non-nutritional bioactive components [28]. Amongst the latter, secretory IgA (sIgA), toll-like receptors (TLRs), lactoferrin, lactadherin, oligosaccharides (HMOs) support the development of the immature immune system of the neonate and confer intrinsic protection against infections [29]. Therefore, HM is a possible source of viral infections, but these substances could directly affect viral infectivity. In the case of flaviviruses, DENV and Japanese encephalitis virus (JEV) are neutralized by the lipid fraction of breast milk and ZIKV and hepatitis C virus (HCV) are destroyed by free-fatty acids released upon storage by milk lipases in a time-dependent manner [30–33]. Herein, we aimed to explore the intrinsic anti-ZIKV and anti-USUV activity of human milk, according to its maturation stage and regardless of the storage affected-lipid fraction.

We also investigated the antiviral contribution of human milk-derived extracellular vesicles (HM-EVs) and human-milk glycosaminoglycans (HM-GAGs). Briefly, EVs are lipid enclosed vesicles, ranging from 30 to 1000 nm in diameter, that are released by most tissues including breast epithelial cells, macrophages and lymphocytes present in breast milk [34–36]. These vesicles can selectively be taken up by other cells, in which they release their molecular cargo (e.g. DNA, RNAs, enzymes, signalling proteins), playing a role in intercellular signalling, immune response, stem cell differentiation, tissue regeneration and viral replication [37,38]. GAGs are other abundant constituents of human milk defined as linear heteropolysaccharides composed of repeating disaccharidic units [39–41]. Detailed analyses performed on HM-GAGs demonstrated the presence of a complex mixture made up of chondroitin sulfate (CS)/dermatan sulfate (DS), heparan sulfate (HS)/heparin (Hep) and a minor percentage of hyaluronic acid (HA), with the CS/DS fraction being the most represented ($\sim$ 55%) followed by HS/Hep ($\sim$ 40%) [39].

HM-GAGs and HM-EVs have recently become the subject of increasing interest for their implication for infants [42,43]. HM-EVs have been demonstrated to be active *in vitro* against human immunodeficiency virus (HIV) [44] and HM-GAGs have also shown anti-bacterial and anti-viral activity due to their ability to act as soluble receptors inhibiting the attachment of different pathogens to the intestinal mucosa [45–47]. Both human milk constituents, have been poorly investigated for their antiviral action so far, therefore their role needs to be clarified.

Here we report that human milk is endowed with anti-ZIKV and anti-USUV activity at all maturation stages and that it acts by altering virus attachment to the host cell. This activity is mostly due to non-specific bioactive factors, including HM-EVs and HM-GAGs.

Methods

Ethic statement

An ethical review process was not required for this study since it was not a clinical trial. Each milk donor involved in this research signed a written consent form, where the mother's and infant's data protection was assured. Moreover, the donors were informed about the study design.

Human milk sample collection and clarification

Thirty-nine healthy mothers were enrolled in the study: 18 mothers donated as many colostrum samples (days 1–5 postpartum), 11 mothers donated colostrum, transitional (days 6–14 postpartum) and mature milk samples (beyond day 15 postpartum), and 10 mothers each donated 15 ml of mature milk that were added in a unique pool. All mothers were admitted to Sant'Anna Hospital (Città della Salute e della Scienza of Turin, Italy). The donors cleaned their hands and breasts according to the Italian HMB guidelines [48], and the milk samples were collected in sterile bisphenol-free polypropylene bottles using a breast pump and immediately stored at -20˚C unless otherwise stated. After thawing, the milk samples were centrifuged at a low speed (2000 x g) for 10 minutes at room temperature to remove the fat globule layer. The defatted milk was then transferred to a new tube and centrifuged at 12000 x g for 30 minutes to obtain the aqueous fraction. The supernatant was filtered through a syringe, equipped with a 0.45 μm pore size sterile filter (Sarstedt, Verona, Italy), to further eliminate any cells and cellular debris.

Cell lines

African green monkey fibroblastoid kidney cells (Vero) (ATCC CCL-81) were cultured in Eagle's minimal essential medium (MEM; Sigma, St. Louis, MO) supplemented with heat-inactivated, 10% (v/v) fetal bovine serum (FBS) (Sigma). The embryonic human kidney cells (293T) (ATCC CRL-3216) were grown as monolayer in Dulbecco's modified Eagle's medium (DMEM; Sigma) supplemented with 10% FBS and 1% Glutamax-I (Invitrogen, Carlsbad, CA) and low-passage-number (<30) human foreskin fibroblasts (HFF-1) (ATCC SCRC-1041) were grown as monolayers in DMEM supplemented with 15% FBS. The media were supplemented with 1% (v/v) antibiotic-antimycotic solution (Zell Shield, Minerva Biolabs, Berlin, Germany) and cells were grown at 37˚C in an atmosphere of 5% of CO_2.

The antiviral assays against ZIKV and USUV were performed on Vero cells using MEM supplemented with 2% of FBS, unless otherwise stated.

Viruses

Two strains of infectious Zika viruses (1947 Uganda MR766 and 2013 French Polynesia HPF2013) were generated by transfection of 293T cells with two plasmids (pCDNA6.2 Zika MR766 Intron3115 HDVr MEG 070916 5 and pCDNA6.2 Zika HPF2013 3864,9388Intron HDVr MEG091316 2) as previously described [49]. The viruses were then propagated in Vero cells and titrated by plaque assay. All the antiviral assays were performed with ZIKV HPF2013 strain, unless otherwise stated.

Usutu virus (Strain: 3345 Isolate: Arb276) was isolated and produced by APHA (Animal & Plant Health Agency–GOV. UK) and kindly provided by the European Viral Archive Global (EVAg). It was propagated in Vero cells and titrated by means of the indirect immunoperoxidase staining procedure, by using a mouse monoclonal antibody direct to flavivirus protein E (D1-4G2-4-15 (4G2), Novus Biological) and a secondary antibody peroxidase-conjugated AffiniPure F(ab')2 Fragment Goat Anti-Mouse IgG (H+L) (Jackson ImmunoResearch Laboratories Inc., 872 W. Baltimore Pike, West Grove, PA 19390).

Extracellular vesicles (EVs) isolation and characterization

Extracellular vesicles were extracted from the aqueous fraction of three colostrum samples before their freezing. The aqueous fraction was obtained as described above and subsequently incubated with 2:1 v/v ratio of colostrum:ExoQuick solution (System Biosciences, CA)

overnight at 4˚C. The extracellular vesicles were then purified, according to the manufacturer's instructions. The EV pellet was resuspended in 1 x PBS, quantified to establish the protein concentration using a protein assay kit (Bio-Rad Laboratories, Munich), aliquoted and stored at -80˚C until use.

The EV protein profile was analyzed by means of western blotting. HFF cell lysate was used to verify the reactivity of the anti-calnexin primary antibody. These cells were chosen as control since they are a reliable and highly standardized human cell line. A RIPA buffer, containing protease inhibitors, was added to the EV pellet, or to the HFF cells, for 10 minutes at RT to allow complete lysis. Soluble proteins were collected, by means of centrifugation at 15,000 $x\,g$, and were then quantified using a protein assay kit. The western blot was performed as previously described [50]. Primary antibodies: anti-CD63, anti-CD9, anti-CD81, anti-calnexin, anti-Hsp70 and anti-caveolin1; secondary antibodies: anti-rabbit and anti-mouse (System Biosciences).

A nanoparticle tracking analysis system (NTA) (NanoSight NS300, Malvern Instruments Ltd., UK) was used to determine particle size and particle concentration per milliliter at the ideal particle per frame value (63–65 particles/ frame).

Human milk glycosaminoglycans (HM-GAGs) isolation and characterization

50 mL of mature milk were defatted with acetone. After centrifugation at 10,000 g for 15 min and drying at 60˚C for 24 h, the pellet was solubilized in 200 mL of distilled water and treated with 100 mg of pancreatin (Sigma-Aldrich, code 1071301000, 350 FIP-U/g Protease, 6000 FIP-U/g Lipase, 7500 FIP-U/g Amylase) at 60˚C for 24 h in a stirrer. After boiling for 10 min and centrifugation at 5,000 g for 20 min, three volumes of ethanol were added to the supernatant and the mixture stored at 4˚C for 24 h. After centrifugation at 10,000 g for 15 min and dried at 60˚C for 6 h, the dried powder was dissolved in 100 ml of 50 mM NaCl and centrifuged at 10,000 g for 10 min. The supernatant was applied to a column (5 x 10 cm) packed with QAE Sephadex A-25 anion-exchange resin equilibrated with the same NaCl solution. GAGs were eluted with a linear gradient of NaCl from 50 mM to 2.0 M from 0 to 200 min using low-pressure liquid chromatography (Biologic LP chromatography system from BioRad) at a flow of 1 ml/min. Fractions positive to uronic acid assay were collected [51]. Three volumes of ethanol were added to the pooled fractions and stored at 4˚C for 24 h. The precipitate was centrifuged and dried at 60˚C. The dried purified HM-GAGs were dissolved in distilled water and lyophilized for the virus inhibition assay or further analysis.

For the antiviral assays, GAGs were dissolved in PBS and stocked at 4˚C until use.

HM-GAGs composition was evaluated by electrophoresis on acetate of cellulose [52]. The purity of the milk extract was evaluated by measuring the protein content by the Folin-Ciocalteu test (Sigma-Aldrich, code MAK365-1KT) and the GAGs content by the uronic acid assay [51].

Structural characterization of the CS/DS and HS/Hep components of HM-GAGs was performed by determining the corresponding constituent disaccharides. Briefly, HM-GAGs were treated with chondroitinase ABC or chondroitinase AC for 10 h at 37˚C in 50 mM Tris-Cl pH 8.0 to produce the CS/DS constituent disaccharides. HM-GAGs were also incubated with a cocktail of heparinases (heparinases I, II and III) in 0.1 M sodium acetate/calcium acetate pH 7.0 at 38˚C overnight to release the HS/Hep disaccharides. The unsaturated disaccharides produced were derivatized with 2-Aminoacridinone (AMAC) as previously described [39] and the fluorotagged disaccharides separated and analysed by capillary electrophoresis equipped with a Laser-Induced Fluorescence (LIF) detector [53]. By this analytical approach we also

determined the HA content besides the structural composition and charge density of the sulphated heteropolysaccharides CS/DS and HS/Hep.

Virus inhibition assay

The anti-ZIKV and anti-USUV activity of human milk (colostrum, transitional or mature milk) was determined by means of plaque reduction assay or focus reduction assay respectively.

Vero cells were seeded at a density of $6,5x10^4$ cells /well in 24 well plate for ZIKV antiviral assays or at a density of $1,3x10^4$/well in 96 well plate for USUV antiviral assays. The following day, cells were pre-treated with serial dilutions of human milk aqueous fraction (from 1:3 to 1:6561 parts) for 1h at 37°C. The virus was pre-treated under the same experimental conditions simultaneously: mixtures of serial dilutions of human milk and the same amount of virus were incubated for 1 h at 37°C at multiplicities of infection (MOIs) of 0.0005 PFU/cell for ZIKV and 0.02 FFU/cell for USUV. After a gentle wash, these mixtures were added to cells for 2h at 37°C. Subsequently, the ZIKV infected cells were washed twice with warm medium and overlaid with a 1.2% methylcellulose medium for 72 h at 37°C. In the case of USUV, infected cells were washed twice and overlaid with fresh medium for 24h at 37°C.

The number of ZIKV plaques were counted after cell fixation and staining with a solution of 0.1% crystal violet in 20% ethanol. The USUV-infected cells were detected by means of indirect immunostaining as described above. The inhibitive dilution that produced a 50% reduction of ZIKV or USUV infection (ID_{50}) was determined by comparing the treated with the untreated wells. GraphPAD Prism 8.0 software (San Diego, CA) was used to fit a variable slope-sigmoidal dose-response curve and calculate the ID_{50} values.

Viability assay

Cell viability was measured using the MTS [3-(4,5-dimethylthia-zol-2-yl)-5-(3-carboxymethox-yphenyl)-2-(4-sulfophenyl)-2H-tetra-zolium] assay. Confluent Vero cells were treated with serial dilutions of colostrum or HM-EVs or HM-GAGs under the same experimental conditions of the virus inhibition assay. Cell viability was determined using the Cell Titer 96 Proliferation Assay Kit (Promega, Madison, WI, USA) according to the manufacturer's instructions. Absorbances were measured using a Microplate Reader (Model680, BIORAD) at 490 nm. The effect on cell viability at different dilutions of colostrum was expressed as a percentage, by comparing absorbances of treated cells with those of cells incubated with culture medium alone. The 50% cytotoxic concentrations (CC_{50}) was determined using Prism software.

Immunofluorescence assay

Subconfluent Vero cells plated on coverslips in 24-well plates were treated with colostrum (ID_{90}) following the virus inhibition assay protocol. The infection was performed with MOI of 3 for both viruses. After 30 h or 24 h for ZIKV or USUV infected cells respectively, cells were washed twice with PBS and then fixed in 4% PAF for 15 min RT. Cells were permeabilized in PBS with Triton 0,1% for 20 minutes on ice and then blocked with 5% BSA for 30 minutes. Next the incubation with the primary antibody (Anti-dsRNA mAb, SCICONS J5 or anti-flavivirus protein E mAb D1-4G2-4-15 (4G2), Novus Biological) diluted in blocking buffer was performed for 1 h RT. After three washes in PBS with 0.05% Tween 20, the secondary antibody (Goat Anti-Mouse IgG Rhodamine conjugated, Santa Cruz Biotechnology) diluted in blocking buffer was added to cells for 1 h RT. Subsequently, three washes with PBS were performed and coverslips were mounted and analyzed on a confocal fluorescence microscope (LSM510, Carl Zeiss, Jena, Germany).

Virus inactivation assay

Approximately 10^6 FFU of ZIKV or USUV were incubated with 100 µl of colostrum for 2h at 37˚C. As control, the same number of viral particles was incubated with fresh medium. After the incubation, both treated and untreated viruses were titrated to the non-inhibitory dilution of colostrum. The residual viral infectivity was determined by plaque assay (ZIKV) or by indirect immunostaining (USUV). Statistical analysis was performed using Student's t-test. Significance was reported for p-values <0.05.

Pre-treatment assay

Confluent Vero cell monolayers in 24 well plate (for ZIKV test) or in 96 well plate (for USUV test) were pre-treated with serial dilutions of colostrum (from 1:3 to 1:6561) for 2 h at 37˚C. After washing, cells were infected with ZIKV (MOI = 0.0005) or USUV (MOI = 0.02) for 2h 37˚C. The viral inoculum was then removed and two gentle washes were performed. The ZIKV infected cells were overlaid with 1.2% methylcellulose medium for 72 h at 37˚C and the USUV infected cells were incubated with fresh medium for 24 h at 37˚C. At the end of the incubation cells were fixed and stained with 0.1% crystal violet in 20% ethanol to count the number of ZIKV plaques or fixed and stained with indirect immunostaining to evaluate the number of USUV infected cells.

Where possible, the ID_{50} values were calculated by means of a regression analysis, using dose–response curves generated by GraphPad Prism version 8.0.

Binding assay

Vero cells were seeded in 24 well plate at a density of $1.1x10^5$ cells/well. The following day, cells and viruses (ZIKV or USUV, MOI = 3) were cooled to 4˚C for 10 minutes. The viruses were then allowed to attach to the cells in the presence of colostrum (ID_{90}). After an incubation of 2 h on ice, the cells were washed with a cold medium to remove any unbound virus. The cells were then subjected to three rounds of freeze-thawing to release any bound virus, and the lysate was clarified by means of low speed centrifugation for 10 minutes. The cell-bound virus titers were determined by means of plaque assay (ZIKV) or indirect immunostaining (USUV), as outlined above. The presence of any significant differences was assessed by means of Student's t-test, using PRISM 8.0 GraphPad Software.

Entry assay

The Vero cells were cultured to confluence in 24-well or 96-well trays. ZIKV (MOI = 0.005) and USUV (MOI = 0.2), which had been cooled to 4˚C, were allowed to attach to pre-chilled cells on ice for 2 h at 4˚C. Unbound viruses were then washed, serial dilutions of colostrum (from 1:3 to 1: 6561) were added to cells and the plates were incubated at 37 ˚C to allow virus entry. After the viral entry, the treatment was aspirated and viral particles still present on the cell surface were inactivated by a wash with citrate buffer (citric acid 40 mM, potassium chloride 10 mM, sodium chloride 135 mM, pH 3) for 1 minute at room temperature, as previously described [49]. Cells were then washed with warm medium 3 times and overlaid with 1.2% methycellulose medium (ZIKV entry assay) for 72h or with fresh medium (USUV entry assay) for 24h. Cells were fixed and stained with 0.1% crystal violet in 20% ethanol to count the number of ZIKV plaques or fixed and stained with the indirect immunostaining procedure to evaluate the number of USUV infected cells. The viral entry blockade was determined and expressed as the mean percentage of the untreated control ± SEM. Where possible, the ID_{50} values were calculated by means of regression analysis using dose–response curves (GraphPad Prism 8.0)

Post-entry assay

Vero cells were seeded in 96-well plates at a density of 1.3×10^4 cells/well. The following day, the viral inoculum (ZIKV at MOI = 0.005 or USUV at MOI = 0.2) was added to cells for 2 h at 37˚C. The unpenetrated viruses were inactivated with citrate buffer for 1 minute at room temperature and cells were then washed with warm medium 3 times and incubated with serial dilutions of colostrum (from 1:3 to 1:6561) for 3 h at 37˚C. Finally, after 2 gentle washes, Vero cells were incubated with warm MEM for 30 h (ZIKV) or 24 h (USUV) at 37˚C. The number of infected cells was determined by indirect immunostaining and the viral inhibition expressed as the mean percentage of the untreated control ± SEM. Where possible, the ID_{50} values were calculated by means of regression analysis using dose–response curves (GraphPad Prism 8.0)

Evaluation of HM-EVs and HM-GAGs antiviral activity: virus inhibition assay

The antiviral activity of colostrum-derived EVs and of HM-GAGs was evaluated by means of the same experimental protocol described under the "virus inhibition assay" subheading. The anti-ZIKV and anti-USUV activity of HM-EVs and HM-GAGs was determined by means of plaque reduction assay (ZIKV) or focus reduction assay (USUV). Vero cells were seeded at a density of $6,5 \times 10^4$ cells /well in 24 well plate for ZIKV antiviral assays or at a density of $1,3 \times 10^4$/well in 96 well plate for USUV antiviral assays. The following day, cells were pre-treated with serial dilutions of HM-EVs (from 423 μg/ml to 0.19 μg/ml) or with dilutions of HM-GAGs (from 10 mg/ml to 0.1 mg/ml) for 1 h at 37˚C. The viruses were pre-treated under the same experimental conditions simultaneously: mixtures of serial dilutions HM-EVs or HM-GAGs and the same amount of virus (MOI of 0.0005 PFU/cell for ZIKV and 0.02 FFU/cell for USUV) were incubated for 1 h at 37˚C. After a gentle wash, these mixtures were added to cells for 2h at 37˚C. Subsequently, the ZIKV infected cells were washed twice with warm medium and overlaid with a 1.2% methylcellulose medium for 72 h at 37˚C. In the case of USUV, infected cells were washed twice and overlaid with fresh medium for 24h at 37˚C. The number of ZIKV plaques were counted after cell fixation and staining with a solution of 0.1% crystal violet in 20% ethanol. The USUV-infected cells were detected by means of indirect immunostaining. The effective concentration that produced a 50% reduction of ZIKV or USUV infection (EC_{50}) was determined by comparing the treated with the untreated wells. GraphPAD Prism 8.0 software was used to fit a variable slope-sigmoidal dose-response curve and calculate the EC_{50} values.

Data analysis

All the results are presented as the mean values of two independent experiments. The ID_{50} values of the inhibition curves were calculated from a regression analysis using GraphPad Prism software, version 8.0 (GraphPad Software, San Diego, California, the U.S.A.) by fitting a variable slope-sigmoidal dose-response curve. Statistical analysis was performed using Student's t-test, ANOVA Analysis of variance or the F-test, as reported in the Figure legends.

Results

Human milk is endowed with an intrinsic anti-ZIKV and anti-USUV activity

The first set of experiments was performed in order to investigate the intrinsic antiviral activity of human colostrum against ZIKV and USUV. Colostrum samples were collected from healthy donor mothers admitted to Sant'Anna Hospital of Turin for term or preterm delivery (Table 1).

Table 1. Main clinical characteristics of the first study group.

Sample n°	Gestational Age	Mother's Age	Parity	Type of delivery
1	35+0	39	2002	CS
2	32+1	33	0000	CS
3	29+1	32	0000	CS
4	39+4	33	1001	CS
5	29+5	38	0000	S
6	38+5	40	0000	CS
7	33+2	35	0000	CS
8	27+3	43	1001	CS
9	30+0	30	1001	CS
10	37+4	35	0000	CS
11	38+4	39	1021	S
12	38+2	39	1001	S
13	38+4	37	0000	S
14	34+1	30	1001	S
15	37+4	23	0000	S
16	38+2	42	0000	CS
F1	40+1	32	0000	S
F2	33+3	39	1001	S

S: spontaneous delivery; CS: cesarean section; F1, F2: Fresh colostrum samples.

The aqueous fraction of these samples was selected as preferred biological matrix, due to its previously described lower impact on cell viability [54], and tested *in vitro* against ZIKV (HPF2013) and USUV. Briefly, cells and viruses were treated with serial dilutions of human colostrum before and during the infection. As reported in Fig 1A and S1 Table, all colostrum
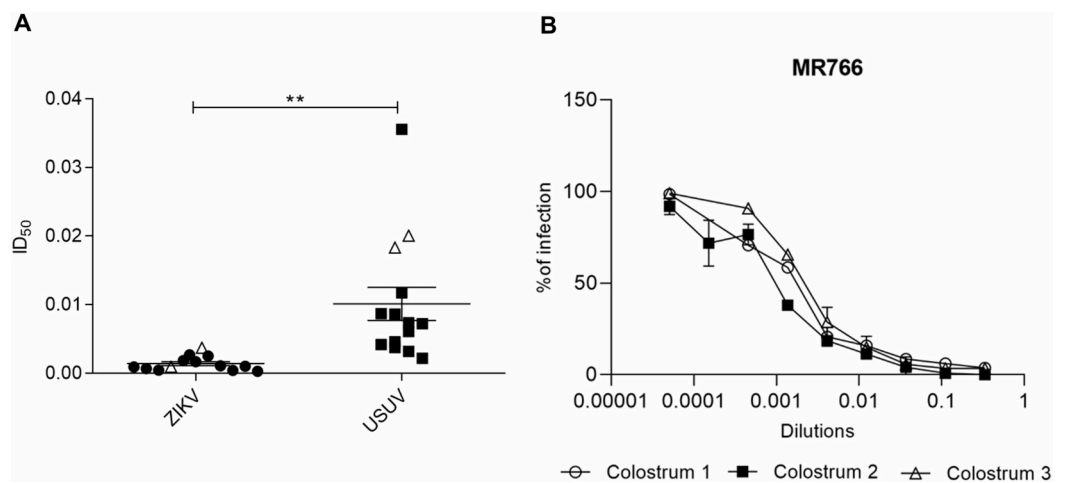

Fig 1. Anti-ZIKV and anti-USUV activities of defatted colostrum samples. Cells and viruses were treated before and during the infection with serial dilutions of human colostrum aqueous fraction (from 1:3 to 1:6561 parts). (A) Anti-ZIKV and anti-USUV inhibitory dilution-50 values obtained from three independent experiments are reported. Results are expressed as mean ± SEM of inhibitory dilution-50 values (Student's t test; ** $p < 0.01$). Results obtained with fresh colostra are indicated with white triangles. (B) Panel B shows the anti-ZIKV activity of three colostrum samples against the African MR766 strain. The dose-response curves are reported. Data are presented as % of control. Values are means ± SEM of three independent experiments performed in duplicate.

samples exhibited antiviral activity against both viruses although to a different extent from mother to mother. The ID_{50s} were ranging from 0.0003 to 0.0026 for ZIKV and from 0.0022 to 0.0355 for USUV indicating that human colostrum is significantly more active against ZIKV. The ID_{50s} obtained with fresh colostra, i.e. with colostra that were clarified and tested *in vitro* within 1 hour after collection, are comparable to those obtained from frozen samples (S1 Fig). Since an incomplete gestational period can affect the maturity of the mammary gland and its ability to secrete milk with the proper composition for the newborn's condition, we stratified the results comparing the antiviral activity of human colostrum from term and preterm mothers, but no significant difference was observed for both viruses (S2 Fig). Furthermore, the antiviral activity of human colostrum against different ZIKV strains was verified by testing 3 colostrum samples against ZIKV MR766 belonging to the African lineage. As shown in Fig 1B, the human colostrum inhibits the MR766 infectivity too, with $ID_{50}s$ comparable to those obtained with the microcephalic HPF2013 strain ($ID_{50\ Colostrum1} = 0.0012$; $ID_{50\ Colostrum2} = 0.0009$; $ID_{50\ Colostrum3} = 0.0023$).

To further confirm the antiviral action of human colostrum against ZIKV and USUV, immunofluorescence experiments detecting the dsRNA (an intermediate in flavivirus replication) and the flavivirus protein E were performed. As shown in Fig 2A and 2B, the synthesis of the dsRNA and the production of the protein E are significantly inhibited by colostrum for both viruses. The same results were obtained with the MR766 ZIKV strain (S3 Fig).

Moreover, in order to exclude the possibility that the observed antiviral action was due to a cytotoxic effect, viability assays were performed by treating cells with human colostrum under the same experimental conditions of the virus inhibition assay described above. As expected, results indicated that colostrum aqueous fraction is not toxic for cells even at the lowest tested dilution (0.33). Results obtained with 3 randomly selected colostrum samples are reported in Fig 3.

Altogether, these results demonstrated that the aqueous fraction of human colostrum is intrinsically endowed with antiviral activity against two emerging flaviviruses without being toxic for cells *in vitro*.

Subsequently, we investigated the variations in the anti-ZIKV and anti-USUV activity of HM according to the different stages of lactation. To this aim, eleven mothers (Table 2) donated samples of colostrum, transitional and mature milk each.

First, the absence of cytotoxicity was verified for transitional and mature milk too (S4 Fig). The virus inhibition assays revealed that all samples exhibit net anti-ZIKV (Fig 4A) and anti-USUV activity (Fig 4B). Within each stage of lactation, milk samples exhibited a wide range of $ID_{50}s$ against both viruses, with mature milk showing the greatest variation. In the anti-ZIKV assays, the ID_{50} values ranged from 0.0004 to 0.004 in colostrum, from 0.0006 to 0.005 in transitional milk and from 0.0003 to 0.007 in mature milk (S2 Table). In the case of USUV, the ID_{50} values ranged from 0.002 to 0.01 in colostrum, from 0.001 to 0.007 in transitional milk and from 0.002 to 0.02 in mature milk (S3 Table). The mean antiviral activity of milk samples appeared to differ according to the stages of lactation with colostrum and transitional milk showing lower mean ID_{50} values than mature milk, but the difference did not reach statistical significance. These results also indicated that human milk is overall more active against ZIKV, confirming what previously demonstrated with colostrum samples and described above. In S5A and S5B Fig, the results obtained from every single mother are separately reported.

Human colostrum alters the binding of ZIKV and USUV to cells

The second goal of this study is to investigate which step of ZIKV and USUV replicative cycle is inhibited by HM. Colostrum was selected for the execution of these tests due to the overall
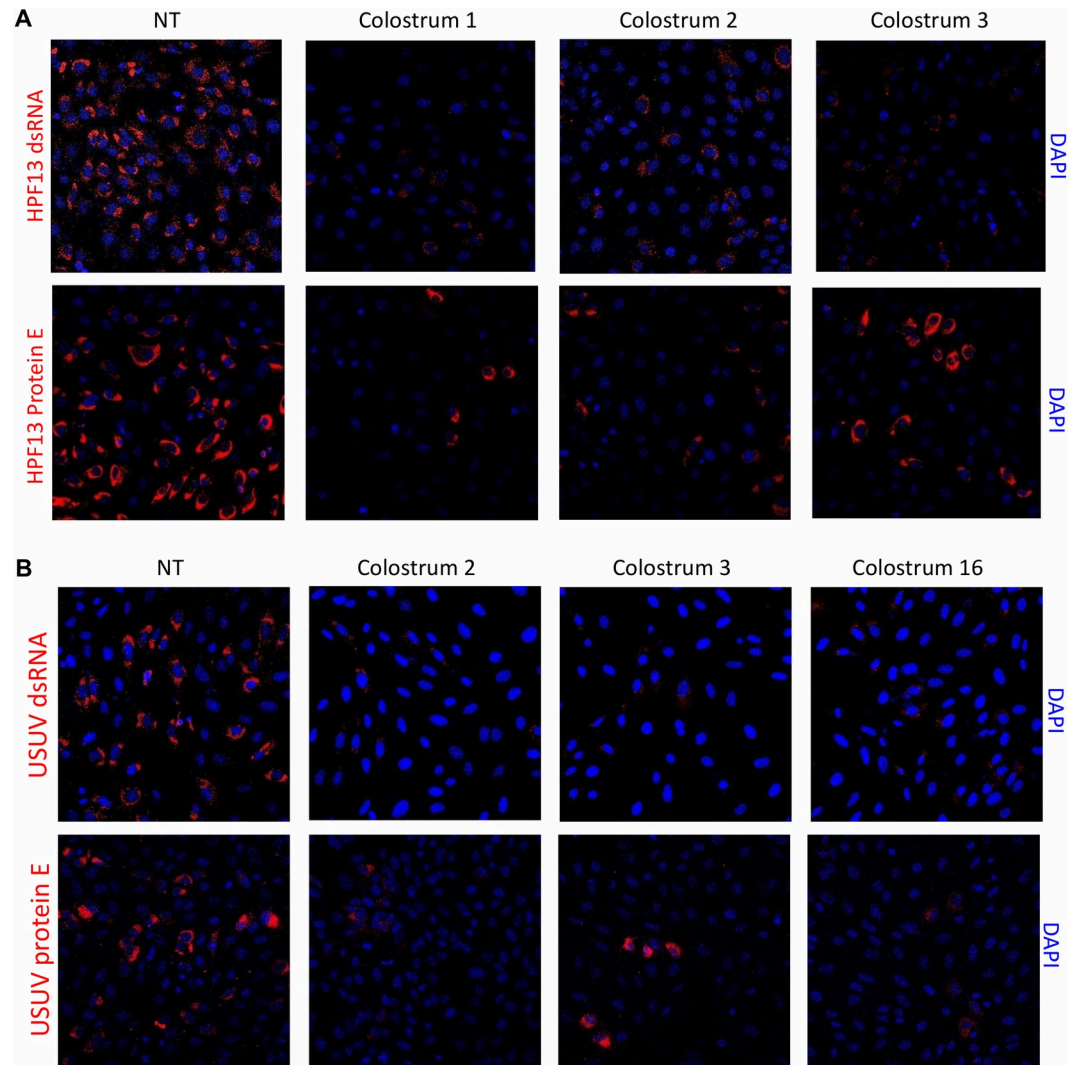
Fig 2. Evaluation of the anti-ZIKV (A) and anti-USUV (B) activity of human colostrum with the immunofluorescence assay detecting the dsRNA intermediate of replication and the flavivirus protein E. Cells and viruses (MOI = 3) were treated before and during the infection with the dilution of colostrum corresponding the ID_{90} in the virus inhibition assay. After 30 h of infection, cells were fixed and subjected to immunofluorescence.

https://doi.org/10.1371/journal.pntd.0008713.g002

lower mean ID_{50} values compared to transitional and mature milk. Three samples of colostrum were randomly selected from the initial screening group for both viruses. First, we investigated whether the aqueous fraction of colostrum is endowed with an intrinsic virucidal activity, i.e. whether colostrum acts by directly inactivating the viral particle. As reported in Fig 5, we did not observe any significant virucidal activity for both viruses.

The pre-treatment of cells with serial dilutions of colostrum for 2 h before infection did not alter ZIKV and USUV infectivity, thus indicating that colostrum does not act directly on cells preventing viral infection (Fig 6).

Subsequently, the early steps of viral replication, i.e. the binding and the entry steps, were evaluated: the treatment with the aqueous fraction of colostrum was performed during the attachment of the virus to cells or during the cell-penetration processes. Results demonstrated that human colostrum does not alter the entry of viruses into cells (Fig 7C and 7D), but it acts by preventing the binding of both viruses to cells. In fact, as reported in Fig 7A and 7B, the
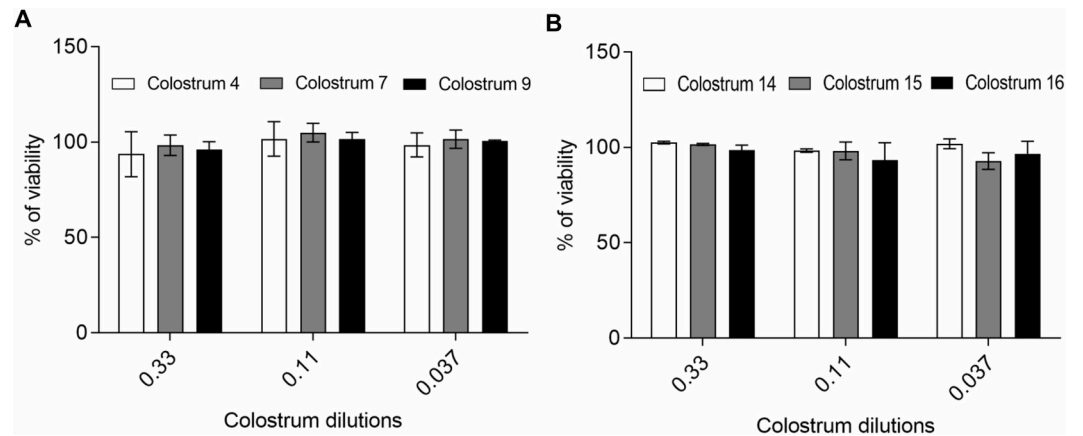
Fig 3. Evaluation of cell viability after colostrum treatment. Cells were treated under the same conditions of the ZIKV (A) and USUV (B) inhibition assay. Results obtained from 3 randomly selected colostrum samples are reported and indicated as % of untreated control. Values are means ± SEM of three independent experiments performed in duplicate.

https://doi.org/10.1371/journal.pntd.0008713.g003

titer of bound ZIKV and USUV to cells is significantly reduced in presence of colostrum. The reduction of ZIKV and USUV titer resulted in more than one order of magnitude between the treated and the untreated samples and was confirmed for all the tested colostrum samples (numerical results are reported in S4 Table).

Lastly, we verified the absence of any additional activity on the later steps of viral replication. When cells were treated with colostrum dilutions after ZIKV or USUV infection for three hours, no reduction in the number of infected cells was observed (Fig 8).

Anti-ZIKV and anti-USUV components of HM: the HM-EVs and the HM-GAGs

Prompted by the above findings, we sought to identify new antiviral components of human milk that could contribute to the antiviral potency of this biofluid. To this aim EVs and GAGs were isolated and characterized.

Colostrum was selected as preferred lactation stage for EVs isolation, due to the previously reported higher concentration of EV in colostrum than transitional and mature milk [34].

Table 2. Main clinical characteristics of the second study group.

Sample n°	Gestational Age	Mother's Age	Parity	Type of delivery
17	41+2	28	0000	CS
18	39+4	26	0000	S
19	39+6	33	1011	CS
20	39+4	30	0010	S
21	40+3	40	1001+1 VTP	S
22	37+1	33	1001	S
23	39+4	34	0000	S
24	38+5	40	1001	S
25	38+2	43	1001	CS
26	40+0	33	2002	S
27	40+4	41	0000	CS

S: spontaneous delivery; CS: cesarean section; VTP: voluntary termination of pregnancy

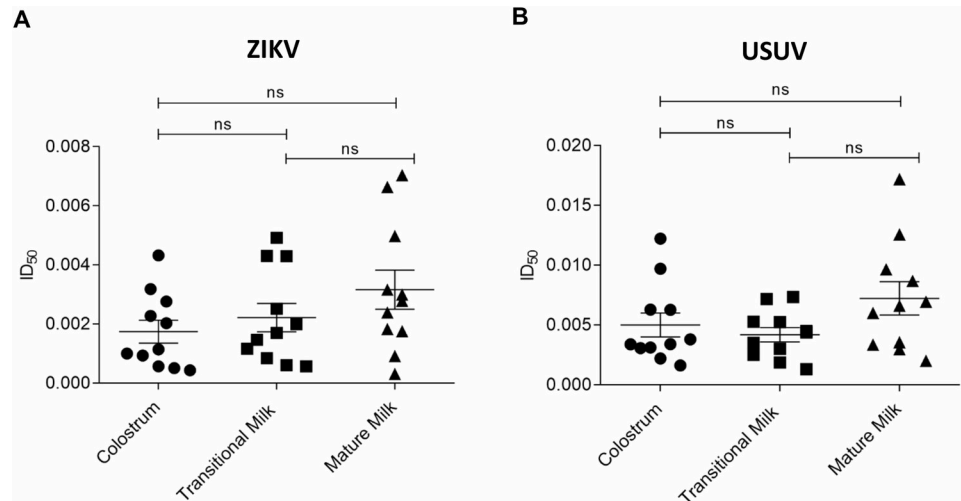https://doi.org/10.1371/journal.pntd.0008713.t002

Fig 4. Anti-ZIKV (A) and anti-USUV (B) activity of defatted human milk samples at different stages of maturation. Cells and viruses were treated before and during the infection with serial dilutions of human milk aqueous fraction (from 1:3 to 1:6561 parts). The inhibitory dilution-50 values for colostrum, transitional milk and mature milk from a cohort of eleven mothers are reported. Results are expressed as mean ± SEM and analyzed by ANOVA followed by Bonferroni post hoc test.

https://doi.org/10.1371/journal.pntd.0008713.g004

The colostrum-derived EVs were characterized according to the "Minimal Information for Studies of Extracellular Vesicles guidelines" (MISEV2018) proposed by the International Society for Extracellular Vesicles (ISEV) [55]. As reported in Fig 9A, the EV-lysate was positive for the three tetraspanines CD63, CD9 and CD81, which are known to be enriched in EVs from multiple tissue sources, and it was positive for two cytosolic proteins (caveolin-1 and HSP70) usually recovered in EVs. Furthermore, the colostrum-derived EV lysate was negative for the contaminating endoplasmatic reticulum-related protein calnexin. We analyzed EV size and concentration by means of the nanoparticle tracking analysis. The NanoSight instrument showed that most EVs were between 100–400 nm in diameter: EVs had a mean diameter of
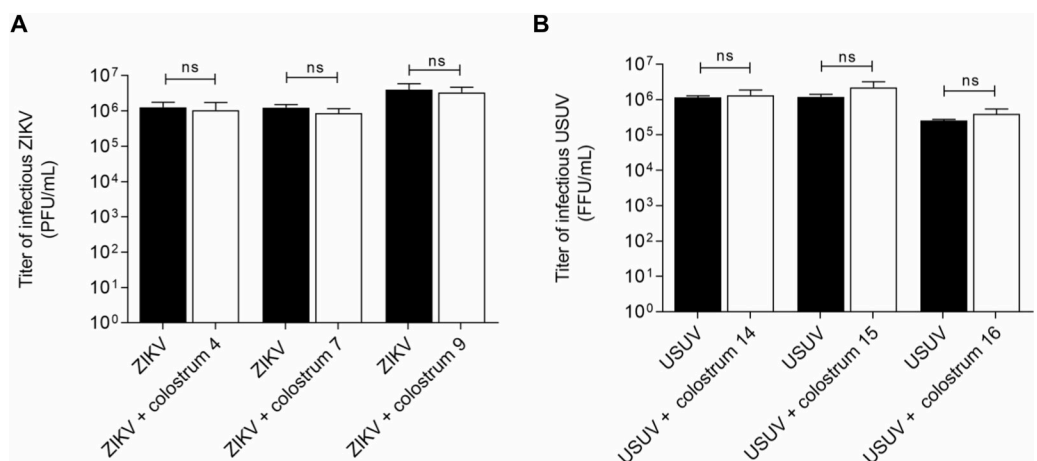
Fig 5. Evaluation of ZIKV (A) and USUV (B) inactivation by human colostrum aqueous fraction. Viruses were incubated with colostrum for 2h at 37°C and subsequently the residual viral infectivity was evaluated. On the y-axis, the infectious titers are expressed as plaque-forming units per ml (PFU/ml) (A) or focus-forming unit per ml (FFU/mL) (B). Error bars represent standard error of the mean of three independent experiments (Student's t test; ns: not significant).

https://doi.org/10.1371/journal.pntd.0008713.g005

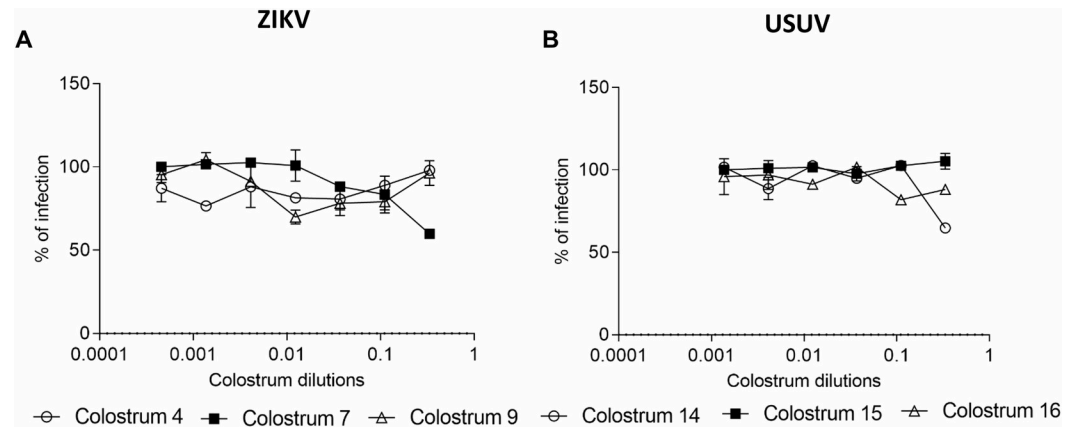**Fig 6. Pre-treatment assay.** Cells were pre-treated with serial dilutions of colostrum for two hours before infection. After washing, cells were infected with ZIKV (A) or USUV (B) and the number of ZIKV plaques or USUV foci was evaluated after 72 or 24 hours respectively. The dose-response curves are reported. Data are presented as % of control. Values are means ± SEM of three independent experiments performed in duplicate.

https://doi.org/10.1371/journal.pntd.0008713.g006

250.0 +/- 8.0 nm (EVs 6), 191.7 +/- 1.5 nm (EVs 7) and 200.3 +/- 2.9 nm (EVs 8) (Mode: 199.4 +/- 16.0 nm, 130.5 +/- 7.9 nm, 137.5 +/- 14.6 nm for sample 6, 7 and 8 respectively). Particle concentration was 7.55×10^{12} (EVs 6), 7.02×10^{12} (EVs 7) and 9.33×10^{12} (EVs 8) particles/ml. A representative analysis is reported in Fig 9B (S6 Fig reports the NTA analysis of EVs 6 and EVs 8).

After the characterization, EVs were tested *in vitro* against ZIKV and USUV. The results (Fig 9C and 9D) demonstrated that colostrum-derived EVs are endowed with a strong antiviral activity against both viruses. Notably, the EC_{50} values of the 3 EV populations were 11.47, 7.04 and 16.22 μg protein/ml for ZIKV and 11.61, 12.33 and 32.57 μg protein/ml for USUV.

Next, the antiviral potency of GAGs isolated from a pool of mature milk samples was evaluated *in vitro*. Mature milk was selected as preferred biological matrix because is more commonly available than colostrum. According to previous studies [39,40,56], the HM-GAGs fraction tested in this study was mainly composed of CS/DS and HS/Hep as evident from the electrophoresis (Fig 10A). Moreover, from the structural characterization analysis (confirmed by the electrophoresis), we obtained a percentage of ~55% CS and 1–2% DS, ~40% HS/low-sulfated Hep (known as fast-moving Hep) and ~2% high-sulfated Hep (known as slow-moving Hep), and trace amount (1–2%) of HA. Additionally, the HM-CS was confirmed to have a very typical low charge density (~0.35) compared to the other known CS [57]. Finally, the purified HM-GAGs were tested to have a purity greater than 98%.

Results from the antiviral assays revealed that HM-GAGs are active against ZIKV and USUV in the range of physiological concentrations detected in term and preterm human colostrum [42] (Fig 10B). The EC_{50} values were 5.8 mg/ml for ZIKV and 3.3 mg/ml for USUV with the higher concentration tested (10 mg/ml) able to completely inhibit USUV infection and to inhibit the 70% of ZIKV infection.

Both EVs samples and HM-GAGs did not show any cytotoxicity (S7 Fig).

Altogether these results demonstrated that colostrum derived EVs and HM-GAGs contribute, at least in part, to the anti-ZIKV and anti-USUV intrinsic action of human milk.

Discussion and conclusion

While the antiviral activity of HM and its components against numerous viral pathogens have been described in literature, its role in protecting against emerging arboviruses has been poorly
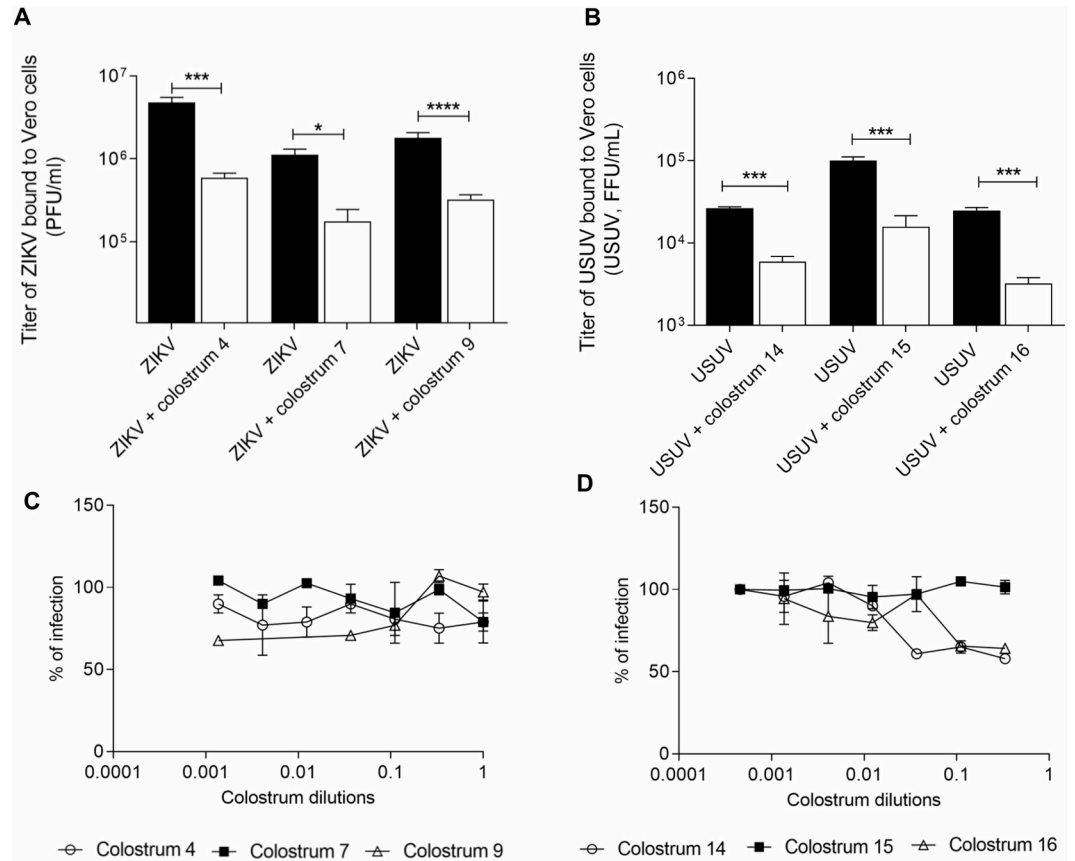
Fig 7. Binding assay (A, B) and entry assay (C, D). ZIKV (A) or USUV (B) (MOI = 3) were allowed to attach to the cells in presence of colostrum (ID$_{90}$) for 2h on ice. The cell-bound virus titers were determined by means of plaque assay (ZIKV) or indirect immunostaining (USUV). On the y-axis, the infectious titers are expressed as plaque-forming units per ml (PFU/ml) (A) or focus-forming unit per ml (FFU/mL) (B). Error bars represent standard error of the mean of three independent experiments (Student's t test; * $p < 0.05$; *** $p < 0.001$; ****$p < 0.0001$); For the entry assay, ZIKV (C) or USUV (D) were absorbed for 2 h at 4°C on pre-chilled Vero cells. After the removal of the unbound virus, the temperature was shifted to 37°C to allow the entry of pre-bound virus in presence of serial dilutions of colostrum for 2h. Unpenetrated virus was inactivated with citrate buffer and the number of ZIKV plaques or the number of USUV foci was evaluated after 72 h or 24 h respectively. The dose-response curves are reported. Data are presented as % of control. Values are means ± SEM of three independent experiments performed in duplicate.

https://doi.org/10.1371/journal.pntd.0008713.g007

investigated so far [25,58,59]. In this study we addressed this issue focusing on two emerging flaviviruses: we assessed the anti-ZIKV and the anti-USUV activity of human milk in its different stages of maturation and we explored the antiviral contribution of specific components, namely the HM-EVs and the HM-GAGs.

The first notable finding is that HM is endowed with antiviral activity against ZIKV and USUV in all the stages of lactation (colostrum, transitional and mature milk) with no significant differences between them. We previously reported a different pattern in the anti-CMV activity of human milk [54]: we demonstrated that colostrum from CMV-IgG+ mothers was significantly more potent than transitional and mature milk and this was due to the higher content of specific immune factors, especially sIgA, in the early stages of lactation. On the contrary, the presence of specific immunoglobulins in the milk samples of the present study is very unlikely, considering the absence of a past travel history in ZIKV endemic areas of the donor mothers and the low seroprevalence of USUV in Europe [11]. The anti-ZIKV and anti-USUV action is attributable to non-specific bioactive factors that act independently from the
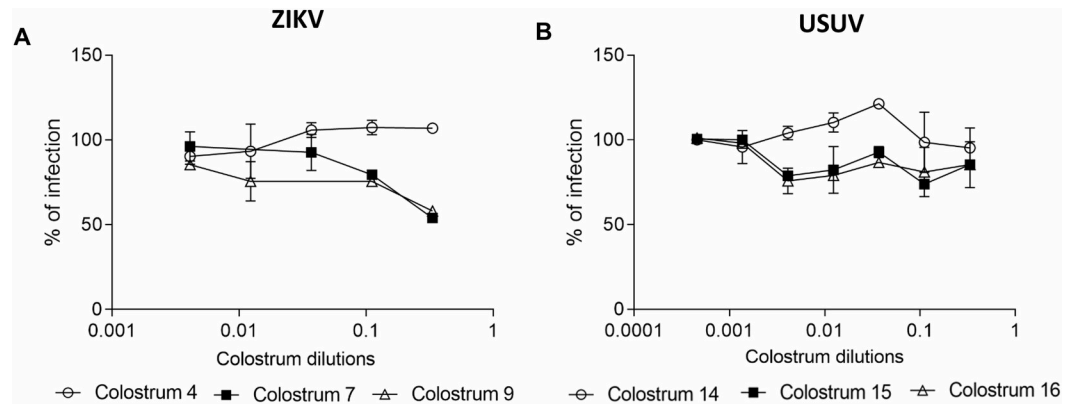
Fig 8. Post-entry assay. Cells were infected with ZIKV (A) or USUV (B) for 2 h at 37˚C. After washing with citrate buffer, cells were treated with serial dilutions of colostrum for 3 h. The number of ZIKV plaques or USUV foci was evaluated after 72 or 24 hours respectively. The dose-response curves are reported. Data are presented as % of control. Values are means ± SEM of three independent experiments performed in duplicate.
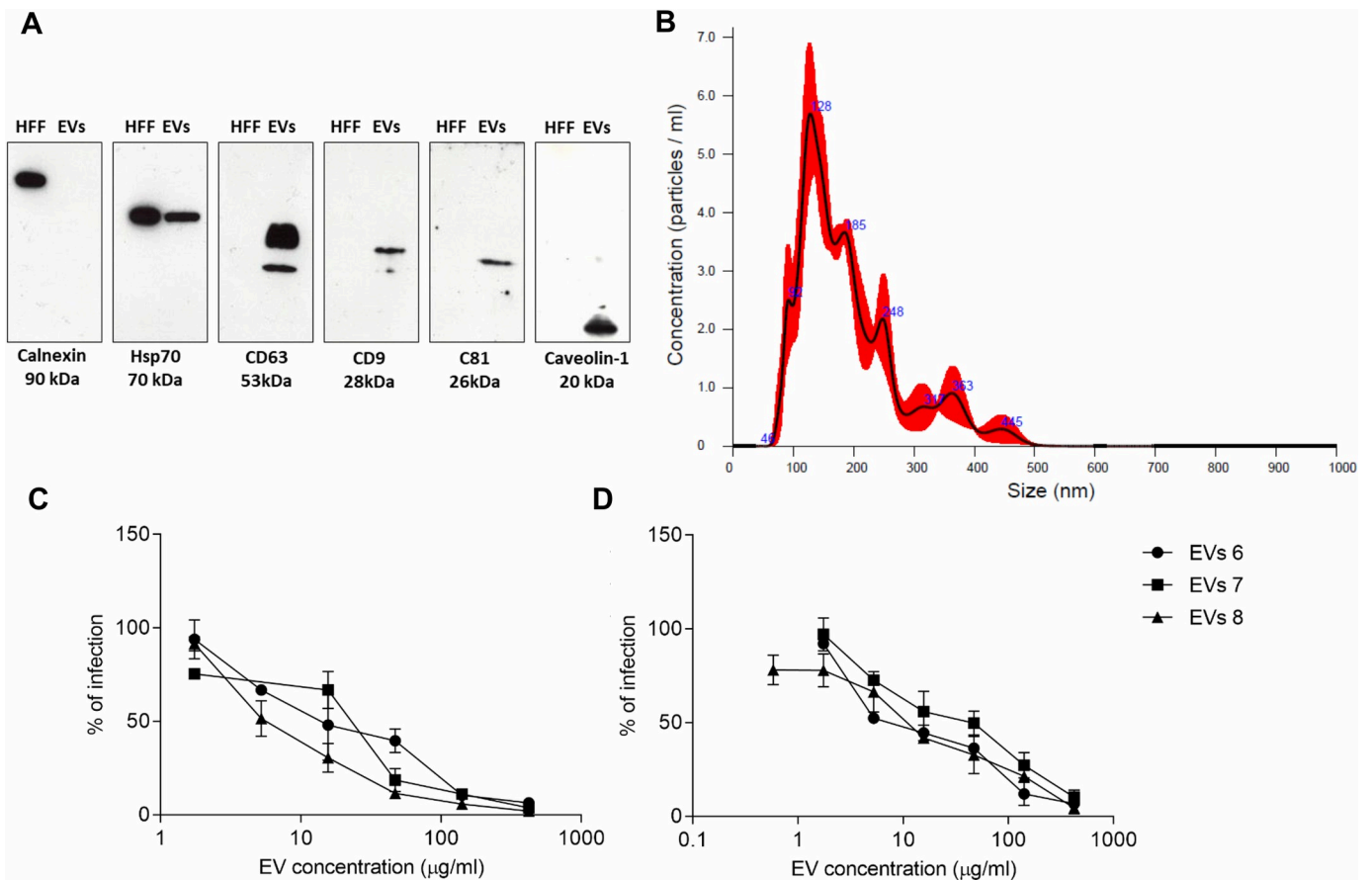
Fig 9. Characterization of colostrum derived-EVs (A, B) and study of their anti-ZIKV (C) and anti-USUV (D) activity. The protein profile of the colostrum-derived EVs was analysed by means of Western blotting using Abs against the endoplasmatic reticulum-related protein calnexin and against the EVs marker proteins CD63, CD9, CD81, Hsp70 and Caveolin-1. HFF cell lysate was used as control (A). In panel B, the Nanoparticle tracking analysis (NTA) is reported. In panels C and D the results obtained from the antiviral assays are reported. Cells and viruses were treated before and during the infection with serial dilutions of EVs. The dose response curves are reported. Data are presented as % of control. Values are means ± SEM of three independent experiments performed in duplicate.
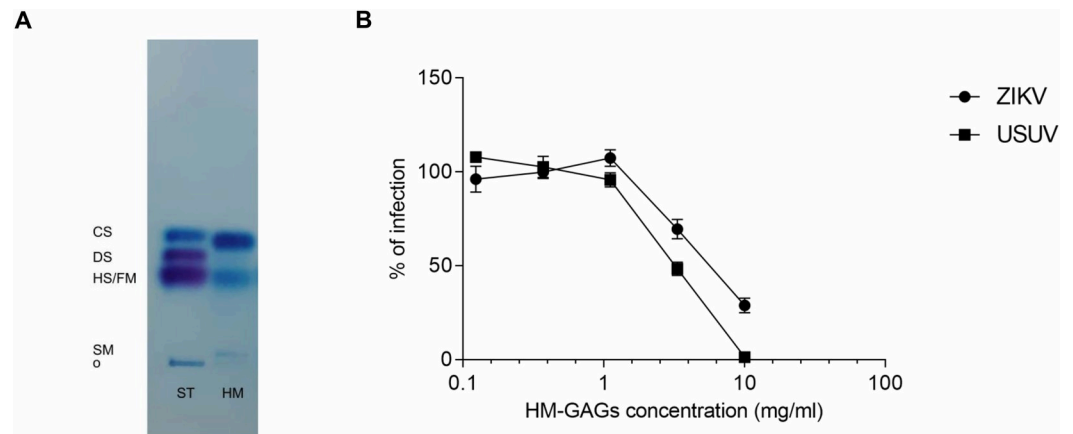
Fig 10. Electrophoresis separation of HM-GAGs (A) and evaluation of their anti-ZIKV and anti-USUV action (B). (A) Purified HM-GAGs were separated by means of acetate of cellulose electrophoresis. CS: chondroitin sulfate; DS: dermatan sulfate; HS: heparan sulfate; FM: fast-moving heparin; SM: slow-moving heparin; o: origin; ST: GAGs standard; HM: human milk; (B) Cells and viruses were treated before and during the infection with serial dilutions of HM-GAGs. Data are presented as % of control and the dose response curves are reported. Values are means ± SEM of three independent experiments performed in duplicate.

mother serostatus. Which is the antiviral potency of colostrum from ZIKV or USUV infected mothers remains an interesting open question.

We also demonstrated that human colostrum exerts an antiviral action against two different ZIKV strains, the HPF2013 and the MR766, belonging to the Asian and African lineage respectively. These results indicate that breast milk could play a protective role against either the microcephalic Asian strains, that have caused the latest epidemics, and the African strains, that have shown to be more infectious *in vitro* and *in vivo*, but have not caused any recently reported human case [60]. To the best of our knowledge, this is the first study reporting the intrinsic anti-USUV activity of human milk. On the contrary, Pang et al. recently indicated a potential anti-ZIKV action of HM in an artificial feeding model mouse [25] and other two reports demonstrated that breast milk is able to inactivate ZIKV in a time-dependent manner. These latter studies attributed the antiviral potential to the fat containing cream fraction of human milk, in which the free fatty acids, released upon storage by milk lipases in a time-dependent manner, incorporate into the viral envelope thereby destroying the viral particle [30,61]. In our experiments, we eliminated the storage affected lipid components from the milk samples and we analyzed the aqueous fractions after having verified that our storage method did not alter the antiviral properties. Our results therefore indicate the presence of an intrinsic anti-ZIKV activity in the aqueous fraction of HM too.

We explored the anti-ZIKV and anti-USUV activity of human milk analyzing the putative step of viral replication inhibited by this biofluid. We focused on the first stage of lactation, because colostrum samples collectively showed the lowest ID_{50} values in the virus inhibition assays. We demonstrated that the aqueous fraction of colostrum acts by altering the binding of ZIKV and USUV to cells, thus preventing cellular infection. Despite the early steps of USUV and ZIKV replicative cycles are not yet fully defined, it has been demonstrated that different molecules play a role in flaviviruses attachment to cells. The most common attachment factors are negatively charged glycosaminoglycans (GAGs), which can be utilized by several flaviviruses, including DENV, WNV, JEV and tick-borne encephalitis virus (TBEV), as low-affinity attachment factors to concentrate the virus on cell surface [62]. Contradictory results have emerged instead from studies about the dependence of ZIKV on cellular GAGs [63–66]. In addition, phosphatidylserine (PS) receptors' families, such as T-cell immunoglobulin (TIM)

and TYRO3, AXL and MERTK (TAM), as well as integrins and C-type lectin receptors (CLRs), have been described as key factors during the initial steps of flavivirus cell invasion [62,67]. Given the extremely complex composition of human milk and the results obtained from the study of its mechanism of action, we could hypothesize the presence of one or more factors in HM able to limit USUV and ZIKV interaction with the above-mentioned cellular receptors. We can exclude a possible action of residual free fatty acids, since the mechanism of action indicated by Conzelmann et al. and attributed to the lipid components consisted of a virucidal activity.

To support our results, we investigated the antiviral activity of two HM components derived from the aqueous fraction of human milk. HM-EVs showed a strong inhibition of ZIKV and USUV infection *in vitro*, suggesting that they could contribute, at least in part, to the overall antiviral action of human milk. Consistently with these findings, previous studies demonstrated the antiviral potency of HM-EVs and indicated that they compete with viruses for the binding to cellular receptors [44,68]. In particular, Näslund and colleagues showed that HM-exosomes compete with HIV-1 for binding to DC-SIGN receptor on monocyte-derived dendritic cells. Even though our results are preliminary and the mechanism of action has not been investigated yet, we speculate that a similar mechanism could be possible against ZIKV and USUV too.

GAGs are other HM components that could contribute in inhibiting the binding of both flaviviruses to cells. Since numerous viruses, including some flaviviruses, attach to cell exploiting cellular GAGs, these complex carbohydrates from different origins have been largely investigated for their ability to act as soluble receptors [69–74]. Notably, the first data available on the antiviral role of GAGs isolated from HM are those reported by Newburg et al. demonstrating that HM-CS was able to inhibit the binding of the HIV envelop glycoprotein gp120 to the cellular CD4 receptor [46]. In this study, HM-GAGs were tested against ZIKV and USUV at concentrations that would be relevant to breastfed infants [40]. In particular, highest GAGs values are present at 4th day after partum (~ 9.3 mg/ml and ~ 3.8 mg/ml in preterm and term milk, respectively), followed by a progressive decrease up to day 30th (~ 4.3 mg/ml and ~ 0.4 mg/ml). Given the possibility that cellular GAGs are low-affinity attachment factors for ZIKV and USUV, the antiviral action of HM-GAGs (potentially acting as decoy receptors) is not as strong as expected, but the EC_{50} values fall within the range of GAG concentrations in preterm and term colostrum. Furthermore, the GAGs concentration detected in preterm mature milk is still partially active against USUV. These results indicate that HM-GAGs could only partially contribute to the overall antiviral action of human milk, mostly acting during the first days after birth. This also highlights that the dependence of ZIKV and USUV on cellular GAGs for their attachment to cells warrant further investigations.

In conclusion, the intrinsic anti-ZIKV activity of human milk here reported, along with the higher viscosity detected in colostrum from ZIKV-infected mothers and the storage-dependent virucidal activity of HM lipid components, are three different factors that hinder the spread of ZIKV through breastfeeding [30,75]. Furthermore, we can now add USUV to the list of viral pathogens inhibited by human milk. Altogether, our data support the WHO recommendations about breast-feeding during ZIKV infection and could contribute to producing new guidelines for a possible USUV epidemic.

Supporting information

S1 Table. Anti-ZIKV and anti-USUV activities of defatted colostrum (numerical results of Fig 1A).
(DOCX)

S2 Table. ID_{50} values of defatted human milk samples at different stages of maturation against ZIKV (numerical results of Fig 5A).
(DOCX)

S3 Table. ID_{50} values of defatted human milk samples at different stages of maturation against USUV (numerical results of Fig 5B).
(DOCX)

S4 Table. Numerical results of the binding assays reported in Fig 8A and 8B (the mean values are reported).
(DOCX)

S1 Fig. Anti-ZIKV (A) and anti-USUV (B) activities of two fresh colostrum samples. Cells and viruses were treated before and during the infection with serial dilutions of colostrum aqueous fraction (from 1:3 to 1:6561 parts). The dose-response curves are reported. Data are presented as % of control. Values are means ± SEM of three independent experiments performed in duplicate. The ID_{50} values obtained from the ZIKV antiviral assays values were 0.0037 (colostrum F1) and 0.00097 (colostrum F2). In the case of USUV, the ID_{50} values were 0.018 (colostrum F1) and 0.02 (colostrum F2).
(PDF)

S2 Fig. Comparison between the antiviral activity of colostrum from term and preterm mothers. Cells and viruses were treated before and during the infection with serial dilutions of human colostrum aqueous fraction (from 1:3 to 1:6561 parts). Anti-ZIKV and anti-USUV inhibitory dilution-50 values obtained from three independent experiments are reported and stratified to compare term and preterm mothers. Panel A reports the results obtained by testing colostra against ZIKV, while panel B shows the results for USUV. Results are expressed as mean ± SEM of inhibitory dilution-50 values (Student's t test; ns: not significant).
(PDF)

S3 Fig. Evaluation of the anti-ZIKV activity of human colostrum against the MR766 strain with immunofluorescence assays detecting the dsRNA and the flavivirus protein E. Cells and viruses (MOI = 3) were treated before and during the infection with the dilution of colostrum corresponding the ID_{90} in the virus inhibition assay. After 30 h of infection, cells were fixed and subjected to immunofluorescence.
(PDF)

S4 Fig. Evaluation of cell viability after the treatment with transitional (A, C) or mature milk (B, D). Cells were treated under the same conditions of the ZIKV (A, B) and USUV (C, D) inhibition assays. Results from 3 randomly selected samples are reported in each graph. Data are indicated as % of untreated control. Values are means ± SEM of three independent experiments performed in duplicate.
(PDF)

S5 Fig. Anti-ZIKV (A) and anti-USUV (B) activity of defatted human milk samples at different stages of maturation. The inhibitory dilution-50 values of colostrum, transitional and mature milk obtained from every single mother are separately reported indicating the sample number.
(PDF)

S6 Fig. Nanoparticle tracking analysis (NTA) of EVs 6 (A) and EVs 8 (B).
(PDF)

S7 Fig. Evaluation of cell viability after EVs (A) or GAGs treatment (B). Cells were treated under the same experimental conditions of the ZIKV and USUV inhibition assay, but without infection. Cell viability was evaluated after 24 h or 72 h, respecting the same experimental timing of USUV or ZIKV antiviral assay respectively. Results obtained with one representative EV population and with the GAGs preparation are reported and indicated as % of untreated control. Values are means ± SEM of three independent experiments performed in duplicate. (PDF)

Author Contributions

Conceptualization: Paola Tonetto, Alessandra Coscia, Guido E. Moro, Enrico Bertino, David Lembo.

Data curation: Rachele Francese, Andrea Civra, Manuela Donalisio, Federica Capitani.

Funding acquisition: Guido E. Moro, David Lembo.

Investigation: Rachele Francese, Andrea Civra, Manuela Donalisio, Nicola Volpi, Federica Capitani, Stefano Sottemano.

Methodology: Rachele Francese, Andrea Civra, Manuela Donalisio, Nicola Volpi, Federica Capitani.

Resources: Stefano Sottemano, Paola Tonetto, Alessandra Coscia, Giulia Maiocco, Enrico Bertino.

Supervision: Guido E. Moro, Enrico Bertino, David Lembo.

Writing – original draft: Rachele Francese.

Writing – review & editing: Nicola Volpi, Paola Tonetto, Alessandra Coscia, Guido E. Moro, Enrico Bertino, David Lembo.

References

1. Ashraf U, Ye J, Ruan X, Wan S, Zhu B, Cao S. Usutu virus: an emerging flavivirus in Europe. Viruses. 2015 Jan 19; 7(1):219–38. https://doi.org/10.3390/v7010219 PMID: 25606971

2. Paixão ES, Barreto F, Teixeira M da G, Costa M da CN, Rodrigues LC. History, Epidemiology, and Clinical Manifestations of Zika: A Systematic Review. Am J Public Health. 2016 Apr; 106(4):606–12. https://doi.org/10.2105/AJPH.2016.303112 PMID: 26959260

3. Weaver SC, Costa F, Garcia-Blanco MA, Ko AI, Ribeiro GS, Saade G, et al. Zika Virus: History, Emergence, Biology, and Prospects for Control. Antiviral Res. 2016 Jun; 130:69–80. https://doi.org/10.1016/j.antiviral.2016.03.010 PMID: 26996139

4. Koppolu V, Shantha Raju T. Zika virus outbreak: a review of neurological complications, diagnosis, and treatment options. J Neurovirol. 2018; 24(3):255–72. https://doi.org/10.1007/s13365-018-0614-8 PMID: 29441490

5. Mlakar J, Korva M, Tul N, Popović M, Poljšak-Prijatelj M, Mraz J, et al. Zika Virus Associated with Microcephaly. N Engl J Med. 2016 Mar 10; 374(10):951–8. https://doi.org/10.1056/NEJMoa1600651 PMID: 26862926

6. Pacheco LD, Weaver SC, Saade GR. Zika Virus Infection—After the Pandemic. N Engl J Med. 2020 09; 382(2):e3.

7. WHO | Zika situation report [Internet]. WHO. [cited 2020 May 4]. Available from: http://www.who.int/emergencies/zika-virus/situation-report/10-march-2017/en/

8. Barzon L. Ongoing and emerging arbovirus threats in Europe. J Clin Virol. 2018; 107:38–47. https://doi.org/10.1016/j.jcv.2018.08.007 PMID: 30176404

9. Clé M, Beck C, Salinas S, Lecollinet S, Gutierrez S, Van de Perre P, et al. Usutu virus: A new threat? Epidemiol Infect. 2019; 147:e232. https://doi.org/10.1017/S0950268819001213 PMID: 31364580

10. Clé M, Barthelemy J, Desmetz C, Foulongne V, Lapeyre L, Bolloré K, et al. Study of Usutu virus neuro-pathogenicity in mice and human cellular models. PLoS Negl Trop Dis. 2020 Apr; 14(4):e0008223. https://doi.org/10.1371/journal.pntd.0008223 PMID: 32324736

11. Roesch F, Fajardo A, Moratorio G, Vignuzzi M. Usutu Virus: An Arbovirus on the Rise. Viruses. 2019 Jul 12; 11(7).

12. Salinas S, Constant O, Desmetz C, Barthelemy J, Lemaitre J-M, Milhavet O, et al. Deleterious effect of Usutu virus on human neural cells. PLoS Negl Trop Dis. 2017 Sep; 11(9):e0005913. https://doi.org/10.1371/journal.pntd.0005913 PMID: 28873445

13. Mann TZ, Haddad LB, Williams TR, Hills SL, Read JS, Dee DL, et al. Breast Milk Transmission of Flavi-viruses in the Context of Zika Virus: A Systematic Review. Paediatr Perinat Epidemiol. 2018 Jul; 32 (4):358–68. https://doi.org/10.1111/ppe.12478 PMID: 29882971

14. Cavalcanti MG, Cabral-Castro MJ, Gonçalves JLS, Santana LS, Pimenta ES, Peralta JM. Zika virus shedding in human milk during lactation: an unlikely source of infection? International Journal of Infectious Diseases. 2017 Apr 1; 57:70–2. https://doi.org/10.1016/j.ijid.2017.01.042 PMID: 28188933

15. Colt S, Garcia-Casal MN, Peña-Rosas JP, Finkelstein JL, Rayco-Solon P, Weise Prinzo ZC, et al. Transmission of Zika virus through breast milk and other breastfeeding-related bodily-fluids: A systematic review. PLoS Negl Trop Dis. 2017 Apr 10; 11(4):e0005528 https://doi.org/10.1371/journal.pntd.0005528 PMID: 28394887

16. Dupont-Rouzeyrol M, Biron A, O'Connor O, Huguon E, Descloux E. Infectious Zika viral particles in breastmilk. The Lancet. 2016 Mar 12; 387(10023):1051.

17. Giovanetti M, Goes de Jesus J, Lima de Maia M, Junior JX, Castro Amarante MF, Viana P, et al. Genetic evidence of Zika virus in mother's breast milk and body fluids of a newborn with severe congenital defects. Clinical Microbiology and Infection. 2018 Oct 1; 24(10):1111–2. https://doi.org/10.1016/j.cmi.2018.06.008 PMID: 29906587

18. Sotelo JR, Sotelo AB, Sotelo FJB, Doi AM, Pinho JRR, Oliveira R de C, et al. Persistence of Zika Virus in Breast Milk after Infection in Late Stage of Pregnancy. Emerg Infect Dis. 2017 May; 23(5):854–6.

19. Besnard M, Lastere S, Teissier A, Cao-Lormeau V, Musso D. Evidence of perinatal transmission of Zika virus, French Polynesia, December 2013 and February 2014. Euro Surveill. 2014 Apr 3; 19(13).

20. Blohm GM, Lednicky JA, Márquez M, White SK, Loeb JC, Pacheco CA, et al. Complete Genome Sequences of Identical Zika virus Isolates in a Nursing Mother and Her Infant. Genome Announc. 2017 Apr 27; 5(17).

21. Blohm GM, Lednicky JA, Márquez M, White SK, Loeb JC, Pacheco CA, et al. Evidence for Mother-to-Child Transmission of Zika Virus Through Breast Milk. Clin Infect Dis. 2018 19; 66(7):1120–1. https://doi.org/10.1093/cid/cix968 PMID: 29300859

22. Hemachudha P, Wacharapluesadee S, Buathong R, Petcharat S, Bunprakob S, Ruchiseesarod C, et al. Lack of Transmission of Zika Virus Infection to Breastfed Infant. Clin Med Insights Case Rep. 2019 Mar 12; 12:1179547619835179 https://doi.org/10.1177/1179547619835179 PMID: 30886528

23. Mello AS, Pascalicchio Bertozzi APA, Rodrigues MMD, Gazeta RE, Moron AF, Soriano-Arandes A, et al. Development of Secondary Microcephaly After Delivery: Possible Consequence of Mother-Baby Transmission of Zika Virus in Breast Milk. Am J Case Rep. 2019 May 21; 20:723–5. https://doi.org/10.12659/AJCR.915726 PMID: 31110169

24. Sampieri CL, Montero H. Breastfeeding in the time of Zika: a systematic literature review. PeerJ. 2019; 7:e6452. https://doi.org/10.7717/peerj.6452 PMID: 30809448

25. Pang W, Lin Y-L, Xin R, Chen X-X, Lu Y, Zheng C-B, et al. Zika virus transmission via breast milk in suckling mice. Clinical Microbiology and Infection [Internet]. 2020 Apr 25 [cited 2020 May 7]; Available from: http://www.sciencedirect.com/science/article/pii/S1198743X20302299

26. Mosca F, Giannì ML. Human milk: composition and health benefits. Pediatr Med Chir. 2017 Jun 28; 39 (2):155. https://doi.org/10.4081/pmc.2017.155 PMID: 28673076

27. WHO | Infant feeding in areas of Zika virus transmission [Internet]. WHO. [cited 2020 May 4]. Available from: http://www.who.int/elena/titles/zika_breastfeeding/en/

28. Ballard O, Morrow AL. Human milk composition: nutrients and bioactive factors. Pediatr Clin North Am. 2013 Feb; 60(1):49–74. https://doi.org/10.1016/j.pcl.2012.10.002 PMID: 23178060

29. Andreas NJ, Kampmann B, Mehring Le-Doare K. Human breast milk: A review on its composition and bioactivity. Early Hum Dev. 2015 Nov; 91(11):629–35. https://doi.org/10.1016/j.earlhumdev.2015.08.013 PMID: 26375355

30. Conzelmann C, Zou M, Groß R, Harms M, Röcker A, Riedel CU, et al. Storage-Dependent Generation of Potent Anti-ZIKV Activity in Human Breast Milk. Viruses. 2019 Jun 28; 11(7).

31. Falkler WA, Diwan AR, Halstead SB. A lipid inhibitor of dengue virus in human colostrum and milk; with a note on the absence of anti-dengue secretory antibody. Arch Virol. 1975; 47(1):3–10. https://doi.org/10.1007/BF01315587 PMID: 1170830

32. Fieldsteel AH. Nonspecific antiviral substances in human milk active against arbovirus and murine leukemia virus. Cancer Res. 1974 Apr; 34(4):712–5. PMID: 4814990

33. Pfaender S, Heyden J, Friesland M, Ciesek S, Ejaz A, Steinmann J, et al. Inactivation of hepatitis C virus infectivity by human breast milk. J Infect Dis. 2013 Dec 15; 208(12):1943–52. https://doi.org/10.1093/infdis/jit519 PMID: 24068703

34. de la Torre Gomez C, Goreham RV, Bech Serra JJ, Nann T, Kussmann M. 'Exosomics'-A Review of Biophysics, Biology and Biochemistry of Exosomes With a Focus on Human Breast Milk. Front Genet. 2018; 9:92. https://doi.org/10.3389/fgene.2018.00092 PMID: 29636770

35. Raposo G, Stoorvogel W. Extracellular vesicles: exosomes, microvesicles, and friends. J Cell Biol. 2013 Feb 18; 200(4):373–83. https://doi.org/10.1083/jcb.201211138 PMID: 23420871

36. Zonneveld MI, Brisson AR, van Herwijnen MJC, Tan S, van de Lest CHA, Redegeld FA, et al. Recovery of extracellular vesicles from human breast milk is influenced by sample collection and vesicle isolation procedures. J Extracell Vesicles. 2014; 3.

37. Abels ER, Breakefield XO. Introduction to Extracellular Vesicles: Biogenesis, RNA Cargo Selection, Content, Release, and Uptake. Cell Mol Neurobiol. 2016 Apr; 36(3):301–12. https://doi.org/10.1007/s10571-016-0366-z PMID: 27053351

38. van der Pol E, Böing AN, Harrison P, Sturk A, Nieuwland R. Classification, functions, and clinical relevance of extracellular vesicles. Pharmacol Rev. 2012 Jul; 64(3):676–705. https://doi.org/10.1124/pr.112.005983 PMID: 22722893

39. Coppa GV, Gabrielli O, Buzzega D, Zampini L, Galeazzi T, Maccari F, et al. Composition and structure elucidation of human milk glycosaminoglycans. Glycobiology. 2011 Mar; 21(3):295–303. https://doi.org/10.1093/glycob/cwq164 PMID: 21030540

40. Coppa GV, Gabrielli O, Zampini L, Galeazzi T, Maccari F, Buzzega D, et al. Glycosaminoglycan content in term and preterm milk during the first month of lactation. Neonatology. 2012; 101(1):74–6. https://doi.org/10.1159/000330848 PMID: 21934331

41. Shimizu M, Uryu N, Yamauchi K. Presence of Heparan Sulfate in the Fat Globule Membrane of Bovine and Human Milk. Agricultural and Biological Chemistry. 1981 Mar 1; 45(3):741–5.

42. Coppa GV, Gabrielli O, Bertino E, Zampini L, Galeazzi T, Padella L, et al. Human milk glycosaminoglycans: the state of the art and future perspectives. Ital J Pediatr. 2013 Jan 15; 39:2. https://doi.org/10.1186/1824-7288-39-2 PMID: 23321150

43. Zempleni J, Aguilar-Lozano A, Sadri M, Sukreet S, Manca S, Wu D, et al. Biological Activities of Extracellular Vesicles and Their Cargos from Bovine and Human Milk in Humans and Implications for Infants. J Nutr. 2017; 147(1):3–10. https://doi.org/10.3945/jn.116.238949 PMID: 27852870

44. Näslund TI, Paquin-Proulx D, Paredes PT, Vallhov H, Sandberg JK, Gabrielsson S. Exosomes from breast milk inhibit HIV-1 infection of dendritic cells and subsequent viral transfer to CD4+ T cells. AIDS. 2014 Jan 14; 28(2):171–80. https://doi.org/10.1097/QAD.0000000000000159 PMID: 24413309

45. Coppa GV, Facinelli B, Magi G, Marini E, Zampini L, Mantovani V, et al. Human milk glycosaminoglycans inhibit in vitro the adhesion of Escherichia coli and Salmonella fyris to human intestinal cells. Pediatr Res. 2016 Apr; 79(4):603–7. https://doi.org/10.1038/pr.2015.262 PMID: 26679156

46. Newburg DS, Linhardt RJ, Ampofo SA, Yolken RH. Human milk glycosaminoglycans inhibit HIV glycoprotein gp120 binding to its host cell CD4 receptor. J Nutr. 1995 Mar; 125(3):419–24. https://doi.org/10.1093/jn/125.3.419 PMID: 7876916

47. Viveros-Rogel M, Soto-Ramirez L, Chaturvedi P, Newburg DS, Ruiz-Palacios GM. Inhibition of HIV-1 infection in vitro by human milk sulfated glycolipids and glycosaminoglycans. Adv Exp Med Biol. 2004; 554:481–7. https://doi.org/10.1007/978-1-4757-4242-8_69 PMID: 15384629

48. Arslanoglu S, Bertino E, Tonetto P, Nisi GD, Ambruzzi AM, Biasini A, et al. Guidelines for the establishment and operation of a donor human milk bank. The Journal of Maternal-Fetal & Neonatal Medicine. 2010 Sep 1; 23(sup2):1–20.

49. Francese R, Civra A, Rittà M, Donalisio M, Argenziano M, Cavalli R, et al. Anti-zika virus activity of polyoxometalates. Antiviral Research. 2019 Mar 1; 163:29–33. https://doi.org/10.1016/j.antiviral.2019.01.005 PMID: 30653996

50. Civra A, Francese R, Gamba P, Testa G, Cagno V, Poli G, et al. 25-Hydroxycholesterol and 27-hydroxycholesterol inhibit human rotavirus infection by sequestering viral particles into late endosomes. Redox Biol. 2018; 19:318–30. https://doi.org/10.1016/j.redox.2018.09.003 PMID: 30212801

51. Cesaretti M, Luppi E, Maccari F, Volpi N. A 96-well assay for uronic acid carbazole reaction. Carbohydrate Polymers. 2003 Oct 1; 54(1):59–61.

52. Volpi N, Maccari F. Electrophoretic approaches to the analysis of complex polysaccharides. J Chromatogr B Analyt Technol Biomed Life Sci. 2006 Apr 13; 834(1–2):1–13. https://doi.org/10.1016/j.jchromb.2006.02.049 PMID: 16530493

53. Mantovani V, Galeotti F, Maccari F, Volpi N. Recent advances in capillary electrophoresis separation of monosaccharides, oligosaccharides, and polysaccharides. Electrophoresis. 2018; 39(1):179–89. https://doi.org/10.1002/elps.201700290 PMID: 28857216

54. Donalisio M, Rittà M, Tonetto P, Civra A, Coscia A, Giribaldi M, et al. Anti-Cytomegalovirus Activity in Human Milk and Colostrum From Mothers of Preterm Infants. J Pediatr Gastroenterol Nutr. 2018; 67 (5):654–9. https://doi.org/10.1097/MPG.0000000000002071 PMID: 30074575

55. Théry C, Witwer KW, Aikawa E, Alcaraz MJ, Anderson JD, Andriantsitohaina R, et al. Minimal information for studies of extracellular vesicles 2018 (MISEV2018): a position statement of the International Society for Extracellular Vesicles and update of the MISEV2014 guidelines. J Extracell Vesicles. 2018; 7(1):1535750. https://doi.org/10.1080/20013078.2018.1535750 PMID: 30637094

56. Coscia A, Peila C, Bertino E, Coppa GV, Moro GE, Gabrielli O, et al. Effect of holder pasteurisation on human milk glycosaminoglycans. J Pediatr Gastroenterol Nutr. 2015 Jan; 60(1):127–30. https://doi.org/10.1097/MPG.0000000000000570 PMID: 25221936

57. Volpi N. Chondroitin Sulfate Safety and Quality. Molecules. 2019 Apr 12; 24(8).

58. Lawrence RM, Lawrence RA. Breast milk and infection. Clin Perinatol. 2004 Sep; 31(3):501–28.

59. Chirico G, Marzollo R, Cortinovis S, Fonte C, Gasparoni A. Antiinfective Properties of Human Milk. J Nutr. 2008 Sep 1; 138(9):1801S–1806S. https://doi.org/10.1093/jn/138.9.1801S PMID: 18716190

60. Beaver JT, Lelutiu N, Habib R, Skountzou I. Evolution of Two Major Zika Virus Lineages: Implications for Pathology, Immune Response, and Vaccine Development. Front Immunol. 2018; 9:1640. https://doi.org/10.3389/fimmu.2018.01640 PMID: 30072993

61. Pfaender S, Vielle NJ, Ebert N, Steinmann E, Alves MP, Thiel V. Inactivation of Zika virus in human breast milk by prolonged storage or pasteurization. Virus Res. 2017 15; 228:58–60. https://doi.org/10.1016/j.virusres.2016.11.025 PMID: 27889615

62. Agrelli A, de Moura RR, Crovella S, Brandão LAC. ZIKA virus entry mechanisms in human cells. Infect Genet Evol. 2019; 69:22–9. https://doi.org/10.1016/j.meegid.2019.01.018 PMID: 30658214

63. Kim SY, Zhao J, Liu X, Fraser K, Lin L, Zhang X, et al. Interaction of Zika Virus Envelope Protein with Glycosaminoglycans. Biochemistry. 2017 28; 56(8):1151–62. https://doi.org/10.1021/acs.biochem.6b01056 PMID: 28151637

64. Gao H, Lin Y, He J, Zhou S, Liang M, Huang C, et al. Role of heparan sulfate in the Zika virus entry, replication, and cell death. Virology. 2019; 529:91–100. https://doi.org/10.1016/j.virol.2019.01.019 PMID: 30684694

65. Cagno V, Tseligka ED, Jones ST, Tapparel C. Heparan Sulfate Proteoglycans and Viral Attachment: True Receptors or Adaptation Bias? Viruses. 2019 Jul 1; 11(7).

66. Ghezzi S, Cooper L, Rubio A, Pagani I, Capobianchi MR, Ippolito G, et al. Heparin prevents Zika virus induced-cytopathic effects in human neural progenitor cells. Antiviral Res. 2017; 140:13–7. https://doi.org/10.1016/j.antiviral.2016.12.023 PMID: 28063994

67. Oliveira LG, Peron JPS. Viral receptors for flaviviruses: Not only gatekeepers. J Leukoc Biol. 2019 Sep; 106(3):695–701. https://doi.org/10.1002/JLB.MR1118-460R PMID: 31063609

68. van Dongen HM, Masoumi N, Witwer KW, Pegtel DM. Extracellular Vesicles Exploit Viral Entry Routes for Cargo Delivery. Microbiol Mol Biol Rev. 2016 Jun; 80(2):369–86. https://doi.org/10.1128/MMBR.00063-15 PMID: 26935137

69. Olofsson S, Bergström T. Glycoconjugate glycans as viral receptors. Ann Med. 2005; 37(3):154–72. https://doi.org/10.1080/07853890510007340 PMID: 16019714

70. Shukla D, Spear PG. Herpesviruses and heparan sulfate: an intimate relationship in aid of viral entry. J Clin Invest. 2001 Aug; 108(4):503–10. https://doi.org/10.1172/JCI13799 PMID: 11518721

71. Spillmann D. Heparan sulfate: anchor for viral intruders? Biochimie. 2001 Aug; 83(8):811–7. https://doi.org/10.1016/s0300-9084(01)01290-1 PMID: 11530214

72. Barth H, Schnober EK, Zhang F, Linhardt RJ, Depla E, Boson B, et al. Viral and cellular determinants of the hepatitis C virus envelope-heparan sulfate interaction. J Virol. 2006 Nov; 80(21):10579–90. https://doi.org/10.1128/JVI.00941-06 PMID: 16928753

73. Cagno V, Andreozzi P, D'Alicarnasso M, Jacob Silva P, Mueller M, Galloux M, et al. Broad-spectrum non-toxic antiviral nanoparticles with a virucidal inhibition mechanism. Nat Mater. 2018; 17(2):195–203. https://doi.org/10.1038/nmat5053 PMID: 29251725

74. Grice ID, Mariottini GL. Glycans with Antiviral Activity from Marine Organisms. Results Probl Cell Differ. 2018; 65:439–75. https://doi.org/10.1007/978-3-319-92486-1_20 PMID: 30083931

75. de Quental OB, França EL, Honório-França AC, Morais TC, Daboin BEG, Bezerra IMP, et al. Zika Virus
Alters the Viscosity and Cytokines Profile in Human Colostrum. J Immunol Res. 2019; 2019:9020519.
https://doi.org/10.1155/2019/9020519 PMID: 31828175

8. ANALYSIS OF THE EFFECT OF HOLDER PASTEURIZATION AND HIGHT TEMPERATURE-SHORT TIME PASTEURIZATION ON MILK'S ANTIVIRAL PROPERTIES

As previously described, recent findings have confirmed the therapeutic properties of human milk components and have left no doubt that it constitutes an indispensable part of newborns' nutritional treatment, especially premature babies with very low (VLBW) and extremely low (ELBW) birth weight. Initiating lactation in preterms' mothers and maintaining mother's milk supply for NICU infants remains challenging. Donor milk has become the standard way of feeding newborns who cannot receive the milk of their biological mothers (149,150). Donor milk administration to prematurely born children needing longer hospital stays requires necessary collecting procedures, freezing, storage and pasteurization. Low temperature long time (LTLT) pasteurization, also known as the holder method (HoP), is considered to be the standard for human milk pasteurization. Milk is incubated for 30 min at 62.5 °C in a water bath or other device that ensures effective heating. Modern milk pasteurizers guarantee precise measurement of the temperature inside the bottle, automatic control of the process and the possibility of efficient and safe milk cooling to low temperature (usually 4 °C) (149). Holder pasteurization destroys vegetative forms of bacteria and most viruses including HIV and CMV. This method is thought to lead to a good compromise between the microbiological safety and nutritional/biological quality of donor milk. Nonetheless, it is also well known that HoP affects some of the nutritional and biological properties of human milk. In particular, water soluble vitamins, and vitamin C are generally reported as significantly decreased and proteins are the components more significantly affected by HoP. Specific proteins with significant immunologic and anti-infective action (such as immunoglobulins and lactoferrin) are reduced by this method and a substantial reduction in the enzymatic activity has also been observed (151). Therefore, Human Milk Banks (HMBs) and researchers are committed to developing novel or enhanced methods to process donor milk that can ensure microbial inactivation, while improving the preservation of its nutritional, immunological, and functional constituents (152). High Temperature Short Time pasteurization (HTST), that consists of heating thin-layered milk in continuous flow systems at 72∘C for 15 seconds, was the first non-HoP technique tested to improve the nutritional and immunological quality of milk, because it has been established in the dairy industry since the 1930s (149). In this context, we investigated and compared the effect of both HoP and HTST on milk's antiviral properties, with the aim to identify the best method to preserve this fundamental quality of human milk.

8.1 Publications

Donalisio M, Rittà M, Francese R, Civra A, Tonetto P, Coscia A, Giribaldi M, Cavallarin L, Moro GE, Bertino E, Lembo D. High Temperature-Short Time Pasteurization Has a Lower Impact on the Antiviral Properties of Human Milk Than Holder Pasteurization. Front Pediatr. 2018 Oct 16;6:304. doi: 10.3389/fped.2018.00304. PMID: 30460212; PMCID: PMC6232822.

In the present study we investigated whether and to which extent HoP and HTST pasteurization have an effect on the antiviral properties of raw human milk against a panel of viral pathogens causing diseases in newborns and children, as Herpes simplex virus type I and II (HSV-1, HSV-2), HCMV, RSV, HRhV, and HRoV. The results indicated that the Holder pasteurization, significantly decrease the milk antiviral activity against HSV-1, HSV-2, HCMV, RSV, and HRhV, but not against HRoV. By contrast, HTST preserved antiviral properties of raw human milk against four out of six viruses analyzed. Our study provided the first evidence that HTST pasteurization preserves milk antiviral activity better than HoP, thus indicating that this method could improve the quality of the final product.

High Temperature—Short Time Pasteurization Has a Lower Impact on the Antiviral Properties of Human Milk Than Holder Pasteurization

Manuela Donalisio[1], Massimo Rittà[1], Rachele Francese[1], Andrea Civra[1], Paola Tonetto[2], Alessandra Coscia[2], Marzia Giribaldi[3,4], Laura Cavallarin[3], Guido E. Moro[5], Enrico Bertino[2] and David Lembo[1]*

[1] Laboratory of Molecular Virology, Department of Clinical and Biological Sciences, University of Turin, Turin, Italy, [2] Neonatal Intensive Care Unit, Department of Public Health and Pediatrics, University of Turin, Turin, Italy, [3] Consiglio Nazionale delle Ricerche-Istituto di Scienze delle Produzioni Alimentari, Bari, Italy, [4] Consiglio per la Ricerca in Agricoltura e l'Analisi dell'Economia Agraria, Centro di Ricerca in Ingegneria e Trasformazioni Agroalimentari, Turin, Italy, [5] Italian Association of Human Milk Banks, Milan, Italy

Holder pasteurization (62. 5°C for 30 min) is recommended by all international human milk bank guidelines to prevent infections potentially transmitted by donor human milk. A drawback is that it affects some human milk bioactive and nutritive components. Recently, High Temperature-Short Time (HTST) pasteurization has been reported to be a valuable alternative technology to increase the retention of some biological features of human milk. Nevertheless, to date, few data are available about the impact of pasteurization methods other than Holder on the antiviral activity of human milk. The present study was aimed at evaluating the antiviral activity of human milk against a panel of viral pathogens common in newborns and children (i.e., herpes simplex virus 1 and 2, cytomegalovirus, respiratory syncytial virus, rotavirus, and rhinovirus), and at assessing the effect of Holder and HTST pasteurization on milk's antiviral properties. The results indicate that human milk is endowed with antiviral activity against all viruses tested, although to a different extent. Unlike the Holder pasteurization, HTST preserved the inhibitory activity against cytomegalovirus, respiratory syncytial virus, rotavirus and herpes simplex virus type 2. By contrast, both methods reduced significantly the antiviral activities against rhinovirus and herpes simplex virus type 1. Unexpectedly, Holder pasteurization improved milk's anti-rotavirus activity. In conclusion, this study contributes to the definition of the pasteurization method that allows the best compromise between microbiological safety and biological quality of the donor human milk: HTST pasteurization preserved milk antiviral activity better than Holder.

Keywords: human milk, HTST, Holder, antiviral activity, virus, pasteurization

INTRODUCTION

A mother's own milk is the first choice for improving the short- and long-term outcomes for all newborns, including preterm infants (1, 2). When a mother's own milk is unavailable or in short supply, a common occurrence in Neonatal Intensive Care Units, the World Health Organization and the American Academy of Pediatrics recommend the use of donor milk (DM)

as the best alternative (2, 3). Human milk (HM) can be considered a species-specific dynamic biological system, known to encompass many kinds of biological functions, including antimicrobial and antiviral properties (2). It is generally agreed that breastfeeding reduces the rate of serious gastroenteritis, especially caused by rotaviruses (HRoVs), and infant respiratory infections, as well as otitis media. The main viruses involved in infant respiratory and middle ear infections are respiratory syncytial virus (RSV) and rhinoviruses (HRhV) (4–7). Furthermore, most herpetic infections are acquired during childhood and their infection is lifelong. The vast majority of herpes simplex virus 1 (HSV-1) infections are oral-labial herpes and they are mainly transmitted by oral-to-oral contact. By contrast, neonatal herpes can occur when an infant is exposed to herpes simplex virus 2 (HSV-2) in the genital tract during delivery. The risk for neonatal herpes is greatest when a mother acquires HSV infection for the first time in late pregnancy (8). Human cytomegalovirus (HCMV) is another herpesvirus, responsible for the most common congenital infection worldwide, affecting 1 out of every 150 live-born infants worldwide (9).

Several specific bioactive and immunomodulatory factors play a role in the milk-mediated defense system against viral infections, including milk proteins, as lactoferrin, lactadherin, lactoperoxidase, lysozyme, and secretory immunoglobulins A (sIgA), but also mucins, sulfated glycolipids, glycosaminoglycans and vitamin A (6, 10–12). Despite the presence of protective factors in HM, some viruses, as human immunodeficiency virus type 1, human T-lymphotrophic virus, zikavirus, and HCMV, are transmitted from mother to infant thus the heat treatment of DM is mandatory in human milk banks (HMBs) to guarantee microbiological safety (13). The ESPGHAN Committee on Nutrition has recently advised that "future research should focus on the improvement of milk processing in HMBs, particularly of heat treatment" (14). Currently, a pasteurization process at 62.5°C for 30 min (the Holder pasteurization method, HoP) is recommended in all international guidelines for the constitution of HMBs (13, 15). However, literature indicates that HoP affects several milk components to variable degrees, with a marked effect on milk protein content and activity (16, 17). Therefore, HMBs and researchers are committed to developing novel or enhanced methods to process DM that can ensure microbial inactivation, while improving the preservation of its nutritional, immunological, and functional constituents (14). High Temperature Short Time pasteurization (HTST) was the first non-HoP technique tested to improve the nutritional and immunological quality of milk, because it has been established in the dairy industry since the 1930s. HTST in food industry is usually performed by heating thin-layered milk in continuous flow systems at 72°C for 15 seconds, although high variability on the processing equipment and conditions was recently observed for HTST when applied to HM pasteurization (18). On the basis of the existing evidence, a new small-scale continuous-flow HTST pasteurizer was recently designed and validated for treating HM by our group (19).

The present research is aimed at assessing whether and to which extent HoP and HTST have an effect on the antiviral

properties of raw HM against a panel of viral pathogens causing diseases in newborns and children, as HSV-1, HSV-2, HCMV, RSV, HRhV, and HRoV.

MATERIALS AND METHODS

HM Samples Collection

HM samples were obtained from the HMB of the Città della Salute e della Scienza of Turin, Italy. An ethical review process was not required for this study, because it was not a clinical trial. Each milk donor involved in this research signed a written consent form, where mother's and infant's data protection was assured. Besides, donors where informed that only milk samples stored in excess to the needs of their infants should have been used for research purposes explaining the study design. Two pools of milk were obtained on two different occasions. Both pools (final volume 250 ml) included colostrum (days 1–5 postpartum), transitional milk (days 6–14 postpartum), and mature milk (beyond day 15 postpartum). Each pool contained milk samples from three donors. The donors of the first pool were different from those of the second pool. The donors cleaned their hands and breasts according to the Italian HMB guidelines (13). The milk specimens were collected in sterile bisphenol-free polypropylene bottles using a breast pump and stored by the HMB at −20°C until processed. The individual specimens were thawed overnight in refrigerated conditions, and then pooled rapidly in the morning in the HMB, and shipped refrigerated within 1 h. Upon arrival, pooled samples were processed according to the appropriate technique, and immediately separated in 10-ml aliquots, which were conveyed to the analyzing laboratory within 1 h. Raw milk was also aliquoted immediately after collection and stored as fresh and/or frozen material, as required.

Milk Pasteurization

The milk samples were processed using either HoP or HTST system. HoP was performed directly in sterile bisphenol-free polypropylene bottles using a standard HM pasteurizer (Metalarredinox, BG, Italy). HTST was performed using a patented proprietary device (European Patent n° 2974603), as previously described (19, 20). HTST-pasteurized milk was collected in sterile bisphenol-free polypropylene bottles. Four mL from each sample were skimmed by centrifugation at 2,000 g for 30 min at 4°C in sterile tubes (Eppendorf S.r.l, Milan, Italy), and then shipped refrigerated within 1 h to the laboratory for antiviral assays.

Cells

African green monkey kidney cells (Vero) (ATCC CCL-81) and human epithelial cells Hep-2 (ATCC CCL-23) were grown as monolayers in Eagle's minimal essential medium (MEM) (Gibco/BRL) supplemented with heat-inactivated 10% fetal calf serum (FCS) (Gibco/BRL) and 1% antibiotic-antimycotic solution (Zell Shield, Minerva Biolab) at 37°C in an atmosphere of 5% of CO_2. Human Foreskin Fibroblasts (HFF-1) (ATCC SCRC-1041) at low-passage-number (<30), African green monkey kidney epithelial cells (MA104) and human epithelial

adenocarcinoma HeLa cells (ATCC CCL-2) were propagated in Dulbecco's Modified Eagle's Medium (DMEM) (Sigma-Aldrich) supplemented with FCS and antibiotic-antimycotic solution.

Viruses

The neurovirulent strains LV (21) and MS (ATCC VR-540) of HSV-1 and HSV-2, were propagated in Vero cells at 37°C (22). HRhV 1A (ATCC VR-1559) was propagated in HeLa cells, at 33°C. HSV-1, HSV-2, and HRhV titers were determined by the standard plaque method and expressed as plaque-forming unit (PFU)/ml. A bacterial artificial chromosome (BAC)-derived HCMV strain Towne incorporating the green fluorescent protein (GFP) sequence (23) was propagated on HFF-1 and viral titres were determined by fluorescent focus assay. RSV strain A2 (ATCC VR-1540) was propagated in Hep-2 and titrated by the indirect immunoperoxidase staining procedure using an RSV monoclonal antibody (Ab35958, Abcam) (24). Human HRoV strain Wa (ATCC VR-2018) was activated with 5 μg/ml of porcine pancreatic trypsin type IX (Sigma) for 30 min at 37°C and propagated in MA104 cells by using MEM containing 0.5 μg of trypsin per ml. HCMV, RSV and HRoV titers were expressed as focus-forming units (FFU)/ml. Virus stocks were maintained frozen (-80°C).

Viral Inhibition Assay

Antiviral activity of milk samples was determined by plaque reduction assays for HSV-1, HSV-2, and HRhV and by focus reduction assays for HCMV, RSV, and HRoV. Antiviral assays were performed by incubating serial dilutions of milk (from 1/1 to 1/1024 parts in medium) with virus for 1 h at 37 °C and then the mixtures were added to cells for 2 h at 37°C. After three washings with medium, monolayers were overlaid with 1.2%-methylcellulose medium with 2% FCS. The effect on HSV and HRhV infections was evaluated on pre-seeded Vero or Hela cells (10×10^4) respectively, in 24-well plates infected with 200 PFU/well of HSV or 30 PFU/well of HRhV; after incubation for 24 h (HSV-2 and HRhV) or 48 h (HSV-1) cells were fixed and stained with 0.1% crystal violet in 20% ethanol and viral plaques were counted. The mean plaque count for each sample dilution was expressed as a percentage of the mean plaque count of the control (25). In HCMV inhibition assay, cells pre-seeded in 96-well plates at a density of 5.0×10^3/well, were infected with 140 PFU/well of GFP-coding HCMV. After 5-day-incubation at 37°C 5% CO_2 atmosphere, infected cells were visualized as green fibroblasts using fluorescence microscopy and counted. In RSV and HRoV inhibition assays, Hep-2 cells and MA104 were pre-seeded at a density of 1×10^4/well and 1.4×10^4, respectively, in 96-well plates. Cells were infected with 60 PFU/well of RSV or 200 PFU/well of HRoV and, after 16 h (HRoV) or 3 days post-infection (RSV), infected cells were fixed with cold methanol and acetone for 1 min and subjected to virus-specific immunostaining as described previously (26, 27). Fluorescent and immunostained viral foci were microscopically counted and results were reported as percentages of foci in comparison to controls. The endpoints of the assays were the effective milk dilution that reduced the viral plaque/focus formation by 50% (inhibitory dilution-50, ID50) in comparison to that in the untreated control. The ID50 of

milk was calculated by using the program PRISM 4 (GraphPad Software) to fit a variable slope-sigmoidal dose–response curve. All data were generated from duplicate wells in at least three independent experiments on each HM pool.

Cell Viability Assay

Cell viability was measured by the MTS [3-(4,5-dimethylthiazol-2-yl)-5-(3-carboxymethoxyphenyl)-2-(4-sulfophenyl)-2H-tetrazolium] assay. Confluent cell cultures seeded in 96-well plates were incubated with different dilutions of milk in triplicate under the same experimental conditions described for the antiviral assays. Cell viability was determined by the CellTiter 96 Proliferation Assay Kit (Promega) according to the manufacturer's instructions. Absorbances were measured using a Microplate Reader (Model 680, BIORAD) at 490 nm. Their effect on cell viability at different milk dilutions was expressed as a percentage, by comparing the absorbances of treated cells with that of the cells incubated with culture medium alone. The 50%-cytotoxic dilutions (CD50) and 95% confidence intervals (CIs) were determined with Prism 4 software.

Statistical Analysis

Statistical analysis was performed using Extra sum-of-square F test as reported in legends of figures, on GraphPad software. Significance was reported for $p < 0.05$.

RESULTS AND DISCUSSION

Antiviral Activity of HM

This paper reports on the antiviral activity of raw milk and investigates the impact of two pasteurization techniques on such biological property. The first set of experiments was dedicated to assess the antiviral activity of two HM raw milk pools against a panel of viral pathogens causing diseases in newborns and children, and representing different viral structures and families: enveloped DNA viruses, as HSV-1, HSV-2, and HCMV (*Herpesviridae* family); enveloped RNA viruses, as RSV (*Paramyxoviridae* family); naked single strand RNA virus, as HRhV (*Picornaviridae* family); naked double strand RNA virus, as HRoV (*Reoviridae* family). **Figure 1A** reports the antiviral activity of the two HM pools, expressed as ID50, i.e., the dilution of milk sample inhibiting the 50% of infectivity. The results revealed that both pools exhibited antiviral activity against all viruses with ID50 ranging from 0.010 to 0.183. As for the viruses belonging to the *Herpesviridae* family, both pools exhibited a similar antiviral activity against HCMV, whereas a statistically significant difference in anti-HSV-1 and anti-HSV-2 activity was observed ($p < 0.05$). These results confirm previous findings that HM samples were endowed with anti-HCMV activity, although to a different extent from sample to sample and from mother to mother (6, 28). Our data evidenced a high activity against HSV-1 and HSV-2, in contrast with other studies that observed weak or no antiviral effect (29–31) for raw HM, whereas, when HM samples were aspirated from the stomachs of the infants within few hours of feeding, they were reported to reduce HSV-1 titers (31). The observed inhibitory activity of milk pools with ID50 around of 0.01 against RSV and 0.05 against HRhV supports
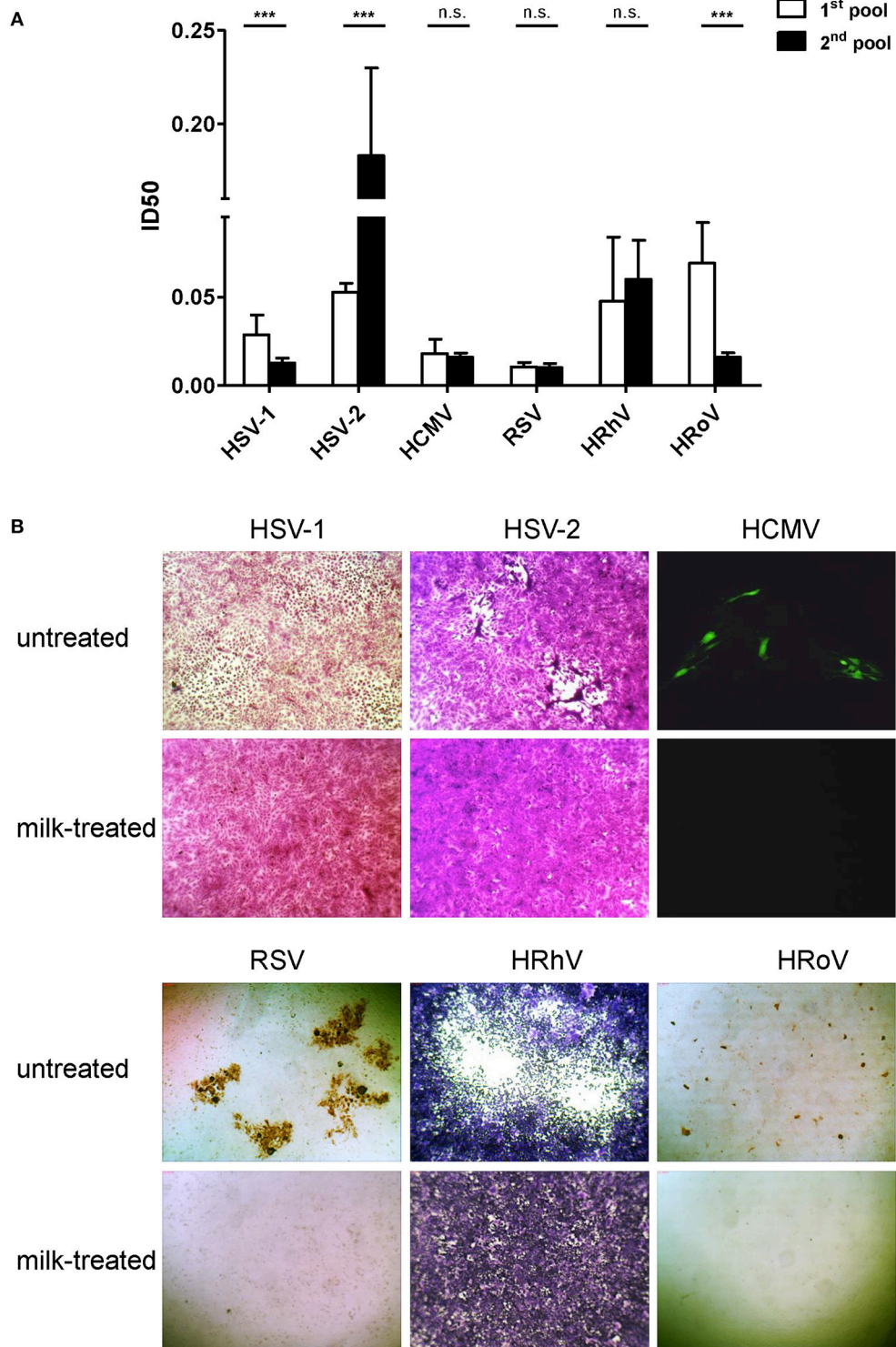
FIGURE 1 | (A) Antiviral activities against HSV-1, HSV-2, HCMV, RSV, HRhV, and HRoV are reported as inhibitory dilution-50 (ID50) values for raw human milk pool #1 (white) and pool #2 (black bar). Data are reported as mean ID50 ± 95% confidence intervals of 4 independent experiments. ID50 values were compared using the sum-of-squares F-test. ***$P < 0.001$; n.s., not significant. (B) Representative examples of plaque reduction assays and fluorescence foci assays of antiviral assays treating infected cells with raw milk samples at a 1:2 dilution, an inhibitory dilution-100 (ID100) for all viruses. Untreated infected (upper row) and milk-treated infected (lower row) fields are reported for HSV-1, HSV-2, HCMV, RSV, HRhV, and HRoV. HSV-1, HSV-2 and HRhV plaques were visualized after crystal violet staining; RSV and HRoV foci were visualized by ICC (magnification 40X). HCMV fluorescent foci were visually counted as green cells at fluorescence microscopy (magnification 100X). HSV-1, HSV-2, and HRhV plaques are violet; HCMV infected cells are green; RSV and HRoV foci are brown.

clinical observations that maternal milk protects infants against respiratory infections, as bronchiolitis, during the first year of life, and encourages breastfeeding as an effective/inexpensive measure of prevention of lower respiratory tract infections in infancy (32, 33). However, a variable antiviral activity of HM was observed against different HRhV serotypes circulating worldwide (6). Although the anti-HRoV activity of lactoferrin and of milk fat globule membrane components that contains bioactive glycoproteins and glycolipids has been widely reported in the past, Pfaender et al. did not evidence a pronounced reduction in viral titers of HRoV by HM (30, 34). By contrast, our study reports a clear anti-HRoV effect for both milk pools, supporting protection of breastfed children against gastrointestinal viral infection. The differences in the serostatus of the donor mothers for each virus along with the interpersonal variability in the content of antiviral components of HM may explain the different

extents of antiviral potencies between the two HM pools, and some inconsistencies with previous literature. **Figure 1B** shows representative images of the total inhibitory effect of raw milk at a 1:2 dilution against all tested viral infections. Of note, all the antiviral activities were not a consequence of cytotoxicity of HM samples, since the CD50 of milk was one or two logarithms greater than the ID50 (data not shown).

Effect of Hop and HTST Methods on Antiviral Activity of HM

The main aim of this work was to assess the impact of two pasteurization methods, HoP and HTST, on the antiviral properties of raw HM. Therefore, in a second set of experiments, aliquots of the HM pools were pasteurized in parallel or left untreated and their antiviral activity was evaluated. **Figure 2**
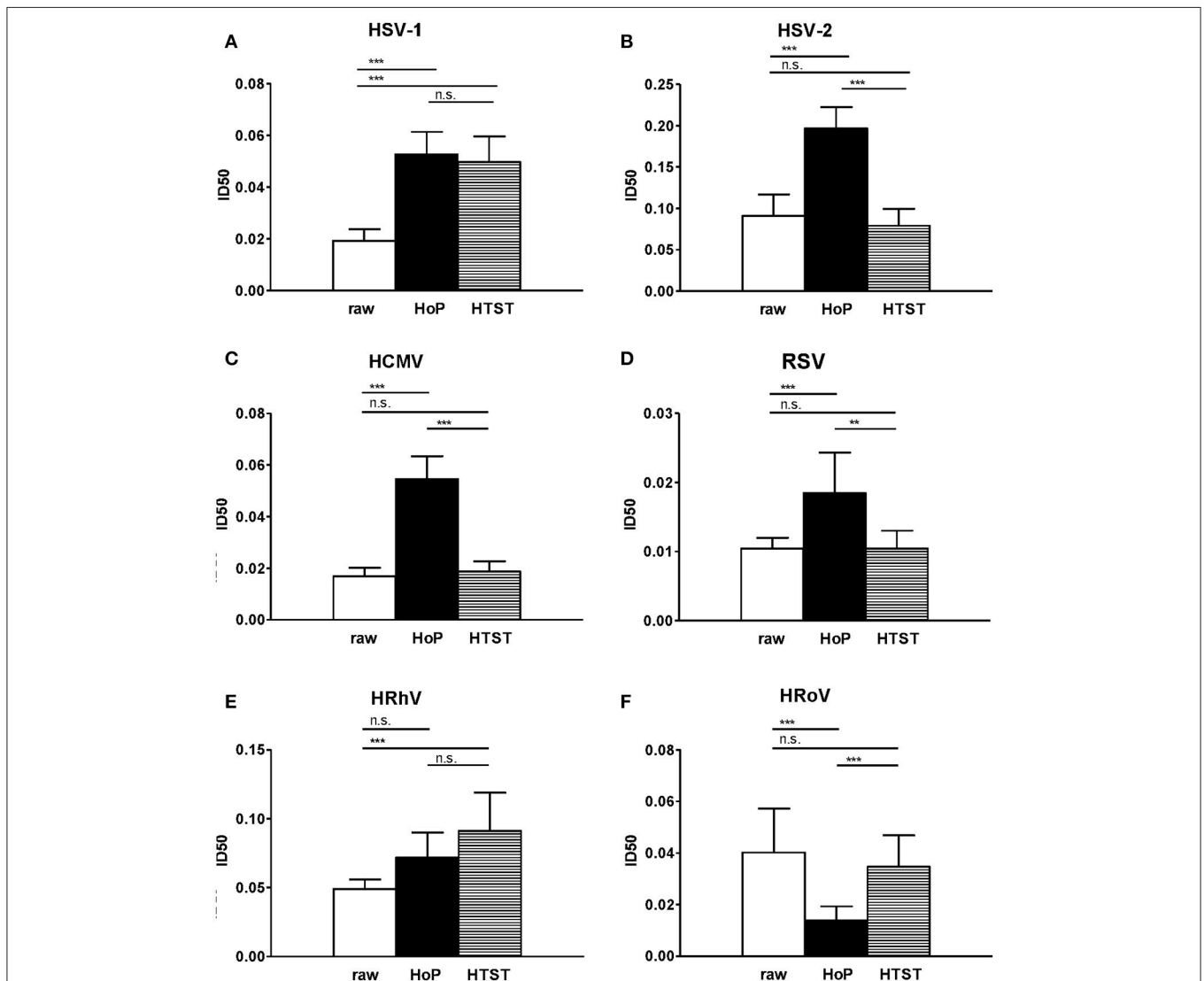
FIGURE 2 | Raw milk (white), Holder pasteurized (HoP, black bar) and HTST pasteurized milk (horizontal striped bar) activities against HSV-1 **(A)**, HSV-2 **(B)**, HCMV **(C)**, RSV **(D)**, HRhV **(E)**, and HRoV **(F)** are reported as a mean ID50 ± 95% confidence intervals of two milk pools. Each pool was tested in 4 independent experiments. ID50 values were compared using the sum-of-squares F-test. $**p < 0.01$; $***P < 0.001$; n.s., not significant.

reports the average of ID50 of the two pools, untreated or pasteurized. The results evidenced a statistically significant reduction of milk antiviral activity following HoP pasteurization against HSV-1, HSV-2, HCMV, RSV, and HRhV infections. These findings may reflect the reduction of specific components with significant immunologic and anti-infective action, such as immunoglobulins and lactoferrin, caused by HoP (16, 17). By contrast, HTST preserved the inhibitory activity of raw milk against most of the tested viruses: no significant difference was evidenced between the ID50 of raw and HTST treated HM samples against HSV-2, HCMV, RSV, and HRoV (**Figure 2**). These data are consistent with previous reports showing that HTST is better than HoP at preserving some biological HM properties, including the antioxidant potential, the lactoferrin content and structure, B and C vitamins, and some cytokines (18). In this experiment, the reliability of such higher biological activity retention is increased by the use of a patented equipment that has a technology readiness level (TRL) of 6, which was directly compared to a commercial HoP device normally used in HMBs. **Figure 2** also showed that HoP and HTST similarly reduced the antiviral activities against HSV-1 and HRhV compared to untreated milk. Unexpectedly, HM anti-HRoV activity was increased by HoP treatment with an ID50 value of 0.014 for pasteurized milk against an ID50 value of 0.04 of raw HM. Although we do not have an explanation for this result, we can speculate that thermal treatment at 62.5°C for 30 min may alter the structure of some HM components thereby increasing their protective activity, such as the release of specific peptides active against HRoV following protein degradation.

CONCLUSION

This study demonstrated that raw HM is endowed with antiviral activity *in vitro* against viral pathogens causing infections in newborns and children. Further studies are needed to investigate the clinical relevance of this activity. HoP method, currently recommended in international guidelines for HMBs, proved to significantly decrease the antiviral activity against HSV-1, HSV-2, HCMV, RSV, and HRhV but not against HRoV. By contrast, HTST preserved antiviral properties of raw HM against four out of six viruses analyzed. These data, along with previous literature, support the HTST as a valid alternative to HoP. Despite the fact that HTST provides a thermal treatment at a higher temperature than HoP (72 vs. 62.5°C, respectively), the far more rapid heating and cooling time of HTST (seconds instead of minutes, respectively) could improve the quality of the final product. This may make HTST suitable for providing the best compromise between microbiological safety and preservation of key biological components and properties of HM, including its antiviral activity.

AUTHOR CONTRIBUTIONS

DL, LC, GM, and EB conceived and designed the study. PT and ACo, collected and pooled the HM samples. MD, MR, RF, and ACi, performed the antiviral assays. LC and MG performed the pasteurizations. MD, LC, and DL analyzed the data. DL, MD, LC, MG, PT, ACo, GM, and EB interpreted the results obtained. MD drafted the manuscript. DL, LC, GM, and EB revised the manuscript. All authors read and approved the final version of the manuscript and agreed to be accountable for all aspects of the work.

FUNDING

REFERENCES

1. Section on Breastfeeding. Breastfeeding and the use of human milk. *Pediatrics* (2012) 129:e827-41. doi: 10.1542/peds.2011-3552
2. WHO/UNICEF. Meeting on infant and young child feeding. *J Nurse Midwifery* (1980) 25:31-8.
3. Horta BL, Victora CG, World Health Organization. Long-term Effects of Breastfeeding: *A Systematic Review*. Geneva:World Health Organization (2013).
4. May JT. Microbial contaminants and antimicrobial properties of human milk. *Microbiol Sci.* (1988) 5:42-6.
5. Yolken RH, Peterson JA, Vonderfecht SL, Fouts ET, Midthun K, Newburg DS. Human milk mucin inhibits rotavirus replication and prevents experimental gastroenteritis. *J Clin Invest.* (1992) 90:1984-91. doi: 10.1172/JCI 116078
6. Clarke NM, May JT. Effect of antimicrobial factors in human milk on rhinoviruses and milk-borne cytomegalovirus in vitro. *J Med Microbiol.* (2000) 49(8):719-23. doi: 10.1099/0022-1317-49-8-719
7. Hanson LA, Lönnroth I, Lange S, Bjersing J, Dahlgren UI. Nutrition resistance to viral propagation. *Nutr Rev.* (2000) 58(2 Pt 2):S31–37. doi: 10.1111/j.1753-4887.2000.tb07801.x
8. Herpes simplex virus [Internet]. World Health Organization. [(Cited Accessed Jun 18, 2018 Jun 18]). Available fromonline at: http://www.who.int/news-room/fact-sheets/detail/herpes-simplex-virus

9. Manicklal S, Emery VC, Lazzarotto T, Boppana SB, Gupta RK. The "silent" global burden of congenital cytomegalovirus. *Clin Microbiol Rev.* (2013) 26(1):86-102. doi: 10.1128/CMR.00062-12
10. Viveros-Rogel M, Soto-Ramirez L, Chaturvedi P, Newburg DS, Ruiz-Palacios GM. Inhibition of HIV-1 infection in vitro by human milk sulfated glycolipids and glycosaminoglycans. *Adv Exp Med Biol.* (2004) 554:481-7.
11. Ng TB, Cheung RCF, Wong JH, Wang Y, Ip DTM, Wan DCC, et al. Antiviral activities of whey proteins. *Appl Microbiol Biotechnol.* (2015) 99(17):6997-7008. doi: 10.1007/s00253-015-6818-4
12. Wakabayashi H, Oda H, Yamauchi K, Abe F. Lactoferrin for prevention of common viral infections. *J Infect Chemother.* (2014) 20(11):666-71. doi: 10.1016/j.jiac.2014.08.003
13. Italian Association of Human Milk Banks Associazione Italiana Banche del Latte Umano Donato (AIBLUD: www.aiblud.com), Arslanoglu S, Bertino E, Tonetto P, De Nisi G, Ambruzzi AM, et al. Guidelines for the establishment and operation of a donor human milk bank. *J Matern-Fetal Neonatal Med.* (2010) 23 (Suppl. 2):1-20. doi: 10.3109/14767058.2010.512414
14. ESPGHAN Committee on Nutrition, Arslanoglu S, Corpeleijn W, Moro G, Braegger C, Campoy C, et al. Donor human milk for preterm infants: current evidence and research directions. *J Pediatr Gastroenterol Nutr.* (2013) 57(4):535-42. doi: 10.1097/MPG.0b013e3182a3af0a
15. Human Milk Banking Association of North America. *Guidelines for the Establishment and Operation of a Donor Human Milk Bank*. Fort Worth, TX, USA. (2018).

16. Peila C, Moro GE, Bertino E, Cavallarin L, Giribaldi M, Giuliani F, et al. The effect of holder pasteurization on nutrients and biologically-active components in donor human milk: a review. *Nutrients* (2016) 8:E477.(8). doi: 10.3390/nu8080477

17. Picaud J-C, Buffin R. Human milk-treatment and quality of banked human milk. *Clin Perinatol.* (2017) 44(1):95–119. doi: 10.1016/j.clp.2016.11.003

18. Peila C, Emmerik NE, Giribaldi M, Stahl B, Ruitenberg JE, van Elburg RM, et al. Human milk processing: a systematic review of innovative techniques to ensure the safety and quality of donor milk. *J Pediatr Gastroenterol Nutr.* (2017) 64(3):353-61. doi: 10.1097/MPG.0000000000001435

19. Giribaldi M, Coscia A, Peila C, Antoniazzi S, Lamberti C, Ortoffi M, et al. Pasteurization of human milk by a benchtop high-temperature short-time device. *Innov Food Sci Emerg Technol.* (2016) 36:228-233. doi: 10.1016/j.ifset.2016.07.004

20. Cavallarin L, Giribaldi M, Antoniazzi S, Bertino E, Coscia A, Gariglio GM. (2015) "*A pasteurizer for continuously treating small volumes of liquid foods*". European Patent n° 2974603, owned by Consiglio Nazionale delle Ricerche, Università degli Studi di Torino, and Giada s.a.s. di Gariglio Gian Marco & C. (Date: Accessed Jan 19.01.17). (2015).

21. Tognon M, Manservigi R, Sebastiani A, Bragliani G, Busin M, Cassai E. Analysis of HSV isolated from patients with unilateral and bilateral herpetic keratitis. *Int Ophthalmol.* (1985) 8(1):13-8.

22. Donalisio M, Quaranta P, Chiuppesi F, Pistello M, Cagno V, Cavalli R, et al. The AGMA1 poly(amidoamine) inhibits the infectivity of herpes simplex virus in cell lines, in human cervicovaginal histocultures, and in vaginally infected mice. *Biomaterials* (2016) 85:40-53. doi: 10.1016/j.biomaterials.2016.01.055

23. Donalisio M, Cagno V, Vallino M, Moro GE, Arslanoglu S, Tonetto P, et al. Inactivation of high-risk human papillomaviruses by Holder pasteurization: implications for donor human milk banking. *J Perinat Med.* (2014) 42(1):1-8. doi: 10.1515/jpm-2013-0200

24. Cagno V, Donalisio M, Civra A, Volante M, Veccelli E, Oreste P, et al. Highly sulfated K5 Escherichia coli polysaccharide derivatives inhibit respiratory syncytial virus infectivity in cell lines and human tracheal-bronchial histocultures. *Antimicrob Agents Chemother.* (2014) 58(8):4782-94. doi: 10.1128/AAC.02594-14

25. Donalisio M, Rusnati M, Cagno V, Civra A, Bugatti A, Giuliani A, et al. Inhibition of human respiratory syncytial virus infectivity by a dendrimeric heparan sulfate-binding peptide. *Antimicrob Agents Chemother* (2012) 56(10):5278-88. doi: 10.1128/AAC.00771-12

26. Donalisio M, Ranucci E, Cagno V, Civra A, Manfredi A, Cavalli R, et al. Agmatine-containing poly(amidoamine)s as a novel class of antiviral macromolecules: structural properties and in vitro evaluation of

infectivity inhibition. *Antimicrob Agents Chemother.* (2014) 58(10):6315-9. doi: 10.1128/AAC.03420-14

27. Lembo D, Donalisio M, Laine C, Cagno V, Civra A, Bianchini EP, et al. Auto-associative heparin nanoassemblies: a biomimetic platform against the heparan sulfate-dependent viruses HSV-1, HSV-2, HPV-16 and RSV. *Eur J Pharm Biopharm.* (2014) 88(1):275-82. doi: 10.1016/j.ejpb.2014.05.007

28. Donalisio M, Rittà M, Tonetto P, Civra A, Coscia A, Giribaldi M, et al. Anti-Cytomegalovirus Activity in Human Milk and Colostrum from Mothers of Preterm Infants. *J Pediatr Gastroenterol Nutr.* (2018) doi: 10.1097/MPG.0000000000002071. [Epub ahead of print].

29. Lopez I, Quibriac M, Petitjean J, Bazin M, Duhamel JF, Freymuth F. Neutralizing activity against herpes simplex in maternal milk. *Arch Fr Pediatr.* (1989) 46(4):263-5.

30. Pfaender S, Heyden J, Friesland M, Ciesek S, Ejaz A, Steinmann J, et al. Inactivation of hepatitis C virus infectivity by human breast milk. *J Infect Dis.s* (2013) 208(12):1943-52. doi: 10.1093/infdis/jit519

31. Isaacs CE, Kashyap S, Heird WC, Thormar H. Antiviral and antibacterial lipids in human milk and infant formula feeds. *Arch Dis Child* (1990) 65(8):861-4.

32. Lanari M, Prinelli F, Adorni F, Di Santo S, Faldella G, Silvestri M, et al. Maternal milk protects infants against bronchiolitis during the first year of life. Results from an Italian cohort of newborns. *Early Hum Dev.* (2013) 89(Suppl. 1):S51–57. doi: 10.1016/S0378-3782(13)70016-1

33. Oddy WH. A review of the effects of breastfeeding on respiratory infections, atopy, and childhood asthma. *J Asthma* (2004) 41(6):605-21.

34. van der Strate BW, Beljaars L, Molema G, Harmsen MC, Meijer DK. Antiviral activities of lactoferrin. *Antiviral Res.* (2001) 52(3):225-39. doi: 10.1016/S0166-3542(01)00195-4

9. AN ALTERNATIVE PREVENTIVE APPROACH AGAINST HUMAN ROTAVIRUS GASTROENTERITIS

In the last study presented in this thesis, we investigated a potential alternative approach, involving bovine milk, to figh HRoV infections. The main characteristics of HRoV and its pathogenesis have been described in section 3.1.

A growing body of literature has documented the protective effect of bovine colostrum against several viral infections in humans (153–157). Furthermore, vaccination of cows against specific human pathogens results in polyclonal pathogen-specific antibodies in bovine colostrum. The antibodies purified from this hyperimmune bovine colostrum (HBC) have been exploited for the treatment of a variety of gastrointestinal infections caused by pathogenic bacteria or viruses (35,157–161), indicating that HBC could be an alternative source for low-cost virus-specific antibodies. This evidence, together with the high content of antimicrobial peptides and proteins that can stimulate innate antiviral pathways and adaptive immune responses, suggests that bovine colostrum could be exploited as a functional food to protect against viral infections. Indeed, ingestion of HBC has been proposed as an alternative prophylactic approach against HRoV gastroenteritis (162,163). To date, HBC containing HRoV-specific, neutralizing IgG has been produced by immunizing pregnant cows with HRoV vaccine and harvesting colostrum after delivery. However, the additional costs and regulatory and safety issues arising from the use of an HRoV vaccine make it impossible to generate HBC on a large scale. Therefore, we investigated whether the conventional bovine rotavirus vaccine is sufficient to enhance the antiviral properties of bovine colostrum against HRoV.

9.1 Publications

Civra A, Altomare A, Francese R, Donalisio M, Aldini G, Lembo D. <u>Colostrum from cows immunized with a veterinary vaccine against bovine rotavirus displays enhanced in vitro anti-human rotavirus activity</u>. J Dairy Sci. 2019 Jun;102(6):4857-4869. doi: 10.3168/jds.2018-16016. Epub 2019 Apr 10. PMID: 30981494; PMCID: PMC7127701.

In this study, we demonstrated *in vitro* that the conventional bovine rotavirus vaccine is sufficient to enhance the anti-human rotavirus protective efficacy of bovine colostrum, thus providing a conservative approach to produce hyperimmune bovine colostrum, making it exploitable as a functional food.

Colostrum from cows immunized with a veterinary vaccine against bovine rotavirus displays enhanced in vitro anti-human rotavirus activity

Andrea Civra,[1]* Alessandra Altomare,[2]* Rachele Francese,[1] Manuela Donalisio,[1] Giancarlo Aldini,[2]† and David Lembo[1]†
[1]Department of Clinical and Biological Sciences, University of Turin, 10043 Orbassano, Italy
[2]Department of Pharmaceutical Sciences, Università degli Studi di Milano, 20133 Milan, Italy

ABSTRACT

Human rotaviruses represent a major cause of severe diarrheal disease in infants and young children. The limited impact of oral vaccines on global estimates of rotavirus mortality and the suboptimal use of oral rehydration justify the need for alternative prophylactic and therapeutic strategies, especially for immunocompromised hosts. The protective effects of colostrum—the first milk produced during the initial 24 to 48 h after parturition—are well documented in the literature. In particular, the ingestion of hyperimmune bovine colostrum has been proposed as an alternative preventive approach against human rotavirus gastroenteritis. Although the immunization of pregnant cows with human rotavirus boosts the release of specific immunoglobulin G in bovine colostrum, it raises regulatory and safety issues. In this study, we demonstrated that the conventional bovine rotavirus vaccine is sufficient to enhance the anti-human rotavirus protective efficacy of bovine colostrum, thus providing a conservative approach to produce hyperimmune bovine colostrum, making it exploitable as a functional food.
Key words: rotavirus, colostrum, cows, hyperimmune, immunoglobulins

INTRODUCTION

Viral gastroenteritis represents a significant economic and public health burden, causing high morbidity and mortality rates, mainly in the poorest countries (Das et al., 2014). Human rotaviruses (**HRoV**) are a major cause of severe diarrheal disease in infants and young children are the second most common cause of death in children less than 5 years old (Marcotte and Hammarström, 2016). Because no specific antiviral drug is available, conventional treatment for HRoV acute gastroenteritis is largely symptomatic and involves fluid and electrolyte replacement and maintenance of nutrition. Despite the introduction of oral HRoV vaccines that have significantly reduced the incidence of the disease in developed countries (Payne et al., 2013), the impact of this active prophylaxis on global estimates of HRoV mortality has been limited (Tate et al., 2016). This is mainly due to inadequate immunization coverage in lower income countries, where the burden of diarrheal disease is higher and vaccines are mostly needed. In fact, oral vaccines are less immunogenic when given to infants in low-income countries compared with high-income countries for a number of reasons, including transplacental maternally acquired antibodies, breastfeeding, histo blood group antigens, malnutrition, microbiota dysbiosis, and environmental enteropathy. Moreover, the scarce availability of vaccines in these areas, along with their contraindications in immunodeficient patients (Babji and Kang, 2012; Binder et al., 2014; Gaspar et al., 2014; Glass et al., 2014), leave between one-third and one-half of children unprotected from severe HRoV disease (Babji and Kang, 2012). These hindrances, together with the suboptimal use of therapeutic oral rehydration solutions, justify the development of effective alternative prophylactic and therapeutic approaches to prevent and control HRoV gastroenteritis disease, especially for immunocompromised hosts.

Colostrum is the first milk produced by mammary glands during the initial 24 to 48 h after parturition (Tokuyama et al., 1990; Stelwagen et al., 2009), and it represents a unique source of highly concentrated nutritional components (Macy, 1949) and growth factors (Pakkanen and Aalto, 1997) for the gastrointestinal development of mammalian newborns.

More importantly, colostrum provides neonates with essential passive immunity against infectious diseases (Ogra and Ogra, 1978; Morris et al., 1980; Majumdar and Ghose, 1982; Stephan et al., 1990; Tokuyama et al., 1990; Ebina et al., 1992; Cohen, 2006; Stelwagen

et al., 2009). In particular, bovine colostrum (**BC**) has evolved into a highly effective host defense mechanism (Rainard and Riollet, 2006). In ruminants, no transplacental exchange of immune factors occurs in utero; therefore, colostrum and, to a lesser extent, mature milk provide protection through a high immunoglobulin content, without which the newborn would not survive (Larson et al., 1980). The immunoglobulins present in BC are IgG_1, IgG_2, IgA, and IgM (Ogra and Ogra, 1978). The abundance of different immunoglobulin classes in colostrum and milk varies among species, with IgA being predominant in human mammary secretions. In contrast, in BC, IgG_1 is the most represented (Barrington et al., 1997), whereas IgA and IgM are present at much lower concentrations. The BC immunoglobulins, in conjunction with the ability of the ruminant neonatal gut to allow unrestricted passage of the large immunoglobulin molecules, provide the young animal with passive immunization (Bush and Staley, 1980; Moore et al., 2005).

Although the effect of colostrum is species-specific, a growing body of literature has documented the protective effect of BC against several viral infections in humans (Bojsen et al., 2007; Ng et al., 2010; Benson et al., 2012; Inagaki et al., 2014; El-Fakharany et al., 2017).

In particular, vaccination of cows against specific human pathogens results in polyclonal pathogen-specific antibodies in BC. The antibodies purified from this hyperimmune BC (**HBC**) have been exploited for the treatment of a variety of gastrointestinal infections caused by pathogenic bacteria (Playford et al., 2000; Kelly, 2003; Hammarström and Weiner, 2008; Struff and Sprotte, 2008) or viruses (Korhonen et al., 2000; Mehra, 2006; Inagaki et al., 2010, 2013; Ng et al., 2010; Byakwaga et al., 2011; Kramski et al., 2012a,b), indicating that HBC could be an alternative source for low-cost virus-specific antibodies. This evidence, together with the high content of antimicrobial peptides and proteins (e.g., lactoferrin, lactoperoxidase, and lysozyme) that can stimulate innate antiviral pathways and adaptive immune responses (Thapa, 2005; Smolenski et al., 2007; Stelwagen et al., 2009), suggests that BC could be exploited as a functional food to protect against viral infections.

Consistently, ingestion of HBC has been proposed as an alternative prophylactic approach against HRoV gastroenteritis (Ebina et al., 1992; Sarker et al., 1998). To date, HBC containing HRoV-specific, neutralizing IgG has been produced by immunizing pregnant cows with HRoV and harvesting colostrum after delivery. However, the additional costs and regulatory and safety issues arising from the use of an HRoV vaccine make it impossible to generate HBC on a large scale.

The alternative use of BC from nonimmunized cows (**NHBC**) may bypass these limits but, as expected, the literature has shown that NHBC has significantly lower anti-HRoV efficacy (Inagaki et al., 2010). In this study, we present proof-of-concept data showing a protective effect of HBC from cows vaccinated with a conventional bovine rotavirus strain (**BRoV**) against different HRoV genotypes.

MATERIALS AND METHODS

Chemicals

Laemmli buffer, molecular mass standards, and electrophoresis apparatus for one-dimensional electrophoresis were supplied by BioRad Laboratories Inc. (Hercules, CA). β-Mercaptoethanol, dithiothreitol, acetonitrile, SDS, iodoacetamide, formic acid, and all other chemicals used in the experimental work were products of pure analytical grade and purchased from Sigma-Aldrich Corp. (St. Louis, MO). Water and acetonitrile (Optima LC/MS grade) for liquid chromatography/MS analyses were purchased from Fisher Scientific (Loughborough, UK).

Bovine Colostrum Collection

Fresh BC and HBC samples were supplied by Advances in Medicine (AIM, Bologna, Italy). According to the supplier, colostrum was collected from both unvaccinated and vaccinated pregnant dairy Holstein cows. Three cows were immunized by subcutaneous inoculation of the inactivated trivalent vaccine Trivacton 6 (Merial Italia SpA, Milan, Italy) to maintain a maximum rate of antibodies in colostral secretions against *Escherichia coli*, rotavirus, and coronavirus, which are implied in the development of neonatal diarrhea. Vaccination was performed with a 2-injection schedule, administered 2 mo and 4 wk before parturition, respectively. Colostrum from the 3 vaccinated cows was collected until 5 h after birth, pooled, and immediately frozen at −20°C. Concentrations of IgG in whole colostrum samples was 50 mg/mL (protein content: 12%), as assessed by previously described methods (Sacerdote et al., 2013).

After a suitable dilution with demineralized water (1 volume), the suspension was introduced into a sterile beaker (controlled continuous stirring) and heated at ~38°C for about 1 h. The suspension was skimmed by removing the fatty layer using a sterile spatula, and caseins were removed by adjusting the pH to their isoelectric point (pH 4.6 with 1 *M* HCl). After 1 h, the product was centrifuged at 2,500 × *g* for 45 min at 25°C to ensure removal of all caseins. Low-molecular-

weight components, including salts and lactose, were then removed by using hollow-fiber cross-flow filtration cartridges (GE Healthcare Bio-Sciences Corp., West-borough, MA.) with a nominal molecular weight cutoff of 4000 coupled to a tangential flow filtration system equipped with a peristaltic pump essential to keep the flow recirculation continuous (Kross Flo-Tangential flow Filtration System Research III, Spectrum Laboratories Inc., Rancho Dominguez, CA). The pH of the retentate was then adjusted to 7.0 ± 0.2 with 1 M NaOH, the neutralized sample was centrifuged at $12,000 \times g$ for 40 min at 25°C, and the supernatant was retained. The next steps consisted of clarification through 0.45- and 0.22-µm filters followed by lyophilization.

Bovine IgG Purification

Affinity Chromatography. Immunoglobulin G was purified by affinity chromatography, using protein G from streptococci as the stationary phase, immobilized in a preparative chromatographic column. In detail, the affinity column was prepared by packing 400 mL of Protein G Sepharose 4 Fast Flow resin (GE Healthcare, Chicago, IL) in a HiScale 50 column support (GE Healthcare), which was connected to a fast protein liquid chromatography (FPLC) system (ÄKTAprime plus, GE Healthcare). Chromatographic purification started by eluting the column with 5 volumes ($5 \times$ chromatographic bed volume) of buffer A (binding buffer: 20 mM sodium phosphate, pH 7), and then the sample was loaded at a flow rate of 20 mL/min. The eluate was monitored by a UV detector at 280 nm, a conductivity meter (0.001–999.9 mS/cm), and a pH meter; all fractions characterized by significant UV absorption were automatically collected (IgG-depleted fractions). The subsequent step consisted of recovering the IgG fractions (IgG-enriched fractions) by eluting the column with 100% elution buffer (1 M glycine hydrochloride pH 2.5). Column regeneration was carried out by eluting 5 volumes ($5 \times$ chromatographic bed volume) of 20% ethanol.

Tangential Flow Filtration. The IgG-enriched and IgG-depleted fractions obtained above were mixed and subjected to concentration and desalting using hollow-fiber cross-flow filtration cartridges with a nominal molecular weight cutoff of 3000 and a surface area of 650 cm^2 (GE Healthcare) coupled to a tangential flow filtration system equipped with a peristaltic pump essential to keep the flow recirculation continuous (Kross Flo- Tangential flow Filtration System Research III). The IgG-enriched and IgG-depleted fractions were concentrated 20 to 30 times, dialyzed with 5 volumes of water, filtered through 0.22-µm membranes in sterile conditions, and finally lyophilized.

Separation of Proteins on Polyacrylamide Gel

One-dimensional (SDS-PAGE) protein separation was performed under reducing conditions; 10-µL aliquots of samples containing 20 to 25 µg of protein were mixed with 10 µL of Laemmli sample buffer containing 50 mM dithiothreitol and heated at 95°C for 5 min. Samples and a standard protein mixture (Precision Plus Protein Standards, BioRad Laboratories Inc.) were loaded on precast gels (Any KD Mini Protean TGX, BioRad Laboratories Inc.) and then placed in the electrophoresis cell (Mini-Protean Tetra) and run at 200 V (constant) for 30 to 40 min. Staining was carried out using Coomassie blue stain (Biosafe G250 Stain, BioRad Laboratories Inc.) and the images acquired by using the BioRad GS800 densitometer and analyzed using the software Quantity One 1-D (BioRad Laboratories Inc.).

IgG and IgM Analysis by Size Exclusion Chromatography

The IgG contents of the IgG-enriched and IgG-depleted fractions were then determined by size exclusion chromatography (**SEC**) according to the method reported by Altomare et al. (2016b); SEC was performed on a Thermo Finnigan Surveyor HPLC system (ThermoFinnigan Italia, Milan, Italy) equipped with a variable wavelength detector and an auto-sampler, controlled by Xcalibur software (version 2.0.7 Thermo Fisher Scientific, Rodano, Italy). The SEC separation was performed on a 4.6- $\times$ 300-mm Phenomenex Yarra 3u SEC-3000 column (Phenomenex Inc., Torrance, CA), with a 4 $\times$ 3 mm GFC4000 pre-column (Phenomenex Inc.), by running an isocratic flow of mobile phase containing 0.1 M sodium phosphate bibasic, 0.025% sodium azide, pH 6.8, at a constant flow rate of 0.5 mL/min. The autosampler temperature was set at 8°C and UV detection was conducted at a wavelength of 280 nm, typical wavelength for protein detection. The dipeptide tyrosine-histidine (**TH**) was chosen as internal standard, because it marks the racing front, being the smallest analyte. All samples were previously spiked with a small amount of TH (10 µL) in order to obtain a final concentration of 0.3 mM.

Cell Lines and Viruses

African green monkey kidney epithelial cells (MA104) and human epithelial adenocarcinoma HeLa cells (ATCC CCL-2) were propagated in Dulbecco's modified Eagle's medium (**DMEM**; Gibco-BRL, Gaithersburg, MD) supplemented with heat-inactivated 10% fetal bovine serum (Gibco-BRL) and 1% antibiotic-antimycotic

solution (Zell Shield, Minerva Biolabs GmbH, Berlin, Germany), at 37°C in an atmosphere of 5% of CO_2. African green monkey kidney cells (Vero cells; ATCC CCL-81) were grown as monolayers in Eagle's minimal essential medium (Gibco/BRL) supplemented with 10% fetal bovine serum and 1% antibiotic-antimycotic solution. The HRoV strains Wa (ATCC VR-2018), HRV408 (ATCC VR-2273), and HRV248 (ATCC VR-2274) and the BRoV strain NCDV (ATCC VR-1290) were activated with 5 µg/mL porcine pancreatic trypsin type IX (Sigma-Aldrich Co.) for 30 min at 37°C and propagated in MA104 cells using DMEM containing 0.5 µg of trypsin per mL as described previously (Civra et al., 2015). Viral titers are expressed as focus-forming units (**FFU**) per milliliter. A serologic characterization of the rotaviruses exploited in this study is provided in Table 1. Human rhinovirus (**HRhV**) 1A (ATCC VR-1559) was propagated in HeLa cells at 34°C in a humidified 5% CO_2 incubator. Clinical isolates of human herpes simplex virus type 1 (**HSV1**) and type 2 (**HSV2**) were provided by M. Pistello (University of Pisa, Italy). Human cytomegalovirus (**HCMV**) strain Towne was provided by W. Brune (Heinrich Pette Institut, Hamburg, Germany). Vesicular stomatitis virus (**VSV**; ATCC VR-1238), HCMV, HSV1, and HSV2 were propagated in Vero cells at 37°C in a humidified 5% CO_2 incubator. When the full cytopathic effect developed, cells and supernatants were harvested, pooled, frozen and thawed 3 times, clarified, and aliquoted. Viruses were stored at −70°C. Viral titers were determined by the standard plaque method as described previously (Civra et al., 2014; Cagno et al., 2017), and expressed as plaque-forming units per milliliter (PFU/mL).

Focus Reduction Assay

Antiviral activity of NHBC, HBC, or IgG against HRoV Wa, HRV408, HRV248, and NCDV was determined by focus reduction assay or plaque reduction assay. Assays of inhibition of rotavirus infectivity were carried out with confluent MA104 cell monolayers plated in 96-well trays, as described elsewhere (Civra et al., 2014). Cells were treated for 2 h at 37°C with serial dilutions of colostrum, at protein concentrations ranging from 0.02 to 3,340 µg of protein/mL in serum-free medium before virus addition. Infection with HRoV was performed at a multiplicity of infection (**MOI**) of 0.02 FFU/mL for 1 h at 37°C, in presence of the colostrums. Infected cells were washed with serum-free medium, fresh methanol extract was added, and cells were incubated in this medium at 37°C in a humidified incubator in 5% (vol/vol) CO_2 in 95% (vol/vol) air. After 16 h of incubation, infected cells were fixed with

Table 1. Rotavirus strains used in this study[1]

Strain	Origin	Serotype[2]
Wa	Human	G1[P8]
HRV408	Human	Natural reassortant G3[P?]
HRV248	Human	Natural reassortant G4[P4]
NCDV	Bovine	G6[P1]

[1]The characteristics of the rotavirus strains are from Parrón et al. (2018) and Rahman et al. (2012).
[2][P?] = P genotype unknown.

cold acetone-methanol (50:50), and viral titers determined by indirect immunostaining by using a mouse monoclonal antibody directed to human rotavirus VP6 (0036; Covalab, Villeurbanne, France), and the secondary antibody peroxidase-conjugated AffiniPure F(ab′)$_2$ Fragment Goat Anti-Mouse IgG (H$^+$L) (Jackson ImmunoResearch Laboratories Inc., West Grove, PA).

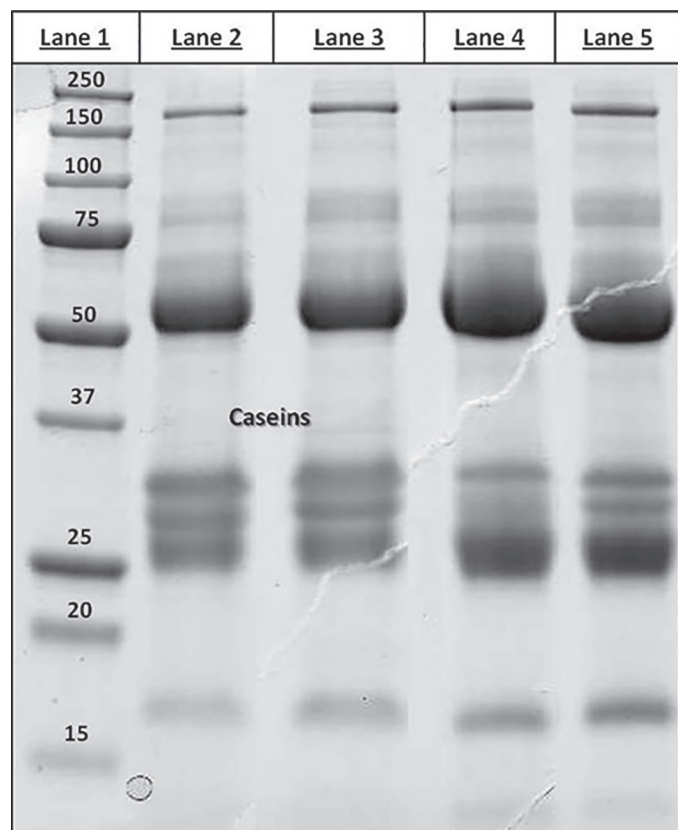**Figure 1.** Sodium dodecyl sulfate-PAGE profiling of colostrum proteins. Lane 1 = Precision Plus Protein Standard (BioRad Laboratories, Hercules, CA); lane 2 = untreated bovine colostrum; lane 3 = untreated hyperimmune bovine colostrum; lane 4 = bovine colostrum defatted, casein-depleted, dialyzed, and filtered; lane 5 = hyperimmune bovine colostrum defatted, casein-depleted, dialyzed, and filtered.

Plaque Reduction Assay

For the plaque reduction assay, HeLa or Vero cells were first seeded (at 8×10^4 cells/well) in 24-well plates. Twenty-four hours later, HBC, NHBC, or IgG was serially diluted in medium (from 0.02 to 3,340 µg of protein/mL) and added to cell monolayers. After 2 h of incubation (37°C, 5% CO_2), medium was removed and infection was performed with 200 µL/well of HRhV 1A, VSV, HSV-1, HSV-2, or HCMV at an MOI of 0.0002 PFU/mL in presence of colostrums. The infected cells were incubated at 34°C for HRhV infections or 37°C for the other viruses for 1 h, washed with medium, and overlaid with a 1:1 combination of 1.6% SeaPlaque Agarose and 2× DMEM containing the colostrums. Control wells (100% of infection) were prepared by treating cells with equal volumes of culture medium. The plates were incubated at 34°C or 37°C for 3 d. After incubation, the plates were fixed with 7.5% formaldehyde (Fluka, Bucharest, Romania) and stained with crystal violet (Sigma-Aldrich Co.). The number of plaques formed was counted.

Rotavirus Neutralization Assay

Immunoglobulin G precipitated with ammonium sulfate (**AS**) was added at a 90% effective concentration (**EC$_{90}$**) to 2×10^5 FFU/mL of trypsin-activated RoV suspension and mixed in a total volume of 200 µL. Untreated or negative controls were performed with an equal volume of culture medium or AS supernatant.
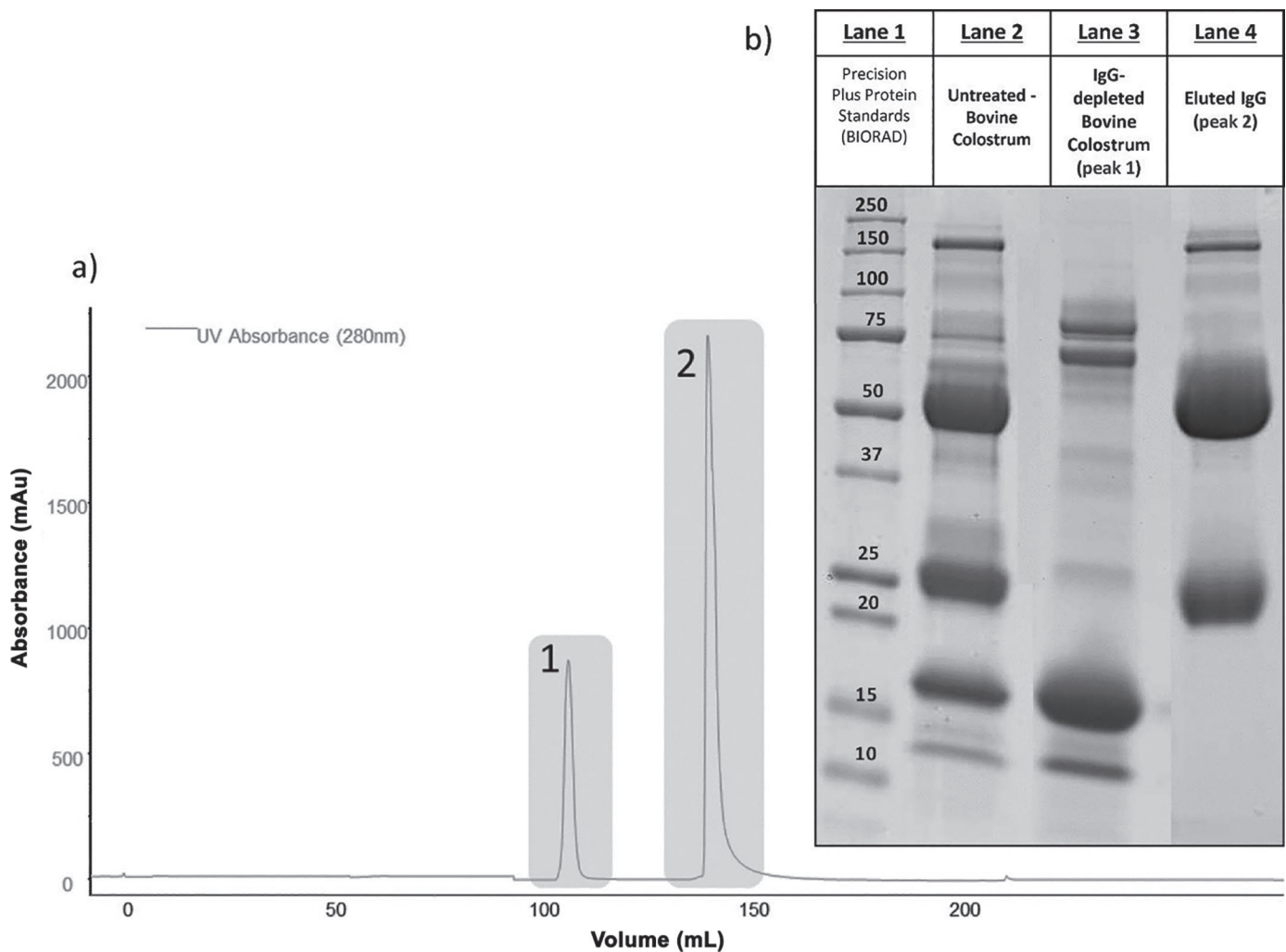
Figure 2. Purification of IgG by affinity chromatography. (a) Fast protein liquid chromatography-UV chromatogram of the untreated-bovine colostrum (casein-depleted and defatted colostrum) obtained by using protein G as affinity stationary phase; peaks 1 and 2 represent, respectively, the IgG-depleted and IgG-enriched fractions as demonstrated by the SDS-PAGE patterns. (b) Gel electrophoretic pattern of peaks 1 (lane 3) and 2 (lane 4) compared with the untreated bovine colostrum pattern, run under reducing conditions. The characteristic bands at 25 and 50 Da are evident in peak 2 and negligible in peak 1. BIORAD = BioRad Laboratories (Hercules, CA).

The virus-compound mixtures were incubated for 1 h at 37°C, serially diluted to the noninhibitory concentration of test IgG, and the residual viral infectivity was determined as previously described (Civra et al., 2014).

Rotavirus-Cell Binding Assay

Rotavirus-cell binding assays were performed as described previously (Civra et al., 2015). Trypsin-activated RoV strains Wa, HRV248, HRV408, and NCDV were treated as described for the neutralization assays. After 1 h, cells were washed with fresh medium and cooled on ice. The RoV were then cooled to 4°C and allowed to attach to cells for 1 h (MOI = 3 FFU/cell) at 4°C. After a wash with cold DMEM, cells were subjected to 2 rounds of freeze/thawing and then incubated at 37°C for 30 min with 10 μg/mL porcine trypsin to release

bound virus. The lysates were then clarified by low-speed centrifugation for 10 min, and cell-bound virus titers were determined by indirect immunostaining as above.

Cell Viability Assay

Cells were seeded at a density of 5×10^3/well in 96-well plates and treated the next day with HBC, NHBC, IgG, or AS supernatant at concentrations ranging from 0.02 to 7,140 μg/mL to generate dose–response curves. Control samples (100% of viability) were prepared by treating cells with culture medium. After 24 or 72 h of incubation, cell viability was determined using a CellTiter 96 Proliferation Assay Kit (Promega, Madison, WI), following the manufacturer's instructions. Absorbances were measured using a Microplate Reader
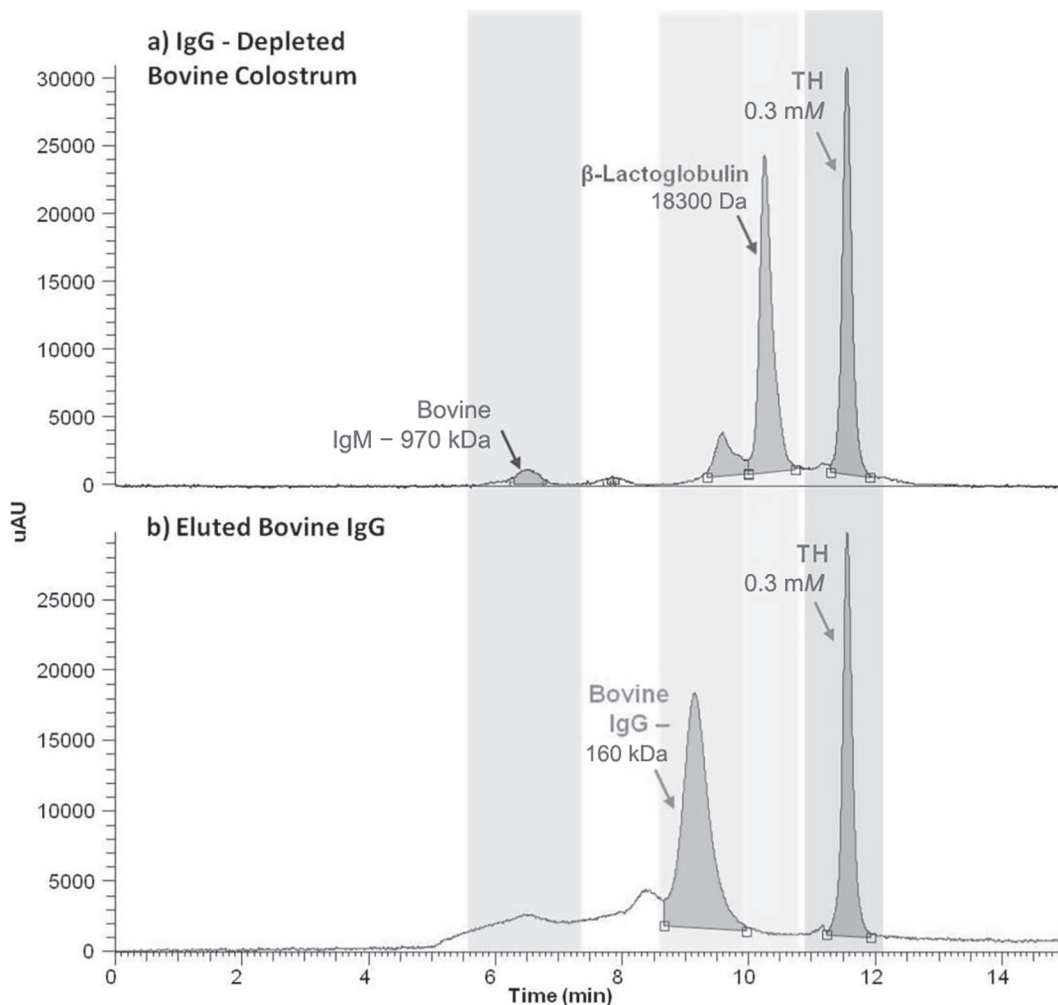

Figure 3. Analysis of IgG by size exclusion chromatography (SEC)-UV; (a) shows the SEC-UV chromatogram of the IgG-depleted bovine colostrum sample, using the dipeptide tyrosine-histidine (TH) as internal standard; (b) shows the SEC-UV chromatogram of IgG purified fraction from bovine colostrum.

(model 680, BioRad Laboratories) at 490 nm. Viability of treated cells was expressed as a percentage relative to cells incubated with culture medium.

Statistical Assessments

Blockades of viral infectivity were expressed as mean percent $\pm$ standard deviation (SD). Where possible, antiviral effective concentration (EC_{50}) values were calculated by regression analysis using the dose–response curves generated from the experimental data, using Prism 4 (GraphPad Software, San Diego, CA). The 50% cytotoxic concentration (CC_{50}) was determined using logarithmic viability curves. Where possible, a selectivity index (SI) was calculated by dividing CC_{50} by EC_{50}. One-way ANOVA followed by Bonferroni test was used to assess the statistical significance of the differences between treated and untreated samples. The EC_{50} values were compared using the sum-of-squares F test. Significance was set at the 95% level.

RESULTS

One-Dimensional Gel Electrophoresis

Figure 1 displays the SDS-PAGE profile of colostrum proteins (under reducing conditions) relative to the following samples: colostrum from nonimmunized (lane 2) and immunized (lane 3) cows and the corresponding defatted, casein-depleted, dialyzed, filtered samples (lanes 4 and 5). As expected, all protein profiles showed 2 intense bands at approximately 50 and 25 kDa, representing the heavy and light IgG chains, respectively. The other bands represent the classical set of high-abundance species normally found in any milk of animal origin (although in colostrum, IgG alone represent ~80% of the total protein mass), including α-lactalbumin (14.1 kDa), β-lactoglobulin (19.9 kDa), serum transferrin (77.7 kDa), and α2-macroglobulin (167.5 kDa). As expected, the protein patterns relative to colostrum samples differed in respect to the corresponding defatted, casein-depleted, dialyzed, filtered samples by a significant reduction in the bands attributable to the caseins (lanes 2 and 3, Figure 1).

Bovine IgG Purification by Affinity Chromatography

Purification of IgG from colostrum collected from nonimmunized and immunized cows was achieved by using a preparative affinity chromatography system based on protein G from streptococci, which is highly selective against bovine IgG.

The affinity chromatogram trace, recorded at 280 nm, displayed 2 peaks: the first (not retained) corresponded to the non-immunoglobulin protein fraction, and the second to the IgG fraction (Figure 2a), the

Table 2. Antiviral activities[1] of bovine colostrums (BC)

BC and virus[2] (strain)	EC_{50} (µg/mL) (95% CI)	EC_{90} (µg/mL) (95% CI)	CC_{50} (µg/mL)	SI
Nonimmune BC				
HSV-1	NA[3]	NA	>6,680	—
HSV-2	NA	NA	>6,680	—
HCMV	NA	NA	>6,680	—
HRhV	NA	NA	>6,680	—
HRoV (Wa)	2.3 (1.6–3.5)	16.3 (6.8–39.1)	>6,680	>2,855
HRoV (HRV408)	12.6 (8.6–18.7)	90 (38–215)	>6,680	>529
HRoV (HRV248)	4.2 (2.4–7.3)	134 (39–454)	>6,680	>1,591
BRoV (NCDV)	61 (44–86)	143 (97–211)	>6,680	>109
VSV	64 (55–75)	343 (252–467)	>6,680	>104
Hyperimmune BC				
HSV-1	NA	NA	>7,140	—
HSV-2	6,018 (2,560–14,110)	NA	>7,140	>1.18
HCMV	NA	NA	>7,140	—
HRhV	NA	NA	>7,140	—
HRoV (Wa)	0.3 (0.3–0.5)	4.5 (2.4–8.5)	>7,140	>21,000
HRoV (HRV408)	2.1 (1.7–2.6)	7.6 (4.7–12.5)	>7,140	>3,449
HRoV (HRV248)	1.6 (1.2–2.8)	8.1 (5.6–11.6)	>7,140	>4,519
BRoV (NCDV)	5.5 (3.7–8.2)	51 (21–122)	>7,140	>1,301
VSV	89 (60–132)	489 (200–1198)	>7,140	>80

[1]EC_{50} = half-maximal effective concentration; EC_{90} = 90% effective concentration; CC_{50} = half-maximal cytotoxic concentration; SI = selectivity index (CC_{50}/EC_{50}).

[22]HSV-1 = herpes simplex type 1; HSV-2 = herpes simplex type 2; HCMV = human cytomegalovirus; HRhV = human rhinovirus; HRoV = human rotavirus; BRoV = bovine rotavirus; VSV = vesicular stomatitis virus.

[3]Not assessable.

peak of which accounted for 80%. The electrophoretic patterns obtained for the 2 collected fractions (Figure 2b) indicated good depletion of immunoglobulins, whose characteristic bands at 160, 50, and 25 kDa were very weak in the aliquot eluted within the first peak and much more intense in the fraction of the second peak, corresponding to the immunoglobulins.

SEC-UV for IgG Analysis

A SEC-UV method was optimized to achieve reproducible separation of the most abundant analytes in bovine colostrum; the method was then applied to

verify the purity of the fractions obtained: the non-immunoglobulin protein fraction and the IgG eluted fraction.

Figure 3 represents typical chromatograms recorded by setting the UV detector at 280 nm and relative to the IgG-depleted (Figure 3a) and IgG-enriched (Figure 3b) fractions, each spiked with the internal standard TH (0.3 mM). The typical retention times for IgG and the dipeptide TH were 9.15 and 11.57 min, respectively. The peak relative to IgG was evident only in the IgG-enriched fraction and absent in the IgG-depleted fraction, which was characterized by other peaks such as representing IgM and β-lactoglobulin
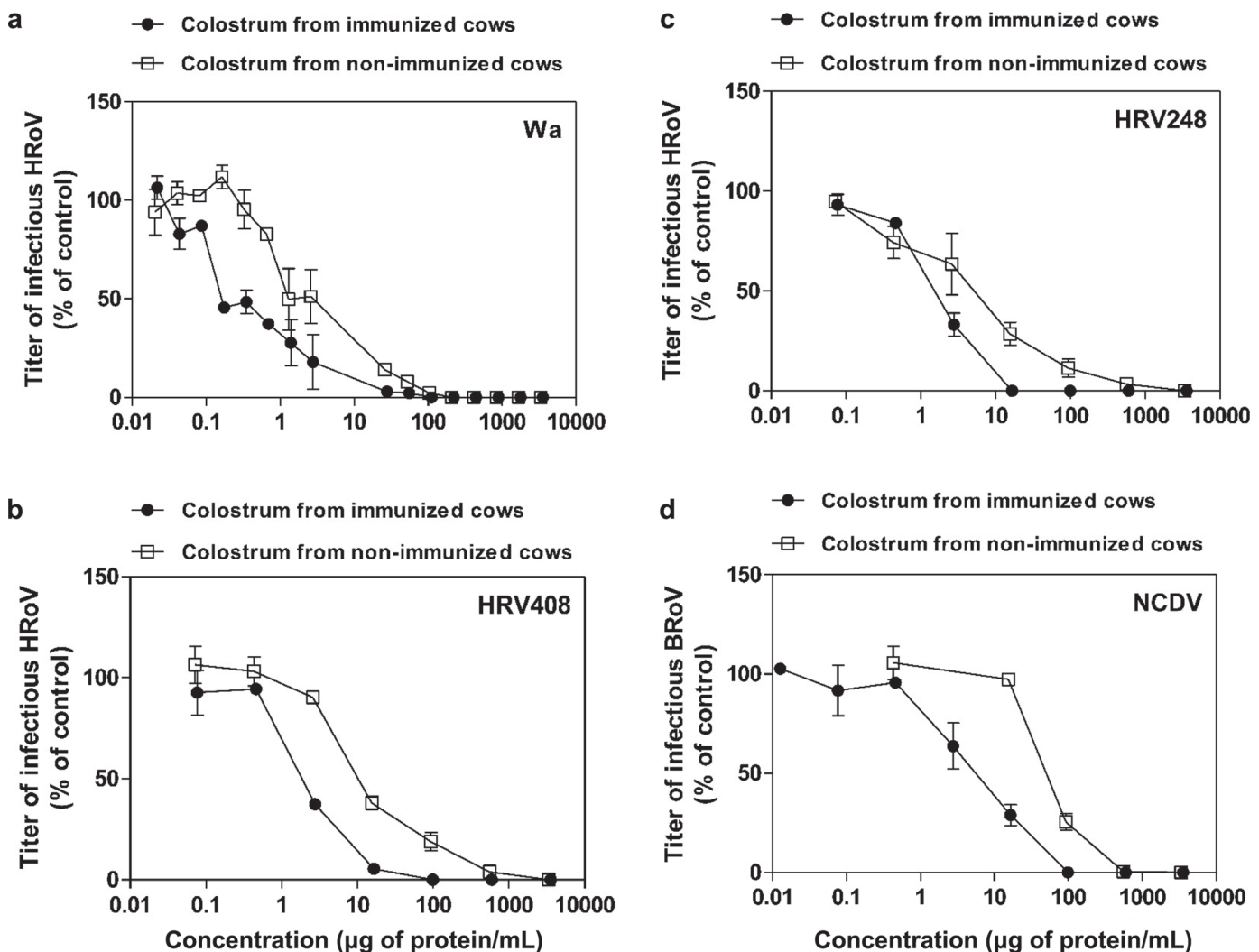
Figure 4. Antiviral activity of colostrum from immunized cows (hyperimmune bovine colostrum, HBC) and colostrum from nonimmunized cows (NHBC) against human rotavirus (HRoV) strains Wa (a), HRV408 (b), and HRV248 (c) and bovine rotavirus (BRoV) strain NCDV (d) on MA104 cells. Cells were treated for 2 h with increasing concentrations of colostrum and then infected in the presence of colostrum. Viral infections were detected as described in the Material and Methods. The percentage infection was calculated by comparing treated and untreated wells. The results are means and SEM for duplicates.

Antiviral Activity Assessment

After their biochemical characterization, colostrums and IgG samples were tested for antiviral activity. The results summarized in Table 2 show that neither NHBC nor HBC had antiviral activity against human pathogens, including HSV-1, HCMV, or HRhV. Although HBC showed a weak antiviral activity against HSV-2, nevertheless it was not able to inhibit viral infectivity to 100%. As expected, NHBC was effective against bovine pathogens such as BRoV NCDV ($EC_{50} = 61.5$ µg of protein/mL) and VSV ($EC_{50} = 64$ µg of protein/mL; Table 2). Of note, NHBC had non-strain-restricted antiviral efficacy against the HRoV strains Wa ($EC_{50} = 2.3$ µg of protein/mL), HRV248 ($EC_{50} = 4.2$ µg of protein/mL), and HRV408 ($EC_{50} = 12.6$ µg of protein/mL) with percentages of inhibition up to 100% (Figure 4). To test the hypothesis that colostrum from cows immunized with a veterinary anti-BRoV vaccine may exert a higher anti-HRoV activity than that from non-immunized cows, we performed a second set of antiviral assays. As expected, HBC exerted significantly ($P < 0.0001$; F test) higher antiviral activity against BRoV NCDV ($EC_{50} = 5.5$ µg of protein/mL), compared with colostrum of nonimmunized cows (Table 2). This result indicates that vaccination elicited an anti-BRoV immune response. Notably, HBC was also significantly ($0.0001 < P < 0.0005$; F test) more effective than NHBC against Wa ($EC_{50} = 0.3$ µg of protein/mL), HRV248 ($EC_{50} = 1.6$ µg of protein/mL), and HRV408 ($EC_{50} = 2.1$ µg of protein/mL; Table 2), suggesting a high titer of cross-reactive IgG in HBC. Therefore, we performed a third set of experiments to test the presence of anti-HRoV IgG in HBC-derived IgG. The results shown in Table 3 and Figure 5 demonstrate that these IgG inhibit the infectivity of BRoV strain NCDV ($EC_{50} = 6.2$ µg of protein/mL) but, more interestingly,

also have strong antiviral activity against HRoV strains Wa ($EC_{50} = 1.9$ µg of protein/mL), HRV248 ($EC_{50} = 0.7$ µg of protein/mL), and HRV408 ($EC_{50} = 1.8$ µg of protein/mL) with percentages of inhibition up to 100%. As a negative control for IgG antiviral assays, we treated cells with equal volumes of IgG-depleted AS supernatant; results shown in Table 3 and Figure 5 show that the IgG-depleted AS supernatant did not have significant antiviral activity. Notably, treatment of the different cell lines with NHBC, HBC, and IgG did not affect cell viability, even at high concentrations, showing that the antiviral activity we observed was not caused by nonspecific cytotoxic effects.

Mechanism of action experiments show that these IgG neutralize virus infectivity by significantly ($0.0103 < P < 0.0155$; ANOVA) inhibiting RoV-cell binding (Figure 6a,b,c). More importantly, the significant ($0.0005 < P < 0.0183$; ANOVA) neutralization of viral infectivity observed in virus inactivation assays (Figure 6d,e,f) was consistent with a neutralizing activity of virus-specific antibodies targeting RoV surface antigens, rather than cellular receptors.

DISCUSSION

The supportive properties of BC when consumed by other mammalian species, including pigs and humans, are well documented in the medical literature (Bridger and Brown, 1981; Pakkanen and Aalto, 1997; Gopal and Gill, 2000; He et al., 2001; Solomons, 2002; Uruakpa et al., 2002; Boudry et al., 2007; Struff and Sprotte, 2007). Emerging evidence indicates that BC is a promising nutraceutical that could prevent or mitigate various diseases in newborns and adults (Bagwe et al., 2015), in particular gastrointestinal infections. Consistent with these findings, in this study we confirmed the protective activity of NHBC against HRoV, which is

Table 3. Antiviral activities[1] of IgG from hyperimmune bovine colostrum

Sample and virus[2] (strain)	EC_{50} (µg/mL) (95% CI)	EC_{90} (µg/mL) (95% CI)	CC_{50} (µg/mL)	SI
IgG				
HRoV (Wa)	1.9 (1.4–2.6)	19.7 (10.4–37.1)	>5,910	>3,110
HRoV (HRV408)	1.8 (0.8–3.9)	12.6 (2.5–63.2)	>5,910	>3,283
HRoV (HRV248)	0.7 (0.6–0.9)	8.2 (4.9–13.9)	>5,910	>8,443
BRoV (NCDV)	6.2 (5.2–7.4)	30.2 (19.7–49.0)	>5,910	>953
Ammonium sulfate supernatant				
HRoV (Wa)	NA[3]	NA	>5,910	NA
HRoV (HRV408)	NA	NA	>5,910	NA
HRoV (HRV248)	NA	NA	>5,910	NA
BRoV (NCDV)	NA	NA	>5,910	NA

[1]EC_{50} = half-maximal effective concentration; EC_{90} = 90% effective concentration; CC_{50} = half-maximal cytotoxic concentration; SI = selectivity index (CC_{50}/EC_{50}).

[2]HRoV = human rotavirus; BRoV = bovine rotavirus.

[3]Not assessable.

well documented in the literature (Inagaki et al., 2010, 2013). Of note, NHBC also showed antiviral activity against several HRoV strains and, as expected, against BRoV strain NCDV, at concentrations comparable to those previously shown (Inagaki et al., 2013).

In our experimental setting, NHBC showed no significant antiviral activity against 4 viral pathogens; namely, HRhV, HCMV, HSV-1, and HSV-2. These results show that BC is not a broad-spectrum antiviral but rather it exerts specific antiviral activities. It is likely that this antiviral specificity and potency reflects the immunological status of the animal.

Boosting the natural concentrations of immune components in colostrum and milk by vaccinating cows offers great potential for their use as prophylactic or therapeutic products in humans. Hyperimmune BC from cows vaccinated with HRoV was an effective

therapeutic approach to reduce the duration and severity of RoV-caused diarrhea in a double-blind controlled clinical study with infants of 6 to 24 mo of age (Mitra et al., 1995). In a second study, Davidson et al. (1989) produced HBC by introducing a vaccine containing 4 HRoV into pregnant Friesian cows. They demonstrated that this HBC administered orally mediated protection by preventing HRoV infection. Efficacy of passive immunization with HBC-derived IgG is documented in the literature. Hilpert et al. (1987) treated infants hospitalized with acute diarrhea with anti-rotavirus immunoglobulin concentrate without observing a significant decrease in duration of diarrhea or excretion of virus. Turner and Kelsey (1993) demonstrated a reduction in incidence and duration of diarrhea in treated infants. Sarker et al. (1998) produced HBC by immunizing pregnant cows with HRoV strains Wa, RV3, RV5, and
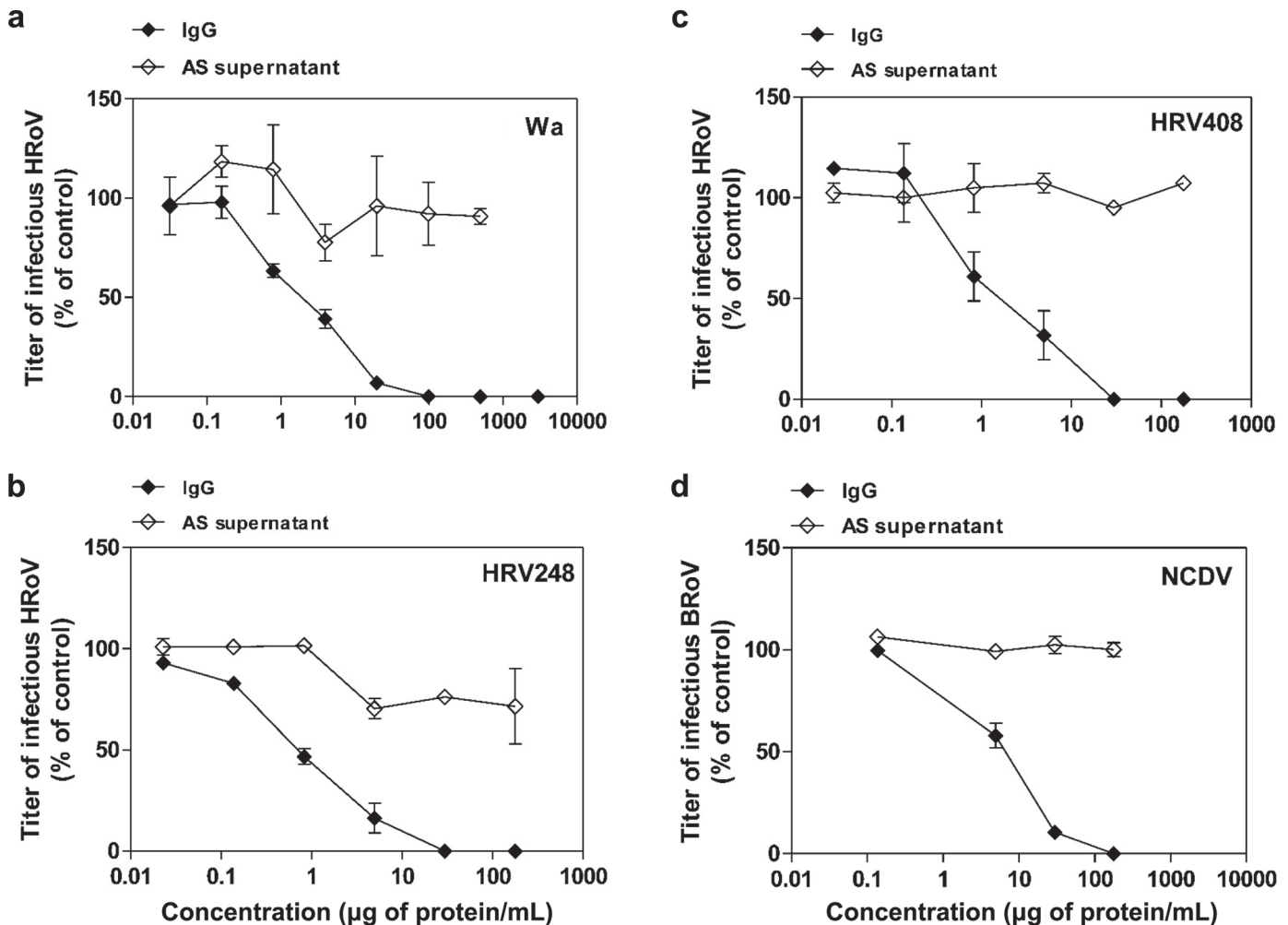
Figure 5. Antiviral activity of hyperimmune bovine colostrum (HBC)-derived IgG or ammonium sulfate (AS) supernatant against human rotavirus (HRoV) strains Wa (a), HRV248 (b), and HRV408 (c) and bovine rotavirus (BRoV) strain NCDV (d) on MA104 cells. Viral infections were detected as described in Material and Methods. The percentage infection was calculated by comparing treated and untreated wells. The results are means and SEM for duplicates.

ST3 (representing serotypes 1 to 4, respectively). The HBC-purified IgG were then administered in a double-blind placebo-controlled trial to children with diagnosed HRoV diarrhea. Children who received HBC-IgG had significantly less daily and total stool output and frequency and required less oral rehydration solution than did children who received placebo. However, it is difficult to generate large-scale amounts of HBC by immunizing cows with an unconventional HRoV vaccine; indeed, the yield is insufficient to cover the global requirement because over 500,000 deaths occur worldwide every year due to rotavirus-induced diarrhea (Bagwe et al., 2015). To overcome these limitations, we proposed and tested

the hypothesis that HBC from cows immunized with a conventional veterinary vaccine against BRoV would exert a higher anti-HRoV activity than NHBC due to a high titer of cross-reactive anti-HRoV IgG. Indeed, our results confirm this hypothesis and indicate an easier and cheaper approach for the production of anti-HRoV HBC or IgG in cows. We demonstrated an in vitro HRoV inhibition efficacy (i.e., EC_{50}) of HBC comparable to that of Inagaki and colleagues, who treated MA104 cells with skimmed and concentrated bovine late colostrum from HRoV-immunized cows (Inagaki et al., 2010, 2013). We demonstrated that HBC and its IgG can inhibit the infectivity of 4 RoV with 4 different
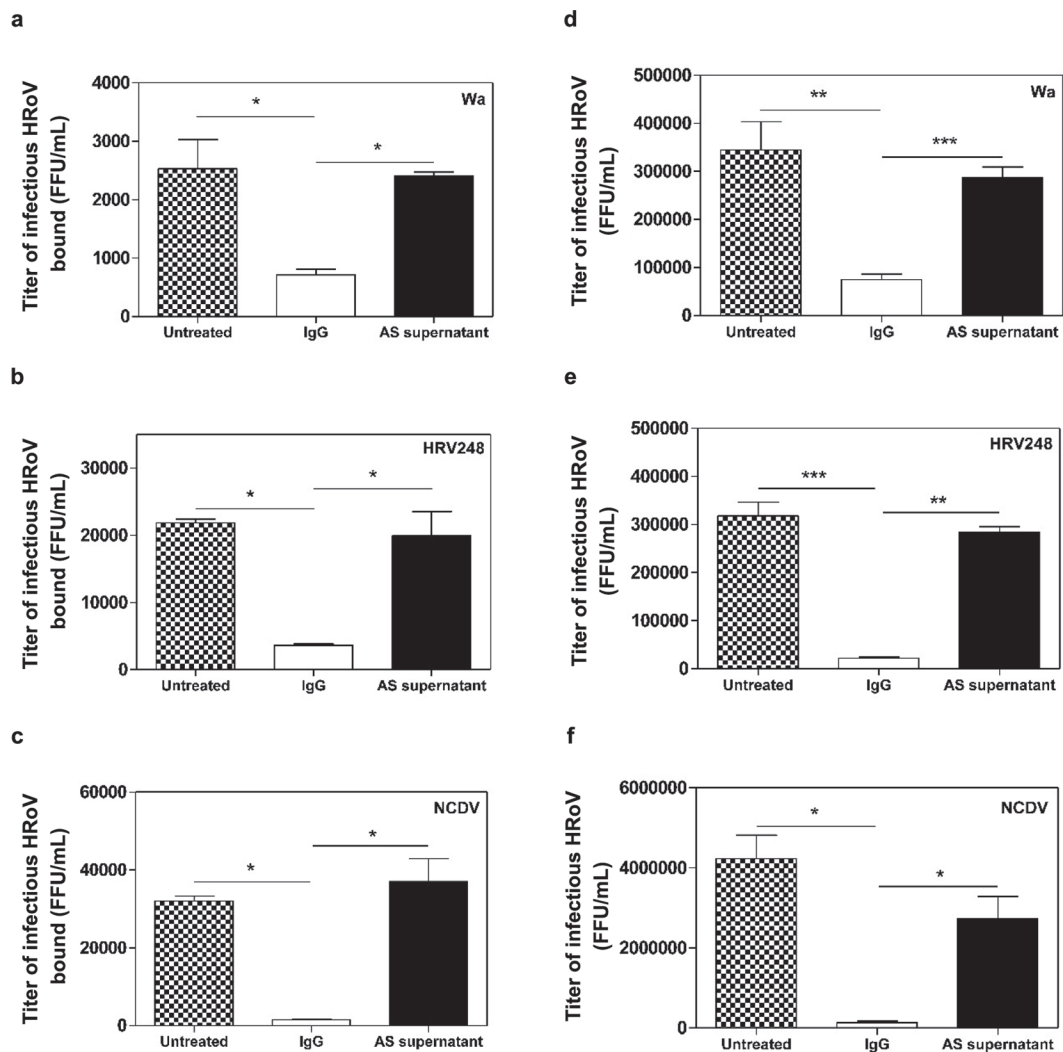
Figure 6. Mechanism of action of hyperimmune bovine colostrum (HBC)-derived IgG, untreated colostrum, or ammonium sulfate (AS) supernatant on rotavirus strains. Panels a, b, and c show the effect of HBC-derived IgG on Wa, HRV248, and NCDV, respectively, binding to the MA104 cell surface. Panels d, e, and f show the results of virus inactivation assays on infectious particles of Wa, HRV248, and NCDV, respectively. On the y-axis, the infectious titers of HRoV are expressed as focus-forming units per milliliter (FFU/mL). Error bars represent the SEM of independent experiments. $*P < 0.05$, $**P < 0.001$, $***P < 0.0001$. HRoV = human rotavirus; BRoV = bovine rotavirus.

GP genotypes (Table 1), suggesting that vaccination with BRoV stimulates the production of cross-reactive neutralizing antibodies.

With a view to exploiting HBC as a source of anti-HRoV IgG, quality assessment procedures are necessary to monitor the IgG content; nevertheless, these techniques are already available and well documented in the literature (Altomare et al., 2016a). Moreover, cows produce BC in large excess respective to the amount needed to feed their calves: cows produce about 33 L of colostrum each day in the first days after parturition, but just 4 to 6 L/d is administered to the calf during the first 2 d (Devery-Pocius and Larson, 1983).

Overall, we demonstrated that the conventional BRoV vaccine is sufficient to boost the anti-HRoV protective efficacy of BC. This represents a conservative, feasible, and not yield-limiting approach to produce HBC that could be exploited as a functional food to prevent and treat HRoV infections.

ACKNOWLEDGMENTS

REFERENCES

Altomare, A., E. Fasoli, M. Colzani, X. M. Paredes Parra, M. Ferrari, F. Cilurzo, C. Rumio, L. Cannizzaro, M. Carini, P. G. Righetti, and G. Aldini. 2016a. An in depth proteomic analysis based on ProteoMiner, affinity chromatography and nano-HPLC-MS/MS to explain the potential health benefits of bovine colostrum. J. Pharm. Biomed. Anal. 121:297–306.

Altomare, A., L. Regazzoni, X. M. P. Parra, F. Selmin, C. Rumio, M. Carini, and G. Aldini. 2016b. Set-up and application of an analytical approach for the quality control of purified colostrum as food supplement. J. Chromatogr. B Analyt. Technol. Biomed. Life Sci. 1028:130–144.

Babji, S., and G. Kang. 2012. Rotavirus vaccination in developing countries. Curr. Opin. Virol. 2:443–448.

Bagwe, S., L. J. Tharappel, G. Kaur, and H. S. Buttar. 2015. Bovine colostrum: An emerging nutraceutical. J. Complement. Integr. Med. 12:175–185.

Barrington, G. M., T. E. Besser, W. C. Davis, C. C. Gay, J. J. Reeves, and T. B. McFadden. 1997. Expression of immunoglobulin G1 receptors by bovine mammary epithelial cells and mammary leukocytes. J. Dairy Sci. 80:86–93.

Benson, K. F., S. G. Carter, K. M. Patterson, D. Patel, and G. S. Jensen. 2012. A novel extract from bovine colostrum whey supports anti-bacterial and anti-viral innate immune functions in vitro and in vivo: I. Enhanced immune activity in vitro translates to improved microbial clearance in animal infection models. Prev. Med. 54:S116–S123.

Binder, H. J., I. Brown, B. S. Ramakrishna, and G. P. Young. 2014. Oral rehydration therapy in the second decade of the twenty-first century. Curr. Gastroenterol. Rep. 16:376–384.

Bojsen, A., J. Buesa, R. Montava, A. S. Kvistgaard, M. B. Kongsbak, T. E. Petersen, C. W. Heegaard, and J. T. Rasmussen. 2007. Inhibitory activities of bovine macromolecular whey proteins on rotavirus infections in vitro and in vivo. J. Dairy Sci. 90:66–74.

Boudry, C., A. Buldgen, D. Portetelle, A. Collard, A. Thewis, and J. P. Dehoux. 2007. Effects of oral supplementation with bovine colostrum on the immune system of weaned piglets. Res. Vet. Sci. 83:91–101.

Bridger, J. C., and J. F. Brown. 1981. Development of immunity to porcine rotavirus in piglets protected from disease by bovine colostrum. Infect. Immun. 31:906–910.

Bush, L. J., and T. E. Staley. 1980. Absorption of colostral immunoglobulins in newborn calves. J. Dairy Sci. 63:672–680.

Byakwaga, H., M. Kelly, D. F. Purcell, M. A. French, J. Amin, S. R. Lewin, H. Haskelberg, A. D. Kelleher, R. Garsia, M. A. Boyd, D. A. Cooper, and S. Emery. 2011. CORAL Study Group. Intensification of antiretroviral therapy with raltegravir or addition of hyperimmune bovine colostrum in HIV-infected patients with suboptimal CD4+ T-cell response: A randomized controlled trial. J. Infect. Dis. 204:1532–1540.

Cagno, V., A. Civra, D. Rossin, S. Calfapietra, C. Caccia, V. Leoni, N. Dorma, F. Biasi, G. Poli, and D. Lembo. 2017. Inhibition of herpes simplex-1 virus replication by 25-hydroxycholesterol and 27 hydroxycholesterol. Redox Biol. 12:522–527.

Civra, A., V. Cagno, M. Donalisio, F. Biasi, G. Leonarduzzi, G. Poli, and D. Lembo. 2014. Inhibition of pathogenic non-enveloped viruses by 25-hydroxycholesterol and 27-hydroxycholesterol. Sci. Rep. 4:7487.

Civra, A., M. G. Giuffrida, M. Donalisio, L. Napolitano, Y. Takada, B. S. Coulson, A. Conti, and D. Lembo. 2015. Identification of equine lactadherin-derived peptides that inhibit rotavirus infection via integrin receptor competition. J. Biol. Chem. 290:12403–12414.

Cohen, S. M. 2006. Jaundice in the full-term newborn. Pediatr. Nurs. 32:202–208.

Das, J. K., R. A. Salam, and Z. A. Bhutta. 2014. Global burden of childhood diarrhea and interventions. Curr. Opin. Infect. Dis. 27:451–458.

Davidson, G. P., P. B. Whyte, E. Daniels, K. Franklin, H. Nunan, P. I. McCloud, A. G. Moore, and D. J. Moore. 1989. Passive immunisation of children with bovine colostrum containing antibodies to human rotavirus. Lancet 2:709–712.

Devery-Pocius, J. E., and B. L. Larson. 1983. Age and previous lactations as factors in the amount of bovine colostral immunoglobulins. J. Dairy Sci. 66:221–226.

Ebina, T., M. Ohta, Y. Kanamaru, Y. Yamamoto-Osumi, and K. Baba. 1992. Passive immunizations of suckling mice and infants with bovine colostrum containing antibodies to human rotavirus. J. Med. Virol. 38:117–123.

El-Fakharany, E. M., V. N. Uversky, and E. M. Redwan. 2017. Comparative analysis of the antiviral activity of camel, bovine, and human lactoperoxidases against Herpes Simplex virus type 1. Appl. Biochem. Biotechnol. 182:294–310.

Gaspar, H. B., L. Hammarström, N. Mahlaoui, M. Borte, and S. Borte. 2014. The case for mandatory newborn screening for severe combined immunodeficiency (SCID). J. Clin. Immunol. 34:393–397.

Glass, R. I., U. Parashar, M. Patel, J. Gentsch, and B. Jiang. 2014. Rotavirus vaccines: Successes and challenges. J. Infect. 68:S9–18.

Gopal, P. K., and H. S. Gill. 2000. Oligosaccharides and glycoconjugates in bovine milk and colostrum. Br. J. Nutr. 84:S69–S74.

Hammarström, L., and C. K. Weiner. 2008. Targeted antibodies in dairy-based products. Adv. Exp. Med. Biol. 606:321–343.

He, F., E. Tuomola, H. Arvilommi, and S. Salminen. 2001. Modulation of human humoral immune response through orally administered bovine colostrum. FEMS Immunol. Med. Microbiol. 31:93–96.

Hilpert, H., H. Brüssow, C. Mietens, J. Sidoti, L. Lerner, and H. Werchau. 1987. Use of bovine milk concentrate containing antibody to rotavirus to treat rotavirus gastroenteritis in infants. J. Infect. Dis. 156:158–166.

Inagaki, M., H. Muranishi, K. Yamada, K. Kakehi, K. Uchida, T. Suzuki, T. Yabe, T. Nakagomi, O. Nakagomi, and Y. Kanamaru. 2014. Bovine κ-casein inhibits human rotavirus (HRV) infection via direct binding of glycans to HRV. J. Dairy Sci. 97:2653–2661.

Inagaki, M., M. Yamamoto, Xijier, Cairangzhuoma, K. Uchida, H. Yamaguchi, M. Kawasaki, K. Yamashita, T. Yabe, and Y. Kanamaru. 2010. In vitro and in vivo evaluation of the efficacy of bo-

vine colostrum against human rotavirus infection. Biosci. Biotechnol. Biochem. 74:680–682.

Inagaki, M., M. Yamamoto, Cairangzhuoma, Xijier, T. Yabe, K. Uchida, M. Kawasaki, T. Nakagomi, O. Nakagomi, N. Minamoto, and Y. Kanamaru. 2013. Multiple-dose therapy with bovine colostrum confers significant protection against diarrhea in a mouse model of human rotavirus-induced gastrointestinal disease. J. Dairy Sci. 96:806–814.

Kelly, G. S. 2003. Bovine colostra: A review of clinical uses. Altern. Med. Rev. 8:378–394.

Korhonen, H., P. Marnila, and H. S. Gill. 2000. Bovine milk antibodies for health. Br. J. Nutr. 84:S135–S146.

Kramski, M., R. J. Center, A. K. Wheatley, J. C. Jacobson, M. R. Alexander, G. Rawlin, and D. F. Purcell. 2012a. Hyperimmune bovine colostrum as a low-cost, large-scale source of antibodies with broad neutralizing activity for HIV-1 envelope with potential use in microbicides. Antimicrob. Agents Chemother. 56:4310–4319.

Kramski, M., G. F. Lichtfuss, M. Navis, G. Isitman, L. Wren, G. Rawlin, R. J. Center, A. Jaworowski, S. J. Kent, and D. F. Purcell. 2012b. Anti-HIV-1 antibody-dependent cellular cytotoxicity mediated by hyperimmune bovine colostrum IgG. Eur. J. Immunol. 42:2771–2781.

Larson, B. L., H. L. Heary, and J. E. Devery. 1980. Immunoglobulin production and transport by the mammary gland. J. Dairy Sci. 63:665–671.

Macy, I. G. 1949. Composition of human colostrum and milk. Am. J. Dis. Child. 78:589–603.

Majumdar, A. S., and A. C. Ghose. 1982. Protective properties of anticholera antibodies in human colostrum. Infect. Immun. 36:962–965.

Marcotte, H., and L. Hammarström. 2016. Immunodeficiencies: Significance for gastrointestinal disease. Pages 47–72 in Viral Gastroenteritis. Molecular Epidemiology and Pathogenesis. L. Svensson, U. Desselberger, H. B. Greenberg, and M. K. Estes, ed. Academic Press, London, UK.

Mehra, R. 2006. Milk Ig for health promotion. Int. Dairy J. 16:1262–1271.

Mitra, A. K., D. Mahalanabis, H. Ashraf, L. Unicomb, R. Eeckles, and S. Tzipori. 1995. Hyperimmune cow colostrum reduces diarrhoea due to rotavirus: A double-blind, controlled clinical trial. Acta Paediatr. 84:996–1001.

Moore, M., J. W. Tyler, M. Chigerwe, M. E Dawes, and J. R. Middleton. 2005. Effect of delayed colostrum collection on colostral IgG concentration in dairy cows. J. Am. Vet. Med. Assoc. 226:1375–1377.

Morris, J. A., C. Wray, and W. J. Sojka. 1980. Passive protection of lambs against enteropathogenic *Escherichia coli*: Role of antibodies in serum and colostra. J. Med. Microbiol. 13:265–271.

Ng, W. C., V. Wong, B. Muller, G. Rawlin, and L. E. Brown. 2010. Prevention and treatment of influenza with hyperimmune bovine colostrum antibody. PLoS One 5:e13622.

Ogra, S. S., and P. L. Ogra. 1978. Immunological aspects of human colostrum and milk. J. Pediatr. 92:550–555.

Pakkanen, R., and J. Aalto. 1997. Growth factors and antimicrobial factors in bovine colostrum. Int. Dairy J. 7:285–297.

Parrón, J. A., D. Ripollés, A. C. Sánchez, M. D. Pérez, M. Calvo, S. López, C. F. Arias, and L. Sánchezm. 2018. Antirotaviral activity of bovine milk components: Extending the list of inhibitory proteins and seeking a better understanding of their neutralization mechanism. J. Funct. Foods 44:103–111.

Payne, D. C., J. A. Boom, M. A. Staat, K. M. Edwards, P. G. Szilagyi, E. J. Klein, and U. D. Parashar. 2013. Effectiveness of pentavalent and monovalent rotavirus vaccines in concurrent use among US children <5 years of age, 2009–2011. Clin. Infect. Dis. 57:13–20.

Playford, R. J., C. E. Macdonald, and W. S. Johnson. 2000. Colostrum and milk-derived peptide growth factors for the treatment of gastrointestinal disorders. Am. J. Clin. Nutr. 72:5–14.

Rahman, S., K. Higo-Moriguchi, K. W. Htun, K. Taniguchi, F. C. Icatlo Jr., T. Tsuji, Y. Kodama, S. V. Nguyen, K. Umeda, H. N. Oo, Y. Y. Myint, T. Htut, S. S. Myint, K. Thura, H. M. Thu, N. N. Dwi Fatmawati, and K. Oguma. 2012. Randomized placebo-controlled clinical trial of immunoglobulin Y as adjunct to standard supportive therapy for rotavirus-associated diarrhea among pediatric patients. Vaccine 30:4661–4669.

Rainard, P., and C. Riollet. 2006. Innate immunity of the bovine mammary gland. Vet. Res. 37:369–400.

Sacerdote, P., F. Mussano, S. Franchi, A. E. Panerai, G. Bussolati, S. Carossa, A. Bartorelli, and B. Bussolati. 2013. Biological components in a standardized derivative of bovine colostrum. J. Dairy Sci. 96:1745–1754.

Sarker, S. A., T. H. Casswall, D. Mahalanabis, N. H. Alam, M. J. Albert, H. Brussow, G. J. Fuchs, and L. Hammerstrom. 1998. Successful treatment of rotavirus diarrhea in children with immunoglobulin from immunized bovine colostrum. Pediatr. Infect. Dis. J. 17:1149–1154.

Smolenski, G., S. Haines, F. Y. Kwan, J. Bond, V. Farr, S. R. Davis, K. Stelwagen, and T. T. Wheeler. 2007. Characterisation of host defence proteins in milk using a proteomic approach. J. Proteome Res. 6:207–215.

Solomons, N. W. 2002. Modulation of the immune system and the response against pathogens with bovine colostrum concentrates. Eur. J. Clin. Nutr. 56:S24–S28.

Stelwagen, K., E. Carpenter, B. Haigh, A. Hodgkinson, and T. T. Wheeler. 2009. Immune components of bovine colostrum and milk. J. Anim. Sci. 87:3–9.

Stephan, W., H. Dichtelmuller, and R. Lissner. 1990. Antibodies from colostrum in oral immunotherapy. J. Clin. Chem. Clin. Biochem. 28:19–23.

Struff, W. G., and G. Sprotte. 2007. Bovine colostrum as a biologic in clinical medicine: A review. Part I: Biotechnological standards, pharmacodynamic and pharmacokinetic characteristics and principles of treatment. Int. J. Clin. Pharmacol. Ther. 45:193–202.

Struff, W. G., and G. Sprotte. 2008. Bovine colostrum as a biologic in clinical medicine: A review—Part II: Clinical studies. Int. J. Clin. Pharmacol. Ther. 46:211–225.

Tate, J. E., A. H. Burton, C. Boschi-Pinto, and U. D. Parashar. 2016. Global, regional, and national estimates of rotavirus mortality in children <5 years of age, 2000–2013. Clin. Infect. Dis. 62:S96–105.

Thapa, B. R. 2005. Health factors in colostrum. Indian J. Pediatr. 72:579–581.

Tokuyama, H., Y. Tokuyama, and S. Migita. 1990. Isolation of two new proteins from bovine colostrum which stimulate epidermal growth factor-dependent colony formation of NRK-49f cells. Growth Factors 3:105–114.

Turner, R. B., and D. K. Kelsey. 1993. Passive immunization for prevention of rotavirus illness in healthy infants. Pediatr. Infect. Dis. J. 12:718–722.

Uruakpa, F. O., M. A. H. Ismond, and E. N. T. Akobundu. 2002. Colostrum and its benefits: A review. Nutr. Res. 22:755–767.

10. DISCUSSION AND CONCLUSION

Due to the epidemiological importance of viral diseases and the difficulties faced in controlling them, the search for new antiviral therapeutic options is essential and urgent. Nevertheless, the discovery of a new antiviral drug is quite challenging. Since viruses are obligatory intracellular pathogens, they are essentially dependent on the machinery and metabolism of a host cell. Therefore, selective toxicity and minimization of major side effects to the host are necessary during the development of new antivirals. In addition to the possibility of resistance presented by certain viral strains, limitations of *in vitro* laboratory techniques and availability of animal models that mimic human infections *in vivo* also hinder the discovery of new candidate molecules for antivirals. For these reasons, the current list of available antivirals is quite limited in terms of number and variety. Moreover, many antiviral drugs on market often present problems that reduce their efficacy, such as limited solubility, a short half-life, or slow, incomplete or highly variable absorption. In this context, research on new antivirals has become extremely important.

During my PhD program, the first line of research was focused on the discovery of new antiviral drugs against both known and emerging viruses. In particular, I focused my attention on the emerging ZIKV and on the well-known HRoV, two viruses that are still without specific antivirals. Compounds of different origins and different properties (chemically synthetized molecules, cholesterol derived molecules, plant extracts and compounds from ethno-medicine) have been investigated.

Two different compounds have been identified as promising antiviral agents against ZIKV and they could be considered a good starting point for the development of novel and efficient antiviral pharmaceuticals. In <u>Francese R et al. (*Antiviral Res*, 2019),</u> we demonstrated that three POMs, TeW_6, $TiW_{11}Co$ and Ti_2PW_{10}, never tested before as antiviral agents, exert a specific and not strain-restricted anti-ZIKV effect. Furthermore, we deeply explored the antiviral mechanism of Ti_2PW_{10}, the POM that showed the most favorable selectivity index, and we demonstrated that it is able to hamper the entry process of ZIKV into the host cells, thus reducing the viral progeny production. These results are in line with the previously reported broad-spectrum antiviral activity and mechanism of action of the POMs class (30,32,164–166). In this study, POMs were tested against ZIKV for the first time and our results indicated that we can include ZIKV in the list of pathogens targeted by the wide spectrum of action of these chemical entities. Further experiments are necessary to identify the cellular localization of this polyanion and to clarify its molecular mechanism of action. Previous POMs studied thus far in biomedical research have exhibited some disadvantages that limited their application in clinical medicine, mainly due to their inorganic nature. At physiological pH, several POM salts are poorly soluble in water or thermodynamically unstable and therefore can undergo

degradation or transformation in toxic metabolites (24,26,167). It's important that POMs used in biological studies are truly solution-stable at physiological pH and in other physico-chemical conditions. POMs of our minilibrary exhibited features that seemed to overcome limitations in the biomedical field. Notably, all three POMs have been found stable in aqueous solution up to 6 months, they showed good biocompatibility in the hemolysis assay, and their tonicity and pH values were suitable for *in vitro* biological studies. Furthermore, a recent study evaluated the toxicity of Ti_2PW_{10} in orally-treated Wistar albino rats. The measurement of biochemical parameters of renal and liver function, and a histopathological analysis of liver tissue showed that the polyanion didn't affect renal function and only induced a mild reversible hepatotoxicity (168). Further studies are required to evaluate the antiviral potency and the biocompatibility in *in vivo* models.

An alternative and complementary strategy to the classical approaches in the antiviral research field, is the study of medicinal plants as natural sources of phytochemicals, such as polyphenols and alkaloids. It is estimated that approximately 25% of modern medicines are derived from natural compounds and hundreds of plant extracts endowed with antiviral properties were recognized by numerous scientific productions reporting both *in vitro* and *in vivo* studies (34). Therefore, in the search for new antiviral candidates against ZIKV, we also explored the antiviral potential of *Punica granatum* derivatives (Acquadro S et al.; *Planta Med*, 2020). We started from the evidence that its extracts exerted inhibitory activity against other viruses, such as HSV-2, HIV-1, and FluV (43–45). We discovered that pomegranate leaf extract and its fractions are active against the MR766 and the HPF2013 ZIKV strains. Moreover, we demonstrated that, between the 11 phenolic and triterpenic compounds isolated from the crude extract, ellagic acid was the one possessing the anti-ZIKV activity and that it acts by preventing ZIKV cell infection. In recent years, this compound has gained attention due to its antioxidant, anticancer, anti-allergic, and anti-inflammatory activities. Its antioxidant properties have been associated with hepatoprotective activity, the attenuation of liver injury during hepatitis B infection, and with therapeutic effects on the survival of influenza-challenged mice, in combination with an antiviral drug and an immunomodulator (169,170). Our data suggested that ellagic acid may be also a promising candidate for the development of a novel anti-ZIKV compound, but we underline that further structural studies and modifications might be needed to improve its selectivity index. Moreover, a key advantage of this approach is that leaf collection is sustainable, as it does not cause damage to the plant during spring pruning or in the fall.

Both Ti_2PW_{10} and ellagic acid have been shown to prevent cell infection and reduce ZIKV progeny production, thus indicating that they could be used for either preventive and therapeutic interventions aimed at impairing the chain of ZIKV congenital transmission. The preventive activity is an important feature in the current context in which an effective vaccine is not available.

Promising compounds active against HRoV were also identified and their mechanism of action was deeply explored. In Civra A et al. (*Redox Biology*, 2018) we found that 25HC and 27HC exerted a remarkable anti-HRoV effect based at least on the impairment of the OSBP/VAP-A interplay and on abnormal cholesterol accumulation within LEs, the last gate for the virus to enter the cytosol. Indeed, since these side chain oxysterols have been shown to drive a number of biochemical reactions within the cells (66), their direct action on LE structure and function cannot be excluded. The substantial accumulation of cholesterol in the late endosomal compartment resulted in sequestering viral particles inside these vesicles thereby preventing cytoplasmic virus replication. We demonstrated, for the first time, that oxysterols can trigger this antiviral mechanism, and that this restriction strategy can block the infectivity of a non-enveloped virus. Notably, the average EC_{50}s of 25HC against HRoV strains, assessed on MA104 and Caco cells, were at supraphysiologic levels, but still in the range of 25HC levels detectable in inflammation-driven processes (171–173). Furthermore, a recent *in vivo* study revealed that the administration of exogenous 25HC at high concentration (50 mg/kg) was not toxic for mice (70). We calculated that the average EC_{50}s of 27HC were, on the contrary, in the physiologic range of concentrations of this oxysterol (173). These considerations means that, theoretically, appropriate stimulation of their enzymatic production or exogenous administration of 25HC and 27HC could be safe antiviral strategies to fight rotavirus gastroenteritis. Finally, our study also provided the proof of concept that accumulation of cholesterol within LEs is an effective anti-HRoV mechanism opening the way to the search for small anti-HRoV molecules endowed with this molecular mechanism.

In line with the previously demonstrated broad-spectrum antiviral activity of oxysterols (57), in Civra A. et al. (*Free Radical Biology and Medicine*, 2020), we demonstrated other two new mechanisms of inhibition of virus entry and diffusion within infected cells mediated by 25HC and 27HC. These molecules were shown able to down-regulate the junction adhesion molecule-A and the cation independent isoform of mannose-6-phosphate receptor, two crucial molecules for a number of viruses to exert infection. This was the first report on cell proteome modulation by two side chain oxysterols, i.e. 25HC and 27HC, certainly of primary interest in human pathophysiology.

As previously performed for ZIKV, we explored medicinal plants as alternative source of antiviral compounds also against the HRoV (Civra A. et al., *BMC Complementary and Alternative Medicine*, 2017). Indeed, several studies reported on anti-HRoV activity by plant extracts (174–178). This second approach resulted in the detection of Rindera lanata (Boraginaceae), a plant from Turkey flora, as possible source of anti-HRoV compounds. We demonstrated that the Rindera lanata extract targets the early steps of HRoV infection, likely by hampering virus penetration into the cells. The favourable selectivity index and the anti-HRoV activity against multiple viral strains make the

Rindera lanata extract a promising starting material for a bioguided-fractionation aimed at identifying anti-HRoV compounds. Among the major phenolic compounds present in the methanol extract of Rindera lanata, hesperidin is known to a have anti-HRoV activity (179) and we could speculate that it might be responsible, at least in part, to the anti-HRoV effect of the extract. Further work remains to be done in order to isolate the active principle, elucidate its mechanism of action and assess its clinical potential. Considering the current problems related to the low efficacy of rotavirus vaccines in some Regions and the relative high mortality rate, a specific anti-HRoV drug is still a necessity. Our works, here discussed, aimed at fulfil this unmet medical need.

Generally, in the absence of an effective vaccine or antiviral drug, the best opportunities to prevent the global spread of a new pathogen or to control new outbreaks of well-known viruses are rapid and early identification systems and individual and government control measures. In this context, we tested the antiviral potential of a nanostructured composite coating deposited on fibre-based air filters (Balagna C. et al., *Surface Coating and Technology*, 2021). We demonstrated that the silver nanocluster/silica coating is endowed with strong virucidal activity against RSV and FluVA, two viruses chosen as representative of the air-transmitted virus category. Our results suggested that this coating deposited on air filters (and cotton textiles) can lead to an important contribution to the viral biological risk restraint, especially but not only, in the health sector. In fact, it can improve the current prevention and safety procedures, also in crowded places or in public transport, kindergartens, offices, gyms, and sports facilities. Furthermore, the antiviral coating can confer an added value to protective clothing such as gowns, masks, or gloves. Recently, in a short communication, our collaborators revealed the virucidal effect of the silver coating (deposited on disposable facemask) also against SARS-CoV-2 (180), underling the importance of this technology in the air-borne pathogen control.

In conclusion, the first line of research of my PhD course resulted in the identification of different antiviral compounds against both known and emerging viruses. Taking into account their good biocompatibility, their high selectivity index and their wide spectrum-antiviral action, Ti_2PW_{10} and the oxysterols, 25HC and 27HC, are the molecules that I consider the most promising for a possible application as antiviral drugs in the near future. Furthermore, we also identified an effective preventive technology against air-borne infections. Ongoing experiments are also testing the antiviral potential of this technology against viruses of the *Coronaviridae* family and are deeply exploring its mechanism of action.

The second line of research of this PhD thesis was aimed at studying the antiviral properties of human milk, both against viruses of pediatric clinical relevance or against recently emerged human

pathogens. Human milk at different stages of maturation and from mothers with term or preterm delivery was employed in the study and we focused on the discovery of milk compounds conferring protection against viral infections.

First, in Donalisio M. et al., *Microorganism*, 2020 and in Civra A. & Francese R., et al., *Journal of Human Lactation*, 2021, we contributed to clarify the mechanisms underlying the protective role of human milk against HCMV, HRoV and RSV infections. We found that HM-EVs are endowed with anti-HCMV, anti-RSV and anti-HRoV activity, although to different extent between different mothers. To the best of our knowledge, these are the first papers reporting the antiviral action of HM-EVs. The results of the antiviral assays indicated that EVs inhibit HCMV, HRoV and RSV by interfering with the early virus-cell interactions. In particular, HCMV attachment to cells and HRoV and RSV entry inside the host cells were the inhibited steps. These results are in line with the previously demonstrated mechanism of action of milk-exosomes (a specific subtype of HM-EVs) against HIV: Näslund and colleagues, indeed, showed that milk exosomes compete with HIV-1 for binding to DC-SIGN receptors on monocyte-derived dendritic cells (181). Furthermore, it was previously demonstrated that cells can take up EVs through a variety of endocytic pathways, including clathrin-dependent endocytosis and clathrin-independent pathways such as macropinocytosis and phagocytosis (182,183). These events may perturb the virus penetration process by inducing a modification of the lipidic composition of cellular membrane, if they occur concomitantly with a virus infection. In addition, it has been demonstrated that EVs exploit viral entry routes to deliver their cargo inside the target cells (184); it is thus likely that EVs compete with HRoV and RSV for the same penetration mechanisms. With the aim of characterizing the potential molecular players of the antiviral activity of HM-EVs, in Donalisio M. et al., we also conducted membrane "shaving" experiments and a proteomic analysis of the shaved peptides. The significant reduction in the antiviral activity of EVs, after shaving experiments, suggested a crucial role of EV surface proteins in inhibiting viral infection. The proteomic analysis of the EV surfaceome revealed the contribution of immune components including antibodies (mainly IgA) and complement component proteins (C9 and C3) to the antiviral activity. We found both milk proteins (caseins, whey proteins and milk fat membrane associated proteins) and proteins shared by different tissue cells and biological fluids. The common feature of the identified proteins is that their glycomoieties seem to play a crucial role in the interference mechanism between a virus and the host cells, acting as a point of cell-specific recognition for the virus particle and inhibiting its attachment on the cell surface.

Additional studies are required to assess whether the EVs could reach the intestinal lumen intact and be absorbed, in order to exert their antiviral action locally, against HRoV, or at distal body sites, against HCMV and RSV. In this regard, recent *in vivo* studies demonstrated that milk exosomes are

long-lasting *in vivo* (185) and accumulate in the intestinal mucosa, spleen, liver, heart or brain when administered orally or intravenously to mice and pigs (138).

Taken together, our results demonstrated that EVs contribute to the overall anti-HCMV, anti-RSV and anti-HRoV activity played by human colostrum *in vitro* and that they should be added to the list of antiviral effectors contained in this complex biofluid. HM-EVs could become a therapeutic option for neonates whose mothers are unable to breastfeed and where receiving donor-expressed breast milk is difficult. This is indeed already a fertile ground for research with multiple neonatal conditions targeted using mesenchymal stem cell (MSC)–derived EVs as "cell free" regenerative medicine (126).

In Francese R. et al., *PLoS Negl Trop Dis,* 2020, we also explored human milk antiviral activity against emerging flaviviruses, namely ZIKV and USUV. We demonstrated that human milk is endowed with antiviral activity against ZIKV and USUV in all the stages of lactation (colostrum, transitional and mature milk) with no significant difference between them. The presence of specific immunoglobulins in the milk samples of the present study was very unlikely, considering the absence of a past travel history in ZIKV endemic areas of the donor mothers and the low seroprevalence of USUV in Europe. The anti-ZIKV and anti-USUV action was therefore attributable to non-specific bioactive factors, acting independently from the mother serostatus. Which is the antiviral potency of colostrum from ZIKV or USUV infected mothers remains an interesting open question. Secondly, we demonstrated that the aqueous fraction of colostrum acts by altering the binding of ZIKV and USUV to cells, thus preventing cellular infection. Given the extremely complex composition of human milk, we hypothesized the presence of one or more factors in human milk able to limit USUV and ZIKV interaction with their cellular receptors. Our hypothesis was confirmed by the demonstration that HM-EVs and HM-GAGs contributed, at least in part, to the anti-flavivirus activity of human milk. Both human milk compounds were previously demonstrated to interfere with the early cell-virus interactions (181,186,187) and, even though our results are preliminary and the mechanism of action has not been investigated yet, we speculate that a similar mechanism of action could be possible against ZIKV and USUV too. Altogether, our data support the WHO recommendations about breast-feeding during ZIKV infection and could contribute to producing new guidelines for a possible USUV epidemic.

Lastly, since human milk from donor milk banks is considered the best alternative when a mother's own milk is not available, in Donalisio M. et al., *Front Pediatr.,* 2018, we investigated the effect of milk pasteurization (a routine procedure in HMBs) on milk's antiviral properties. HoP method, currently recommended in international guidelines for HMBs, proved to significantly decrease the antiviral activity against HSV-1, HSV-2, HCMV, RSV, and HRhV but not against

HRoV. By contrast, HTST preserved the antiviral properties of raw human milk against four out of six viruses analyzed. These data, along with previous literature, supported the HTST as a valid alternative to HoP. Despite the fact that HTST provides a thermal treatment at a higher temperature than HoP (72 vs. 62.5°C, respectively), the far more rapid heating and cooling time of HTST (seconds instead of minutes, respectively) could improve the quality of the final product. This may make HTST suitable for providing the best compromise between microbiological safety and preservation of key biological components and properties of human milk, including its antiviral activity.

In the last article presented in this thesis (Civra A. et al., *J. Dairy Sci*, 2019) we explored the antiviral potential of bovine milk against human viruses. We proposed and tested the hypothesis that hyperimmune bovine colostrum (HBC) from cows immunized with a conventional veterinary vaccine against bovine rotavirus (BRoV) would exert a higher anti-HRoV activity than BC from nonimmunized cows (NHBC), due to a high titer of cross-reactive anti-HRoV IgG. Indeed, our results confirmed this hypothesis and indicated an easier and cheaper approach for the production of anti-HRoV HBC or IgG in cows. We demonstrated an *in vitro* HRoV inhibition efficacy (i.e., EC_{50}) of HBC comparable to that of Inagaki and colleagues (188,189), who treated MA104 cells with skimmed and concentrated bovine late colostrum from HRoV-immunized cows. We demonstrated that HBC and its IgG can inhibit the infectivity of 4 RoV with 4 different GP genotypes, suggesting that vaccination with BRoV stimulates the production of cross-reactive neutralizing antibodies. Moreover, cows produce BC in large excess respective to the amount needed to feed their calves: cows produce about 33 L of colostrum each day in the first days after parturition, but just 4 to 6 L/d is administered to the calf during the first 2 d (190). Overall, we demonstrated that the conventional BRoV vaccine is sufficient to boost the anti-HRoV protective efficacy of BC. This represents a conservative, feasible, and not yield-limiting approach to produce HBC that could be exploited as a functional food to prevent and treat HRoV infections.

In conclusion, the second line of research of my PhD course resulted in the identification of new antiviral compounds, i.e., HM-EVs and HM-GAGs, that are conferred by the mother to the child through lactation. Our results contributed to clarifying the mechanisms underlying the protective effect of human milk against viral infections. Furthermore, we discovered that the antiviral activity of this biofluid can be extended to two emerging flaviviruses, namely ZIKV and USUV, thus underling the importance of supporting breastfeeding even when these infections occur. We gave also a contribution to the HMB field, indicating the pasteurization method that better preserve the antiviral properties of human milk. Generally, our data contributed to gain knowledge in the intricate world of human milk benefits and represented an additional reason to sustain breastfeeding worldwide.

11. REFERENCES

1. Antiviral Agents | DrugBank Online [Internet]. [citato 22 ottobre 2020]. Available at: https://go.drugbank.com/categories/DBCAT000066

2. Commissioner O of the. U.S. Food and Drug Administration [Internet]. FDA. 2020 [citato 22 ottobre 2020]. Available at: https://www.fda.gov/home

3. Gonçalves BC, Lopes Barbosa MG, Silva Olak AP, Belebecha Terezo N, Nishi L, Watanabe MA, et al. Antiviral therapies: advances and perspectives. Fundam Clin Pharmacol. 4 ottobre 2020;

4. Chaudhuri S, Symons JA, Deval J. Innovation and trends in the development and approval of antiviral medicines: 1987-2017 and beyond. Antiviral Res. 2018;155:76–88.

5. DrugVirus.info [Internet]. [citato 22 ottobre 2020]. Available at: https://drugvirus.info/

6. Andersen PI, Ianevski A, Lysvand H, Vitkauskiene A, Oksenych V, Bjørås M, et al. Discovery and development of safe-in-man broad-spectrum antiviral agents. Int J Infect Dis. 1 aprile 2020;93:268–76.

7. Nováková L, Pavlík J, Chrenková L, Martinec O, Červený L. Current antiviral drugs and their analysis in biological materials—Part I: Antivirals against respiratory and herpes viruses. J Pharm Biomed Anal. 5 gennaio 2018;147:400–16.

8. Nováková L, Pavlík J, Chrenková L, Martinec O, Červený L. Current antiviral drugs and their analysis in biological materials – Part II: Antivirals against hepatitis and HIV viruses. J Pharm Biomed Anal. 5 gennaio 2018;147:378–99.

9. Saiz J-C, Vázquez-Calvo Á, Blázquez AB, Merino-Ramos T, Escribano-Romero E, Martín-Acebes MA. Zika Virus: the Latest Newcomer. Front Microbiol. 2016;7:496.

10. Musso D, Roche C, Robin E, Nhan T, Teissier A, Cao-Lormeau V-M. Potential sexual transmission of Zika virus. Emerg Infect Dis. febbraio 2015;21(2):359–61.

11. Motta IJF, Spencer BR, Cordeiro da Silva SG, Arruda MB, Dobbin JA, Gonzaga YBM, et al. Evidence for Transmission of Zika Virus by Platelet Transfusion. N Engl J Med. 15 settembre 2016;375(11):1101–3.

12. Heinz FX, Stiasny K. The Antigenic Structure of Zika Virus and Its Relation to Other Flaviviruses: Implications for Infection and Immunoprophylaxis. Microbiol Mol Biol Rev [Internet]. 1 marzo 2017 [citato 4 dicembre 2020];81(1). Available at: https://mmbr.asm.org/content/81/1/e00055-16

13. Sirohi D, Kuhn RJ. Zika Virus Structure, Maturation, and Receptors. J Infect Dis. 15 dicembre 2017;216(Suppl 10):S935–44.

14. Agrelli A, de Moura RR, Crovella S, Brandão LAC. ZIKA virus entry mechanisms in human cells. Infect Genet Evol J Mol Epidemiol Evol Genet Infect Dis. 2019;69:22–9.

15. Paixão ES, Barreto F, Teixeira M da G, Costa M da CN, Rodrigues LC. History, Epidemiology, and Clinical Manifestations of Zika: A Systematic Review. Am J Public Health. aprile 2016;106(4):606–12.

16. Pacheco LD, Weaver SC, Saade GR. Zika Virus Infection - After the Pandemic. N Engl J Med. 09 2020;382(2):e3.

17. Zika virus [Internet]. [citato 22 ottobre 2020]. Available at: https://www.who.int/news-room/fact-sheets/detail/zika-virus

18. WHO | Zika epidemiology update [Internet]. WHO. [citato 23 ottobre 2020]. Available at: http://www.who.int/emergencies/diseases/zika/epidemiology-update/en/

19. Agarwal A, Chaurasia D. The expanding arms of Zika virus: An updated review with recent Indian outbreaks. Rev Med Virol. n/a(n/a):e2145.

20. Saiz J-C, Martín-Acebes MA. The Race To Find Antivirals for Zika Virus. Antimicrob Agents Chemother [Internet]. 1 giugno 2017 [citato 23 ottobre 2020];61(6). Available at: https://aac.asm.org/content/61/6/e00411-17

21. Silva NM, Santos NC, Martins IC. Dengue and Zika Viruses: Epidemiological History, Potential Therapies, and Promising Vaccines. Trop Med Infect Dis. dicembre 2020;5(4):150.

22. Simonin Y, van Riel D, Van de Perre P, Rockx B, Salinas S. Differential virulence between Asian and African lineages of Zika virus. PLoS Negl Trop Dis. 2017;11(9):e0005821.

23. Pope MT, Kortz U. Polyoxometalates. In: Encyclopedia of Inorganic and Bioinorganic Chemistry. Chichester, UK: John Wiley & Sons, Ltd; 2012.

24. Čolović M, Lacković M, Lalatović J, Mougharbel AS, Kortz U, Krstić DZ. Polyoxometalates in Biomedicine: Update and Overview. Curr Med Chem. 2019;26:1–18.

25. Geisberger G, Paulus S, Gyenge EB, Maake C, Patzke GR. Targeted delivery of polyoxometalate nanocomposites. Small. 2011;7(19):2808–14.

26. Čolović MB, Lacković M, Lalatović J, Mougharbel AS, Kortz U, Krstić DZ. Polyoxometalates in Biomedicine: Update and Overview. Curr Med Chem. 2020;27(3):362–79.

27. Zhao J, Li K, Wan K, Sun T, Zheng N, Zhu F, et al. Organoplatinum-Substituted Polyoxometalate Inhibits β-amyloid Aggregation for Alzheimer's Therapy. Angew Chem - Int Ed. 2019;18032–9.

28. Bijelic A, Aureliano M, Rompel A. The antibacterial activity of polyoxometalates: Structures, antibiotic effects and future perspectives. Chem Commun. 2018;54(10):1153–69.

29. Bijelic A, Aureliano M, Rompel A. Polyoxometalates as Potential Next-Generation Metallodrugs in the Combat Against Cancer. Angew Chem - Int Ed. 2019;58(10):2980–99.

30. Shigeta S, Mori S, Yamase T, Yamamoto N, Yamamoto N. Anti-RNA virus activity of polyoxometalates. Biomed Pharmacother. 2006;60(5):211–9.

31. Wang J, Liu Y, Xu K, Qi Y, Zhong J, Zhang K, et al. Broad-spectrum antiviral property of polyoxometalate localized on a cell surface. ACS Appl Mater Interfaces. 2014;6(12):9785–9.

32. Qi Y, Han L, Qi Y, Jin X, Zhang B, Niu J, et al. Anti-flavivirus activity of polyoxometalate. Antiviral Res. 2020;179:104813.

33. WHO | Herbal medicine research and global health: an ethical analysis [Internet]. WHO. [citato 26 ottobre 2020]. Available at: https://www.who.int/bulletin/volumes/86/8/07-042820/en/

34. Mukhtar M, Arshad M, Ahmad M, Pomerantz RJ, Wigdahl B, Parveen Z. Antiviral potentials of medicinal plants. Virus Res. febbraio 2008;131(2):111–20.

35. Akram M, Tahir IM, Shah SMA, Mahmood Z, Altaf A, Ahmad K, et al. Antiviral potential of medicinal plants against HIV, HSV, influenza, hepatitis, and coxsackievirus: A systematic review. Phytother Res PTR. maggio 2018;32(5):811–22.

36. Frederico ÉHFF, Cardoso ALBD, Moreira-Marconi E, de Sá-Caputo D da C, Guimarães CAS, Dionello C da F, et al. ANTI-VIRAL EFFECTS OF MEDICINAL PLANTS IN THE

MANAGEMENT OF DENGUE: A SYSTEMATIC REVIEW. Afr J Tradit Complement Altern Med AJTCAM. 2017;14(4 Suppl):33–40.

37. Batista MN, Braga ACS, Campos GRF, Souza MM, Matos RPA de, Lopes TZ, et al. Natural Products Isolated from Oriental Medicinal Herbs Inactivate Zika Virus. Viruses. 11 2019;11(1).

38. Benarba B, Pandiella A. Medicinal Plants as Sources of Active Molecules Against COVID-19. Front Pharmacol. 2020;11:1189.

39. Adhikari B, Marasini BP, Rayamajhee B, Bhattarai BR, Lamichhane G, Khadayat K, et al. Potential roles of medicinal plants for the treatment of viral diseases focusing on COVID-19: A review. Phytother Res [Internet]. [citato 26 ottobre 2020];n/a(n/a). Available at: https://onlinelibrary.wiley.com/doi/abs/10.1002/ptr.6893

40. Fellah B, Bannour M, Rocchetti G, Lucini L, Ferchichi A. Phenolic profiling and antioxidant capacity in flowers, leaves and peels of Tunisian cultivars of Punica granatum L. J Food Sci Technol. settembre 2018;55(9):3606–15.

41. Vučić V, Grabež M, Trchounian A, Arsić A. Composition and Potential Health Benefits of Pomegranate: A Review. Curr Pharm Des. 2019;25(16):1817–27.

42. Howell AB, D'Souza DH. The pomegranate: effects on bacteria and viruses that influence human health. Evid-Based Complement Altern Med ECAM. 2013;2013:606212.

43. Arunkumar J, Rajarajan S. Study on antiviral activities, drug-likeness and molecular docking of bioactive compounds of Punica granatum L. to Herpes simplex virus - 2 (HSV-2). Microb Pathog. maggio 2018;118:301–9.

44. Haidari M, Ali M, Ward Casscells S, Madjid M. Pomegranate (Punica granatum) purified polyphenol extract inhibits influenza virus and has a synergistic effect with oseltamivir. Phytomedicine Int J Phytother Phytopharm. dicembre 2009;16(12):1127–36.

45. Neurath AR, Strick N, Li Y-Y, Debnath AK. Punica granatum (pomegranate) juice provides an HIV-1 entry inhibitor and candidate topical microbicide. Ann N Y Acad Sci. novembre 2005;1056:311–27.

46. Bekir J, Mars M, Souchard JP, Bouajila J. Assessment of antioxidant, anti-inflammatory, anti-cholinesterase and cytotoxic activities of pomegranate (Punica granatum) leaves. Food Chem Toxicol Int J Publ Br Ind Biol Res Assoc. maggio 2013;55:470–5.

47. Sadiq A, Bostan N, Yinda KC, Naseem S, Sattar S. Rotavirus: Genetics, pathogenesis and vaccine advances. Rev Med Virol. 2018;28(6):e2003.

48. Rodríguez JM, Luque D. Structural Insights into Rotavirus Entry. In: Greber UF, curatore. Physical Virology: Virus Structure and Mechanics [Internet]. Cham: Springer International Publishing; 2019 [citato 27 ottobre 2020]. pag. 45–68. (Advances in Experimental Medicine and Biology). Available at: https://doi.org/10.1007/978-3-030-14741-9_3

49. Rotavirus ~ ViralZone page [Internet]. [citato 28 dicembre 2020]. Available at: https://viralzone.expasy.org/107?outline=all_by_species

50. Tate JE, Burton AH, Boschi-Pinto C, Parashar UD, World Health Organization–Coordinated Global Rotavirus Surveillance Network. Global, Regional, and National Estimates of Rotavirus Mortality in Children <5 Years of Age, 2000-2013. Clin Infect Dis Off Publ Infect Dis Soc Am. 1 maggio 2016;62 Suppl 2:S96–105.

51. Gleizes O, Desselberger U, Tatochenko V, Rodrigo C, Salman N, Mezner Z, et al. Nosocomial rotavirus infection in European countries: a review of the epidemiology, severity and economic burden of hospital-acquired rotavirus disease. Pediatr Infect Dis J. gennaio 2006;25(1 Suppl):S12-21.

52. Prameela KK, Vijaya LR. The importance of breastfeeding in rotaviral diarrhoeas. Malays J Nutr. aprile 2012;18(1):103–11.

53. Krawczyk A, Lewis MG, Venkatesh BT, Nair SN. Effect of Exclusive Breastfeeding on Rotavirus Infection among Children. Indian J Pediatr. marzo 2016;83(3):220–5.

54. Disease factsheet about rotavirus [Internet]. European Centre for Disease Prevention and Control. [citato 29 ottobre 2020]. Available at: https://www.ecdc.europa.eu/en/rotavirus-infection/facts

55. Folorunso OS, Sebolai OM. Overview of the Development, Impacts, and Challenges of Live-Attenuated Oral Rotavirus Vaccines. Vaccines [Internet]. 27 giugno 2020 [citato 29 ottobre 2020];8(3). Available at: https://www.ncbi.nlm.nih.gov/pmc/articles/PMC7565912/

56. Burnett E, Parashar UD, Tate JE. Real-world effectiveness of rotavirus vaccines, 2006-19: a literature review and meta-analysis. Lancet Glob Health. 2020;8(9):e1195–202.

57. Lembo D, Cagno V, Civra A, Poli G. Oxysterols: An emerging class of broad spectrum antiviral effectors. Mol Aspects Med. 2016;49:23–30.

58. Luu-The V. Assessment of steroidogenesis and steroidogenic enzyme functions. J Steroid Biochem Mol Biol. settembre 2013;137:176–82.

59. Jakobsson T, Treuter E, Gustafsson J-Å, Steffensen KR. Liver X receptor biology and pharmacology: new pathways, challenges and opportunities. Trends Pharmacol Sci. luglio 2012;33(7):394–404.

60. Lappano R, Recchia AG, Francesco EMD, Angelone T, Cerra MC, Picard D, et al. The Cholesterol Metabolite 25-Hydroxycholesterol Activates Estrogen Receptor α-Mediated Signaling in Cancer Cells and in Cardiomyocytes. PLOS ONE. 31 gennaio 2011;6(1):e16631.

61. Raccosta L, Fontana R, Maggioni D, Lanterna C, Villablanca EJ, Paniccia A, et al. The oxysterol-CXCR2 axis plays a key role in the recruitment of tumor-promoting neutrophils. J Exp Med. 26 agosto 2013;210(9):1711–28.

62. Radhakrishnan A, Ikeda Y, Kwon HJ, Brown MS, Goldstein JL. Sterol-regulated transport of SREBPs from endoplasmic reticulum to Golgi: oxysterols block transport by binding to Insig. Proc Natl Acad Sci U S A. 17 aprile 2007;104(16):6511–8.

63. Infante RE, Abi-Mosleh L, Radhakrishnan A, Dale JD, Brown MS, Goldstein JL. Purified NPC1 protein. I. Binding of cholesterol and oxysterols to a 1278-amino acid membrane protein. J Biol Chem. 11 gennaio 2008;283(2):1052–63.

64. Leonarduzzi G, Sottero B, Poli G. Oxidized products of cholesterol: dietary and metabolic origin, and proatherosclerotic effects (review). J Nutr Biochem. dicembre 2002;13(12):700–10.

65. Leonarduzzi G, Gamba P, Sottero B, Kadl A, Robbesyn F, Calogero RA, et al. Oxysterol-induced up-regulation of MCP-1 expression and synthesis in macrophage cells. Free Radic Biol Med. 1 novembre 2005;39(9):1152–61.

66. Vurusaner B, Leonarduzzi G, Gamba P, Poli G, Basaga H. Oxysterols and mechanisms of survival signaling. Mol Aspects Med. 2016;49:8–22.

67. Blanc M, Hsieh WY, Robertson KA, Kropp KA, Forster T, Shui G, et al. The transcription factor STAT-1 couples macrophage synthesis of 25-hydroxycholesterol to the interferon antiviral response. Immunity. 24 gennaio 2013;38(1):106–18.

68. Zhao J, Chen J, Li M, Chen M, Sun C. Multifaceted Functions of CH25H and 25HC to Modulate the Lipid Metabolism, Immune Responses, and Broadly Antiviral Activities. Viruses [Internet]. 6 luglio 2020 [citato 3 novembre 2020];12(7). Available at: https://www.ncbi.nlm.nih.gov/pmc/articles/PMC7411728/

69. Li C, Deng Y-Q, Wang S, Ma F, Aliyari R, Huang X-Y, et al. 25-Hydroxycholesterol Protects Host against Zika Virus Infection and Its Associated Microcephaly in a Mouse Model. Immunity. 21 2017;46(3):446–56.

70. Tricarico PM, Caracciolo I, Gratton R, D'Agaro P, Crovella S. 25-hydroxycholesterol reduces inflammation, viral load and cell death in ZIKV-infected U-87 MG glial cell line. Inflammopharmacology. giugno 2019;27(3):621–5.

71. Liu S-Y, Aliyari R, Chikere K, Li G, Marsden MD, Smith JK, et al. Interferon-inducible cholesterol-25-hydroxylase broadly inhibits viral entry by production of 25-hydroxycholesterol. Immunity. 24 gennaio 2013;38(1):92–105.

72. Zhao J, Chen J, Li M, Chen M, Sun C. Multifaceted Functions of CH25H and 25HC to Modulate the Lipid Metabolism, Immune Responses, and Broadly Antiviral Activities. Viruses [Internet]. 6 luglio 2020 [citato 3 novembre 2020];12(7). Available at: https://www.ncbi.nlm.nih.gov/pmc/articles/PMC7411728/

73. Civra A, Cagno V, Donalisio M, Biasi F, Leonarduzzi G, Poli G, et al. Inhibition of pathogenic non-enveloped viruses by 25-hydroxycholesterol and 27-hydroxycholesterol. Sci Rep. 15 dicembre 2014;4:7487.

74. Roulin PS, Lötzerich M, Torta F, Tanner LB, van Kuppeveld FJM, Wenk MR, et al. Rhinovirus uses a phosphatidylinositol 4-phosphate/cholesterol counter-current for the formation of replication compartments at the ER-Golgi interface. Cell Host Microbe. 12 novembre 2014;16(5):677–90.

75. Arita M, Kojima H, Nagano T, Okabe T, Wakita T, Shimizu H. Oxysterol-binding protein family I is the target of minor enviroxime-like compounds. J Virol. aprile 2013;87(8):4252–60.

76. Bigazzi M, Nardi E, Selvi F. Palynological Contribution to the Systematics of Rindera and the Allied Genera Paracaryum and Solenanthus (Boraginaceae-Cynoglosseae). Willldenowia. 2006;36(1):37–46.

77. Altundag E, Ozturk M. Ethnomedicinal studies on the plant resources of east Anatolia, Turkey. Procedia - Soc Behav Sci. 1 gennaio 2011;19:756–77.

78. Mosaddegh M, Naghibi F, Moazzeni H, Pirani A, Esmaeili S. Ethnobotanical survey of herbal remedies traditionally used in Kohghiluyeh va Boyer Ahmad province of Iran. J Ethnopharmacol. 7 maggio 2012;141(1):80–95.

79. Hodinka RL. Respiratory RNA Viruses. Microbiol Spectr [Internet]. 22 luglio 2016 [citato 5 novembre 2020];4(4). Available at: https://www.asmscience.org/content/journal/microbiolspec/10.1128/microbiolspec.DMIH2-0028-2016

80. Kutter JS, Spronken MI, Fraaij PL, Fouchier RA, Herfst S. Transmission routes of respiratory viruses among humans. Curr Opin Virol. febbraio 2018;28:142–51.

81. Shi T, McLean K, Campbell H, Nair H. Aetiological role of common respiratory viruses in acute lower respiratory infections in children under five years: A systematic review and meta-analysis. J Glob Health. giugno 2015;5(1):010408.

82. Burk M, El-Kersh K, Saad M, Wiemken T, Ramirez J, Cavallazzi R. Viral infection in community-acquired pneumonia: a systematic review and meta-analysis. Eur Respir Rev Off J Eur Respir Soc. giugno 2016;25(140):178–88.

83. Jung HE, Kim TH, Lee HK. Contribution of Dendritic Cells in Protective Immunity against Respiratory Syncytial Virus Infection. Viruses [Internet]. 15 gennaio 2020 [citato 8 novembre 2020];12(1). Available at: https://www.ncbi.nlm.nih.gov/pmc/articles/PMC7020095/

84. Griffiths C, Drews SJ, Marchant DJ. Respiratory Syncytial Virus: Infection, Detection, and New Options for Prevention and Treatment. Clin Microbiol Rev. 1 gennaio 2017;30(1):277–319.

85. Schweitzer JW, Justice NA. Respiratory Syncytial Virus Infection. In: StatPearls [Internet]. Treasure Island (FL): StatPearls Publishing; 2020 [citato 7 novembre 2020]. Available at: http://www.ncbi.nlm.nih.gov/books/NBK459215/

86. RSV | Home | Respiratory Syncytial Virus | CDC [Internet]. 2019 [citato 7 novembre 2020]. Available at: https://www.cdc.gov/rsv/index.html

87. Walsh EE. Respiratory Syncytial Virus infection: an illness for all ages. Clin Chest Med. marzo 2017;38(1):29–36.

88. Global, regional, and national disease burden estimates of acute lower respiratory infections due to respiratory syncytial virus in young children in 2015: a systematic review and modelling study - The Lancet [Internet]. [citato 7 novembre 2020]. Available at: https://www.thelancet.com/journals/lancet/article/PIIS0140-6736(17)30938-8/fulltext

89. Elawar F, Oraby AK, Kieser Q, Jensen LD, Culp T, West FG, et al. Pharmacological targets and emerging treatments for respiratory syncytial virus bronchiolitis. Pharmacol Ther. 27 ottobre 2020;107712.

90. CDC. Types of Influenza Viruses [Internet]. Centers for Disease Control and Prevention. 2019 [citato 13 novembre 2020]. Available at: https://www.cdc.gov/flu/about/viruses/types.htm

91. Hutchinson EC. Influenza Virus. Trends Microbiol. 1 settembre 2018;26(9):809–10.

92. Taubenberger JK, Morens DM. The Pathology of Influenza Virus Infections. Annu Rev Pathol. 2008;3:499–522.

93. Influenza (Seasonal) [Internet]. [citato 13 novembre 2020]. Available at: https://www.who.int/news-room/fact-sheets/detail/influenza-(seasonal)

94. Kumar B, Asha K, Khanna M, Ronsard L, Meseko CA, Sanicas M. The emerging influenza virus threat: status and new prospects for its therapy and control. Arch Virol. 2018;163(4):831–44.

95. Jacobs SE, Lamson DM, St. George K, Walsh TJ. Human Rhinoviruses. Clin Microbiol Rev. gennaio 2013;26(1):135–62.

96. Edwards MR, Ritchie AI, Johnston SL. Exacerbations of chronic respiratory diseases. Rhinovirus Infect. 2019;137–68.

97. Bennett L, Waterer G. Control Measures for Human Respiratory Viral Infection. Semin Respir Crit Care Med. agosto 2016;37(4):631–9.

98. Ferraris M, Balagna C, Perero S. Method for the Application of an Antiviral Coating to a Substrate and Relative Coating [Internet]. 2019 [citato 18 novembre 2020]. Available at: https://patentscope.wipo.int/search/en/detail.jsf;jsessionid=0CD93875A06C45293CD6ABFDC7CF9E36.wapp1nA?docId=WO2019082001&tab=PCTDESCRIPTION

99. Ciriminna R, Albo Y, Pagliaro M. New Antivirals and Antibacterials Based on Silver Nanoparticles. ChemMedChem. 2020;15(17):1619–23.

100. Chen N, Zheng Y, Yin J, Li X, Zheng C. Inhibitory effects of silver nanoparticles against adenovirus type 3 in vitro. J Virol Methods. novembre 2013;193(2):470–7.

101. Xiang D, Chen Q, Pang L, Zheng C. Inhibitory effects of silver nanoparticles on H1N1 influenza A virus in vitro. J Virol Methods. dicembre 2011;178(1–2):137–42.

102. Yang XX, Li CM, Huang CZ. Curcumin modified silver nanoparticles for highly efficient inhibition of respiratory syncytial virus infection. Nanoscale. 7 febbraio 2016;8(5):3040–8.

103. Synthesis and Application of Silver Nanoparticles (Ag NPs) for the Prevention of Infection in Healthcare Workers - PubMed [Internet]. [citato 19 novembre 2020]. Available at: https://pubmed-ncbi-nlm-nih-gov.bibliopass.unito.it/31344881/

104. Lara HH, Garza-Treviño EN, Ixtepan-Turrent L, Singh DK. Silver nanoparticles are broad-spectrum bactericidal and virucidal compounds. J Nanobiotechnology. 3 agosto 2011;9:30.

105. Antiviral and Immunomodulatory Activity of Silver Nanoparticles in Experimental RSV Infection - PubMed [Internet]. [citato 19 novembre 2020]. Available at: https://pubmed-ncbi-nlm-nih-gov.bibliopass.unito.it/31398832/

106. Bahl R, Frost C, Kirkwood BR, Edmond K, Martines J, Bhandari N, et al. Infant feeding patterns and risks of death and hospitalization in the first half of infancy: multicentre cohort study. Bull World Health Organ. giugno 2005;83(6):418–26.

107. Duijts L, Jaddoe VWV, Hofman A, Moll HA. Prolonged and exclusive breastfeeding reduces the risk of infectious diseases in infancy. Pediatrics. luglio 2010;126(1):e18-25.

108. Collins A, Weitkamp J-H, Wynn JL. Why are preterm newborns at increased risk of infection? Arch Dis Child Fetal Neonatal Ed. luglio 2018;103(4):F391–4.

109.   Breastfeeding [Internet]. [citato 19 novembre 2020]. Available at: https://www.who.int/westernpacific/health-topics/breastfeeding

110.   Andreas NJ, Kampmann B, Mehring Le-Doare K. Human breast milk: A review on its composition and bioactivity. Early Hum Dev. 1 novembre 2015;91(11):629–35.

111.   Eriksen KG, Christensen SH, Lind MV, Michaelsen KF. Human milk composition and infant growth. Curr Opin Clin Nutr Metab Care. 2018;21(3):200–6.

112.   Ballard O, Morrow AL. Human Milk Composition: Nutrients and Bioactive Factors. Pediatr Clin North Am. febbraio 2013;60(1):49–74.

113.   Blackshaw K, Valtchev P, Koolaji N, Berry N, Schindeler A, Dehghani F, et al. The risk of infectious pathogens in breast-feeding, donated human milk and breast milk substitutes. Public Health Nutr. 16 giugno 2020;1–16.

114.   Lanzieri TM, Dollard SC, Josephson CD, Schmid DS, Bialek SR. Breast milk-acquired cytomegalovirus infection and disease in VLBW and premature infants. Pediatrics. giugno 2013;131(6):e1937-1945.

115.   Kurath S, Halwachs-Baumann G, Müller W, Resch B. Transmission of cytomegalovirus via breast milk to the prematurely born infant: a systematic review. Clin Microbiol Infect Off Publ Eur Soc Clin Microbiol Infect Dis. agosto 2010;16(8):1172–8.

116.   Henrick BM, Yao X-D, Nasser L, Roozrogousheh A, Rosenthal KL. Breastfeeding Behaviors and the Innate Immune System of Human Milk: Working Together to Protect Infants against Inflammation, HIV-1, and Other Infections. Front Immunol. 2017;8:1631.

117.   Crough T, Khanna R. Immunobiology of human cytomegalovirus: from bench to bedside. Clin Microbiol Rev. gennaio 2009;22(1):76–98, Table of Contents.

118.   Tomtishen JP. Human cytomegalovirus tegument proteins (pp65, pp71, pp150, pp28). Virol J. 17 gennaio 2012;9:22.

119.   Human cytomegalovirus entry into cells - PubMed [Internet]. [citato 30 novembre 2020]. Available at: https://pubmed-ncbi-nlm-nih-gov.bibliopass.unito.it/22440964/

120.   Beltran PMJ, Cristea IM. The life cycle and pathogenesis of human cytomegalovirus infection: lessons from proteomics. Expert Rev Proteomics. dicembre 2014;11(6):697–711.

121. Cytomegalovirus (CMV) and Congenital CMV Infection | CDC [Internet]. 2020 [citato 1 dicembre 2020]. Available at: https://www.cdc.gov/cmv/index.html

122. Gugliesi F, Coscia A, Griffante G, Galitska G, Pasquero S, Albano C, et al. Where do we Stand after Decades of Studying Human Cytomegalovirus? Microorganisms [Internet]. 8 maggio 2020 [citato 1 dicembre 2020];8(5). Available at: https://www.ncbi.nlm.nih.gov/pmc/articles/PMC7284540/

123. Hamprecht K, Goelz R. Postnatal Cytomegalovirus Infection Through Human Milk in Preterm Infants: Transmission, Clinical Presentation, and Prevention. Clin Perinatol. 2017;44(1):121–30.

124. Britt WJ, Prichard MN. New therapies for human cytomegalovirus infections. Antiviral Res. 2018;159:153–74.

125. Introduction to Extracellular Vesicles: Biogenesis, RNA Cargo Selection, Content, Release, and Uptake - PubMed [Internet]. [citato 1 dicembre 2020]. Available at: https://pubmed-ncbi-nlm-nih-gov.bibliopass.unito.it/27053351/

126. O'Reilly D, Dorodnykh D, Avdeenko NV, Nekliudov NA, Garssen J, Elolimy AA, et al. Perspective: The Role of Human Breast-Milk Extracellular Vesicles in Child Health and Disease. Adv Nutr [Internet]. [citato 2 dicembre 2020]; Available at: http://academic.oup.com/advances/advance-article/doi/10.1093/advances/nmaa094/5896686

127. C A, Sm J, Kr Q, Jj F, R L, M N, et al. Exosomes with immune modulatory features are present in human breast milk [Internet]. Vol. 179, Journal of immunology (Baltimore, Md. : 1950). J Immunol; 2007 [citato 2 dicembre 2020]. Available at: http://pubmed.ncbi.nlm.nih.gov/17641064/

128. C M, M P, S W, H A, K B, B S. Human breast milk-derived exosomes attenuate cell death in intestinal epithelial cells [Internet]. Vol. 24, Innate immunity. Innate Immun; 2018 [citato 2 dicembre 2020]. Available at: http://pubmed.ncbi.nlm.nih.gov/29991305/

129. O K, Rs R, C J, Kj B, Ro W, Aa B, et al. Detection of long non-coding RNAs in human breastmilk extracellular vesicles: Implications for early child development [Internet]. Vol. 11, Epigenetics. Epigenetics; 2016 [citato 2 dicembre 2020]. Available at: http://pubmed.ncbi.nlm.nih.gov/27494402/

130. N K, H I, K S, T O. microRNA as a new immune-regulatory agent in breast milk [Internet]. Vol. 1, Silence. Silence; 2010 [citato 2 dicembre 2020]. Available at: http://pubmed.ncbi.nlm.nih.gov/20226005/

131. T C, Qy X, Rs Y, X C, Qe Q, Sb W, et al. Exploration of microRNAs in porcine milk exosomes [Internet]. Vol. 15, BMC genomics. BMC Genomics; 2014 [citato 2 dicembre 2020]. Available at: http://pubmed.ncbi.nlm.nih.gov/24499489/

132. A L, J S, R G, J C, J A, J Z. A diet defined by its content of bovine milk exosomes and their RNA cargos has moderate effects on gene expression, amino acid profiles and grip strength in skeletal muscle in C57BL/6 mice [Internet]. Vol. 59, The Journal of nutritional biochemistry. J Nutr Biochem; 2018 [citato 2 dicembre 2020]. Available at: http://pubmed.ncbi.nlm.nih.gov/29986306/

133. Bc M, Sm J, G S. Milk is not just food but most likely a genetic transfection system activating mTORC1 signaling for postnatal growth [Internet]. Vol. 12, Nutrition journal. Nutr J; 2013 [citato 2 dicembre 2020]. Available at: http://pubmed.ncbi.nlm.nih.gov/23883112/

134. Mj van H, Mi Z, S G, En N-'t H, J G, B S, et al. Comprehensive Proteomic Analysis of Human Milk-derived Extracellular Vesicles Unveils a Novel Functional Proteome Distinct from Other Milk Components [Internet]. Vol. 15, Molecular & cellular proteomics : MCP. Mol Cell Proteomics; 2016 [citato 2 dicembre 2020]. Available at: http://pubmed.ncbi.nlm.nih.gov/27601599/

135. Y L, X D, J L, B L. Human milk exosomes and their microRNAs survive digestion in vitro and are taken up by human intestinal cells. Mol Nutr Food Res [Internet]. 15 agosto 2017 [citato 2 dicembre 2020];61(11). Available at: https://europepmc.org/article/med/28688106

136. Exosomal MicroRNAs in Milk from Mothers Delivering Preterm Infants Survive in Vitro Digestion and Are Taken Up by Human Intestinal Cells - Kahn - 2018 - Molecular Nutrition & Food Research - Wiley Online Library [Internet]. [citato 2 dicembre 2020]. Available at: https://onlinelibrary-wiley-com.bibliopass.unito.it/doi/full/10.1002/mnfr.201701050

137. L L, J D, Pt S, P Y, E F, Kl M, et al. Antigen presentation by exosomes released from peptide-pulsed dendritic cells is not suppressed by the presence of active CTL [Internet]. Vol. 179, Journal of immunology (Baltimore, Md. : 1950). J Immunol; 2007 [citato 2 dicembre 2020]. Available at: http://pubmed.ncbi.nlm.nih.gov/17911587/

138. Manca S, Upadhyaya B, Mutai E, Desaulniers AT, Cederberg RA, White BR, et al. Milk exosomes are bioavailable and distinct microRNA cargos have unique tissue distribution patterns. Sci Rep. 27 luglio 2018;8(1):11321.

139. Ashraf U, Ye J, Ruan X, Wan S, Zhu B, Cao S. Usutu Virus: An Emerging Flavivirus in Europe. Viruses. 19 gennaio 2015;7(1):219–38.

140. Oliveira LG, Peron JPS. Viral receptors for flaviviruses: Not only gatekeepers. J Leukoc Biol. 2019;106(3):695–701.

141. Clé M, Beck C, Salinas S, Lecollinet S, Gutierrez S, Van de Perre P, et al. Usutu virus: A new threat? Epidemiol Infect [Internet]. 4 luglio 2019 [citato 3 dicembre 2020];147. Available at: https://www.ncbi.nlm.nih.gov/pmc/articles/PMC6625183/

142. Roesch F, Fajardo A, Moratorio G, Vignuzzi M. Usutu Virus: An Arbovirus on the Rise. Viruses [Internet]. 12 luglio 2019 [citato 3 dicembre 2020];11(7). Available at: https://www.ncbi.nlm.nih.gov/pmc/articles/PMC6669749/

143. Vilibic-Cavlek T, Petrovic T, Savic V, Barbic L, Tabain I, Stevanovic V, et al. Epidemiology of Usutu Virus: The European Scenario. Pathogens [Internet]. 26 agosto 2020 [citato 3 dicembre 2020];9(9). Available at: https://www.ncbi.nlm.nih.gov/pmc/articles/PMC7560012/

144. Benzarti E, Garigliany M. In Vitro and In Vivo Models to Study the Zoonotic Mosquito-Borne Usutu Virus. Viruses. 30 2020;12(10).

145. Mann TZ, Haddad LB, Williams TR, Hills SL, Read JS, Dee DL, et al. Breast Milk Transmission of Flaviviruses in the Context of Zika Virus: A Systematic Review. Paediatr Perinat Epidemiol. luglio 2018;32(4):358–68.

146. Hubert M, Jeannin P, Burlaud-Gaillard J, Roingeard P, Gessain A, Ceccaldi P-E, et al. Evidence That Zika Virus Is Transmitted by Breastfeeding to Newborn A129 (Ifnar1 Knock-Out) Mice and Is Able to Infect and Cross a Tight Monolayer of Human Intestinal Epithelial Cells. Front Microbiol [Internet]. 22 ottobre 2020 [citato 3 dicembre 2020];11. Available at: https://www.ncbi.nlm.nih.gov/pmc/articles/PMC7649816/

147. Pang W, Lin Y-L, Xin R, Chen X-X, Lu Y, Zheng C-B, et al. Zika virus transmission via breast milk in suckling mice. Clin Microbiol Infect Off Publ Eur Soc Clin Microbiol Infect Dis. 25 aprile 2020;

148. Sampieri CL, Montero H. Breastfeeding in the time of Zika: a systematic literature review. PeerJ [Internet]. 19 febbraio 2019 [citato 3 dicembre 2020];7. Available at: https://www.ncbi.nlm.nih.gov/pmc/articles/PMC6385688/

149. Wesolowska A, Sinkiewicz-Darol E, Barbarska O, Bernatowicz-Lojko U, Borszewska-Kornacka MK, van Goudoever JB. Innovative Techniques of Processing Human Milk to Preserve Key Components. Nutrients [Internet]. 24 maggio 2019 [citato 4 dicembre 2020];11(5). Available at: https://www.ncbi.nlm.nih.gov/pmc/articles/PMC6566440/

150. Breastfeeding SO. Breastfeeding and the Use of Human Milk. Pediatrics. 1 marzo 2012;129(3):e827–41.

151. Peila C, Moro GE, Bertino E, Cavallarin L, Giribaldi M, Giuliani F, et al. The Effect of Holder Pasteurization on Nutrients and Biologically-Active Components in Donor Human Milk: A Review. Nutrients [Internet]. 2 agosto 2016 [citato 4 dicembre 2020];8(8). Available at: https://www.ncbi.nlm.nih.gov/pmc/articles/PMC4997390/

152. ESPGHAN Committee on Nutrition, Arslanoglu S, Corpeleijn W, Moro G, Braegger C, Campoy C, et al. Donor human milk for preterm infants: current evidence and research directions. J Pediatr Gastroenterol Nutr. ottobre 2013;57(4):535–42.

153. Bojsen A, Buesa J, Montava R, Kvistgaard AS, Kongsbak MB, Petersen TE, et al. Inhibitory activities of bovine macromolecular whey proteins on rotavirus infections in vitro and in vivo. J Dairy Sci. gennaio 2007;90(1):66–74.

154. Ng WC, Wong V, Muller B, Rawlin G, Brown LE. Prevention and treatment of influenza with hyperimmune bovine colostrum antibody. PloS One. 26 ottobre 2010;5(10):e13622.

155. Benson KF, Carter SG, Patterson KM, Patel D, Jensen GS. A novel extract from bovine colostrum whey supports anti-bacterial and anti-viral innate immune functions in vitro and in vivo: I. Enhanced immune activity in vitro translates to improved microbial clearance in animal infection models. Prev Med. maggio 2012;54 Suppl:S116-123.

156. El-Fakharany EM, Uversky VN, Redwan EM. Comparative Analysis of the Antiviral Activity of Camel, Bovine, and Human Lactoperoxidases Against Herpes Simplex Virus Type 1. Appl Biochem Biotechnol. maggio 2017;182(1):294–310.

157.   Inagaki M, Yamamoto M, Xijier null, Cairangzhuoma null, Uchida K, Yamaguchi H, et al. In vitro and in vivo evaluation of the efficacy of bovine colostrum against human rotavirus infection. Biosci Biotechnol Biochem. 2010;74(3):680–2.

158.   Playford RJ, Macdonald CE, Johnson WS. Colostrum and milk-derived peptide growth factors for the treatment of gastrointestinal disorders. Am J Clin Nutr. luglio 2000;72(1):5–14.

159.   Kelly GS. Bovine colostrums: a review of clinical uses. Altern Med Rev J Clin Ther. novembre 2003;8(4):378–94.

160.   Struff WG, Sprotte G. Bovine colostrum as a biologic in clinical medicine: a review. Part I: biotechnological standards, pharmacodynamic and pharmacokinetic characteristics and principles of treatment. Int J Clin Pharmacol Ther. aprile 2007;45(4):193–202.

161.   Byakwaga H, Kelly M, Purcell DFJ, French MA, Amin J, Lewin SR, et al. Intensification of antiretroviral therapy with raltegravir or addition of hyperimmune bovine colostrum in HIV-infected patients with suboptimal CD4+ T-cell response: a randomized controlled trial. J Infect Dis. 15 novembre 2011;204(10):1532–40.

162.   Ebina T, Ohta M, Kanamaru Y, Yamamoto-Osumi Y, Baba K. Passive immunizations of suckling mice and infants with bovine colostrum containing antibodies to human rotavirus. J Med Virol. ottobre 1992;38(2):117–23.

163.   Sarker SA, Casswall TH, Mahalanabis D, Alam NH, Albert MJ, Brüssow H, et al. Successful treatment of rotavirus diarrhea in children with immunoglobulin from immunized bovine colostrum. Pediatr Infect Dis J. dicembre 1998;17(12):1149–54.

164.   Qi Y, Xiang Y, Wang J, Qi Y, Li J, Niu J, et al. Inhibition of hepatitis C virus infection by polyoxometalates. Antiviral Res. novembre 2013;100(2):392–8.

165.   Barnard DL, Hill CL, Gage T, Matheson JE, Huffman JH, Sidwell RW, et al. Potent inhibition of respiratory syncytial virus by polyoxometalates of several structural classes. Antiviral Res. marzo 1997;34(1):27–37.

166.   Wang J, Liu Y, Xu K, Qi Y, Zhong J, Zhang K, et al. Broad-spectrum antiviral property of polyoxometalate localized on a cell surface. ACS Appl Mater Interfaces. 25 giugno 2014;6(12):9785–9.

167.   Rhule JT, Hill CL, Judd DA, Schinazi RF. Polyoxometalates in Medicine. Chem Rev. 5 febbraio 1998;98(1):327–58.

168.   Čolović MB, Medić B, Ćetković M, Kravić Stevović T, Stojanović M, Ayass WW, et al. Toxicity evaluation of two polyoxotungstates with anti-acetylcholinesterase activity. Toxicol Appl Pharmacol. 15 2017;333:68–75.

169.   García-Niño WR, Zazueta C. Ellagic acid: Pharmacological activities and molecular mechanisms involved in liver protection. Pharmacol Res. luglio 2015;97:84–103.

170.   Pavlova EL, Simeonova LS, Gegova GA. Combined efficacy of oseltamivir, isoprinosine and ellagic acid in influenza A(H3N2)-infected mice. Biomed Pharmacother Biomedecine Pharmacother. febbraio 2018;98:29–35.

171.   Upston JM, Niu X, Brown AJ, Mashima R, Wang H, Senthilmohan R, et al. Disease stage-dependent accumulation of lipid and protein oxidation products in human atherosclerosis. Am J Pathol. febbraio 2002;160(2):701–10.

172.   Leonarduzzi G, Poli G, Sottero B, Biasi F. Activation of the mitochondrial pathway of apoptosis by oxysterols. Front Biosci J Virtual Libr. 1 gennaio 2007;12:791–9.

173.   Honda A, Yamashita K, Hara T, Ikegami T, Miyazaki T, Shirai M, et al. Highly sensitive quantification of key regulatory oxysterols in biological samples by LC-ESI-MS/MS. J Lipid Res. febbraio 2009;50(2):350–7.

174.   Alfajaro MM, Kim H-J, Park J-G, Ryu E-H, Kim J-Y, Jeong Y-J, et al. Anti-rotaviral effects of Glycyrrhiza uralensis extract in piglets with rotavirus diarrhea. Virol J. 18 dicembre 2012;9(1):310.

175.   Gonçalves JLS, Lopes RC, Oliveira DB, Costa SS, Miranda MMFS, Romanos MTV, et al. In vitro anti-rotavirus activity of some medicinal plants used in Brazil against diarrhea. J Ethnopharmacol. 14 luglio 2005;99(3):403–7.

176.   Knipping K, Garssen J, van't Land B. An evaluation of the inhibitory effects against rotavirus infection of edible plant extracts. Virol J. 26 luglio 2012;9:137.

177.   Roner MR, Tam KI, Kiesling-Barrager M. Prevention of rotavirus infections in vitro with aqueous extracts of Quillaja Saponaria Molina. Future Med Chem. luglio 2010;2(7):1083–97.

178. Téllez MA, Téllez AN, Vélez F, Ulloa JC. In vitro antiviral activity against rotavirus and astrovirus infection exerted by substances obtained from Achyrocline bogotensis (Kunth) DC. (Compositae). BMC Complement Altern Med. 3 dicembre 2015;15(1):428.

179. Bae EA, Han MJ, Lee M, Kim DH. In vitro inhibitory effect of some flavonoids on rotavirus infectivity. Biol Pharm Bull. settembre 2000;23(9):1122–4.

180. Balagna C, Perero S, Percivalle E, Nepita EV, Ferraris M. Virucidal effect against coronavirus SARS-CoV-2 of a silver nanocluster/silica composite sputtered coating. Open Ceram. maggio 2020;1:100006.

181. Näslund TI, Paquin-Proulx D, Paredes PT, Vallhov H, Sandberg JK, Gabrielsson S. Exosomes from breast milk inhibit HIV-1 infection of dendritic cells and subsequent viral transfer to CD4+ T cells. AIDS Lond Engl. 14 gennaio 2014;28(2):171–80.

182. Feng D, Zhao W-L, Ye Y-Y, Bai X-C, Liu R-Q, Chang L-F, et al. Cellular internalization of exosomes occurs through phagocytosis. Traffic Cph Den. maggio 2010;11(5):675–87.

183. Yang M, Song D, Cao X, Wu R, Liu B, Ye W, et al. Comparative proteomic analysis of milk-derived exosomes in human and bovine colostrum and mature milk samples by iTRAQ-coupled LC-MS/MS. Food Res Int Ott Ont. febbraio 2017;92:17–25.

184. Tian T, Zhu Y-L, Zhou Y-Y, Liang G-F, Wang Y-Y, Hu F-H, et al. Exosome uptake through clathrin-mediated endocytosis and macropinocytosis and mediating miR-21 delivery. J Biol Chem. 8 agosto 2014;289(32):22258–67.

185. Luketic L, Delanghe J, Sobol PT, Yang P, Frotten E, Mossman KL, et al. Antigen presentation by exosomes released from peptide-pulsed dendritic cells is not suppressed by the presence of active CTL. J Immunol Baltim Md 1950. 15 ottobre 2007;179(8):5024–32.

186. van Dongen HM, Masoumi N, Witwer KW, Pegtel DM. Extracellular Vesicles Exploit Viral Entry Routes for Cargo Delivery. Microbiol Mol Biol Rev MMBR. giugno 2016;80(2):369–86.

187. Newburg DS, Linhardt RJ, Ampofo SA, Yolken RH. Human milk glycosaminoglycans inhibit HIV glycoprotein gp120 binding to its host cell CD4 receptor. J Nutr. marzo 1995;125(3):419–24.

188. Inagaki M, Muranishi H, Yamada K, Kakehi K, Uchida K, Suzuki T, et al. Bovine κ-casein inhibits human rotavirus (HRV) infection via direct binding of glycans to HRV. J Dairy Sci. maggio 2014;97(5):2653–61.

189. Inagaki M, Yamamoto M, Xijier null, Cairangzhuoma null, Uchida K, Yamaguchi H, et al. In vitro and in vivo evaluation of the efficacy of bovine colostrum against human rotavirus infection. Biosci Biotechnol Biochem. 2010;74(3):680–2.

190. Devery-Pocius JE, Larson BL. Age and previous lactations as factors in the amount of bovine colostral immunoglobulins. J Dairy Sci. febbraio 1983;66(2):221–6.

ACKNOWLEDGEMENTS

Poco prima di iniziare questo percorso di Dottorato, sono stata catapultata dagli eventi nella cruda realtà di questo mondo. La caduta è stata fragorosa, ma mi ha permesso di vedere sfumature che ignoravo del tutto. Con il tempo ho anche capito che se ti aggrappi alle cose belle tutto diventa più facile e ci si rialza più in fretta. Bisogna trovare il bello e saperne gioire.

Una delle cose belle di questi 4 anni è stato il mio Laboratorio. Nel Laboratorio di Virologia Molecolare e Ricerca Antivirale ho trascorso un'infinità di ore che paiono, al contrario, essere volate come un soffio di vento. Ho lavorato tanto, ho faticato, ma l'ho fatto in un ambiente sano ed equilibrato che mi ha sempre fatto sentire a casa. Devo quindi ringraziare dal profondo del cuore tutte le persone che compongono il gruppo di laboratorio, perché sono figure preziose che hanno contribuito a fare di me quello che sono.

Ringrazio il mio Maestro, il Prof. David Lembo, per essere il capo che molti vorrebbero e che tanti ci invidiano. Grazie per la sua profonda empatia e per aver curato la nostra parte umana ancor prima del nostro essere scienziati. Grazie per aver saputo cogliere e valorizzare i punti forti di ognuno di noi e per aver creato un gruppo di persone che, seppur profondamente diverse, sono estremamente unite. Grazie per non essersi mai stancato di ripeterci di sognare in grande e sognare sempre, nonostante le evidenti avversità. Grazie per aver trovato puntualmente le parole giuste sia per rincuorarci, sia per spronarci a migliorare ogni giorno. Grazie, infine, per aver creduto in me e per avermi fatto crescere professionalmente più di quanto potessi immaginare all'inizio del mio percorso. Guardandomi indietro vedo 4 anni di successi e sono certa che il Professore ci guiderà, nel futuro prossimo, verso altri traguardi ambiziosi.

Ringrazio la Prof.ssa Manuela Donalisio per incarnare l'ideale di donna moderna che ho sempre ammirato: forte, decisa, indipendente, appassionata, in carriera e madre. Grazie per essere stata per me un punto di riferimento, sempre pronta ad aiutarmi e sostenermi. Grazie per il bel rapporto, professionale e di amicizia, che si è creato tra noi.

Ringrazio il Dott. Andrea Civra, per essere stato come un fratello maggiore. Grazie per avermi insegnato molti trucchi del mestiere fin da quando ero studentessa e per continuare a farlo instancabilmente. Grazie per aver condiviso le sue idee brillanti e per essere la forza innovativa del nostro gruppo. Ammiro la sua profonda e radicata passione per la Virologia che è in grado di trasmettere a quanti ci circondano. Grazie per essere diametralmente opposto alla mia persona e per

avermi così fornito un diverso punto di vista su cui ragionare e con cui crescere. Grazie, infine, per aver sempre mantenuto il sorriso, anche nei miei tempi più bui.

Ringrazio il Dott. Massimo Rittà per la sua indistruttibile gentilezza, per la sua sensibilità e la sua preziosa amicizia. Grazie per non avermi mai negato un consiglio o un incoraggiamento.

Ringrazio anche tutti gli altri compagni di viaggio. Ringrazio la dolce Irene e le auguro che il suo percorso di dottorato sia tanto bello quanto il mio e ringrazio Matteo, Federica, Eleonora e Natalie per essere stati parte del bello che mi ha circondata.

Ringrazio la mia bella e grande famiglia, in cui includo i miei numerosi amici. In particolare ringrazio la donna più forte che io conosca, mia madre, che si piega, ma so che non si spezzerà mai. Ringrazio la mia roccia, mio papà. E ringrazio mio fratello, Edoardo, per lottare ogni giorno e per resistere al richiamo degli abissi dell'animo umano.

Infine ringrazio Dario, infinito amore mio.